# REFINEMENT OF MODELLING TOOLS TO ASSESS POTENTIAL AGROHYDROLOGICAL IMPACTS OF CLIMATE CHANGE IN SOUTHERN AFRICA

by

Lucille Annalise Perks

Submitted in partial fulfilment of
the academic requirements for the degree of
Doctor of Philosophy of Science in Hydrology
in the
School of Bioresources Engineering and Environmental Hydrology
University of Natal

Pietermaritzburg
2001

# ABSTRACT

Changes in climate due to anthropogenic influences are expected to affect both hydrological and agricultural systems in southern Africa. Studies on the potential impacts of climate change on agrohydrological systems had been performed previously in the School of Bioresources Engineering and Environmental Hydrology (School of BEEH). However, refinement of these modelling tools and restructuring of the databases used was needed to enable more realistic and dynamic simulations of the impacts of changes in climate. Furthermore, it was realised that modifications and linkages of various routines would result in a faster processing time to perform climate impact assessments at the catchment scale.

Baseline ("present") climatic information for this study was obtained from the School of BEEH's database. Scenarios of future climate were obtained from six General Circulation Models (GCMs). Output from the five GCMs which provided monthly climate output was used in the climate impact assessments carried out. Potential changes in variability of rainfall resulting from climate change was assessed using the daily climate output from the sixth GCM. As the spatial resolution of the climatic output from these GCMs was too coarse for use in climate impact studies the GCM output was interpolated to a finer spatial resolution.

To assess the potential impact of climate change on water resources in southern Africa the *ACRU* hydrological modelling system was selected. The *ACRU* model was, however, initially modified and updated to enable more dynamic simulation of climate change. In previous hydrological studies of climate change in southern Africa Quaternary Catchments were modelled as individual, isolated catchments. To determine the potential impact of changes in

climate on accumulated flows in large catchments the configuration of the Quaternary Catchments needed to be determined and this configuration used in *ACRU*.

The changes in hydrological responses were calculated both as absolute differences between future and present values and the ratio of future hydrological response to the present response. The large degree of uncertainty between the GCMs was reflected in the wide range of results obtained for the water resources component of this study. In addition to the climate impact studies, sensitivity and threshold studies were performed using *ACRU* to assess the vulnerability of regions to changes in climate.

Potential change in the yields and distributions of parameters important to agriculture, such as heat units, crops, pastures and commercial tree species were assessed using simple crop models at a quarter of degree latitude / longitude scale. Most species were simulated to show decreases in yields and climatically suitable areas. There are many sources of uncertainties when performing climate impact assessments and the origins of these uncertainties were investigated. Lastly, potential adaptation strategies for southern Africa considering the results obtained are presented.

# PREFACE

The research work presented in this thesis was carried out in the School of Bioresources Engineering and Environmental Hydrology, University of Natal, Pietermaritzburg, from August 1997 to December 2000, under the supervision of Prof. Roland E. Schulze and the co-supervision of Dr Gregory A. Kiker.

I wish to certify that the research reported in this thesis is my own original and unaided work except where specific acknowledgement is given, and that no part of the thesis has been submitted in any form for any degree or diploma to another University.

Signed

Lucille A. Perks

# ACKNOWLEDGEMENTS

The author wishes to express her sincere appreciation for the assistance and advice given by the following:

Prof. R.E. Schulze (Professor of Hydrology in the School of Bioresources Engineering and Environmental Hydrology, University of Natal, Pietermaritzburg) for his supervision, guidance and encouragement regarding the research presented in this thesis;

Dr G. A. Kiker (Lecturer in the School of Bioresources Engineering and Environmental Hydrology, University of Natal, Pietermaritzburg) for his co-supervision, expertise and guidance in the fields of computer programming and Geographical Information Systems;

The staff of the Computing Centre for Water Research (CCWR, University of Natal, Pietermaritzburg) for their advice and assistance and use of their computing facilities. Particular thanks to Mr A. Kure and Mr R. de Vos for their assistance in Fortran programming and guidance in the use of the UNIX system;

Prof. B. C. Hewitson (Department of Environmental and Geographical Science, University of Cape Town), for data and information on climate change;

Mr M. J.C. Horan for his invaluable expertise and help in the field of Geographic Information Systems;

Mrs M. Maharaj for her assistance in running the Smith Crop Models for various agricultural impacts of climate change and use of program to generate daily temperature estimates;

The National Research Foundation (NRF) for the provision of a post-graduate grant;

The Water Research Commission (WRC) for funding the research presented in Chapter 7 in this thesis; and

The United States Country Studies Programme and Eskom for funding research on impacts of climate change on water resources and agriculture in southern Africa.

# LIST OF ABBREVIATIONS

The following abbreviations are frequently used in this dissertation:

| | |
|---|---|
| 1X $CO_2$ | present climatic conditions |
| 2X $CO_2$ | effective doubling of atmospheric carbon dioxide concentrations, representing a future climate scenario |
| $CO_2$ | carbon dioxide |
| CSM (1998) | 1998 version of the Climate Systems Model General Circulation Model |
| Genesis (1998) | 1998 version of the Genesis General Circulation Model |
| GCMs | General Circulation Models |
| HadCM2-S | second version of the Hadley Centre General Circulation Model using the scenario of greenhouse gases only and excluding sulphate feedbacks |
| HadCM2+S | second version of the Hadley Centre General Circulation Model using the scenario of greenhouse gases and sulphate feedbacks |
| HadCM3-S | third version of the Hadley Centre General Circulation Model using the scenario of greenhouse gases only and excluding sulphate feedbacks |
| $I_l$ | rainfall interception loss (mm) |
| IPCC | Intergovernmental Panel on Climate Change |
| $K_{cm}$ | crop water use coefficient on a monthly basis (-) |
| $K_d$ | crop water use coefficient on a daily basis (-) |
| LAI | leaf area index (-) |
| MAR | mean annual runoff (mm) |
| ppmv | part per million by volume |
| $R_A$ | fraction of roots in the A horizon (-) |
| $T_{max}$ | maximum temperature (°C) |
| $T_{min}$ | minimum temperature (°C) |
| UKTR-S | first version of the Hadley Centre General Circulation Model using the scenario of greenhouse gases only and excluding sulphate feedbacks |

# TABLE OF CONTENTS

# LIST OF TABLES

# LIST OF FIGURES

# 1. INTRODUCTION AND OBJECTIVES

There is clear evidence that increases in the concentrations of certain gases in the atmosphere have resulted in an increase of the temperature of the earth over the past century (IPCC, 2000a). The seven warmest recorded years occurred during the past decade (1990 to 1999) with the warmest having been 1998. In addition, 1999 was the 21st consecutive year with an above-normal globally averaged surface temperature (World Climate News, 2000). Although the earth's climate has always experienced natural fluctuations in temperature over time the changes in temperatures presently being experienced are, firstly, human induced and not a result of natural influences and, secondly, the rate of temperature change is set to be unprecedented (Rowlands, 1998).

The concentrations of the gases which regulate the temperature of the earth, known as greenhouse gases, have been increasing exponentially since the beginning of the Industrial Revolution in the 1800s owing to anthropogenic activities such as fossil fuel burning and the use of man-made gases in industry (Westmacott and Burn, 1997; Piltz, 1998). This disturbance of the natural controls of the earth's temperature by anthropogenic activities is termed the enhanced greenhouse effect and is described in greater detail in Chapter 2.

Although scientists agree that concentrations of greenhouse gases are rising, there remain major uncertainties about the magnitude of the impact of these gases, in particular that of carbon dioxide ($CO_2$), on the earth's climate. These uncertainties are reflected in a wide range of estimates of future global mean temperature and precipitation changes and in uncertainties about regional climate alterations (IPCC, 2000a).

Relatively small changes in temperature and precipitation, together with their non-linear effects on evapotranspiration and soil moisture, can cause significant dynamic response changes on water quantity, quality and distribution. Such changes in the future could lead to an intensification of the global hydrological cycle and could have major impacts on regional water resources (IPCC, 2000a). In addition, rising concentrations of $CO_2$ have the potential to affect plant growth and transpiration rates, thereby affecting the productivity of agricultural

systems (Rosenzweig and Hillel, 1998). Thus, considering the socio-economic implications of changes in agrohydrological systems, impact studies are needed to assess what the potential impact of changes in climate could be on these systems.

Initially, the emphasis of the global change research community was on understanding global scale aspects of climate change. However, more recently there has been growing interest in the regional and local implications of climate change (Yarnal, 1998). Africa could be considered the continent most vulnerable to climate change. Compared to most industrialised countries, developing countries are generally more dependent on climatic resources and have a lower adaptive capacity at present (Downing *et al.*, 1997). Southern Africa, defined in this study as the contiguous area covered by the Republic of South Africa and the Kingdoms of Lesotho and Swaziland, is characterised by a general scarcity of water, exacerbated by a high temporal and spatial variability of rainfall, thus rendering it a high risk natural environment (Basson, 1997; Schulze, 1997a). Anticipated climate changes over South Africa are expected to be different from global means (Schulze and Kunz, 1996).

The research presented in this thesis builds on from previous research in the School of Bioresources Engineering and Environmental Hydrology at the University of Natal, Pietermaritzburg (School of BEEH) on climate change impacts on agricultural and hydrological systems in southern Africa (e.g. Schulze *et al.*, 1993; Kunz, 1993; Lowe, 1997). From this previous research, relatively simple techniques had been developed to assess the potential agrohydrological impacts of climate change in southern Africa. However, it was realised that refinement of these tools would enable more realistic simulations of the impacts of changes in climate as well as a more efficient method of obtaining results.

The primary objective of this thesis was the refinement of modelling tools, primarily the *ACRU* model, and fundamental review of the spatial databases used to in this study. Following this primary objective were the secondary objectives of applying these refined tools and restructured databases to assess potential agrohydrological impacts of climate change in southern Africa as well as the evaluation of uncertainties in climate impact assessments and possible adaptation strategies for southern Africa considering the results obtained. An overview of the layout of this thesis is presented in Figure 1.1.

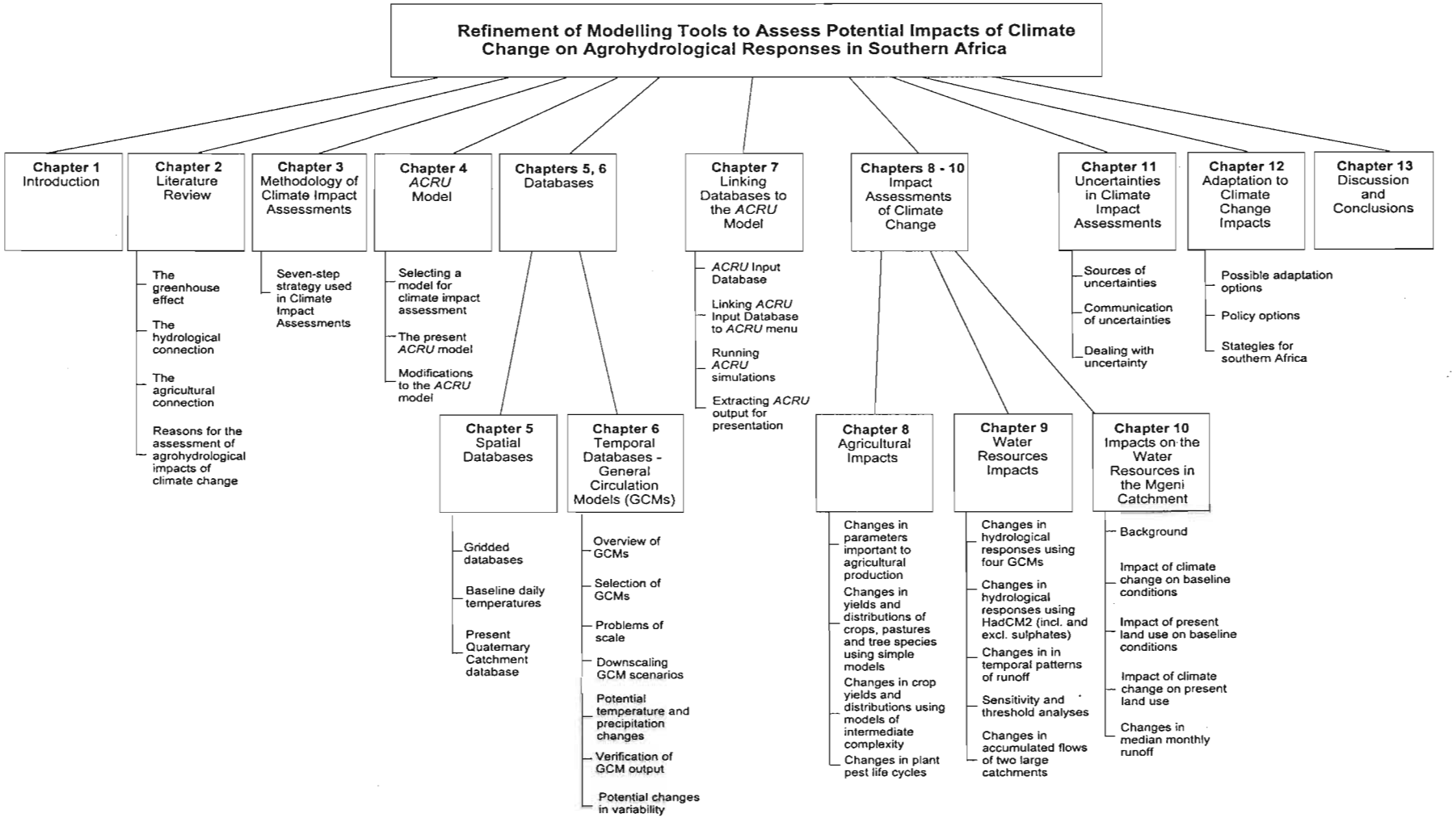


Figure 1.1 Layout plan of thesis

With the primary objective, sub-objectives of this study include

i) the selection of a suitable agrohydrological model to assess the potential impacts of climate change on water resources in the study region and modification of the model to enable, *inter alia*, more dynamic simulation of impacts of changes in climate on the agrohydrological system;

ii) the interpolation of monthly temperature and precipitation estimates of projected future climate scenarios to a scale suitable for use in climate impact assessments;

iii) the extraction of daily estimates of projected future temperature and precipitation scenarios for southern Africa to assess potential changes in, *inter alia*, climatic and hence hydrological variability in the study area;

iv) the preparation of a spatial database structure which would allow flexibility and ease of use for storage and manipulation of input variables for the agrohydrological model used in many instances in this study for simulating potential climate change impacts;

v) the linkages of operational catchments in the study area to assess potential changes in accumulated streamflows at any point in a large catchment owing to changes in climate;

as part of the secondary objective, *viz.* applying refinements in impact studies, were

vi) the assessment of potential changes in crop yields and the climatically optimum cultivation areas of selected crops, commercial tree species and planted pastures resulting from climate change using models of varying complexity;

vii) an assessment of sensitivities, thresholds of change and potential impacts of climate change on hydrological responses and water resources in southern Africa;

viii) a detailed case study of an operational catchment in southern Africa to simulate potential changes in supply and demand of water with a change in climate and assess the relative impact of climate change versus land use change on the water resources of this catchment;

and finally

ix) the assessment of the sources of uncertainty which are inherent in climate change impact assessments; and

x) suggestions on potential adaptation strategies for southern Africa based on the results obtained.

The 10 points listed above are now discussed more fully in the light of the sequence and contents of chapters making up this thesis.

An initial objective of any regional study of the impacts of climate change is the selection of a model, in this case an agrohydrological one, considered suitable for assessing climate change impacts. The daily time step *ACRU* agrohydrological modelling system (Schulze, 1995a) has been selected for reasons given in Chapter 4 and modified to enable more dynamic simulation of water and agriculture responses with changes in temperature, precipitation and $CO_2$ concentrations.

When conducting experiments to assess the potential impacts of climate change, it is necessary to obtain

i) values of baseline conditions of the present climate in order to provide a reference against which to compare impacts of predictions of future climates; as well as

ii) quantitative representations of the predicted changes in climate.

The spatial databases of baseline climatic conditions used in this study are described in Chapter 5. Baseline climate information was required in the form of gridded values, used in most of the agricultural impacts assessments, and on a Quaternary Catchment scale, which is the finest scale of operational catchment subdivision used in hydrological studies in southern Africa, at which the water resources, maize and winter wheat yield assessments are conducted.

At present no method exists of providing confident predictions of future climates and therefore climate scenarios are generally used. Such scenarios present coherent, systematic and physically plausible descriptions of future climate which may be used as input into climate change assessments (Parry and Carter, 1998). Climate change scenarios can help identify potential directions of effects and the potential magnitudes of impacts. The use of scenarios can also help identify the sensitivity of agrohydrological responses to changes in different climatological variables. There are numerous ways in which climate change scenarios can be constructed, although the most widely favoured methods use results from large scale atmospheric models, known as General Circulation Models (GCMs). Outputs from GCMs are, at present, usually applied as monthly or seasonal adjustments to the baseline

climatic conditions rather than daily adjustments, assuming no change in climatic variability and sequences of events between the baseline and future climates (Parry and Carter, 1998).

General Circulation Models produce estimates of climatic variables for a regular network of points across the globe. The most reliable spatial scales of GCMs are continental to global, where the grid cells are tens, or hundreds, of kilometres across, whereas simulation models to assess potential climate change impacts generally have an ideal spatial resolution of 10 km or less (Bass, 1993). To allow GCM output of temperature and precipitation to be used in simulation models, several methods have been adopted for developing regional GCM-based scenarios at a finer grid scale, frequently through a process of interpolation. Thus, the next objective of this study was the interpolation of the GCM output to a finer spatial resolution for use in impact studies. The six GCMs selected for use in this study and the interpolation of the monthly temperature and precipitation output from these GCMs are described in Chapter 6. Furthermore, daily information on present and future climatic conditions as simulated by the HadCM3 GCM of the Hadley Centre in the United Kingdom was obtained towards the end of this study and this information was used in a preliminary analysis of potential changes in climate variability and climatic extremes resulting from climate change.

Previously the inputs into the *ACRU* model for each Quaternary Catchment were stored in ASCII files and the input information was extracted based on each catchment's numerical identity. This information storage structure was found to be limiting owing to, *inter alia*, the restrictions imposed by linking the *ACRU* input information for each catchment via a numerical identity which is restricting if the Quaternary Catchments are subdivided and the new information pertaining to these catchments needs to be added to the database. In addition, the initial structure did not allow for easy manipulation and addition of new information to the database. Thus, the *ACRU* Input Database structure for application with the *ACRU* model has been completely revised to allow for greater flexibility of this input information, as described in Chapter 7.

The new database structure was used for to store the relevant *ACRU* input information for each of the 1946 Quaternary Catchments making up the study region as a pre-populated database which multiple users could access when simulating agrohydrological responses at

a Quaternary Catchment level. The information in the Quaternary Catchment Input Database has also been enhanced to allow studies of, say, potential changes in sediment yield, extreme value distributions or crop yields to be carried out.

In previous hydrological studies in southern Africa each Quaternary Catchment was modelled as an individual catchment without considering upstream runoff contributions. In reality, however, the Quaternary Catchments are hydrologically linked and simulated streamflows should be cascaded from one Quaternary Catchment to the next one downstream, using catchment configuration and flow routing procedures available in *ACRU*. In order to be able to simulate the runoff of the Quaternary Catchments as they would flow naturally into the next downstream Quaternary Catchment, the Quaternary Catchments had to be configured to determine the sequencing of cascading catchments. This configuration facilitates the determination of changes in the total (accumulated) available water at any point within a large catchment with and without changes in climate. The methods used for simulating agrohydrological responses to changes in climate and the extraction of the results for display purposes are described in Chapter 7.

Once the baseline and climate change scenarios had been prepared, this information can to be utilised in conjunction with selected models to assess the potential impacts of climate change on agricultural production and water resources systems in southern Africa (Chapters 8 and 9). For this purpose the daily time step *ACRU* model is used in conjunction with the Quaternary Catchment Input Database. However, for certain agricultural impact assessments simple unidirectional, monthly models are used in conjunction with the School of BEEH's gridded climatic database (baseline database). The exceptions are the maize and winter wheat yield analyses which were carried out using submodels of intermediate complexity which have been imbedded within the *ACRU* modelling system.

The results of the water resources assessments presented in Chapter 9 are carried out assuming baseline catchment land cover conditions to assess relative changes in water resources in the study area. However, a detailed study is carried out on the Mgeni Catchment in KwaZulu-Natal, South Africa which displays complex present land use and water transfer patterns, to assess potential changes in water supply and demand with changes in climate, as well as

evaluating the relative impacts of climate change compared with that of land use change from a baseline to the present land use, on water resources in this catchment. This was achieved by including dams, abstractions from dams and rivers, return flows, irrigation demand / supply as well as domestic water use in the model simulations of this catchment. The results from this detailed study of an operational catchments' responses are presented in Chapter 10.

There are many uncertainties in climate impact assessments. These uncertainties need to be understood and communicated to the users of the climate impact assessment. Uncertainties in impact assessments are derived from numerous sources including the output from the GCMs, the downscaling procedure used and the model used in the impacts assessments. The sources of these uncertainties and the methods suggested to convey these uncertainties in climate impact assessments are reviewed in Chapter 11.

Various adaptation measures can be applied in both the agricultural and water resources sectors to reduce any potential negative effects of climate change. Examples of potential adaptation strategies which could be applied in southern Africa, considering the results obtained from this and various other studies carried out, are highlighted in Chapter 12. Finally, in Chapter 13 the thesis is concluded with a review of the objectives of the research, conclusions that can be drawn from the results obtained and recommendations for future research.

* * * * * * *

The chapter which follows describes the natural greenhouse effect and how the anthropogenically induced increases in certain atmospheric trace gases may augment this effect. Only general background information on the mechanisms of climate change is provided, and the reader is referred to the comprehensive report by the Intergovernmental Panel on Climate Change (IPCC) on the science of climate change (IPCC, 1996a) for greater detail. Following this short description of the greenhouse effect is an overview of recent findings of how changes in climate, induced by the greenhouse effect, could affect hydrological and agricultural responses, with particular reference to potential impacts in developing countries.

# 2. GLOBAL CLIMATE CHANGE AND ITS LINKS TO HYDROLOGICAL AND AGRICULTURAL SYSTEMS

Data from the turn of the century to the end of 1995 for Africa south of the equator (Jones, 1994; Hulme, 1996) show that, except for a hot 1941, the 10 years with the highest average annual temperatures have all occurred since 1983, with the hottest year being 1987. Among South Africa's most severe droughts of this century have been those in the 1982/3 and 1991/2 summer seasons. Many statistical tests indicate that much of the warming can be attributed to human activities (Piltz, 1998). Changes in temperature and subsequent changes in precipitation and evaporation rates are expected to affect both hydrological and agricultural systems.

As an introduction to the potential impacts on these two systems, the greenhouse effect and the natural and anthropogenic influences on climate are briefly reviewed. This is followed by an overview of potential changes in climatic variables, catchment processes and water resources resulting from climate change. In regard to anticipated effects on agricultural systems, potential changes in physiological processes of crops, competition from weeds, insect pests and plant diseases are subsequently highlighted.

## 2.1 Global Climate Change

For several decades scientists have been searching for evidence that climate is changing and that these changes are primarily a result of human activities (Piltz, 1998). Scientific observations from ships and land-based stations have shown that the average air temperature of the earth has increased by between 0.3 and 0.6 °C during the past 100 years and by 0.2 and 0.4 °C over the past 40 years (IPCC, 1996a; Hudson, 1997). Precipitation patterns, amounts and intensities have also changed globally (IPCC, 2000a). Such changes in climate over the recent past are termed climate change.

### 2.1.1 The greenhouse effect

The greenhouse effect is a natural process responsible for regulating the earth's surface temperature and is influenced primarily by the concentration of atmospheric trace gases known as greenhouse gases. The atmospheric concentrations of active greenhouse gases, such as carbon dioxide ($CO_2$), methane ($CH_4$) and chlorofluorocarbons (CFCs) have been increasingly exponentially since the beginning of the Industrial Revolution (19th century), thereby augmenting the natural greenhouse effect (IPCC, 1996a).

This anthropogenic disturbance of the natural greenhouse effect is termed the augmented, or enhanced, greenhouse effect (Graedel and Crutzen, 1993). Elevated concentrations of greenhouse gases from anthropogenic activities are associated with an increasing global population, fossil fuel combustion, biomass burning, land use changes such as deforestation, agricultural practices, industrialisation and the use of CFCs for propellants, solvents and refrigerants (Sulzman *et al.*, 1995).

These greenhouse gases in the atmosphere absorb and partially re-emit outgoing infra-red radiation from the earth's surface while allowing for the penetration of incoming short wave solar radiation through the atmosphere, as depicted in Figure 2.1 (Sulzman *et al.,* 1995).

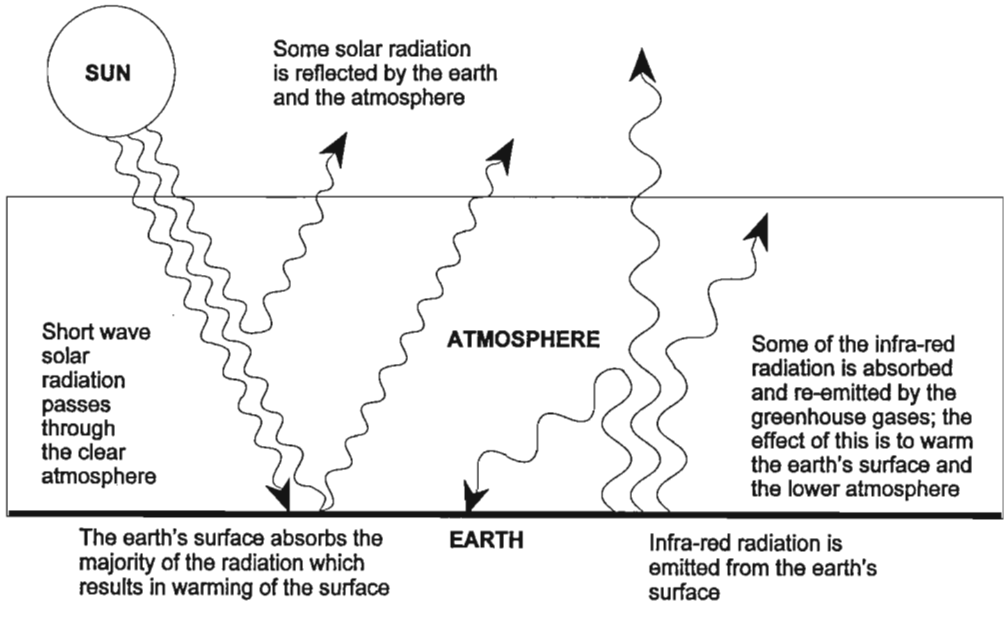


Figure 2.1 Schematic diagram of the greenhouse effect

The augmented greenhouse effect results in increased warming at the earth's surface, which in turn affects other climatic variables such as atmospheric humidity, cloudiness, rainfall and evaporation. This warming may, however, be partly offset by anthropogenic aerosols which produce a negative radiative forcing or cooling effect. Examples of aerosols which result in a cooling of the atmosphere are sulphate aerosols, soot, organics, mineral dust and sea salt. The quantities of these aerosols can vary considering over space and respond quickly to changes in emissions. The quantification of the impact these aerosols have on the climate is less certain than the impact of the greenhouse gases which have a positive radiative forcing. The rapid accumulation of greenhouse gases resulting from human activities and development of the planet can have a variety of impacts from local to regional and global scales (Graedel and Crutzen, 1993; IPCC, 1996a; IPCC, 2000a).

### 2.1.2 Natural and anthropogenic influences on climate

Any anthropogenic influences on climate will be superimposed on the natural variability of the present climate (IPCC, 1996a). While considerable progress has been made since the early 1990s in distinguishing between natural and anthropogenic influences on climate, this distinction, however, remains difficult as both influences have an impact on climate (Piltz, 1998). However, recent findings have been able to consistently find evidence for an anthropogenic signal in the record of climate over the past 50 years (IPCC, 2000a). The problem of attribution of causal blame for any unusual changes in climate is termed the attribution problem (Risbey *et al.*, 2000).

The most significant natural contributor to the enhanced greenhouse effect is water vapour, while the main anthropogenic contributor is $CO_2$, the atmospheric concentration of which has increased by 30% since the Industrial Revolution (Shackleton *et al.*, 1996; Peixoto, 1997). The atmospheric concentration of $CO_2$ at present has not been exceeded in the past 420 000 years and the rate of increase over recent decades has not been evident in the past 20 000 years (IPCC, 2000a). There is an important symbiosis which exists between atmospheric $CO_2$ and water vapour. The abundance of water vapour is ultimately controlled by surface temperature. Any increases in $CO_2$, which raises temperature, augments atmospheric water vapour, which in turn eventually raises temperature even further (Hare, 1988).

The concentration of $CO_2$ before the Industrial Revolution was estimated at 280 ppmv. The common climate change scenario of an effective doubling of $CO_2$ ($2X\ CO_2$) is made up of the combined effects of all greenhouse gases (Pittock, 1991). This effective atmospheric doubling of $CO_2$ from Pre-Industrial times to 560 ppmv could take place during the latter part of the 21st century (Shackleton *et al.*, 1996).

The products of certain greenhouse gases destroy the ozone layer, an important filter of ultraviolet radiation from the sun. Its destruction reduces the atmosphere's ability to filter incoming solar radiation, thus further disturbing the radiation budget (Graves and Reavey, 1996).

One of the most significant impacts of the augmented greenhouse effect is anticipated to be on water resources which includes changes in water supply and demand, irrigation demand and water quality (Arnell, 1995). The anticipated responses of the hydrological cycle to changes in precipitation and temperature are reviewed in the following section.

## 2.2 Climate Change: The Hydrological Connection

Southern Africa's natural environment is characterised by a scarcity of water and a high temporal and spatial variability of runoff, making it a high risk natural environment (Schulze, 1997a). Relatively small changes in temperature and precipitation, together with their non-linear effects on evapotranspiration and soil moisture, can cause significant dynamic response changes on water quantity, quality and distribution, especially in arid and semi-arid regions. Such changes in the future could lead to an intensification of the global hydrological cycle and have major impacts on regional water resources (IPCC, 1996b; MacIver, 1998). Water is considered to be one of the most critical factors associated with climate change impacts and adaptability.

### 2.2.1 The hydrological equation

In order to quantify the potential impacts of climate change on the hydrological system, an understanding of the workings of the hydrological equation and how it will be affected by climate change is needed (Rosenberg *et al.*, 1990). It is important to distinguish between hydrological effects and water resources impacts owing to climate change. Hydrological effects are those changes in the primary hydrological system (e.g. rainfall, evapotranspiration, infiltration and runoff) that are caused by global warming. Water resources, however, connotes the control, use and distribution of the available water supply for society's purposes.

Changes in climate variables need to be translated into hydrological responses changes. For example, changes in precipitation ($\Delta P$), temperature ($\Delta T$) or potential evaporation ($\Delta E_p$) have to be converted to changes in soil moisture ($\Delta S$), streamflow volume ($\Delta Q$), peak discharge ($\Delta q_p$) or sediment yield ($\Delta S_y$). In addition, hydrological responses have to be translated into water resources related changes, for example of reservoir yield, stormwater design or irrigation water demands (Beran, 1989; Schulze, 1997a). Reduced to its barest form for a given catchment undisturbed by hydraulic alterations such as dams, abstractions or interbasin water transfers, the hydrological equation in relation to climate change can be expressed in the form presented in Figure 2.2 (Schulze, 1991).

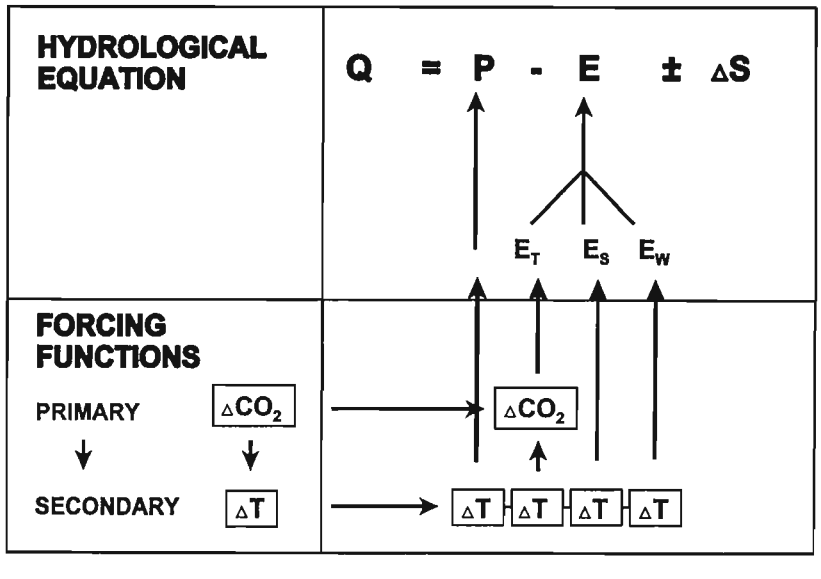


Figure 2.2 Climate change and the hydrological equation (after Schulze, 1991)

where $Q$ = runoff (mm equivalent)

$P$ = precipitation (mm)

$E$ = total evaporation (mm), made up of three components, *viz.*

$E_t$ = plant transpiration

$E_s$ = soil water evaporation

$E_w$ = evaporation from open water surfaces and / or intercepted water

$\Delta S$ = changes in the water storage (surface, soil and groundwater in mm)

$\Delta CO_2$ = changes in carbon dioxide (ppmv)

$\Delta T$ = changes in temperature (°C).

This simple hydrological equation describes a dynamic, non-linearly lagged and cascading hydrological system consisting of complex feedforwards and feedbacks, with any perturbations to inputs or stores interacting or cascading throughout the system (Schulze, 1998). A change to either of the two forcing functions, *viz.* precipitation or temperature, could therefore impact the response function, *viz.* runoff as shown in Figure 2.2 (Schulze, 1997a).

Any change in the distribution of precipitation will affect soil moisture storage, runoff processes and groundwater recharge (IPCC, 1996b). The factors which govern runoff may be divided into two categories (Kunz and Schulze, 1993), *viz.* climatic variables (e.g. precipitation and evaporation) and catchment processes (e.g. vegetation and soil characteristics). Potential changes in climatic variables, catchment processes and water storage owing to changes in climate are reviewed in Sections 2.2.2 to 2.2.4 which follow. Potential changes in water resources resulting from changes in climate will be summarized in Sections 2.2.5 to 2.2.7.

### 2.2.2 Changes in climatic variables

The most important climatic variable which induces changes in catchment responses is precipitation. Changes in the seasonal distribution or intensity of precipitation will change soil water storage, runoff processes and groundwater recharge. Projections of regional

changes in precipitation from climate models are less certain than changes in temperature. Climate models project an increase in global mean precipitation of about 3 - 15% for a temperature increase of 1.5 - 4.5 °C. However, on a regional scale, it is likely that precipitation will increase in some areas while decreasing in others (IPCC, 1996b). Precipitation is influenced on a local scale by factors such as altitude, distance from physiographic barriers and direction of rain-bearing winds which, due to the coarse spatial scale of the GCM grids simulations, is often not represented in the simulations of climate. Temperature pattens, however, are more predictable over space.

There is a sensitive, non-linear relationship between precipitation and runoff, with small changes in precipitation being amplified in changes in runoff (Schulze *et al.*, 1995a). Arid and semi-arid regions, which cover nearly half of South Africa, are particularly sensitive to changes in precipitation because the fraction of rainfall that runs off or percolates to groundwater is small (Lins *et al.*, 1991) and hence, any small absolute change in streamflow is likely to be significant in relative terms.

Probably equally important hydrological consequences of global warming are potential changes in the intensity and seasonality of rainfall (Schulze, 1997a). Increased convective activity could increase the frequency and intensity of rainfall events, augmenting runoff volumes, peak discharges and sediment yields from a catchment (Kunz, 1993).

In southern Africa, over 90% of all precipitation evaporates and transpires again, with only about 10% converted to runoff (Whitmore, 1971). Relatively small changes in evaporation and transpiration could have significant effects on surface runoff (Schulze, 1997a). Changes in both temperature and $CO_2$ concentrations can affect evaporation rates. The capacity of the air to hold water vapour increases by approximately 5 - 6% per °C increase in temperature (Rosenberg *et al.*, 1990), and therefore an increase in evaporation can be expected in a warmer climate.

The greenhouse effect may alter humidity, windspeed and cloudiness which also affect atmospheric evaporative demand (Rosenberg *et al.*, 1990). Increases in evaporative demand influence soil water storage through changes in evapotranspiration (Hulme, 1996) and could

affect open-water evaporation losses from water impoundments in South Africa by up to 10% (Schulze, 1991).

### 2.2.3 Changes in catchment processes

Changes in climate also significantly affect certain other processes within the hydrological system. Important in regard to catchment processes are possible changes in catchment vegetative cover and soil properties. The changes in vegetative cover and distribution are difficult to quantify as vegetation dynamics and species interactions are complex (Hulme, 1996; Schulze, 1998).

Soil properties such as bulk density, porosity, moisture content, infiltration rate, permeability and nutrient content may change with an evolving climate, perhaps slowly over decades, and also with changing vegetation cover (Rosenzweig and Hillel, 1998). Soils containing clays prone to swelling, might, with increased temperatures and soil water dehydration, encourage soil cracking, increase infiltrability and hence reduce surface runoff. Alternatively, longer wet periods could lead to waterlogging and higher surface runoff responses (Schulze, 1997a).

In addition, the increased organic matter decomposition, induced by higher temperatures, could increase the potential for soil crusting. These crusted surfaces inhibit seedling emergence, reduce infiltration rates and enhance surface runoff generation (Valentin, 1996). The overall change in runoff, due to changes in evaporation and precipitation, will depend on the individual catchment characteristics (Schulze, 1997a).

### 2.2.4 Potential changes in water storage

Soil water storage plays an important role in evaporation and evapotranspiration for plants. Any change in seasonal distribution of precipitation will change soil water storage and hence groundwater recharge (IPCC, 1996b). There are discrepancies among climate models in the prediction of regional soil moisture changes due to climate change (Rosenzweig and Hillel, 1998).

Soil moisture content is dependent on, *inter alia*, the thickness of the respective soil horizons, its texture (and hence the permanent wilting point, drained upper limit and porosity) and the interplay of the local climate regime and vegetative cover (Lowe, 1997). Soil moisture content in the A and B horizon influences a range of hydrological responses. Generally, soil moisture content in the A horizon (i.e. topsoil horizon) may influence the rate of evaporation from the soil surface, stormflow generation and the amount of saturated drainage from the A horizon to the B horizon. However, soil moisture content in the B horizon (i.e. subsoil horizon) plays a role in plant transpiration and controls the amount and rate of saturated drainage from the B horizon to the intermediate or groundwater store (Schulze, 1995b).

Groundwater plays an important role in the supply of domestic and agricultural water in many areas. Changes in precipitation patterns or magnitude could affect recharge to groundwater. There have been very few studies into the effect of climate change on groundwater recharge, with predictions of impacts and changes in recharge rates varying depending on the climate change scenario considered (IPCC, 1996b).

The occurrence of groundwater in South Africa is relatively limited compared to world averages. Already many farms, rural settlements and villages are primarily dependent on groundwater, and groundwater is destined to play an increasingly important role, particularly in the drier parts of the country. Groundwater is likely to be vital to upgrading basic drinking water supplies and sanitation services for developing communities, particularly in rural areas. It is therefore important to know the extent to which climate change may modify the availability and quality of groundwater, which is already poor in some critical areas such as the in the northern parts of the study area (Conley, 1996). It is apparent that more studies into the potential impact of climate change on groundwater recharge are needed.

### 2.2.5 Potential climate change effects on water demand and supply

South Africa experiences a high inter-annual variability of runoff, thereby placing significant demands on surface water supplies. Increasing rainfall and runoff variability and high evaporation losses will in future place a greater demand than at present on costly surface water impoundments to ensure supply of water (Conley, 1996; Mirza, 1998). Thus, the impact of

global climate change on water supply in southern Africa will depend strongly on reservoir yield (Shackleton *et al.*, 1996).

Changes in precipitation could affect water availability in soils, rivers and dams, with implications for water supplies for domestic, industrial and agricultural uses as well as ecological requirements (IPCC, 1996a). In many of the smaller settlements and farms in the drier parts of southern Africa, water supply is dependent on single sources such as rivers or groundwater from boreholes. Rural communities are expected to place a high demand on groundwater supplies in the future because of its cost effectiveness in many circumstances (Conley, 1996). Water supply situations which rely on a single local source will be particularly vulnerable to any changes in water availability. This is also the case for rural water supply in underdeveloped areas, even in the wetter parts of the country, because of the high costs of piped surface water (Conley, 1996).

Developments such as urbanisation, afforestation and overgrazing already have major impacts on runoff responses (Schulze, 1998). Implications of changes in supply and demand owing to climate change impacts give rise to potentially serious conflicts between users. The impacts of climate change on water supply systems will depend on the ability of water resources managers to respond not only to climate change, but also to population growth and changes in demands and technology.

Generally, users may be protected from climate change impacts on water supply by effective management of water resources. However, there could be substantial economic, social and environmental costs, particularly in regions that already are water-limited and where there is considerable competition among users. It is uncertain as to whether water supply systems could be adapted enough in the future to compensate for any negative impacts of climate change on water resources and potential increases in demand, should these occur (IPCC, 1996b).

### 2.2.6 Potential impacts of climate change on irrigation demand

Irrigation is the largest consumptive user of water in South Africa, using 52% of all stored water (Basson, 1997). Variability of rainfall is expected to increase with climate change, therefore to assure high crop yields, there will be the need for reliable water supply for irrigation to reduce the vulnerability of rainfed agriculture (Shackleton *et al.*, 1996). Farmers who practice irrigation should be less vulnerable to climate change than dryland farmers, provided they are assured an adequate supply of water (Rosenzweig and Hillel, 1998). However, both rainfed and irrigated crops would require more water if temperature and evaporative demand were to increase, although this demand could be offset in certain regions by the effects of increased rainfall (Arnell, 1995) and / or by the suppression of transpiration (cf. Section 2.3.1.1) induced by increased atmospheric $CO_2$ concentrations (IPCC, 1996b).

The amount of water needed to irrigate a crop (the irrigation requirement) depends principally on crop evapotranspiration. Rising air temperatures generally increase water vapour pressure deficits and consequently increase the potential crop evapotranspiration (Rosenzweig and Hillel, 1998). Rosenberg *et al.* (1990) conducted a detailed study on a grassland in Kansas, USA, and estimated that a 1 °C rise in mean air temperature could result in a 4 - 8% increase in evapotranspiration.

Water use efficiency may be defined as the amount of accumulated dry matter yield (carbon) per unit of water utilised by the plant in the evapotranspiration process (Acock, 1990). It is expected that plant water use efficiency will increase for constant temperature conditions in a future climate, as a result of the $CO_2$ fertilisation effect (cf. Section 2.3.1.1) which increases the photosynthesis rate while simultaneously reducing stomatal conductance, which has the effect of suppressing transpiration (IPCC, 1996b). An increase in water use efficiency could have important bearing on the soil moisture distribution over time, hence plant available water as well as net irrigation demand in a future climate. However, if increasing temperatures are taken into account, water use efficiency may decrease, owing to greater vapour pressure deficits (Bazzaz *et al.*, 1996). The complex feedforwards and feedbacks brought about by plant : $CO_2$ : temperature interactions make to difficult to estimate potential changes in water use efficiency and irrigation demand (Wolfe and Erickson, 1993).

### 2.2.7 Potential impacts of climate change on water quality

The conservation of the natural environment is becoming an increasing concern. Rivers, groundwater, wetlands and estuaries constitute important components of the water resources of southern Africa. Many of these systems, e.g. the Vaal or the Mgeni (Kienzle *et al.*, 1997) already have water quality and sedimentation problems (Shackleton *et al.*, 1996). The potential result of particularly severe water quality deterioration could lead to a reduction in riverine species diversity and changes in essential aquatic ecological processes (McAnally *et al.*, 1997).

Water quality depends on a complex system of inputs, feedbacks, water temperature as well as anthropogenic factors such as water transfers and releases, abstractions and land use. Changes in water quality which result from changes in climate are expected to be site specific, depending on the current water quality, anthropogenic impacts of land use and amount and direction of climate change (Arnell, 1995).

Climate change could have a range of impacts on the water quality of streams and impoundments in southern Africa. Water quality changes that might be expected are alterations in the physical (e.g. sediment), chemical (e.g. in the dissolved salts) and biological (e.g. algae, *E. coli*) status of the water systems (Arnell, 1995; Ashton, 1996). In addition, there is evidence of possible changes in the occurrence of water-bourne diseases in a warmer climate (UKMO, 2000). The possible alterations to each of these components will be reviewed in the following sections.

#### 2.2.7.1 Possible alterations in the physical status of water systems

Any changes in air temperature and precipitation interact with water systems to alter, for example, the seasonal maximum and minimum temperatures, the daily cycles and the timing and duration of seasonal thermal patterns of these systems. There is a strong likelihood that climatic changes will affect rainfall patterns, which will include not only magnitude, but also the timing, intensity and duration of rainfall events. Changes in rainfall patterns resulting from climate change would result in changes in the quantity, quality and timing of runoff to

river systems. This would affect the quantities of suspended material transported by rivers, thus affecting the transportation of nutrients and salts (Ashton, 1996).

In China, for example, the regional effects of climate change on sedimentation were studied using the Yellow River Basin as a case study. Results from the conceptual model used indicate that runoff would tend to decrease with a resultant increase in sedimentation owing to increased storm intensity during the flood season (Shiklomanov, 1999).

#### 2.2.7.2 Possible alterations in the chemical status of water systems

Water temperature exerts a control over the quantities of gases and ions in solution, including dissolved oxygen concentrations (Ashton,1996). Climate induced changes in the magnitude and timing of runoff will impact water temperature, salinity, turbidity, nutrient carrying capacity and dissolved oxygen levels of these systems (Ashton, 1996; McAnally *et al.*, 1997). Increased temperatures could have the effect of altering chemical reactions which take place in reservoirs, which in turn could cause gradual changes in the regional chemical characteristics. These changes, combined with altered solubility characteristics, could change rates of decomposition with significant changes in water chemistry expected to occur (Ashton, 1996).

#### 2.2.7.3 Possible alterations in the biological status of water systems

Changes in water temperature exert profound effects of the biological components of water ecosystems. Effects of changes in water temperature could be changes in rates of metabolic processes, in the creation of preferential habitats and in changes in species and population composition (Ashton, 1996). Changes in the physical and chemical status of a water body could affect the development of phyto-plankton and aquatic plants as well as organisms which rely on these components for habitat and food supplies. An example of such a biological change could be the change in the distribution patterns of the snail vectors of the Bilharzia parasite.

One of the potential consequences of heavy rains and flooding is an increase in the occurrence of water-bourne diseases (Patz *et al.*, 2000). For example, the floods in the Horn of Africa and East Africa during the 1997 - 98 El Niño episode, led to an increase in the incidence of mosquito-, rodent- and water-bourne diseases with resultant outbreaks of malaria, cholera and Rift Valley fever killing an estimated 5 000 people. An increase in flood events with climate change could increase the incidence of such outbreaks. The UKMO (2000) project that by 2080 an estimated 290 million additional people will be at risk of contracting falciparum malaria (clinically more dangerous than the more widespread vivax malaria) as a result of climate change with no mitigation of emissions (UKMO, 2000). Such changes could have implications for human health, especially in rural areas (Ashton, 1996).

These potential changes to natural systems and reservoirs could affect the use of the water for domestic and agricultural applications, which could, in turn, have repercussions on the cost of water treatment. If water quality decreases to the extent that treatment is no longer feasible, the water supply effectively decreases (Shackleton *et al.*, 1996). Therefore, a better understanding of the processes regulating water quality is essential for successful management of water resources in a changing climate.

### 2.2.8 Potential changes in extreme events

One of the most difficult climatic changes for most regions to adapt to would be increased climatic variability and thus more frequent extreme events, i.e. higher peak floods, more persistent and severe droughts and greater uncertainty about the timing of the rainy season. Few such changes are likely to be beneficial (Gleick, 1990). As floodplains become more developed and populated, the loss of life and damage to property is bound to increase as a result of enhanced flood events in the future (Shackleton *et al.*, 1996).

Small changes in the total amount, frequency and intensity of precipitation can directly affect the magnitude and timing of runoff and the intensity of floods and droughts (IPCC, 1996a). However, there is still debate as to how extreme events are expected to change in future. Convective activity could increase as a direct result of the larger amounts of water vapour that can be held in a warmer atmosphere. The higher amounts of water vapour would be fed by

increased sea surface temperatures and evapotranspiration. The higher precipitable water contents of the atmosphere could result in increases in the size and intensity of thunderstorms and subsequently a greater risk of local flash flooding. Convective activity has not yet been analysed in detail in climate change simulations with coupled atmosphere / ocean models (cf. Chapter 3, Section 3.5) and therefore this is considered to be a subject requiring further analysis by Brinkop (2000).

In 1991 Pittock and collaborators suggested that there is increasing evidence that paths and intensities and convective activity of storms may change in the future (Pittock *et al.*, 1991). However, it is difficult to establish if there has been an increase in extreme events over the last few decades. This is partly due to the fact that a long time series is required to distinguish between inter-decadal variability and climate change and long data series are often not available (Frigon and Caya, 2000). In addition, catchments under pristine conditions, against which the hydrological effects of increased convectivity could be assessed, are rare with most gauged catchments having been urbanised, afforested or having their streamflows altered through construction of dams or abstractions for irrigation, industrial and domestic use. This makes it more difficult to establish whether the occurrence of extreme events is increasing (Kundzewicz, 2000). In a recent review by Kundzewicz (2000) he stated that with climate change there could be

i) more frequent wet spells in the mid to high latitudes;
ii) an increased frequency of high rainfall intensity events;
iii) an increase in the intensity of mid-latitude cyclones;
iv) a rise in sea-level which would result in coastal flooding and
v) increased exposure of populations to vulnerability.

He concluded that in many places the occurrence of extreme events was likely to increase in the future owing to a combination of anthropogenic and climate induced impacts (Kundzewicz, 2000).

Voss *et al.* (2000) noted in the presentation of their study of potential changes in extreme events that it was important to assess the change in number of wet days to establish if the occurrence of floods and droughts was increasing. They concluded that there could be

decreases in the number of light precipitation events but an increase in the number of heavy precipitation events with climate change.

Numerous devastating climate related events were reported across the world in 1999 and 2000. In south-eastern Australia the driest period on record (since 1895) occurred between April and July 1999. In contrast, Venezuela, India, Vietnam and southern Africa, in particular Mozambique, experienced severe flooding. Other significant events included tropical cyclones in Australia, tornadoes in the USA and heavy snow and early avalanches in Europe (World Climate News, 2000). It is, however, still to speculative to suggest scientifically that these are manifestations of climate change. The projected increased variability and convective intensity of storms that are expected in a future climate could add to the flood risk in southern Africa; however, the inherent variability of extreme events makes it difficult to isolate and quantify this risk (Shackleton *et al.*, 1996).

The agricultural and socio-economic conditions in South Africa make it vulnerable to droughts and floods (Joubert and Hewitson, 1997). During the past two decades, most of the African continent has experienced extensive, severe and prolonged droughts (Kayane, 1996). South Africa is a semi-arid country, with large areas under rain-fed subsistence agriculture, making the country's agricultural sector particularly vulnerable to drought (Gibberd *et al.*, 1996). If the 1991 - 92 or 1997 - 98 drought experienced over southern Africa, for example, became more frequent, perhaps occurring every five years instead of every 20 or so, the consequences on rural agriculture and settlement would be significant. As precipitation patterns in the future are difficult to project at this time, it is difficult to predict the frequency, intensity, duration and location of drought in the future (Downing *et al.*, 1997). In most cases, however, it is true to state that changes in variation and frequency of extreme events have a greater impact on hydrological responses, in the short and middle term, than changes in means.

Thus, it has been illustrated how hydrological systems, and subsequently water resources, are expected to be affected by changes in climate. The second resource sector under consideration which will potentially be affected by climate change is the agricultural sector. Potential physiological changes of plants, effects on agricultural production and potential

changes in plant diseases and life cycles of plant pests owing to climate change are reviewed in the following sections.

## 2.3 Climate Change: The Agricultural Connection

Climate change is expected to affect plant physiological processes, which in turn affect crop yields and distribution. Thus, to understand potential changes in agricultural yields which could take place in the future, an understanding of how plant responses are expected to change is needed.

### 2.3.1 Potential effects of climate change on plant response

Increases in temperature and changes in precipitation could have biological impacts on plants and, of particular interest in this study, crop production. These impacts could range from alterations in metabolism, nutrient requirements and biochemical activities of organisms to changes in patterns of activity within communities and geographical distribution of ecosystems (Bloomgarden, 1995). Changes in atmospheric $CO_2$ concentrations have been shown to have the potential to affect plant processes such as photosynthesis, stomatal resistance, respiration and transpiration (Rosenberg *et al.*, 1990). Ultimately, it is the combined effects of increases in atmospheric $CO_2$ and changes in climatic variables that contribute to the responses of plants to climate change (Bloomgarden, 1995). The potential effects of increased $CO_2$ and temperature on plants are expanded upon in the following sections.

#### 2.3.1.1 Physiological effects of increased atmospheric carbon dioxide on plants

Plant processes that are affected by enhanced $CO_2$ concentrations include photosynthesis, stomatal resistance, respiration and transpiration. Experimental evidence shows that as atmospheric $CO_2$ concentrations increase, certain plants use water more efficiently due to suppression of transpiration resulting from reduced stomatal conductance, while some plants display more rapid growth rates through enhanced photosynthetic rates (IPCC, 1996b).

This enhanced plant growth rate is known as the $CO_2$ fertilisation effect. When atmospheric $CO_2$ concentrations increase, more $CO_2$ diffuses into the leaf of the plant and the photosynthetic rate increases because of the increased gradient between the leaf and air resistance (Wolfe and Erickson, 1993). The result of the $CO_2$-induced increase in photosynthesis is more rapid plant development and growth, with plants reaching full leaf area and biomass sooner than plants grown in ambient $CO_2$ concentrations (IPCC, 1990). The result of this increased leaf area could be decreased soil water evaporation and changes in transpiration, assuming temperature remained constant (Rosenberg *et al.*, 1990).

Not all plants respond equally to an increase in $CO_2$ concentrations. Most tree and grass species follow a C3 photosynthetic pathway and show a significant increase in their photosynthetic rate from an increase in $CO_2$ concentrations. C3 plants constitute 95% of the world's plants, including wheat, rice, soybean and most horticultural crops. Some plants, *viz.* those with a C4 photosynthetic pathway, while constituting only a small percentage of the world's plants do, however, include important agricultural crop species such as maize, millet, sorghum, sugarcane and most weed species. In these plants the effect of enhanced $CO_2$ concentrations on photosynthesis is not as marked as in their C3 counterparts (Rosenzweig and Hillel, 1998).

An important agricultural as well as hydrological effect of atmospheric $CO_2$ enrichment is the suppression of transpiration. Transpiration is suppressed as a result of the partial closure of stomata, the small openings in the leaf surface through which $CO_2$ is absorbed and water vapour is released. Exposure to elevated levels of $CO_2$ causes plants to close their stomata in an attempt to balance the rates of water, $CO_2$ and nutrient use, even while promoting photosynthesis (Rosenzweig and Hillel, 1998). Transpiration suppression through the decrease in stomatal conductance (i.e. increase in stomatal resistance) implies a decrease in plant water use and a consequent potential increase in runoff because the soil is likely to be relatively wetter with the onset of a rainfall event (Kunz and Schulze, 1993).

Enhanced stomatal resistance is more pronounced in C4 plants than in C3 plants, indicating that the decrease in plant water use will be more pronounced in C4 than C3 plants. There are, however, feedbacks in the stomatal response to $CO_2$. The closure of the stomata, and

consequent reduction in transpiration, could result in a rise in leaf temperature and an increase in transpiration (Hulme, 1996).

The physiological mechanisms and complex feedbacks involved in stomatal response are still not completely understood and estimates of transpiration suppression vary at present. Most experiments seem to show a net decrease in transpiration with an increase in $CO_2$ concentrations (Wolfe and Erickson, 1993; Rosenzweig and Hillel, 1998). However, such experiments do not simulate the natural environment and, at present, it is unclear what plant responses will be when space, light, nutrient, water and other resources are taken into account in field conditions (Körner, 1993).

Considering the complex feedforwards and feedbacks involved, the overall change in runoff resulting from changes in climate is difficult to simulate realistically. Higher temperatures result in enhanced growth rates, increases in the evaporative demand for water vapour, increased plant water use and therefore would tend to decrease runoff. However, transpiration suppression implies a decrease in plant water use and a consequent potential increase in runoff because the soils are likely to be relatively wetter.

Kunz (1993) simulated hydrological conditions at seven sites in South Africa using the *ACRU* model (cf. Chapter 4) to determine whether the influence of transpiration suppression had a greater influence on runoff change than increased potential evaporation. Results showed that changes were site specific and that each location had different climatic thresholds for changes in hydrological response.

#### 2.3.1.2 Plant responses to increased temperature

Atmospheric temperature affects not only the distribution of plants but also affects the plant performance within the geographical range (Ennos and Bailey, 1995). Temperature plays an important role in the regulation of photosynthesis in a plant. Different plant species have differing optimum minimum and maximum temperatures for photosynthesis, usually related to their climate of origin. However, plants can acclimatise to changes in temperature through an alteration in the thermal stability of enzymes involved in photosynthetic reactions (Graves

and Reavey, 1996). The range of temperature regimes over which a species can successfully maintain photosynthesis is dependent on genetic variation within the species and the degree to which individual plants can adjust their photosynthetic physiology (Graves and Reavey, 1996). This will be an important factor in determining the competitive advantage of plants in a changing, natural ecosystem.

In an agricultural system, however, crop plants are often hybrids which lack the genetic variation of natural plants requiring breeders of crop plants to continually develop new hybrids which can thrive under a variety of climatic conditions. Thus, breeding and gene manipulation of successful crop plants may play an important role in food production in a changing environment (Graves and Reavey, 1996).

During certain stages of growth, such as during grain fill or pollen maturation, plants are sensitive to the temperature range (Domleo, 1990) and therefore an increase in temperature may disrupt these critical stages in the plant's growth cycle. For example, warmer winters may also stimulate earlier bud burst and flowering of plants. However, a period of frost after a warmer period may result in the destruction of vulnerable plant tissues (Graves and Reavey, 1996) with a subsequent decline in crop production.

### 2.3.2 Potential effects of climate change on agricultural production

Increases in the concentration of atmospheric $CO_2$ and in temperature have the effect of increasing plant growth and development, thereby reducing the time the crop spends in the ground. The number of heat units (cf. Chapter 8, Section 8.1.1) required to reach various phenological stages in the crop would thus be reduced resulting in the crop reaching maturity in a shorter period of time. In addition, warmer conditions may reduce the mean start and end dates of frost occurrence, thereby lengthening the growing season of a crop. Avoidance strategies, such as planting earlier or later, could be implemented to avoid peak periods of pest and disease incidences (Lowe, 1997). However, some crops require a period of chilling to stimulate growth, develop leaves, flower or set fruit (Schulze, 1997b) and increases in temperatures may make the cultivation of such crops unviable in present climatically suitable areas in a future warmer climate.

Generally, plant responses in natural and commercial agricultural environments to changing climatic conditions remain unclear, but some reduction in transpiration may be expected and there is evidence that senescence may be delayed. Both of these factors indicate that $CO_2$ enhancement and warming could cause an increase in biomass accumulation (IPCC Agricultural Impacts, 1995).

Weeds, insects and pest diseases are affected by changes in climate. The resultant changes in the activity and distribution of these crop pests will likely affect crop production, as the following sections set out to review.

#### 2.3.2.1 Competition from weeds

Weeds growing amongst agricultural crops compete for the same essential water and nutrients as the crop resulting in a likely reduction in crop yields (IPCC Agricultural Impacts, 1995). Changes in climate and atmospheric $CO_2$ concentrations will not only affect crop production but also affect weed growth and weed-crop competition (Ennos and Bailey, 1995). Most of the world's agriculturally important crops are C3 plants, whilst the majority of the competitive weeds are C4 plants (Rosenzweig and Hillel, 1998).

As established previously (cf. Section 2.3.1.1) $CO_2$ enrichment is likely to benefit C3 plants more than C4 plants, indicating that crops may show greater photosynthetic rate increases than weeds and thus a net beneficial effect is likely to take place in many cases. However, in a drier future climate, agriculturally competitive C4 weeds may be more competitive due to their ability to survive better in more arid conditions (Hulme, 1996). However, at slightly higher, cooler altitudes C3 crops may be better suited to future climatic conditions than C4 weeds (Ennos and Bailey, 1995).

Uncertainty regarding the magnitude and the potential effects of climate change on agriculturally competitive weeds remains an obstacle to accurately predicting the potential effects of weeds on crop production.

### 2.3.2.2 Effects of climate change on agricultural insect pests

Agricultural insect pests tend to have a broad host range and their geographical distribution is limited primarily by their host. Insects have high rates of reproduction and mobility allowing them to acclimatise rapidly to changes in climate and to migrate, should unfavourable conditions arise.

Agricultural pests and the pathogens they may carry are strongly influenced by weather conditions. Temperature is an important factor in determining mortality and reproductive rates of many insects. A warmer environment may favour the development of certain insect species, resulting in a greater number of life cycles per season. However, species with minimum critical temperature thresholds for development may be adversely affected with a resultant decrease in populations.

Changes in precipitation could also affect insect populations. An increase in heavy rainfall events, for example, can drown soil-dwelling insects, in addition to creating a moist environment in which insect predators, parasites and pathogenic organisms such as fungi and bacteria can proliferate. However, drought favours aphids and locusts, which have the potential to devastate crops and vegetables and thus have a marked effect on food security (IPCC Agricultural Impacts, 1995).

### 2.3.2.3 Effects of climate change on plant diseases

An increasing amount of ultraviolet-B (UV-B) radiation is currently reaching the earth's surface compared to levels experienced prior to the 1930s owing to stratospheric ozone depletion. This, coupled with higher concentrations of atmospheric $CO_2$, has a direct biological effect on plants enrichment (Manning and Tiedemann, 1994).

Ozone adversely affects plant growth and provides pathogenic organisms with an opportunity to colonise the weakened plant. The exact effect of ozone depletion on plants and their resulting response to plant diseases is uncertain (Manning and Tiedemann, 1994).

Enhanced UV-B radiation can stunt plant growth, increase branching and canopy size. This would have the effect of increasing the humidity of the microclimate, thereby favouring the development of bacterial or fungal infections. Enhanced UV-B may also reduce net photosynthesis in many plants (Manning and Tiedemann, 1994), resulting in a reduction in carbohydrate stores, which will reduce the incidence of high sugar diseases such as rusts and mildews (Agrios, 1988).

The increase in plant canopy size expected as a result of $CO_2$ enrichment is likely to create a much more humid microclimate within the plant than is currently present (IPCC, 1990). This, coupled with the expected increase in plant biomass provides an improved nutrient base for pathogens, could favour the incidence of plant diseases such as rusts, powdery mildews, leaf spots and blights. However, the increased stomatal resistance associated with $CO_2$ enrichment could reduce the incidence of stomata-invading aerial pathogens such as downy mildews (Manning and Tiedemann, 1994). The expected increase in winter temperatures resulting from the greenhouse effect could increase the overwintering potential of certain diseases, resulting in a greater concentration of reproductive spores in the spring, which could have widespread economic implications for agriculture (Agrios, 1988).

## 2.4 Reasons for the Assessment of Hydrological and Agricultural Impacts of Climate Change: A Summary of Findings

There are many uncertainties with regard to the directions, magnitudes and rates of change of hydrological and agricultural systems potentially resulting from climate change. Hydrological and agricultural systems are affected directly by changes in temperature and precipitation as well as by the frequency of extreme events such as floods and droughts. In addition, rising concentrations of $CO_2$ have the potential to affect plant growth and transpiration rates to enhance the productivity of agricultural systems, thereby affecting hydrological processes such as runoff.

Climate change is likely to have marked effects on the terrestrial hydrological system. It could affect inputs to the system (e.g. rainfall, temperature and through cloudiness, wind and

vapour pressure, the reference potential evaporation), processes within the system (e.g. vegetation dynamics, soil surface changes) and output (e.g. runoff volume, peak discharge as well as soil water recharge and sediment yield). The hydrological system is believed to amplify responses to climate change. Hydrologists' risk analyses are based on the assumption of climatic stationarity which would be invalidated by climate change.

The possible feedbacks, spatial shifts in agricultural belts, sensitivity of crop yields and vulnerabilities of crops to failure have ramifications on, *inter alia*, food production, food supply, its distribution and trade. Thus, climate change poses a threat to food security and a region's economic viability. This is a strong motivation to assess the impacts of climate change on agricultural systems (Schulze *et al.*, 1993). Climate change may also result in changes in the occurrence of pests and diseases, planting dates of crops, occurrence of frost and length of crop cycles (Schulze, 1993; Adams *et al.*, 1998).

As agricultural systems are managed systems, it is important to understand the human response to the effects of climate change on production and food supply. They are dynamic systems where the producers continuously respond to changes in, *inter alia*, crop yields, food prices and technological change. Thus, failure to account for human adaptations, either in short-term adaptative measures or long-term technological changes, will overestimate the potential damage from climate change and underestimate its potential benefits (Adams *et al.*, 1998).

The projected increase in world population combined with a change in the climate will stress the existing food production regions to increase their output. This may result in increased demand for irrigation in some regions. If the climate shifts or changes, existing irrigation systems may not be adequate to accommodate the increased demand. Resource allocations to these systems will have to be adjusted, which will be difficult without accurate hydrological predictions. In addition, agricultural areas that have traditionally not required irrigation may, under changed climatic conditions, require irrigation (McAnally, 1997).

* * * * * * *

In this chapter some of the potential impacts of climate change on hydrological and agricultural systems were reviewed. It is important to understand how these systems have been shown, through experiments, to respond or how they are expected to respond to changes in climate to enable future climatic conditions to be simulated with greater certainty. However, it is clear that there still remains a large degree of uncertainty as to the direction and magnitude of potential impacts of climate change on hydrological and agricultural systems.

The IPCC (IPCC, 1994) suggests a seven step strategy for climate impact assessment. In Chapter 3 the methodologies used in climate impact assessment will be outlined and the seven steps generally used in these assessments will be reviewed.

# 3. METHODOLOGIES AND CONCEPTS RELATED TO CLIMATE CHANGE IMPACTS STUDIES

At different spatial and temporal scales, the impacts of climate change, and the adaptations to these impacts, vary greatly. Over the past 20 - 30 years, scientists have developed a variety of methods to assess potential climate change impacts (Parry and Carter, 1998). Although these methods differ widely, they have features in common and the general approach is termed climate impact assessment.

There are seven steps that are generally followed when undertaking climate impact assessment. These steps were used as a guideline when evaluating the potential impacts of climate change on agrohydrological systems in this study. This chapter will be introduced with a brief background on climate impact assessment, followed by an outline of each of the seven steps as suggested by Parry and Carter (1998).

## 3.1 Climate Impact Assessment

Policy makers require climate impact assessments to provide them with the necessary scientific information for policy decisions. The goal of climate impact assessment is to ensure optimal use of the available climatic resources, through the assessment of both positive and negative impacts, and the evaluation of the possible options to adapt in response to climate change (Parry and Carter, 1998). Following this broad objective are more specific objectives of identifying regions that are particularly sensitive to climate change, assessment of vulnerabilities in these regions and identification of thresholds in biological systems to change (Benioff *et al.*, 1996; MacIver, 1998).

When assessing the potential hydrological impacts of climate change, it is necessary to identify and evaluate possible scenarios of climatic change, to include the effect of carbon dioxide ($CO_2$) enrichment on plants and potential changes in land cover. It is also important to provide integrated assessments which include alternative strategies and projections of

effects on water users and ecosystems (Cohen, 1995). Up until the 1970s, the focus of climate impact assessment was on the uni-directional influence of climate on human activity. However, in the past few decades, greater emphasis is being placed on the interaction between climate and human activity (Parry and Carter, 1998).

Comparability between impact assessments is important. Decision makers using the impact assessments should be confident that, at a minium, basic assumptions are uniform (such as the use of a common set of climate change scenarios) and that models and analytical tools were used correctly. Parry and Carter (1998) suggest a seven step strategy of assessment for climate impact and adaptation assessment adopted by the IPCC (IPCC, 1994), but which has been applied in climate impact assessment since the early 1990s (e.g. Carter *et al.*, 1992), as outlined in Figure 3.1.

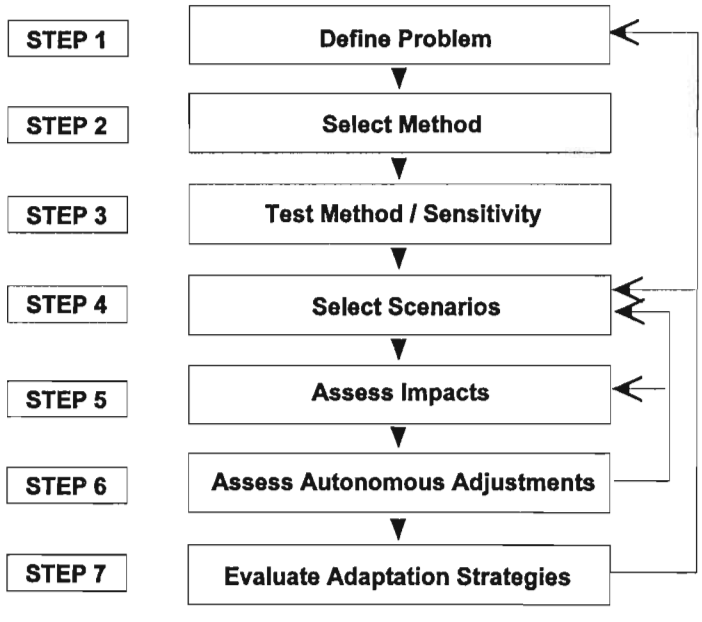


*Note*: The thin arrowed lines indicate steps that may need to be repeated

Figure 3.1 Seven steps of climate impact assessment as adopted by the IPCC (after Parry and Carter, 1998, adapted from Carter *et al.*, 1994)

The first five steps are common to most impact assessments whereas the last two steps are included in fewer studies. These seven steps will be described in more detail in the subsequent sections, following the general guidelines given by Parry and Carter (1998), with particular reference to hydrological and agricultural impacts.

## 3.2 Step 1: Defining the Problem

The first step of climate impact assessment is to define the nature of the problem. This includes an explanation of who the intended users are and of the temporal and spatial scales of the assessment. The study area and time frame of the assessment will generally be guided by the goal of the assessment. It is important to identify the main data requirements in an impact assessment, as the availability of data often limits many impact studies (Parry and Carter, 1998). The databases used in this regional study are described in Chapter 5.

The main features of the data requirements are

i) type of data required;
ii) duration of record;
iii) spatial coverage and resolution;
iv) sources and format of the data;
v) quantity and quality of the data; and
vi) the availability and cost of the data (Benioff *et al.*, 1996; Parry and Carter, 1998).

## 3.3 Step 2: Selection of the Method to Assess Potential Impacts of Climate Change

To date, the conventional approach adopted in climate impact assessments has been the assumption that certain changes in climate take place whereafter the impacts implied by these changes are evaluated. However, since the mid 1990s emphasis is being placed on the assessment of the sensitivity and / or vulnerability of systems to climate change. A combination of the two can be effectively adopted by establishing the vulnerability of various sectors and identifying the types of climate change most likely to affect these sectors (Parry and Carter, 1998). A literature review should be performed to provide a background understanding of the study region, the system (e.g. hydrology) or the activity being investigated, as well as an examination of related studies to obtain an overview of methods that are available and to identify possible research collaborators. Although there are various methods available to assess climate impacts, the most common method is the use of

simulation models to simulate a variety of responses to climate change scenarios (Parry and Carter, 1998).

## 3.4 Step 3: Testing the Method

Various feasibility studies could be adopted as a preliminary stage of large projects. Given the uncertainties in both the magnitude and direction of impacts of climate change, a key issue is the assessment of sensitivity and vulnerability of hydrological systems to possible changes in climate.

### 3.4.1 Vulnerability of agricultural and hydrological systems to climate change

The US Country Studies Program defines a country's vulnerability to climate change as "an evaluation of how changes in climate may affect segments of the natural environment, elements of the national economy and human health and welfare" (Benioff *et al.*, 1996; p 6). Vulnerability depends not only on a system's sensitivity, but also on the system's ability to adapt to new climatic conditions (IPCC, 1995).

#### 3.4.1.1 Vulnerability of regions to changes in climate

Defining a region as being vulnerable is not a prediction of negative consequences of climate change; rather, it is an indication that, across the range of possible climate changes there are some climatic outcomes that would lead to relatively more serious consequences for that particular region, than for other regions (Reilly, 1996). Some regions have become more vulnerable to hazards such as floods, droughts and storms as a result of increasing population densities in sensitive areas such as floodplains and coastal zones (IPCC, 1996b). Other regions which could be particularly vulnerable to climate change are those which at present are already

i) arid or semi-arid areas, and in which small changes in climate could have major repercussions in water resources;

ii) areas of large water demand relative to supply;

iii) areas which have water quality problems;

iv) areas which are dependent on groundwater supplies or where groundwater is already being pumped faster than the natural recharge rates;

v) areas with limited water supplies and that are already prone to interruption of supply caused by floods or prolonged droughts (Gleick, 1990);

vi) areas which have suffered major land use change such as deforestation or urbanisation;

vii) areas which high population densities; and

viii) areas with limited economic resources to cope with extreme events (Liu, 2000).

Many countries in the world are already suffering from serious water shortages, which have become a limiting factor in their economic and social development and renders them vulnerable to changes in climate. Africa may be particularly vulnerable to climate change. For example, African countries tend to have a much higher share of their economy in climate-sensitive areas. Most African countries have at least one-third to one-half of their GNP in agriculture (World Bank, 1992). Major cities such as Lagos, Nigeria, with a population of eight million people and Alexandria, Egypt with a population of three million are vulnerable to sea-level rise (El-Raey *et al.*, 1995, French *et al.*, 1995). River basins such as the Nile and Zambezi are critical sources of water for irrigation and hydropower and their river flows are quite sensitive to climate variability and, hence, change (Gleick, 1993). Africa also experiences widespread poverty, recurrent droughts and over-dependence of rainfed agriculture (Watson *et al.*, 1997).

Vulnerability can also arise from the fact that many of the worlds water resources are shared. For example, water in the Nile River is shared by nine countries. This could potentially led to water conflicts in times of water shortages (Morehouse and Diaz, 1999).

#### 3.4.1.2 Qualitative vulnerability analysis

Parry and Carter (1998) suggest performing a qualitative vulnerability analysis of, say, a region's hydrological or agricultural response to climate change. This technique makes use of a matrix format, where different exposure units, classified by type or scale (e.g. villages, town and cities, or agricultural activities such as agricultural production or size of reservoir)

are entered on one axis. On the other axis, some effects of climate are categorized, for example the effects of floods or droughts or changes in means or variabilities on water supply or demand or agriculture. Qualitative ratings are then assigned to each cell in the matrix, indicating both the likely size of the effect and the probability of occurrence. Preliminary assessments of this kind can help identify which units are considered potentially most vulnerable to climate change.

Table 3.1 Example of a qualitative vulnerability analysis of different sized settlements to droughts and floods (Parry and Carter, 1998)

| Settlement | Climate Vulnerability Rating | | |
|---|---|---|---|
| | Drought Effects on Agriculture | Drought Effects on Water Supply | Flooding Effects on Buildings |
| Villages | 1, U | 2, U | 4, L |
| Towns | 2, U | 2, U | 4, L |
| Cities | 4, U | 3, U | 4, L |

Ratings: 1 = Large or very important, 5 = Trivial L = Likely, U = Unlikely

### 3.4.2 Analogue studies

Temporal analogues make use of climatic information from the past as an analogue of possible future climate. These temporal analogues can be used to identify climatic events and their impacts in the past as analogues of events which could occur in the future, possibly with an altered frequency under a changed climate. This is a useful tool to illustrate the possible extent of future climate change (Carter, 1998; Parry and Carter, 1998; Bonell *et al.*, 1999).

The major disadvantage of using temporal analogues for climate change scenarios is that past changes in climate would have been unlikely to be caused by increasing concentrations of greenhouse gases and hence the affects of increased $CO_2$ concentrations on plants would not be taken into account (Carter, 1998).

### 3.4.3 Model testing

This could be considered the most critical stage of the impact assessment. Most studies rely almost exclusively on the use of simulation models to estimate future impacts. Two main procedures, *viz.* verification and sensitivity analysis, are recommended to precede formal impact assessments.

#### 3.4.3.1 Model selection

When choosing a hydrological and / or agricultural simulation model to mimic possible effects of climate change, it is important to keep the following criteria in mind (Schulze, 1997a):

i) The model's structure needs a sound physical and conceptual basis to enable it to reproduce responses associated with changes in (say) land use, vegetative growth rates, $CO_2$ concentrations, transpiration rates and feedbacks, climatic variables and / or soil properties.

ii) The model should reproduce the non–linear hydrological and agricultural process responses under a variety of conditions, both geographical and in terms of extremes. Hence, Schulze (1997a) recommends that deterministic models, using short time steps, be applied in climate impact studies. Models that require any form of external calibration cannot be used for climate change studies as these model outputs are calibrated against historical data for conditions prevailing for a certain time period, and therefore those models cannot be used to extrapolate for future climatic or land use conditions.

iii) Atmospheric $CO_2$ concentrations are certain to increase in future and therefore $CO_2$ enrichment effects should be included in any assessment of climate change. However, the effects of $CO_2$ on plant responses remain difficult to express in climate change impact studies, due mainly to the complexity of the processes involved and the incomplete understanding of the many feedforwards and feedbacks in the natural environment (Cohen, 1995).

Verification, or history matching, involves the comparison of model simulations with real world observations to assess statistically the performance of the model chosen. Both the

model's end products (e.g. runoff, sediment yield, crop yield) as well as its internal state variables (e.g. soil moisture, evapotranspiration, interception) should be verified (Schulze, 1998). Verifying a model for climate change conditions can be difficult, as there are often few adequate data sets available to test the behaviour of the system in conditions resembling the future about which much uncertainty still exists (Parry and Carter, 1998).

For this particular study the *ACRU* agrohydrological model was selected for the water resources component of this study (results provided in Chapters 9 and 10), the simulation of maize yield, the staple food crop in the study area, and winter wheat yield (results provided in Chapter 8, Section 8.3). Details on the selection of this model and modifications to the model to enable more dynamic simulation of climate change are provided in Chapter 4.

#### 3.4.3.2 Sensitivity analysis

Hydrological sensitivity analyses can be performed by applying a simulation model to a particular point or catchment under analysis and then incrementally perturbing the historical input data (e.g. precipitation and / or temperature) one variable at a time to represent the range of climatic conditions likely to occur in a region. Through such an analysis, information can be gained on the direction and sensitivity of the outputs to unit changes in the inputs, as well as on the model's robustness (Parry and Carter, 1998; Schulze, 1998). Details on the techniques and results from sensitivity analyses performed in this study are provided in Chapter 9, Section 9.4

### 3.4.4 Thresholds of response of hydrological and agricultural systems

In climate change studies thresholds represent magnitudes of a response variable (e.g. runoff, crop yield) to a change in the driving variable (e.g. rainfall, temperature, $CO_2$ concentration) at which that response becomes significant in its difference to that under present climatic conditions. The implication of significant could be

i) that a discrete discontinuity in the response appears, e.g. a certain level of curvilinearity (steepening or flattening) is attained; or

ii) that a certain level of relative change has occurred that is considered critical, e.g. when mean annual runoff change has reached 10% or 20% or one standard derivation from the present; or that a certain level of absolute change has occurred, e.g. when mean annual runoff has changed by 50 mm or 100 mm (Jones, 2000; Schulze and Perks, 2000).

Other aspects of threshold analysis could include ascertaining at what stage during a change in climate the hydrological or agricultural system would start responding, to what extent the responses may be non-linear, to what extent responses may be discrete rather than taking place in a continuum, and to what extent feedbacks may cancel feedforwards (Schulze and Perks, 2000).

The methodology used in the threshold analyses for the study is given in Section 7.6 of Chapter 7. The results from threshold analyses of mean annual runoff and mean annual percolation into the vadose zone are presented in Chapter 9, Section 9.5 and that of median maize yield in Chapter 8, Section 8.3.6.

## 3.5 Step 4: Scenarios of Change

In order to conduct simulation experiments to assess the potential impacts of climate change, it is necessary to obtain quantitative representations of the anticipated changes in climate. At present, no method exists of providing confident predictions of future climates and therefore climate scenarios are generally used (Parry and Carter, 1998). Such scenarios present coherent, internally consistent and physically plausible descriptions of future climate, which may be used as input into climate change assessments (Carter *et al.*, 1994). Climate change scenarios can help identify potential direction of effects and the potential magnitude of impacts. The use of scenarios can also help identify the sensitivity of a sector such as hydrology or agriculture to changes in different climatological variables (Ringius *et al.*, 1996).

There are numerous of ways in which climate change scenarios can be constructed. One of the earliest scenarios constructed for use in impact assessments appeared in the 1970s and was

based on expert judgement. A panel of experts were requested to give estimates for a future climate and these responses were averaged and weighted according to the level of expertise of the panel members and a frequency distribution constructed. These methods were criticised, for amongst other reasons, their potential bias and lack of transparency (Hulme and Carter, 1999).

The most widely favoured methods for generating scenarios at present use results from large scale atmospheric General Circulation Models, or GCMs (Hulme, 1996). Outputs from GCMs are usually applied as monthly or seasonal adjustments to the baseline conditions, assuming no change in climatic variability between the baseline and future climate (Parry and Carter, 1998).

There are four criteria which been suggested should be met by climate change scenarios if they are to be useful in climate impact assessments:

i) It is important that scenarios chosen are consistent with global projections, e.g. the IPCC estimates a 1.5 - 4.5 °C increase in temperature for an effective doubling of $CO_2$ concentrations.

ii) The GCM simulations should be physically plausible, i.e. they should not violate any basic laws of physics, have sufficient number of variables to be usable in climate impact assessment and be representative of the potential range of future regional climate change (Carter, 1998).

iii) In order to provide reference points with which to compare future predictions, current baseline climatic conditions need to be specified (Parry and Carter, 1998). It is important to use a sufficient duration of recent historical climate data which includes a number of significant climate anomalies. The US Country Studies Program suggests that a 30 year period of data is sufficient to give a good representation of wet, dry, warm and cool periods at a location. The quality of the data is important and for this reason it is usually (but not always) better to use a recent record, as these data are expected to be more accurate. The World Meteorological Organization's recommended period of record is 1961 - 1990 (Benioff *et al.*, 1996; Carter, 1998), however, a longer period of record may be needed in some regions depending on the climate of that location.

iv) Any changes in climate should be representative of the potential range of future regional climate change.

General Circulation Models which are presently used in climate impact assessments internationally include the Hadley Centre GCM (Murphy and Mitchell, 1995), Genesis GCM (Thompson and Pollard, 1995), Climate System Model, GISS Ocean-Atmosphere Model (Russell *et al.*, 1995), ECHAM (Roeckner *et al.*, 1996) and Geophysical Fluid Dynamics Laboratory (GFDL) GCM (Manabe, 1991). More details on the selection and use of GCMs in this study are provided in Chapter 6.

## 3.6 Step 5: Assessing the Impacts

It is important for the impact assessor to express the results of a climate impact assessment in a from that is valuable to the end users. A common feature of all climate impact assessments is that they have a geographical dimension. Since climate varies over space, climate change impacts will vary spatially and thus a good way to represent these impacts is in the form of maps (Parry and Carter, 1998), which are commonly created using a computer-based Geographical Information System (GIS). In addition, changes in climate occur over time and thus results are presented as a time series in certain cases.

There are many uncertainties when modelling climate change impacts. These could include errors due to inaccurate present climate data observations, lack of data, assumptions or estimates that have been used in the analysis. Where quantification of uncertainties is possible, they are usually expressed as confidence limits around the estimate (Parry and Carter, 1998). Results from this regional study of potential climate change impacts on agricultural and hydrological systems are provided in Chapters 8 and 9 respectively.

## 3.7 Steps 6 and 7: Evaluating Adaptive Responses

The impacts on current climate of increases in greenhouse gas concentrations already in the atmosphere, could be felt for several generations yet to come, even in the unlikely event that

greenhouse gas emissions were to be stabilised or reduced in the future (Downing *et al.*, 1997). The reason for this is that many greenhouse gases have a long chemical half life in the atmosphere and it can therefore take many years for the climate system to return to its original state (Ringius *et al.*, 1996). The enhanced greenhouse effect has the potential to cause climatic change impacts across the range of human and natural systems. The severity of the impacts will vary and not all impacts will constitute damage to the environment, with some sectors being more resilient and robust to climate change impacts (Ringius *et al.*, 1996), or even benefiting from them. However, most natural systems are sensitive to changes in climate because of their limited adaptive capacity. Natural systems considered particularly vulnerable to climatic changes are glaciers, coral reefs, mangroves, arctic and montane ecosystems, wetlands and native grasslands (IPCC, 2000b).

Adaption can be applied to lessen harmful effects and potentially enhance beneficial effects (IPCC, 2000b). Adaptation can be either spontaneous or planned and can be carried out in response to, or in anticipation of, changes in conditions (MacIver, 1998; Pittock and Jones, 1998). Most ecological, economic and social systems will undergo some natural, i.e. spontaneous, adjustments as the climate changes. Thus, a distinction needs to be made between such spontaneous responses to climate change, termed autonomous adjustments, and responses that require deliberate policy decisions, described as adaptation strategies (Parry and Carter, 1998). Responding to climate change will consist of abatement, i.e. controlling of greenhouse gases in order to try and stabilise climate change at an acceptable level and adaptation (Downing *et al.*, 1997).

In a particular situation, the question arises as to whether or not it is necessary to respond to the potential impacts of climate change. The chosen climate change response strategy may involve implementation of cost-effective anticipatory adaptation ("no regrets" strategy / policy) or a no response policy ("business as usual", or "wait and see") or seek to undertake research for better information policy (Ringius *et al.*, 1996). The argument for adaptation is related to the extent of vulnerability to present climatic conditions and the potential for further impacts which may be induced by climate change.

There are various options on how to adapt to the effects of climate change. Implementation of cost-effective anticipatory adaptation may be warranted in situations where changes in mean climate and climatic hazards may be rapid, where the consequences would be significant, or the risk is very high, especially for vulnerable populations. It may also be suggested in cases where the marginal cost of adaptation is small, where adaptation brings benefits regardless of climate change, or for protection against extreme events and to prevent irreversible impacts (Ringius *et al.*, 1996). The cost of anticipatory responses may be less than suffering the consequences later or undertaking remedial relief (Downing *et al.*, 1997).

In cases where adequate technologies and responses already exist, there may not be a need for specific immediate action. There are various arguments for the postponement of adaptation to climate change, including the following:

i) Many key factors in climate change predictions are still uncertain.

ii) Better and cheaper technology will be available in the future and future generations could have greater financial resources than at present that can be used for adaptive purposes (Downing *et al.*, 1997).

iii) Hydrologists already generally over design hydraulic structures to accommodate the present variability of streamflow and therefore present structures could possibly cope with any additional climate change impacts (Beran, 1989).

iv) The GCMs do not appear to represent present conditions with a high degree of accuracy at present (cf. verification studies results in Chapter 6, Section 6.6), especially in Africa, which makes it difficult to have full confidence in the predictions of future climates (Schulze, 1997a).

v) Another argument for delaying adaptation is that climate change is likely to take place gradually and therefore society could adapt as the climate changes. Some responses may be easily implemented by existing institutions and could therefore be implemented as the effects of climate change arise.

If the present scope for adaptation is limited, investment in research and education are warranted to develop new solutions to accommodate climate change (Downing *et al.*, 1997). The IPCC (2000b) identify water resources, forestry and agriculture as systems that are sensitive to change. Agrohydrological management and modelling may assist in prediction

of climate change impacts and assist in adaptation strategies. Adaptation may not be necessary in all cases (Ringius *et al.*, 1996). If adaptation is the chosen response, however, there is a strong justification to react at an early stage before the costs of climate change become substantial, because by such anticipatory adaptation costs could be avoided or even reduced (Downing *et al.*, 1997).

Potential adaptation strategies that might be applicable in southern Africa, stakeholders in adaptation strategies and policy options for adaptation are discussed in Chapter 12.

* * * * * * *

The seven steps described in this chapter provide an outline of procedures that are generally followed when conducting climate impact assessment. Conventionally certain changes in climate are assumed and then the effects of these climatic changes are simulated using a suitable model. The *ACRU* agrohydrological model is considered suitable for climate change impact studies and was selected for the hydrological impact studies, maize and winter wheat yield analyses performed.

Chapter 4 provides an introduction to hydrological modelling and the selection of a suitable hydrological model for climate change impact studies. This is followed with the basic concepts of the *ACRU* model and the modifications made to the model to allow for improved climate change impact studies to be performed using the model.

# 4. THE *ACRU* AGROHYDROLOGICAL MODELLING SYSTEM AND MODIFICATIONS TO THE MODEL

In order to simulate possible impacts of climate change on hydrological responses, the *ACRU* agrohydrological modelling system (Schulze, 1995a) was chosen. Other models which have been applied in agriculture and water resources studies in southern Africa include the CERES model for crop yield simulations (Jones and Kiniry, 1986) and the SWAT model which has be used in hydrological simulations (Arnold *et al.*, 1996). Some of the features of the *ACRU* model that render it suitable for climate change impact studies will be reviewed. The many equations which describe the processes relevant to climate change studies which are represented in the *ACRU* model, including definitions of their initial and boundary conditions, are given and explained in detail in Chapters 2, 4 - 7, 10, 12, 13 and 16 - 19 of Schulze (1995a) and will not be repeated here.

## 4.1 Simulation Modelling of Hydrological Responses

Many functional and structural conceptualizations of simulation models have been formulated. However, the emphasis in this instance is on hydrological models which can realistically simulate the impacts of climate changes on hydrological responses. In broad concept, such models are quantitative expressions of observation, analysis and prediction of the time variant interactions of various hydrological processes (for example, rainfall, infiltration, evaporation or streamflow). Such models are structured collections of physical laws and empirical observations written in mathematical terminology and combined in such a way as to produce a set of results (the model's outputs, e.g. runoff), based on a set of known and / or assumed conditions (the model's inputs, e.g. rainfall, soils or land use). Ultimately, in hydrology, such models are applied as real world decision tools in the planning, design and operation of hydrologically related systems and structures (such as reservoirs or irrigation projects). Because the natural and altered prototypes of hydrological systems are complex ones, the models abstract, i.e. they simplify, the behaviour of the prototypes (Schulze, 1995c).

The hydrological processes of greatest relevance in any change in climate are those involving interactions of exchanges of water vapour and heat (condensation, precipitation, runoff, evaporation and transpiration), characteristics of the soil (surface infiltrability, subsurface transmissivity / redistribution of soil water and water holding capacity), of land cover (above-ground attributes related to biomass, physiology and structure, as well as below-ground attributes relating to root structure and distribution) and of topographic features of the landscape such as altitude, slope and aspect (Schulze, 1998).

There are several advantages to modelling the components of the climate change problem, including the ability to analyse dynamic behaviour among various issues, and treat uncertainties explicitly (Yarnal, 1998). To model this system realistically

i) the model structure needs a sound physical and conceptual basis to enable it to reproduce responses associated with changes in land use and / or carbon dioxide ($CO_2$) concentrations on transpiration rates, and / or changes in temperature on evaporation rates, and / or changes in rainfall characteristics or soil properties on runoff generation or soil water redistribution mechanisms; furthermore,

ii) the model should also reproduce the other non-linear process responses (both of internal state variables and final model output) with inherent and intuitive accuracy and sensitivity, giving the right answer for the right hydrological reason under a range of climatic, land use and physiographic conditions. Hence, only deterministically based models operating in relatively short time steps should be used in such impact studies, since models requiring any form of external calibration, particularly of location-specific exponents or physically non-meaningful parameters, are inherently not usable for land use or climate change-driven hydrological impact studies because those parameters are representative of the state (i.e. condition) of the catchment at the time of calibration and not of the catchment under altered conditions (Schulze, 1997a).

## 4.2 Selection of a Hydrological Model for Climate Change Impact Studies

In order to assess the climate change impacts for this study, the *ACRU* agrohydrological simulation model was selected. The acronym *ACRU* was originally derived from the

Agricultural Catchments Research Unit which was founded in 1974 in the erstwhile Department of Agricultural Engineering, now the School of Bioresources Engineering and Environmental Hydrology of the University of Natal, Pietermaritzburg. *ACRU* is a deterministically based, physical-conceptual and integrated multi-purpose modelling system, revolving around a daily time step multi-layer soil water budget. Internal state variables (for example, soil moisture), model components (for example, interception) as well as end-product model output (for example, streamflow or sediment yield) have been widely verified (Schulze *et al.*, 1995b) under different hydrological regimes in Africa (Republic of South Africa, Kingdom of Lesotho, Zimbabwe), Europe (Germany) and the Americas (USA, Chile).

*ACRU* complies with many of the model attribute criteria set out in Section 4.1 earlier. In its routines total evaporation is partitioned into soil water evaporation and transpiration, thus rendering it sensitive to temperature change as well as accommodating a transpiration suppression function associated with increases in $CO_2$. In runoff generating routines account is taken of land use / tillage induced changes in initial infiltration and soil water redistributions as well as of rainfall characteristics while the stormflow and baseflow components of runoff are modelled separately and explicitly.

## 4.3 Present Operational Version of the *ACRU* (1995) Agrohydrological Modelling System

*ACRU* uses daily time steps, although some more conservative climatic variables such as temperature and reference potential evaporation may be input as monthly values if daily values are unavailable and these are then transformed internally in the model to daily values by Fourier Analysis and then adjusted for the presence of rainfall. Daily multi-layer soil water budgeting forms the core of the model, which is structured to be responsive and sensitive to climate and land use changes on the soil water and runoff regimes (Schulze *et al.*, 1995b). The general structure of the model is illustrated in Figure 4.1, in which the partitioning of soil water as well as the evaporation pathways are shown schematically. What follows below is an abbreviated qualitative description of the major soil budgeting processes of *ACRU*, with

equations given only in those sections describing changes made to the model in this study in order to enhance its application to climate change studies.

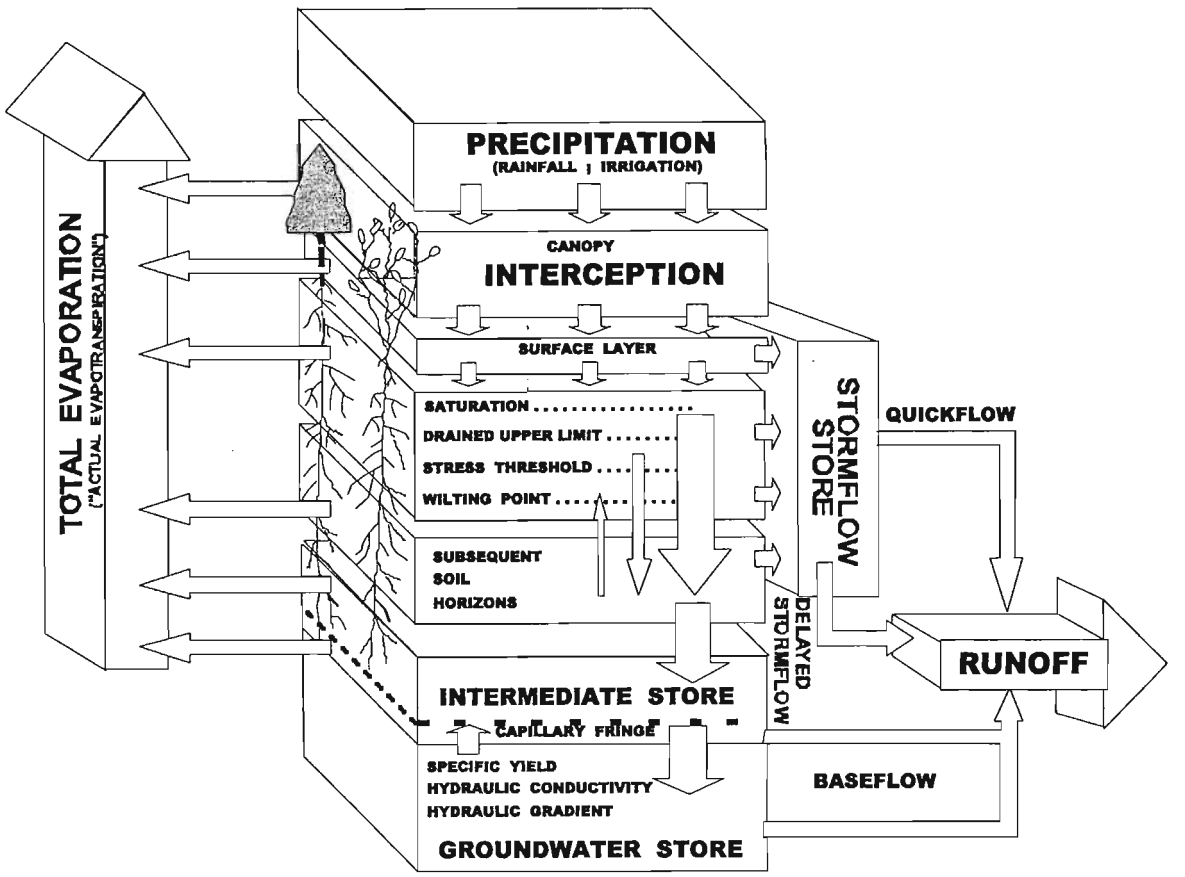


Figure 4.1 General structure of the *ACRU* agrohydrological modelling system (Schulze *et al.,* 1995b)

In *ACRU*, soil water partitioning and redistribution involves that portion of the rainfall that was not intercepted, or released as stormflow (either quickflow or delayed flow), and which resides in the topsoil, i.e. the so-called A horizon. Once filled to beyond its drained upper limit (i.e. field capacity), the remaining soil water percolates into the subsoil, i.e. the B horizon, as saturated drainage as a function of horizon textural differences and the soil horizons' relative wetness. If the soil water content of the subsoil exceeds its drained upper limit, then saturated vertical drainage into the intermediate or groundwater store occurs. It is from this store that delayed baseflow may be generated as a decay function. In *ACRU*, upwards unsaturated soil water redistribution functions include capillary action (Schulze, 1995b).

Evaporation from *ACRU* occurs from both soil horizons simultaneously, either in the form of soil water evaporation from the topsoil or as plant transpiration from all soil horizons containing actively growing roots (Schulze *et al.*, 1995b). It is possible to estimate total evaporation as an entity or to compute soil water evaporation and plant transpiration separately within the model structure. The latter option is employed when simulating climate change impacts, so as to be able to account for the stomatal increase in stomatal conductance and corresponding transpiration suppression in plants resulting from enhanced atmospheric $CO_2$ concentrations.

## 4.4 Modifications Made in this Study to the *ACRU* Model to Enhance Climate Change Impact Simulations

Although *ACRU* has been used to simulate the effect of climate change on hydrological and agricultural responses in previous studies (e.g. Schulze, 1991; Kunz, 1993; Schulze, 1993; Lowe, 1997; Schulze,1997a; Schulze, 1998), there were certain routines which either needed to be updated, or modified, or added to the model for the first time to enable more realistic simulations of the agrohydrological processes involved in climate change.

### 4.4.1 Reasons for modifications

Modifications to *ACRU* were made for the following reasons:

i) Hydrologically important biomass indicators such as the crop's water use coefficient ($K_{cm}$ , i.e. the amount of water evapotranspired by the crop or vegetation at a given stage of its growth cycle under optimum soil water conditions), canopy interception of rainfall on raindays and root development are generally input into *ACRU* on a month-by-month basis. Under natural conditions the onset of a vegetation's growth cycle, either after a period of dormancy (senescence) or following planting, and hence the corresponding biomass indicators, are triggered largely by critical minimum temperatures being exceeded, while the seasonal development of the crop is also thermally, i.e. temperature, driven when plants are not water stressed. Thus, dynamic

changes in these indicators with changing temperature needed to be incorporated in routines in *ACRU* when simulating varying seasonal climatic conditions.

ii) Previously the monthly input values of $K_{cm}$ were disaggregated to daily values of the water use coefficient ($K_d$) using a six-harmonic Fourier Analysis imbedded in the *ACRU* model. However, on a given day of the year these values of $K_d$ would then be the same (i.e. re-cycled) for every year of simulation. This technique did not account for dry periods during which the plant would be experiencing soil water stress and the $K_d$ would effectively decline with sustained wilting as a consequence, nor for conditions of the soil's wetting up again after a dry spell, in which case the plant would take some time to recover either fully or partially from soil water stress to its original $K_d$ value. It was considered conceptually more correct to account for these stresses and recoveries, especially when simulating hydrological processes in a perturbed climate in which influences of changes in evaporative demands and precipitation amounts have to be accounted for.

iii) Recent experiments have given new estimates for the magnitudes of transpiration suppression under conditions of $CO_2$ enrichment than the ones contained in *ACRU* (Goudriaan and Unsworth, 1990). These new estimates needed to be incorporated into *ACRU* (Schulze and Perks, 2000).

Each of the modifications outlined above is described in more detail in the following sections.

### 4.4.2 Temperature driven biomass indicators

The onset of a vegetation growth cycle (and hence corresponding hydrologically important biomass indicators such as the water use coefficient, $K_d$, rainfall interception loss, $I_l$, and root development, $R_A$) is triggered largely by critical minimum temperatures, while the seasonal development of the crop is also temperature driven when plants are not water stressed.

If, therefore, temperature was to increase in future, the values for these variables are expected to change and algorithms for these dynamic changes need to be included in *ACRU* when simulating future climatic conditions. Various linear functions were developed to represent the changes in these parameters expressed as a function of minimum temperature.

#### 4.4.2.1 Modifications to *ACRU* to incorporate temperature driven biomass indicators

Relationships were first developed by Schulze and Lynch (1992) to represent changes to the $K_{cm}$ , $I_l$ and $R_A$ for natural vegetation as function of minimum temperature. These variables could thus change dynamically over a growing season, dependent on temperature input to the model. These relationships were, however, never incorporated into *ACRU* and the assumptions on which they were based have never been published. The biomass relationships are illustrated schematically in Figure 4.2.

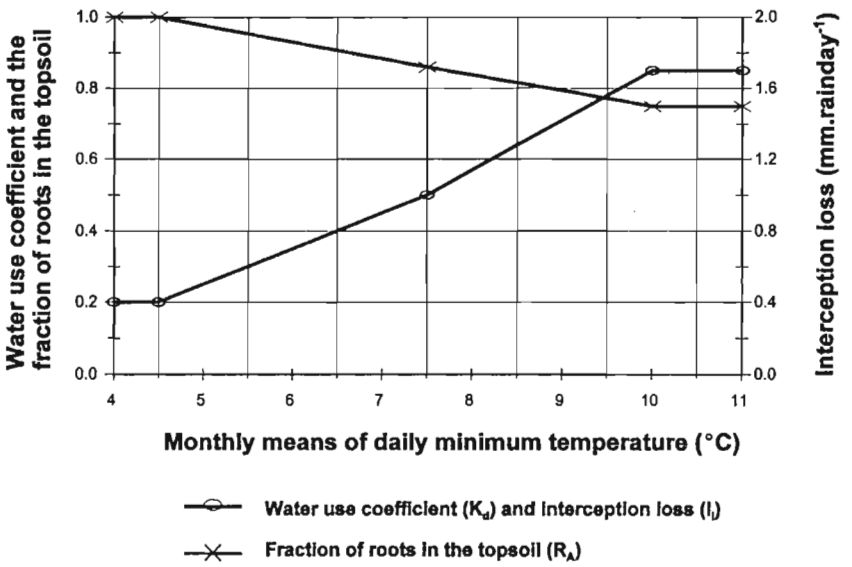


Figure 4.2 Generalised biomass attribute values for the *ACRU* modelling system, generated for non-water stressed conditions and derived from minimum temperature (modified by Schulze and Lynch, 1992)

The biomass relationships, which are used as a proxy to real values when simulating conditions of a natural grassland type vegetation, imply that there is no soil water stress, and are based on the following assumptions:

i) Vegetative growth follows an annual growth cycle.

ii) Seasonal vegetative growth follows a temperature driven sigmoidal curve. Such a growth pattern has been shown in many studies, including Hughes' (1992) thermally driven derivation of the $K_d$ for sugarcane in South Africa.

iii) There is effectively no growth when monthly minimum temperatures are below 4.5 °C, up to which temperature $K_d$ is assigned a value of 0.2 (Schulze *et al.*, 1995c), while above a minimum temperature of 10 the value of $K_d$ remains 0.85.

iv) Canopy interception loss (mm.rainday$^{-1}$) takes place in a direct proportion to the above ground biomass index, *viz.* the daily value of the $K_d$, but with a lower limit of 0.4 mm.rainday$^{-1}$ when biomass is at a minimum and an upper limit of 1.7 mm.rainday$^{-1}$ when natural grassland vegetation is considered to be at full canopy cover.

v) At full canopy cover it is estimated that 75% of the active root mass distribution is in the topsoil and the remaining 25% in the subsoil.

vi) As above ground biomass increases, so root development takes place and the roots which initially colonised only the topsoil extend to the lower soil horizons. Effectively the fraction of roots in the topsoil therefore decreases. Hence the inverted relationship between topsoil root fraction and biomass. Furthermore, roots die off with plant die-back which may result from cold (frost) related senescence, and once monthly means of daily maximum temperature are at 4.5 °C or below, the plant is assumed to no longer transpire actively. Under such conditions evaporative losses therefore take place via the soil and thus from the topsoil only, effectively therefore giving the topsoil a rooting fraction equal to 100%, i.e. 1.0.

vii) When soil water stress occurs, the potential biomass values for the $K_d$ are subjected to stress related reductions and recovery rates described in Section 4.4.3.

#### 4.4.2.2 Algorithms for temperature driven biomass indicators

The algorithms introduced into *ACRU* for this new option to estimate biomass indicators when no actual values are available are as follows (in each case with minimum temperature, $T_{min}$, in °C):

i) For the water use coefficient, $K_d$:

| | | | | |
|---|---|---|---|---|
| If | | $T_{min} \leq$ | 4.5, | $K_d = 0.20$ |
| If | $4.5 \leq$ | $T_{min} \leq$ | 7.5, | $K_d = 0.20 + 0.10\ (T_{min} - 4.5)$ |
| If | $7.5 \leq$ | $T_{min} \leq$ | 10.0, | $K_d = 0.50 + 0.14\ (T_{min} - 7.5)$ |
| If | | $T_{min} >$ | 10.0, | $K_d = 0.85$ |

ii) For canopy interception loss, $I_l$ (mm.rainday$^{-1}$):

If $T_{min} \leq 4.5$, $I_l = 0.40$

If $4.5 \leq T_{min} \leq 7.5$, $I_l = 0.40 + 0.20 (T_{min} - 4.5)$

If $7.5 \leq T_{min} \leq 10.0$, $I_l = 1.00 + 0.28 (T_{min} - 7.5)$

If $T_{min} > 10.0$, $I_l = 1.70$

iii) For the fraction of roots in the topsoil, $R_A$:

If $T_{min} \leq 4.5$, $R_A = 1.00$

If $4.5 \leq T_{min} \leq 10.0$, $R_A = 1.00 - 0.045 (T_{min} - 4.5)$

If $T_{min} > 10.0$, $R_A = 0.75$

These equations represent what is depicted diagrammatically in Figure 4.2. As shown in the figure, both $K_d$ and the interception loss increase with an increase in minimum temperatures, whereas the fraction of roots in the topsoil decreases with an increase in minimum temperatures.

#### 4.4.2.3 Illustration of changes to temperature driven biomass indicators

To examine the changes in daily water use coefficient, rainfall interception loss and fraction of roots in the topsoil when this new option was activated in *ACRU,* four sample points located in different climate zones were selected across the study area, *viz.* in the

i) winter rainfall region (32°30'S, 18°45'E);

ii) summer rainfall region, subtropical (22°30'S, 30°00'E);

iii) summer rainfall region, coastal (30°00'S, 30°00'E); and

iv) summer rainfall region, interior (30°00'S, 26°15'E).

The summer season in the study area is from October to March and the winter season is April through September. Two simulations using *ACRU* were performed at each point, *viz.* one with observed present minimum temperatures and the other with a 2 °C increase in minimum temperatures.

The biomass indicators for non-soil water stressed conditions for each of the four locations were plotted for the two simulations and are illustrated in Figures 4.3 to 4.6.

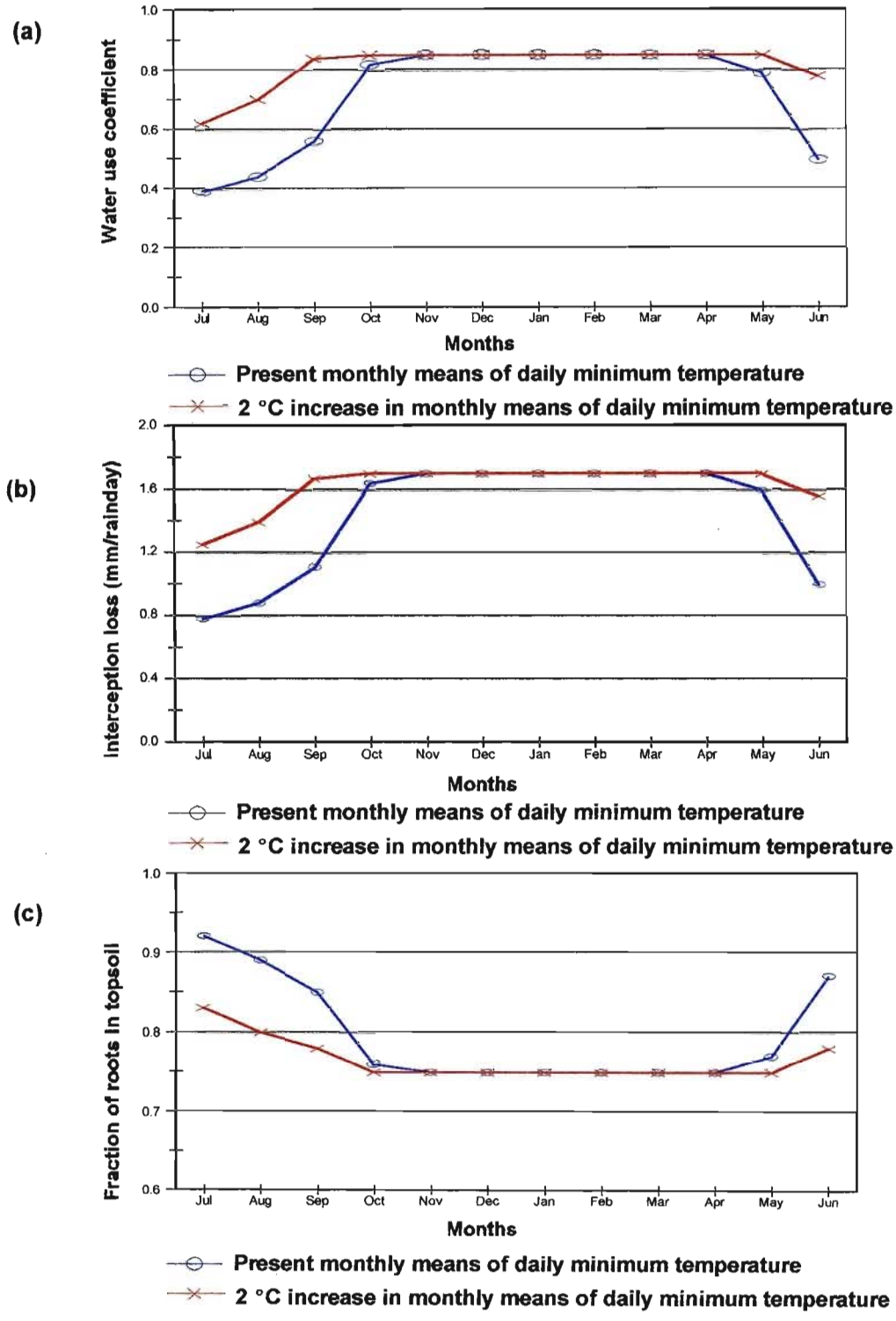


Figure 4.3 Illustration of temperature driven biomass indicators for present monthly means of daily minimum temperature and a 2 °C increase in minimum temperatures for sample point 32°30'S and 18°45'E in the winter rainfall region: (a) water use coefficient (b) canopy interception loss and (c) fraction of roots in topsoil

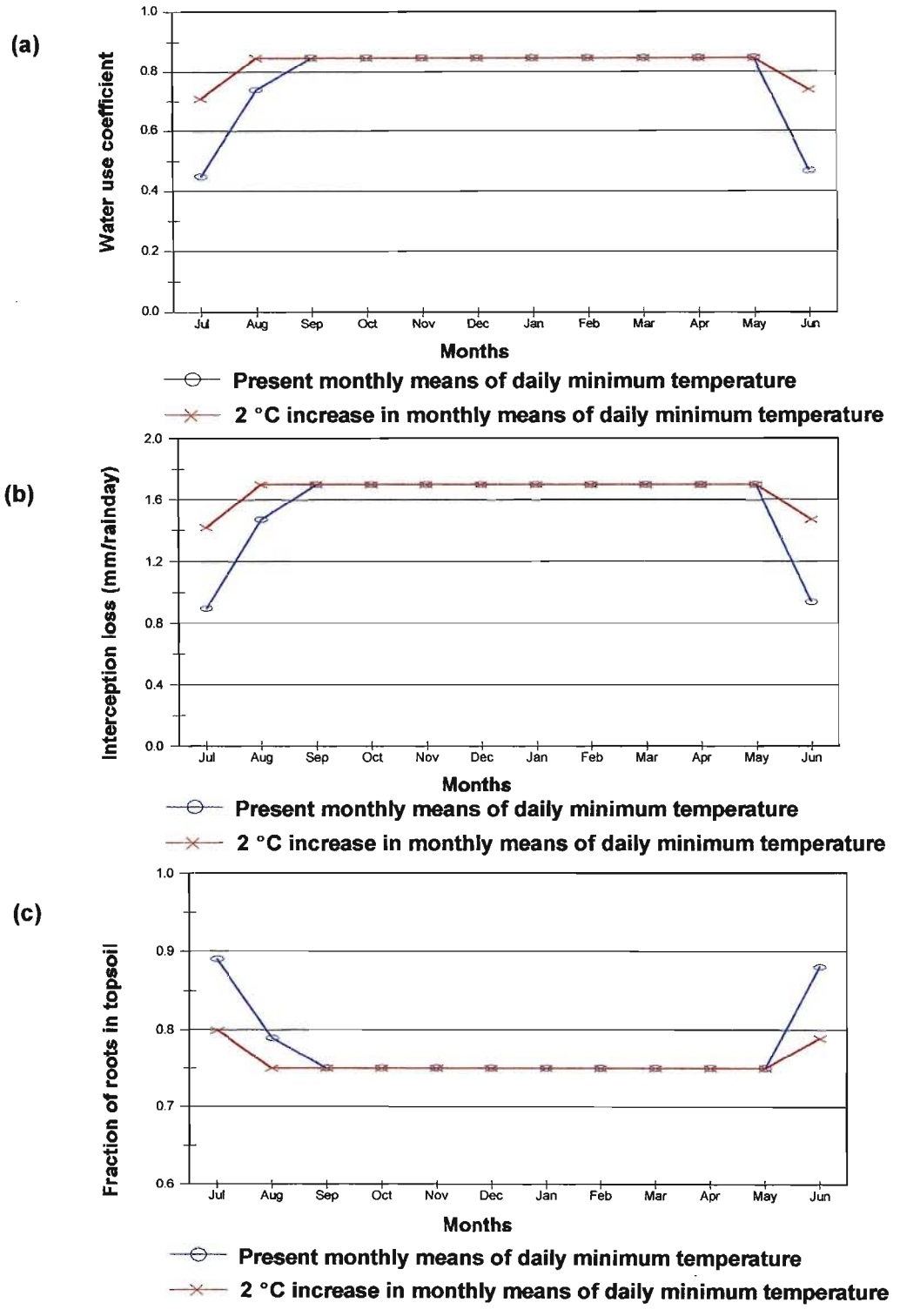


Figure 4.4 Illustration of temperature driven biomass indicators for present monthly means of daily minimum temperature and a 2 °C increase in minimum temperatures for sample point 22°30'S and 30°00'E in the subtropical summer rainfall region: (a) water use coefficient (b) canopy interception loss and (c) fraction of roots in topsoil

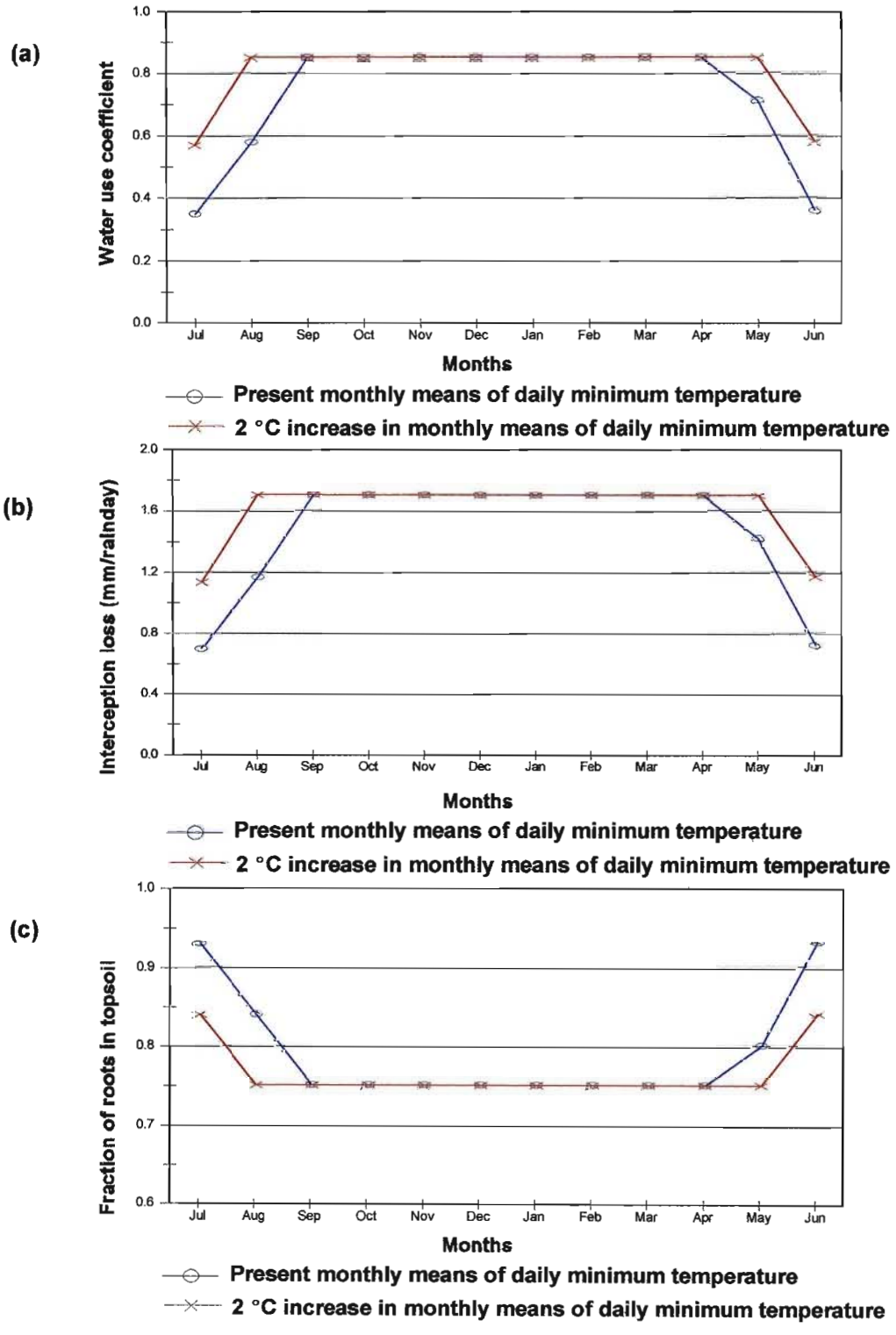


Figure 4.5 Illustration of temperature driven biomass indicators for present monthly means of daily minimum temperature and a 2 °C increase in minimum temperatures for sample point 30°00'S and 30°00'E in the coastal summer rainfall region: (a) water use coefficient (b) canopy interception loss and (c) fraction of roots in topsoil

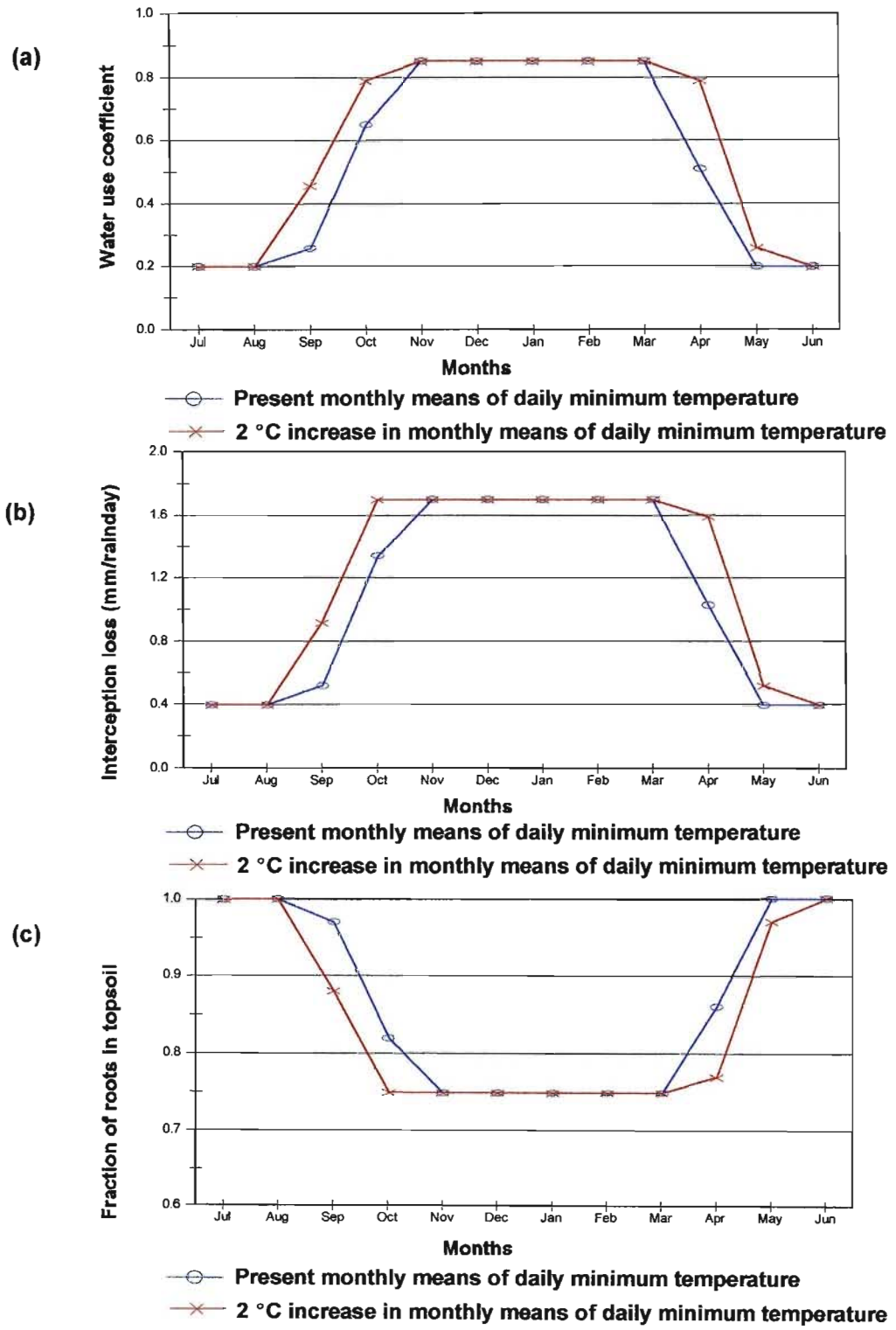


Figure 4.6 Illustration of temperature driven biomass indicators for present monthly means of daily minimum temperature and a 2 °C increase in minimum temperatures for sample point 30°00'S and 26°15'E in the interior summer rainfall region: (a) water use coefficient (b) canopy interception loss and (c) fraction of roots in topsoil

It should, furthermore, be remembered that the dynamically simulated values of $K_d$ and $I_l$ are for optimum conditions of soil water and that the further modifications to these variables under conditions of soil water stress are discussed in Section 4.4.3.

The biomass indicators for the winter rainfall region for the two simulations are illustrated in Figure 4.3. The duration of the $K_d$ at its maximum of 0.85 is from November to April with present minimum temperatures. This duration is extended to a month earlier in October and a month later to May in a 2 °C warmer climate (Figure 4.3, a). In a warmer climate the increases in interception loss, which is now related directly to the biomass indicator $K_d$, from May to October are substantial, with increases of 0.5 mm.rainday$^{-1}$ shown for August and September (Figure 4.3, b). The fraction of roots in the topsoil, on the other hand, decreases in these months (Figure 4.3, c), indicating a more rapid root development into the subsoil horizon.

In the warm, subtropical summer rainfall region (Figure 4.4), the duration of the $K_d$ at its maximum of 0.85 is already long (September to May) for present climatic conditions. The only change to $K_d$ with a 2 °C increase in minimum temperature in this region is that the $K_d$ in August also reaches the maximum possible of 0.85 (Figure 4.4, a). The duration of maximum interception loss (1.7 mm.rainday$^{-1}$) is also longer in this region than in the winter rainfall region (Figure 4.4, b). The patterns of the biomass indicators of the warm coastal summer rainfall (Figure 4.5) area are similar to those of the subtropical summer rainfall region.

Increases in the value of $K_d$ of the interior summer rainfall region due to a 2 °C increase in minimum temperature occur particularly in the springtime month of October (Figure 4.6, a). The increases in interception loss occur in the months of April to October for a warmer climate (Figure 4.6, b). The fraction of roots in the topsoil for a 2 °C increase in minimum temperatures is the same for most months with the exception of April, September and October, where the decreases reflect the more rapid root development in a warmer climate (Figure 4.6, c).

### 4.4.3 Soil water stress related water use coefficient

Evaporation from a vegetated surface comprises of evaporation from the soil surface and transpiration from the plant. These two interlinked processes are often termed evapotranspiration. When the plant experiences no soil water stress, maximum transpiration rates are expected to occur. The maximum transpiration of a crop cover at any stage in its growth cycle depends on its above ground biomass, which is expressed either by its $K_d$, or its leaf area index (LAI).

At full canopy cover (i.e. when $K_d \geq 1.0$ or LAI $\geq 2.7$) it is assumed in *ACRU* that transpiration makes up 95% of the total evaporation loss and the soil water evaporation component the remaining 5%, while with partial vegetation cover the partitioning of total evaporation into transpiration and soil water evaporative losses is a non-linear function of the $K_d$, using an equation modified from Ritchie (1972) such that the fraction of evaporative energy available for transpiration ($F_t$) is given as

$$F_t = 0.7 \ LAI_d^{0.5} - 0.21$$

where $LAI_d$ = daily value of the leaf area index

which is derived as a function of $K_d$ (Schulze *et al.*, 1995c) as

$$LAI_d = [\ln (K_d - 1.0932) / -0.7947] / - 0.6513.$$

#### 4.4.3.1 Modification to the water use coefficient routine in *ACRU*

In *ACRU* the daily value of a vegetated cover's potential $K_d$ is used to determine the maximum soil water evaporation and transpiration loss by vegetation. The potential $K_d$ can be expressed as a ratio of maximum evaporation ($E_m$) from the plant and soil to a reference potential evaporation ($E_r$) such that

$$K_d = E_m / E_r.$$

The upper boundary limit of the potential $K_d$ is set at 1.02 at full canopy while its lower boundary, when no canopy cover occurs, is set at 0.2 (Schulze *et al.*, 1995c). During a period of soil water stress, a plant loses its ability to transpire at maximum rate and also its ability to recover immediately again to the maximum rate when the plant water stress is relieved by rainfall or irrigation. A stress induced reduction in the effective $K_d$ therefore takes place, while a recovery period is required for the crop to attain its maximum transpiration rate again.

From experimental trials, a curvilinear $K_d$ reduction function was developed for sugarcane by Hughes (1992) for conditions of varying soil water stress. This curve was adapted by Kunz (1993) to reduce the $K_d$ under times of stress using a stress index. Because sugarcane is considered to be a physiologically simple plant which is similar in its water use responses to most grasses, this stress index (SI) has been generalised for use with natural vegetation. It follows an exponential decay function using the previous day's water use coefficient value ($K_{d-1}$) as follows

$$SI = EXP\ (-K_{d-1}/10) + 0.02.$$

This equation allows for a relatively higher daily reduction in $K_d$ by plants which are stressed at or near full canopy (i.e. $K_d \sim 1.0$), with relatively little daily reduction in $K_d$ for stressed plants with an already low water use coefficient (i.e. $K_d \sim 0.4$). This change in the rate of $K_d$ reduction is important in an anticipated warmer future climate where plants are expected to increase their potential rate of growth due to higher temperatures, while at the same time possibly experiencing changes in plant stress patterns.

Hughes' (1992) observation based research on water use coefficients of sugarcane included the development of a recovery curve for water use coefficients when dry soils wetted up again. His original equation was modified by Kunz (1993) to make it season and location independent. The daily recovery index (RI) of the $K_d$ is based on the finding from the data sets used by Hughes (1992) that $K_d$ recovers at a linear rate as a function of the mean daily air temperature, $T_{m10}$, for values of $T_m \geq 10$ °C. Thus, the recovery of $K_d$, and hence an increase in transpiration, will be faster in the warmer summer months than during the cooler winter

months and in a warmer location compared with a cooler location, and also would not take place unless a threshold mean daily temperature of 10 °C was reached. In an anticipated warmer future climate, a stressed crop will therefore recover more rapidly than at present following the release of soil water stress through rainfall. The daily recovery index is calculated as

$$RI = 0.002333 \times T_{m10}.$$

The stress thresholds of both the A and B horizons of the soil are calculated to gauge whether the plant is considered to be under soil water stress or not. For example, the stress threshold for the A horizon ($SL_A$) is calculated as

$$SL_A = ( \theta_{PAW(A)} \times f_s ) + \theta_{LL(A)}$$

where $\theta_{PAW(A)}$ = plant available water soil water content (mm equivalent)

$f_s$ = fraction of the plant available water of a soil horizon at which total (i.e. actual) evaporation is assumed to drop below the maximum evaporation during drying of soil (0.4 is a typical value)

$\theta_{LL(A)}$ = soil water content (mm equivalent) at the lower limit of soil water (i.e. at permanent wilting point) for the A horizon.

On a given day, if the soil water contents of both the A and B horizons of the previous day are less than their respective stress thresholds, plant stress is assumed to occur.

The $K_d$ is then reduced by

$$K_d = K_{d-1} \times SI.$$

When the soil water content of either the A or B horizons of the previous day is above the stress threshold, the plant's $K_d$ recovers at the following rate

$$K_d = K_{d-1} + RI.$$

On condition that $K_d$ does not exceed the potential $K_d$, with these modifications now in *ACRU*, the model facilitates a dynamic change in a biomass indicator which can vary dynamically with climate change and associated changes in soil water stress.

#### 4.4.3.2 Illustration of the modification to the stress related water use coefficient

To illustrate the effect of the application of stress indices and recovery rates on $K_d$ in *ACRU*, an example from a catchment near Pietermaritzburg was used to simulate the differences in patterns of $K_d$ between the previous and now modified routines (Figure 4.7).

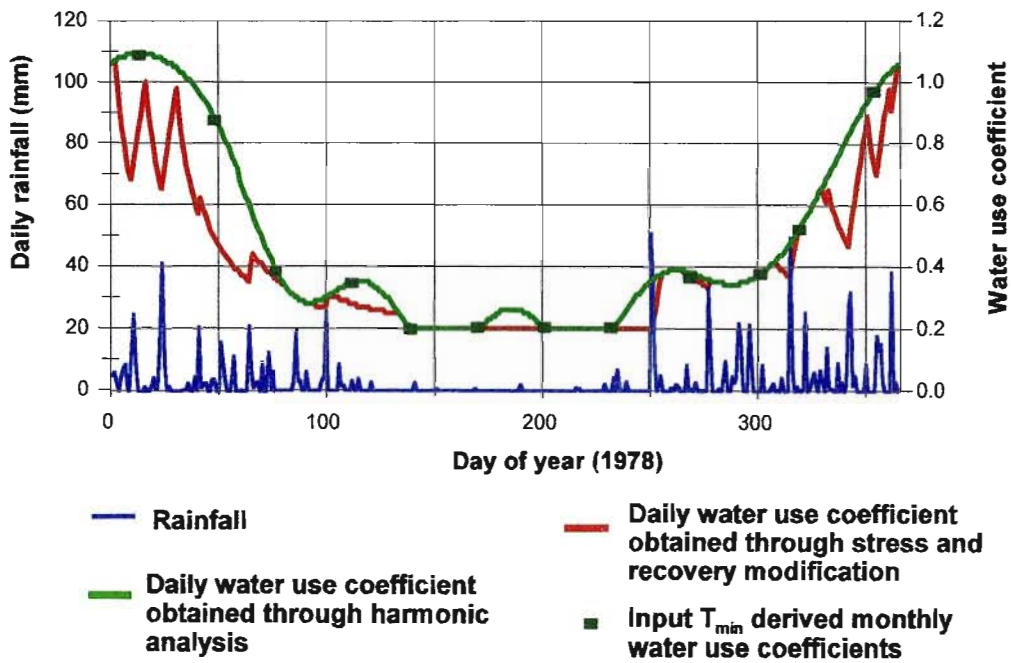


Figure 4.7 Original and modified curves of the water use coefficient for a catchment near Pietermaritzburg showing the influence of soil water induced stress and stress recovery

As shown in Figure 4.7 the modified $K_d$ (red line) can never exceed the potential $K_d$ established through the six-harmonic Fourier Analysis (green line) and can never decrease

below a $K_d$ value of 0.2. Figure 4.7 shows clearly the influence of soil water stress and stress relief on $K_d$, particularly from day of year 1 - 100 and again 320 - 365.

### 4.4.4 Carbon dioxide feedbacks to transpiration losses

When exposed to higher levels of atmospheric $CO_2$, plants close their stomata in an attempt to balance the rates of water, $CO_2$ and nutrient use (cf. Chapter 2, Section 2.3.1.1). Stomatal closure is more pronounced in C4 than in C3 plants because C4 plants do not reproduce $CO_2$ by photorespiration and therefore the concentration of $CO_2$ in the stomatal cavities is much lower than for C3 plants (Acock, 1990). Hence, the $CO_2$ gradient from air to leaf cavity is steeper for C4 plants, resulting in greater stomatal closure in an attempt to reduce the $CO_2$ gradient (Schulze, 1995b).

To account for the day-to-day effects of this phenomenon, maximum transpiration suppression rates in *ACRU* for a doubling of atmospheric $CO_2$ levels had previously been set at 22% for C3 plants and 33% for C4 plants, based on values suggested by Idso and Brazel (1984) and other literature sources summarized in IPCC (1990).

#### 4.4.4.1 Modifications to carbon dioxide feedbacks

However, these transpiration suppression rates have subsequently been superceded by the findings, summarized in IPCC (1995), of more recent research which shows that acclimation (i.e. adaption) to $CO_2$ enhancement over time reduces the impact of $CO_2$ on stomatal conductance and hence transpiration suppression. Thus, the maximum transpiration suppression values in *ACRU* have now been modified to 15% for C3 plants and 22% for C4 plants to reflect these recent findings. These changes are important in calculating water budgets in an anticipated warmer future climate, where plants are expected to increase their rates of growth, but at the same time experience changes in plant stress patterns while simultaneously being subjected to $CO_2$ induced transpiration loss feedbacks.

#### 4.4.4.2 Illustration of modified carbon dioxide feedbacks to account for reduced transpiration losses

To examine the effect of $CO_2$ induced transpiration suppression on maximum transpiration, actual transpiration and soil water content, the same catchment near Pietermaritzburg as used in Section 4.3.3.2 was used in simulation to assess changes between the original (1995) and newly modified $CO_2$ suppression amounts in *ACRU*. *ACRU* simulations were therefore carried out on this catchment conditions assuming

i) no $CO_2$ transpiration suppression;

ii) original $CO_2$ transpiration suppression amounts of 33% for C4 plants; and

iii) modified $CO_2$ transpiration suppression amounts of 22% for C4 plants.

It was assumed that maize (a C4 plant) was planted on 1 November in the catchment. The option for computing soil water evaporation and plant transpiration as separate processes in *ACRU* was selected. Figure 4.8 shows the effect of activating transpiration suppression in *ACRU* on maximum transpiration from the A horizon during January 1981 using both the original and modified suppression values. Maximum transpiration occurs when the plant is under no soil water stress (Schulze, 1995b). As shown in the figure the modified transpiration suppression amounts are less than the original amounts.

Figure 4.9 shows the actual transpiration amounts determined by *ACRU* for this catchment under the varying modes of transpiration suppression. Actual transpiration can either be equal to maximum transpiration under conditions of no soil water stress or less than maximum transpiration either because of a deficiency of available soil water or an excess of soil water (Schulze, 1995b). The difference in the three transpiration suppression scenarios is most distinct when the soil is wetted after rainfall and the actual transpiration is high (18th - 21st January 1981). The scenario of no $CO_2$ transpiration suppression resulted in the highest actual transpiration during this period, with progressively decreasing actual transpiration simulated for the modified and original scenarios respectively.

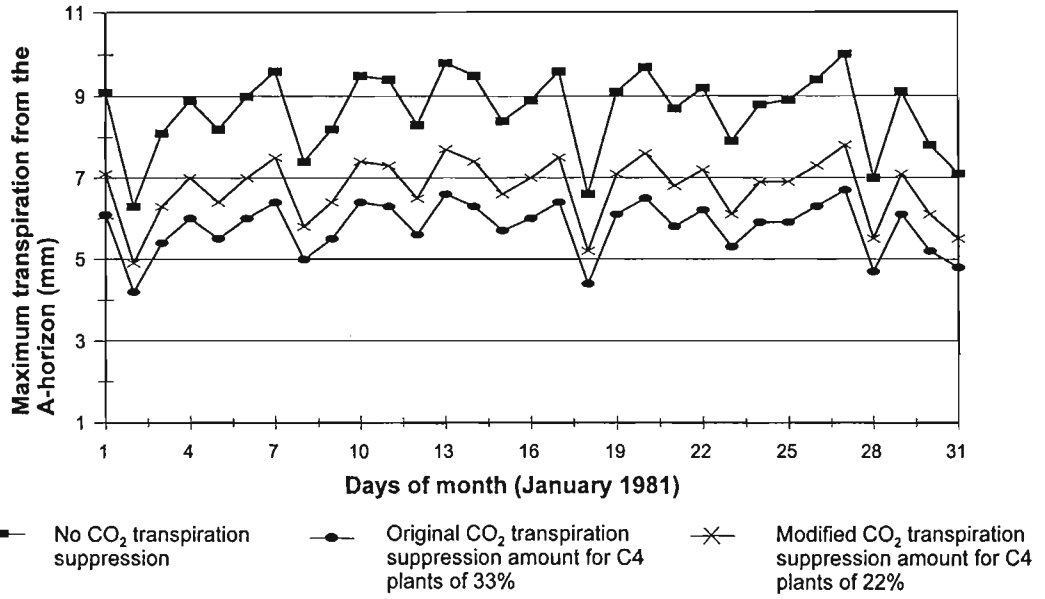


Figure 4.8 Maximum transpiration from the A horizon for a catchment near Pietermaritzburg for simulations with no transpiration suppression, original transpiration suppression amounts and modified transpiration suppression amounts for C4 plants

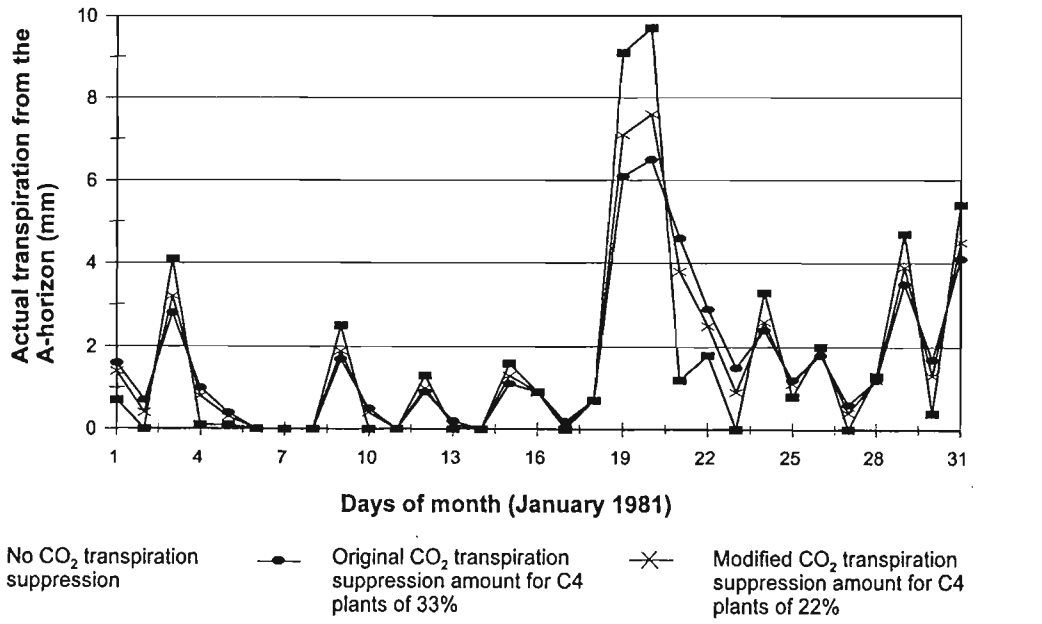


Figure 4.9 Actual transpiration from the A horizon for a catchment near Pietermaritzburg for simulations with no transpiration suppression, original transpiration suppression amounts and modified transpiration suppression amounts for C4 plants

There was not much difference in the simulated soil water content for the first 18 days of the month under the three scenarios as the soil was relatively dry (Figure 4.10). Following the sharp increase in soil water content on 18 January 1981 after a rainfall event, the rate of decrease in soil water content is different for the three transpiration suppression scenarios. During the period following this rainfall event the soil water content was simulated to be highest using the original $CO_2$ transpiration suppression amounts. The simulated soil water content was not as high using the modified transpiration suppression amounts compared to that using the original transpiration suppression amounts.

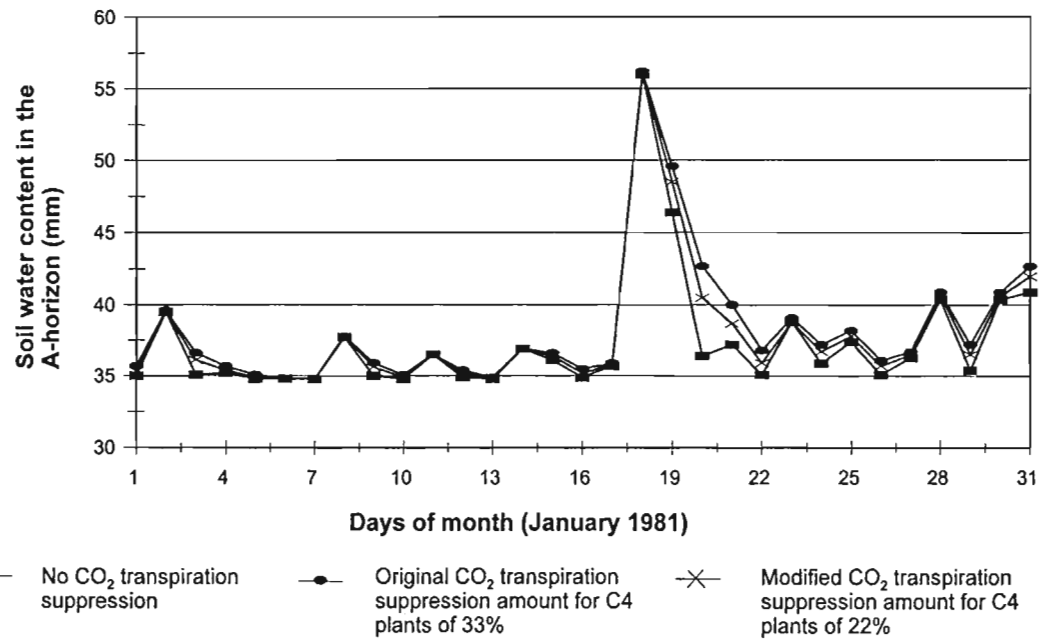


Figure 4.10 Soil water content in the A horizon for a catchment near Pietermaritzburg for simulations with no transpiration suppression, original transpiration suppression amounts and modified transpiration suppression amounts for C4 plants

### 4.4.5 Modifications to the winter wheat submodel in *ACRU*

Potential changes in winter wheat yield were simulated using the winter wheat submodel in *ACRU*. The results from these simulations are presented in Chapter 8, Section 8.3. However, modifications were first needed to the winter wheat submodel to enable changes in temperature and atmospheric $CO_2$ concentration to be taken into account as described below.

The phenology based winter wheat submodel in *ACRU* (Schulze *et al.*, 1995d) takes the general form

$$Y_w = Y_{pw} (E_{t1} / E_{tm1})^{\alpha w1} \times (E_{t2} / E_{tm2})^{\alpha_{w2}} \times (E_{t3} / E_{tm3})^{\alpha w3}$$

where

| | | | |
|---|---|---|---|
| | $Y_w$ | = | seasonal winter wheat grain yield ($t.ha^{-1}$) |
| | $Y_{pw}$ | = | potential winter wheat grain yield ($t.ha^{-1}$) for the season |
| | $E_{ti}$ | = | accumulated ("actual") daily crop transpiration (mm) for a given growth stage, *i*, from all soil horizons |
| | $E_{tmi}$ | = | accumulated daily maximum transpiration (mm) for a given growth stage, *i*, from all soil horizons |
| | $\propto_{wi}$ | = | exponent to allow for stress weighting in growth stage *i* in winter wheat |
| | 1 | = | growth stage 1: emergence to jointing |
| | 2 | = | growth stage 2: jointing to soft dough and |
| | 3 | = | growth stage 3: soft dough to maturity. |

For southern Africa different empirical values of the exponent $\propto_{wi}$ have been derived for use with *ACRU*'s soil water budgeting procedures, dependent on the availability of A-pan equivalent information as given in Table 4.1 (Domleo, 1990; Schulze *et al.*, 1995d). In the absence of A-pan evaporation data the Linacre (1984) temperature based equation for potential evaporation equivalents have been used in the derivation of the exponents - this method should therefore be applied in winter wheat simulations with *ACRU* (Schulze *et al.*, 1995d).

Presently in the winter wheat submodel of *ACRU* the determination of maximum crop transpiration, $K_{cm}$ , is performed by starting with the winter wheat crop coefficients for different growth stages which are triggered by days after planting and not by a more dynamic degree-day procedure. The value of $E_{tm}$ for winter wheat is assumed zero from planting to emergence at 15 days, increasing linearly to 0.5 $K_{cm}$ at jointing after 30 days, then increasing linearly to 0.9 $K_{cm}$ at heading when maximum leaf area is attained, thereafter remaining at 0.9

$K_{cm}$ until the soft dough stage is reached 80 days after planting. This technique of obtaining $E_{tm}$ from $K_{cm}$ was adapted from research by Childs and Hanks (1975).

Table 4.1 Present default values derived empirically for use with the *ACRU* winter wheat yield model in southern Africa (after Domleo, 1990; Schulze *et al.*, 1995d)

| Phenological State | Growth Stage | Days Since Planting | Exponent to be Used in *ACRU* With | |
|---|---|---|---|---|
| | | | Daily A-pan Observations | A-pan Equivalent by Linacre (1984) |
| Emergence | | 15 | | |
| | 1 | | 0.10 | 0.20 |
| Jointing | | 30 | | |
| | 2 | | 0.10 | 0.20 |
| Soft Dough | | 80 | | |
| | 3 | | 0.60 | 0.75 |
| Maturity | | 120 | | |

However, when simulating winter wheat yield for a future climate scenario, this present method could not take into account

i) the increases in temperature expected with climate change which would affect both the starts of the phenological growth periods as well as the varying lengths of the growing season; and

ii) the expected suppression of transpiration resulting from increases in atmospheric $CO_2$ concentrations as in the *ACRU* winter wheat model evapotranspiration was computed as an entity and not with transpiration and soil water evaporation separately, which would facilitate a transpiration suppression for the C3 wheat to be determined.

Therefore, modifications needed to be made to the *ACRU* wheat submodel to allow these factors to be taken into account and allow more realistic simulations of potential winter wheat yields in a future climate.

First, the *ACRU* model was adjusted to be able to allow for the anticipated increases in temperature. The phenological growth stages were set to rather be activated by the number of growing degree days (accumulated heat units) rather than on days after planting. This is

a similar technique to that used in the maize yield submodel of *ACRU* (cf. Table 8.11). To determine the anticipated number of accumulated heat units that were required to reach each phenological stage, five wheat growing sites in southern Africa were identified, *viz.* Glen, Bethlehem, Sandvet, Bergville and Marquard (Domleo, 1990). At each of these sites the mean daily temperatures were calculated from daily maximum and minimum temperatures generated using the latitude, longitude and elevation at each site (Table 4.2), following the technique described in Chapter 5, Section 5.2.

Table 4.2 The latitudes, longitudes and elevations of the five sites selected to represent winter wheat cultivation areas in southern Africa (Domleo, 1990)

| Station | Latitude | Longitude | Elevation | Quaternary Catchment |
|---|---|---|---|---|
| Bethlehem | 28°10' | 28°18' | 1638 | C60A |
| Marquard | 28°41' | 27°21' | 1572 | C42E |
| Glen | 28°57' | 26°20' | 1304 | C52H |
| Sandvet | 28°08' | 26°41' | 1290 | C43A |
| Bergville | 28°46' | 29°22' | 1158 | C81C |

Using a biofix for wheat of 4.4 °C (cf. Chapter 8, Section 8.1.1) the accumulated number of growing degree days were determined from the assumed plant date of 15 May. The median number of accumulated growing degree days for the start of each phenological stage for the five sites was identified. In Table 4.3 the accumulated growing degree days calculated for each site as well as the number of accumulated growing degree days expected in a growing season, calculated as the sum of the four phenological periods, are listed.

The median number of accumulated growing degree days (rounded off) used to start each phenological stage of winter wheat in the modified *ACRU* winter wheat submodel are shown in Table 4.4.

Table 4.3 Estimated accumulated growing degree days for each phenological period in the growth of winter wheat for five sites in southern Africa

| Station | Planting to Emergence | Emergence to Jointing | Jointing to Soft Dough | Soft Dough to Maturity | Length of Season |
|---|---|---|---|---|---|
| Bethlehem | 87 | 186 | 303 | 562 | 1138 |
| Marquard | 88 | 209 | 318 | 587 | 1202 |
| Glen | 102 | 235 | 353 | 672 | 1362 |
| Sandvet | 120 | 301 | 462 | 803 | 1686 |
| Bergville | 143 | 423 | 679 | 1052 | 2297 |

Table 4.4 Estimated values of accumulated growing degree days after planting used to activate the various phenological periods and length of growing season

| Phenological State | Growing Degree Days |
|---|---|
| Planting to Emergence | 100 |
| Emergence to Jointing | 240 |
| Jointing to Soft Dough | 350 |
| Soft Dough to Maturity | 670 |
| Length of Season | 11360 |

Therefore, accumulated growing degree days have replaced the number of days of growth used to activate the various phenological periods as well as the length of the growing season, allowing the growth of winter wheat to occur faster than at present and the duration of the growing season to be shorter in a anticipated warmer climate in future.

Secondly, transpiration suppression could not be taken into account. The winter wheat submodel in *ACRU* was therefore modified for climate change simulations such that once maximum transpiration is calculated it is suppressed by 15% as wheat is classified as a C3 plant (cf. Section 4.4.4).

* * * * * * *

In this chapter a brief introduction to the *ACRU* agrohydrological model and the modifications to the model to enable dynamic simulations of water resources resulting from changes in climate have been presented. The modifications include the introduction of temperature driven biomass indicators whereby the crop water use coefficient, vegetation interception loss and fraction of roots in the A horizon can be derived automatically using minimum monthly temperatures, the refinement of the daily value of the water use coefficient to account for stresses and recovery of the plant and the adjustment of the suppression of plant transpiration owing to increased atmospheric $CO_2$ concentrations. In addition, the winter wheat submodel imbedded in the *ACRU* model was revised. The phenological growth stages of the plant are now activated by accumulated growing degree days facilitating faster development of the crop in a warmer 2X $CO_2$ climate.

In order to simulate both present and future climate scenarios with *ACRU*, spatial information on the study area is required. In Chapter 5 the various spatial databases that were used to perform climate change impact studies for the study area are outlined. The methodology used for the generation of daily maximum and minimum temperatures for use in this study is also described.

# 5. SPATIAL DATABASES FOR CLIMATE CHANGE IMPACT STUDIES IN SOUTHERN AFRICA

In order to evaluate the impacts of climate change on agriculture, hydrological responses and water resources, it is necessary to have spatial information on physiographic variables as well as present (baseline) and future climatic parameters throughout southern Africa as input into the *ACRU* model. To provide reference points with which to compare future climate predictions, current baseline climate conditions need to be specified (Parry and Carter, 1998). These conditions assume climatic stationarity over time, with no trends of general increases or decreases being detectable (Benioff *et al.*, 1996).

## 5.1 Gridded Databases

In order to study the impacts of climate change on water resources and agriculture, it was necessary to have information on various climatic and physiographic parameters for southern Africa. Use was made of the School of BEEH's gridded altitude and climate databases and the establishment of these databases is described in detail in the *South African Atlas of Agrohydrology and -Climatology* (Schulze, 1997b).

This gridded database of southern Africa is made up of one minute of a degree by one minute of a degree (1' x 1') latitude / longitude grid blocks (equating to approximately 1 600 m x 1 600 m), comprising 437 000 pixels in a digital database covering South Africa, Lesotho and Swaziland. The primary database has been derived from various sources and serves to determine primary locational, physiographic and climatic attributes used in subsequent analyses. These attributes include

i) latitude;
ii) longitude;
iii) altitude;
iv) aspect;
v) a continentality index;
vi) a topographic exposure index;
vii) a terrain roughness index; and
viii) extraterrestrial radiation for each month.

To obtain secondary climatic parameters for each month, southern Africa was delineated into regions of relatively homogenous responses to those factors affecting a climatic variable (e.g. for rainfall mapping 34 regions were identified, for temperature and potential evaporation 12). Using stepwise multiple regression techniques with the primary attributes listed above as variables, equations were developed for the secondary climatic parameters of maximum and minimum temperature and precipitation for each month of the year.

Finally, the primary variables together with the derived secondary variables were used to develop tertiary sets of information (e.g. heat units, relative humidity, potential evaporation) which could then be used in determining, for example, crop yields (Schulze, 1997b). More detail on the preparation of baseline climate information is provided in Perks *et al.* (2000).

## 5.2 Generation of Baseline Daily Maximum and Minimum Temperature Series

The procedure to generate baseline daily maximum and minimum temperature given the latitude, longitude and elevation of a point in southern Africa was completed by the School of BEEH in September 2000. The impact assessments in this study were generally conducted using monthly temperature, however, the development of this procedure facilitated the option of using daily temperatures in the impact assessments. Whereas the monthly temperatures remain constant from year to the year, daily temperatures reflect the intra-monthly and inter-annual variability in temperature which exists.

This automated procedure to infill periods of missing data, and to extend records at stations with a minimum of 5 years of observed temperature data to a common record of 45 years' (1950 - 1994) daily maximum and minimum temperature values is described below. Records of over 600 temperature stations in South Africa, Lesotho and Swaziland were used in this research (Perks *et al.*, 2000).

The procedure adopted was as follows:

i) First the available temperature data at each qualifying station were throughly quality checked. This included flagging days as having missing data when daily minimum

temperature ≥ daily maximum temperature values, or correcting temperature for those days on which obvious data transposing errors had occurred (e.g. an error of 10 °C when 18 °C was recorded, instead of a 28 °C).

ii) Each station, in turn, was selected to be a "target" station, i.e. the stations for which its record had to be either infilled or extended.

iii) For each target station nine "control" stations were selected, i.e. stations from which data would be used to infill or extend the target station's missing daily temperature values for the 45 year period 1951 - 1994.

iv) These nine control station stations were selected according to criteria of inverse of distance from, and difference in altitude to, the target station, and they were then ranked from best to ninth. Where fewer than nine control stations were found with a radius of 50 km of the target station, only those qualifying control stations were considered.

v) For each month of the year, as well as for the summer season (October - March) and winter season (April - September), the means and standard deviations of the daily maximum and minimum temperatures within that month / season were determined for both target and control stations.

vi) The control station with a monthly standard deviation closest to that of the target station was selected to infill / extend the target station records which were missing for the selected 1950 - 1994 period. In each case the control station's mean for that month was adjusted up or down to correspond with the mean of the target station for that month, and any missing records infilled. Infilled values were flagged as such.

vii) If there remained any missing periods of daily temperature values of the target station, the next best control station in terms of corresponding standard deviation was selected and the procedure above repeated.

viii) The reason for corresponding standard deviations rather than means being the criteria for selecting 'best' control stations was that the 'best' means frequently displayed marked differences in variance of temperature (Hewitson, 1997, pers. comm.), and whereas differences in variance cannot easily be 'corrected' meaningfully, difference in means can.

ix) If, after the nine qualifying control stations had not infilled the entire 45 year daily record at the target station, the remaining missing values were 'patched' by using Fourier Analysis.

x) In that procedure the 12 monthly means of the observed daily maximum and minimum temperatures were subjected to a Fourier Analysis using six harmonics to generate 365 daily values. These were then used to infill the remaining missing days' values. Values derived by Fourier Analysis were assigned a separate flag, since the same values are "recycled" for the same day year after year and therefore do not display natural day-to-day variability. The procedure was repeated for minimum temperature.

xi) The result of the above procedures was 600 temperature stations each with a 45 year daily time sequence of maximum and minimum temperature.

xii) In order to generate 45 year time series of daily temperature at locations other than at the climate stations, southern Africa was delineated into 12 regions of similar temperature lapse rates. For each of the 12 regions and for each month of the year a separate lapse rate was computed according to procedures outlined in Schulze (1995a; 1997a) for maximum and minimum temperatures separately.

xiii) For any specific location the lapse rate region is first determined. Thereafter the altitude difference between the location in question and the closest temperature station within that region is calculated, and by applying the respective regional / monthly lapse rate a 45 year series of daily maximum and minimum temperatures can then be generated (Perks *et al.*, 2000).

## 5.3 Present Quaternary Catchments' Database

The Department of Water Affairs and Forestry (DWAF) has delineated southern Africa into 22 so-called Primary Catchments which are each subdivided into Secondary, then Tertiary and finally into interconnected Quaternary Catchments, of which 1946 have been delineated. The Quaternary Catchment is the smallest catchment which the DWAF uses for general planning purposes (Midgely *et al.*, 1995).

From the 1' x 1' gridded databases, values of median monthly rainfall, monthly means of daily maximum and minimum temperatures, monthly totals of reference potential evaporation (A-pan equivalent) as well as a mean altitude were calculated for each Quaternary Catchment using the *ZONALSTATS* command in ARC/INFO. The result was that for each Quaternary Catchment month-by-month representative values for these baseline climate variables were obtained. The same procedure was followed to obtain a representative value of mean annual precipitation for each Quaternary Catchment. The water resources impact studies of climate change (cf. Chapter 9), the maize and winter wheat yield analyses (cf. Chapter 8, Section 8.3) were performed at the Quaternary Catchment scale.

The GCM output was interpolated to a quarter of a degree by quarter of a degree ($^1/_4°$ x $^1/_4°$) latitude / longitude resolution for use in the impact assessment conducted in this study. Figure 5.1 shows the Quaternary Catchment configuration for the study region and the resolution of the $^1/_4°$ x $^1/_4°$ as well as 1' x 1' gridded values, using the mean annual precipitation grid as an example.

| | |
|---|---|
| Figure 5.1 | Quaternary Catchment configuration for the study region (after SRK and DWAF, 1994) and the resolution of the quarter degree latitude / longitude gridded values using the mean annual precipitation grid as an example |

The Quaternary Catchments are numbered in a downstream order. By way of example, the Quaternary Catchment which is numbered W51F, which lies to the north of the town of Piet Retief in Mpumalanga province, would be interpreted as follows:

i) The letter "W" denotes that the Quaternary catchment is in the Primary drainage region W. There are 22 Primary drainage regions which cover southern Africa, numbered alphabetically from A to X, but excluding the letters I and O.

ii) The number "5" denotes that the Quaternary Catchment is in Secondary drainage region number five of Primary region W. There are, at maximum, nine Secondary drainage regions (1 - 9) per Primary drainage region.

# QUATERNARY CATCHMENTS, ¼° AND 1' x 1' GRIDS : EXAMPLE USING MEAN ANNUAL PRECIPITATION.

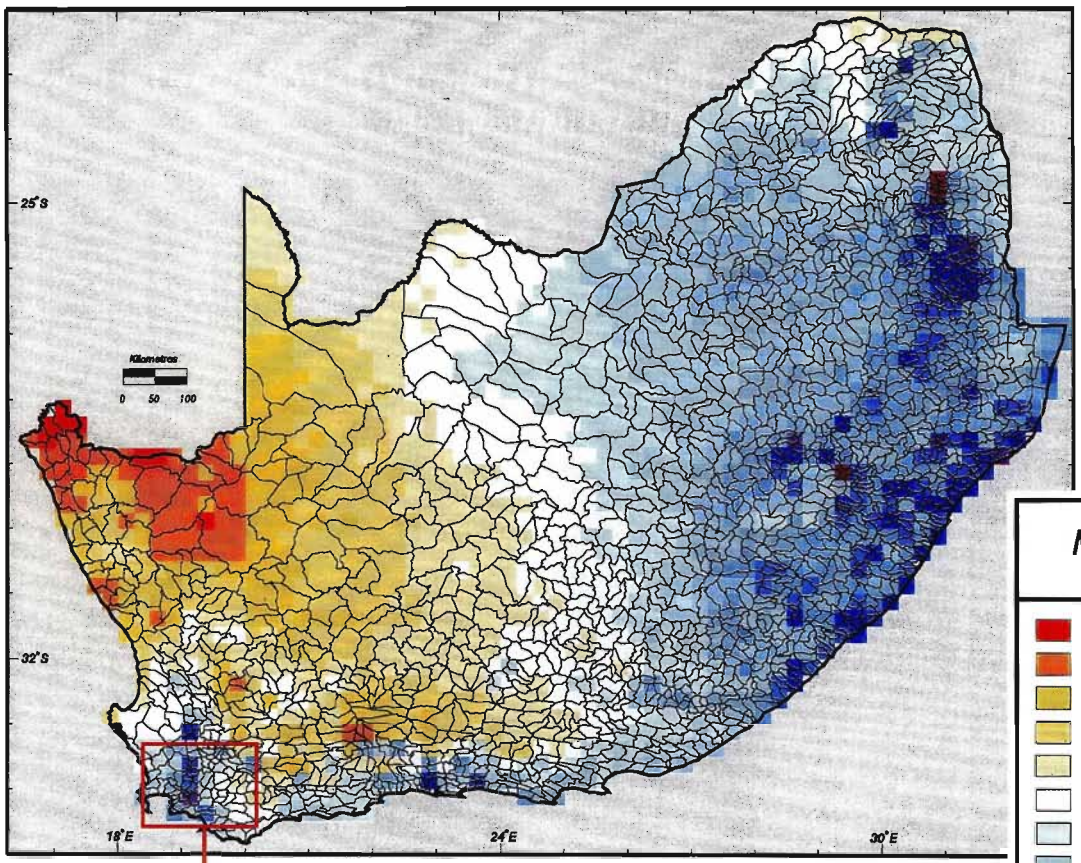


MAP (mm)

- 0 - 50
- 50 - 100
- 100 - 150
- 150 - 200
- 200 - 300
- 300 - 400
- 400 - 500
- 500 - 600
- 600 - 700
- 700 - 800
- 800 - 900
- 900 - 1000
- 1000 - 1200
- 1200 - 1400
- 1400 - 1600
- > 1600

Quaternary Catchments and ¼° Grid Cells

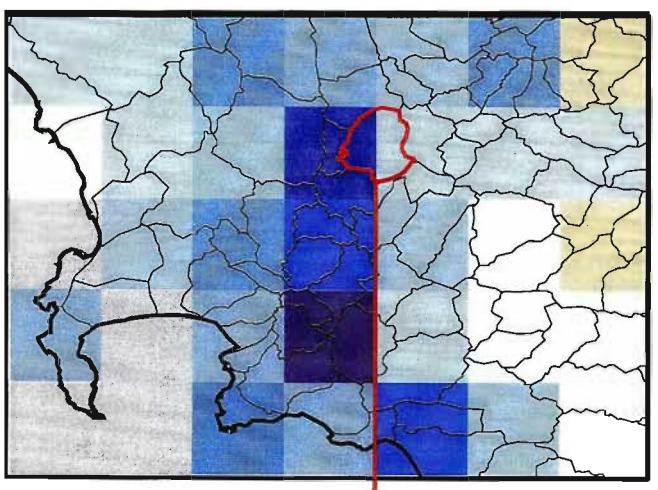

Location Map

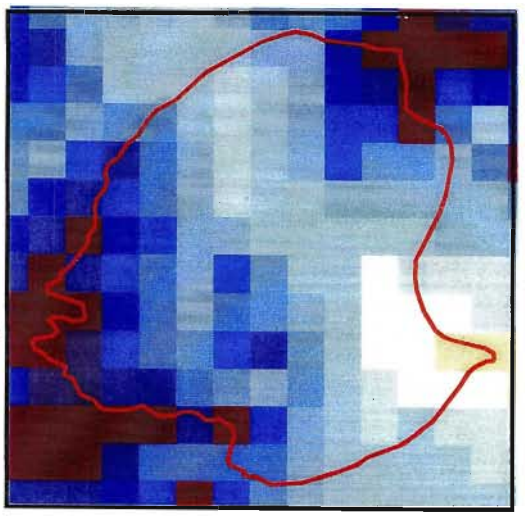

1' x 1' Grid and Quaternary Catchment

iii) The number "1" denotes that the Quaternary Catchment is in Tertiary drainage region number one of Secondary region 5. There are, at maximum, nine Tertiary drainage regions (1 - 9) per Secondary drainage region.

iv) The letter "F" now denotes the Quaternary Catchment F of Tertiary drainage region 1. There are, at maximum, 12 Quaternary Catchments (A to M, with I omitted) per Tertiary drainage region (Midgley *et al.*, 1995).

Figure 5.2 shows the 22 Primary Catchments in the study area and lists the drainage regions that these Primary Catchments fall into (after Midgely *et al.*, 1995).

| Figure 5.2 | The Primary Catchments and drainage regions of southern Africa (after Midgely *et al.*, 1995) |
|---|---|

The School of BEEH's Quaternary Catchment database presently in use was primarily established by Meier (1997), building on structures already established in the erstwhile Department of Agricultural Engineering, UNP (now School of BEEH). The most important input variable required by the *ACRU* model is daily rainfall. A so-called driver rainfall station has been assigned with a continuous and quality checked 44 year daily rainfall record from 1950 - 1993 to each Quaternary Catchment (Meier and Schulze, 1995). As rainfall-runoff models are particularly sensitive to rainfall input, data from over 9000 daily rainfall stations were considered in the process of selecting driver rainfall stations for the respective Quaternary Catchments (Meier, 1997).

Land cover information on the water use coefficient, canopy interception loss per rainday and fraction of roots in the topsoil horizon is required by the *ACRU* model on a month-by-month basis for hydrological modelling purposes. In this climate change study it was either assumed that each Quaternary Catchment was under grassland in fair hydrological condition (i.e. 50 - 75% plant cover) or, alternatively, the land cover attributes were generalised by the temperature driven procedures outlined in Chapter 4, Section 4.4.2.

# PRIMARY CATCHMENTS OF SOUTHERN AFRICA (after SRK & DWAF, 1994)

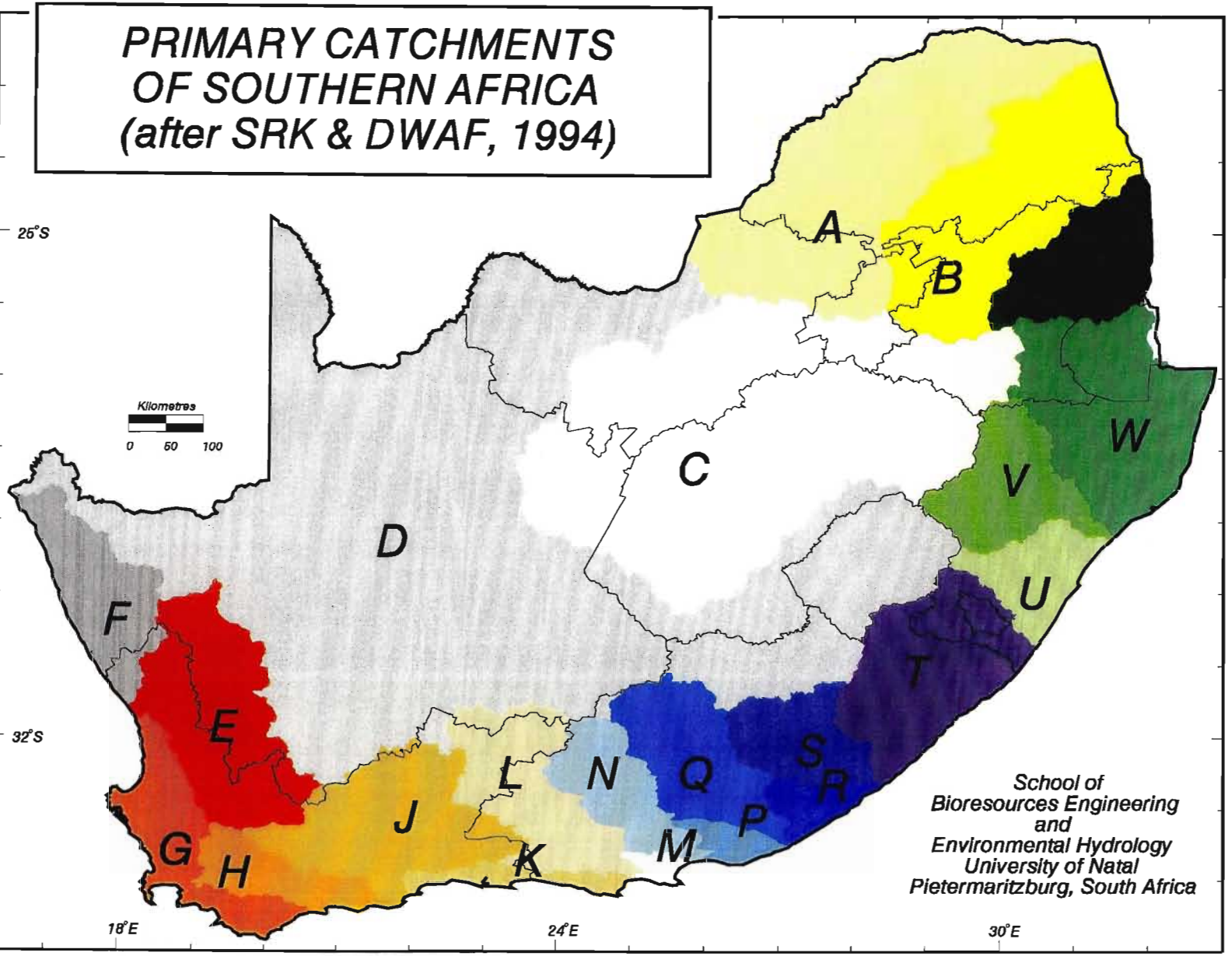


School of
Bioresources Engineering
and
Environmental Hydrology
University of Natal
Pietermaritzburg, South Africa

## Drainage Regions

*Limpopo - Olifants : A, B*

*Vaal : C*

*Orange (excl. Vaal) : D, F*

*Western Cape : E, G, H, J, K, L*

*Eastern Cape : M, N, P, Q, R, S, T*

*Eastern Escarpment : U, V, W, X*

In regard to the soils attributes, *ACRU* requires information for both top- and subsoil, on the thickness (m) of the soil horizon, as well as soil water contents ($m.m^{-1}$) at saturation, drained upper limit (field capacity) and the lower limit of available soil water (i.e. permanent wilting point). These values were derived by Schulze and Lynch (1992) from information on 84 broad homogenous soil zones identified by the Institute of Soil Climate and Water over southern Africa. All the 1946 Quaternary Catchments' databases are linked to the *ACRU* agrohydrological model. The database and modelling system are, in turn, linked with a Geographic Information System (GIS) for mapping and analytical purposes as explained in Chapter 7. The School of BEEH database used in this study as baseline information will hereafter be referred to as the baseline database.

* * * * * * *

In this short chapter the data available in the gridded and Quaternary Catchment databases was reviewed. The methodology used to derive daily baseline maximum and minimum temperatures was also explained. In the following chapter the future climate scenarios used in this study are described as well as the interpolation techniques used to develop regional General Circulation Model scenarios at a spatial scale suitable for use in the *ACRU* model.

# 6. TEMPORAL DATABASES FOR CLIMATE CHANGE IMPACT STUDIES IN SOUTHERN AFRICA

There are numerous ways by which climate change scenarios can be constructed, although the most widely favoured methods use output from large scale atmospheric models, known as General Circulation Models, or GCMs. Outputs from GCMs which have been run for a scenario of effective doubling of atmospheric carbon dioxide concentrations (2X $CO_2$) are, for present-day impact studies, usually converted for application as monthly adjustments to daily, or as seasonal adjustments to monthly baseline climate conditions, assuming no change in climatic variability and sequences of wet / dry days between the baseline and future climates.

In this chapter a brief review of GCMs and a short description of those GCMs whose output was selected for the assessment of climate impacts on agrohydrological responses over southern Africa are presented in Section 6.1 and Section 6.2 respectively. The GCMs have a coarse spatial resolution and some of the scale problems that arise though using GCM output in agrohydrological models are discussed in Section 6.3. This is followed by a description of the techniques used in this study to downscale the GCM output to a finer spatial resolution (Section 6.4). The resultant gridded output of temperature and precipitation provided by the GCMs selected for the climate impact assessments is explained in Section 6.5.

It is important to select GCMs that reflect current climatic conditions realistically. This is assessed by comparing the output from present climate (1X $CO_2$) scenarios from the GCM with observed climate data. In order to assess the ability of GCMs to reflect present climatic conditions three verification studies were performed. The first two verification studies were conducted on the 1X $CO_2$ *monthly* climatic output given by HadCM2 from the Hadley Centre in the United Kingdom which is taken to represent the period 1961 to 1990. The third verification study was carried out on the *daily* output produced by the latest (year 2000) version of the Hadley Centre GCM, *viz.* HadCM3, to assess the ability of this GCM to mimic the rainfall variability in the study area. The results from these verification studies are

summarised in Section 6.6. Finally, in Section 6.7 potential changes in variability of precipitation owing to changes in climate, as simulated by the HadCM3, are presented.

## 6.1 General Circulation Models (GCMs)

General Circulation Models represent the most sophisticated attempt to date to simulate climate on a global scale. General Circulation Models are computerised, three-dimensional, mathematical representations of the earth's atmosphere and are based on fundamental laws governing atmospheric physics (Ringius *et al.*, 1996). They describe physical relationships such as the processes governing clouds, precipitation and radiation. General Circulation Models calculate wind, temperature and moisture distributions in the atmosphere as well as surface climate parameters. Equations for the above variables are solved for a number of vertical layers in the atmosphere and for grid points in finite difference models at the surface of the earth (Rosenzweig and Hillel, 1998).

General Circulation Models were originally designed to simulate atmospheric circulation patterns for specified conditions of external forcing (Sulzman *et al.*, 1995). However, since the 1970s they have been used to provide estimates of the response of certain climatological variables to different levels of greenhouse forcing (Joubert and Tyson, 1996).

The major advantage of using GCMs as the basis for creating climate change scenarios is that they are, according to Benioff *et al.* (1996), the only credible tool to estimate changes in climate due to increased greenhouse gases in a physically consistent manner for a large number of climate variables. Although outputs from GCMs seem unanimous in their projections that an effective doubling of atmospheric $CO_2$ concentrations would lead to an increase in global mean temperature and precipitation, they differ considerably in their predictions at a regional scale (IPCC, 1996a). Output from GCMs should therefore be treated as large-scale sets of possible future climatic conditions and should not be regarded as forecasts (Parry and Carter, 1998). Pielke (2000a) concurs with this view suggesting that as factors such as human induced land use change have not been included in the GCMs

simulations and, thus, the output from the model runs can only be interpreted as sensitivity experiments and not as forecasts or projections of future climate.

General Circulation Models usually provide outputs from a simulation of present, i.e. 'control', conditions and from a 'perturbation' experiment which assumes a climate associated with future greenhouse gas concentrations, usually for an effective doubling of $CO_2$ from pre-Industrial Revolution levels of 280 ppmv to the equivalent of 560 ppmv (Parry and Carter, 1998).

The US Country Studies Program suggests that at least three GCMs should be used for creating 2X $CO_2$ scenarios of climate change. Using output from one GCM only can create the impression of a prediction which has a certainty to it, while using output from only two GCMs could be interpreted as giving only a slight variation among scenarios (Benioff *et al.*, 1996). New and Hulme (1999) add that using several climate change scenarios provides a range of possible outcomes, however, there is no attached probability to the outcomes.

Once the GCMs have been selected, gridded future climate scenarios can be created by combining monthly GCM output with output from the baseline climate period. In the case of temperature the change predicted by the 2X $CO_2$ GCM output minus the 1X $CO_2$ output can be applied. For impact studies involving precipitation, however, the ratio change in precipitation (2X $CO_2$ / 1X $CO_2$) predicted by the GCM, must be multiplied by the baseline precipitation to represent a future scenario.

## 6.2 Selection of GCMs for Impact Studies

At least 10 different GCMs have been developed by atmospheric scientists in various research groups and have been used to simulate the effects of greenhouse gas increases (Rosenzweig and Hillel, 1998). General Circulation Models are used to conduct two types of simulation experiments for estimating future climates, *viz.* equilibrium and transient experiments. Initially most calculations were made in equilibrium mode, implying that the models are subjected to an instantaneous (rather than gradual time dependent) effective doubling of $CO_2$

concentrations relative to a base year and are then run to simulate an equilibrium climate under those hypothetical conditions (Loaiciga *et al.*, 1996). These conditions are usually taken to represent the combined effects of all the greenhouse gases that would be equivalent to the radiative forcing of a doubled concentration of atmospheric $CO_2$. However, the results from these equilibrium GCMs did not contain information about the time of realisation (Hulme and Carter, 1999).

Technological advancements since the early 1990s have allowed for the implementation of time dependent transient GCMs, in which the ambient $CO_2$ level is increased at a fixed rate, for example 1% per annum, compounded until doubling has occurred. Transient experiments are generally performed using high resolution, fully coupled global ocean-atmosphere GCMs (Joubert and Tyson, 1996). These GCMs introduce a time dimension to, and hence rates of, climate change (Hulme and Carter, 1999).

A distinction is made between GCM simulations which include and exclude sulphate forcing. Greenhouse gases cause a warming effect whereas sulphate aerosols can cause a cooling effect by scattering and absorbing solar radiation and altering the properties and lifetimes of clouds (Carter, 1998; Piltz, 1998). Therefore, the effect on climate simulations which include sulphate aerosol forcing, compared to those forced by greenhouse gases only, is to suppress global warming.

There does not currently (end of year 2000) appear to be consensus as to whether to use output from GCM simulations which include or exclude sulphate forcing. It is argued on the one hand that including sulphate forcing in the GCM simulation is a more accurate representation of climatic conditions. However, although sulphate aerosols may partially offset greenhouse warming, these aerosols have a very short lifetime of only several days in the atmosphere compared with that of $CO_2$ , which could remain in the atmosphere for around a hundred years. Therefore, on the other hand, it is argued that it is better to use output from GCM simulations which exclude sulphate aerosols as it is unsure as to whether sulphate aerosols will increase or decrease in future, with a resultant uncertainty as to the net change in climate and atmospheric chemistry (IPCC, 2000a).

It is only in recent years that aerosols have been included in certain GCM simulations of future climate. However, it is believed that the earlier GCM simulations overestimated sulphate aerosol concentrations as there has been a significant decline in these aerosols over recent years through newer and cleaner industrial technologies (Carter, 1998). This finding may indicate a preference to use output from simulations which exclude sulphate forcing in the earlier versions of the GCMs. New and Hulme (1999), for example, chose GCM simulations which did not consider sulphate aerosol feedbacks owing to the uncertainty inherent in aerosol emissions compared to greenhouse gas forcing. The sulphate forcing in the HadCM3 GCM has been reduced by half from that used in the second version (UKMO, 2000). Therefore, results from simulations which are forced using output from GCMs which included sulphate forcing need to be viewed in the light of these recent findings.

The climate impact assessments in this study were carried out using five GCM scenarios, *viz.*

i) UKTR GCM (first version from the Hadley Centre), excluding sulphate forcing;
ii) HadCM2 GCM (second version from the Hadley Centre), excluding sulphate forcing;
iii) HadCM2 GCM, including sulphate forcing;
iv) Climate System Model (1998 version) GCM, excluding sulphate forcing; and
v) Genesis GCM (1998 version), excluding sulphate forcing.

In addition, output from the HadCM3 (third version from the Hadley Centre), excluding sulphate forcing, which only obtained in October 2000, was used in an analysis of potential changes in variability of rainfall emanating from to climate change (Section 6.7).

In the assessment of potential impacts of climate change on agriculture in the study area the UKTR GCM, excluding sulphate forcing, based on its reputation as one of the world's leading models at the time that these impact studies were performed in 1997 (Hulme, 1996). However, the second version of this GCM was obtained in 1999 and therefore an investigation was carried out comparing results obtained using the two versions of this GCM as well as making a comparison of results obtained by including or excluding the cooling effect of sulphates in the GCM simulations on agricultural production. Results of the agricultural assessment are presented in Chapter 8. The assessment of potential changes in water resources in southern Africa was conducted using the *ACRU* model driven by climate scenarios from the two HadCM2 GCM scenarios, the Genesis GCM and the Climate System

Model for three key hydrological responses. However, the majority of the water resources assessment were carried out using the HadCM2, both including and excluding sulphate forcing (Chapters 9 and 10). The four GCMs used in the impact assessments in this study are the HadCM2 GCM excluding sulphate forcing, HadCM2 including sulphate forcing, the Climate System Model (1998) GCM and the Genesis (1998) GCM and these four GCMs will often hereafter be referred to as the selected GCMs. More detail on each of the GCMs mentioned is provided in the following sections.

### 6.2.1 UKTR GCM excluding sulphate forcing

The UKTR GCM was developed by the UK Meteorological Office and the Hadley Centre and is based on the Unified Model and this version was released in 1992 (Murphy and Mitchell, 1995). This GCM includes a coupled dynamical ocean model and runs at a spatial resolution of 2.50° latitude and 3.75° longitude. The UKTR represented the first generation of transient climate change experiments (Gates *et al.*, 1992).

Two simulation periods were provided by Hewitson *et al.* (1998, pers. comm.), *viz.*

i) a control simulation of 75 years representing present climatic conditions (1X $CO_2$); and

ii) a second simulation of 75 years including greenhouse gas forcing, through a 1% per year compounded increase in atmospheric $CO_2$ concentrations (2X $CO_2$).

GCM point output of mean monthly values of precipitation, maximum and minimum temperature for these two simulation periods was provided. This output did not include the effect of sulphate forcing. The simulations from the UKTR GCM, excluding sulphate feedback, will hereafter be termed UKTR-S.

### 6.2.2 HadCM2 GCM excluding sulphate forcing

Simulations using an updated version of the Hadley Centre GCM, HadCM2, were released in 1995. This second version of the GCM runs at the same spatial resolution of 2.50° latitude by 3.75° longitude as the 1992 version (UKTR). Two integrations of HadCM2 were provided

by Hewitson *et al.* (1998, pers. comm.), *viz.* including greenhouse gases, which is referred to as HadCM2GGa1, and an integration which included sulphate forcing which is termed HadCM2GSa1 by the Hadley Centre (Viner, 2000a). The simulations from the HadCM2 GCM which exclude sulphate feedback will, hereafter, be termed HadCM2-S.

Monthly mean values of precipitation, maximum and minimum temperatures for three simulation periods were provided (Hewitson *et al.,* 1998, pers. comm.), *viz.*

i) a control simulation representing present climatic conditions (1X $CO_2$);

ii) a second simulation which includes greenhouse gas forcing through a 1% per year increase in atmospheric $CO_2$ concentrations, with the future 2X $CO_2$ scenarios being estimated to represent the period 2030 - 2059; and

iii) a third simulation period presuming $CO_2$ levels to have reached triple the Pre-Industrial levels, which could occur at approximately 2070 - 2099. However, this last output was not used in this study.

### 6.2.3 HadCM2 GCM including sulphate forcing

Output from the HadCM2 included simulations which incorporated sulphate forcing. As sulphates have a cooling effect on the atmosphere, it is presumed that predicted future temperatures from these simulations will be lower than temperatures from the simulations that exclude sulphate forcing. The simulations were performed using a resolution of 2.50° latitude by 3.75° longitude for the same three monthly variables and simulation periods as described in Section 6.2.2 (Hewitson *et al.,* 1998, pers. comm.). The simulations from the HadCM2 GCM which include sulphate feedback will, hereafter, be termed HadCM2+S.

### 6.2.4 HadCM3 GCM with individual greenhouse gases only included

The third version of the Hadley Centre GCM (HadCM3) was released in the 1998 (Gordon *et al.*, 2000). The output is given at the same spatial resolution of 2.50° latitude by 3.75° longitude as the earlier versions. However, in addition to monthly changes in temperature and precipitation, daily values of climate variables were also provided. The information obtained for this study was daily precipitation, maximum and minimum temperature for

i) a control simulation representing present climatic conditions; and

ii) a second simulation which includes greenhouse gas forcing through a 1% per year increase in atmospheric $CO_2$ concentrations, with

iii) the information from the HadCM3 provided for each month as standerdised 30 day data sets irrespective of the actual number of days in the month (Viner, 2000a).

The future climate scenario is estimated to represent the period 2071 to 2099 as this was the data time frame that was provided. Unlike the output of future climate conditions from the aforementioned GCMs (cf. Sections 6.2.1 to 6.2.3) this period is not taken to represent an effective doubling of $CO_2$ scenario but merely a scenario of future climate conditions.

In HadCM3, the ocean is represented at a much higher resolution than it was in the previous two versions, *viz.* at 1.25° latitude x 1.25° longitude, thus resulting in six ocean grid cells to one atmosphere grid cell (Viner, 2000a). The first two versions required flux corrections to be applied to prevent the simulated climate from drifting as a result of an imbalance between the implied and actual ocean heat transports. The HadCM3 gives a greatly improved representation of ocean currents such as the Gulf Stream. This, together with improvements in the representation of processes in the atmosphere and on land, has allowed the model's climate to remain stable without the need for flux-adjustments (UKMO, 2000).

Output from two climate change scenarios have been generated by the University of East Anglia in the United Kingdom (Viner, 2000a). The first is referred to as HadCM3GGa1 which includes greenhouse gas forcing only. The HadCM3GGa1 was forced using the historical increase in the individual greenhouse gases from 1860 - 1990 and after 1990 was forced using the individual increases in greenhouse gases of 1% per year compounded rise in radiative forcing. The HadCM3 has, very recently, also been run including changes in sulphate aerosols from revised projections of $SO_2$ emissions corresponding to about half of the concentrations estimated by IS92a (IPCC, 1995). This scenario is termed HadCM3AAa1 and includes all anthropogenic gases. Although the direct cooling effect of sulphate aerosols is much reduced, cooling from the indirect effect via changes in cloud brightness is also included (UKMO, 2000).

For this study only output from the HadCM3GGa1 was provided (Viner, 2000a). As the climate change scenarios generated by this GCM were only obtained two months before completion of this study, only limited results could be generated using output from this GCM. This GCM will be hereafter be referred to as HadCM3-S.

### 6.2.5 Climate System Model (1998 version) GCM excluding sulphate forcing

The Climate System Model (CSM) project of the National Center for Atmospheric Research (NCAR) began formally in January 1994 with the long-term goal of building, maintaining, and continually improving a comprehensive model of the climate system, including both physical and biogeochemical aspects (Hewitson *et al.*, 1998, pers. comm.). This transient GCM includes a coupled dynamical ocean model and operates at a resolution of 2.79° latitude by 2.81° longitude in southern Africa. Sulphate forcing is not included and, in addition to monthly means of precipitation, only means of monthly temperatures, and not yet maximum and minimum temperature values separately, were output (Hewitson *et al.*, 1998, pers. comm).

Two simulation periods were provided by Hewitson *et al.* (1998, pers. comm.), *viz.*

i) a control simulation representing present climatic conditions (1X $CO_2$); and

ii) a future simulation (2X $CO_2$), including greenhouse gas forcing through a 1% per year increase in atmospheric $CO_2$ concentrations.

### 6.2.6 Genesis (1998 version) GCM excluding sulphate forcing

The Global Environmental and Ecological Simulation of Interactive Systems (Genesis) model was developed by the Interdisciplinary Climate Systems section of the Climate and Global Dynamics Division at NCAR. Genesis is now, however, also being hosted by the Pennsylvania State University. This quasi-equilibrium GCM uses a coupled mixed layer slab and is run at a spatial resolution of 3.71° latitude by 3.75° longitude. Sulphate forcing was not included and, in addition to monthly means of precipitation, only means of monthly temperature were provided and not maximum and minimum temperatures separately (Thompson and Pollard, 1995; Hewitson *et al.*, 1998, pers. comm.). Genesis was run for two 10 year simulation periods, *viz.*

i) for a simulation using present day levels of atmospheric $CO_2$; and

ii) for a simulation assuming effectively doubled atmospheric $CO_2$ concentrations.

There are spatial mismatches between output from GCMs and input into many impacts simulation models. For example, the hydrological importance of climatic change increases from global to regional to local scales, whereas the accuracy of climate change predictions generally declines from global through regional to local scales (Schulze, 1997a). Scale problems will be expanded upon in the following section.

## 6.3 Problems of Scale in Assessing Climate Change Impacts

General Circulation Models produce estimates of climatic variables for a large, regular network of grid cells across the globe (Parry and Carter, 1998). The most reliable spatial scales for the application of GCMs output are therefore continental to global, where the grid cells are tens or hundreds of kilometres across. However, agrohydrological simulation models used for operational decisions have an ideal linear spatial resolution of 10 km or less (Bass, 1993; Hulme, 1996; Schulze, 1997a). Thus, a major disadvantage is that the spatial scale of the output from the GCMs is not fine enough for impact assessments and as input into agrohydrological models (Benioff *et al.*, 1996; Schulze, 1997a). The usefulness and limitations of GCMs therefore need to be understood (Rosenzweig and Hillel, 1998) when applying their output in climate change impact studies.

The hydrological cycle plays a significant role in many natural processes, both physical and geobiochemical. This cycle is, however, highly sensitive to short term temporal and local scale spatial changes in precipitation. General Circulation Models were not originally designed for regional to local scale climate change impact studies in hydrology. Their direct representations of hydrological quantities such as runoff are generally highly simplified large-scale averages with little spatial reliability or relevance to specific regions (Schulze, 1997a). For the purpose of example the hydrological cycle was selected to illustrate need to use grids finer than those derived from GCMs for meaningful regional impacts assessment.

### 6.3.1 The scale dilemma in applying GCM output in hydrological impact studies

Primary output from GCMs includes precipitation and temperature, while runoff is a secondary output from a GCM. The runoff estimations derived directly from the GCMs are generally still coarse (Loaiciga *et al.*, 1996). Therefore, in simulations of potential changes in runoff and other responses from the hydrological system, the temperature and precipitation output from GCMs is rather input into credible and tested hydrological models, for the hydrological models to then output hydrological responses to climate change.

According to Schulze (1997a), a number of scale paradoxes, or mismatches, exist in regard to the application of GCM-derived climate change scenarios in hydrological impacts studies. These are summarized below:

i) *Spatial and temporal scale mismatches exist between GCMs and catchment models:* GCMs use short time steps, commonly 10 - 30 minutes, cascading through 10 or more atmospheric layers and then provide information for a range of climatic variables (including temperature and precipitation) for either an equilibrium or a transient climate at a grid cells, typically at a spatial resolution of 250 - 300 km. Multi-purpose hydrological impacts models, on the other hand, typically use a time step of one day, commonly cascading rainfall through two or three soil layers to produce output on hydrological variables such as runoff, sediment yield, evaporation and change in soil water storage at spatial units with a resolution ideally around 10 km or smaller (Bass, 1993; Hulme, 1996). The most reliable spatial scales of GCMs, however, are continental to global and their most reliable temporal scale to date remains seasonal. Thus, these resolutions are far too coarse for meaningful hydrological applications without appropriate spatial and temporal downscaling (Benioff *et al.*, 1996; Schulze, 1997a).

ii) *A precipitation response mismatch exists between GCM output and its hydrological importance*: Hydrological responses are highly sensitive of any local changes in precipitation, with small changes resulting in amplified changes in runoff, both positively and negatively. The ability of GCMs to predict spatial and temporal change in precipitation declines from global to regional to local scales. However, the

importance in hydrological responses to change in precipitation increases from global to regional to local scales.

iii) A *paradox exists between changes in means vs the importance of variability*: Most GCMs at present generally give broad indications only of directions and magnitudes of means of predicted changes in monthly temperature or change in precipitation for, say, a 2X $CO_2$ scenario. However, for impact studies hydrological models require detailed information on the variability of change in temperature or change in precipitation, at time scales ranging from intra-daily, inter-daily to inter-seasonal levels, as well as information on persistency of events, i.e. sequences of hot/hot days, cool/hot, hot/cool or cool/cool days in the case of temperature, or of wet/wet, wet/dry, dry/dry or dry/wet days in the case of precipitation. It is these sequences which determine largely the runoff potential prior to a given rainfall event or the need to irrigate, because they will have largely determined antecedent catchment wetness conditions, which are crucial to local runoff responses and irrigation requirements.

iv) *A transient vs invariate climate control paradox exists*: With global warming, climate is assumed to change slowly and near-linearly over a timespan of decades at macro or subcontinental scales. In a catchment hydrological response situation this transient climate change is superimposed over important invariate (i.e. non-changing) controls of regional to meso-scale climate such as the influences of altitude, topographic roughness or continentality on local precipitation patterns (orographic influences) as well as on temperature patterns (e.g. lapse rates, cold air drainage). These invariate controls and their significance to hydrological responses are likely to persist, irrespective of any larger synoptic pattern shifts associated with climate change, and their profound local influences will have to be separated out from more synoptic scale climatic perturbations.

### 6.3.2 The GCM-hydrology upscaling-downscaling cycle

The cycle of spatial upscaling and climatic downscaling (Schulze, 1993; Schulze, 1997a) depicted in Figure 6.1 highlights the dilemma faced when using currently available GCM climate change scenarios in hydrological impact studies.

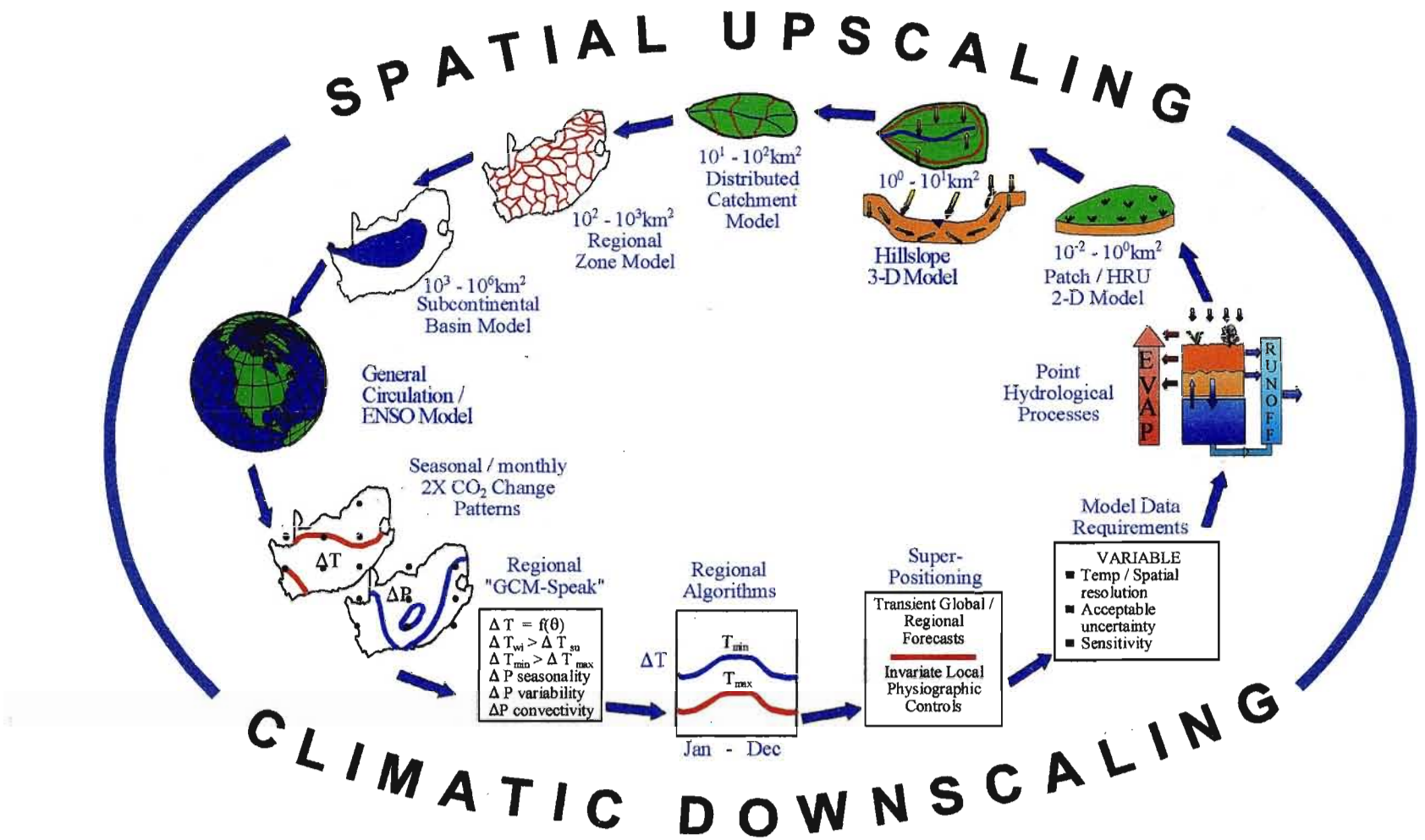


Figure 6.1 The GCM-hydrology climatic downscaling-spatial upscaling cycle (after Schulze, 1993)

Spatial upscaling problems as reviewed by Schulze (1997a) are discussed first:

i) Hydrological processes such as infiltration, soil water redistribution, soil water evaporation or transpiration are usually measured in one dimension (vertically up and down) at one or more individual points in a landscape (right hand side of Figure 6.1).

ii) Already at the hydrological response unit, or patch, scale ($10^{-2}$ - $10^{0}$ $km^2$), where uniform soils and vegetation conditions are assumed, the point processes are no longer spatially representative.

iii) Point processes are even less representative at the hillslope hydrology scale ($10^{0}$ - $10^{1}$ $km^2$), where a second (horizontal) dimension introduces advective processes and a third spatial dimension accounts for uneven solar radiation loadings on slopes (and hence different evaporation demands) as well as lateral soil water flows which are dependent, *inter alia*, on gradient and changes in the soil profile's hydraulic properties down a toposequence from crest through convexo-concave midslopes to valley bottoms.

iv) Operational hydrology models, set up typically at spatial scales from $10^{1}$ - $10^{2}$ $km^2$, attempt to disaggregate, for example, Quaternary Catchments into interlinked subcatchments at this areal scale. While sub-Quaternary level subcatchments of 10 - 100 $km^2$ may be perceived to be ideal operational water planning units, in being relatively homogeneous in terms of broad land uses or rainfall receipt, they are nevertheless, on the whole, hydrologically artificial. This is so because two sets of scalar processes, namely hillslope hydrological processes, which repeat themselves spatially in a landscape, and hydraulic processes, which are additive down the stream channel, but are attenuated over channel distance (or by reservoir construction), are mixed yet are often viewed as a single process in hydrological models.

v) An example of further spatial upscaling would be a country-level delimitation of relatively homogenous zones of (say) $10^{2}$ - $10^{3}$ $km^2$, with zonation in terms of broad climatic and physiographic uniformity. Quaternary Catchments have been delimited at this level in southern Africa. At this level, the detailed point hydrological processes imbedded in physical-conceptual models are no longer truly hydrologically valid and model output should ideally be used for interzonal comparisons only, rather than for absolute hydrological responses. Resolving scale issues at this spatial level then often consists of multiplying answers by area-related exponential functions which have little

real physical meaning. The alternative is to employ flow routing procedures in conjunction with catchment generated runoff.

vi) Subcontinental catchment models, operating at scales of $10^3$ - $10^6$ km$^2$ and larger, display considerable spatial averaging of regional hydrological regimes, usually transcending a number of climatic hydrological regimes, each of which responds to different dominant hydrological processes. It is really only at this scale that boundary conditions imposed by GCMs become applicable and the broad-scale GCM output at monthly time resolution are, in any way, usable as direct input to the models. Even at this scale, however, major discrepancies exist between observed and GCM-predicted regional precipitation and streamflow responses (Schulze, 1997a).

Climatic downscaling problems from GCM output to a level required by hydrological impacts models, as conceptualised by Schulze (1993, 1997a) are summarized below in the context of Figure 6.1:

i) While present generation GCMs predict broad subcontinental seasonal or monthly changes in temperature and changes in precipitation patterns for a climate change scenarios, different GCMs are still giving significantly different magnitudes of expected rainfall change over southern Africa, and even different signs of changes in precipitation (Hulme, 1996; Joubert and Hewitson, 1997; cf. Section 6.5.2). For the sensitive hydrological system such broad spatial prognoses are often meaningless at local level when, for example, observed rainfall in southern Africa between adjacent GCM points some 300 km apart (and even for locations < 50 km apart) may range from 50 to 3000 mm per annum, as is the case in the Western Cape Province (cf. Dent *et al.*, 1989).

ii) Current downscaling research (e.g. Hewitson, 1999) is, however, starting to provide hydrologically useful regional algorithms through regionally nested models.

iii) As one moves to hydrological responses from synoptic (e.g. GCM grid) to regional to more local scale, the superpositioning of transient global-scale climate changes on physiographic, but time invariant, controls of local climate (such as altitude) may be dominated by the latter (cf. Section 6.3.1), and downscaling procedures even beyond those reported by Hewitson (1999) may need to be addressed for hydrological impact studies of climate change.

To facilitate the use of GCM-derived climatic output in simulation models for climate change, the large grid cells output by the GCMs therefore have to be interpolated to a finer spatial scale. There are numerous techniques available for downscaling output from GCMs as discussed in the following section.

## 6.4 Techniques of Downscaling GCM Scenarios

As described in the previous section the hydrological importance of climatic change increases from global to regional to local scale, whereas the accuracy of climate change predictions generally declines from global to local scales (Schulze, 1997a). To allow GCM output of temperature and precipitation to be used in agrohydrological models, several methods have been adopted for developing regional GCM-based scenarios at a smaller grid scale, a procedure known as downscaling (Carter, 1998).

Without downscaling the GCM output for use in hydrological models, sudden changes in modelled climate could occur at the boundaries of GCM grid cells. This is known as the edge-effect. However, downscaling GCM output to a level suitable for input into hydrological models may affect the quality of the information obtained from the hydrological model due to the sensitivity of the hydrological system to changes in climatic variables (Schulze, 1997a).

### 6.4.1 Downscaling options

Schulze (2000a) has summarized the five downscaling methods which Hostetler (1999) has identified. The methods are given below in increasing levels of complexity and cost, but also (hopefully) with an increase in the signal of regional to local accuracy (Hostetler, 1999). Advantages and disadvantages methods are noted below each technique.

i) The first is simply using the *nearest point values*, i.e. effectively applying no downscaling at all

   This method is criticised because of the inherent inaccuracies of the GCMs at the regional level and therefore it is suggested that at least four GCM points should be used in downscaling. Secondly, areas in close proximity to one another, but falling

in two adjacent grid cells may have similar climates, but could be assigned very different climate forcing scenarios with resultant significant impacts on, say, the hydrological simulations in this area (Carter, 1998).

ii) *Appending anomalies*, i.e. changes to observations between (say) 2X $CO_2$ - 1X $CO_2$ scenarios

This method has the advantage of being very simple, with minimal computational requirements, with the method maintaining the inter-correlation structure of variables (diurnal and seasonal cycles), although the last named point may also be seen as a disadvantage.

iii) *Regional bilinear interpolation*, either simple or weighted (e.g. by the inverse of the distance squared from the point estimate)

This is a simple method which is easy to use for gridded application. It eliminates the problems of discontinuities between GCM grid cells. This method has the advantage that regional structure is maintained and can be used to correct temperature for elevation, but with the inherent disadvantages that raw GCM parameters may be inadequate for the intended use in impacts models and that smoothed, large-scale features such as changes in precipitation fields are interpolated (Carter, 1998; Hostetler, 1999).

iv) *Statistical downscaling*, of which four submethods have been used, *viz.* linear and non-linear regression techniques, weather typing (whereby statistical characteristics of precipitation and temperature are associated with present day circulation patterns, on the assumption that GCMs reproduce circulation patterns better that outputing actual climatic values and that downscaling of 2X $CO_2$ scenarios can be achieved in this way), stochastic weather generators (which use monthly climate change output to generate daily climate change scenarios in which variability and not only means are accounted for) and the use of probability distributions

When applied to daily GCM data statistical downscaling can provide daily scenarios for specific regions. Statistical downscaling associates real circulation features with surface fields and is considered a relatively straightforward method. However, these methods do made assumptions about underlying distributions and these assumptions of stationarity under changing climatic conditions in regard to extremes may be questioned, because physical processes are ascribed to relations. Wilby *et al.* (1999)

concluded in a recent study that statistical downscaling of GCM output had various advantages including that it is less data intensive and computational demanding than other methods such as nested or regional climate models. This results in a shorter time to obtain results as well as making multiple scenarios possible (Arnitt, 2000). However, this method assumes, firstly, that the GCMs produce accurate representations of the future and secondly, that the statistical equations used for downscaling remain invariant under changed regional atmospheric and land-surface conditions and this hypothesis cannot be tested (Polcher, 1999) In addition, large amounts of observational data are often required (Carter, 1998; Pielke 2000b, pers. comm.).

v) *Regional meso-scale climate downscaling*, i.e. a numerical technique using GCM outputs as initial and boundary conditions for regional scale models; also termed dynamical downscaling

This method reveals high resolution processes and feedbacks and is amenable to interactive surface processes modelling as well as being applicable to any type of climate change and using time as well as space resolutions. Dynamical downscaling is a method which remains computationally very expensive, time consuming and requires associated GCM simulation, which may introduce another level of model bias or error. Owing to the time constraints this technique in often limited to a single scenario (Arnitt, 2000). The spatial resolution of the GCM is generally inadequate to define the lateral boundary conditions of the regional model (Polcher, 1999; Pielke, 2000b, pers. comm.) and the lateral boundary conditions are the dominant forcing of regional atmospheric models.

For this study downscaling was achieved by a weighted bilinear interpolation technique as described below as it is a relatively simple method and is not computationally intensive.

### 6.4.2 Downscaling GCM grid output to quarter degree latitude / longitude values using interpolation by inverse distance weighting

Text files containing information on the latitude and longitude positions of the GCM points in and around southern Africa were provided for the UKTR-S GCM by Hewitson (1997, pers.

comm.) for use in the agricultural impact assessment component of this study. Similar ASCII files containing the location of the GCM points for the CSM (1998), Genesis (1998) and HadCM2 GCMs were downloaded from an Internet website established by Hewitson *et al.* (1998, pers. comm.).

For each of the aforementioned GCMs, ASCII data files were provided on GCM generated values of temperature and precipitation at each GCM point, for each month of the year, for both present and future (i.e. effective doubling of $CO_2$ concentrations) simulations. Furthermore, differences in parameter values between future and present conditions of the climate parameters were also given. As the precipitation difference values from the GCMs were in mm per day, their values were multiplied by the number of days in the month to create new values of simulated precipitation change in mm per month. From the values contained in the control file and the accompanying ASCII files, points coverages were created using the *GENERATE* command in ARC/INFO.

Similar text files on the latitude and longitudes of the point estimates generated by the HadCM3-S were obtained. Simulated daily precipitation, maximum temperature and minimum temperature was provided by Viner (2000a) for 7008 points across the globe for the time periods 1960 to 1989 and 2070 to 2099, representing present and future climate scenarios respectively. Files of daily values were provided in 10 year time frames for each variable. From these files the daily information corresponding to the GCM points falling in and around southern Africa was extracted for the analyses of potential changes in variability (cf. Section 6.7). This daily information was stored in an ASCII file for each variable for each year for the 64 points falling in and around southern Africa.

In the assessments of potential changes in variability, the daily values of precipitation for a summer and winter month for present climatic conditions (represented by the period 1961 - 1989) and future climatic conditions (2071 - 2099) were used. From these original files various statistics were calculated for present climate and future climatic conditions at each point selected for southern Africa for analysis and mapping.

The spatial resolution of the GCMs is very coarse with the rectangular grid cells ranging from 2.81° to 3.75° longitude and by 2.50° to 3.71° latitude. The information at each point was interpolated to a quarter degree ($^1/_4$°) latitude / longitude resolution, a resolution considered suitable for biodiversity and certain agrohydrological impact studies. For the purposes of this study an inverse distance weighting (IDW) technique available in the ARC/INFO GIS was used for weighted bilinear interpolation of the information at each point to a $^1/_4$° resolution.

The IDW interpolation technique determines grid values using a linearly weighted combination of a set of sample points, with the weighting being a function of the inverse of the distance from control points. This gives the closest point the highest, and the furthest point the lowest, relative weighting. In this study, the inverse of the square of the distance was used, so as to give the closest point an even higher relative representation. Thus, IDW allows for the control of the significance of known input points upon the interpolated values, based on their distance from the output point (ESRI, 1991).

The characteristics of the interpolated surface can be controlled by limiting the number of input points in the IDW process. For the interpolation between GCM points a radius of the closest four surrounding points was used. This will, on one hand, maintain spatial variation in the representation of climate, yet on the other, will prevent points that are too far from the point of interpolation, and which thus have little influence on the local climate, from being included in the process.

Caution must, however, be exercised when implementing this IDW technique. Since IDW is an inverse distance weighted average (ESRI, 1991) the implications of this are that the interpolated values obtained cannot ever be higher than the highest, or lower than the lowest, input values. Hence, by implication, any spatial extremes in climate relative to localised geographical features such as mountain ranges either must have been reflected in the original (i.e. GCM) input points in order to be reflected in the interpolation or, alternatively, have to be considered in a subsequent computational step. Furthermore, the influence of an input point on an interpolated value is distance related. Consequently, IDW may smooth out features such as physiographic discontinuities.

However, the detailed, i.e. one minute by one minute of a degree latitude / longitude (1' x 1' latitude / longitude) grid, baseline values of present climate parameters given, for example, in the *South African Atlas of Agrohydrology and -Climatology* (Schulze, 1997b) already reflect all the major physiographic determinants in their derivation, with both temperature and precipitation cell values having been determined separately for each month by regionalised step-wise multiple regression techniques using, *inter alia*, altitude, distance from the sea, a topographic valley index and distance from mountain barriers as variables. Physiographic influences will, therefore, also reflect these physiographic influences proportionally at local scale (i.e. 1' x 1' latitude / longitude grid) in impact studies of climate change scenarios, on the assumption that on a local scale these invariate characteristics such as altitude or topographic valley index will act similarly on perturbed climates as they do on present ones.

For each of the GCMs which provided monthly climatic information $^1/_4°$ x $^1/_4°$ grids were created for southern Africa for each month of the year by the IDW interpolation technique discussed above, *viz.*

i) present precipitation (mm);
ii) future precipitation (mm);
iii) change in precipitation (future minus present, mm);
iv) ratio change in precipitation (future / present);
v) present temperature (°C);
vi) future temperature (°C); and
vii) change in temperature (future minus present, °C).

Figure 6.2 illustrates the large grid cells obtained by the GCM (Figure 6.2, top) and the resultant interpolation of these grid cells to the finer spatial resolution of the $^1/_4°$ x $^1/_4°$ grid (Figure 6.2, bottom), using the example of present precipitation for January as simulated by HadCM2-S. The large grid cells shown in Figure 6.2 are not the true cells of the GCMs as the true cells were rectangular and, for schematic purposes, the longer side of the rectangle was used to obtain square cells.

| Figure 6.2 | The large grid cells obtained by a GCM and the resultant interpolation of these grid cells to the finer spatial resolution of the quarter degree longitude / latitude grid |
|---|---|

In Figure 6.2 (top) adjacent grid cells can have very large differences in rainfall. For example the purple grid cell which falls over Mpumalanga represents a rainfall in January of greater than 175 mm and the cell that lies north of it represents a rainfall of between 50 and 75 mm in this month. These large differences in rainfall in the vicinity of the edges of these grid cells would have significant impacts on the simulation of hydrology in these regions. Thus, by interpolating the large grid cells to a $^1/_4°$ x $^1/_4°$ resolution these edge effects are reduced.

### 6.4.3 Conversion of quarter degree latitude / longitude grids to one minute by one minute of a degree latitude / longitude grids

The analyses of potential agricultural impacts of climate change (cf. Chapter 8) and the verification study described in Section 6.6 required the GCM output to be of a finer spatial resolution of 1' x 1' latitude / longitude. Thus, it was necessary to disaggregate the $^1/_4°$ x $^1/_4°$ grids of GCM output into 1' x 1' grids.

The climate change values for individual $^1/_4°$ x $^1/_4°$ grid cells were disaggregated to a 1' x 1' resolution grid using the *RESAMPLE* command in ARC/INFO. The grid cells were *RESAMPLED* such that each 1' x 1' grid value would retain the same absolute change as the $^1/_4°$ x $^1/_4°$ grid in the case of temperature and the same fractional change in the case of precipitation, as demonstrated in Figure 6.3.

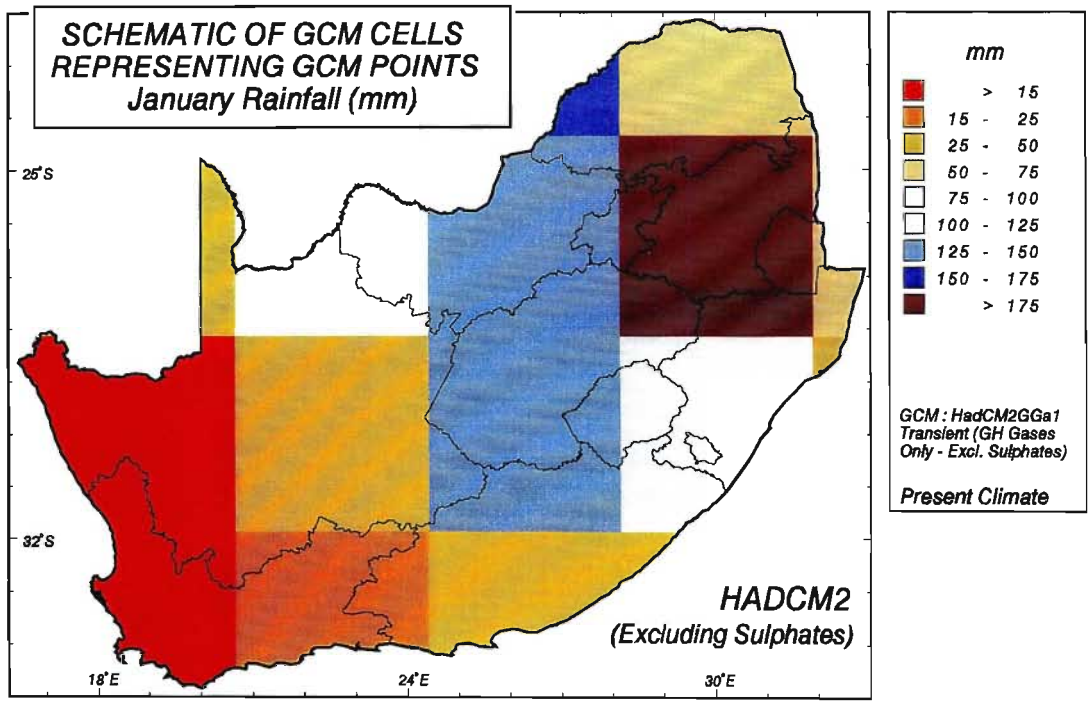
SCHEMATIC OF GCM CELLS
REPRESENTING GCM POINTS
January Rainfall (mm)
25°S
32°S
18°E
24°E
30°E
HADCM2
(Excluding Sulphates)
mm
> 15
15 - 25
25 - 50
50 - 75
75 - 100
100 - 125
125 - 150
150 - 175
> 175
GCM : HadCM2GGa1
Transient (GH Gases
Only - Excl. Sulphates)
Present Climate

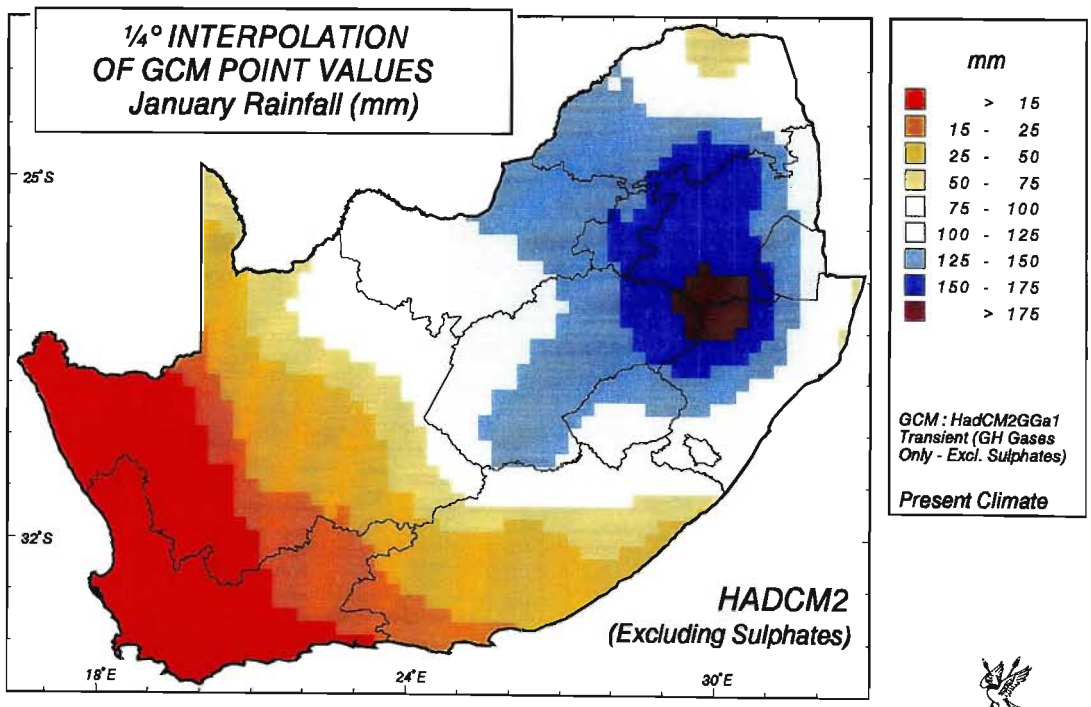
¼° INTERPOLATION
OF GCM POINT VALUES
January Rainfall (mm)
25°S
32°S
18°E
24°E
30°E
HADCM2
(Excluding Sulphates)
mm
> 15
15 - 25
25 - 50
50 - 75
75 - 100
100 - 125
125 - 150
150 - 175
> 175
GCM : HadCM2GGa1
Transient (GH Gases
Only - Excl. Sulphates)
Present Climate

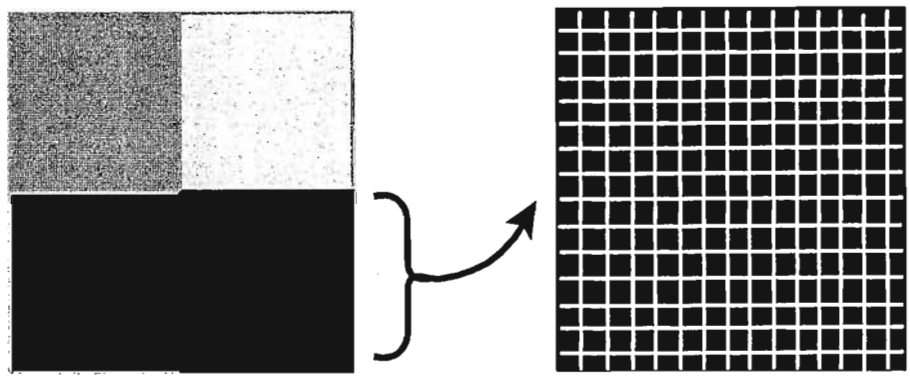

(a) (b)

Figure 6.3 (a) An example of the quarter degree longitude / latitude grid and (b) the resultant *RESAMPLED* one minute by one minute of a degree longitude / latitude grids of one of the quarter degree grid cells

### 6.4.4 Determination of GCM predicted change in precipitation and temperature at Quaternary Catchment level

The hydrological and water resource climate change impact assessments were performed at a Quaternary Catchment scale and thus estimates of changes in temperature and precipitation as simulated by the four GCMs selected for this component of the study were needed for each Quaternary Catchment. When determining the predicted magnitude of change of temperature and precipitation for each Quaternary Catchment, the centroid of each Quaternary Catchment was first determined. The $^1/_4°$ x $^1/_4°$ grid value of either temperature or precipitation closest to the centroid's point location was then the value which was used to estimate the change in climate for that Quaternary Catchment. More detail on the extraction of future climate scenarios from the GCMs for use in *ACRU* is described in Chapter 7, Section 7.4.

## 6.5 Results of Interpolation of GCM Output

To obtain a visual impression of the changes in climate suggested for 2X $CO_2$ climate scenarios by the four GCMs selected for the water resources impact assessment, maps of

monthly, seasonal and mean annual changes in temperature and precipitation were generated. A brief interpretation of these maps is provided in the following sections.

### 6.5.1 Interpolated output of temperature changes downscaled from GCM points

For the HadCM2 GCMs both maximum and minimum temperature output was available on a mean monthly basis, whereas for the CSM and Genesis GCMs only mean temperature output values were available for this research.

#### 6.5.1.1 Changes in maximum and minimum temperature as simulated by the HadCM2 GCMs

Figure 6.4 depicts changes in means of daily maximum temperatures for January (an example of a summer month in southern Africa) and minimum temperatures for July (an example of a winter month) between 2X $CO_2$ simulations by HadCM2 (both excluding and including sulphates) and present climatic conditions (1X $CO_2$).

| | |
|---|---|
| Figure 6.4 | Changes in means of daily maximum temperatures for January and in minimum temperatures for July simulated by HadCM2 for 2X $CO_2$ - 1X $CO_2$ conditions, excluding and including sulphates |

All four maps making up Figure 6.4 show a predicted increase in temperature for all regions within southern Africa, with the highest increase in temperature (over 4 °C) being simulated for maximum temperatures for January by HadCM2-S (Figure 6.4, top left). There appears to be a similarity in pattern in the four maps with the highest predicted increases in temperatures occurring over the north-central parts of the study area. This could be attributed to the influence of continentality because these areas are very distant from the moderating influences of the Indian and Atlantic oceans.

As would be generally expected, the potential changes in maximum and minimum temperatures simulated by HadCM2-S are higher than the simulations where the negative

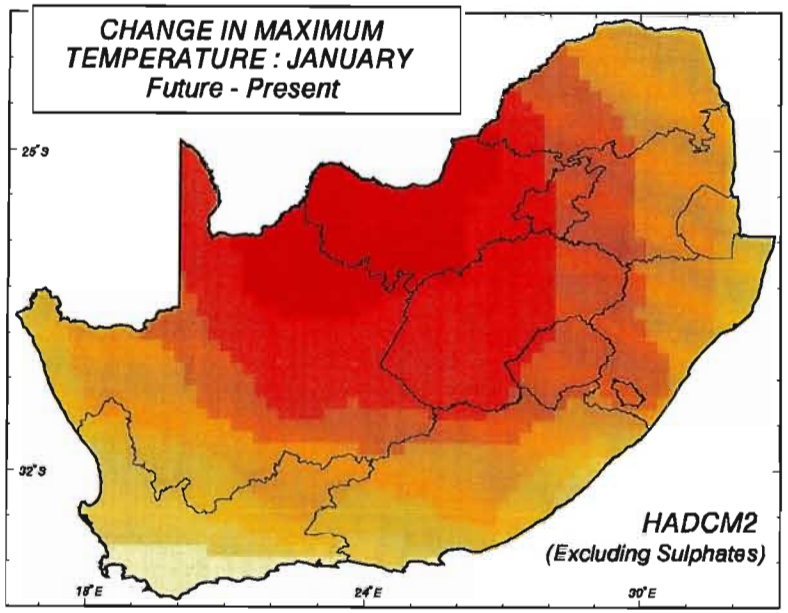


°C
< 1.5
1.5 - 2.0
2.0 - 2.5
2.5 - 3.0
3.0 - 3.5
3.5 - 4.0
> 4.0

GCM : HadCM2GGa1
Transient (GH Gases
Only - Excl. Sulphates)

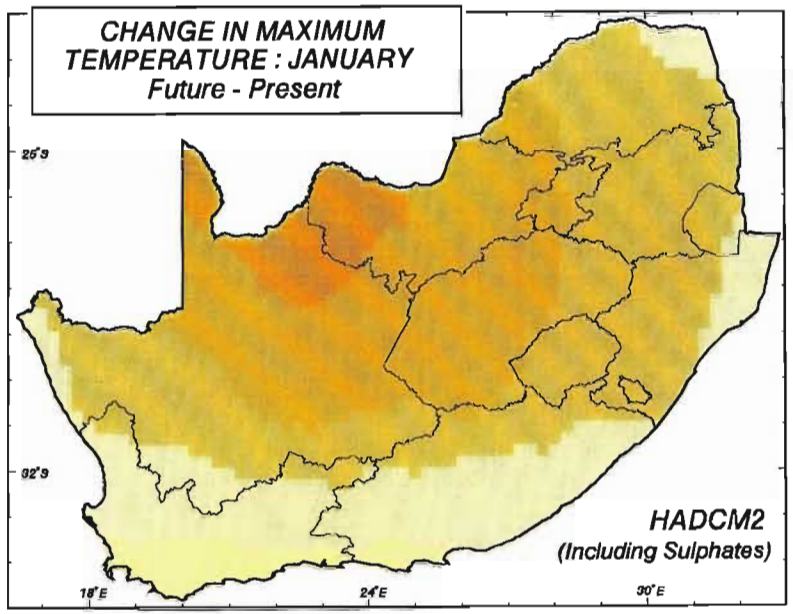


°C
< 1.0
1.0 - 1.5
1.5 - 2.0
2.0 - 2.5
> 2.5

GCM : HadCM2GSa1
Transient (GH Gases
& Sulphate Feedback)

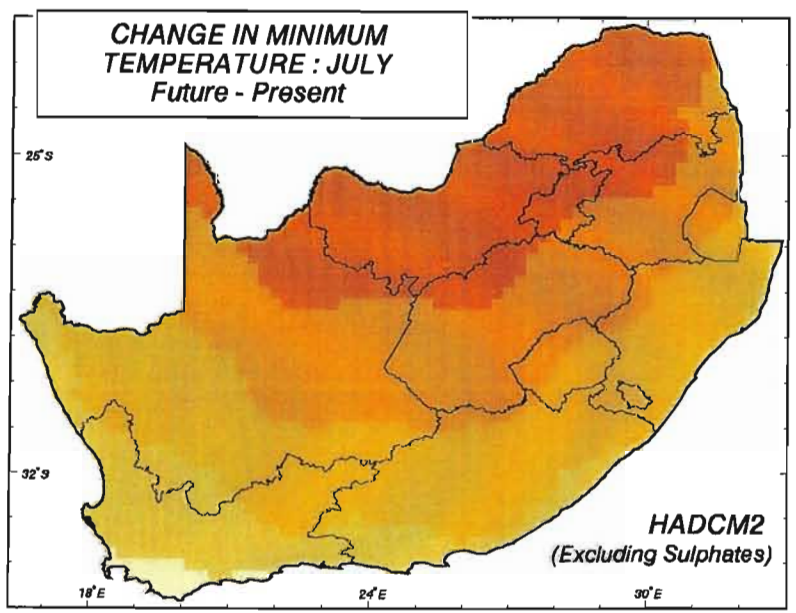


°C
< 1.5
1.5 - 2.0
2.0 - 2.5
2.5 - 3.0
> 3.0

GCM : HadCM2GGa1
Transient (GH Gases
Only - Excl. Sulphates)

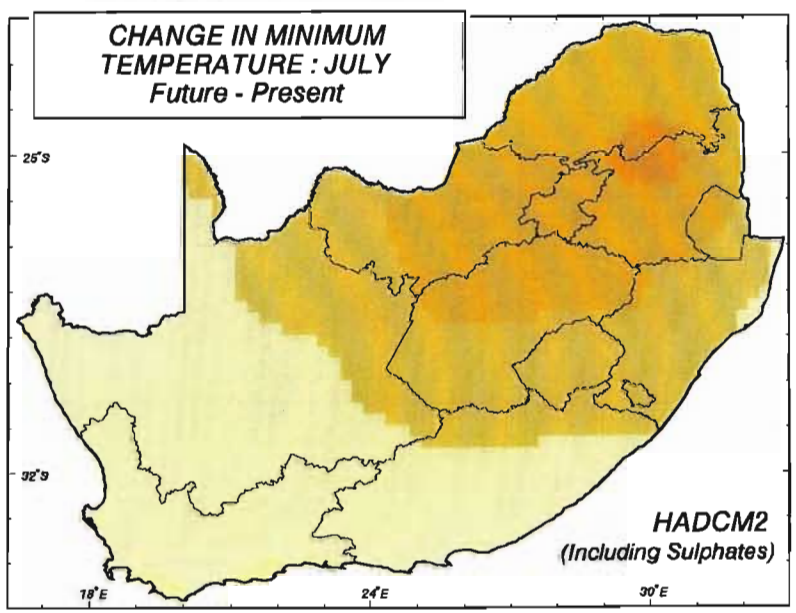


°C
< 1.0
1.0 - 1.5
1.5 - 2.0
2.0 - 2.5
> 2.5

GCM : HadCM2GSa1
Transient (GH Gases
& Sulphate Feedback)

School of
Bioresources Engineering
and
Environmental Hydrology
University of Natal
Pietermaritzburg
South Africa

(cooling) feedback of atmospheric sulphates is included. The simulations excluding sulphates predicted temperature increases between 1 °C and 4.5 °C for January and July whereas the simulations including sulphates predicted increases only between 0.5 °C and 2.5 °C change. The overall predicted increases in maximum temperatures are higher than the predicted increases in minimum temperatures for both simulations, although this is particularly noticeable in the HadCM2 GCM simulation in which sulphate forcing was excluded. This trend is opposite to what would have been anticipated (IPCC, 1990).

#### 6.5.1.2 Changes in mean temperature as simulated by the CSM (1998) and Genesis (1998) GCMs

Only changes in means of monthly temperatures were provided from CSM (1998) and Genesis (1998), compared with maxima and minima being given separately in the case of the two HadCM2 GCMs. The increases in mean temperatures for January and July for these two GCMs are shown for a 2X $CO_2$ - 1X $CO_2$ climate change scenario in Figure 6.5.

Figure 6.5 Changes in mean temperatures for January and July simulated by CSM (1998) and Genesis (1998) for 2X $CO_2$ - 1X $CO_2$ conditions

When comparing the simulated changes in temperature by Genesis (1998) and CSM (1998), the simulated increases in mean temperatures are, on average, higher by Genesis (1998). However, the range of temperature change is greater by CSM (1998). The spatial patterns displayed by HadCM2 in Figure 6.4 are not as distinct as those illustrated for Genesis (1998) and CSM (1998) in Figure 6.5. On average highest predicted increases in temperature are between 2.5 and 3.0 °C.

### 6.5.2 Interpolated output of precipitation changes downscaled from GCM points

The summer (October - March), winter (April - September) and annual values for precipitation for 2X $CO_2$ and 1X $CO_2$ climate scenarios were calculated for each set of GCM output

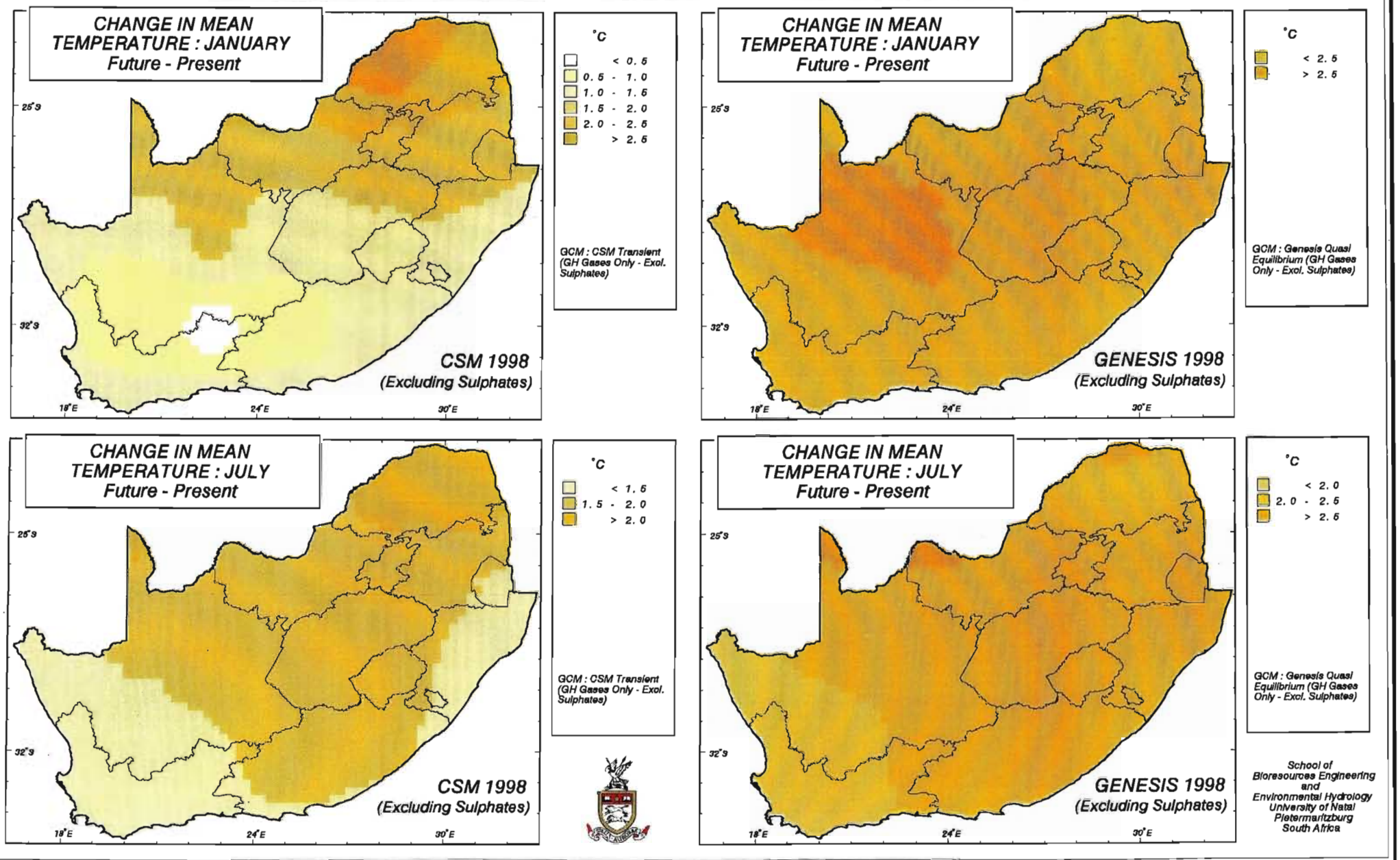
CHANGE IN MEAN TEMPERATURE : JANUARY
Future - Present
25°S
32°S
18°E
24°E
30°E
CSM 1998
(Excluding Sulphates)
°C
< 0.5
0.5 - 1.0
1.0 - 1.5
1.5 - 2.0
2.0 - 2.5
> 2.5
GCM : CSM Transient (GH Gases Only - Excl. Sulphates)
CHANGE IN MEAN TEMPERATURE : JANUARY
Future - Present
GENESIS 1998
(Excluding Sulphates)
°C
< 2.5
> 2.5
GCM : Genesis Quasi Equilibrium (GH Gases Only - Excl. Sulphates)
CHANGE IN MEAN TEMPERATURE : JULY
Future - Present
CSM 1998
(Excluding Sulphates)
°C
< 1.5
1.5 - 2.0
> 2.0
GCM : CSM Transient (GH Gases Only - Excl. Sulphates)
CHANGE IN MEAN TEMPERATURE : JULY
Future - Present
GENESIS 1998
(Excluding Sulphates)
°C
< 2.0
2.0 - 2.5
> 2.5
GCM : Genesis Quasi Equilibrium (GH Gases Only - Excl. Sulphates)
School of Bioresources Engineering and Environmental Hydrology
University of Natal
Pietermaritzburg
South Africa

provided and mapped, in order to compare the relative increases and decreases across southern Africa as predicted by the four selected GCMs.

#### 6.5.2.1 Relative changes in accumulated summer rainfall as simulated by the four selected GCMs

Those regions of the study area which experience their rainy season in summer will be more sensitive to changes in summer rainfall than those regions where the rain falls mostly at other times of year. The rainfall seasonality map for the study area for present climatic conditions (Figure 6.6) shows the dominant seasons in which rain falls within the study area. For example, the north-eastern part of the study area experiences most of its rainfall in summer and therefore this area will be more sensitive to changes in summer rainfall.

| Figure 6.6 | Rainfall seasonality for present climatic conditions (Schulze, 1997b) |
|---|---|

The summer rainfall changes at each $^1/_4°$ grid cell were calculated by adding the rainfall values for October to March for a 2X $CO_2$ climate scenario and dividing that by the sum of the October to March grid values for a 1X $CO_2$ scenario to obtain relative changes. As depicted in Figure 6.7, all four GCMs predict both relative increases and decreases in precipitation in the summer months in the future. However, both HadCM2 GCMs predict that most of the study area is likely to experience decreases, while Genesis (1998) predicts that most parts of southern Africa could expect increases in rainfall in the future for the summer months.

| Figure 6.7 | Relative changes in accumulated summer rainfall, as simulated by four selected GCMs |
|---|---|

HadCM2-S simulates a reduction in the summer months' rainfall in the Eastern Cape and the tip of the western part of southern Africa in excess of 25%. However, from the same GCM most of the north-eastern regions could expect a reduction of only 5% in summer rainfall.

# RAINFALL SEASONALITY

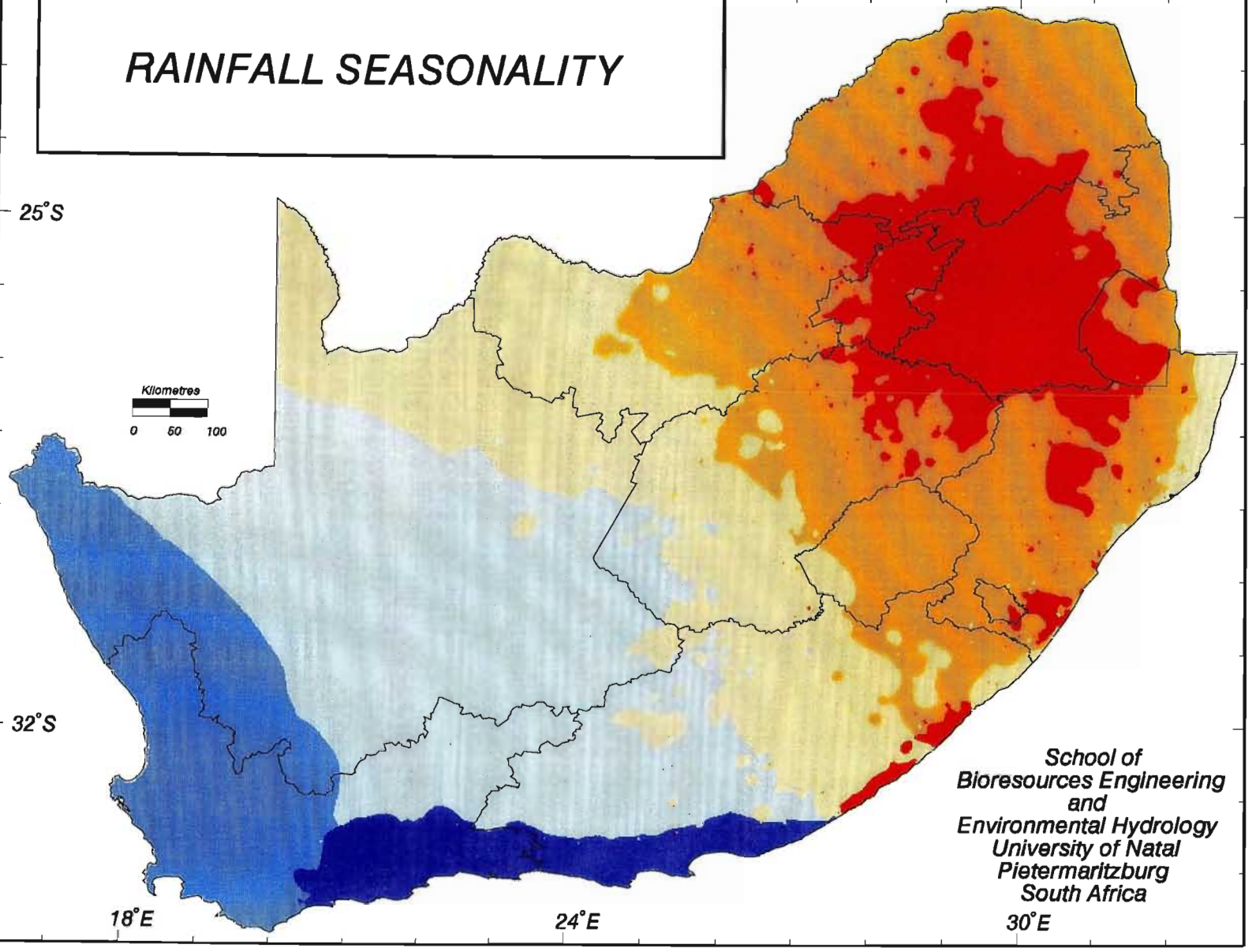


ALL YEAR

WINTER

EARLY SUMMER
- December

MID SUMMER
- January

LATE SUMMER
- February

VERY LATE SUMMER
- March to May

School of
Bioresources Engineering
and
Environmental Hydrology
University of Natal
Pietermaritzburg
South Africa

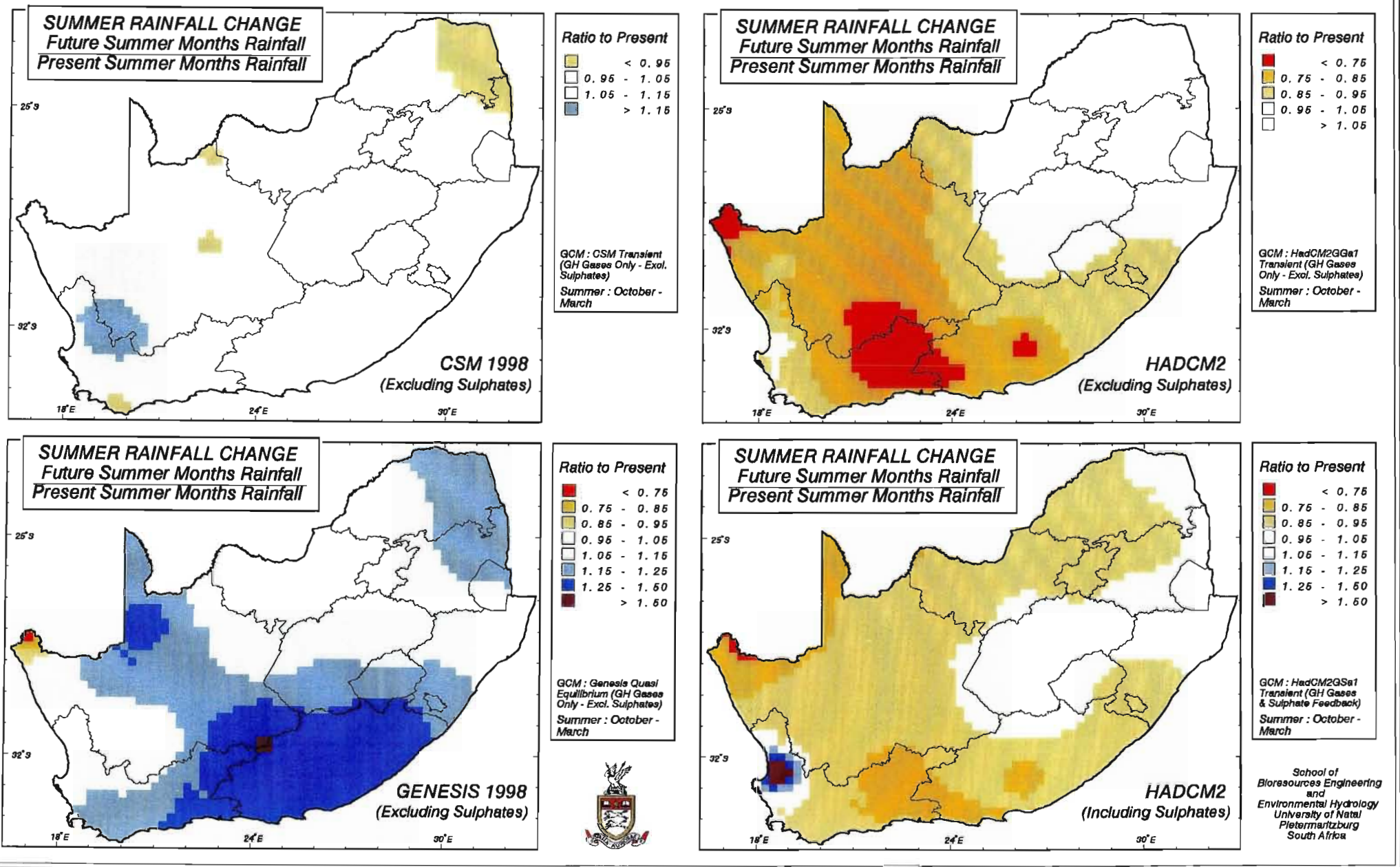
SUMMER RAINFALL CHANGE
Future Summer Months Rainfall
Present Summer Months Rainfall
25°S
32°S
18°E
24°E
30°E
CSM 1998
(Excluding Sulphates)
Ratio to Present
< 0.95
0.95 - 1.05
1.05 - 1.15
> 1.15
GCM : CSM Transient (GH Gases Only - Excl. Sulphates)
Summer : October - March
SUMMER RAINFALL CHANGE
Future Summer Months Rainfall
Present Summer Months Rainfall
HADCM2
(Excluding Sulphates)
Ratio to Present
< 0.75
0.75 - 0.85
0.85 - 0.95
0.95 - 1.05
> 1.05
GCM : HadCM2GGa1 Transient (GH Gases Only - Excl. Sulphates)
Summer : October - March
SUMMER RAINFALL CHANGE
Future Summer Months Rainfall
Present Summer Months Rainfall
GENESIS 1998
(Excluding Sulphates)
Ratio to Present
< 0.75
0.75 - 0.85
0.85 - 0.95
0.95 - 1.05
1.05 - 1.15
1.15 - 1.25
1.25 - 1.50
> 1.50
GCM : Genesis Quasi Equilibrium (GH Gases Only - Excl. Sulphates)
Summer : October - March
SUMMER RAINFALL CHANGE
Future Summer Months Rainfall
Present Summer Months Rainfall
HADCM2
(Including Sulphates)
Ratio to Present
< 0.75
0.75 - 0.85
0.85 - 0.95
0.95 - 1.05
1.05 - 1.15
1.15 - 1.25
1.25 - 1.50
> 1.50
GCM : HadCM2GSa1 Transient (GH Gases & Sulphate Feedback)
Summer : October - March
School of
Bioresources Engineering
and
Environmental Hydrology
University of Natal
Pietermaritzburg
South Africa

Increases of up to 50% in summer precipitation are predicted by HadCM2+S in northern parts of the Western Cape coastline. As this is an arid area which experiences predominantly winter rainfall, this predicted increase is unlikely to result in any significant changes in, for example, the water resources of this region. This GCM estimates that most areas in the study region could expect a change in summer months' precipitation ranging from a 15% decrease to a 5% increase.

CSM (1998) simulates most regions in southern Africa to expect summer rainfall changes to range from a 10% increase to a 10% decrease, whereas, Genesis (1998) simulates increases in summer rainfall over almost the whole study area. The exception is a small region in the western part of the study area where a 25% decrease in summer rainfall is predicted by Genesis (1998). Significant increases (25 to 50%) in the summer months rainfall in the Eastern Cape are simulated by this GCM.

#### 6.5.2.2 Relative changes in accumulated winter rainfall as simulated by the four selected GCMs

The winter rainfall change at each $^1/_4°$ grid cell was calculated by adding the rainfall values for April to September for a 2X $CO_2$ climate scenario and dividing that by the sum of the April to September grid values for a 1X $CO_2$ scenario. Figure 6.8 shows the changes in precipitation predicted by the four selected GCMs for the winter months. The increases and decreases in winter rainfall simulated by the four GCMs are quite different to those of the summer rainfall changes.

| | |
|---|---|
| Figure 6.8 | Relative changes in accumulated winter rainfall as simulated by four selected GCMs |

CSM (1998) simulates large decreases in winter rainfall (to < 75% of present) over the northern parts of the study area. Only the south-western and south-eastern regions are predicted to receive small increases in winter rainfall according to CSM (1998).

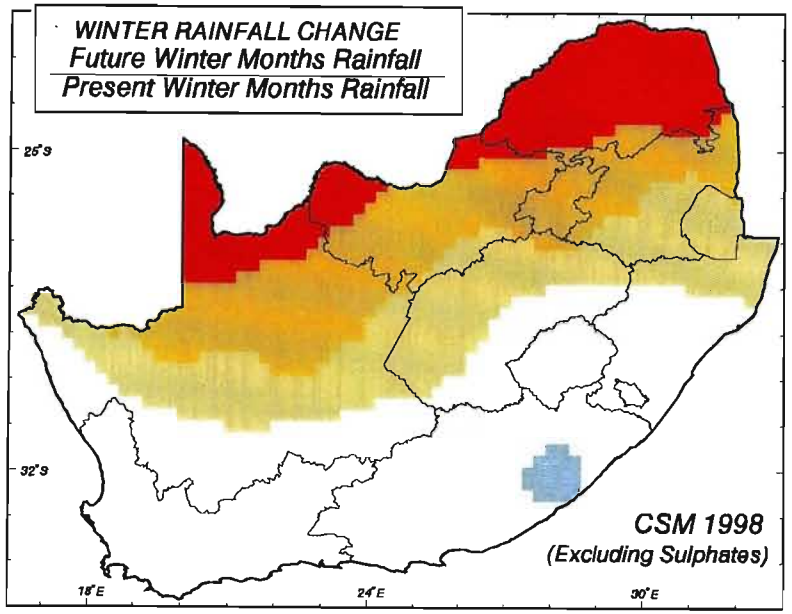


Ratio to Present

< 0.75
0.75 - 0.85
0.85 - 0.95
0.95 - 1.05
1.05 - 1.15
> 1.15

GCM : CSM Transient (GH Gases Only - Excl. Sulphates)
Winter : April - September

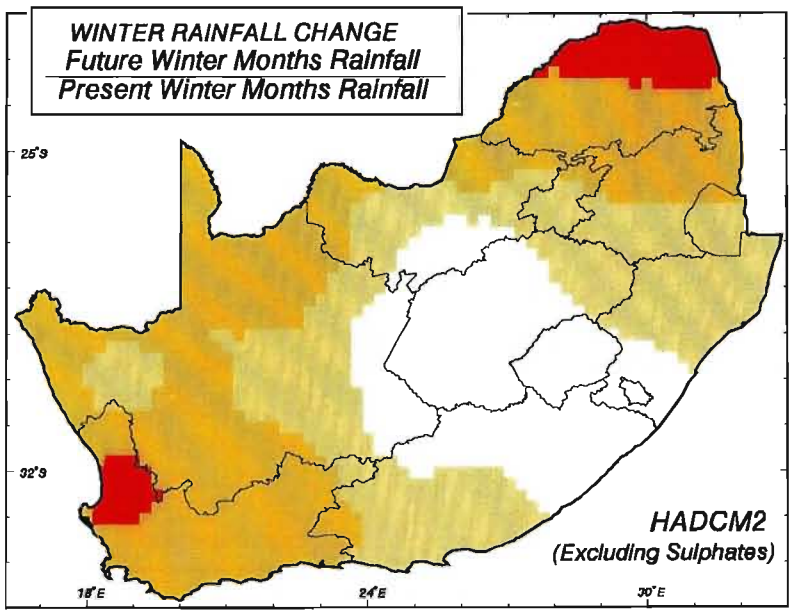


Ratio to Present

< 0.75
0.75 - 0.85
0.85 - 0.95
0.95 - 1.05
> 1.05

GCM : HadCM2GGa1 Transient (GH Gases Only - Excl. Sulphates)
Winter : April - September

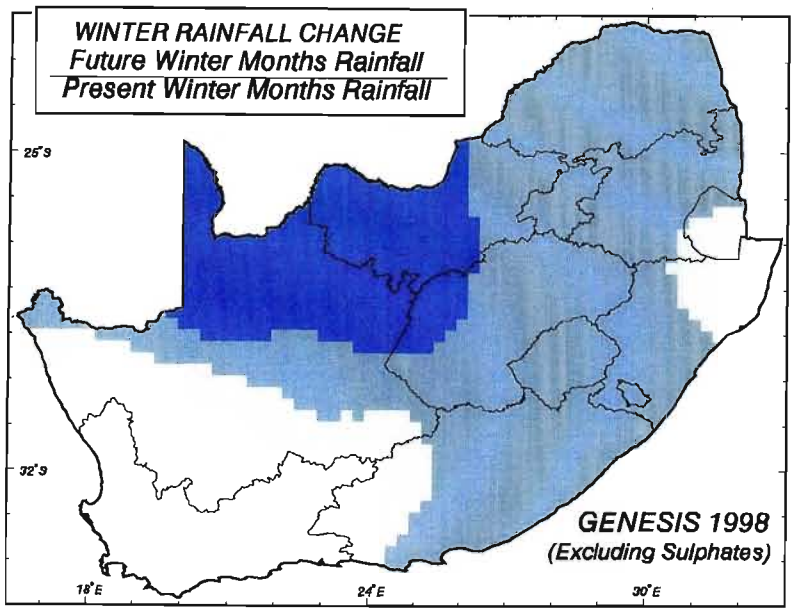


Ratio to Present

< 1.05
1.05 - 1.15
1.15 - 1.25
> 1.25

GCM : Genesis Quasi Equilibrium (GH Gases Only - Excl. Sulphates)
Winter : April - September

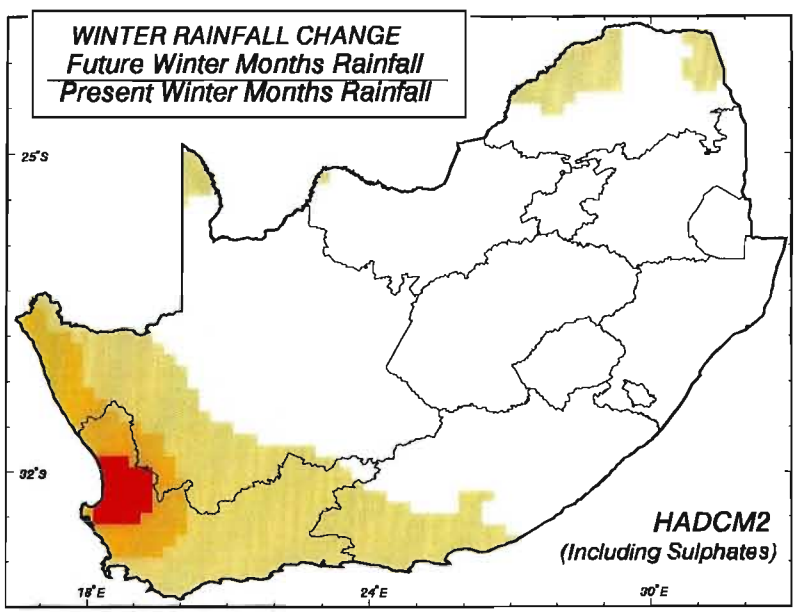


Ratio to Present

< 0.75
0.75 - 0.85
0.85 - 0.95
0.95 - 1.05
> 1.05

GCM : HadCM2GSa1 Transient (GH Gases & Sulphate Feedback)
Winter : April - September

School of
Bioresources Engineering
and
Environmental Hydrology
University of Natal
Pietermaritzburg
South Africa

An overall decrease in winter season rainfall is also simulated by HadCM2-S. This GCM predicts that the central region, however, could experience a slight increase in winter rainfall of approximately 5%. The HadCM2+S shows similar patterns to those excluding sulphates, although the scale of change is much less. Most of the study area is simulated to have very little change (5% increase or decrease) in winter rainfall, except for the south- western areas which could experience a decrease of over 25% in winter season rainfall. Such a decrease in winter rainfall is considered hydrological and agriculturally highly significant as this area receives most of its rainfall in the winter season.

Genesis (1998) simulates increases in winter rainfall throughout the study area. This is quite different to the results from the other three GCMs. The greatest increases, of over 25%, are predicted for the northern-central regions.

#### 6.5.2.3 Relative changes in annual rainfall as simulated by the four selected GCMs

The annual rainfall changes at each $^1/_4°$ grid cell were calculated by adding the rainfall values for January to December for a 2X $CO_2$ climate scenario and dividing that by the sum of the January to December grid values for a 1X $CO_2$ scenario (Figure 6.9).

| Figure 6.9 | Relative changes in annual rainfall as simulated by four selected GCMs |
|---|---|

Both HadCM2 GCM simulations predict decreases in annual rainfall resulting from climate change. Future annual rainfall could be less than 85% of present annual rainfall in certain western parts of the study area. The central regions could expect a relatively small decrease in annual precipitation according to the two HadCM2 GCMs.

Genesis (1998) predicts a relative increase in annual precipitation for the entire study area, with the greatest predicted increases, of over 25%, in the north-central and eastern areas of the study region. CSM (1998), on the other hand, predicts increases of over 5% in the southern regions and decreases of over 15% in the northern regions of the study area.

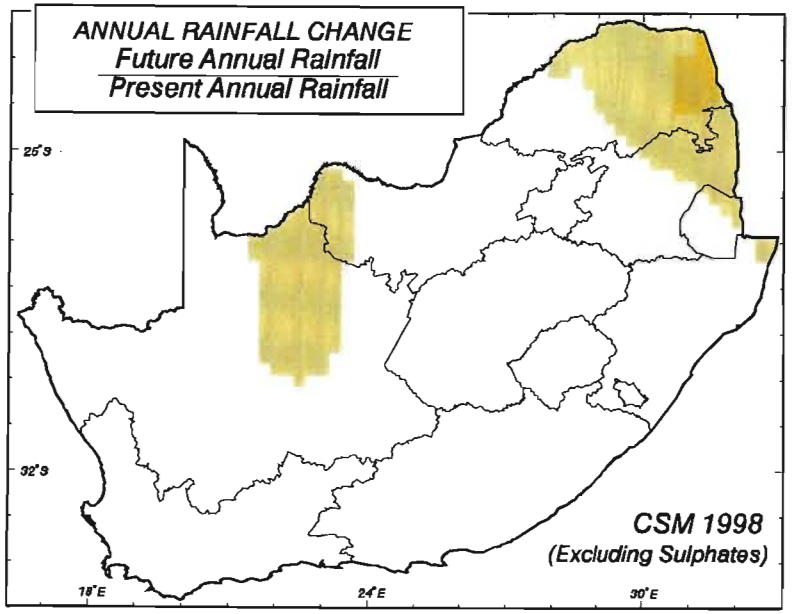


Ratio to Present

< 0.85
0.85 - 0.95
0.95 - 1.05
> 1.05

GCM : CSM Transient (GH Gases Only - Excl. Sulphates)

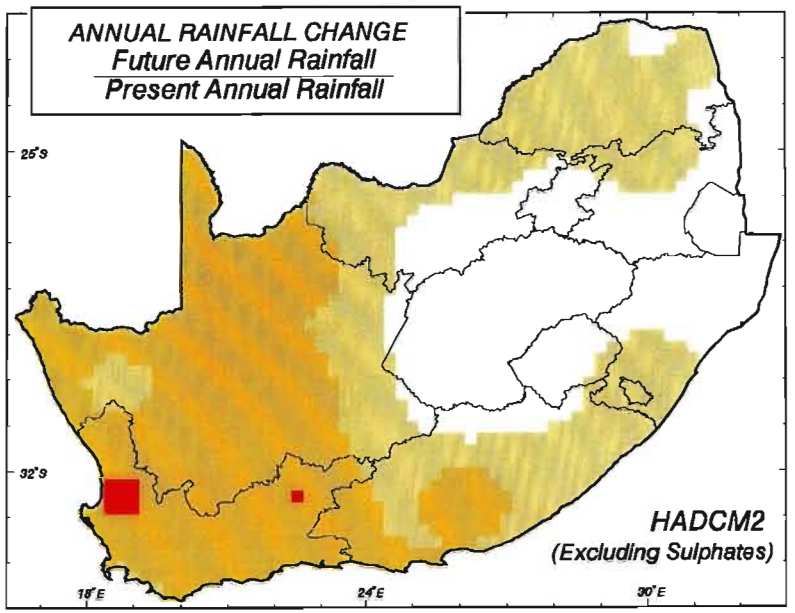


Ratio to Present

< 0.75
0.75 - 0.85
0.85 - 0.95
> 0.95

GCM : HadCM2GGa1 Transient (GH Gases Only - Excl. Sulphates)

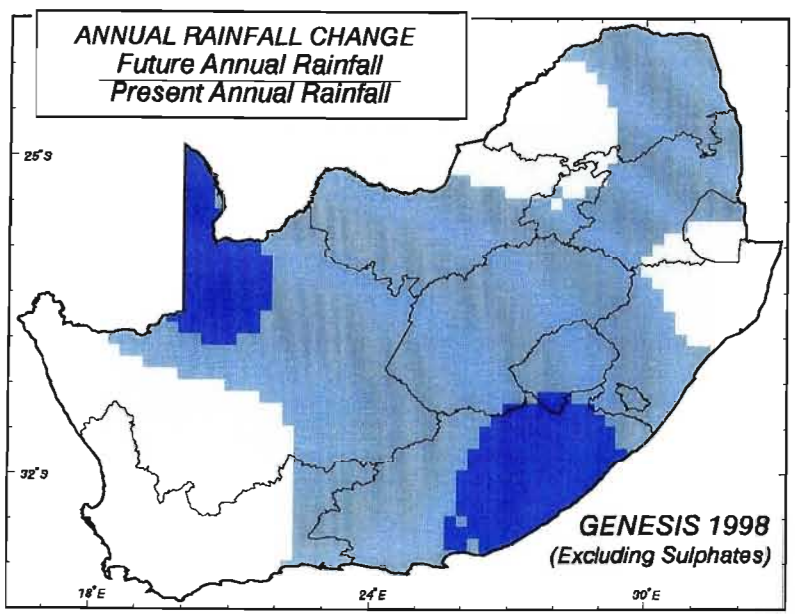


Ratio to Present

< 1.05
1.05 - 1.15
1.15 - 1.25
> 1.25

GCM : Genesis Quasi Equilibrium (GH Gases Only - Excl. Sulphates)

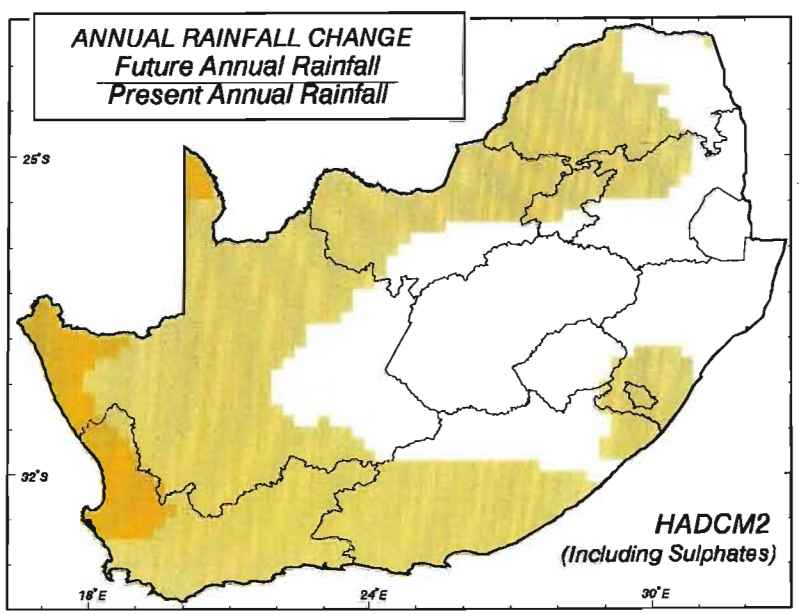


Ratio to Present

< 0.85
0.85 - 0.95
> 0.95

GCM : HadCM2GSa1 Transient (GH Gases & Sulphate Feedback)

School of
Bioresources Engineering
and
Environmental Hydrology
University of Natal
Pietermaritzburg
South Africa

From these maps of temperature and rainfall changes simulated by the four selected GCMs it is evident that there is a large degree of uncertainty as to the magnitude and direction of changes in climate. This will expanded upon in Chapter 11. The selected GCMs all simulate increases in temperatures, with the increases in maximum temperatures in summer (January) on average higher than the increases in minimum temperature in winter (July).

The changes in precipitation resulting from climate change appear less certain and this is shown in the differences in summer, winter and annual precipitation changes simulated by the four selected GCMs. Generally Genesis (1998) predicts large increases in precipitation for most of the study area compared to present climatic conditions. HadCM2-S, on the other hand, simulates decreases in precipitation in a future climate for most regions in the study area. When sulphate forcing is included in HadCM2 simulations of future climatic conditions, the decreases in precipitation for the study region are not as large. CSM (1998) simulates significant decreases in winter rainfall in the northern half of the study area, however, the range of summer rainfall change only varies between a 10% decrease and 20% increase in rainfall.

## 6.6 Verification of GCM Output

Although observed data for future scenarios obviously do not exist, verification studies of GCMs can be undertaken to assess their performance of present-day climate representation (i.e. 1X $CO_2$) output against observed historical records (Carter, 1998). In order to assess how well the GCMs selected might perform for scenarios of climate change, two types of comparison, or history matching studies, were performed. The first verification study was an analysis of the residuals between the gridded monthly output of temperature and precipitation from HadCM2-S for 1X $CO_2$ scenarios (representing present conditions) versus equivalent values obtained from the baseline 1' x 1' gridded database for observed climate (cf. Chapter 5, Section 5.1) for the study area as described in Section 6.6.1.

The second verification study involved a comparison of GCM output for four sample points across southern Africa which were chosen to represent four different climatic zones. The

monthly output of precipitation as well as maximum and minimum temperature simulated by HadCM2-S was compared to the monthly output from the baseline database for present climatic conditions. Output from HadCM3+S was not obtained in this study and, therefore, only the output from HadCM3-S could be assessed. In addition, statistics (e.g. mean and coefficient of variation) computed from the daily precipitation values generated for present climatic conditions by HadCM3-S were compared to those calculated from observed daily precipitation records representing the four selected sample points (Section 6.6.2).

### 6.6.1 Residuals between GCM output for present climatic conditions and observed climate

In a residual study the modelled and observed values are projected to the same grid resolution and statistical methods are then employed to compare, for example, monthly mean values and / or climatic patterns. For the residual verification analyses employed for this study the 1' x 1' grid values (cf. Section 6.4.3) of monthly precipitation and temperature output from HadCM2-S for a 1X $CO_2$ scenario were subtracted from the corresponding averaged gridded values derived from the baseline 1' x 1' gridded databases (cf. Chapter 5, Section 5.1) as described in Dent *et al.* (1989) and Schulze (1997b). The residuals of the grid values show the magnitude of errors which may be incurred as a result of the coarse resolution of, in this example the HadCM2-S output. Examples are presented for monthly means of daily maximum temperature for January, minimum temperature for July and precipitation totals for January and July.

#### 6.6.1.1 Residuals of maximum temperature for January and minimum temperature for July

The monthly means of maximum temperatures for January and of minimum temperatures for July from the 1X $CO_2$ HadCM2-S GCM scenario were subtracted from the corresponding gridded values from the baseline gridded database. The regions of greatest error are shown as the red and purple areas in Figure 6.10, where the red areas represent areas where the observed temperatures are more than 6 °C higher than those simulated by the GCM for that

region and the purple areas are those regions where the observed temperatures are greater than 6 °C lower than those from the GCM.

| Figure 6.10 | Residual grids of observed present temperature minus present (1X $CO_2$) temperature simulated by HadCM2-S for monthly means of daily maximum temperatures in January (top) and minimum temperatures in July (bottom) |
|---|---|

From the residual grid of maximum temperature in January (Figure 6.10, top) it appears that the GCM is generally overestimating maximum temperatures in summer, with the greatest errors being incurred in the central regions of the study area. The exception is Lesotho, where the GCM estimates are lower than the observed baseline monthly means of daily maximum temperatures. There are areas of both underestimation and overestimation by HadCM2-S for minimum temperatures in July (Figure 6.10, bottom), although the magnitude of the underestimation is higher (> than 6 °C in Lesotho) than that of the overestimation (> 2 °C).

#### 6.6.1.2 Residuals of precipitation totals for January and July

The errors incurred in the precipitation values are shown in the residual map for January's mean precipitation (Figure 6.11, top) and that for July (Figure 6.11, bottom). The red areas indicate areas where the observed precipitation amounts are over 60 mm higher that those from the GCM simulations and the purple areas represent areas where the observed rainfall is over 60 mm lower than those from the GCM simulations.

| Figure 6.11 | Residual grids of observed present precipitation minus present (1X $CO_2$) precipitation simulated by HadCM2-S for mean precipitation totals in January (top) and in July (bottom) |
|---|---|

The residuals are high in January, with the GCM generally underestimating the rainfall for most areas, particularly in the central parts of the study area. It is, however, overestimating rainfall amounts along the eastern and southern coastline by significant amounts. The GCM's

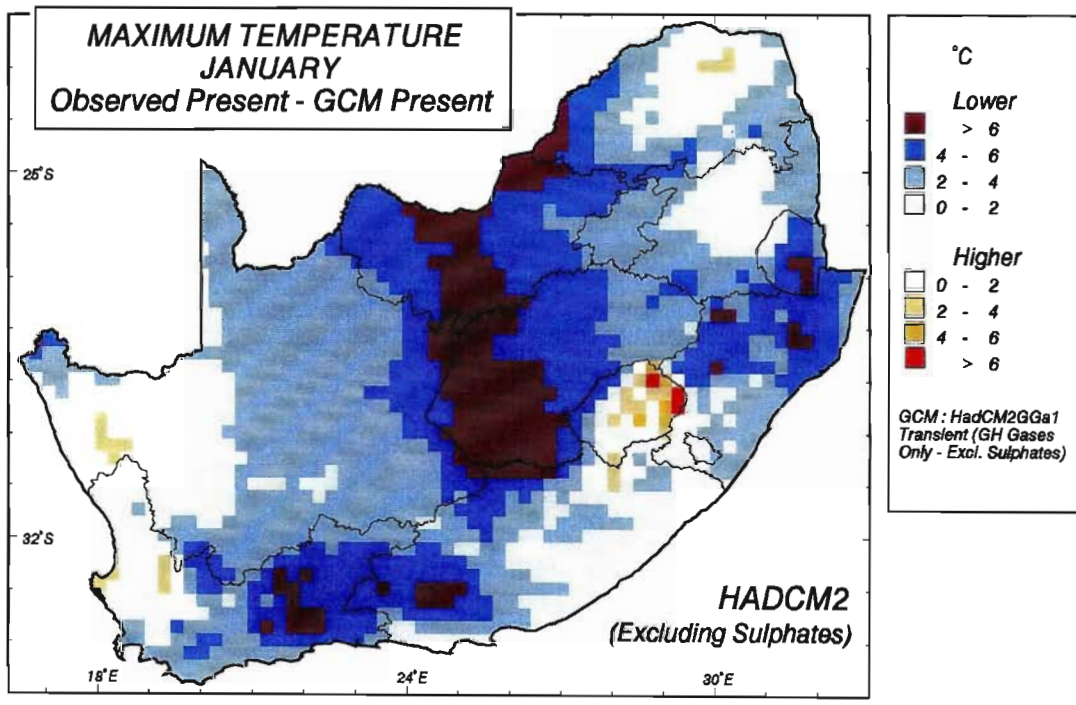
MAXIMUM TEMPERATURE
JANUARY
Observed Present - GCM Present
25°S
32°S
18°E
24°E
30°E
HADCM2
(Excluding Sulphates)
°C
Lower
> 6
4 - 6
2 - 4
0 - 2
Higher
0 - 2
2 - 4
4 - 6
> 6
GCM : HadCM2GGa1
Transient (GH Gases
Only - Excl. Sulphates)

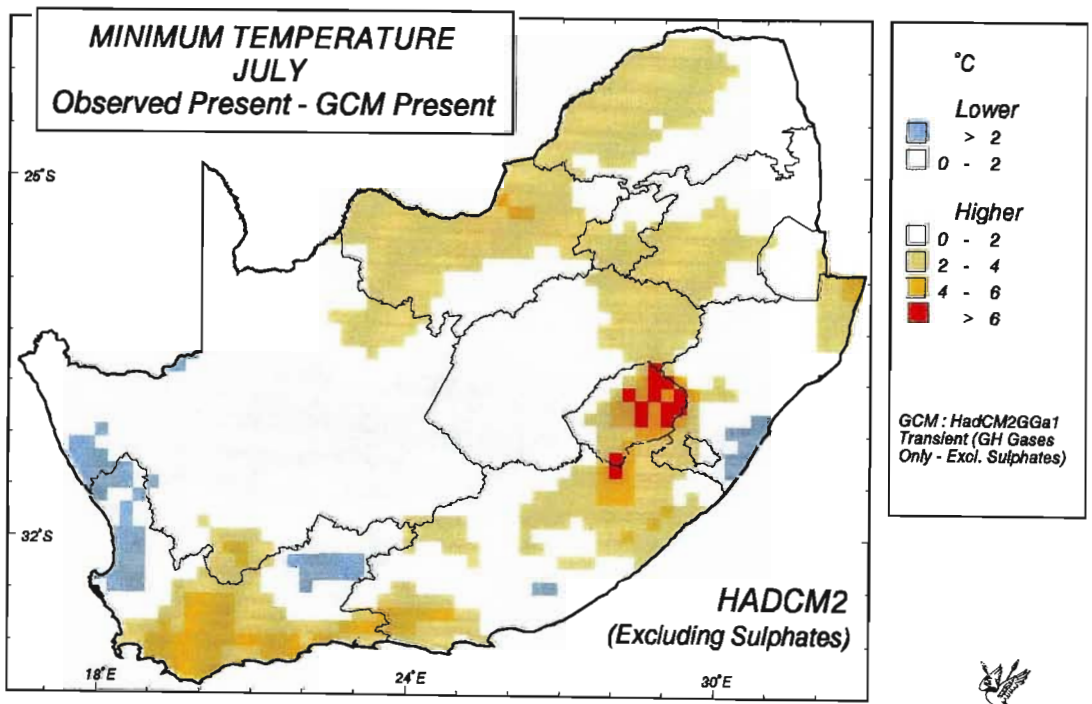
MINIMUM TEMPERATURE
JULY
Observed Present - GCM Present
25°S
32°S
18°E
24°E
30°E
HADCM2
(Excluding Sulphates)
°C
Lower
> 2
0 - 2
Higher
0 - 2
2 - 4
4 - 6
> 6
GCM : HadCM2GGa1
Transient (GH Gases
Only - Excl. Sulphates)

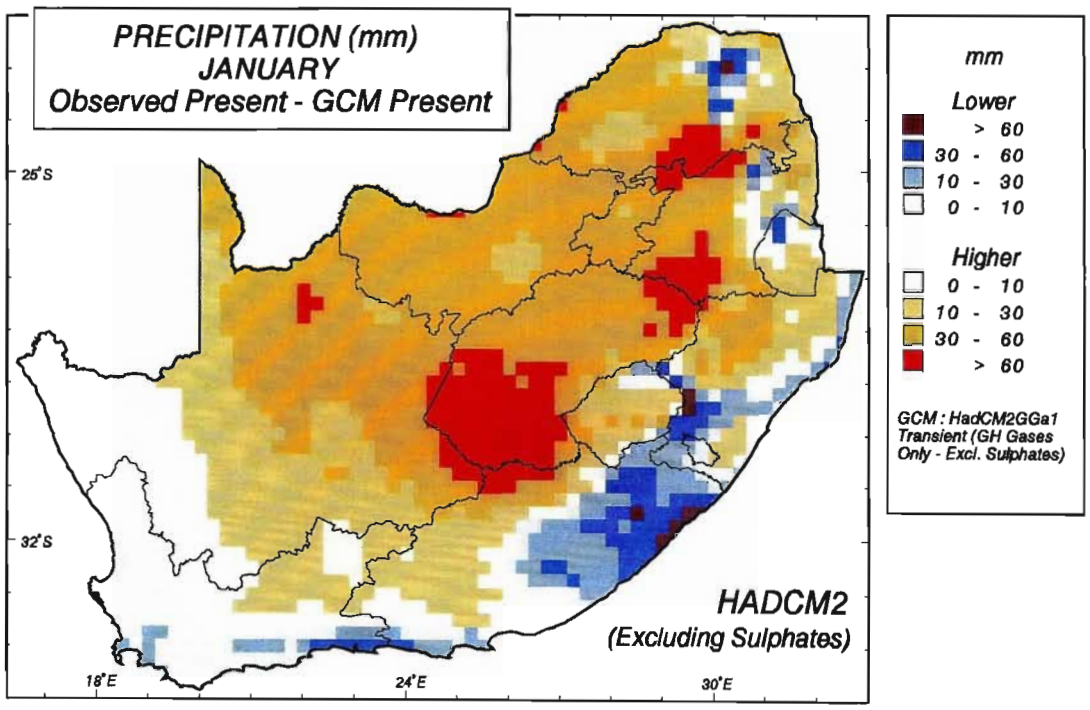
PRECIPITATION (mm)
JANUARY
Observed Present - GCM Present
25°S
32°S
18°E
24°E
30°E
HADCM2
(Excluding Sulphates)
mm
Lower
> 60
30 - 60
10 - 30
0 - 10
Higher
0 - 10
10 - 30
30 - 60
> 60
GCM : HadCM2GGa1
Transient (GH Gases
Only - Excl. Sulphates)

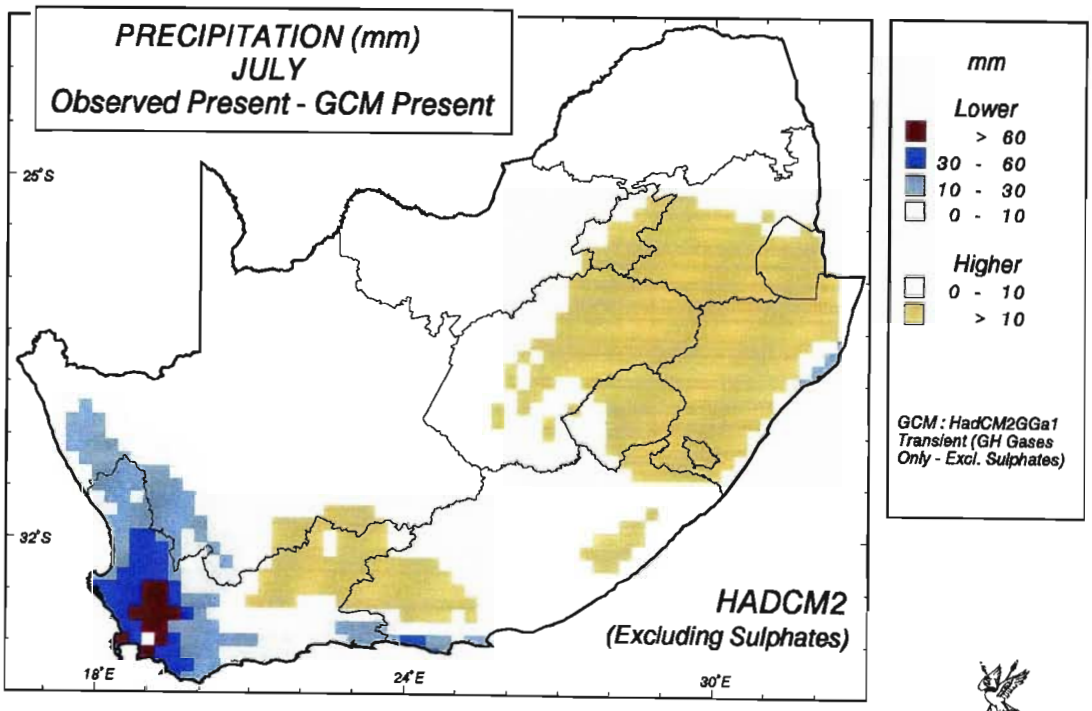
PRECIPITATION (mm)
JULY
Observed Present - GCM Present
25°S
32°S
18°E
24°E
30°E
HADCM2
(Excluding Sulphates)
mm
Lower
> 60
30 - 60
10 - 30
0 - 10
Higher
0 - 10
> 10
GCM : HadCM2GGa1
Transient (GH Gases
Only - Excl. Sulphates)

estimates of present July precipitation are not notably different from those of the observed values for much of the study region, although the GCM is significantly overestimating rainfall in the Western Cape. This is a winter rainfall region and the magnitude of this error could be the cause of significant errors if used in analyses of water resources.

### 6.6.2 Comparison of GCM output for present climatic conditions vs observed climate values at four selected points in southern Africa

The point output of temperature and precipitation from the GCM simulations from the Hadley Centre is at a spatial resolution of 2.50° latitude and 3.75° longitude. For the second assessment of history matching four representative sample points from the HadCM2-S were selected across southern Africa, *viz.* in the

i) winter rainfall region (32°30'S, 18°45'E);
ii) summer rainfall region, subtropical (22°30'S, 30°00'E);
iii) summer rainfall region, coastal (30°00'S, 30°00'E); and
iv) summer rainfall region, interior (30°00'S, 26°15'E).

Firstly the monthly output of precipitation and temperature from HadCM2-S was compared to the monthly climate information from the baseline database for these four sample points as presented in Sections 6.6.2.1 to 6.6.2.3. Secondly, daily precipitation output for present climatic conditions from the HadCM3-S was compared to observed daily precipitation at the four sample points to assess the accuracy of this GCM at simulating rainfall variability in the four selected climate zones in southern Africa (Sections 6.6.2.4. to 6.6.2.6).

#### 6.6.2.1 Methodology used for comparison of monthly climate from GCM output vs observed climate

At each of the four GCM points the 1' x 1' gridded temperature and rainfall values from the baseline climate database for each month of the year were plotted against the respective HadCM2-S temperature and rainfall values for a 1X $CO_2$ scenario (i.e. representative of present climatic conditions) at that point.

The baseline gridded temperature values were determined by stepwise multiple regression according to procedures outlined in Schulze (1997b). The precipitation values extracted from the baseline gridded database are *median* monthly values and were established by methods outlined in Dent *et al.* (1989).

#### 6.6.2.2 Plots of monthly means of daily maximum and minimum temperatures from GCM output vs those from observed climate

The plot of the 12 monthly means of daily maximum temperature for the winter rainfall region shows a good correspondence with a high coefficient of determination, $r^2 = 0.98$ (Figure 6.12). The scatter of GCM maximum temperatures vs those from observed climate for this region plot at a slope of 1.03. The east coast summer rainfall region also shows a good correspondence ($r^2 = 0.98$ and slope = 1.24). In the interior summer rainfall region HadCM2-S visually appears to underestimate daily means of maximum temperature, $r^2 = 0.96$ and the slope = 0.76, because the negative intercept introduces a systematic bias. HadCM2-S thus tends to underestimate maximum temperatures in the interior summer rainfall area by a margin of approximately 1 - 2 °C. The area with the lowest correspondence between the HadCM2-S estimates and baseline database values is the northern subtropical rainfall area ($r^2 = 0.68$ and slope = 0.61).

There is also a good correspondence between the HadCM2-S estimates of monthly means of daily minimum temperatures and the corresponding observed minima from the baseline database ($r^2$ values range from 0.96 to 0.99) as shown in Figure 6.13. HadCM2-S slightly underestimates minimum temperatures in the interior, with a slope of 0.87, and slightly overestimates minimum temperatures in the northern subtropical rainfall area (slope = 0.75).

#### 6.6.2.3 Plots of monthly precipitation totals from GCM output vs those from observed climate

There is, however, only a weak overall relationship between the monthly precipitation estimates from the GCM and those from the present climate database at the four selected GCM points (Figure 6.14). HadCM2-S consistently overestimates monthly precipitation totals

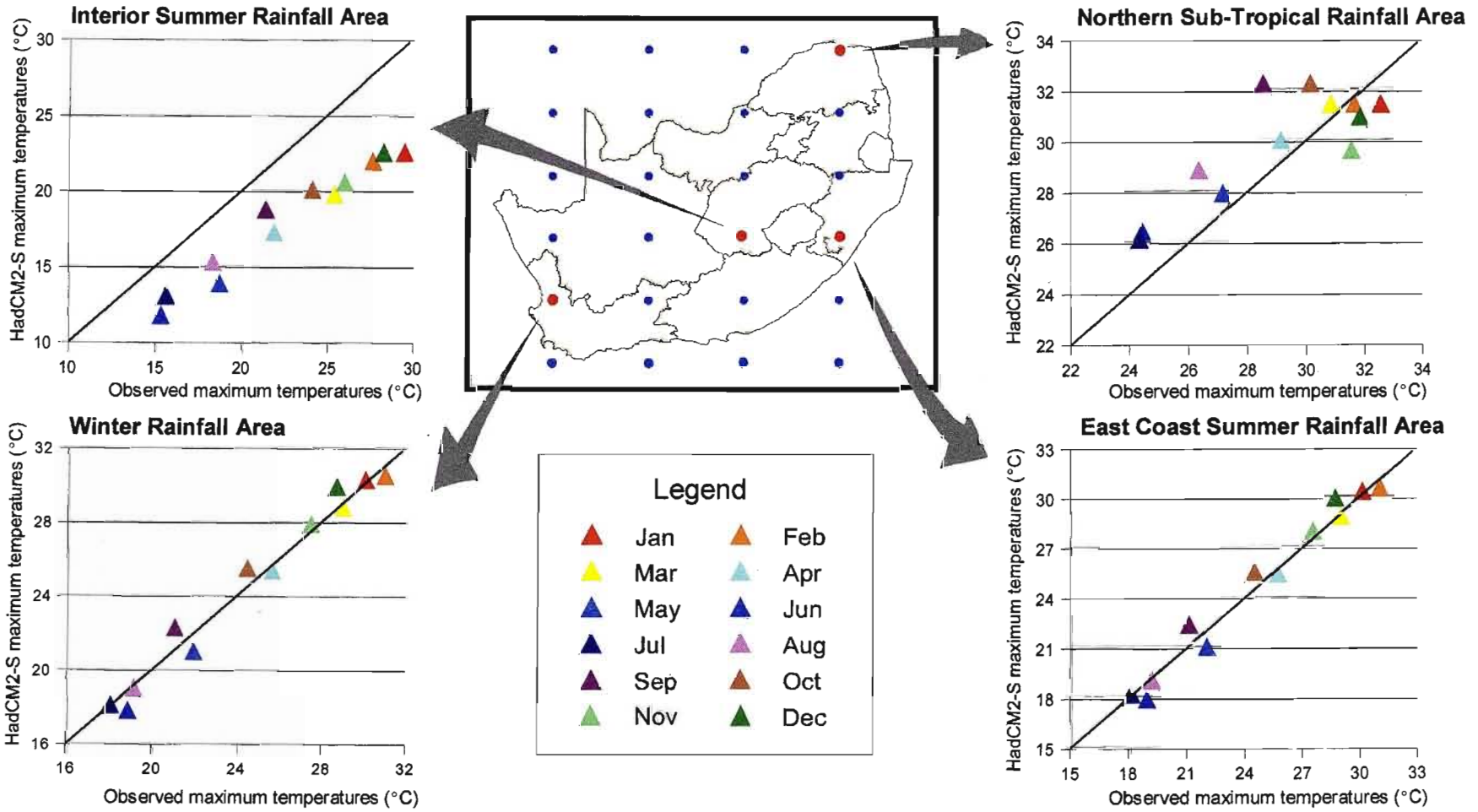


Figure 6.12 Comparison of monthly means of daily maximum temperature between values from HadCM2-S for a "present" (1X $CO_2$) climate and values from the baseline database at four GCM points across southern Africa

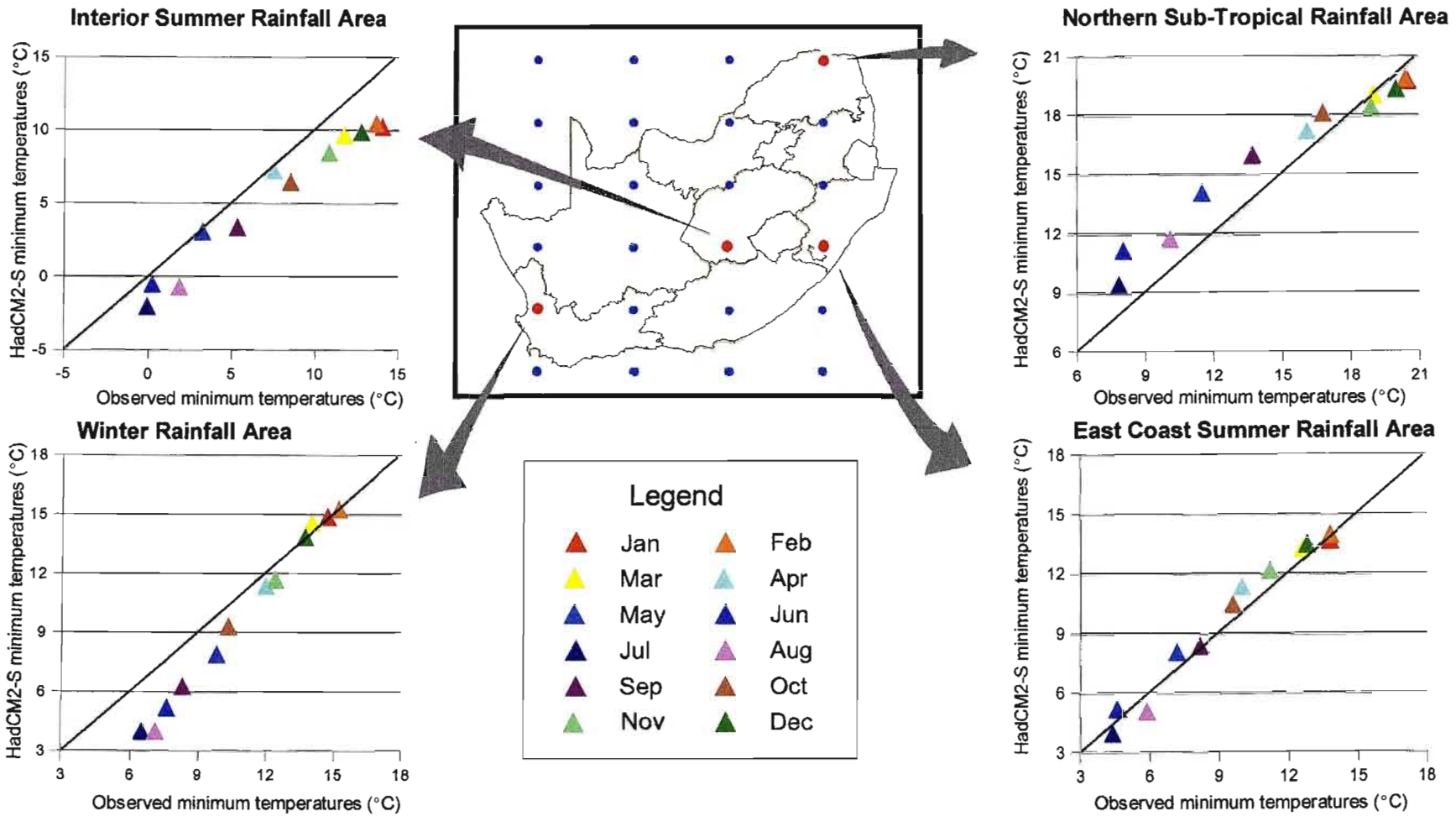


Figure 6.13 Comparison of monthly means of daily minimum temperature between values from HadCM2-S for a "present" (1X $CO_2$) climate and values from the baseline database at four GCM points across southern Africa

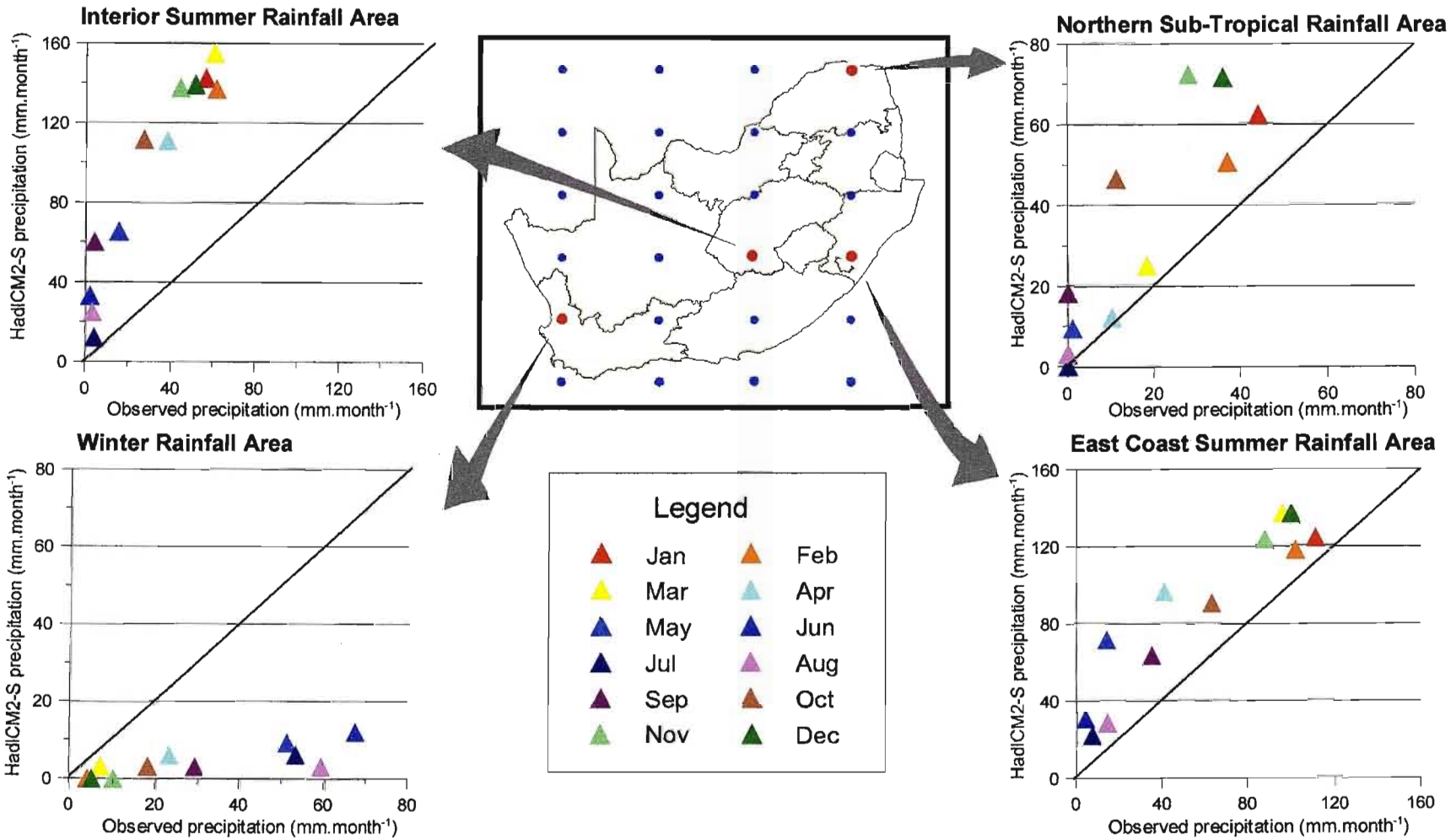


Figure 6.14 Comparison of monthly means of daily precipitation between values from HadCM2-S for a "present" (1X $CO_2$) climate and values from the baseline database at four GCM points across southern Africa

in the interior ($r^2 = 0.91$ and slope = 2.07) and consistently underestimates precipitation in the winter rainfall region ($r^2 = 0.66$ and slope = 0.14).

At the other two sample points HadCM2-S estimations are too high and display little correspondence, with the scatter plot for the northern subtropical rainfall area having a $r^2 = 0.79$ and a slope = 1.47 and the east coast summer rainfall area having a $r^2 = 0.88$ and a slope = 0.97.

From the two verification studies of monthly climate presented in this chapter it is clear that large errors may be incurred by the output from the GCMs when comparing the interpolated values from the GCM for a present climate (1X $CO_2$) scenario to values of present climate generated by the baseline database. While significant *absolute differences* may have been identified between point output from a GCM for a 1X $CO_2$ climate scenario, which is taken to represent present climatic conditions, and parameter estimates derived from climate observations at the same points, it must be assumed that there will be little or no *relative* change in the magnitude of any error at a given GCM point estimate for a 2X $CO_2$ climate scenario of a certain GCM and the 1X $CO_2$ scenario for the same GCM.

For that reason it is argued that in the case of temperatures, the *difference* between predictions from 2X $CO_2$ and 1X $CO_2$ climate scenarios may be considered a plausible temperature scenario for assessments of relative change. Similarly, in the case of precipitation, it is argued that the *ratios* between GCM outputs for future and present climates may be used as an index of relative changes in precipitation. Ratios rather than absolute differences are used to depict relative changes in precipitation, because they would better reflect response changes for non-continuous episodic and pulsar events such as rainfall and can be applied as a multiplier to gridded present day precipitation values, which have influences of local topographic and other effects inherently built in when equations for their gridded spatial representation were developed.

#### 6.6.2.4 Methodology used for comparison of statistics calculated from daily precipitation from GCM output vs those from observed climate

The daily climatic output at each GCM point given by HadCM3-S is representative of the average of the climate over the 3.75° latitude by 2.50° longitude rectangle that it represents for that day. Each GCM point is located in the centre of the rectangle it delineates. The daily precipitation output from HadCM3-S was compared to the daily precipitation from observed climate records in southern Africa at the four selected GCM points across southern Africa. The raingauges selected as driver stations for the Quaternary Catchments database of southern Africa were selected for use in this component of the study (cf. Chapter 5, Section 5.3).

In order to compare the daily output from the GCM for present climate conditions to the observed climate, a data set had to be created from the observed climate rainfall records which was representative of each of the rectangles delimited by the GCM for the period 1961 to 1989. This was achieved by firstly isolating the Quaternary Catchments' centroids which were located inside each rectangle. The raingauges used to drive those Quaternary Catchments were used to generate the statistics for each GCM delimited rectangle. If a raingauge was found to drive more than one Quaternary Catchment in a rectangle, the repeated rainfall data sets were excluded in the calculation of the statistics so as to avoid repetition of rainfall information.

The daily rainfall from 1961 to 1989 was averaged from the selected raingauges which had been isolated for each rectangle to obtain a mean daily rainfall for each day for the period representing present climatic conditions. There are 26 GCM points whose rectangles or parts thereof are located within the study area of southern Africa, as shown in Figure 6.15. The number of Quaternary Catchment rainfall stations falling in each rectangle ranges from 1 to 252. The four selected points are marked as squares in the figure. The number of raindays calculated for any rectangle is expected to be influenced by the number of raingauges falling with the rectangle, because if rainfall is recorded at any one raingauge within the rectangle, that day will be identified as a rainday in the file of mean rainfall for that rectangle for that day.

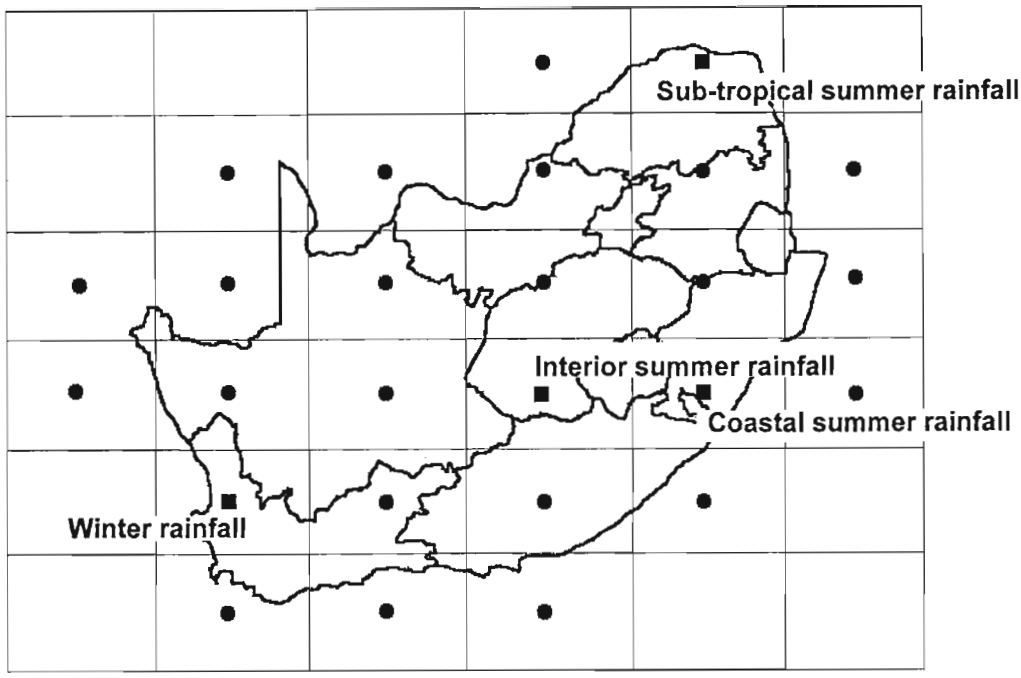


Figure 6.15 The 26 points used to generate daily observed data sets for southern Africa and the four sample points selected for the verification analysis

Two months representative of the winter and summer seasons in the study area were selected for analysis. Information for these two months was isolated from the GCM daily ASCII files described in Section 6.4.2. January was selected to verify GCM results representative of summer months and June selected as representative of the winter months. June was selected instead of July, which has been previously chosen as the representative winter month in the study area, owing to the many missing data values recorded for July from the HadCM3-S. However, as mentioned previously in Section 6.2.4, the GCM rainfall was provided as standardised 30 day data sets per month, irrespective of the month of the year. In order to allow the observed and GCM present climate data sets to be comparable it was assumed that in January only the first 30 days from the observed recorded should be used. In this way a comparable data set for the time period representing present climate was established for each of the GCM points falling in and around southern Africa.

From these data sets established for each GCM point from the Quaternary Catchment rainfall database statistical information could be computed at each of the four sample points in order to compare the observed variability of rainfall to the GCM simulated variability in the four

climate zones in the study area. However, the following considerations should be borne in mind when using the statistics derived from the observed rainfall records:

i) Owing to time constraints only rainfall records from the Quaternary Catchments database were used, whereas in reality more representative stations may exist.

ii) Some data were lost from the rainfall records in the month of January as only the rain falling over the first 30 days was used.

iii) In addition, the number of days with observed rain may be strongly dependent on the number of raingauges located in a rectangle.

The mean, percentage coefficient of variation (CV %) of rainfall, percentage of days with zero precipitation and percentage of days with precipitation exceeding 25 mm were calculated for January and June from the HadCM3-S output and compared to the statistics determined from observed precipitation representing the period 1961 - 1989, as discussed in the following sections.

#### 6.6.2.5 Comparison of statistics derived from daily precipitation from HadCM3 and observed climate for January

The statistics calculated for the four sample points for January are presented in Table 6.1. Assuming the statistics of present climate from the observed records to be accurate, the HadCM3-S appears to provide a good simulation of daily rainfall variability for the winter rainfall area in January. This would be expected as the majority of the rainfall in this area falls in June and therefore the rainfall in January is low.

The simulations of daily precipitation in the subtropical summer and coastal summer rainfall areas are also reasonably good, with the GCM slightly over simulating mean daily rainfall. However, the coefficient of variation calculated from the two data sets is very similar.

The greatest discrepancies are noted in the interior summer rainfall region and this could be due in part to the coarse resolution of the GCM. The rainfall information pertaining to the high rainfall area of Lesotho appears to be displaced and reflected in the GCM point in question in the southern Free State. At this point the GCM is underestimating the number of

days with no rain by 63% and over simulating the number of days with rainfall exceeding 25 mm by 167%.

Table 6.1 Comparison of statistics derived at four sample points in southern Africa from observed daily precipitation and GCM simulated daily precipitation for present climatic conditions for January (GCM: HadCM3-S)

| Sample Points | January | | | |
|---|---|---|---|---|
| | Observed Daily Precipitation: Present | GCM Daily Precipitation: Present Climatic Conditions | Absolute Difference (Observed Present - GCM Present) | Percentage Difference (Observed Present - GCM Present) |
| **Winter Rainfall Region (32°30'S 18°45'E)** | | | | |
| Mean daily rainfall (mm.day$^{-1}$) | 0.3 | 0.2 | 0.1 | 33% |
| CV of rainfall | 4.5 | 5.3 | -0.8 | -18% |
| Percentage of days > 25 mm (%) | 0.0 | 0.0 | 0.0 | 0% |
| Percentage of days with no rainfall (%) | 69.8 | 72.9 | -3.1 | 4% |
| **Subtropical Summer Rainfall Region (22°30'S 30°00'E)** | | | | |
| Mean daily rainfall (mm.day$^{-1}$) | 3.5 | 4.6 | -1.1 | -31% |
| CV of rainfall | 1.6 | 1.4 | 0.2 | 13% |
| Percentage of days > 25 mm (%) | 1.1 | 1.5 | -0.4 | 36% |
| Percentage of days with no rainfall (%) | 17.6 | 20.0 | -2.4 | 14% |
| **Coastal Summer Rainfall Region (30°00'S 30°00'E)** | | | | |
| Mean daily rainfall (mm.day$^{-1}$) | 4.6 | 4.8 | -0.2 | -4% |
| CV of rainfall | 1.1 | 1.2 | -0.1 | -9% |
| Percentage of days > 25 mm (%) | 1.4 | 0.9 | 0.5 | 36% |
| Percentage of days with no rainfall (%) | 0.9 | 3.1 | -2.2 | -244% |
| **Interior Summer Rainfall Region (30°00'S 26°15'E)** | | | | |
| Mean daily rainfall (mm.day$^{-1}$) | 2.3 | 4.8 | -2.5 | -109% |
| CV of rainfall | 1.8 | 1.1 | 0.7 | 39% |
| Percentage of days > 25 mm (%) | 0.3 | 0.8 | -0.5 | -167% |
| Percentage of days with no rainfall (%) | 20.7 | 7.7 | -13.0 | -63% |

### 6.6.2.6 Comparison of statistics derived from daily precipitation from HadCM3 and observed climate for June

In June, HadCM3-S appears to provide a reasonably good representation of variability for present climatic conditions for the winter rainfall, subtropical summer rainfall and coastal summer rainfall points (Table 6.2).

Table 6.2 Comparison of statistics derived at four sample points in southern Africa from observed daily precipitation and GCM simulated daily precipitation for present climatic conditions for June (GCM: HadCM3-S)

| Sample Points | June | | | |
|---|---|---|---|---|
| | Observed Daily Precipitation: Present | GCM Daily Precipitation: Present Climatic Conditions | Absolute Difference (Observed Present - GCM Present) | Percentage Difference (Observed Present - GCM Present) |
| **Winter Rainfall Region (32°30'S 18°45'E)** | | | | |
| Mean daily rainfall (mm.day$^{-1}$) | 0.3 | 0.6 | -0.3 | -100% |
| CV of rainfall | 2.2 | 2.6 | -0.4 | 18% |
| Percentage of days > 25 mm (%) | 0.5 | 0.0 | 0.5 | 100% |
| Percentage of days with no rainfall (%) | 44.5 | 45.2 | -0.7 | -2% |
| **Subtropical Summer Rainfall Region (22°30'S 30°00'E)** | | | | |
| Mean daily rainfall (mm.day$^{-1}$) | 0.3 | 0.3 | 0.0 | N/A |
| CV of rainfall | 4.4 | 3.0 | 1.4 | 32% |
| Percentage of days > 25 mm (%) | 0.0 | 0.0 | 0.0 | 0% |
| Percentage of days with no rainfall (%) | 76.8 | 62.3 | 14.5 | 19% |
| **Coastal Summer Rainfall Region (30°00'S 30°00'E)** | | | | |
| Mean daily rainfall (mm.day$^{-1}$) | 0.6 | 0.5 | 0.1 | 17% |
| CV of rainfall | 4.4 | 3.7 | 0.7 | 16% |
| Percentage of days > 25 mm (%) | 0.1 | 0.0 | 0.1 | N/A |
| Percentage of days with no rainfall (%) | 57.2 | 57.5 | -0.3 | 0% |
| **Interior Summer Rainfall Region (30°00'S 26°15'E)** | | | | |
| Mean daily rainfall (mm.day$^{-1}$) | 0.5 | 2.1 | -1.6 | -320% |
| CV of rainfall | 3.7 | 1.9 | 1.8 | 49% |
| Percentage of days > 25 mm (%) | 0.0 | 0.2 | -0.2 | N/A |
| Percentage of days with no rainfall (%) | 71.6 | 17.6 | 54.0 | 75% |

However, as in the case of January, the statistics calculated for the interior summer rainfall point show a large discrepancy between the GCM generated daily precipitation and the observed precipitation in June. HadCM3-S appears to underestimate the percentage of days with no rainfall by 75% and overestimate the mean daily rainfall by 320%. This is again attributed to the coarse resolution of the GCM.

Assuming HadCM3-S represents rainfall variability in a future climate relatively as accurately as it does present climate, potential changes in variability of rainfall simulated by this GCM for southern Africa can be assessed. This assessment is presented in the following section, Section 6.7.

## 6.7 Potential Changes in Climate Variability

Most impact assessments that have been carried out have perturbed a baseline daily climate data set according to changes in mean monthly climate from climate change scenarios. This technique does not, however, allow for the assessment of potential changes in variability of climate from day to day and year to year with climate change (Arnell, 1999). More recent studies have used either weather generators or stochastic daily information to assess the effects of changes in variability on the hydrology of a region, however, as Arnell points out, it can be difficult to create a realistic weather generator (Arnell, 1999).

To assess potential changes in variability with climate change, daily output from HadCM3-S was used (cf. Section 6.2.4). The extraction of daily precipitation and temperature information from this GCM for southern Africa is discussed in Section 6.4.2.

The first objective of this analysis of potential changes in variability with climate change was to assess the hydrological differences in rainfall between a present and future climate scenario simulated by HadCM3-S. This included the assessment of potential changes, for both January and June, in

i) mean precipitation;
ii) coefficient of variation of daily precipitation;
iii) percentage of days with no precipitation;
iv) percentage of days with 10 to 25 mm of precipitation;
v) percentage of days with precipitation greater than 25 mm; and
vi) percentage of days with precipitation greater than 50 mm.

With the exception of the mean and coefficient of variation of rainfall, the number of days calculated for a given statistic was converted to a percentage of total possible number of days for both the present and future climate for that month (e.g. 29 years of 30 days per month = 870 days). Changes in rainfall amounts and numbers of raindays in January are critical in the summer rainfall zones located on the eastern half of the country, whereas changes in rainfall characteristics in June are considered important for the western coastline of southern Africa (cf. Figure 6.6). The results from this first assessment are presented in Sections 6.7.1 to 6.7.6.

### 6.7.1 Potential changes in mean precipitation

The mean precipitation amounts for January and June simulated by HadCM3-S were calculated by multiplying the mean daily precipitation by 30 days to obtain a mean monthly precipitation. At present the mean precipitation for January as simulated by HadCM3-S ranges from more than 225 mm in the north-east of KwaZulu-Natal to less than 45 mm in the west of the study area (Figure 6.16, top). However, in a future climate simulated by this GCM there is a decrease in areas with an average rainfall of over 225 $mm.day^{-1}$ in January and an increase in areas potentially experiencing less than 45 $mm.day^{-1}$ of mean precipitation in this month (Figure 6.16, middle).

Figure 6.16 Mean precipitation (mm) for January: Present climate (top), future climate (middle) and change in mean daily precipitation (bottom). Both climate scenarios from HadCM3-S

In the map of potential change in mean daily precipitation (Figure 6.16, bottom) the reductions in mean daily precipitation for January equate to a decrease of over 48 mm in the far north of the study area and a reduction in mean precipitation of between 0 and 24 mm for the majority of southern Africa. There are, however, areas simulated to have increases in mean daily precipitation in January, with the largest increases of over 12 $mm.day^{-1}$ in southern KwaZulu-Natal. This is significant as KwaZulu-Natal experiences most of its rain in summer.

The mean rainfall amounts in June in the study area are lower and the rainfall patterns are distinctly different compared to those in January. According to HadCM3-S (Figure 6.17, top), the highest mean rainfall in the present climate occurs in southern Free State, northern KwaZulu-Natal and along the southern coastline. The rainfall amounts, of over 85 mm, simulated by this GCM along the southern coastline are compared to the results obtained by Schulze (1997b) where the highest rainfall area in June, of over 100 mm, is located in the Western Cape. Although a zone of high rainfall in June is shown on the map over southern Free State, this presumably represents the higher rainfall area of the Lesotho highlands, but is displaced owing to the coarse spatial resolution of the GCM output.

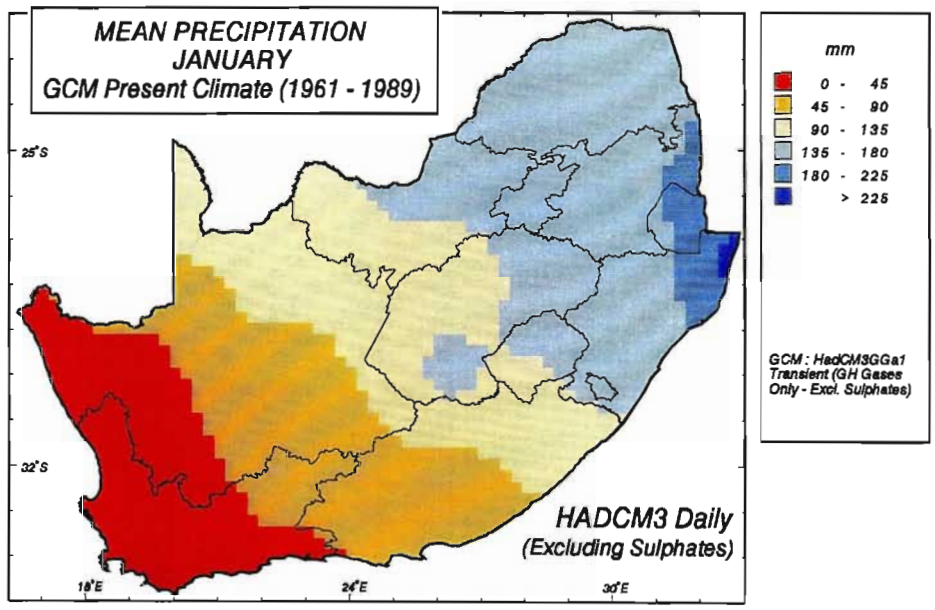


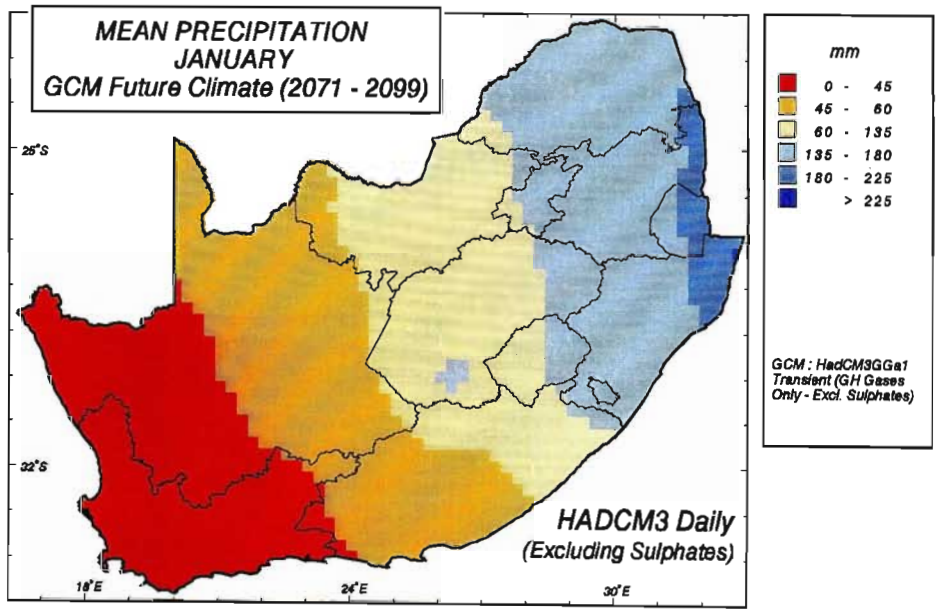


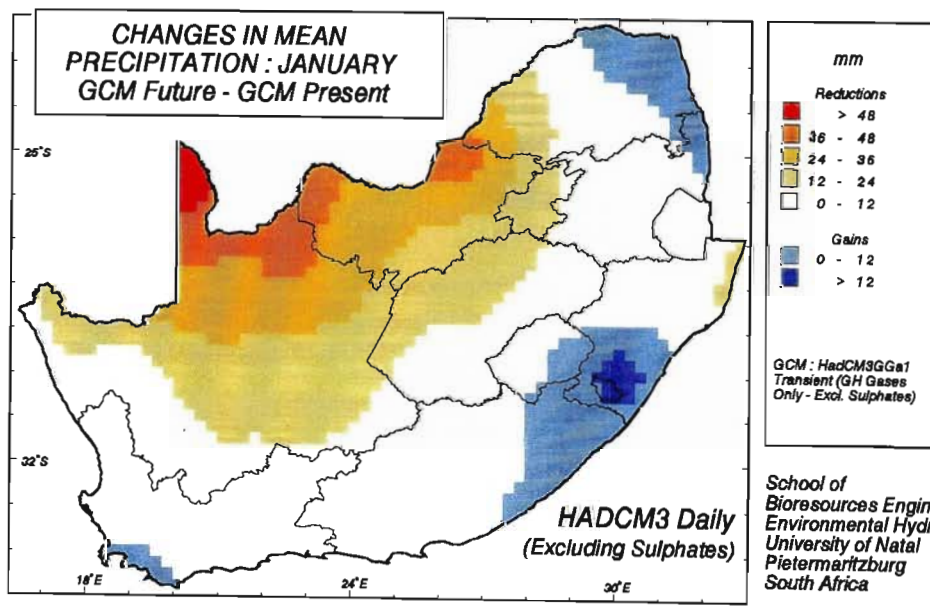


School of
Bioresources Engineering and
Environmental Hydrology
University of Natal
Pietermaritzburg
South Africa

Figure 6.17 Mean precipitation (mm) for June: Present climate (top), future climate (middle) and change in mean daily precipitation (bottom). Both climate scenarios from HadCM3-S

For a future climate scenario (Figure 6.17, middle), a greater part of the study area was simulated by this GCM to experience an average rainfall of less than 15 mm when compared to present climatic conditions. The western parts of the study area experience winter rainfall (cf. Figure 6.6) and decreases of between 6 to 12 mm were simulated for large parts of this western area. In addition, the high rainfall zone identified in the centre of the study area in the GCM present climate is simulated to have more than a 12 mm reduction in mean precipitation in June (Figure 6.17, bottom). However, from observed records this area only receives approximately 18 mm of rainfall a month under present climate conditions (Schulze, 1997b) which again highlights the coarse resolution of the GCM.

### 6.7.2 Potential changes in the coefficient of variation of daily precipitation

Potential changes in natural variability of rainfall for southern Africa were mapped for January and June using output from HadCM3-S. This natural variability is expressed in terms of a coefficient of variation, as a percentage. The higher the coefficient of variation, the higher the inter-daily variability. This statistic is calculated by dividing the standard deviation by the mean and thus the variation around the mean is plotted and changes in the mean in a future climate are accounted for. In addition, this statistic allows for relative comparisons between regions of high and low rainfall (Schulze, 1997b). The coefficient of variation is expressed as a percentage on the maps which follow.

The map of present coefficient of variation of daily precipitation for January, as simulated by HadCM3-S, shows a general increase in variability from east to west of the study area with the highest coefficients of variation calculated for the central west coast of the study area (Figure 6.18, top). The majority of the study area shows a coefficient of variation of daily rainfall in January of less than 200%.

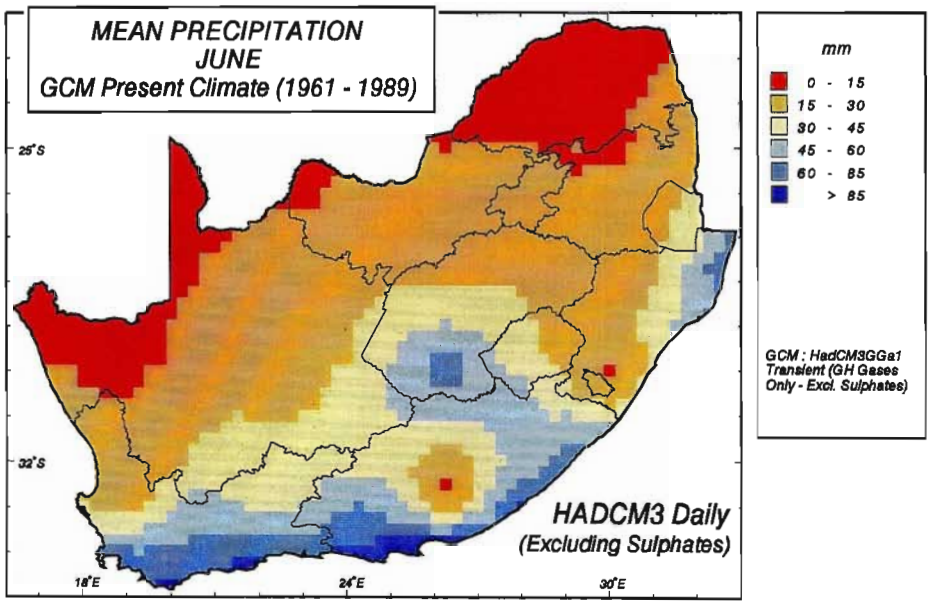


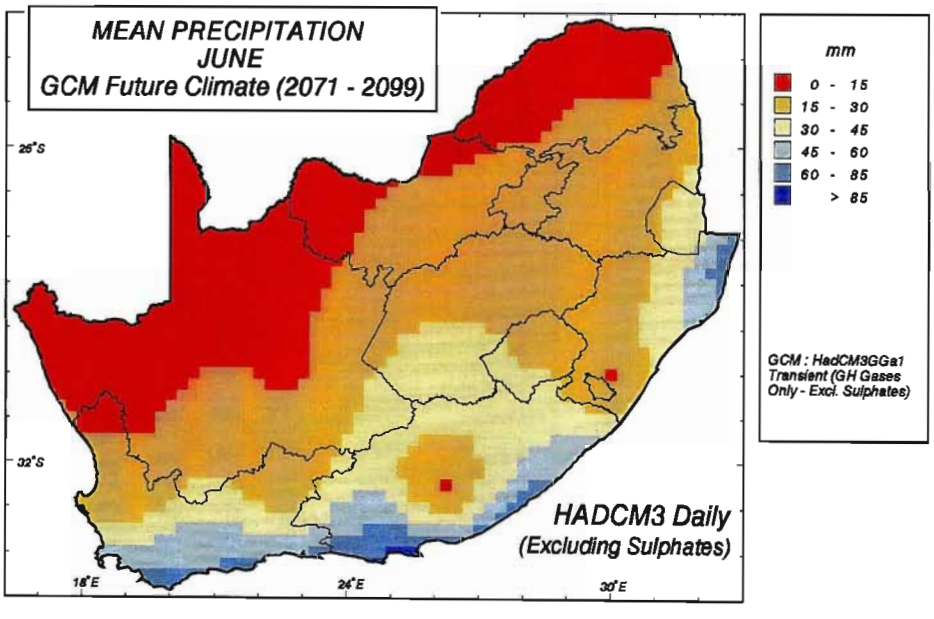


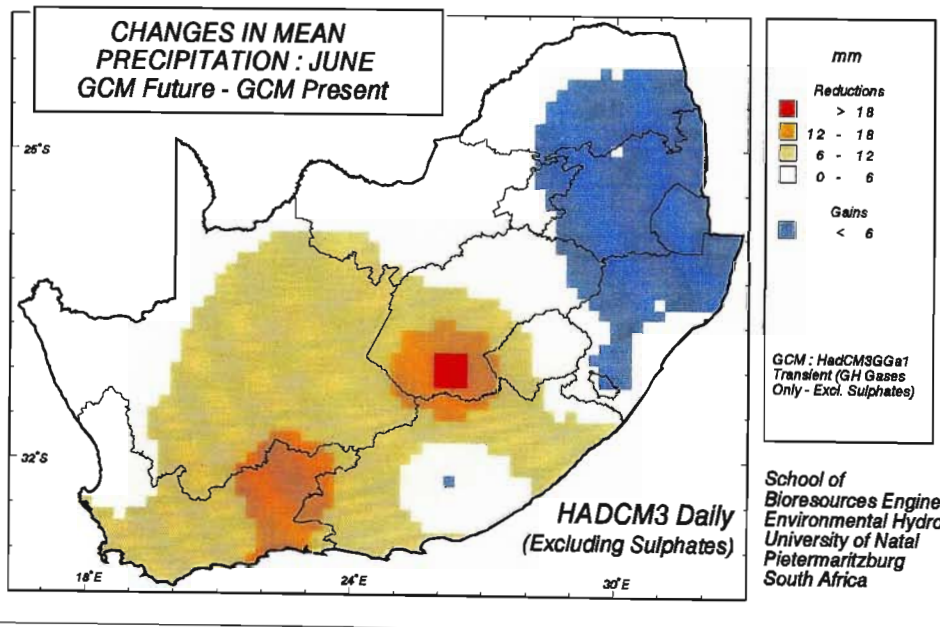


School of
Bioresources Engineering and
Environmental Hydrology
University of Natal
Pietermaritzburg
South Africa

Figure 6.18 Coefficient of variation of daily precipitation (%) for January: Present climate (top), future climate (middle) and change in the coefficient of daily precipitation (bottom). Both climate scenarios from HadCM3-S

In a future climate, the majority of southern Africa retains an inter-daily coefficient of variation of less than 200%. However, the most significant difference is in the central west coast region where a reduction in the area with a coefficient of variation of greater than 500% in January is evident (Figure 6.18, middle). In absolute millimetres terms this may not be significant, as this is a winter (April - September) rainfall area.

In the map of change in the coefficient of variation of daily precipitation in January (Figure 6.18, bottom) the highest increases in coefficient of variation occur in the north-western Cape area and the highest decreases in coefficient of variation were simulated by this GCM in the south-west of southern Africa. The summer rainfall zone in the east of the study area could experience less than a 40% increase in coefficient of variation in January if the results from this GCM are assumed to be accurate.

In comparison, the coefficient of variation of present precipitation in June simulated by HadCM3-S shows the highest coefficients of variation in the north and east and the lowest coefficients of variation in the south of the study area (Figure 6.19, top). The range of coefficients of variation from less than 200% to greater than 400% experienced in the study area for June, however, remain similar to those of January's.

Figure 6.19 Coefficient of variation of daily precipitation (%) for June: Present climate (top), future climate (middle) and change in the coefficient of daily precipitation (bottom). Both climate scenarios from HadCM3-S

Increases in the coefficient of variation in June are simulated with climate change for many areas by this GCM, particularly in the western two-thirds of the study area (Figure 6.19,

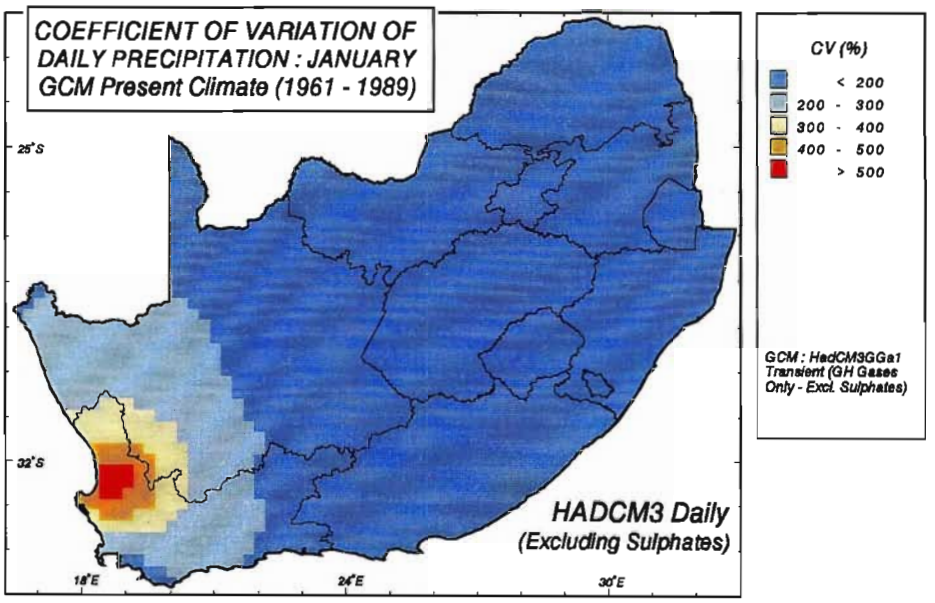


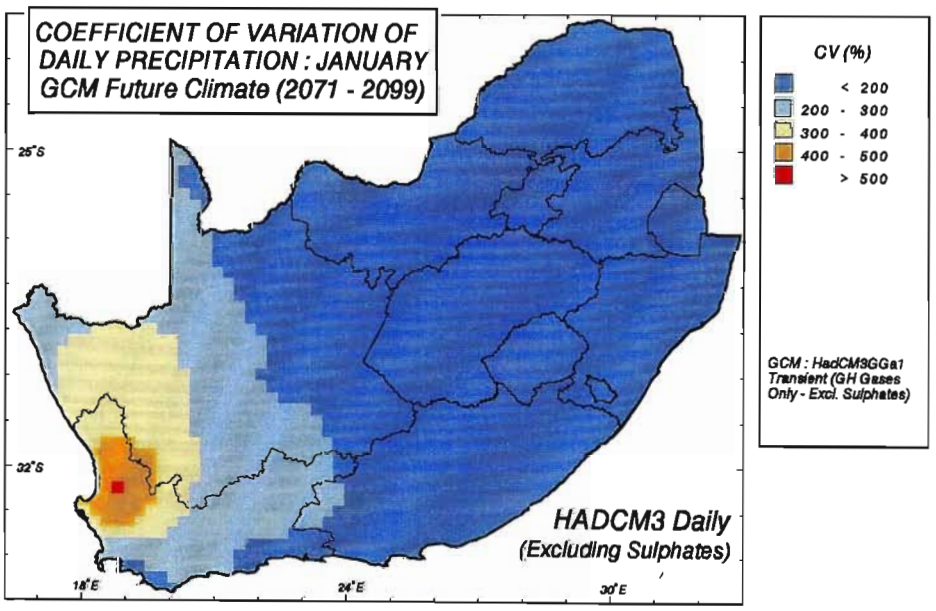


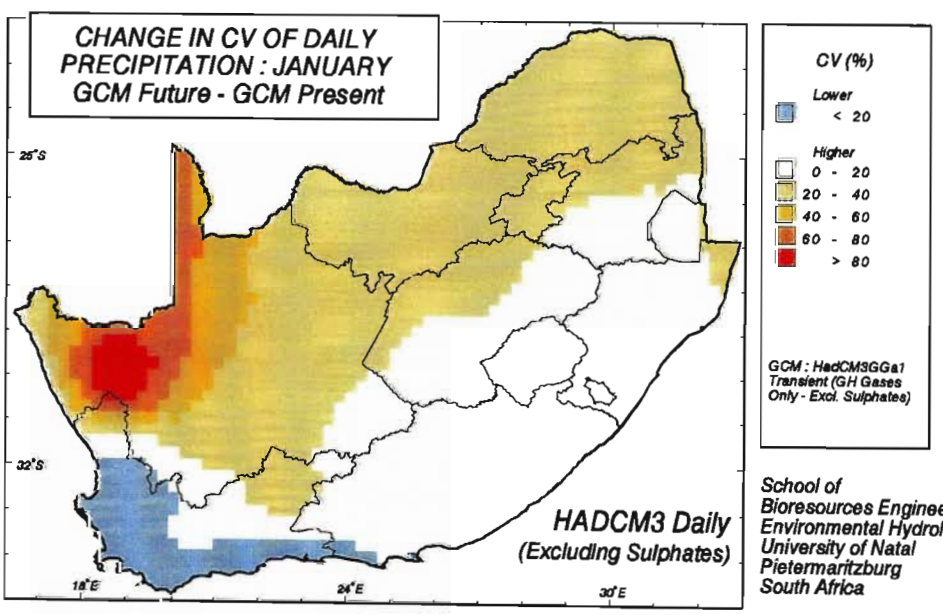


School of
Bioresources Engineering and
Environmental Hydrology
University of Natal
Pietermaritzburg
South Africa

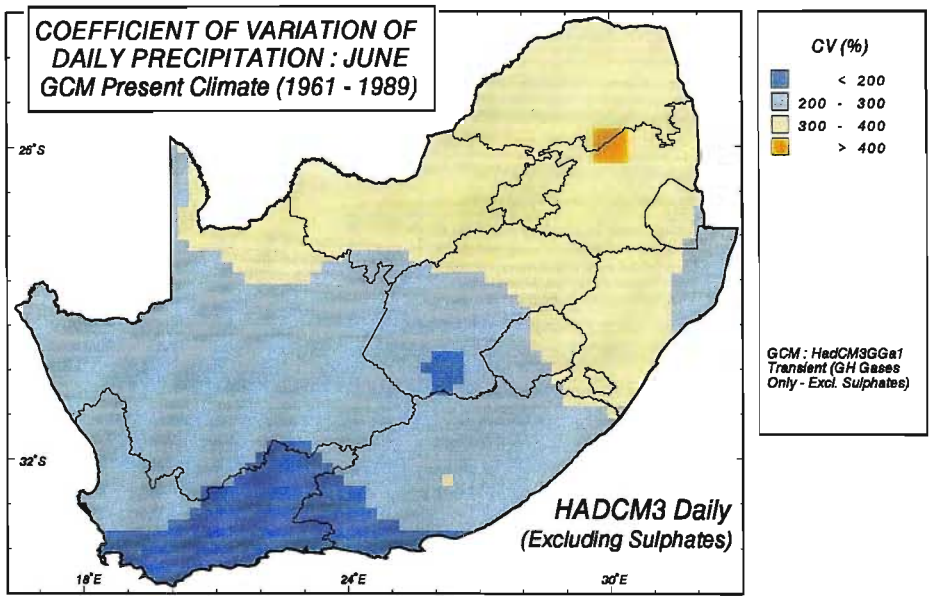


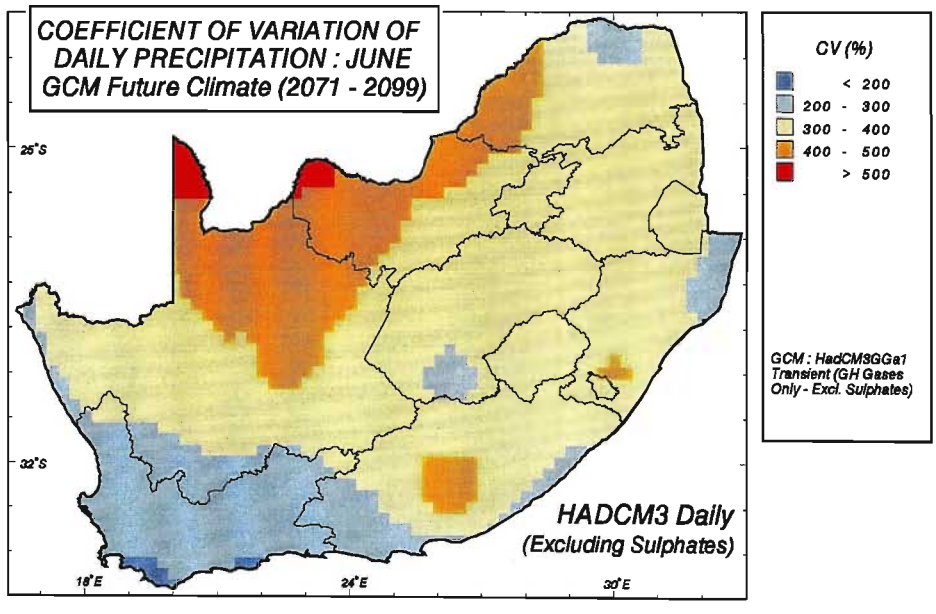


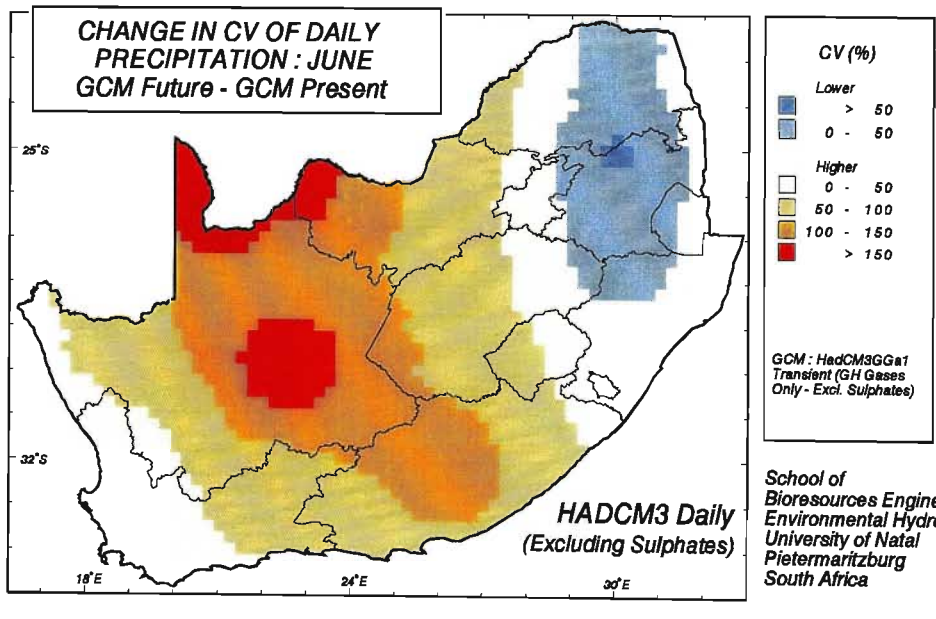


School of
Bioresources Engineering and
Environmental Hydrology
University of Natal
Pietermaritzburg
South Africa

bottom). In the north-east HadCM3-S simulations indicate a slight decrease in the coefficient of variation of daily precipitation in June.

### 6.7.3 Potential changes in percentage of days with no precipitation

For a present climate scenario HadCM3-S simulates a decrease in percentage of days with no precipitation in January from west to east (Figure 6.20, top). Seventy per cent of days are simulated to have no precipitation in the west of the study in this month for present climatic conditions, whereas the eastern half of the study area is shown to have between 10 and 20% of days with no precipitation. In reality the number of days with no precipitation is much higher but this statistic is influenced by the fact each GCM point represents a large area around the point in which rainfall will be recorded if it rains anywhere in the rectangle it delimits.

| | |
|---|---|
| Figure 6.20 | Percentage of days with no precipitation in January: Present climate (top), future climate (middle) and per cent change in days with no precipitation (bottom). Both climate scenarios from HadCM3-S |

In a future climate scenario this pattern could change according to output from simulations by HadCM3-S. The eastern half of the study area could have a higher percentage of days with no rainfall (Figure 6.20, middle). The overall trend appears to be increases in rain-free days in the north and decreases of days with no rain in the south.

The per cent change in days with no precipitation (Figure 6.20, bottom) was determined by calculating the difference in percentages of rain-free days in the future and in the present and dividing this by the percentage of rain-free days under present climatic conditions. The northern areas could potentially experience 75 to 100% more rainless days compared to the present. On the other hand, the southern coastal belt could experience less than 25% fewer rainless days in January that at present, according to output from HadCM3-S.

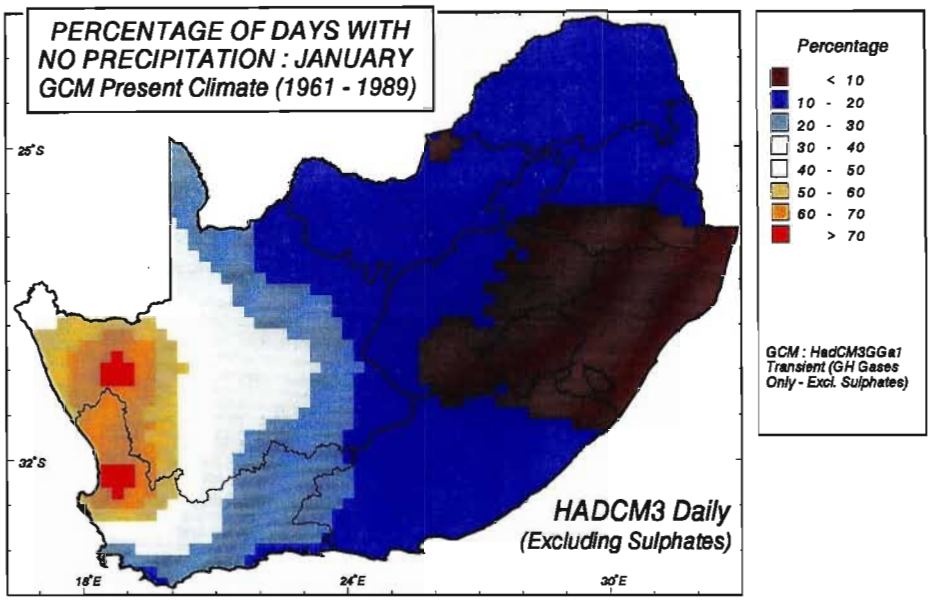


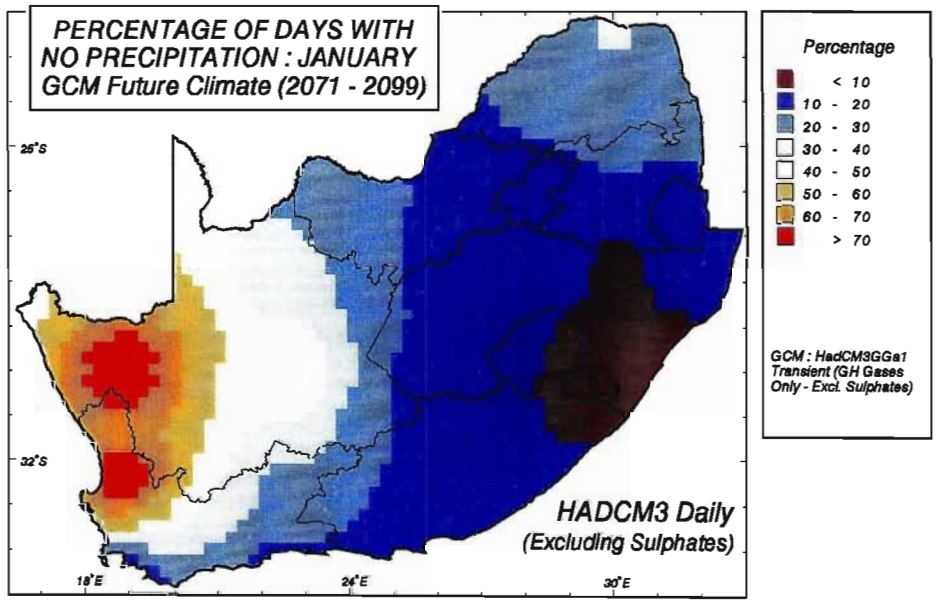


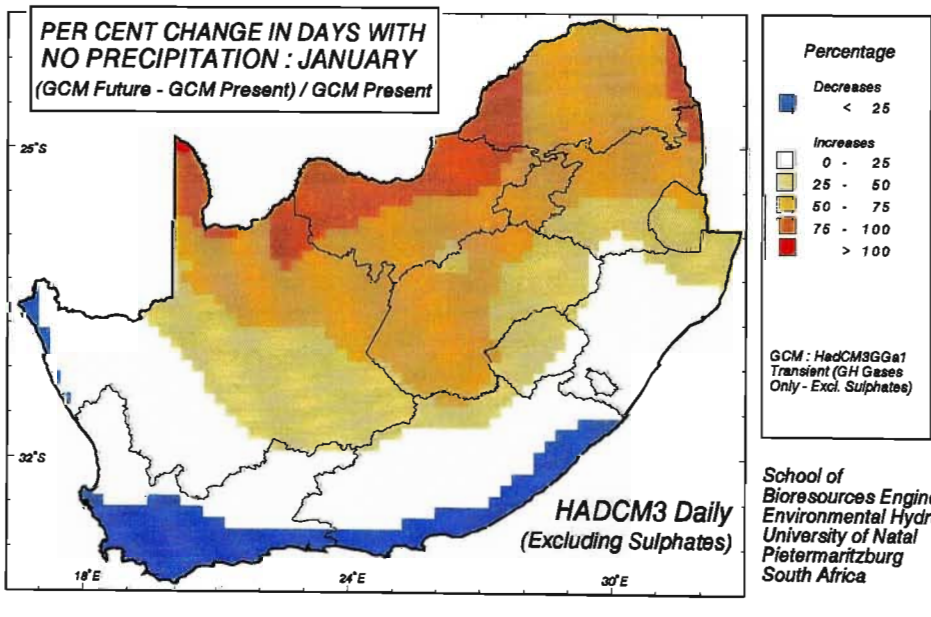


School of
Bioresources Engineering and
Environmental Hydrology
University of Natal
Pietermaritzburg
South Africa

The percentage of days with no rainfall in June for the present climate ranges from less than 30% in the central and south-western parts of the study area to more than 60% in the north, according to HadCM3-S simulations (Figure 6.21, top). However, assuming future climatic conditions simulated by HadCM3-S to be realistic, large increases in rainless days could occur in the central parts of the study area (Figure 6.21, middle). Increases in days with no rain in excess of 75% under present conditions are simulated in this central areas which is already very dry and, therefore, this decrease could have a significant impact on the water resources of this region. In the Western Cape Province, which receives the majority of its rainfall in winter, there could be around a 10 to 20% increase in number of days with rain relative to present conditions. This could be beneficial for the fruit and vegetable cultivation areas in this province. Similarly, an increase in the number of raindays is projected to occur in a north-south strip in the eastern third of the study area.

Figure 6.21 Percentage of days with no precipitation in June: Present climate (top), future climate (middle) and per cent change in days with no precipitation (bottom). Both climate scenarios from HadCM3-S

### 6.7.4 Potential changes in number of days with 10 - 25 mm precipitation

Ten millimetres is a generally accepted threshold amount of precipitation per day for stormflow as well as sediment yield to be generated (Schulze, 1983). The 10 - 25 mm magnitude range of daily precipitation is also an indicator of number of days on which tillage practices cannot be carried out.

In a present climate scenario the percentage of days with 10 to 25 mm rainfall in January ranges from less than 4% in the west to more than 16% in the north-east of southern Africa, using output from HadCM3-S (Figure 6.22, top).

Figure 6.22 Percentage of days with 10 to 25 mm precipitation in January: Present climate (top), future climate (middle) and per cent change in days with 10 to 25 mm precipitation (bottom). Both climate scenarios from HadCM3-S

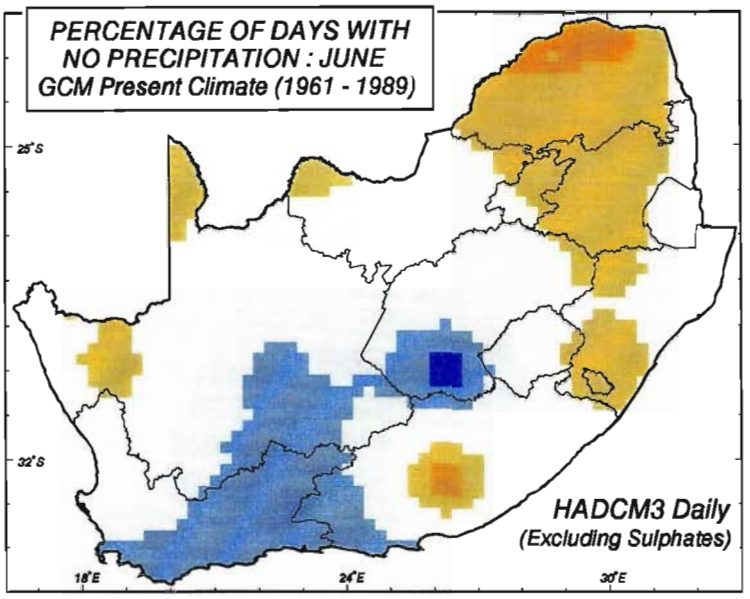


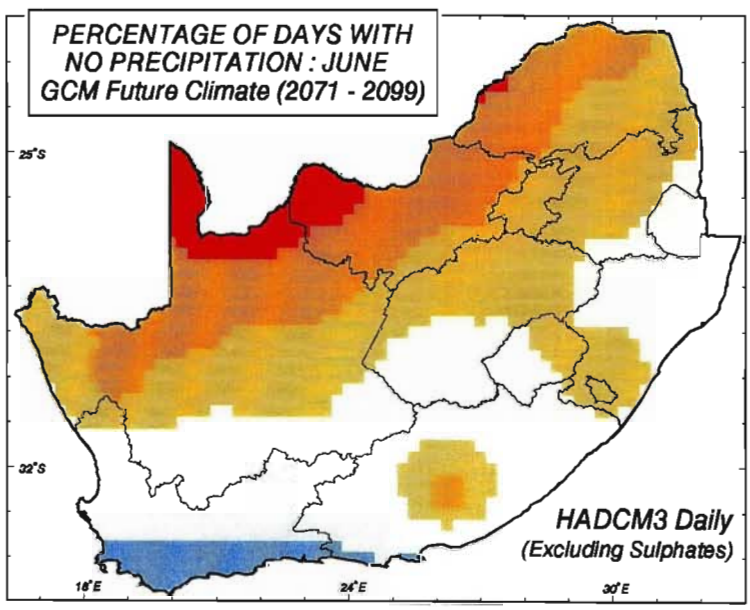


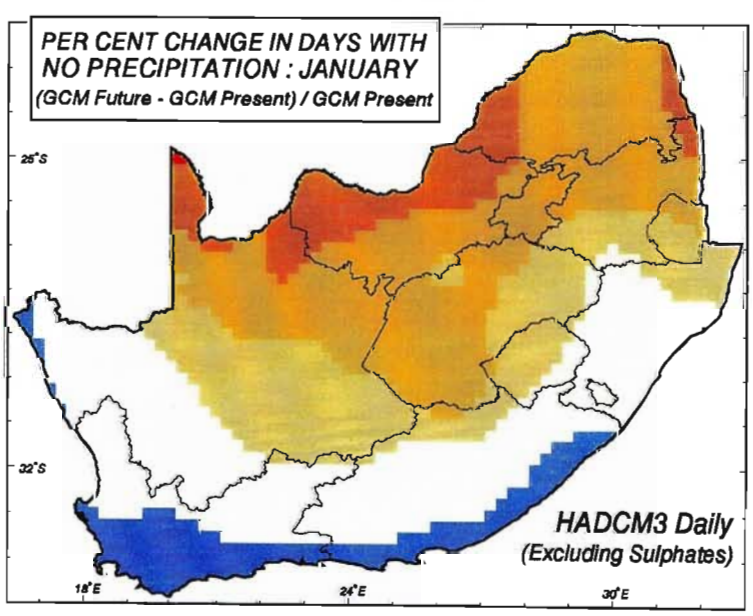


School of
Bioresources Engineering and
Environmental Hydrology
University of Natal
Pietermaritzburg
South Africa

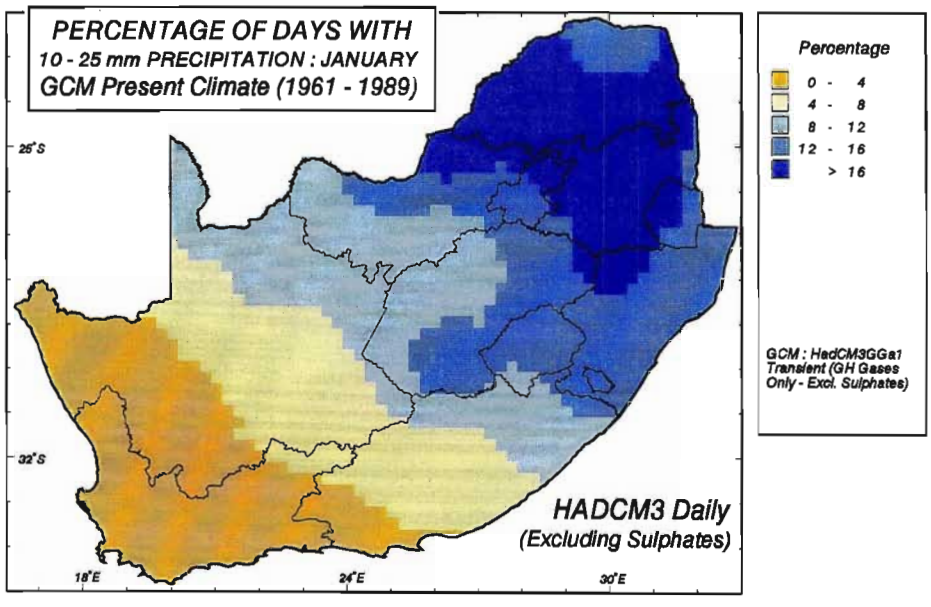


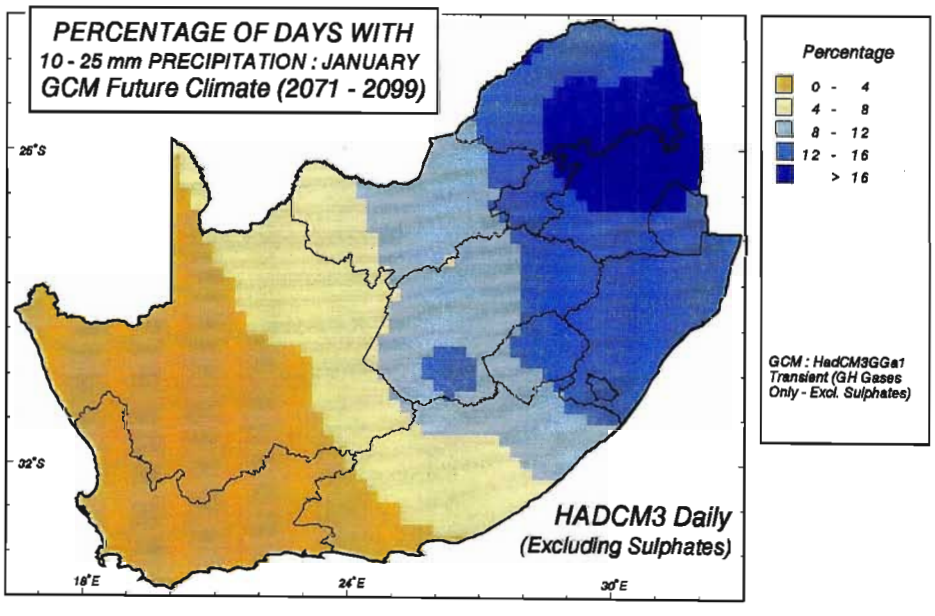


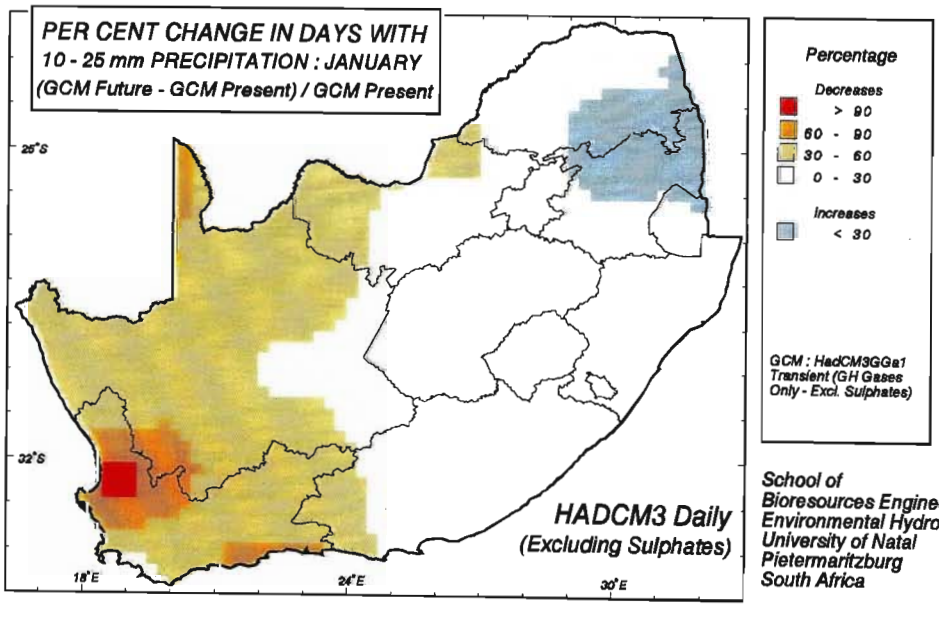


School of
Bioresources Engineering and
Environmental Hydrology
University of Natal
Pietermaritzburg
South Africa

Using HadCM3-S, an overall decrease in the number of days with precipitation between 10 and 25 mm in a future climate is simulated for January under future climatic conditions (Figure 6.22, middle). The largest decreases in days with rainfall of this magnitude range are simulated in the south-west of southern Africa. Most of the study area is simulated by this GCM to have a 30 - 60% decrease in days experiencing 10 to 25 mm rainfall, however, small increases in days with this magnitude could occur in the north-east of the study area (Figure 6.22, bottom). For the month of June a large portion of the study area is simulated to have less than 2% of its precipitation falling in the 10 - 25 mm per day category in the present climate scenario by HadCM3-S (Figure 6.23, top). Higher percentages of days of this rainfall range (over 6%) in June are possible along the southern coastline under present climatic conditions, according to this GCM.

Figure 6.23 Percentage of days with 10 to 25 mm precipitation in June: Present climate (top), future climate (middle) and per cent change in days with 10 to 25 mm precipitation (bottom). Both climate scenarios from HadCM3-S

In June, there is a simulated decrease in percentage of days classified in this rainfall category in the south of southern Africa, using the future climate generated by HadCM3-S (Figure 6.23, middle). The winter rainfall areas in the west of the study area could have more than a 30% decrease in days with 10 - 25 $mm.day^{-1}$ events in June (Figure 6.23, bottom). This decrease and could have significant implications for the water resources and winter wheat yields in these areas.

Time series were prepared for present and future climatic conditions for January and June for the HadCM3-S GCM point located at 30°00'S 30°00'E to examine potential changes in daily rainfall amounts for this point generated by this GCM. Figure 6.24 shows the daily rainfall amounts for June for the period 1961 - 1989. This is a dry time of year at this GCM point, which experiences the majority of its rainfall in summer. Five rainfall events over 10 mm were simulated for the 29 year period by HadCM3-S. However, the future climate simulations produced eight rainfall events over 10 mm for June from 2071 - 2099 (Figure 6.25). This

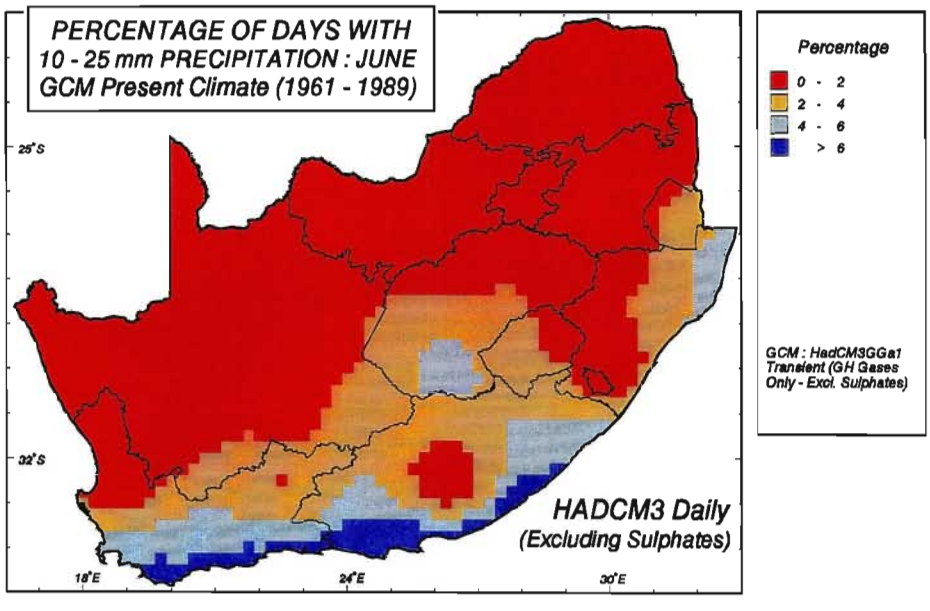


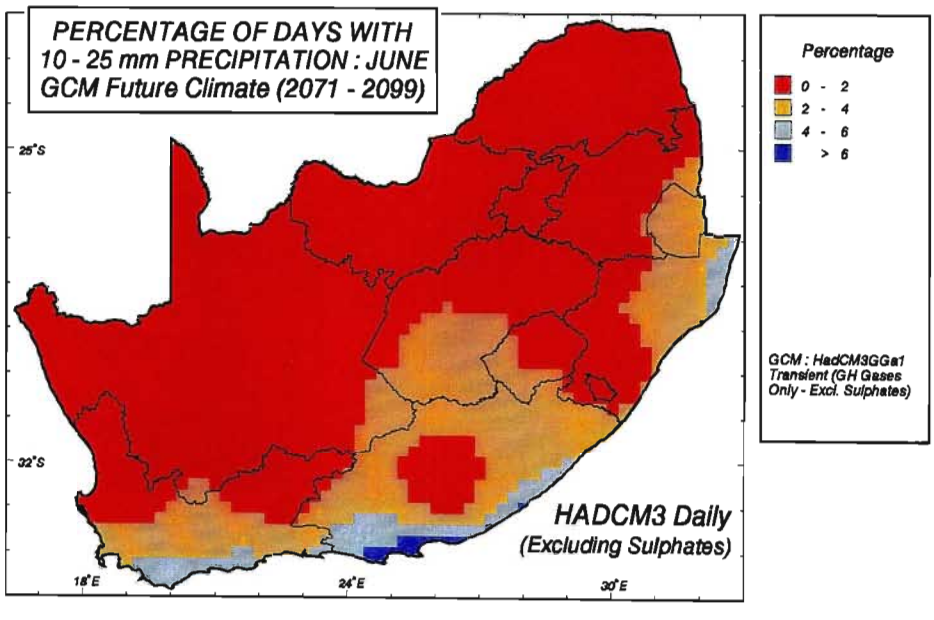


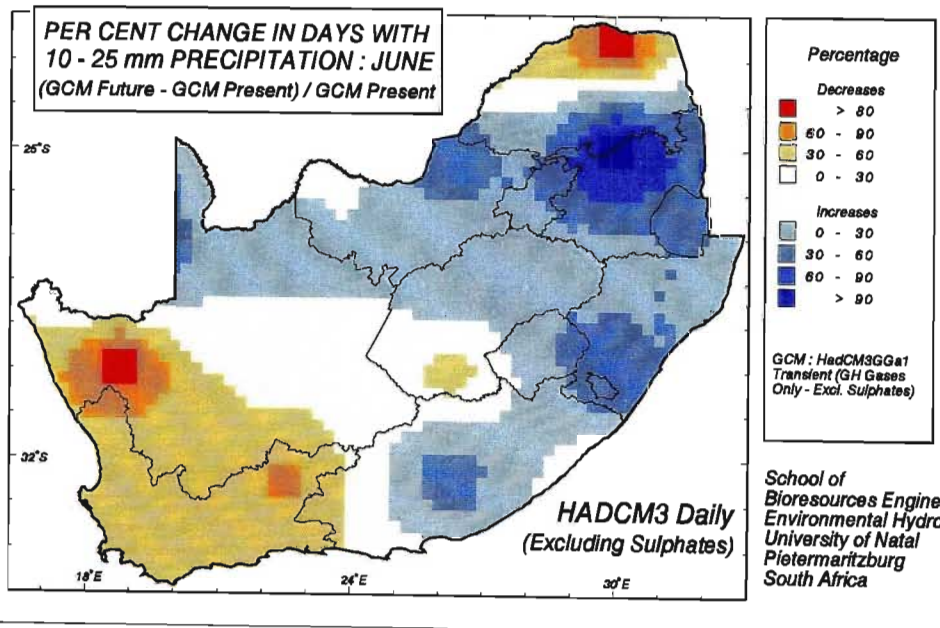


School of
Bioresources Engineering and
Environmental Hydrology
University of Natal
Pietermaritzburg
South Africa

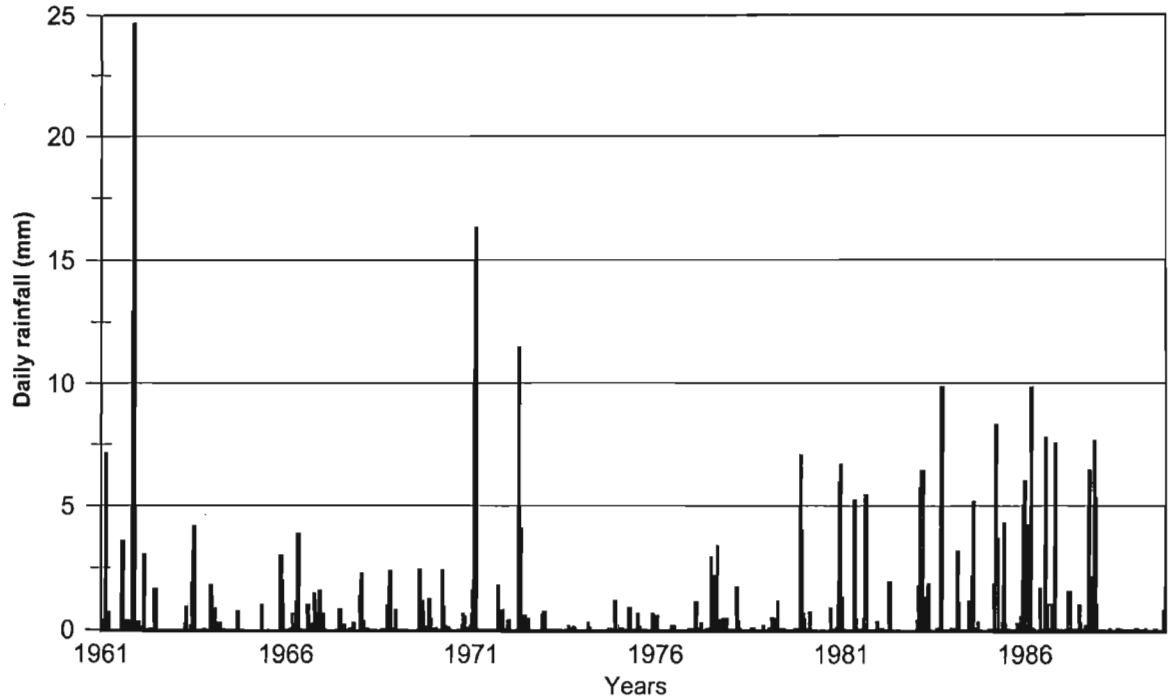


Figure 6.24 Daily rainfall amounts simulated by HadCM3-S for present climatic conditions (1961 - 1989) for the month of June for the GCM point located in the coastal summer rainfall zone (30°00'S 30°00'E)

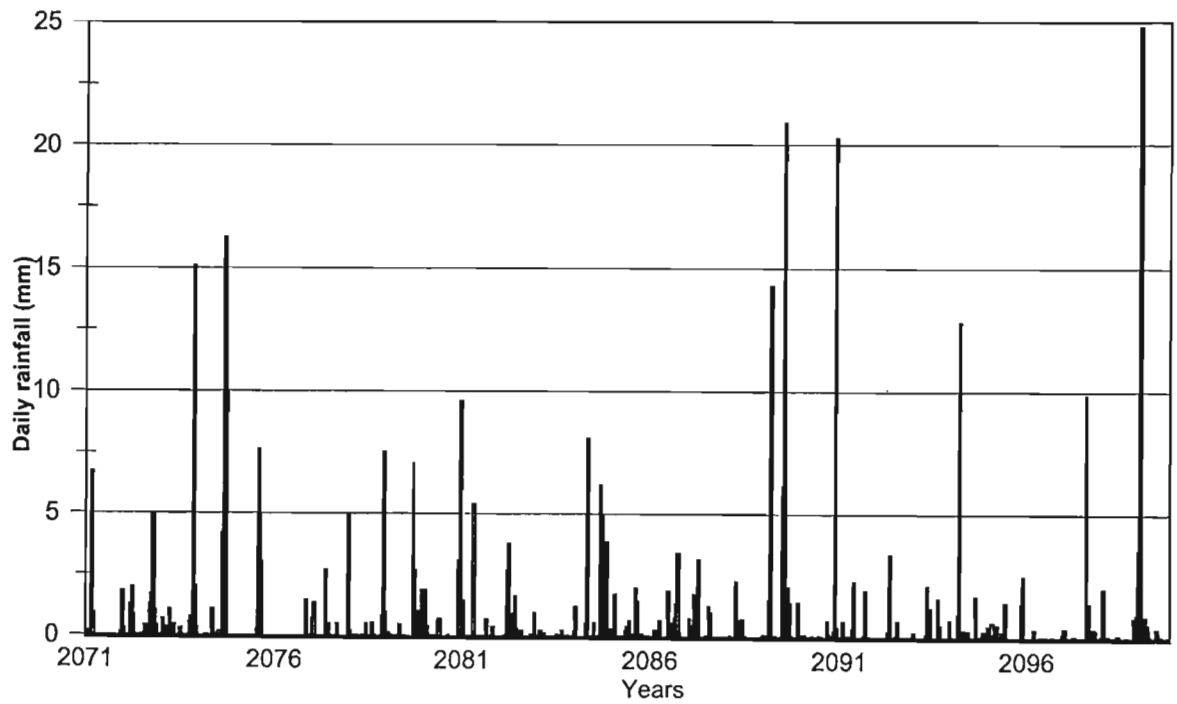


Figure 6.25 Daily rainfall amounts simulated by HadCM3-S for future climatic conditions (2071 - 2099) for the month of June for the GCM point located in the coastal summer rainfall zone (30°00'S 30°00'E)

equates to a 58% increase in days with this magnitude of rainfall in a future climate scenario. This would indicate a possible significant increase in medium to high rainfall events in June in the eastern, coastal region of the study area in a future climate.

### 6.7.5 Potential changes in number of days with more than 25 mm precipitation

Raindays with greater than 25 mm can produce marked hydrographs as well as generating significant amounts of sediment in a catchment. In January, most of southern Africa is simulated to have fewer than 2% of days with precipitation recording above 25 mm. The exceptions to this trend are the most easterly regions of KwaZulu-Natal which, according to HadCM3-S, record over 6% of raindays in this category (Figure 6.26, top).

| | |
|---|---|
| Figure 6.26 | Percentage of days with more than 25 mm precipitation in January: Present climate (top), future climate (middle) and per cent change in days with more than 25 mm precipitation (bottom). Both climate scenarios from HadCM3-S |

This could potentially change in future with a greater portion of the study area experiencing 2 to 4% of days with greater than 25 mm precipitation in January (Figure 6.26, middle). This equates to large increases in days with rain exceeding 25 mm in the eastern half of the study area, with the western part of KwaZulu-Natal potentially experiencing 80 to 120% more days with greater than 25 mm precipitation than at present. This is a significant increase in rainfall events of this magnitude, particularly as the majority of the rain falls in summer in this part of southern Africa. If this future scenario from HadCM3-S is assumed realistic, the net result from these increases in rainfall of this magnitude could be an increases in stormflow and sediment yield generation in this Province.

In June, only a small percentage of days are simulated with raindays greater than 25 mm using output from the HadCM3-S for present climatic conditions (Figure 6.27, top). However, the percentage of events of this magnitude appears to increase in many areas in a future climate (Figure 6.27, middle), particularly in the southern and eastern parts of the study area.

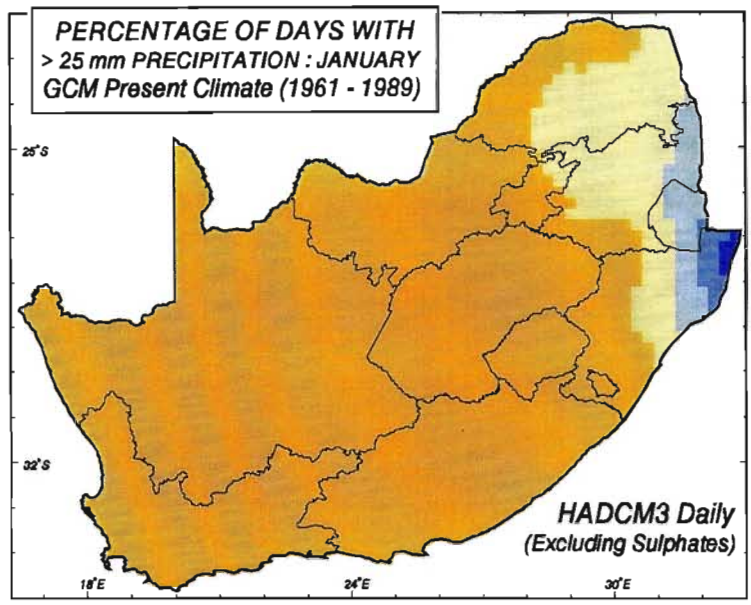


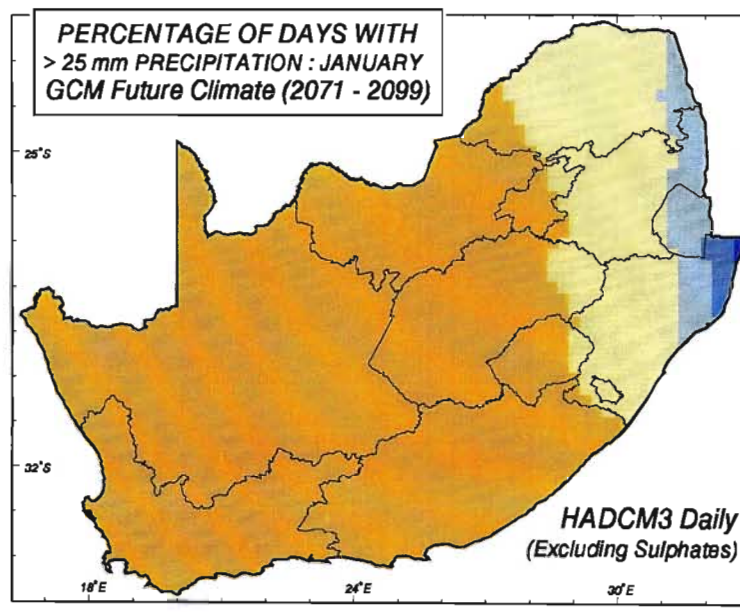


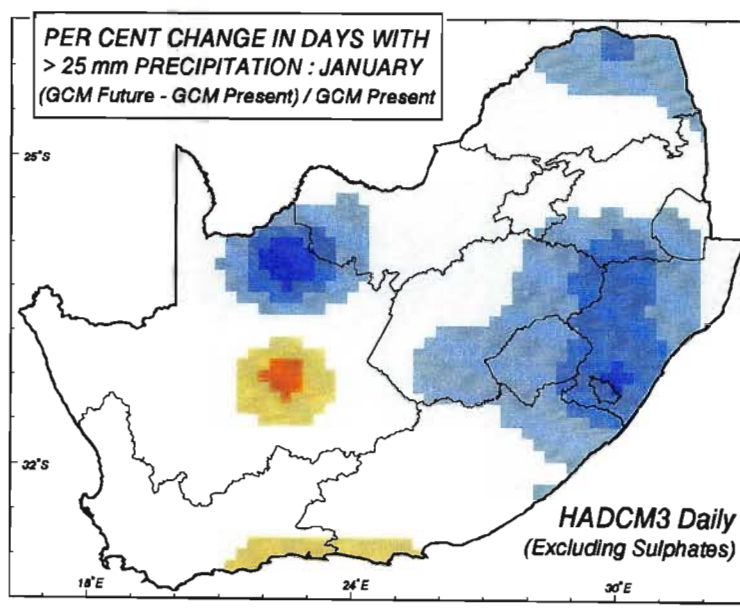


School of
Bioresources Engineering and
Environmental Hydrology
University of Natal
Pietermaritzburg
South Africa

Significant increases (over 200%) in the number of days with rainfall over 25 mm are simulated in the central parts of the study area compared to present climatic conditions. In addition, increases in rainfall events of this magnitude area simulated by HadCM3-S in the winter rainfall areas which could negatively impact the hydrology in these western areas (Figure 6.27, bottom).

| | |
|---|---|
| Figure 6.27 | Percentage of days with more than 25 mm precipitation in June: Present climate (top), future climate (middle) and per cent change in days with more than 25 mm precipitation (bottom). Both climate scenarios from HadCM3-S |

In the graph shown in Figure 6.28 nine rainfall events exceeding 25 mm of rainfall were simulated by HadCM3-S for present climatic conditions in January for the years 1961 to 1989 for the GCM point 30°00'S 30°00'E. However, using output from HadCM3-S it is evident that under future climatic conditions (2071 - 2099) the number of occurrences of rainfall events of greater than 25 mm per day in January appears to increase to more than 15 events for the 29 year time period (Figure 6.29). This equates to a 66% increase in days with more than 25 mm rainfall compared to present climatic conditions. This is significant as this is a summer rainfall area. The highest simulated value for the present climatic conditions in January is around 40 mm in 1966 (cf. Figure 6.28). In comparison the highest value simulated by HadCM3-S for future climatic conditions is over 60 mm in 2085 (cf. Figure 6.29).

### 6.7.6 Potential changes in number of days with more than 50 mm precipitation

High magnitude events (classified here as over 50 mm per day) cause flooding under certain conditions and therefore changes in these extreme events can be significant from a flood protection perspective. Only results from potential changes in these high magnitude events in January are presented, as the number of events greater than 50 mm per day in June was very small.

According to results from HadCM3-S less than 1% of days receive are over 50 mm for most parts of the study area in January (Figure 6.30, top). For a future climate scenario the north-

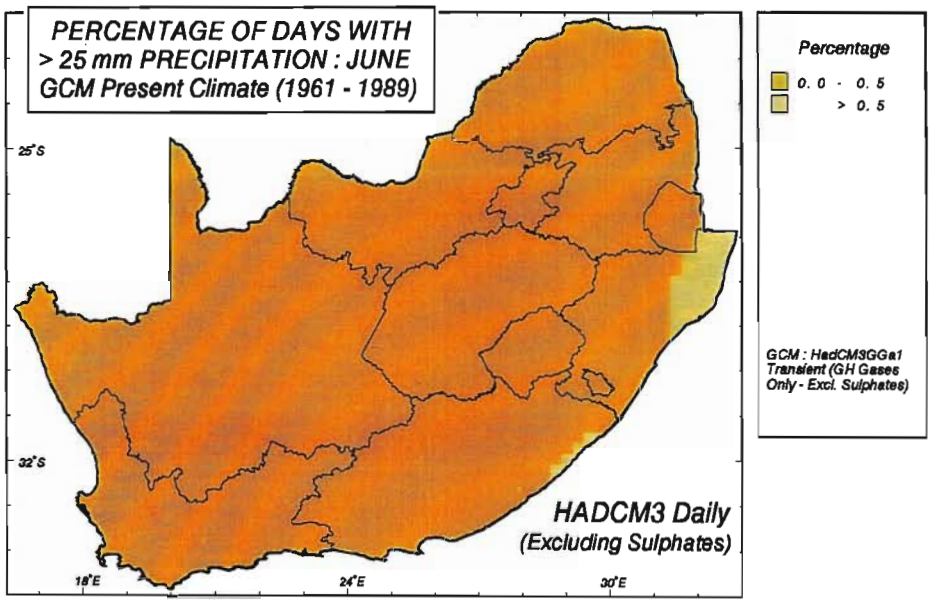


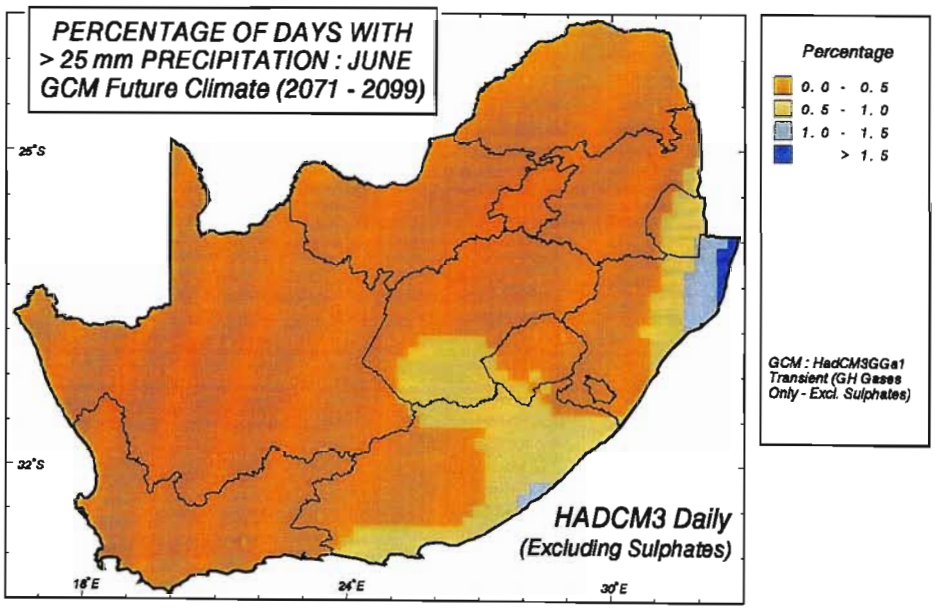


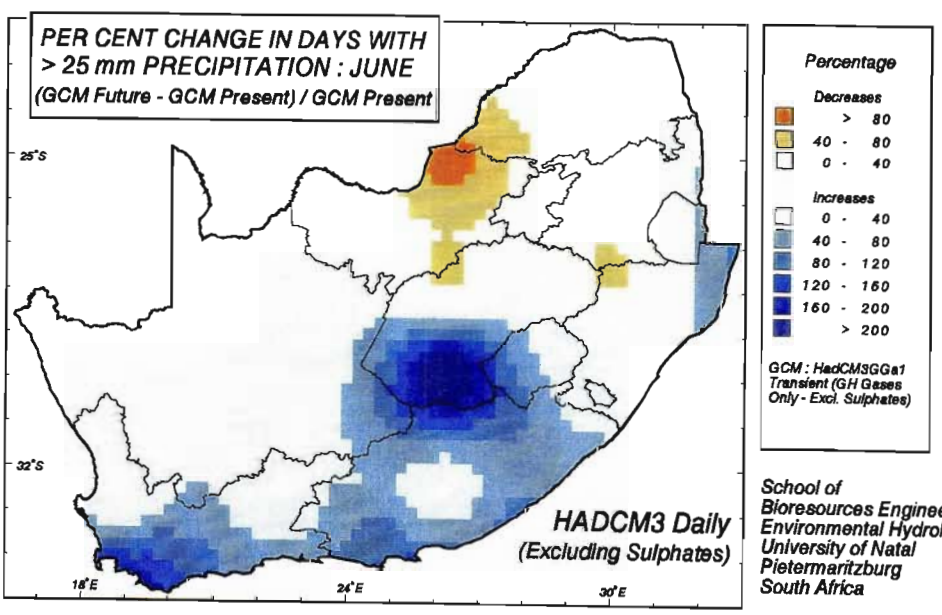


School of
Bioresources Engineering and
Environmental Hydrology
University of Natal
Pietermaritzburg
South Africa

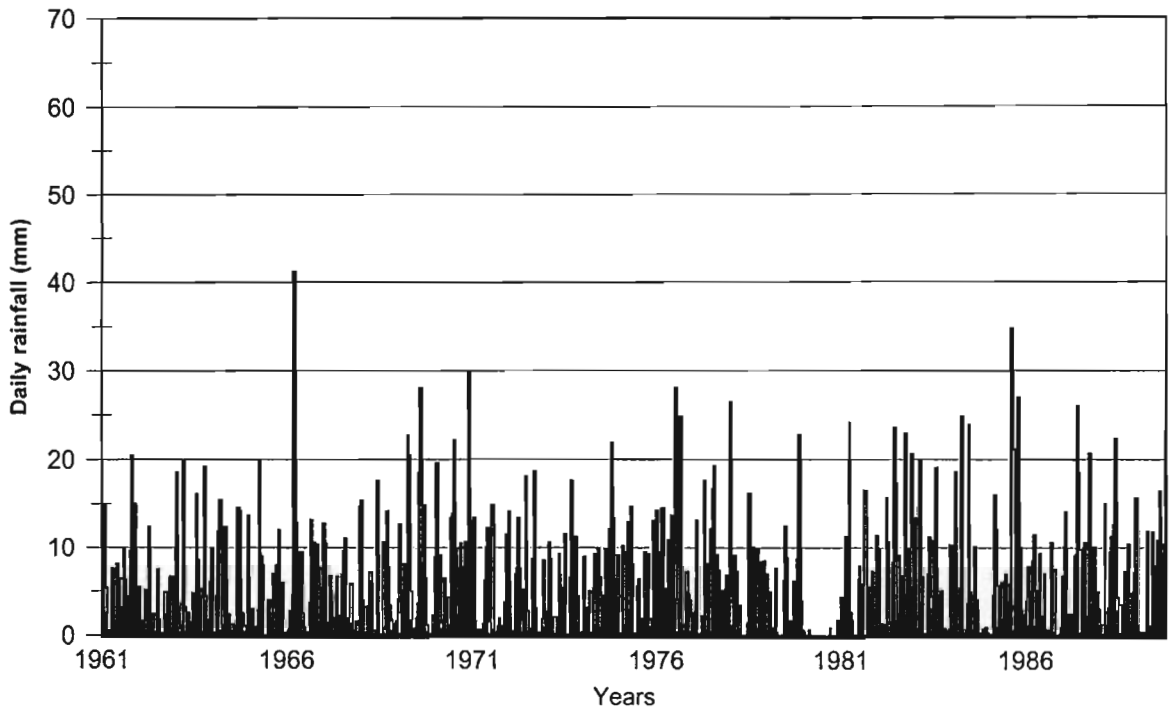


Figure 6.28 Daily rainfall amounts simulated by HadCM3-S for present climatic conditions (1961 - 1989) for the month of January for the GCM point located in the coastal summer rainfall zone (30°00'S 30°00'E)

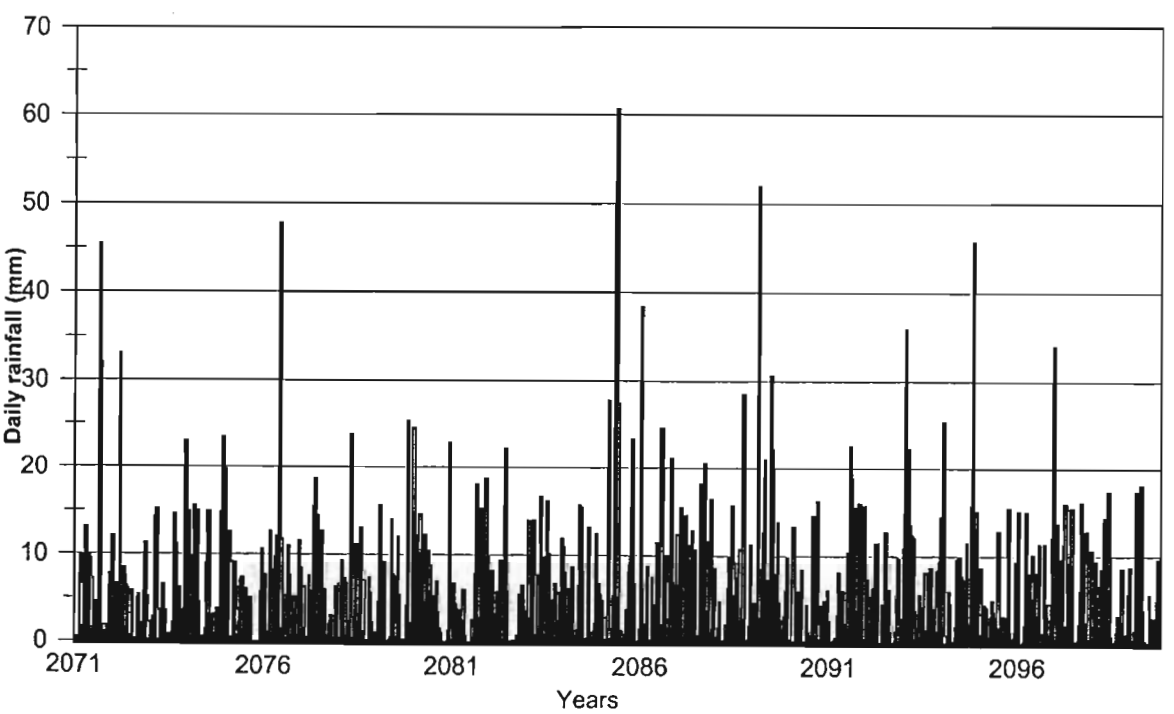


Figure 6.29 Daily rainfall amounts simulated by HadCM3-S for future climatic conditions (2071 - 2099) for the month of January for the GCM point located in the coastal summer rainfall zone (30°00'S 30°00'E)

eastern parts of the study area could receive an increase of rainfall events of this magnitude in the order of 0 - 120%, which could be significant as this is a summer rainfall area. The western two-thirds of the study area could experience decreases up to 40% in high magnitude rainfall events in January (Figure 6.30, middle and bottom).

| | |
|---|---|
| Figure 6.30 | Percentage of days with more than 50 mm precipitation in January: Present climate (top), future climate (middle) and per cent change in days with more than 50 mm precipitation (bottom). Both climate scenarios from HadCM3-S |

From this analysis of potential changes in rainfall variability, HadCM3-S simulates

i) an overall decrease in mean daily rainfall for January and June with the exception of KwaZulu-Natal, in particular, which could have small increases in mean daily precipitation;

ii) an increase in the coefficient of variation for the summer rainfall zones in summer and winter rainfall zones in winter;

iii) increases in the percentage of days in January with no rainfall in the north of between 25% and 100% compared to present climatic conditions and small decreases in the south of the study area;

iv) large decreases in the percentage of days with no rainfall in the central parts of southern Africa in June;

v) a decrease in the percentage of days with 10 - 25 mm rainfall in the winter rainfall region in June;

vi) significant changes in the percentage of days with more than 25 mm of rainfall over southern Africa in January with an increase in the number of events of this intensity particularly in the summer rainfall areas in the north and east of the study area;

vii) increases in the number of days in June with events greater than 25 mm, particularly in the central and southern parts of southern Africa; and

viii) a significant increase in January of high magnitude rainfall events (> 50 mm) in the far east of southern Africa and a small decrease in rainfall events over 50 mm in the western two-thirds of the study area.

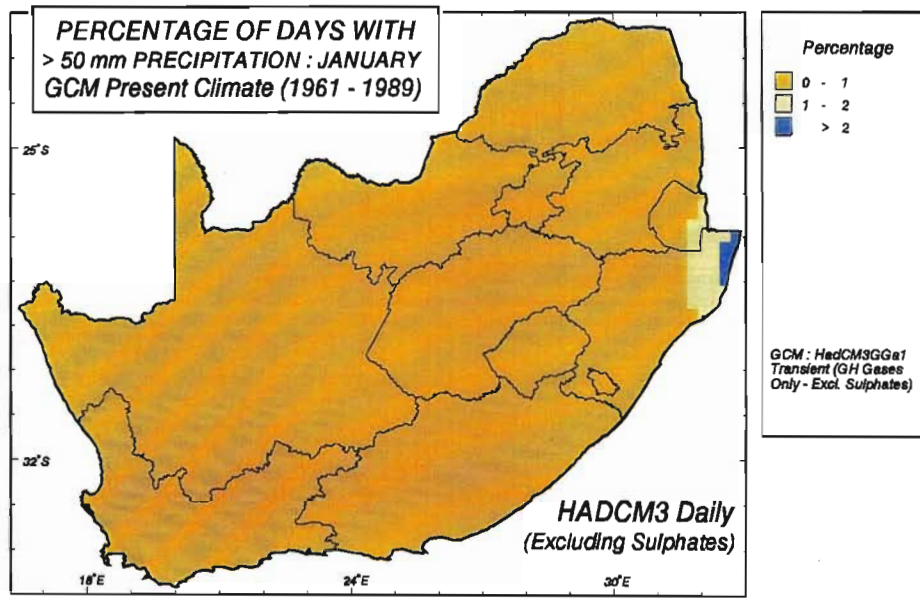


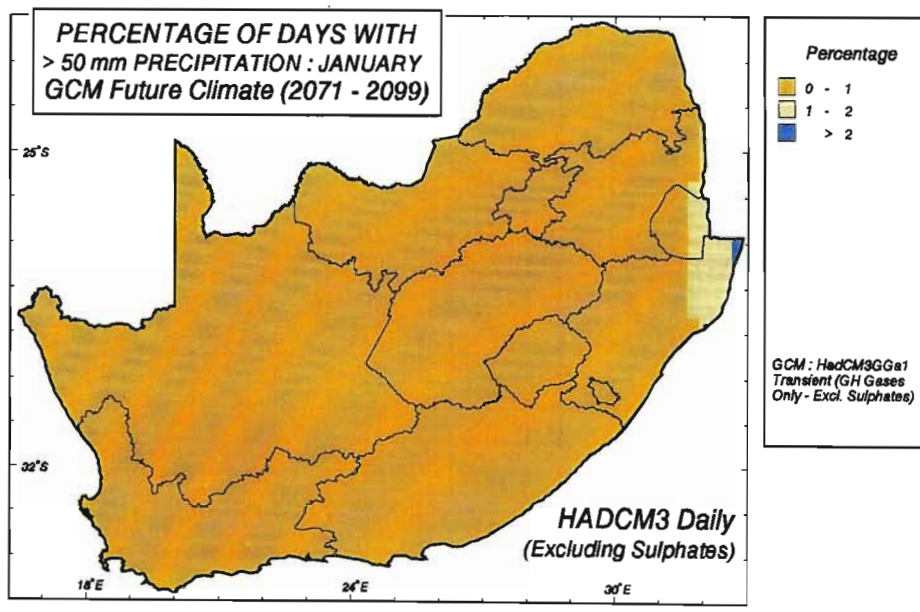


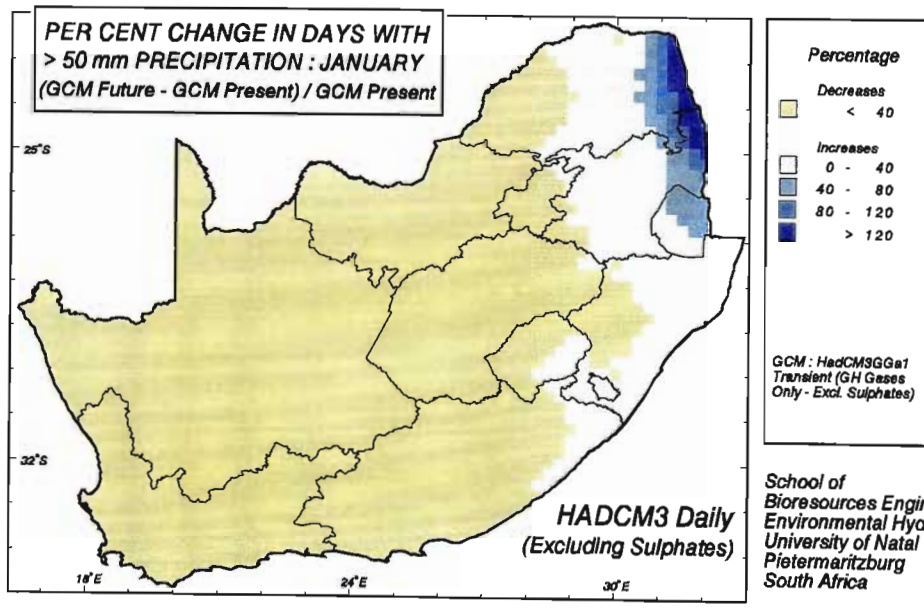


School of
Bioresources Engineering and
Environmental Hydrology
University of Natal
Pietermaritzburg
South Africa

These findings could indicate a possible increase in extreme events in a future climate with an associated increase in flood risk. An increase in extreme events would increase financial demands on the public and private sectors to cover insured and uninsured weather related losses.

* * * * * * *

This chapter has described the methodology of interpolating the coarse GCM grid output of temperature and precipitation to a finer spatial resolution through inverse distance weighting for application in agrohyrological models. The maps of predicted seasonal changes in temperature and precipitation illustrate the large discrepancies between the four GCMs and the uncertainties associated with using output from the GCMs.

Various analyses were undertaken to assess the performance of the GCM output for present climatic conditions against observed climate. In the case of monthly output from the GCMs, there are significant discrepancies in the 1X $CO_2$ climate output from the GCM compared with values from present-day observations and, therefore, it is considered more correct to use the *absolute differences* in the case of temperature, but the *relative differences* in the case of precipitation, in conjunction with the baseline climate estimates to obtain future scenarios of temperature and precipitation. The verification study of the daily variability simulated by HadCM3-S showed a potentially significant increase in variability in a future climate and a possible increase in the higher intensity rainfall events particularly in the eastern half of the study area. Output from the HadCM3-S only was verification as output from the HadCM3+S was unavailable at the time these analyses were carried out.

The analyses of potential changes in rainfall variability in the study area point to an change in the coefficient of variation of daily rainfall as well as the increase in high magnitude events. However, the interpolation of these grid surfaces from a few points across southern Africa leads to uncertainty in the use of these surfaces in the climate impact assessments. Uncertainties in these assessments which will be discussed in greater detail in Chapter 11.

The following chapter outlines the structure of the *ACRU* Input Database, the refinement of tools to use the Input Database in conjunction with the *ACRU* model to simulate potential impacts of climate change on the agrohydrological system at both the Quaternary and Quinary Catchment scale, and the subsequent process of extracting the results for presentation using a GIS.

# 7. LINKING THE *ACRU* INPUT DATABASE TO THE *ACRU* MODEL AND GIS

The inputs required for the *ACRU* model need to be written into the model's input menu prior to simulation of any catchment. Instead of storing the information pertaining to each catchment in the *ACRU* input menu in preparation to perform climate impact assessment in southern Africa, the information required for the *ACRU* simulations has been stored in a database. An interface has been developed whereby information can be selected from an *ACRU* Input Database and automatically read into the *ACRU* model's input menu for the model to run.

Briefly, an *ACRU* Input Database is established containing information required by the *ACRU* model for agrohydrological simulations. A variety of climate information can be used in the simulation, which includes the option of using a future climate scenario from a selected GCM. Relevant catchment information stored in the database can be extracted for simulation. Selected output from the model runs can be displayed in the form of maps or time series. This process will be expanded upon in greater detail in subsequent sections of this chapter.

As shown in Figure 7.1 four main themes constitute Chapter 7. The first theme is the *ACRU* Input Database structure developed for use with the *ACRU* model. The next theme is the interface between this Input Database and the model. The third theme is the simulation of agrohydrological responses for climate impact assessment using *ACRU* and lastly the extraction of output from the model for presentation of results.

In Section 7.1 the initial structure of the *ACRU* Input Database used to simulate agrohydrological responses of the Quaternary Catchments is outlined (cf. Figure 7.1). This database structure was found to be limiting and was subsequently revised, as described in Section 7.2. The new database structure allows for greater flexibility when carrying out an *ACRU* simulation for climate impact assessments or other agrohydrological simulation. In addition, this revised structure facilitates the option of subdividing the Quaternary Catchments

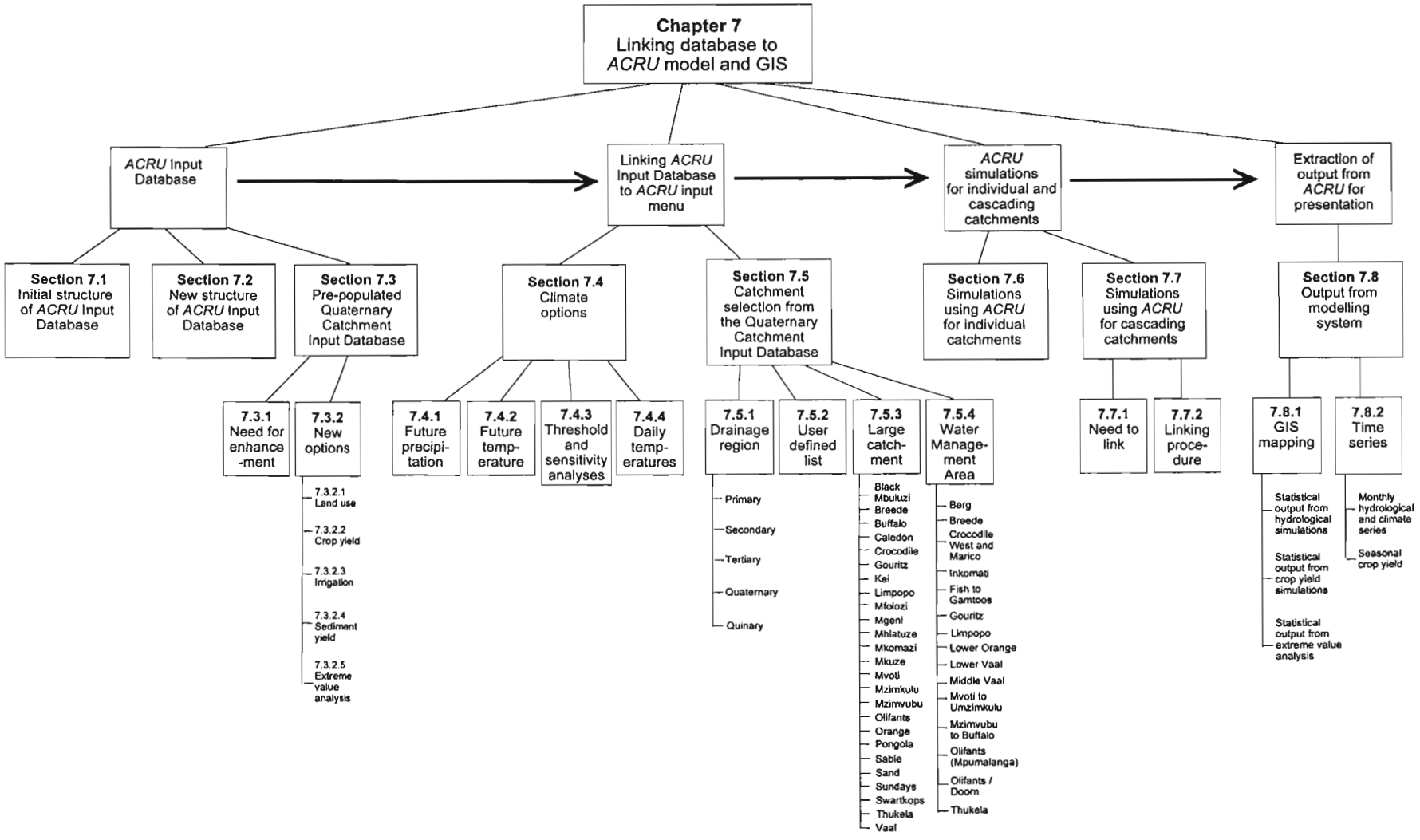


Figure 7.1 Layout plan of Chapter 7: Linking the *ACRU* Input Database to the *ACRU* model and GIS

into Quinary Catchments in those Quaternaries with a high intra-catchment variability which, through subdivision, may result in a more realistic hydrological simulation.

The new database structure was used to store the *ACRU* input parameters for the 1946 Quaternary Catchments in southern Africa as a pre-populated database which can be accessed by multiple users. However, the information stored in the *ACRU* Input Database for each Quaternary Catchment needed enhancement, as highlighted in Section 7.3.

The next objective was to develop an interface to link the *ACRU* Input Database to the *ACRU* model's input menu. This interface facilitates the incorporation of future climate scenarios, different levels of temperature input (Section 7.4) and the quick selection of catchments whose information has been stored in the database (Section 7.5). When using this interface there is the choice of simulations methods, i.e. simulating the hydrology of selected catchments individually or as cascading interlinked catchments. The methodology used for the simulation of catchments in *ACRU* is explained in Sections 7.6 and 7.7. Lastly, the extraction of output from *ACRU* for input into a GIS or for display as a time series is described in Section 7.8.

## 7.1 Initial Structure of the *ACRU* Input Database

The *ACRU* agrohydrological model (described in Chapter 4) was used for various components of this assessment. Various inputs, *viz.* information on soils, land use and climate for each catchment being simulated are required for the *ACRU* model and are input into the model's input menu. The *ACRU* input menu is a formatted ASCII file in which the various hydrological variables required by *ACRU* are entered prior to simulation. Meier (1997) established an *ACRU* Input Database structure for the input data required for simulating hydrological responses from the Quaternary Catchments using the *ACRU* model.

This database structure was used for the initial climate impact assessments. However, this structure was found to be limiting when subdivision of the Quaternary Catchments was potentially required and, therefore, the *ACRU* Input Database was restructured to allow for the

inclusion of information on the subdivided Quaternary Catchments, as expanded upon in Section 7.2.

The procedure of storing the Quaternary Catchment database information in direct access ASCII files and reading them into an *ACRU* input menu was automated by Meier (1997). Each Quaternary Catchment was assigned a numerical identity as a reference. The input information for *ACRU* could then be written to a direct access ASCII file in the order of the numerical identity, such that each line number represented a particular Quaternary Catchment. Thus, once the Quaternary Catchment in question had been selected, it was possible to identify its corresponding numerical identity and, using this number, directly access the hydrological information pertaining to it from the respective files (Meier, 1997). Using this method of reference to the numerical identification number, seven ASCII files were created for each Quaternary Catchment by Meier (1997) containing information on

i) the daily rainfall station file number;
ii) 12 values of monthly means of daily maximum temperature;
iii) 12 values of monthly means of daily minimum temperature;
iv) 12 values of monthly totals of A-pan equivalent reference potential evaporation;
v) catchment attributes (e.g. area, mean altitude, mean annual precipitation, centroid latitude and longitude);
vi) soils attributes (e.g. horizon thicknesses, soil water contents at the lower limit, drained upper limit and porosities of the top- and subsoil horizons, termed hereafter A and B horizons, as well as saturated drainage redistribution rates from the A to B horizons and from the B horizon into the intermediate groundwater zone); and
vii) land cover attributes required by the *ACRU* model (e.g. monthly values water use coefficient, vegetation interception losses per rainday, rooting distributions of the A horizon).

Meier (1997) compiled a UNIX script whereby the Quaternary Catchment database information could be extracted and be written to the *ACRU* menu. The menu consists of a set number of lines with each line having the same length. The *ACRU* model can then use the menu as a direct access file to read input information from any required line number. The

running of the *ACRU* model and subsequent saving of portions of the output could then be performed automatically on each Quaternary Catchment, as indicated in Figure 7.2.

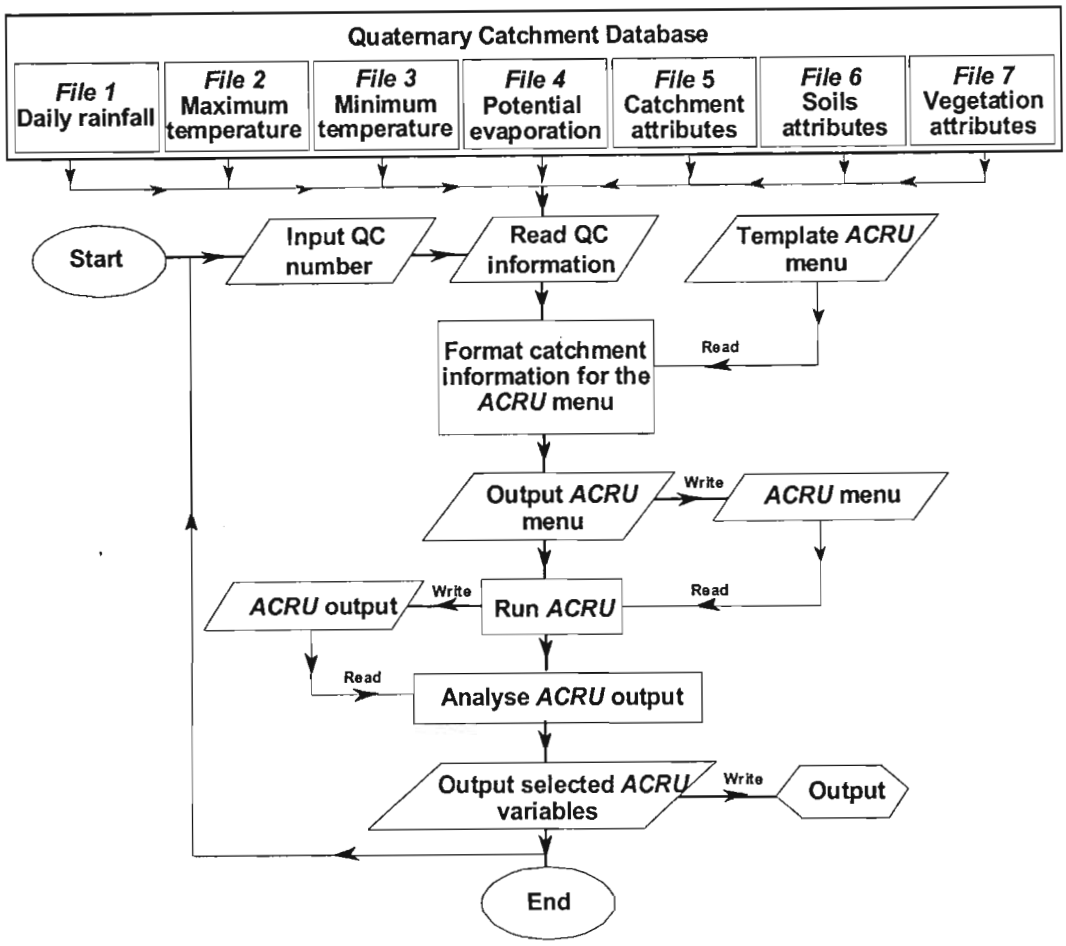


Figure 7.2 Linking the Quaternary Catchment Input Database to the *ACRU* model, as established by Meier (1997)

## 7.2 Revised Structure of *ACRU* Input Database

Assigning each Quaternary Catchment a numerical identity from which all information pertaining to that Catchment could be identified via direct access became limiting when additional catchments needed to be added to the database. In addition, this database structure could only be used for simulating agrohydrological responses of the Quaternary Catchments and not, say, Quinary Catchments. Therefore, the *ACRU* Input Database was restructured to allow for both information on additional catchments to be added as well to allow flexibility

of the system to be able to store *ACRU* input information on any catchment in southern Africa in a database.

The first stage of this restructuring involved reorganising the *ACRU* input information into a single file. The single file is stored in a spreadsheet, thereby allowing more flexible modification and manipulation of the *ACRU* input information in a familiar format. Each row in the spreadsheet refers to a catchment and each column contains input data for the *ACRU* model. The column names follow the parameter names used in the *ACRU* input menu, however, the columns need not be in the same order as they occur in the input menu. The first column is the name of the catchment, e.g. U10A. In total there are 612 *ACRU* inputs possible into the *ACRU* input menu. However, not every input is used in a simulation, for example, if no irrigation is specified in a catchment then irrigation information is not required by the model.

Once the database has been established it is exported from the spreadsheet in comma delimited format and is subsequent converted to an array through a Fortran script. The row containing the *ACRU* input information pertaining to the catchment selected for simulation can be extracted by matching the catchment selected with the catchment name recorded in the first column of the database. This allows for greater flexibility with the naming of the catchments using either alphabetic or numerical identity.

In the previous database structure the seven ASCII files mentioned in Section 7.1 stored the information which pertained to the Quaternary Catchments, and any additional information, e.g. inputs required to carry out a sediment yield analysis, that had to be hard-coded into the Fortran program used in creating the *ACRU* input menus. This system is restricting and the problem was addressed when establishing the new database structure. Greater flexibility in adding new *ACRU* input information was achieved by giving each new *ACRU* input variable added to the database, over and above the original input information, a new input name. For example, the standard name for the *ACRU* input name referring to the raingauge used to "drive" the hydrology of a particular catchment is RAINSTA. However, the situation might arise that an improved driver station is found and, therefore, this new raingauge name needs

to be recorded in the database as an new option. This updated list of rain gauges could be added to the Input Database under the header of, say, RAINSTA2.

The user can then create another spreadsheet file which contains the list of

i) the standard *ACRU* input variable name;

ii) the additional *ACRU* input variable name; and

iii) a description of what information is containing under this new heading.

Multiple new options can be added to what is termed the New Options File. This file is also exported as a comma delimited file from the spreadsheet package and converted to an array using a Fortran script. The various additional options available in the database can be selected or deselected depending on the information required for the simulation as is expanded upon in Section 7.7.

The information pertaining to each Quaternary Catchment stored in the ASCII files, as well as the information that had been hard-coded in the original linking program, was imported into the new database structure and this pre-populated database is described in the following section.

## 7.3 The Pre-Populated Quaternary Catchment Input Database

The Quaternary Catchment Input Database can be used as input to simulate agrohydrological responses of Quaternary Catchments in southern Africa. As updated information is obtained for each Quaternary Catchment it can be included in the database and become available to users of this Input Database.

### 7.3.1 Need for enhancement of the Quaternary Catchment Input Database

The linkage of the *ACRU* Input Database to the *ACRU* model marked a continuation of work on agrohydrological regionalisation previously undertaken by the School of BEEH (e.g. Dent *et al.*, 1989; Schulze and Lynch, 1992; Schulze *et al.*, 1993). However, the operational

facilities for simulating the responses from the Quaternary Catchments were limiting, for the following reasons:

i) There was no direct facility to easily change the land use attributes of, say, veld in fair hydrological condition to, for example, veld in poor or good condition in a Quaternary Catchment.

ii) No direct option was available for the simulation of crop yield or irrigation requirement estimations.

iii) There was no option to perform any extreme value analysis of, say, floods or perform sediment yield analysis.

Each of these limitations was addressed, as described in the following section.

### 7.3.2 Enhancement of the Quaternary Catchment input information

Enhancements to the Quaternary Catchment Input Database included the incorporation of information on different land use options as well as the *ACRU* inputs required to carry out crop yield simulations, irrigation scenarios, sediment yield estimates and extreme value analysis.

#### 7.3.2.1 Land use options

Previously all simulations undertaken for climate change studies at a southern Africa scale in the School of BEEH assumed a baseline land cover of veld in fair hydrological condition, as described by Schulze *et al.* (1993) and Schulze *et al.* (1995c). As an additional option it was felt necessary to allow the user to at least be able to specify the land use as being the equivalent of veld in poor or good hydrological condition in addition to veld in fair condition, in order for simple impact studies of grazing management on, say sediment yield, to be undertaken. This required changes to the monthly values of the water use coefficient, $K_d$ (Table A1 in Appendix), leaf area index, LAI (Table A2 in Appendix) and the coefficient of initial abstraction, COIAM (Table A3 in Appendix), depending on the condition of the veld specified. The values for these new parameters were added to the Quaternary Catchment Input Database as options for simulations and are recorded in the New Options File for the Quaternary Catchment Input Database.

The monthly values of the coefficient of initial abstraction have been calculated for typical rainfall intensity characteristics depending on which rainfall seasonality region the Quaternary Catchment falls into, as shown in Tables A4 and A5 of the Appendix.

#### 7.3.2.2 Crop yield options

Information on plant dates, length of growing season and biomass indicators for maize, winter wheat, sugarcane and primary production have been added to the Quaternary Catchment Input Database. The default plant dates and lengths of the growing seasons that are used for the Quaternary Catchments are given in Table 7.1. However, if updated input information is obtained for different regions these can be incorporated into the Input Database for use.

Table 7.1 Default values of plant dates and lengths of growing season for various crops yields which can be simulated using *ACRU* at a Quaternary Catchment scale

| Crop | Plant Date | Length of Growing Season |
|---|---|---|
| Maize | 15 November | 150 days |
| Sugarcane | 1 July | N/A (yields annualised) |
| Winter Wheat | 15 May | 150 days |
| Primary Production | 1 August | N/A (yields annualised) |

Maize yield is estimated in *ACRU* using the *ACRU* maize yield model (Schulze *et al.*, 1995d). A detailed study of potential change in maize yield resulting from changes in climate was carried out using the *ACRU* maize yield model and the 2X $CO_2$ climatic conditions as estimated by HadCM2. When maize is specified to be planted in the Quaternary Catchment then the month-by-month values of water use coefficient ($K_d$), vegetation interception loss ($I_l$) and roots in A horizon ($R_A$) that have been used in the Quaternary Catchment Input Database are input. These are given in Table A6 in the Appendix. A description of the *ACRU* maize yield model and results from assessments of potential changes in maize and winter wheat with climate change are presented in Section 8.3 of Chapter 8.

Brief descriptions are given below of the sugarcane and primary production submodels in *ACRU*.

Thompson (1976) developed an equation for estimating sugarcane yield in southern Africa for a 12 month (annualised) period (July to June) which is expressed as

$$Y_c = 9.53 (E_{an} / 100) - 2.36$$

where $Y_c$ = annual sugarcane yield ($t.ha^{-1}$)

$E_{an}$ = total evaporation (mm) for that year.

This sugarcane yield model is imbedded in *ACRU* (Schulze *et al.*, 1995d), where $E_{an}$ is calculated from *ACRU*'s daily multi-layer soil water budget.

In *ACRU*, primary production is estimated using a generic and widely applicable soil water budget submodel which uses the Rosenzweig (1968) equation of

$$\log_{10} P_{pr} = 1.66 \log_{10} E_{an} - 1.66$$

in which $P_{pr}$ = net annual above-ground production ($g.m^{-2}$) and

$E_{an}$ = annual total evaporation (mm).

The estimation of primary production is explained in more detail in Schulze *et al.* (1995d).

When simulating maize yield in *ACRU*, crop transpiration and soil water evaporation are modelled separately according to the Ritchie (1972) method (cf. Chapter 4, Section 4.4.3) and the *ACRU* variable EVTR is set to 2. The winter wheat model also separates transpiration from soil water evaporation on a daily basis, but this done internally within the routine and variable EVTR is specified as equal to 1. For the sugarcane and primary production options transpiration and evaporation are modelled as a single entity (EVTR = 1).

#### 7.3.2.3 Irrigation option

*ACRU* contains routines which can simulate irrigation water requirements for a range of crops under a variety of soil conditions and different modes of applying, i.e. scheduling, the irrigated water.

When the irrigation option is selected for Quaternary Catchment comparisons, a number of simplifying assumptions are, however, made for the sake of convenience. First, irrigation in *ACRU* is activated for each month of the year assuming an areal unit of irrigation (e.g. per hectare) within each Quaternary Catchment. The mode of scheduling is specified as demand irrigation, i.e. applying irrigation water to refill the soil profile to the drained upper limit with an unlimited supply of water for irrigation once profile plant available water has been depleted to 50%. The other simplifying assumptions that are made when the irrigation option is selected are given in Table A7 of the Appendix.

In the water resources component of the study, potential changes in stormflow and percolation from irrigation areas were simulated using *ACRU* and the results are presented in Chapter 9, Sections 9.1.3 and 9.2.3 respectively.

#### 7.3.2.4 Sediment yield analysis

Soil erosion is a serious problem in southern Africa (Lorentz and Schulze, 1995). Rooseboom (1992) estimated that the average annual sediment yield in southern Africa varies between 30 and 330 $t.km^{-2}$. To date a simple method has not been found to estimate sediment yield from a catchment. Complex deterministic models are available to estimate erosion processes and sediment transport, however, these models are limited in their application owing to their reliance on calibration.

The Universal Soil Loss Equation, USLE (Wischmeier and Smith, 1978), is an equation which has received recognition as an empirical method useful for initial planning and design purposes. This method is the foundation for other empirical equations which can be applied at a catchment scale to estimate sediment yield, such as the daily stormflow event based

Modified Universal Soil Loss Equation, MUSLE (Williams, 1975), which has been widely verified world-wide and also in South Africa (Kienzle *et al.*, 1997).

Sediment yield at any Quaternary Catchment outlet may be estimated in *ACRU* using the MUSLE, expressed as

$$Y_{sd} = \alpha_{sy} (Q_v \times q_p)^{\beta sy} K \times LS \times C \times P$$

where
- $Y_{sd}$ = sediment yield from an individual stormflow event (t)
- $Q_v$ = stormflow volume for the event ($m^3$)
- $q_p$ = peak discharge for the event ($m^3.s^{-1}$)
- K = soil erodibility factor ($t.h.N^{-1}.ha^{-1}$)
- LS = slope length and gradient factor (-)
- C = cover and management factor (-)
- P = support practice factor (-).

The MUSLE coefficients, $\alpha_{sy}$ and $\beta_{sy}$ are location specific (Simons and Sentürk, 1992) and are determined for specific climatic zones. However, default values in *ACRU* set at 8.934 for $\alpha_{sy}$ and 0.56 for $\beta_{sy}$ were assumed in this study.

At a Quaternary Catchment scale for southern Africa sediment yield can now be estimated for veld being either in good, fair or poor hydrological condition. A cover factor is required for the calculation of the MUSLE and the values were obtained from the *ACRU* User Manual (Smithers and Schulze, 1995), depending on the veld type, as shown in Table 7.2. The same cover factor is used in all months of the year.

Table 7.2 Cover factor and runoff curve numbers used in the determination of sediment yield at Quaternary Catchment scale depending on the veld type selected

| Hydrological Condition of the Veld | Cover Factor | Curve Number |
|---|---|---|
| Veld in Poor Hydrological Condition | 0.17 | 83 |
| Veld in Fair Hydrological Condition | 0.07 | 75 |
| Veld in Good Hydrological Condition | 0.02 | 68 |

When the sediment yield option is selected, then the peak discharge for each Quaternary Catchment needs to be simulated for each stormflow event. For these simulations the SCS peak discharge as equation modified by Schulze and Schmidt (1995) is used, in which

$$q_p = \frac{0.2083\ QA}{1.83\ L}$$

where $q_p$ = peak discharge ($m^3.s^{-1}$)

$Q$ = stormflow depth (mm)

$A$ = catchment area ($km^2$)

$L$ = catchment lag (response) time (h)

$$= \frac{H_l^{\ 0.8}\ (S' + 25.4)^{\ 0.7}}{7069\ S_{\%}^{\ 0.5}}$$

with $H_l$ = hydraulic length (m) of the main channel of the catchment

$S'$ = catchment retardance factor

$$= \frac{25400}{CN_{II}} - 254$$

$S_{\%}$ = average catchment slope (%)

$CN_{II}$ = Runoff Curve Number unadjusted for catchment antecedent wetness.

Information needed for each Quaternary Catchment thus includes

i) the mean catchment slope, $S_{\%}$, which was obtained from the previously established database (Meier, 1997) using a 1' x 1' digital elevation model;

ii) the hydraulic length, $H_l$ (m), of the main channel, which was estimated from an SCS derived default equation given in the *ACRU* User Manual (Smithers and Schulze, 1995) using catchment area ($km^2$) as

$$H_l\ (m) = 1738 \times A^{\ 0.6}$$

and

iii) the SCS Runoff Curve Number, $CN_{II}$ , unadjusted for antecedent soil moisture conditions of the catchment. The Curve Number is given for various land / use treatment classes, hydrological soil groups and stormflow potentials by the SCS and the *ACRU* User Manual (Smithers and Schulze, 1995). The default $CN_{II}$ values selected for the various veld types are given in Table 7.2.

The values for the vegetation interception loss ($I_l$) and coefficient of initial abstraction (COIAM) used when either an extreme value analysis or a sediment yield analysis is performed are given in Tables A8 and A9 respectively of the Appendix.

#### 7.3.2.5 Extreme value analysis

Predicting the expected magnitude of a rainfall and flood amount of a given recurrence interval is an important component of hydrological planning and design. When performing simulations at a Quaternary Catchment scale using the *ACRU* model, extreme value analyses can be performed on the various variables, *viz.*

i) observed daily rainfall depth (mm);
ii) observed streamflow depth (mm);
iii) simulated streamflow depth (mm);
iv) observed peak discharge ($m^3.s^{-1}$); and
v) simulated peak discharge ($m^3.s^{-1}$).

However, as observed streamflow and peak discharge information are not available in the present Quaternary Catchment Input Database, whenever the option to perform an extreme value analysis is selected it is for either

i) maximum daily rainfall (mm);
ii) maximum daily simulated streamflow depth (mm); or
iii) maximum daily simulated peak discharge ($m^3.s^{-1}$)

using the Annual Maximum Series (Schulze *et al.*, 1995e).

The Annual Maximum Series takes the largest event from each '*n*' years of record and the extreme values are calculated for either one or all of the Gumbel, Log-Normal and Log-

Pearson Type III extreme value distributions using this sample of $n$ values, which represent the design magnitude in the $n$ year record.

The information pertaining to these additional options has been added to the Quaternary Catchment Input Database and can be selected via the New Options File for use in an *ACRU* simulation of selected Quaternary Catchments.

## 7.4 Incorporation of Future Climate Scenarios and Daily Temperatures

Previously there was no facility available in *ACRU* to perform simulations directly at the Quaternary Catchment or smaller scale using future projected temperature and precipitation changes as simulated by large scale atmospheric models (GCMs). Monthly output for 2X $CO_2$ scenarios from five GCMs, *viz.*

i) UKTR, excluding sulphate forcing (UKTR-S);
ii) HadCM2, excluding sulphate forcing (HadCM2-S);
iii) HadCM2, including sulphate forcing (HadCM2+S);
iv) CSM (1998), excluding sulphate forcing; and
v) Genesis (1998), excluding sulphate forcing

was selected for application in this study, as described in Chapter 6. The daily output from HadCM3-S has been yet been included as an option in this interface. When performing an *ACRU* simulation with the assumption of future climatic conditions, one of the GCMs available must be chosen as the future climate scenario.

The methodology of including future scenario values precipitation and temperature in an *ACRU* simulation is described in Sections 7.4.1 and 7.4.2. The options of performing a sensitivity or threshold analysis have also been included and the methodology used to perform these studies is presented in Section 7.4.3. In addition, the option of using daily values of maximum and minimum temperatures instead of monthly means of daily temperature inputs for the present climate scenario has also been included as an option for use with the *ACRU* Input Database in conjunction with the *ACRU* model, as explained in Section 7.4.4.

### 7.4.1 Incorporation of monthly future precipitation estimates

Rainfall data from the daily rainfall station selected as the driver station for each catchment are frequently not representative of the rainfall of the catchment in question because of some systematic error (e.g. station located on the watershed, or in a valley). This necessitates an adjustment to be applied to the rainfall (Smithers and Schulze, 1995). Therefore, in *ACRU* a precipitation adjustment factor can be specified when adjusting rainfall from a point estimate to that representing the catchment scale and is calculated for the *i*th month as

$$\text{precipitation adjustment factor } i = \frac{\text{catchment rainfall } i}{\text{station rainfall } i}$$

The catchment rainfall for a given month is usually calculated using the *ZONALSTATS* command in ARC/INFO and is obtained by finding the average rainfall for the catchment from the 1' x 1' of a degree latitude / longitude grid of median monthly and mean annual rainfalls developed for South Africa, Lesotho and Swaziland by Dent *et al.* (1989). Therefore, the rainfall on any day is multiplied by the precipitation correction factor to obtain a representation of the catchment rainfall for that day.

In order to perturb the present day daily values to reflect future estimates of precipitation given by the GCMs the precipitation correction factor has to be adjusted again. It is necessary to extract the ratio change in precipitation (future / present climate) for each month as simulated by the GCM selected. To achieve this, each $^1/_4°$ grid of monthly change in precipitation for each GCM (as described in Chapter 6, Section 6.4.2) was converted to an ASCII file using the *GRIDASCII* command in ARC/INFO.

Using a Fortran program written by Kiker (1999, pers. com) and modified for use in this study, the ratio change in precipitation for the GCM selected for each month of the year is extracted from the 12 ASCII files using the centroid of each catchment. In the example shown in Figure 7.3 the ratio change in precipitation extracted for this catchment would be 1.2 (i.e. a 20% increase in precipitation is simulated by the GCM).

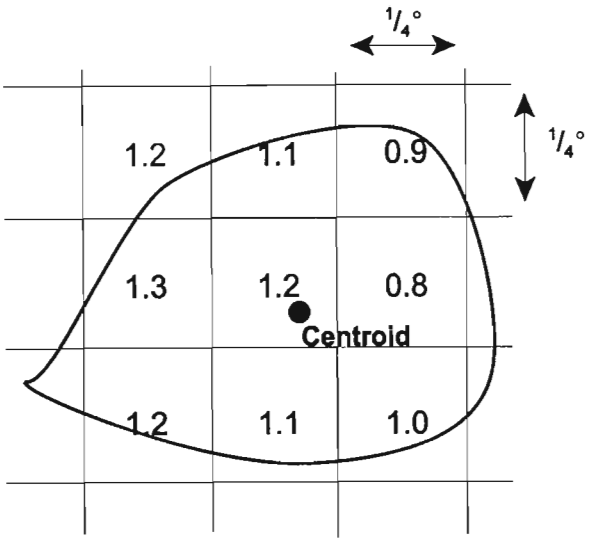


Figure 7.3 A schematic example of the use of the centroid of a catchment to isolate the ratio change in precipitation from an ASCII file representing the quarter of a degree grid for a GCM for a particular month

Thus, the adjustment factor for each month ($i$) for future precipitation is calculated as

future precipitation adjustment factor $i$ = present precipitation adjustment factor $i$ x ratio change in precipitation $i$

The future precipitation adjustment factor is then input into the *ACRU* input menu to replace the precent precipitation adjustment factor when simulating hydrological responses under a future climate. In this way both the catchment adjustment from the point to areal rainfall estimate, and the change in precipitation resulting from climate change, are taken into account in a single step.

### 7.4.2 Incorporation of monthly future temperature estimates

For this study, monthly means of daily maximum and minimum temperatures are entered for each month of the year. Future temperatures are then calculated using the difference in temperature between the future and present estimates of temperature provided by the GCMs. The differences in temperature at the centroid of each catchment for each month of the year

are extracted from ASCII files of the gridded temperature changes using the procedure described in Section 7.4.1 above.

All five GCMs predict an increase in temperature with climate change (cf. Chapter 6, Section 6.5.1). Thus, future temperature for each month of the year (*i*) to be input into the *ACRU* input menu was calculated as

future temperature *i* = present temperature *i* (from the baseline database) + difference in temperature *i* from GCM.

The UKTR-S and HadCM2 GCMs output simulated changes of both maximum and minimum temperature. However, only simulated changes in mean temperatures were available from the CSM (1998) and Genesis (1998) GCMs. As maximum and minimum temperature inputs are required in *ACRU*, it was assumed for these two GCMs that the same difference between future and present mean temperatures could be applied to both maximum and minimum temperature.

### 7.4.3 Performing a threshold or sensitivity analysis

Three threshold analyses (cf. Section 3.4.4 of Chapter 3) were carried out in this study, *viz.* on mean annual runoff, mean annual percolation into the vadose zone and median maize yield. Figure 7.4 illustrates the methodology used in the threshold analyses of climate change on hydrological responses and maize yield in southern Africa.

The results for the threshold analyses were generated using *ACRU* with the GCM predicted changes in precipitation and temperature which were extracted for each Quaternary Catchment using the method described in Sections 7.4.1 and 7.4.2. Five simulations were carried out using

i) present precipitation and temperature;
ii) $^1/_4$ change in GCM predicted precipitation, temperature and $CO_2$;
iii) ½ change in GCM predicted precipitation temperature and $CO_2$;
iv) $^3/_4$ change in GCM predicted precipitation temperature and $CO_2$; and

v) GCM future precipitation, temperature and $CO_2$ as climatic input.

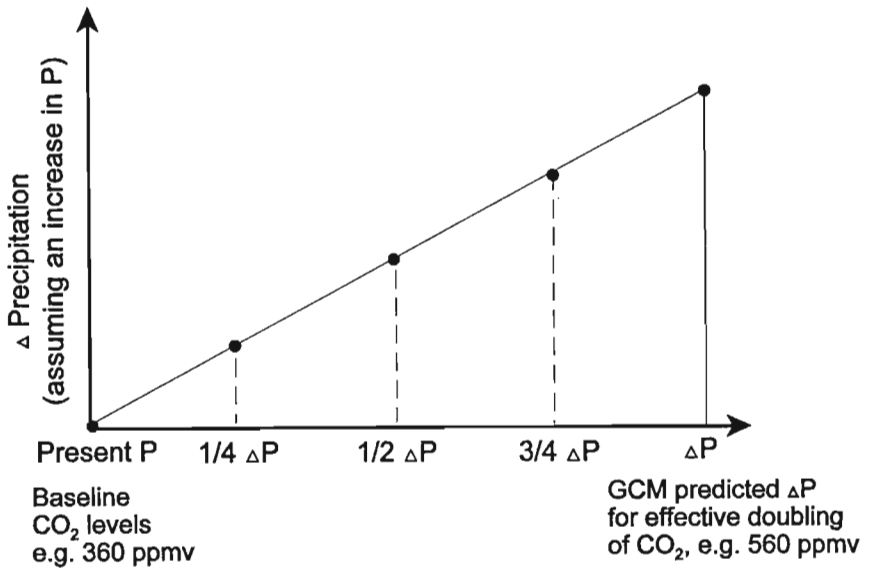


Figure 7.4 Methodology used in the threshold analysis, using precipitation (P) as an example

In the case of $^1/_4$ change in GCM predicted climate, when subscripts 'p' and 'f' denote present and future (2X $CO_2$) climates, then

$^1/_4 \Delta P = [^1/_4 (P_f / P_p - 1) + 1] \times P_p$ for each month of the year

$^1/_4 \Delta T = [^1/_4 (T_f - T_p) + T_p$ for each month of the year

$^1/_4 \Delta CO_2$ = $^1/_4$ of 15% transpiration suppression in *ACRU* for C3 plants

= $^1/_4$ of 22% transpiration suppression in *ACRU* for C4 plants.

In the case of the other fractional changes in GCM predicted variables, the $^1/_4$ in the above equations was substituted by $^1/_2$, $^3/_4$ and 1 respectively.

If estimated dates are assigned to the $^1/_4$, $^1/_2$, $^3/_4$ and 1X change simulations points (marked as dots in Figure 7.4), maps can be created showing when, in future, a critical change in response of a variable might occur; or alternatively, what the anticipated magnitude of change of a hydrological response would be by a certain year.

A study analogous to that of the threshold analyses undertaken in this study was carried out by Parry *et al.* (1999) to assess potential economic implications of climate change on

agriculture in England and Wales. Output from the Basic Linked System (BLS) world food trade model was linked to a British model of agricultural production and land use, the Climate Land Use Allocation Model (CLUAM), to provide projections of agricultural land use under a number of scenarios.

Baseline climate information was obtained for the period 1961 - 1990. Climate output of future climate scenarios was obtained from the GISS couple ocean-atmosphere transient GCM. This is a transient GCM that runs at the spatial resolution of 7.83° latitude by 10.00° longitude. As this is a transient GCM where concentrations of greenhouse gases are increased steadily through time, climatic output at points in time during the simulation could be extracted from the GCM, as opposed to climate output from a fixed future date. Thus, the climatic output for three time slices, *viz.* 2010, 2030 and 2050 was extracted (Parry *et al.*, 1999). The $CO_2$ concentrations were assumed to be 405 ppm, 460 ppm and 530 ppm for the three time slices respectively (Fischer *et al.*, 1996). These time slices are analogous to the $^1/_4$, $^1/_2$, $^3/_4$ change in climate threshold approach used in this study.

The climate change yield impacts were gradually incorporated into the experiments during the periods between the climate time slices. The mean global warming for the GISS for the three time slices was found to be 1.2 °C for 2010, 2.4 °C for 2030 and 3.8 °C for 2050. This is a fairly linear change, which would indicate that the assumption of linearity of climatic change used for the threshold analysis in this particular study is a reasonable assumption (Parry *et al.*, 1999).

In the case of the sensitivity studies the options are to perform a sensitivity analysis of changes in temperature, precipitation and $CO_2$. The monthly temperatures input for a catchment can be increased by 1.5, 2.0, 2.5, 3.0 or 3.5 °C to assess the sensitivity of hydrological response to a change in temperature (cf. Section 3.4.3.2 in Chapter 3). In the case of precipitation, the precipitation correction factor can be increased or decreased by 10 or 20%. To perform a sensitivity analysis of $CO_2$, the $CO_2$ transpiration suppression option in *ACRU* can be included or excluded from the simulation.

### 7.4.4 Incorporation of daily maximum and minimum temperatures

The centroid latitude, longitude and mean elevation can be extracted from the *ACRU* Input Database for a particular catchment and used to generate daily maximum and minimum temperatures following the procedure described in Chapter 5, Section 5.2. This method of deriving daily temperatures can be applied to any catchment where the aforementioned parameters are available. If daily temperatures are required, then a composite file is created containing the daily rainfall and temperatures for each catchment selected for the period of simulation.

If a future climate scenario simulation is selected and the option of daily temperatures is required, then the daily temperature values for the month are increased by the monthly GCM predicted change in precipitation for every day of the month.

## 7.5 Selections of Catchments from the Quaternary Catchment Input Database

Using the *ACRU* model, the hydrological responses of catchments can be generated either with the catchments operating as

i) individual (i.e. non-linked) catchments, which is suited for determining where, within a region, streamflow is actually generated (Section 7.6); or as

ii) cascading (i.e. hydrologically connected, linked) catchments, used to determine cumulative flows down a river system, and hence the total available water at any point within a large catchment (Section 7.7).

Previously the user of the interface could only simulate the hydrology of all the Quaternary Catchments in southern Africa as individual entities and was not able to isolate a cluster of Quaternary Catchments to model them as individual lumped or as cascading interlinked Quaternary Catchments.

The facility has now been incorporated whereby the user can select to model hydrological responses from a group of Quaternary Catchments which can be delimited by

i) drainage region (any Primary, Secondary, Tertiary or Quaternary Catchment within southern Africa);

ii) a user specified list of Quaternary Catchments;

iii) a large catchment in southern Africa; or

iv) a Water Management Area.

These options are described in the sections which follow.

### 7.5.1 Delineation of southern Africa into drainage regions

If, for example, the Primary Catchment "A" is selected then, using a Fortran script, all the Quaternary Catchments that start with the letter "A" are isolated in an ASCII file and the number of Quaternary Catchments in the selected Primary Catchment written to the screen. Each Quaternary Catchment in that Primary Catchment can then be modelled as an individual, lumped catchment using *ACRU*. The same procedure applies for Secondary and Tertiary Catchments, using the first two and first three characters respectively of the Quaternary Catchment numbering system. In addition, a Quaternary Catchment or a cluster of Quaternary Catchments can be selected, based on the numerical identities assigned to them. The option remains to select all the Quaternary Catchments in southern Africa for simulation.

### 7.5.2 A user defined list of Quaternary Catchments

The situation may arise where a selection of Quaternary Catchments is required for simulation, however, they may be situated in scattered locations across southern Africa. In this instance, the user can enter the name of a pre-prepared list of the catchments required.

### 7.5.3 Option of selecting a large catchment in southern Africa

Files containing lists of the Quaternary Catchments which fall into large catchments in southern Africa were created to allow the following catchments to be selected for simulation using *ACRU*:

i) Black Mbuluzi

ii) Breede

xiv) Mvoti

xv) Mzimkulu

iii) Buffalo
iv) Caledon
v) Crocodile
vi) Gouritz
vii) Kei
viii) Limpopo
ix) Mfolozi
x) Mgeni
xi) Mhlatuze
xii) Mkomazi
xiii) Mkuze
xvi) Mzimvubu
xvii) Olifants
xviii) Orange
xix) Pongola
xx) Sabie
xxi) Sand
xxii) Sundays
xxiii) Swartkops
xxiv) Tugela
xxv) Vaal

This eliminates the need for the user to know which Quaternary Catchments fall into the large catchment of interest as the names of these catchments are stored and automatically extracted.

### 7.5.4 Option of selecting a Water Management Area in southern Africa

South Africa has been divided into 19 Water Management Areas (WMAs), as shown in Figure 7.5. Similar ASCII files as those described in Section 7.5.3 were created for each WMA. In future each WMA is to be operated by a Catchment Management Agency (CMA) in accordance with the new National Water Act (NWA, 1998).

Figure 7.5 The Water Management Areas of South Africa (after DWAF, 2000)

The option of individually simulating the hydrology of the Quaternary Catchments that are located in each Water Management Agency is therefore available for decisions to be made by the future CMAs.

# WATER MANAGEMENT AREAS OF SOUTH AFRICA (after DWAF, 2000)

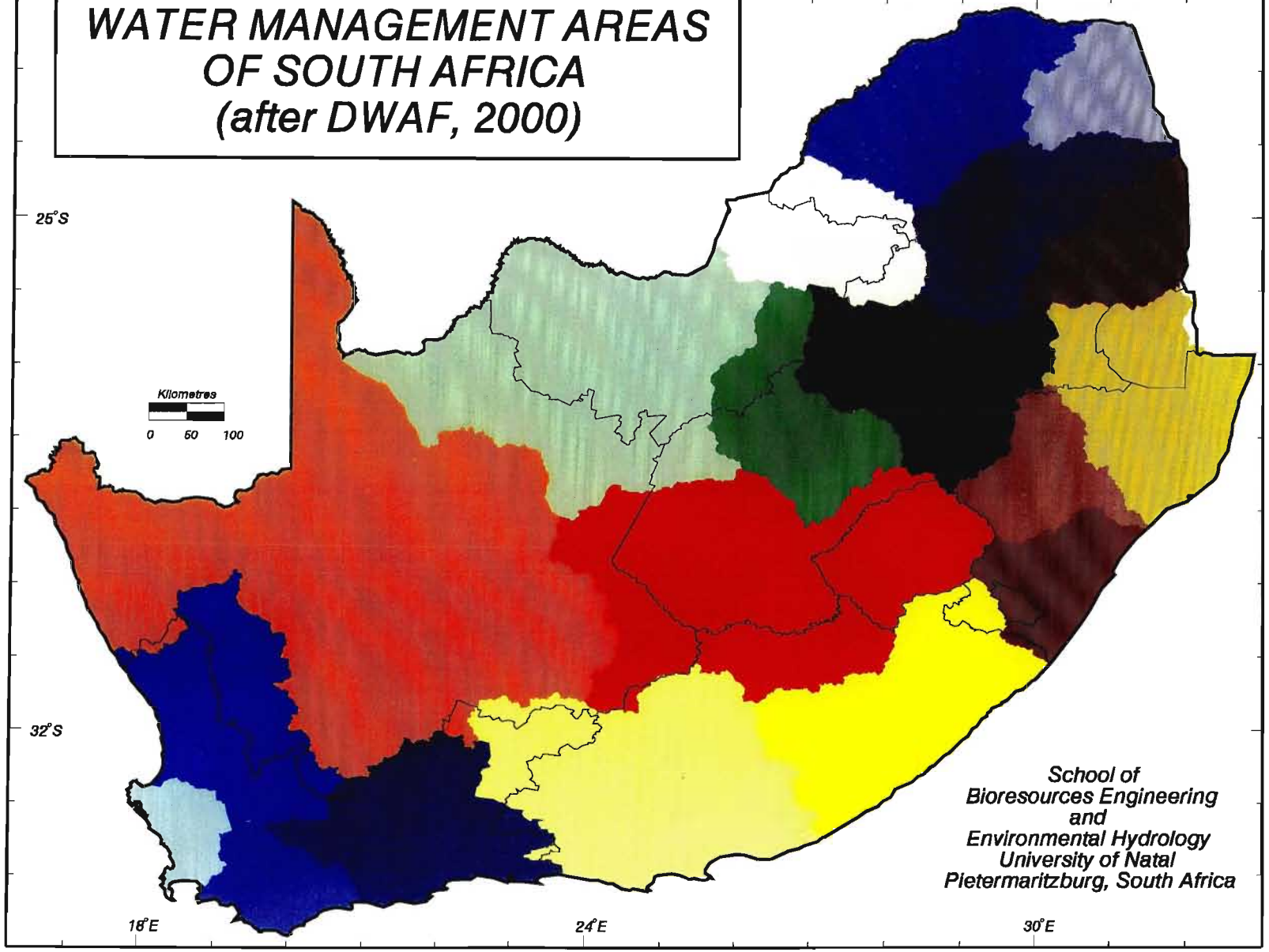


- Limpopo
- Luvuvhu / Letaba
- Crocodile West
- Olifants
- Inkomati
- Usutu to Mhlathuze
- Mvoti to Mzimkulu
- Thukela
- Lower Vaal
- Middle Vaal
- Upper Vaal
- Lower Orange
- Upper Orange
- Mzimvubu to Buffalo
- Fish to Gamtoos
- Gouritz
- Breede
- Berg
- Olifants / Doorn

School of
Bioresources Engineering
and
Environmental Hydrology
University of Natal
Pietermaritzburg, South Africa

## 7.6 Simulation of Agrohydrological Responses of Individual Catchments

The flow chart in Figure 7.6 illustrates the steps taken to enable automated generation of *ACRU* input menus using the *ACRU* Input Database. Firstly, the name of the database being used must be specified, as shown in Figure 7.6. Any new input options that are required must be selected from the New Options File. Options of the hydrological condition of the veld, crops planted or irrigation being applied can be activated for use from the Quaternary Catchment Input Database, for example. In addition, the options of performing a sediment yield analysis and / or an extreme value analysis could be selected (cf. Section 7.3).

The climate input to be used must also be specified. Agrohydrological responses can then be simulated using *ACRU* for

i) present climatic conditions;

ii) perturbed future climatic conditions, using estimates of temperature and rainfall from the selected GCM for a 2X $CO_2$ equivalent climate scenario (cf. Sections 7.4.1 and 7.4.2);

iii) a sensitivity analysis where the temperature or precipitation output can be perturbed and with the option to activate $CO_2$ transpiration suppression only (cf. Section 7.4.3); or

iv) a threshold analysis for different threshold levels (cf. Section 7.4.3).

A choice must be made as to whether daily or monthly temperatures are to be used (cf. Figure 7.6). If daily temperatures are selected then these temperatures are generated using the methodology described in Section 7.4.4 for the period of simulation.

Next, the catchments required for simulation must be identified. If the Quaternary Catchment Input Database is being used, then the Quaternary Catchments can be selected by choosing a drainage region, a large catchment or a Water Management Area in southern Africa (cf. Section 7.5). All the Quaternary Catchments that fall into the selected group will automatically be isolated and the list written to an ASCII file. If the Input Database being used is not the Quaternary Catchment Input Database then an ASCII file needs to be created with a list of the catchments required for simulation.

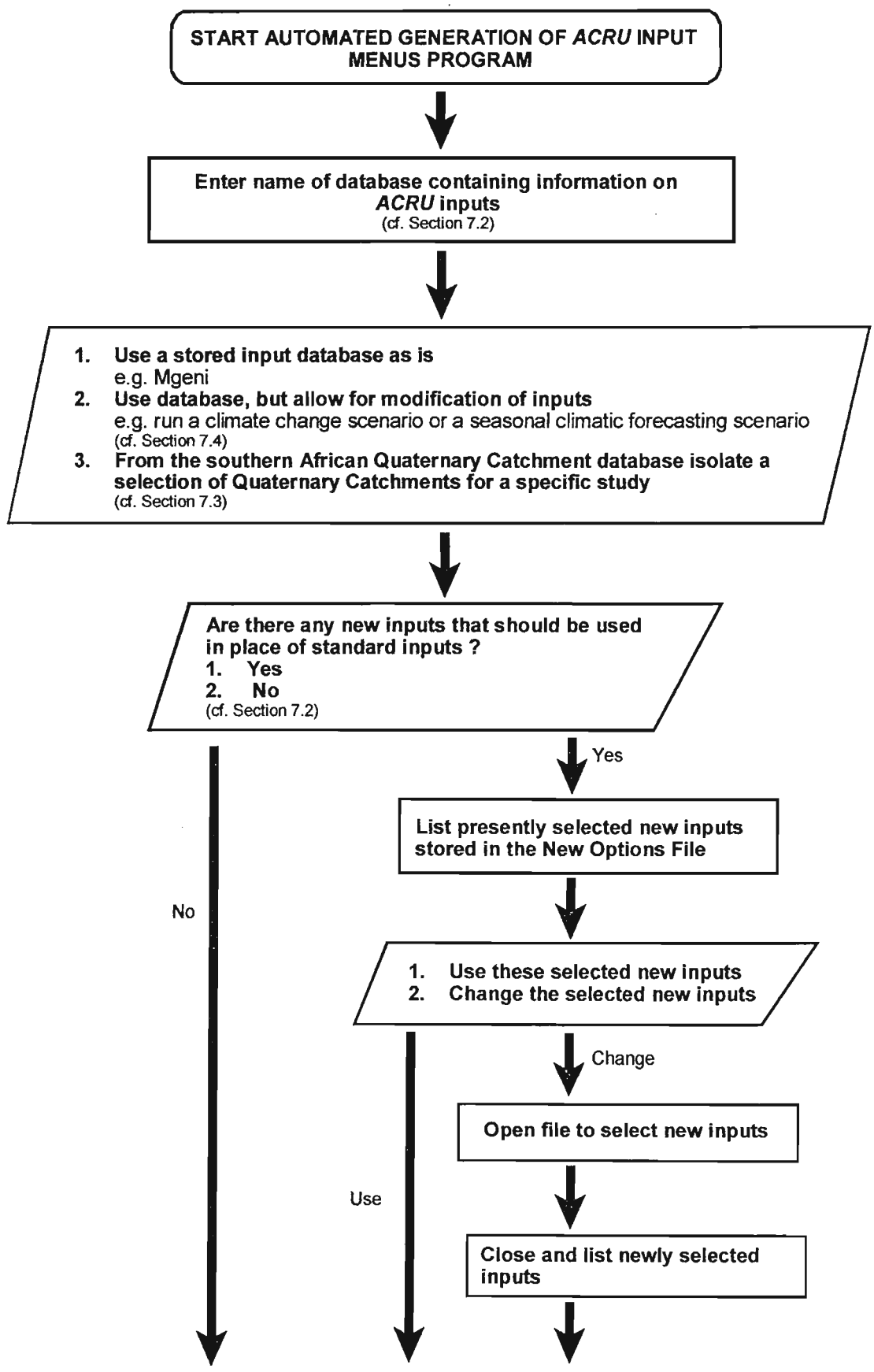


Figure 7.6 Refinements to the linking of the Quaternary Catchments Input Database to the *ACRU* model and GIS

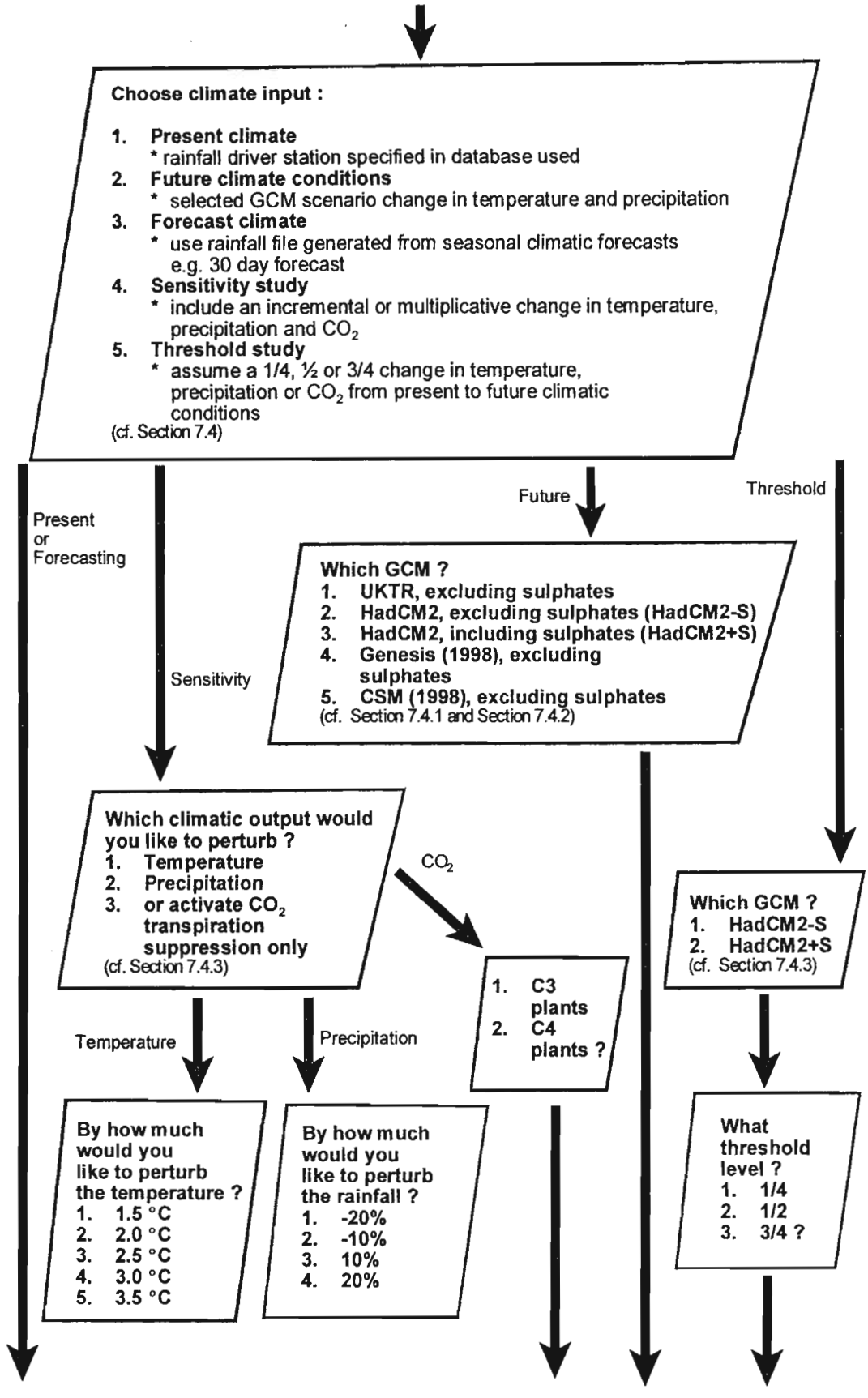


Figure 7.6 Refinements to the linking of the Quaternary Catchments Input Database to the *ACRU* model and GIS (cont.)

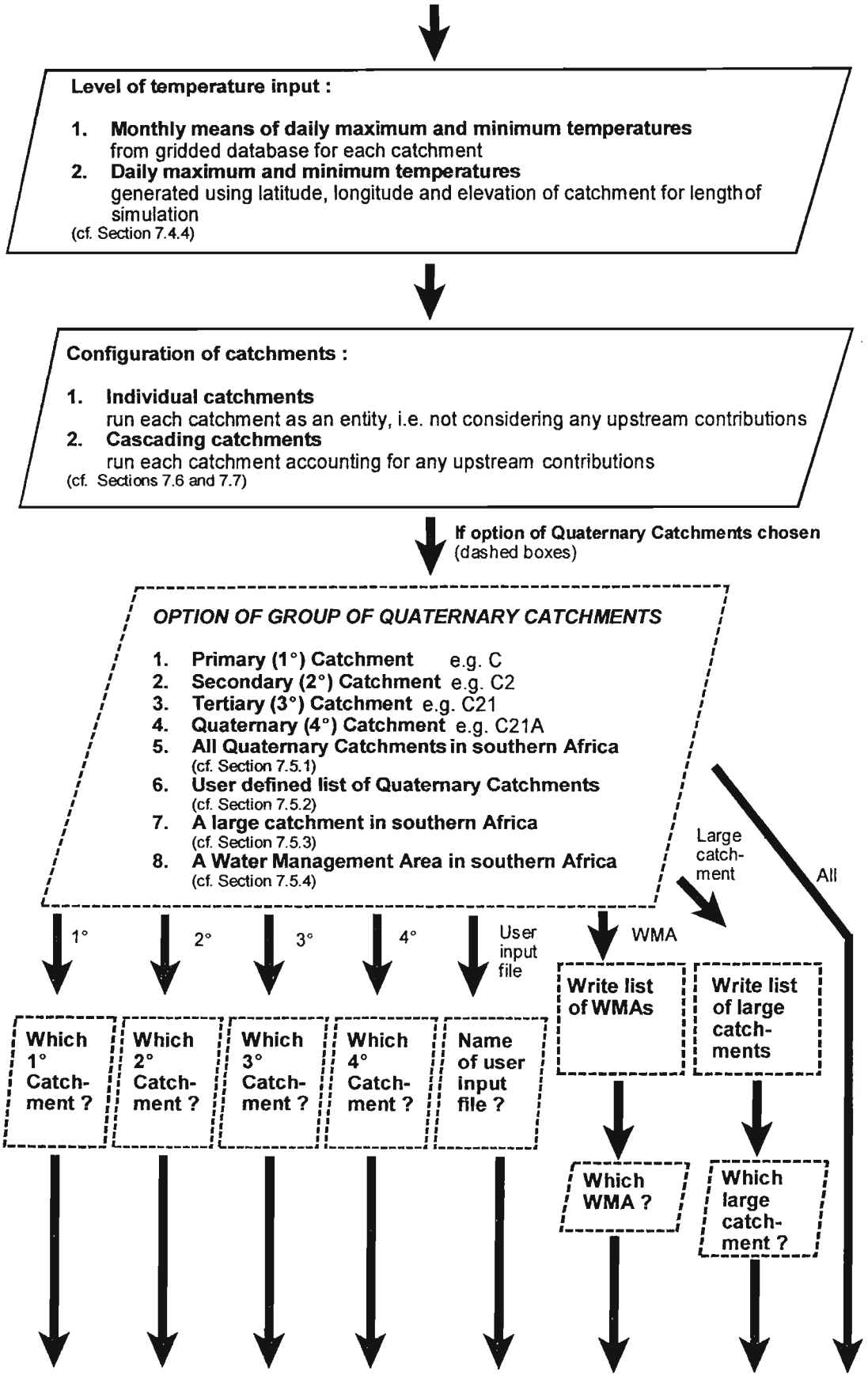


Figure 7.6 Refinements to the linking of the Quaternary Catchments Input Database to the *ACRU* model and GIS (cont.)

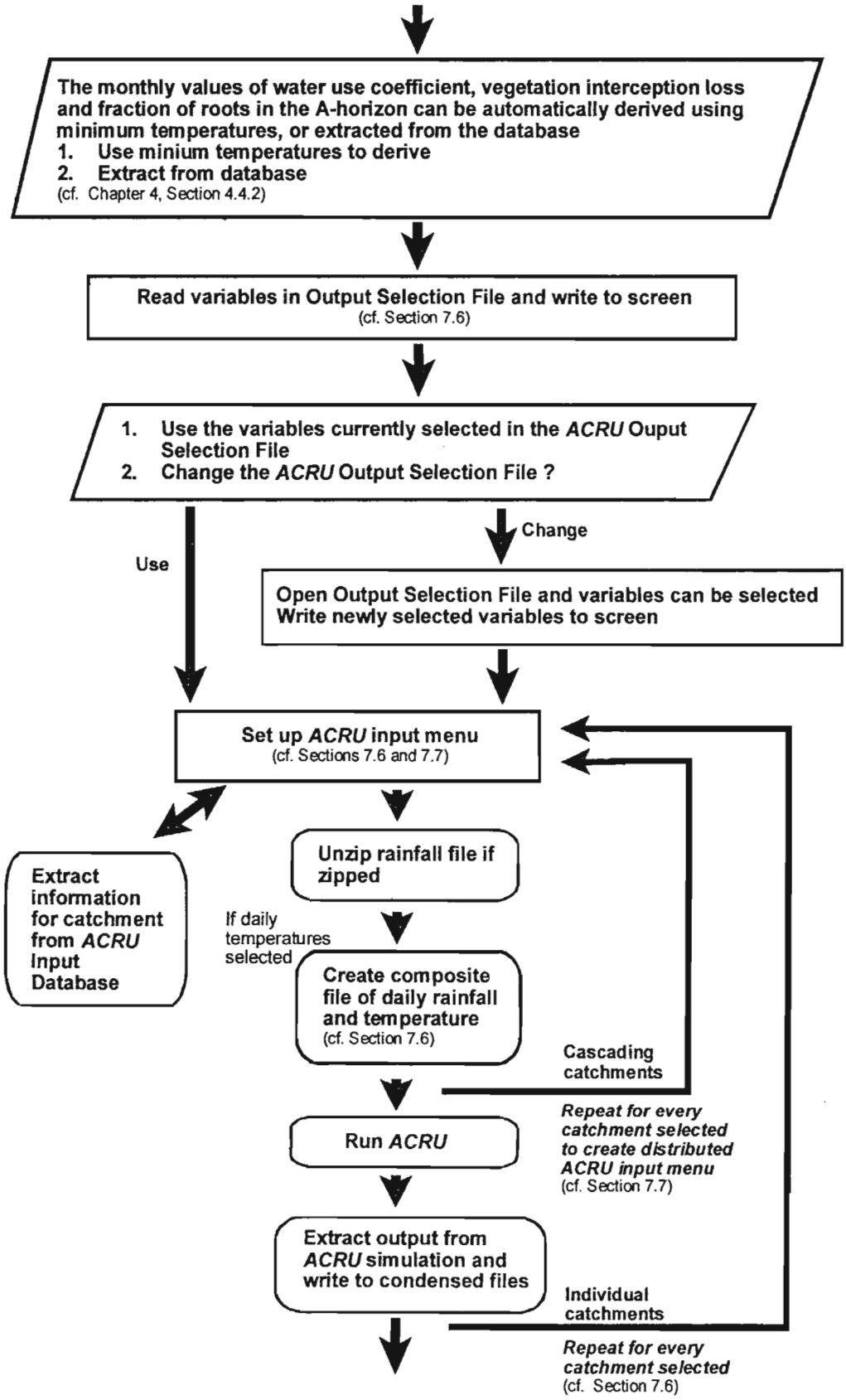


Figure 7.6 Refinements to the linking of the Quaternary Catchments Input Database to the *ACRU* model and GIS (cont.)

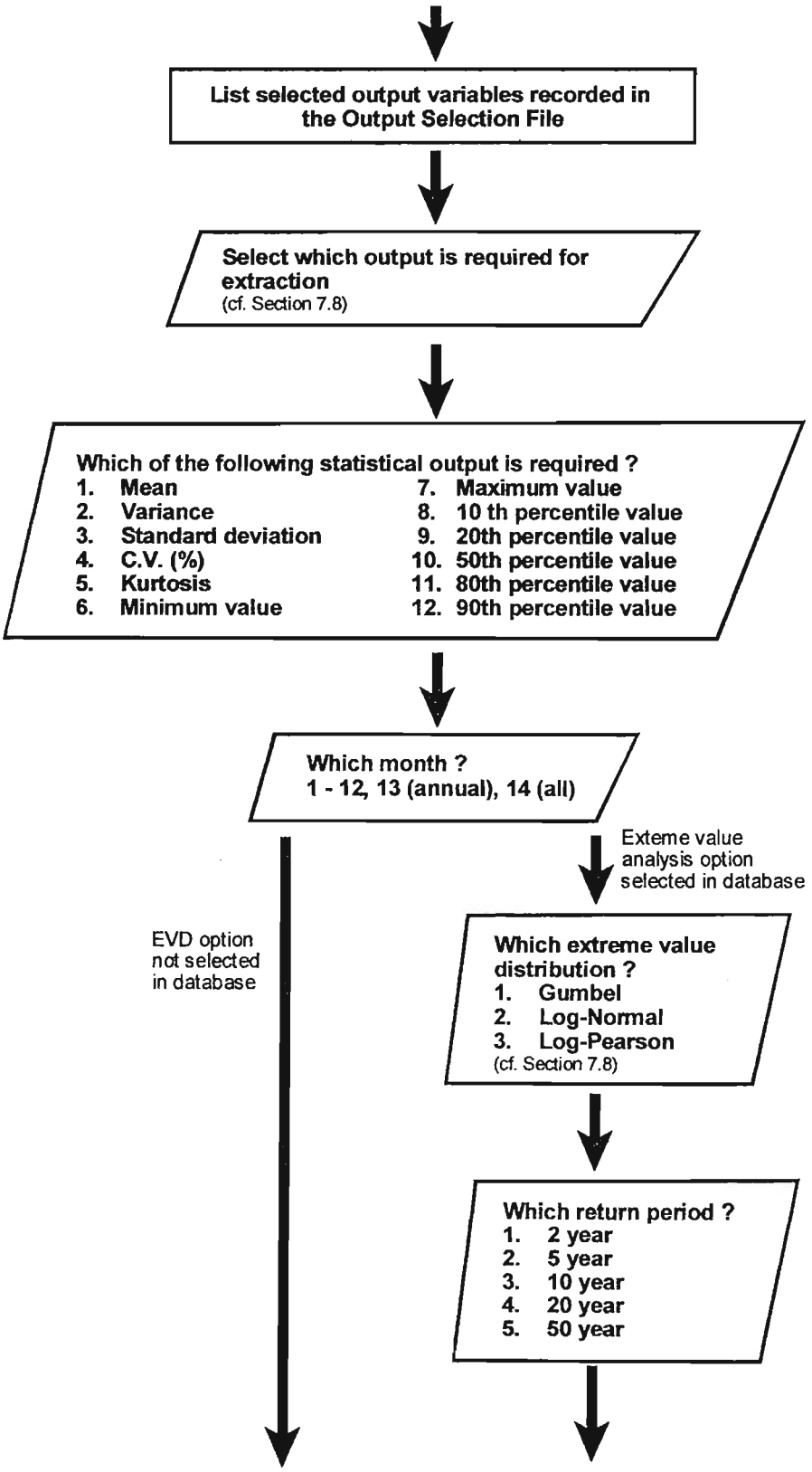


Figure 7.6 Refinements to the linking of the Quaternary Catchments Input Database to the *ACRU* model and GIS (cont.)

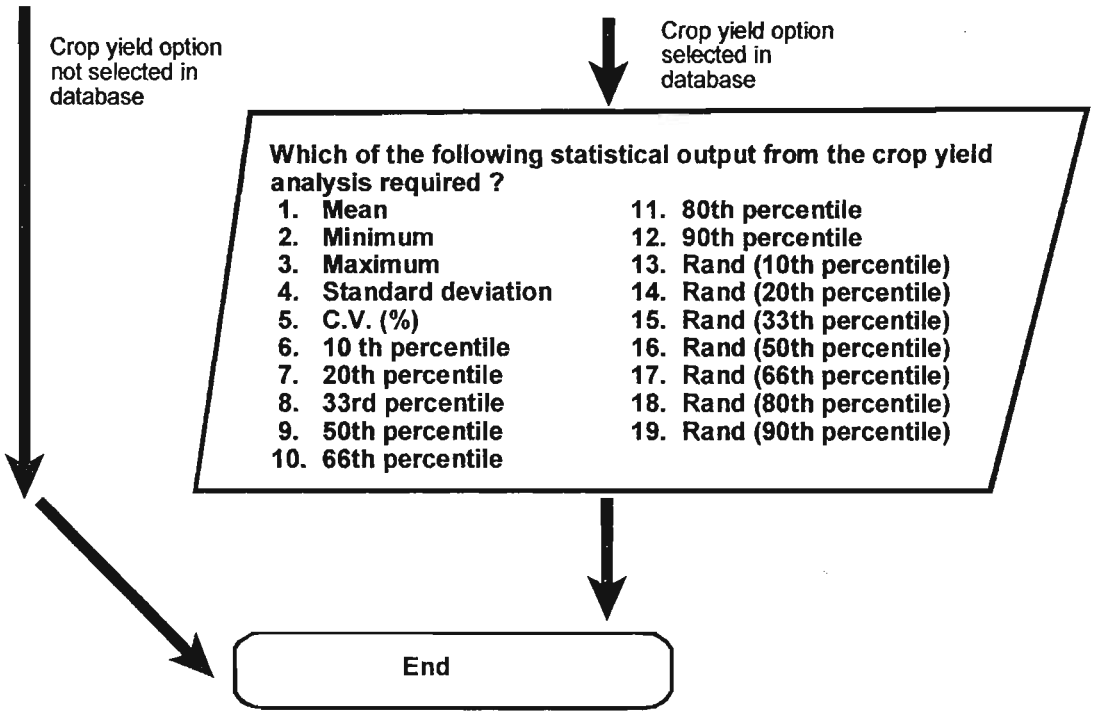


Figure 7.6 Refinements to the linking of the Quaternary Catchments Input Database to the *ACRU* model and GIS (cont.)

There is the option for generating the monthly values of the water use coefficient, vegetation interception loss and fraction of roots in the A horizon from minimum temperatures (cf. Chapter 4, Section 4.4.2), alternatively the monthly parameter values set in the database can be used.

Various output from an *ACRU* simulation can be stored for analysis, e.g. rainfall, simulated runoff or stormflow. The various options available are listed in the *ACRU* Output Selection File and can be identified depending on the output required (cf. Figure 7.6). For each output option selected from this list a file containing monthly and annual statistical information can be derived upon completion of the *ACRU* simulation for each catchment selected via a separate executable program available with the *ACRU* model. Details on the extraction of the statistical output for presentation in a GIS are given in Section 7.8.1.

An *ACRU* input menu is automatically created for each catchment selected containing information (e.g. climate, soils, land cover) pertaining to that catchment, as extracted from the *ACRU* Input Database using a Fortran script. The file containing the daily rainfall information for the simulation period is unzipped in the case of Quaternary Catchments (cf. Figure 7.6) using a Fortran program established by Meier (1997). If the option of using daily temperatures was selected, then composite files are created containing the daily rainfall and temperatures for each catchment selected for simulation.

In climate change impact studies reference potential evaporation for both present and future climate simulations is calculated using the Linacre (1991) equation which is given by Schulze and Kunz (1995) as

$$E_r = [0.015 + 4 \times 10^{-4} T_a + 10^{-6} z] [480 (T_a + 0.006z) / (84 - \phi_d - 40 + 2.3u_{2ms}) (T_a - T_d)]$$

with

| | | | |
|---|---|---|---|
| | $E_r$ | = | reference potential evaporation from an extended water surface (mm) |
| | $T_a$ | = | mean air temperature (°C) |
| | $z$ | = | altitude (m) |
| | $\phi_d$ | = | latitude (°) |

| | | | |
|---|---|---|---|
| | $u_{2ms}$ | = | windspeed at 2 m ($m.s^{-1}$) |
| | $(T_a - T_d)$ | = | $0.023z + 0.37T_a + 0.53\ (T_{mx} - T_{mn}) + 0.35\ T_{ra} - 10.9$ |
| where | $T_{mx}$ | = | maximum air temperature (°C) |
| | $T_{mn}$ | = | minimum air temperature (°C) |
| | $T_{ra}$ | = | range between mean air temperature of hottest and coldest months of the year (°C). |

In this equation potential evaporation is derived using the principles of the physically based Penman (1948) equation, yet it uses only maximum and minimum temperatures (to estimate solar radiation and vapour pressure deficit), together with latitude (to modulate the radiation component for day length) and altitude (which influences the psychrometric constant, net radiation and vapour pressure). Changes in mean annual reference potential evaporation were investigated for conditions of climate change and the results are presented in Chapter 9, Section 9.2.1.

The *ACRU* input menu established for each catchment is used for a individual *ACRU* simulation for each catchment required. The selected output from *ACRU* is written to files which are later used for extraction of the required output for display purposes as explained in Section 7.8.

## 7.7 Simulation of Agrohydrological Responses of Cascading Catchments

Initially, in the School of BEEH, climate change and other impact assessments of water resources had been made using *ACRU* with Quaternary Catchments modelled as individual, catchments which were unconnected hydrologically to other downstream Quaternary Catchments (e.g. Kunz, 1993; Lowe, 1997). In reality, both Quaternary Catchments and Quinary Catchments are, however, hydrologically linked and simulated streamflows should be cascaded from one catchment to the next one downstream, using flow routing procedures available in *ACRU*.

### 7.7.1 Need to link catchments

This cascading option in *ACRU* is useful to determine cumulative flows and total available water under different climate or land use scenarios. This option of simulating a cluster of catchments, such that the streamflow from one catchment flows to its immediate downstream catchment, is modelled in *distributed* mode in *ACRU* as opposed to each catchment being modelled individually, termed *lumped* mode. The procedure of linking catchments to determine accumulative flows is described below.

### 7.7.2 Procedure of linking catchments

When modelling catchments in distributed mode in *ACRU* the total number of subcatchments making up the entire catchment needs to be known and used as input into the *ACRU* menu. In addition, each subcatchment has to be assigned an unique numerical identifier, with the number assigned increasing as the catchments cascades downstream, in such a way that a catchment with a smaller numerical identifier always flows into a catchment with a larger numerical identifier. This ordering, or configuration, of the subcatchments is entered into the *ACRU* input menu. Figure 7.7 illustrates how a catchment might be delineated and each subcatchment assigned a numerical identifier. Subcatchment 8 in the figure would be the exiting subcatchment and if only Catchments 1 through 4 are required for simulation, then Catchment 4 would be the end catchment in the simulation.

To enable the modelling of streamflow from catchments to determine cumulative flows for a selected area, an ASCII file needs to be created listing all the catchments on the left-hand side with their respective downstream catchment listed on the right-hand side. This file is termed the Catchment Ordering File. If a catchment flows into the ocean or another country, for example Mozambique, then that is noted on the right-hand side instead of the catchment name. An example of the format of writing the sequence of the cascading Quaternary Catchments is given in Table 7.3.

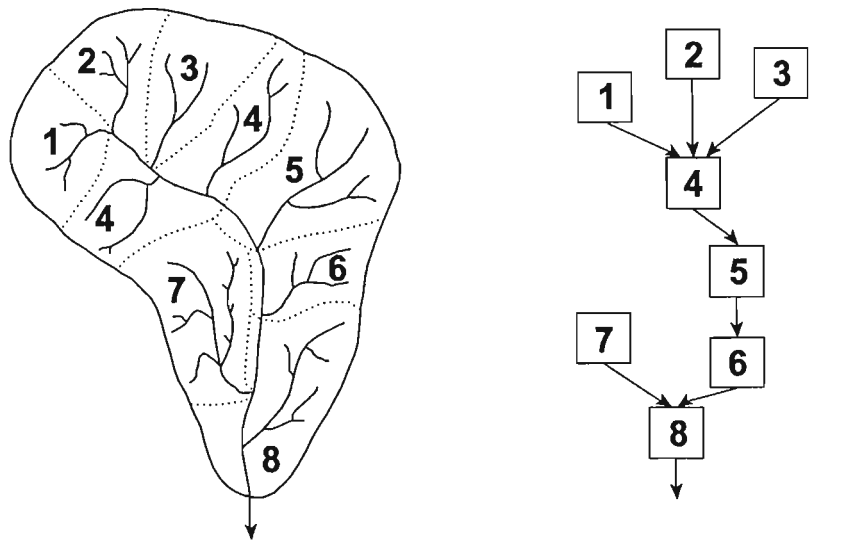


**(a) Subcatchment delineation** **(b) *ACRU* Configuration**

Figure 7.7 An example of (a) the delineation of a catchment into subcatchments and (b) the configuration of the catchment for distributed mode simulation in *ACRU* (after Schulze *et al.*, 1995b)

Table 7.3 Example of list showing the Quaternary Catchments on the left hand side and their downstream Quaternary Catchments or exit on the right hand side

| Upstream Quaternary Catchment | Downstream Quaternary Catchment or Exit |
|---|---|
| M10A | M10B |
| M10B | M10D |
| M10C | M10D |
| M10D | SEA |

In the case of the Quaternary Catchments, this Catchment Ordering File has been created and is automatically accessed if the option of using the Quaternary Catchment Input Database for cascading catchments is selected.

A similar procedure is followed to model catchments as linked catchments in *ACRU* for climate impact assessment as for individual catchments as described in Section 7.6 (cf. Figure 7.6). Once the database has been specified and the level of climate input identified, the end

catchment for the simulation needs to be specified. However, if the option of using the Quaternary Catchment Input Database has been chosen, then there is the option of choosing an exiting Quaternary Catchment from a larger Catchment Division, *viz.* Primary, Secondary or Tertiary Catchment. There may be a single exit from the selected catchment cluster or there may be multiple Quaternary Catchments that exit from the selected catchment cluster, as shown in Figure 7.8.

| | |
|---|---|
| Figure 7.8 | An example of a Primary Catchment with a single Quaternary Catchment at the exit into the sea (Primary Catchment V) and a Primary Catchment with multiple Quaternary Catchments exiting into the sea (Primary Catchment U) |

If this option is chosen a list is written to the screen of all the Quaternary Catchments that exit from that selected Primary, Secondary or Tertiary Catchment. Provided with the list are

i) the total number of Quaternary Catchments that contribute to that exit;
ii) the total drainage area of all the Quaternary Catchments that contribute to that exit;
iii) whether the exiting Quaternary Catchment exits into the sea or another country;
iv) the total area of all the Quaternary Catchments in the selected range; and
v) the total number of Quaternary Catchments in the selected range.

From this information the user can select one exiting Quaternary Catchment, whereby an ASCII file containing a list of all the Quaternary Catchments that feed that exit is automatically established.

Alternatively, any end Quaternary Catchment is entered and through a recursive loop in a Fortran script the catchments that feed that selected end catchment are identified using the Catchment Ordering File. Any end catchment for a group of Quinary Catchments can be selected and the feeding catchments will be identified in a similar manner.

# An Example of a Primary Catchment with a Single Exit (V) and a Primary Catchment with Multiple Exits (U) into the Sea

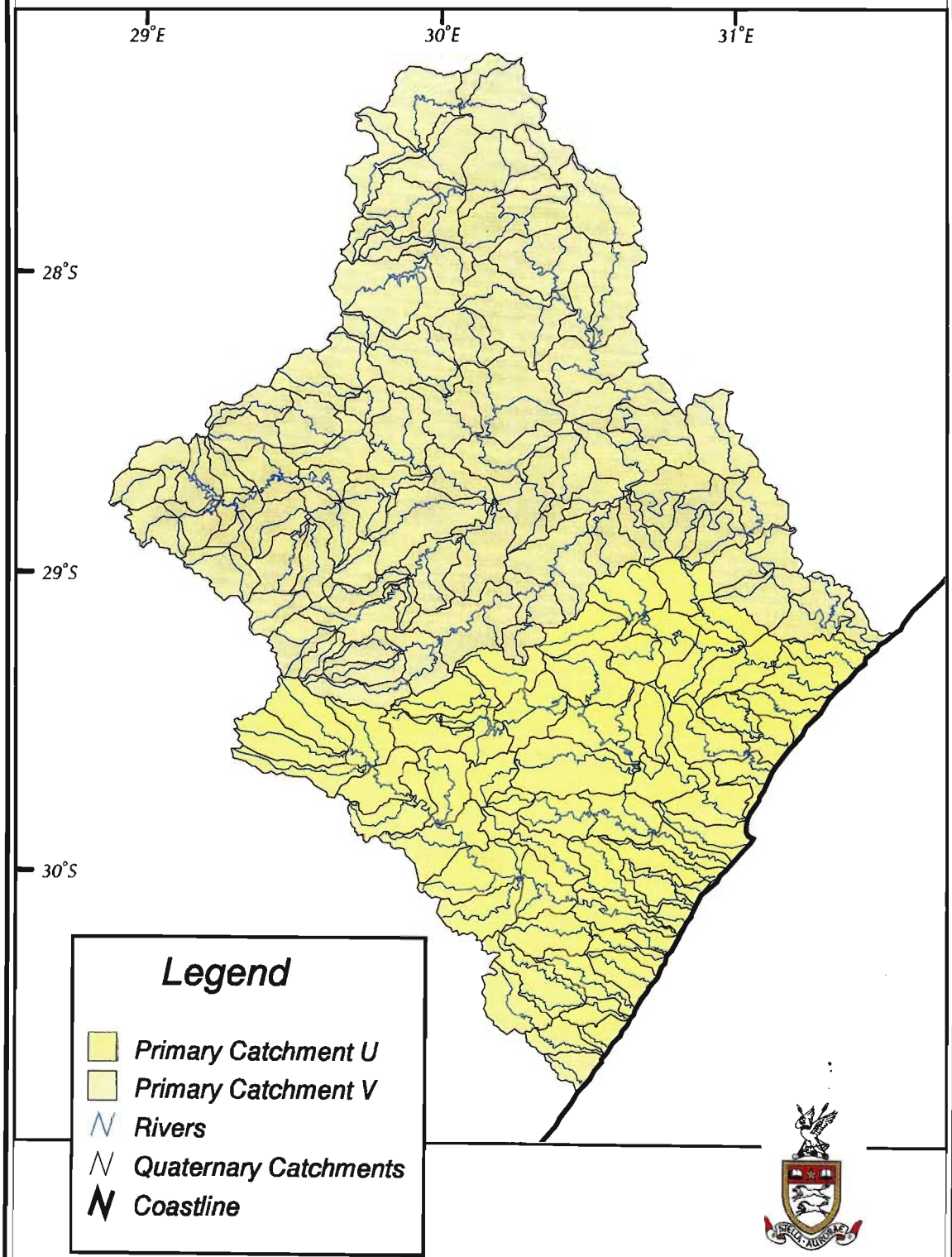

From this list of contributing catchments the total number of catchments that are to be modelled using *ACRU* can be determined and the numerical ordering identity of each catchment, needed for the *ACRU* input menu, can be assigned via a Fortran script.

The other options available for an *ACRU* simulation described in Section 7.6, such as using assuming a future climate scenario, are available when simulating the catchments as cascading catchments, as shown in Figure 7.6. An *ACRU* input menu is established for each catchment by extracting the relevant information from the *ACRU* Input Database specified. All the rainfall files required for the catchments selected are prepared for use.

To model the isolated catchments with *ACRU* when determining accumulated flows, one distributed *ACRU* menu is established using the individual *ACRU* menus that have been created for each catchment selected. This distributed menu contains the details of all the catchments that feed the selected end catchment and the ordering of the catchments to route the streamflow from one catchment to its downstream catchment. Therefore, the structures are in place to perform *ACRU* simulations on Quaternary or Quinary Catchments with the option of the catchments' cascading from the upstream catchment to their downstream catchments.

Output from a simulation of cascading catchments can also be extracted for import into a GIS or spreadsheet, as detailed in the following section.

## 7.8 Extraction of Output from *ACRU* for Presentation

Once the *ACRU* simulations have been performed the output that was required from any simulation needs to be extracted and imported into the ARC/INFO GIS or a spreadsheet for display purposes.

### 7.8.1 Graphical display of output from *ACRU* using the ARC/INFO GIS

The original extraction of output from the *ACRU* model for import into the ARC/INFO GIS for display purposes was time consuming. Routines needed to be written to easily extract output from the *ACRU* model for each catchment for import into GIS for display purposes.

To achieve this, the monthly statistical output generated by *ACRU* is extracted via a Fortran script and is stored in a condensed ASCII file per output variable. The ASCII files are in a column format, with each column representing a statistical output for a month of the year and each row representing a catchment.

A Fortran script was written to read the Output Selection File. This file records which output variables were initially selected. These variables are then written to the screen and information from one of the output variables can be selected. This identifies which stored ASCII file to use to extract the relevant statistical information. Various statistical output is computed by *ACRU*, *viz.*

i) mean;
ii) coefficient of variation CV (%);
iii) minimum value;
iv) maximum value;
v) 10th percentile value;
vi) 20th percentile value;
vii) 50th percentile value;
viii) 80th percentile value; and
ix) 90th percentile value

and one of the these statistics can be extracted, in turn, for the output variable selected

Either the output for any specified month, the annual total or output for all the months can be selected for extraction from the isolated ASCII file.

Similarly, the extreme value analysis output can be extracted for use in the GIS. Output from either the Gumbel, Log-Normal or Log-Pearson analyses can be selected. Consequently, the

return period of 2, 5, 10, 20 or 50 years must be chosen. The desired column from the ASCII file for the selected output is extracted and this information can then easily be imported into the GIS using the *JOINITEM* command in ARC/INFO which joins the extracted column of information to the coverage of the catchment under investigation.

The output from a crop yield analysis is also extracted using a similar program. The options for extraction include the same statistical options as available for the hydrological output, as well as the percentiles (10, 20, 33, 50, 66, 80 and 90%) output from the economic analysis, as shown in Figure 7.6.

In the case of sediment yield, $S_y$, the output from *ACRU* is recorded in tonnes sediment for the entire catchment. Therefore, in order to calculate the sediment yield from a catchment in tonnes per hectare, the output is converted by

$$S_y / \text{area (km}^2\text{) x100.}$$

A similar procedure using the catchment area is used to convert the accumulated streamflow from mm per catchment to $m^3$, in this case

accumulated streamflow ($m^3 \times 10^6$) = (accumulated streamflow (mm) / 1000) x area ($km^2$).

### 7.8.2 Graphical display of a time series from *ACRU*

A monthly or daily output file can also be generated from an *ACRU* simulation for the variables selected in the Output Selection File. This information can be imported into a spreadsheet and plotted as a time series to illustrate a temporal change in response of, say, runoff over time.

* * * * * * *

This chapter has described the refinements made to the procedures which were previously existing for simulating of agrohydrological responses at a Quaternary Catchment scale. With

these refinements the hydrology of both Quaternary Catchments or Quinary Catchments can be simulated as either individual or cascading catchments for both present and future climatic conditions. There are also a greater variety of options that can be specified for the *ACRU* simulations of the Quaternary Catchments. With these structures in place, not only is a greater versatility achieved, but also a more efficient way of obtaining results in assessments of climate change and other impacts for southern Africa.

In the following chapter the techniques developed to assess climate change impacts are applied and the results from the assessment of the agricultural impacts of changes in climate, as simulated using output from the UKTR-S and HadCM2 GCMs, are presented.

# 8. APPLICATION OF TECHNIQUES TO ASSESS POTENTIAL IMPACTS OF CLIMATE CHANGE ON AGRICULTURE IN SOUTHERN AFRICA

The primary objective of this thesis is the refinement of modelling tools and restructuring of databases used in this study as described in Chapters 4 to 7 (greyed out in Figure 8.1). The secondary objectives include the assessment of potential impacts on agriculture (Chapter 8) and water resources (Chapters 9 and 10) by using these fundamentally revised tools in southern Africa, as well as the analysis of uncertainties in the impact assessments and suggested adaptation strategies for southern Africa (Chapters 11 and 12).

At present cultivated areas occupy almost half of the total land area in southern Africa (Hulme, 1996) and the agricultural sector employs an estimated 16.5% of South Africa's economically active population. Agriculture contributes approximately 4.4% directly to South Africa's Gross Domestic Product (1995) and when processing and adding value have been taken into account this figure rises to 13% (Schulze, 1997b). In relative terms agriculture is even more important in Lesotho, constituting 19% of its GDP, and Swaziland where it constitutes 23% of the country's GDP (Schulze, 1997b). In addition, an increasing population places demands on the agricultural sector to increase production at a rate of around 3% per annum (Schulze *et al.*, 1996).

Throughout the southern African region the staple crops are cereals complemented by legumes and pulses. The staple food is maize and almost all of the region's production is rainfed, however, irrigation is critical in certain zones and for some crops. Southern Africa's agricultural productions is vulnerable to climatic variations, with Lesotho having the highest vulnerability according to Hulme (1996).

The impacts of climate change on agricultural production can be significant (Rosenzweig and Hillel, 1998), especially in climatically marginal areas such as southern Africa. Changes in temperature, precipitation and $CO_2$ are expected to affect plant physiological processes and

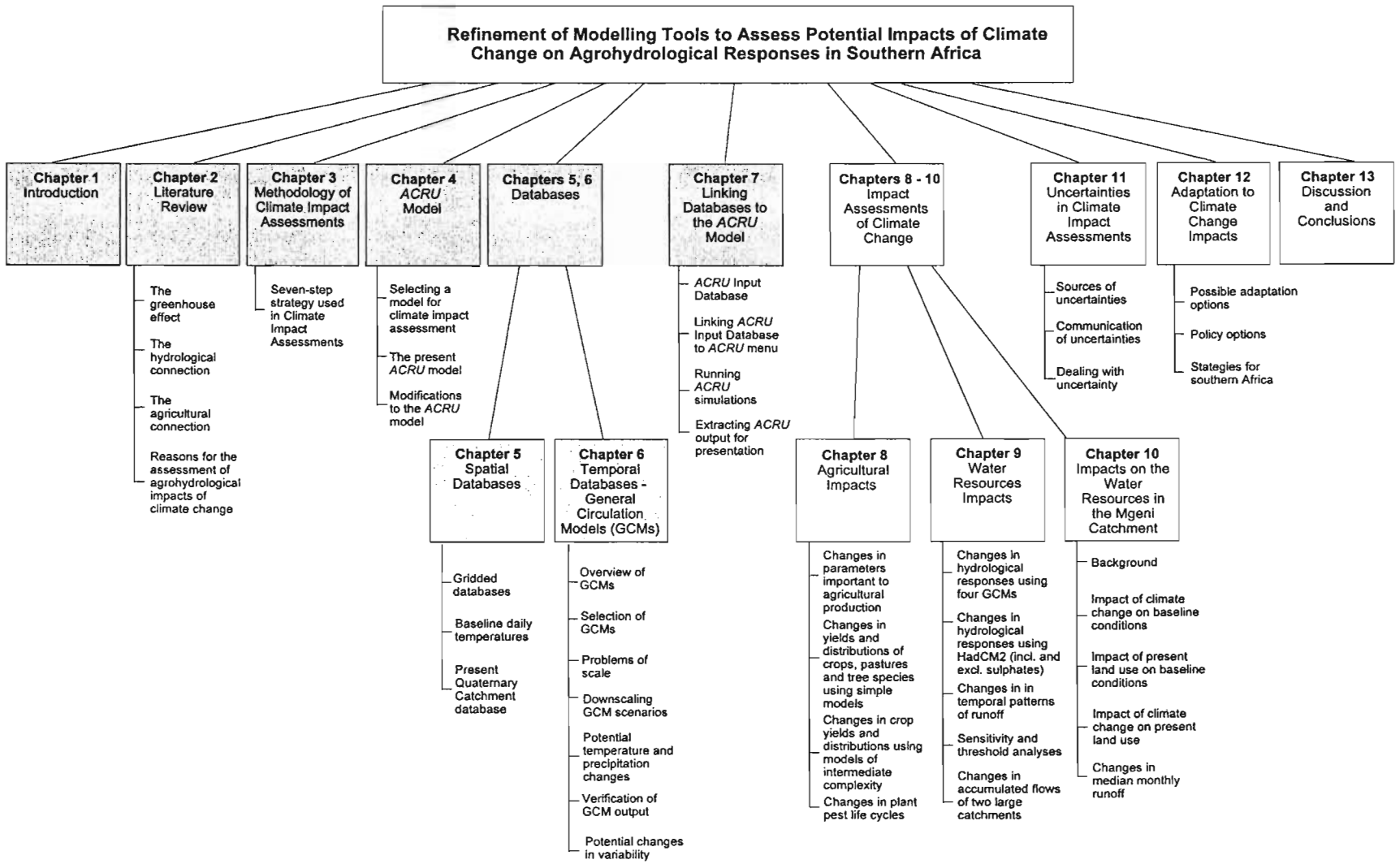


Figure 8.1 Layout plan of thesis

hence agricultural production in the study region (cf. Chapter 2, Section 2.3) and also the life cycles of plant pests (cf. Chapter 2, Section 2.3.2.2).

The structure of this chapter is given in Figure 8.2. It comprises four main sections. The first section (Section 8.1) comprises of an assessment of potential impacts of climate change on climatic parameters important to agricultural production, *viz.* heat units, frost, positive chill units and moisture growing season.

In Section 8.2 simple crop models are used to determine potential changes in yield and climatically optimum growth areas of selected crops, pastures and commercial tree species under conditions of potential climate change. The assessments described in Sections 8.1 and 8.2 were conducted using climatic output from UKTR-S which excluded sulphate forcing (cf. Chapter 6, Section 6.1.2.1) and two versions of HadCM2, one including and the other excluding sulphate forcing (cf. Chapter 6, Section 6.1.2.2 and Section 6.1.2.3 respectively). By using these three GCM scenarios, comparisons could be made between the agricultural impacts from different GCMs as well as from the inclusion and exclusion of the cooling effects of sulphate aerosols.

The *ACRU* maize and winter wheat yield submodels, which are considered models of intermediate complexity and include $CO_2$ fertilisation feedback effects, were used to simulate potential changes in maize and winter wheat yield respectively in southern Africa using future climate scenarios generated by HadCM2 as described in Section 8.3. Since maize is the staple food crop of southern Africa, a more detailed study was undertaken for this crop, including a sensitivity and economic analysis using HadCM2 output as input into the *ACRU* model. The maize yield submodel in *ACRU* can account for $CO_2$ feedbacks and, therefore, results were obtained for both inclusion and exclusion of the potential fertilisation effects associated with increases in atmospheric $CO_2$ concentrations on crop yield (cf. Chapter 2, Section 2.3.1.1). Simulations were carried out in the study area to investigate potential changes in winter wheat yield resulting from climate change, using the modified version of *ACRU* winter wheat submodel (Chapter 4, Section 4.5.5).

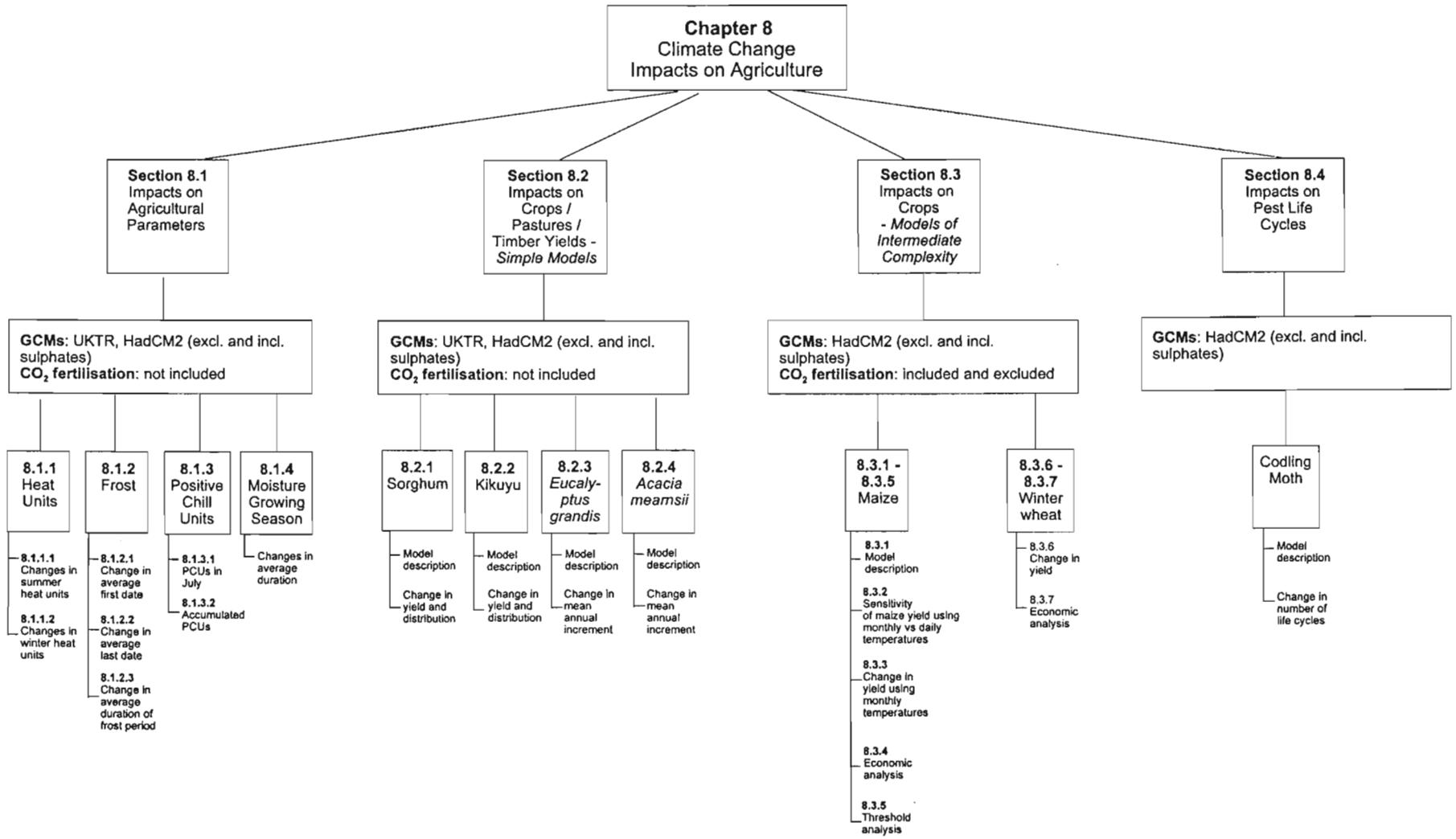


Figure 8.2 Layout plan of Chapter 8: Application of techniques to assess impacts of climate change on agriculture in southern Africa

Finally, the potential changes in the number of life cycles per annum of a plant pest, the codling moth, were analysed and these results are described in Section 8.4.

For many of the climate change assessments statistical tables were prepared. These statistical tables provide information on mean, maximum and minimum values, the coefficient of variation and on a frequency analysis of the parameters being mapped, for each of the nine provinces in South Africa as well as for Swaziland and Lesotho. All values for each province / country are calculated from all the gridded values falling within the respective province or country.

The coefficient of variation (CV) is a measure of the variability of grid cells within the province / country. For the frequency analysis the 20%, 50% and 80% exceedence probabilities were calculated. In the case of the 20% exceedence probability column, this means that for that province / country at least 20% or $^{1}/_{5}$ of the province has grid cells with values exceeding the given figure. Similarly the 50% percentile designates the median value. Where extrapolation procedures have taken place, these values may be considered unreliable and are sometimes truncated. In such cases this is designated with an asterisk (*) followed by a warning below the table. Statistics calculated for the various parameters under present climatic conditions were obtained from Schulze (1997b).

## 8.1 Potential Impacts of Climate Change on Parameters Important to Agricultural Production

Certain climatic parameters such as heat units, positive chill units and frost affect the growth of a plant (Schulze, 1997b). Changes particularly in temperature and to a lesser extent precipitation will affect these parameters, thus affecting locations where certain crops can be grown and their productivity. Soil moisture and the duration moisture growing season are also expected to change in a future climate. Potential changes in these agriculturally important parameters were simulated using output from the UKTR-S and HadCM2, excluding sulphate forcing (HadCM2-S), and the HadCM2, including sulphate forcing (HadCM2+S), in conjunction with the baseline database and the results are presented in the following sections.

### 8.1.1 Potential changes in heat units

The concept of the heat unit revolves around the development a plant or organism being dependent upon the total heat to which it is subjected during its growth cycle, or during certain critical developmental stages. In general, the lower the temperature the slower the rate of growth and development of plants and invertebrate animals (Schulze, 1997b).

Heat units are expressed as degree days (°days), where these are expressed as an accumulation of mean temperatures above a certain lower threshold value (below which active development is considered not to take place), and below an upper limit (above which growth is considered to remain static or even decline), over a period of time. For example, if the threshold temperature is 10 °C and the mean temperature of a given day is 22 °C, then 12 °days, or heat units, are accumulated for that day to a previous total (Schulze, 1997b).

The lower and upper (in brackets) threshold limits vary with crop or pest, e.g. for

| | | | |
|---|---|---|---|
| i) | peas | : | 4 °C (26 °C) |
| ii) | maize | : | 10 °C (30 °C) |
| iii) | citrus, sugarcane | : | 13 °C |
| iv) | oriental fruit moth | : | 7 °C (32 °C) |
| v) | codling moth | : | 11 °C (34 °C) |

Degree days are accumulated from a starting date known as the biofix, which varies from species to species (Schulze, 1997b). Potential changes in the accumulated heat units for the summer and winter seasons in the study area were calculated and mapped.

#### 8.1.1.1 Heat units in the summer season, October to March

Using a minimum threshold daily average of 10 °C, which is applicable to southern Africa's staple food crop of maize, heat units were mapped and intra-provincial statistics prepared, for the six months constituting the summer half of the year, *viz.* October to March, for present and future climatic conditions. In addition, the changes in heat units from present to future climate were mapped.

The map of heat units for the summer season under the present climate (Figure 8.3, top) shows a range from less than 1 200 °days in Lesotho to more than 2 800 °days in the most northerly regions (maize requires, for example, 1 500 - 1 770 ° days to ripen). Using future temperatures as simulated by UKTR-S, the entire study area showed increases in heat units although large parts of Lesotho are expected to still receive less than 1 200 °days in summer (Figure 8.3, middle). The hot northern and eastern perimeter of southern Africa could expect heat units in excess of 3 000 °days in the summer season using future estimates of temperature. This equates to an increase of 500 to 600 °days in these northern regions (Figure 8.3, bottom). The smallest increases of less than 200 °days are expected to occur in the north-eastern parts of Lesotho and the Western Cape Province according to future temperatures simulated by UKTR-S.

| | |
|---|---|
| Figure 8.3 | Heat units (°days) for the summer period of October to March: for present climate (top), future climate (middle) and the difference in heat units between future and present climates (bottom). Future climate scenario from UKTR-S |

The statistics calculated using present climatic conditions show that in parts of the Free State, KwaZulu-Natal and Lesotho no heat units with a base temperature of 10 °C are accumulated in the entire summer (see present minimum values in Table 8.1). Using future climatic information from UKTR-S only KwaZulu-Natal and Lesotho are predicted to have some areas with no heat units accumulating for the summer period (see future minimum values in Table 8.1).

With temperature output from HadCM2-S (Figure 8.4, top left), the pattern of increases in summer heat units are similar to those results obtained using the earlier version of this GCM, the UKTR-S (Figure 8.3, middle). However, fewer areas are simulated to experience increases in excess of 600 °days in summer (Figure 8.4, bottom left).

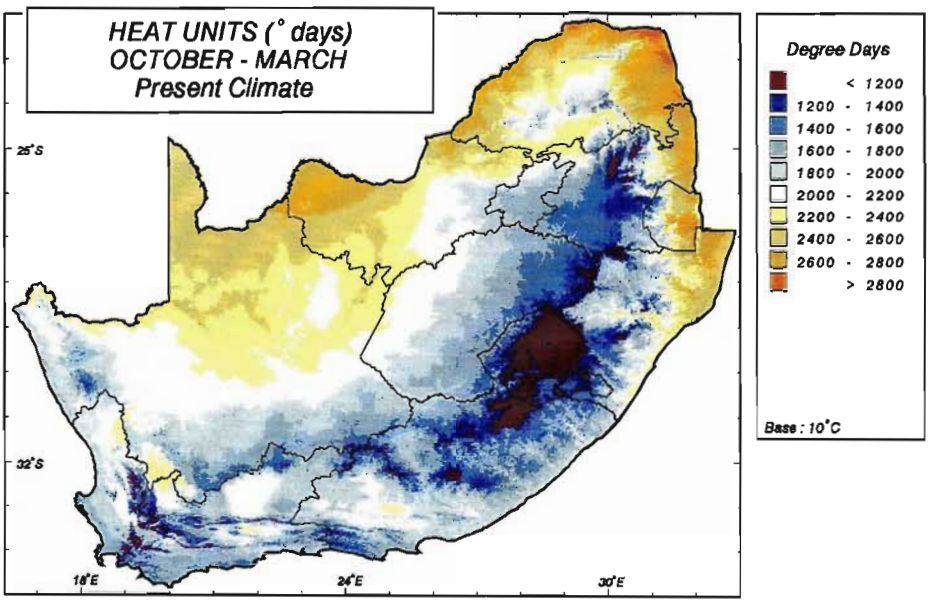


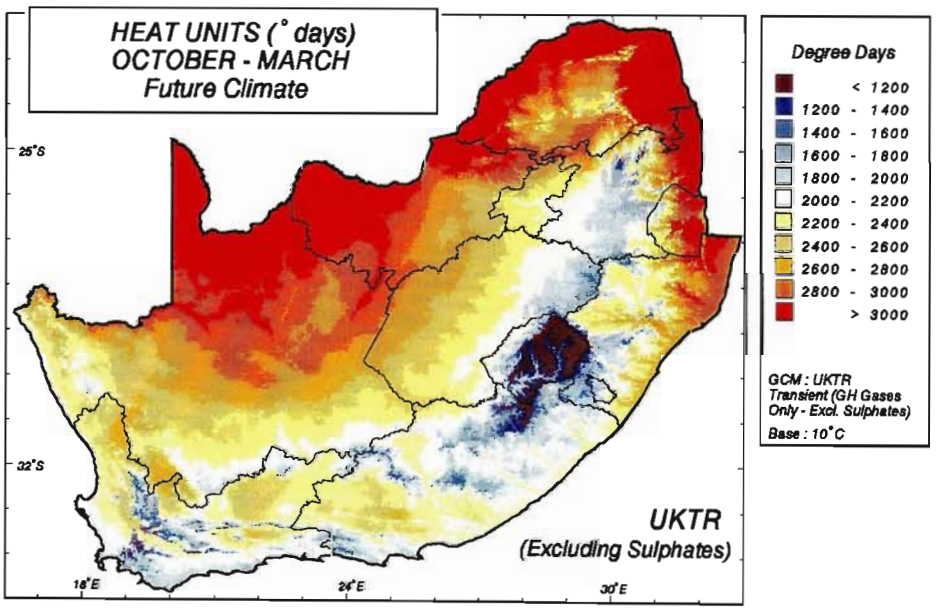


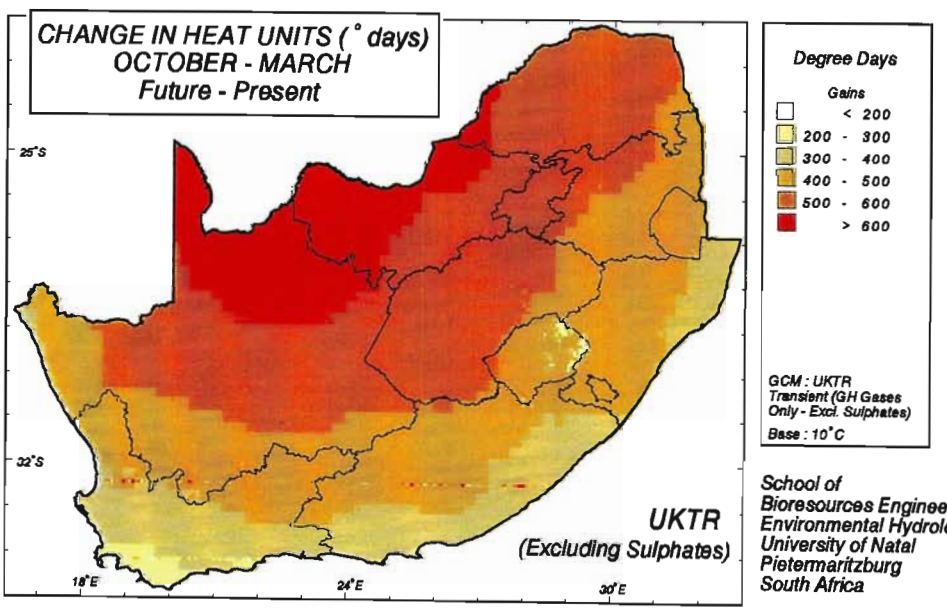


School of
Bioresources Engineering and
Environmental Hydrology
University of Natal
Pietermaritzburg
South Africa

Table 8.1 Statistics for heat units in the summer season (October to March) for present climatic conditions and a future (2X $CO_2$) climate scenario from UKTR-S

| Heat Units (° days, Base 10°C), October - March | | | | | | | | | | | | | | |
|---|---|---|---|---|---|---|---|---|---|---|---|---|---|---|
| Province / Country | Mean Value | | CV (%) | | Maximum Value | | Minimum Value | | Exceedence Probability | | | | | |
| | | | | | | | | | 20% | | 50% | | 80% | |
| | Present | Future | Present | Future | Present | Future | Present | Future | Present | Future | Present | Future | Present | Future |
| Northern Province | 2400 | 2946 | 13 | 11 | 3053 | 3583 | 1114 | 1636 | 2681 | 3230 | 2474 | 3024 | 2126 | 2674 |
| Mpumalanga | 1812 | 2297 | 25 | 20 | 2857 | 3336 | 273 | 774 | 2282 | 2795 | 1645 | 2141 | 1439 | 1918 |
| North-West | 2344 | 2951 | 10 | 9 | 2806 | 3456 | 1612 | 2186 | 2585 | 3214 | 2357 | 2958 | 2119 | 2702 |
| Northern Cape | 2129 | 2671 | 12 | 12 | 2844 | 3314 | 790 | 1239 | 2384 | 2984 | 2158 | 2702 | 1879 | 2358 |
| Gauteng | 1825 | 2364 | 9 | 7 | 2326 | 2862 | 1539 | 2052 | 1944 | 2489 | 1793 | 2335 | 1691 | 2228 |
| Free State | 1793 | 2322 | 14 | 12 | 2273 | 2859 | 0 | 7 | 2031 | 2586 | 1810 | 2344 | 1584 | 2089 |
| KwaZulu-Natal | 1937 | 2355 | 23 | 18 | 2817 | 3216 | 0 | 0 | 2391 | 2779 | 1905 | 2342 | 1565 | 2002 |
| Eastern Cape | 1669 | 2072 | 17 | 13 | 2322 | 2717 | 6 | 259 | 1905 | 2302 | 1699 | 2101 | 1479 | 1885 |
| Western Cape | 1798 | 2178 | 15 | 13 | 2446 | 2787 | 394 | 621 | 2021 | 2431 | 1829 | 3209 | 1613 | 1957 |
| Swaziland | 2311 | 2741 | 15 | 12 | 2836 | 3257 | 1174 | 1635 | 2613 | 3037 | 2411 | 2840 | 1984 | 2425 |
| Lesotho | 824 | 1253 | 65 | 49 | 1890 | 2356 | 0 | 0 | 1400 | 1881 | 814 | 1278 | 164 | 594 |



Table 8.2 Statistics for heat units in the winter season (April to September) for present climatic conditions and future (2X $CO_2$) climate scenario from UKTR-S

| Heat Units (° days, Base 10°C), April - September | | | | | | | | | | | | | | |
|---|---|---|---|---|---|---|---|---|---|---|---|---|---|---|
| Province / Country | Mean Value | | C.V. (%) | | Maximum Value | | Minimum Value | | Exceedence Probability | | | | | |
| | | | | | | | | | 20% | | 50% | | 80% | |
| | Present | Future | Present | Future | Present | Future | Present | Future | Present | Future | Present | Future | Present | Future |
| Northern Province | 1236 | 1830 | 25 | 16 | 1972 | 2539 | 335 | 876 | 1566 | 2137 | 1194 | 1810 | 964 | 1566 |
| Mpumalanga | 791 | 1322 | 60 | 37 | 1884 | 2421 | 14 | 294 | 1225 | 1784 | 595 | 1164 | 378 | 863 |
| North-West | 707 | 1345 | 24 | 15 | 1253 | 1916 | 413 | 958 | 882 | 1557 | 656 | 1313 | 550 | 1152 |
| Northern Cape | 607 | 1158 | 38 | 25 | 1704 | 2174 | 0 | 132 | 835 | 1450 | 589 | 1170 | 400 | 901 |
| Gauteng | 594 | 1132 | 27 | 16 | 1069 | 1669 | 355 | 846 | 693 | 1299 | 496 | 1068 | 443 | 980 |
| Free State | 399 | 896 | 29 | 20 | 615 | 1253 | 0 | 0 | 512 | 1094 | 381 | 878 | 282 | 722 |
| KwaZulu-Natal | 1026 | 1511 | 47 | 31 | 1832 | 2274 | 0 | 0 | 1538 | 2006 | 960 | 1469 | 592 | 1119 |
| Eastern Cape | 597 | 1024 | 57 | 36 | 1510 | 1966 | 0 | 0 | 925 | 1370 | 563 | 1041 | 268 | 677 |
| Western Cape | 601 | 998 | 42 | 29 | 1310 | 1671 | 0 | 49 | 829 | 1236 | 636 | 1035 | 356 | 765 |
| Swaziland | 1360 | 1866 | 23 | 16 | 1824 | 2309 | 437 | 964 | 1635 | 2128 | 1474 | 1979 | 1053 | 1576 |
| Lesotho | 94 | 324 | 111 | 77 | 579 | 1110 | 0 | 0 | 204 | 591 | 51 | 300 | 0 | 21 |

Figure 8.4 Heat units (°days) for the summer period of October to March: future climate (top left) and the difference in heat units between future and present climates (bottom left) using the future climate scenario from HadCM2-S. Future climate (top right) and the difference in heat units between future and present climates (bottom right) using the future climate scenario from HadCM2+S

Much smaller increases in summer heat units were calculated using changes in temperature as simulated by HadCM2+S (Figure 8.4, top right). This is to be expected as sulphate aerosols have a net cooling effect in the atmosphere. The increases in heat units in summer range from less than 300 °days in parts of Lesotho and along the eastern and southern coastlines of southern Africa, to more than 500 °days in isolated regions of Lesotho (Figure 8.4, bottom right). The northern parts of the study could have gains of between 400 and 500 summer °days if sulphate forcing is considered compared to gains in excess of 600 °days if the feedbacks of these aerosols are excluded.

#### 8.1.1.2 Heat units in the winter season, April to September

The mapped patterns of heat units in the winter half of the year, *viz.* April to September, for present climatic conditions broadly follow the same patterns as those for the summer season (Figure 8.5, top). However, the number of °days in the winter season are far lower, with much of Lesotho, for example, experiencing on average less than 200 °days the entire winter season (see Table 8.2).

Figure 8.5 Heat units (°days) for the winter period of April to September: for present climate (top), future climate (middle) and the difference in heat units between future and present climates (bottom). Future climate scenario from UKTR-S

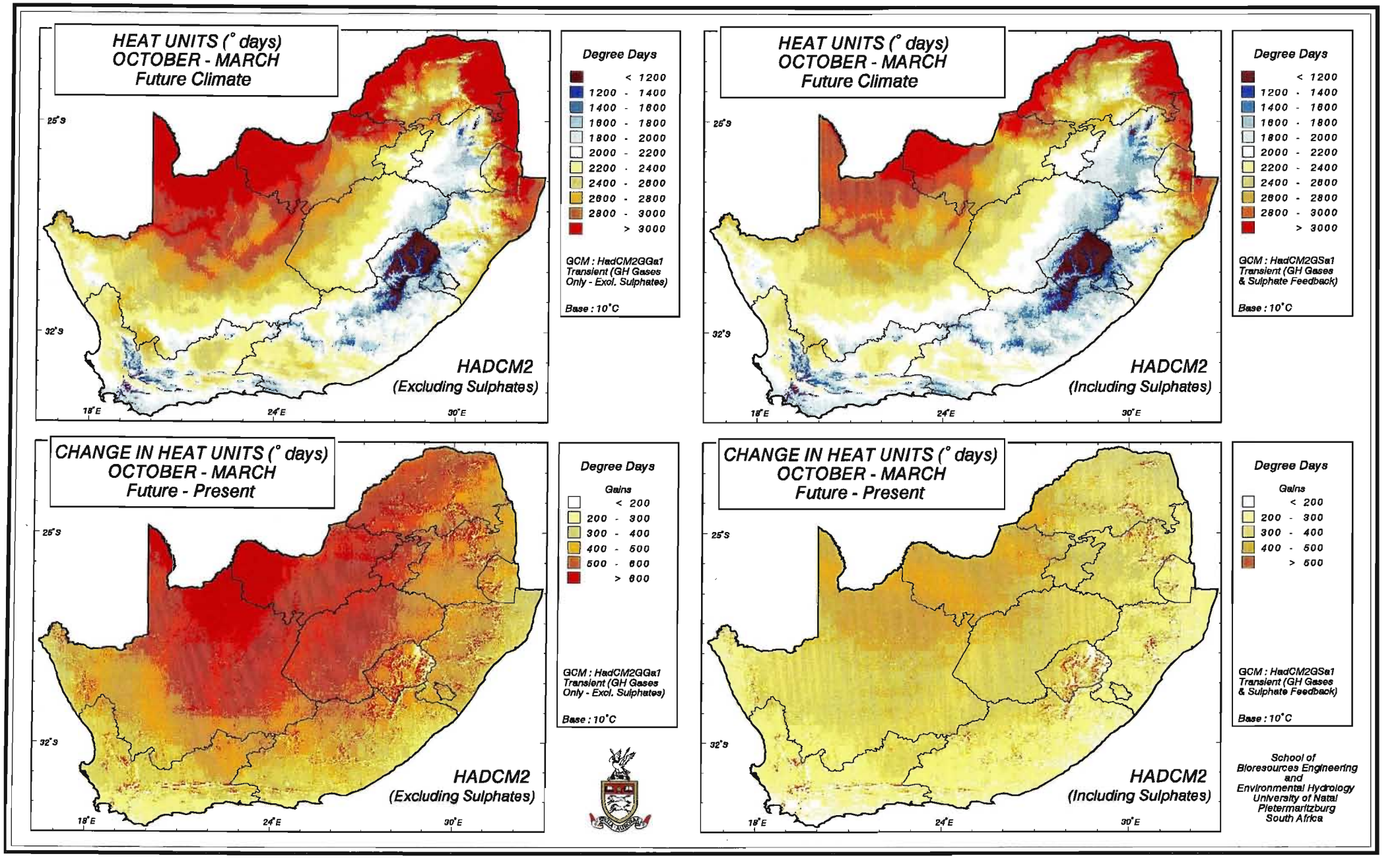
HEAT UNITS (° days)
OCTOBER - MARCH
Future Climate
25°S
32°S
18°E
24°E
30°E
HADCM2
(Excluding Sulphates)
Degree Days
< 1200
1200 - 1400
1400 - 1600
1600 - 1800
1800 - 2000
2000 - 2200
2200 - 2400
2400 - 2600
2600 - 2800
2800 - 3000
> 3000
GCM : HadCM2GGa1
Transient (GH Gases
Only - Excl. Sulphates)
Base : 10°C
HEAT UNITS (° days)
OCTOBER - MARCH
Future Climate
HADCM2
(Including Sulphates)
Degree Days
< 1200
1200 - 1400
1400 - 1600
1600 - 1800
1800 - 2000
2000 - 2200
2200 - 2400
2400 - 2600
2600 - 2800
2800 - 3000
> 3000
GCM : HadCM2GSa1
Transient (GH Gases
& Sulphate Feedback)
Base : 10°C
CHANGE IN HEAT UNITS (° days)
OCTOBER - MARCH
Future - Present
HADCM2
(Excluding Sulphates)
Degree Days
Gains
< 200
200 - 300
300 - 400
400 - 500
500 - 600
> 600
GCM : HadCM2GGa1
Transient (GH Gases
Only - Excl. Sulphates)
Base : 10°C
CHANGE IN HEAT UNITS (° days)
OCTOBER - MARCH
Future - Present
HADCM2
(Including Sulphates)
Degree Days
Gains
< 200
200 - 300
300 - 400
400 - 500
> 600
GCM : HadCM2GSa1
Transient (GH Gases
& Sulphate Feedback)
Base : 10°C
School of
Bioresources Engineering
and
Environmental Hydrology
University of Natal
Pietermaritzburg
South Africa

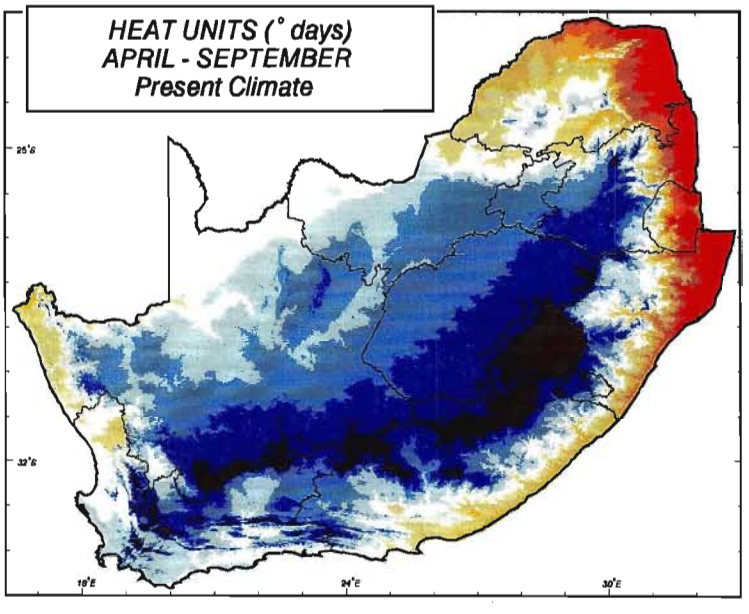


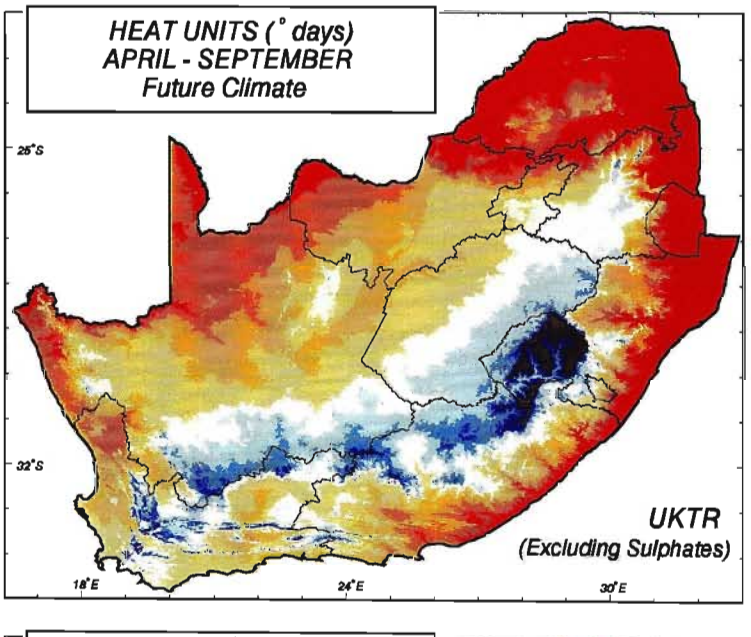


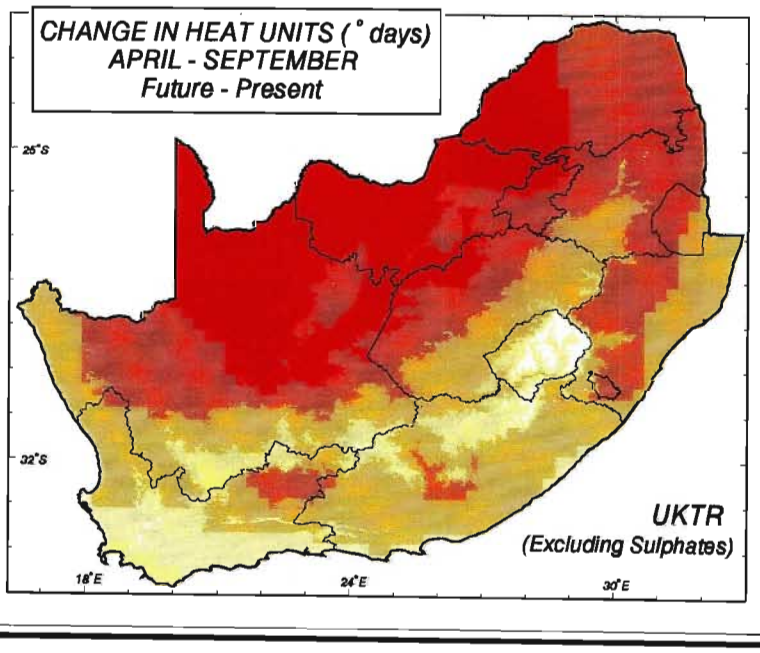


School of
Bioresources Engineering and
Environmental Hydrology
University of Natal
Pietermaritzburg
South Africa

As in the case of the summer season, large increases in the number of °days are expected in a future warmer climate using information from the UKTR-S (Figure 8.5, middle). There appears to be a similar pattern and range of increase as was found in the simulations of the summer season (Figure 8.5, bottom).

There are numerous provinces which have certain areas with no accumulated heat units for the winter season, *viz.* parts of the Northern Cape, Free State, KwaZulu-Natal, Eastern Cape and Western Cape as well as Lesotho (see present minimum values in Table 8.2). In a future climate, the Northern Cape and Western Cape provinces could expect to have heat units accumulating in the winter season (see future minimum values in Table 8.2).

Similar results of potential changes in winter heat units to those obtained using UKTR-S (Figure 8.5, middle and bottom) are obtained using HadCM2-S output (Figure 8.6, top left and bottom left).

| | |
|---|---|
| Figure 8.6 | Heat units (°days) for the winter period of April to September: future climate (top left) and the difference in heat units between future and present climates (bottom left) using the future climate scenario from HadCM2-S. Future climate (top right) and the difference in heat units between future and present climates (bottom right) using the future climate scenario from HadCM2+S |

However, when the cooling influence of sulphates is included in this GCM, the increases in heat units simulated are much lower (Figure 8.6, top right and bottom right). In the central regions of the study area increases of less than 200 °days could be expected and in the northern regions increases of between 300 and 400 °days were simulated using output from HadCM2+S.

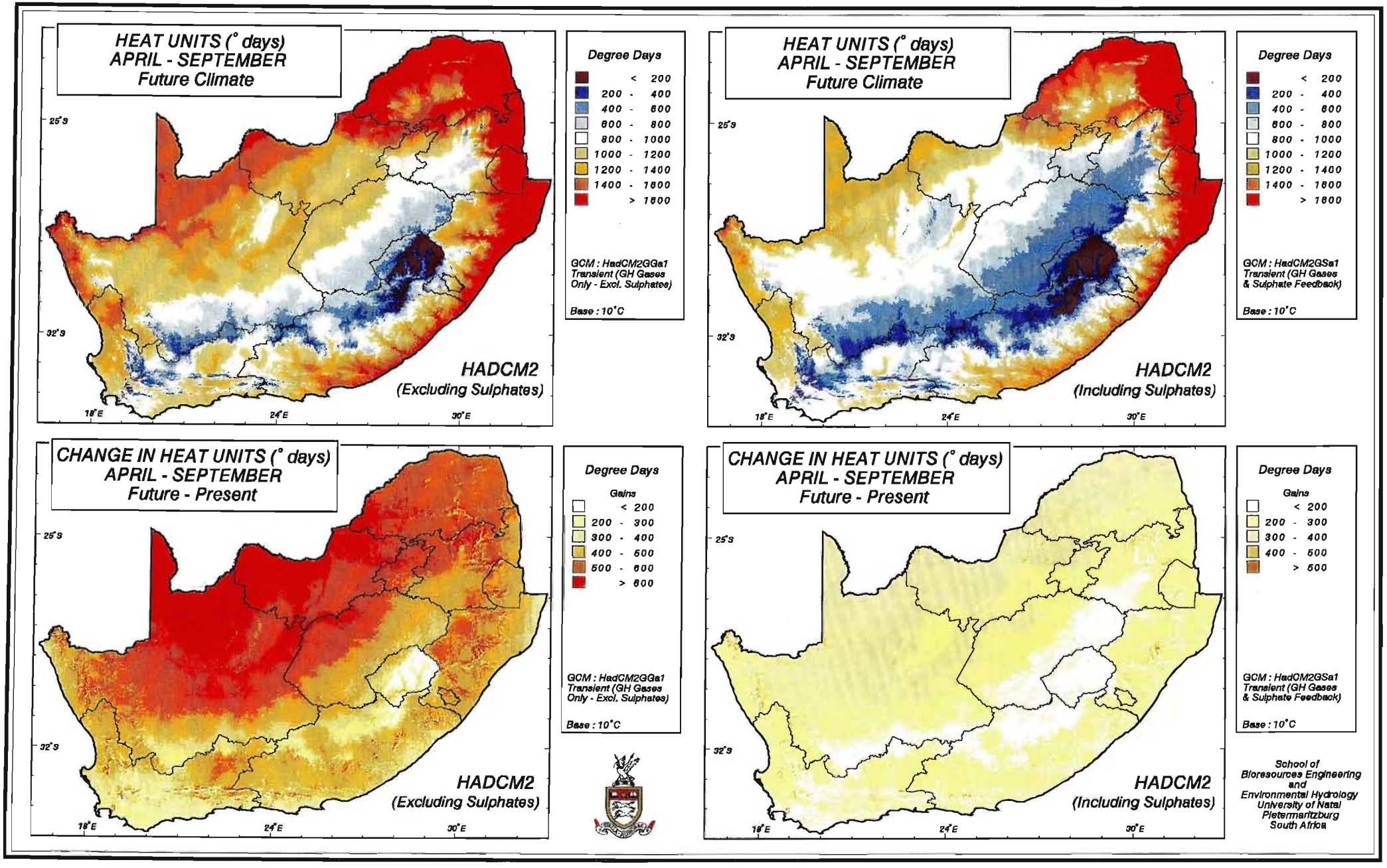
HEAT UNITS (° days)
APRIL - SEPTEMBER
Future Climate
25°S
32°S
18°E
24°E
30°E
HADCM2
(Excluding Sulphates)
Degree Days
< 200
200 - 400
400 - 600
600 - 800
800 - 1000
1000 - 1200
1200 - 1400
1400 - 1600
> 1600
GCM : HadCM2GGa1
Transient (GH Gases
Only - Excl. Sulphates)
Base : 10°C
HEAT UNITS (° days)
APRIL - SEPTEMBER
Future Climate
HADCM2
(Including Sulphates)
Degree Days
< 200
200 - 400
400 - 600
600 - 800
800 - 1000
1000 - 1200
1200 - 1400
1400 - 1600
> 1600
GCM : HadCM2GSa1
Transient (GH Gases
& Sulphate Feedback)
Base : 10°C
CHANGE IN HEAT UNITS (° days)
APRIL - SEPTEMBER
Future - Present
HADCM2
(Excluding Sulphates)
Degree Days
Gains
< 200
200 - 300
300 - 400
400 - 500
500 - 600
> 600
GCM : HadCM2GGa1
Transient (GH Gases
Only - Excl. Sulphates)
Base : 10°C
CHANGE IN HEAT UNITS (° days)
APRIL - SEPTEMBER
Future - Present
HADCM2
(Including Sulphates)
Degree Days
Gains
< 200
200 - 300
300 - 400
400 - 500
> 500
GCM : HadCM2GSa1
Transient (GH Gases
& Sulphate Feedback)
Base : 10°C
School of
Bioresources Engineering
and
Environmental Hydrology
University of Natal
Pietermaritzburg
South Africa

### 8.1.2 Potential changes in frost

While plants possess a number of physical and biological mechanisms which serve to avoid freezing (e.g. solute accumulation within the cell serving to depress freezing points by 2 to 3 °C; supercooling of water; facilitation of extra-cellular freezing), these mechanisms do not provide complete protection from below zero minimum temperatures. Frost can cause formation of ice within the plant cell and outside the cell. Fundamental biological changes can take place under conditions of frost (Levitt, 1980), including

i) accumulation of water soluble solutes such as sugars and sugar alcohols;
ii) accumulation of membrane proteins; and sometimes
iii) irreversible cell membrane injury (Schulze, 1997b).

Whereas, certain plants suffer some damage by frost, such as complete defoliation, from which they can recover, others are killed outright by frost. Low temperatures and frost are, therefore, often critical in determining plant survival and hence their distribution (Schulze, 1997b). Frost is also frequently the limiting factor for growing season length (IPCC, 1996b).

In this study the potential changes in average first date, last date and duration of the period of heavy frost were calculated using predictive equations developed by Schulze (1997b) as described in the following sections.

#### 8.1.2.1 Average first date of heavy frost

In order to estimate and map the average first date of heavy frost, i.e. when daily Stevenson screen minimum temperatures are less than 0 °C, Schulze (1997b) used data from 216 climate stations in southern Africa, each with long term (> 10 years) daily minimum temperatures, to develop a predictive equation which took account of the five factors below. In this equation

$$F_{fd} = - 0.00712Z - 0.01311\phi - 0.00047D_s + 0.05010T_{in} - 0.35391DT_{mn6} + 216.9$$
$$(n = 216; r^2 = 0.83)$$

where $F_{fd}$ = average first date of heavy frost (day of year from January 1)

$Z$ = altitude (m)

$\phi$ = latitude (° South)

$D_s$ = distance from sea (km)

$T_{in}$ = topographic valley index (-)

$DT_{mn6}$ = number of days per year with minimum temperatures ≤ 6 °C.

Using this equation Schulze (1997b) produced a map of the present average first date of heavy frost in the study area (Figure 8.7, top left). This map shows that the eastern seaboard and north-eastern lowveld areas experience either very late first frosts (July) or no frost occurrence at all, whereas, the high lying areas of the Drakensberg experience heavy frost as early as March (Schulze,1997b).

Figure 8.7 Average first date of heavy frost: for present climate (top left), future climate (bottom left), shift in areas experiencing heavy frost (top right) and change in average first date of heavy frost between future and present climates (bottom right). Future climate scenario from UKTR-S

Assuming this predictive equation to be valid for changed climatic conditions and using future minimum temperatures from UKTR-S, the map of average first date of heavy frost in a future climate was generated (Figure 8.7, bottom left). There is a predicted increase in the total area that is frost free under a future climate scenario (Figure 8.7, top right). In addition, the average first date of heavy frost is later in a future warmer climate, with many regions of the study area only receiving their first heavy frost in June or July in future. Most areas could expect the first heavy frost in the future to occur three to four weeks later than at present (Figure 8.7, bottom right). However, in the north-west of the study area there is an estimated delay of over five weeks in the start of heavy frost when using future minimum temperatures obtained from UKTR-S. For example, at present 50% of the Northern Cape experiences their first heavy frost by the 26 May however the date by which this occurs could move to around mid-June in the future (see 50% exceedence probability columns in Table 8.3).

## AVERAGE FIRST DATE OF HEAVY FROST
### Present Climate

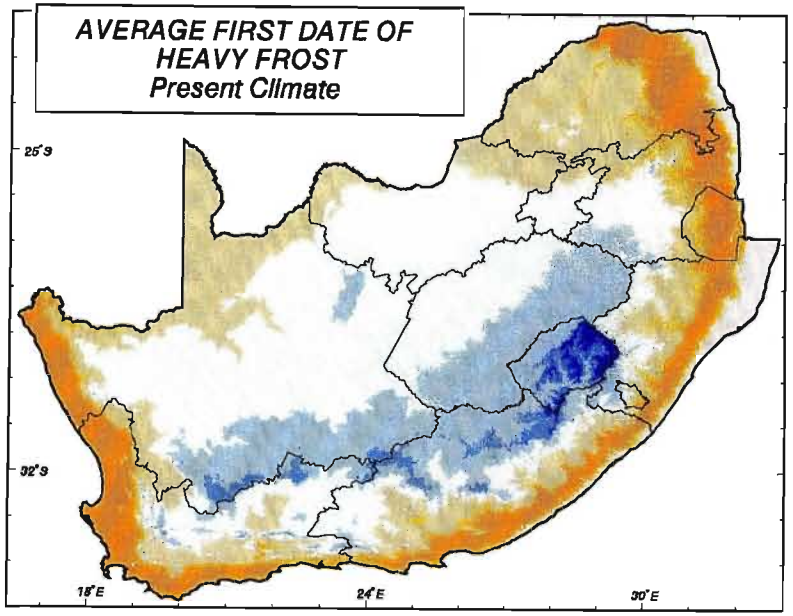


**Month**

- Frost free area
- March
- April
- May 1-15
- May 16-31
- June
- July

(Screen Minimum Temperature < 0 °C)

## SHIFT IN AREAS EXPERIENCING HEAVY FROST

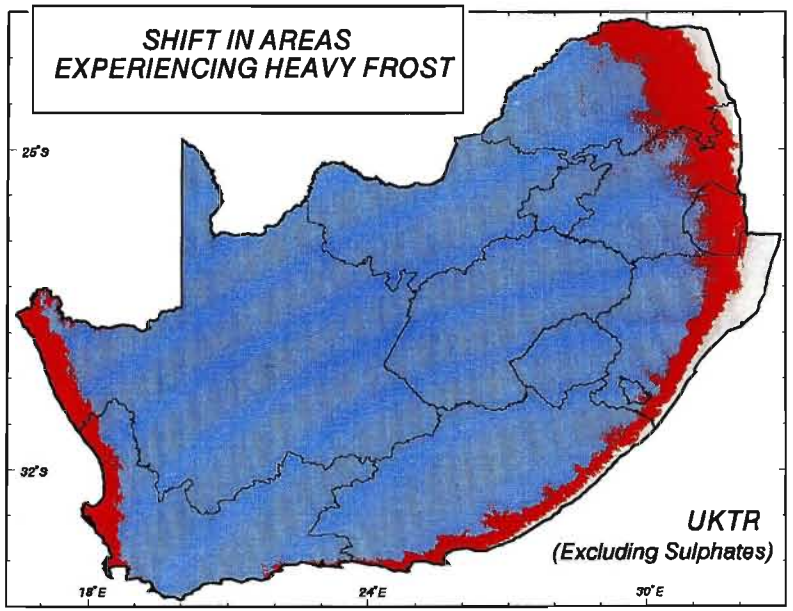


- Frost in present climate but frost free in future climate
- Frost can occur in present and future climate
- Frost free area, present and future climate

GCM : UKTR Transient (GH Gases Only - Excl. Sulphates)

(Screen Minimum Temperature < 0 °C)

## AVERAGE FIRST DATE OF HEAVY FROST
### Future Climate

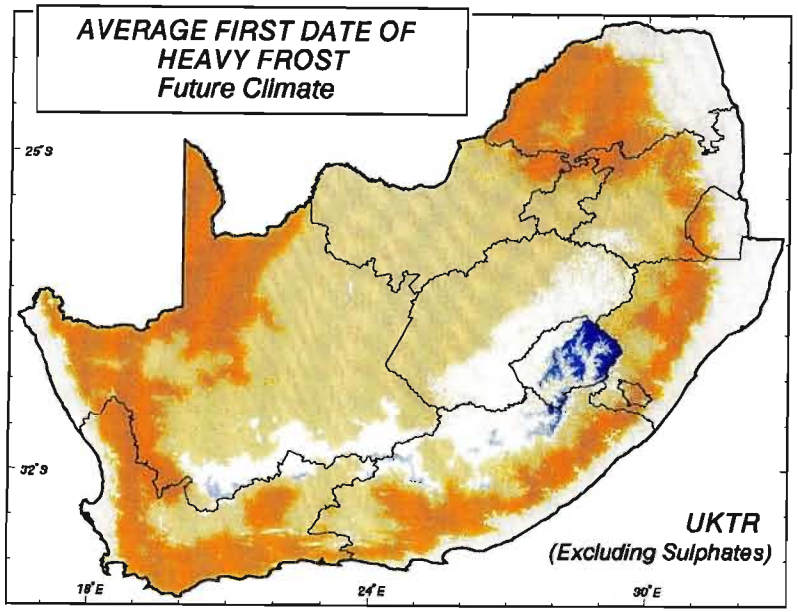


**Month**

- Frost free area
- March
- April
- May 1-15
- May 16-31
- June
- July

GCM : UKTR Transient (GH Gases Only - Excl. Sulphates)

(Screen Minimum Temperature < 0 °C)

## CHANGE IN AVERAGE FIRST DATE OF HEAVY FROST
### Future - Present

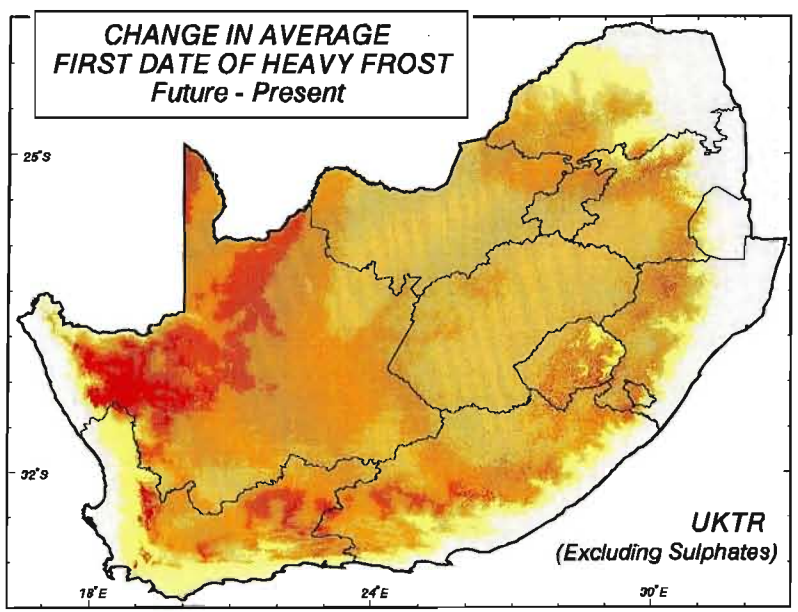


**Weeks**

- Frost free area in future climate

Later

- < 2
- 2 - 3
- 3 - 4
- 4 - 5
- > 5

GCM : UKTR Transient (GH Gases Only - Excl. Sulphates)

(Screen Minimum Temperature < 0 °C)

School of Bioresources Engineering and Environmental Hydrology
University of Natal
Pietermaritzburg
South Africa

Table 8.3 Statistics for average first date of heavy frost for present climatic conditions and a future (2X $CO_2$) climate scenario from UKTR-S

| First Date of Heavy Frost | | | | | | |
|---|---|---|---|---|---|---|
| Province / Country | Date by which at least x% of Province / Country will experience first heavy frost on average | | | | | |
| | 20% | | 50% | | 80% | |
| | Present | Future | Present | Future | Present | Future |
| Northern Province | 8 June | Frost free | 19 June | Early July | Early July | Early July |
| Mpumalanga | 17 May | Frost free | 29 May | 10 June | 1 July | Early July |
| North-West | 22 May | 10 June | 26 May | 15 June | 2 June | 24 June |
| Northern Cape | 16 May | 4 July | 26 May | 19 July | 3 June | Early July |
| Gauteng | 19 May | 7 June | 24 May | 14 June | 1 June | 24 June |
| Free State | 11 May | 28 May | 16 May | 3 June | 22 May | 12 July |
| KwaZulu-Natal | Frost free | Frost free | 2 June | 6 June | Early July | Early July |
| Eastern Cape | 8 May | 16 May | 26 May | 10 June | 29 June | Early July |
| Western Cape | 21 May | 5 June | 9 June | Early July | Early July | Early July |
| Swaziland | 20June | Frost free | Early July | 5 April | Early July | 17 May |
| Lesotho | 12 March | 5 April | 24 April | 17 April | 8 May | 27 May |

The delay in the average first date of heavy frost is not expected to be as long in many parts of the study area using output from the more recent HadCM2-S GCM in comparison to results obtained using the UKTR-S GCM (Figure 8.8, middle). The decrease in areas that could experience heavy frost in future, however, is fairly similar when using output from the two versions (Figure 8.8, bottom).

Figure 8.8 Average first date of heavy frost: for future climate (top), the change in average first date of heavy frost between future and present climates (middle) and shift in areas experiencing heavy frost (bottom). Future climate scenario from HadCM2-S

There is a notable difference in the results when including the effect of sulphate forcing in HadCM2. The delay in the start of heavy frost is expected to be less when including the influence of sulphates as the increases in temperature are not as significant. These occur, for example, the Free State was found to potentially have a two to three week delay in the onset of heavy frost using output from HadCM2-S (Figure 8.8, middle) compared to a less than a two week delay when including sulphate forcing in this GCM (Figure 8.9, middle).

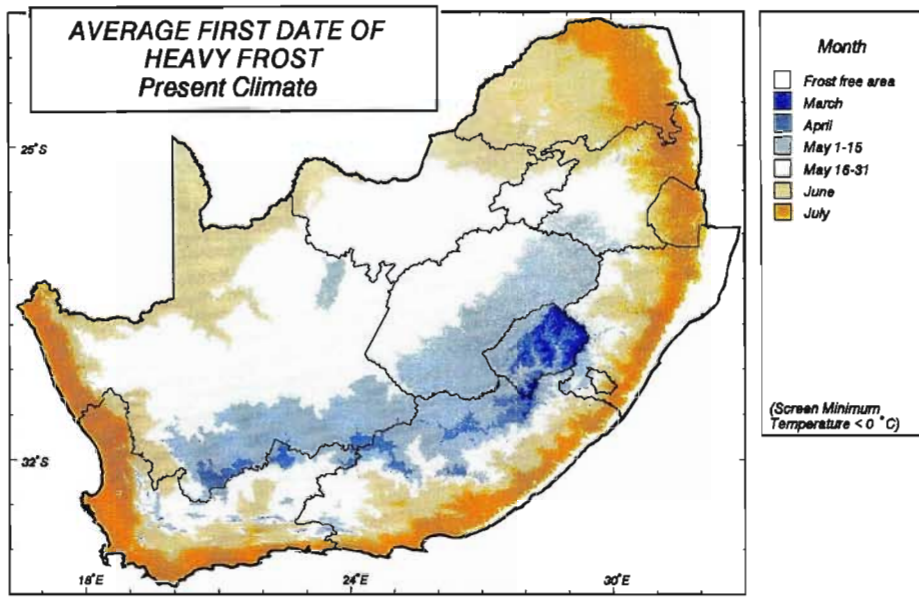


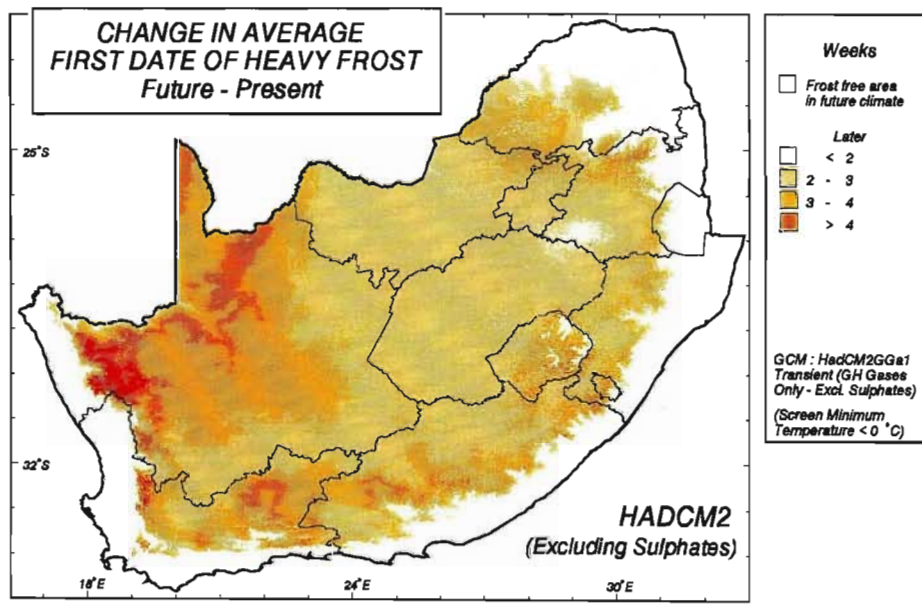


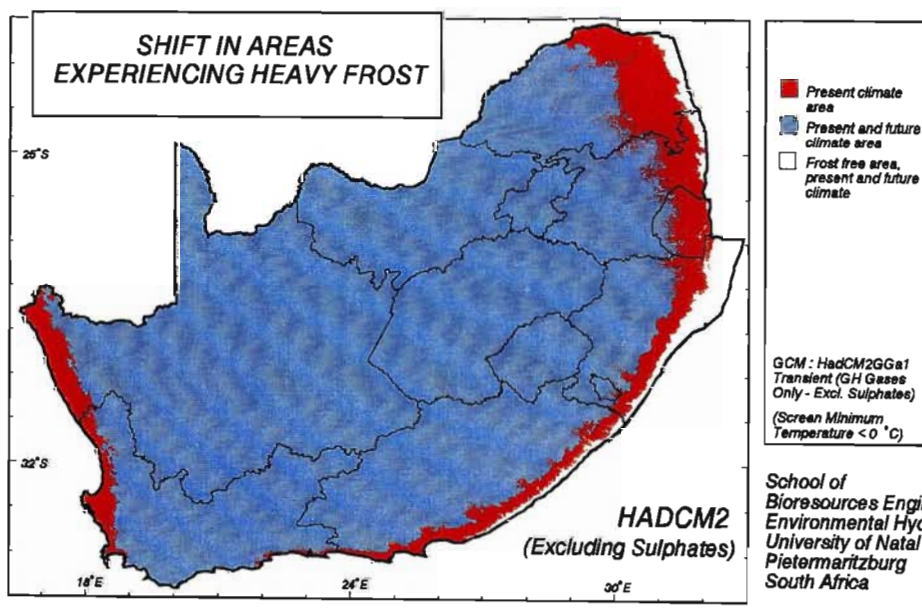


School of
Bioresources Engineering and
Environmental Hydrology
University of Natal
Pietermaritzburg
South Africa

Figure 8.9 Average first date of heavy frost: for future climate (top), the change in average first date of heavy frost between future and present climates (middle) and shift in areas experiencing heavy frost (bottom). Future climate scenario from HadCM2+S

There are only marginal differences in areas experiencing heavy frost between the two scenarios, *viz.* excluding and including sulphate forcing, for example along the western coast of the study area (Figure 8.8, bottom and Figure 8.9, bottom respectively).

### 8.1.2.2 Average last date of heavy frost

Using the same observed data set of minimum temperatures as for the assessment of average first frost occurrence, and the same five factors, the equation for average last date of heavy frost was found by Schulze (1997b) to be

$$L_{fd} = 0.01405Z + 0.05952\phi + 0.01674D_s - 0.02166T_{in} + 0.39817DT_{mn6} + 69.7$$

where $L_{fd}$ = average last date of heavy frost (day of year from January 1)

while the other variables remain as defined previously.

As expected, the + and - signs associated with the variables are reversed from the ones which defined the average first date of heavy frost. Patterns of average last date of heavy frost are, effectively, a reversal of those of the first heavy frost date in the present climate (Figure 8.5, top). Most of the interior experiences last frosts towards the end of August and early September, however, in the high Drakensberg frosts are predicted to persist into early December at present (Schulze, 1997b) as shown in Figure 8.10 (top).

Figure 8.10 Average last date of heavy frost: for present climate (top), future climate (middle) and the change in average last date of heavy frost between future and present climates (bottom). Future climate scenario from UKTR-S

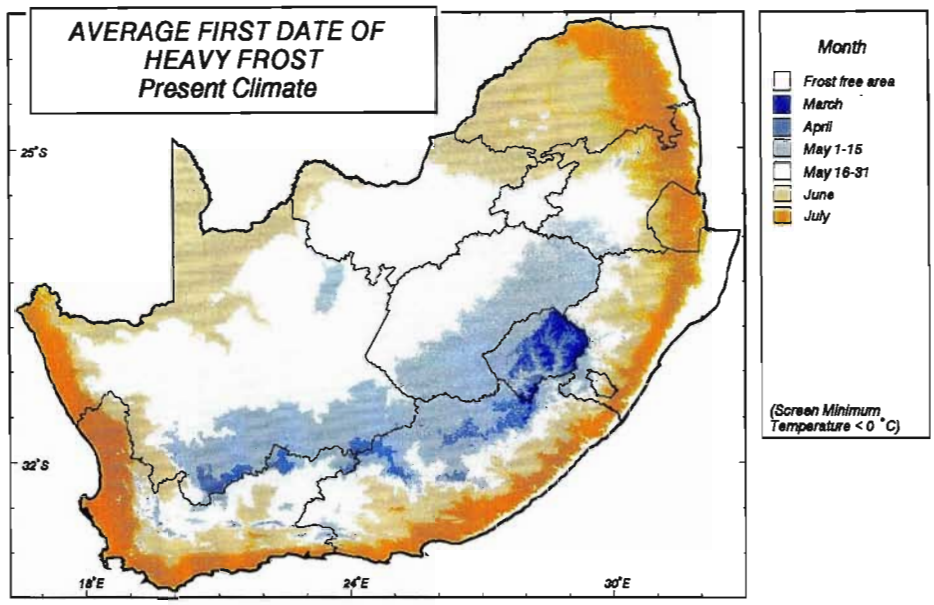


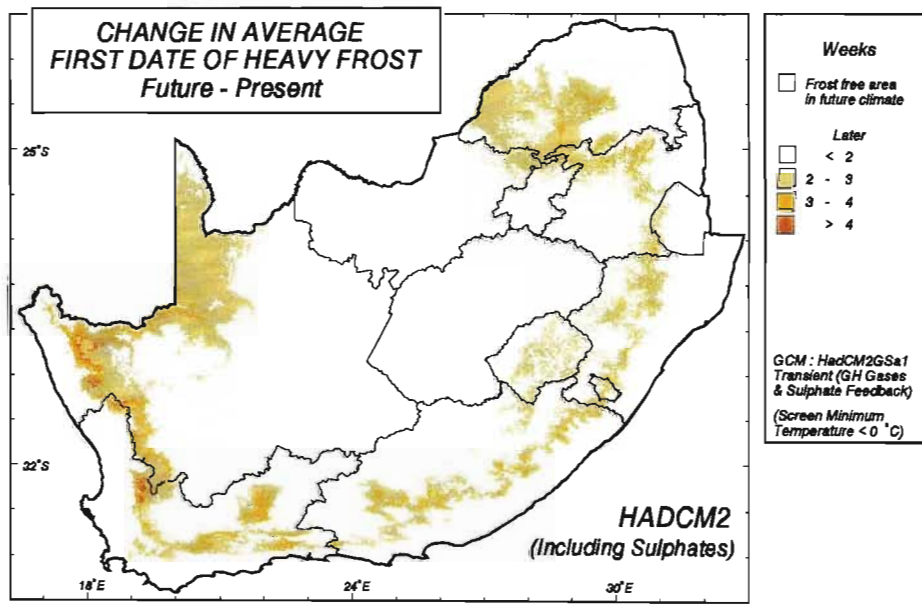


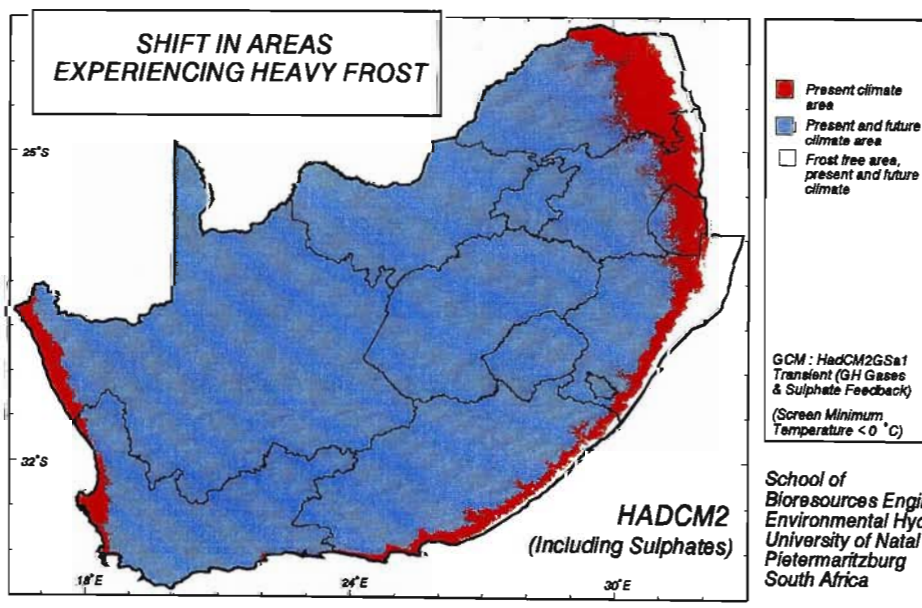


School of
Bioresources Engineering and
Environmental Hydrology
University of Natal
Pietermaritzburg
South Africa

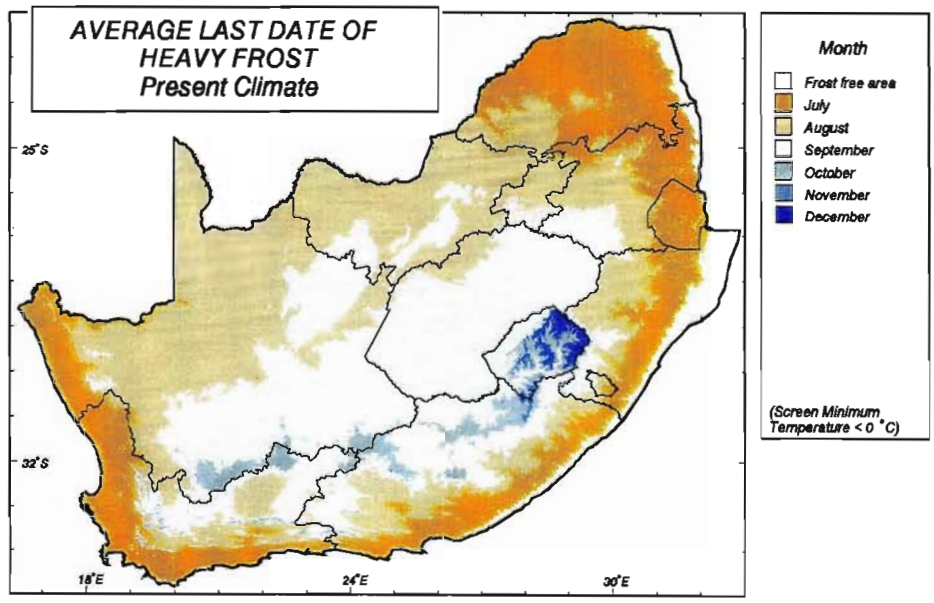


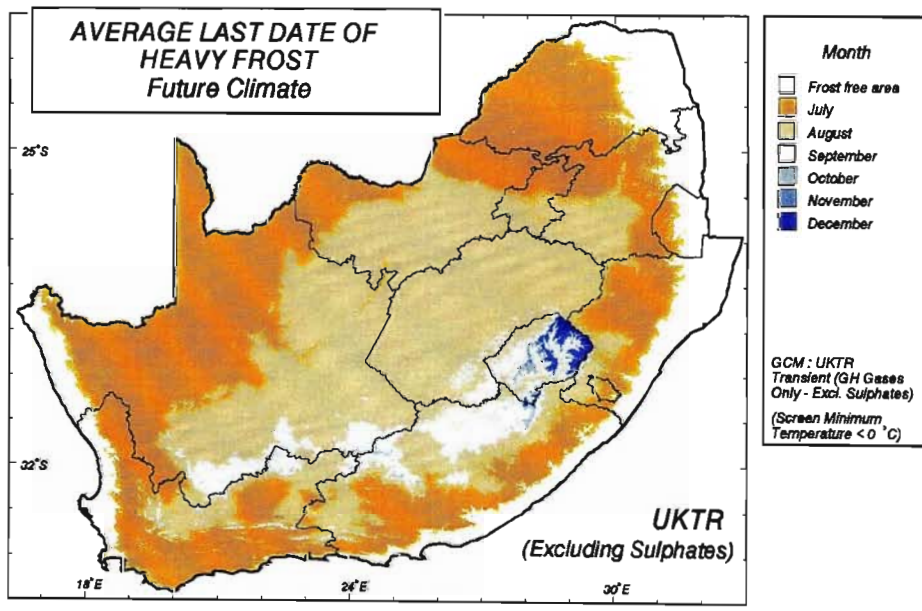


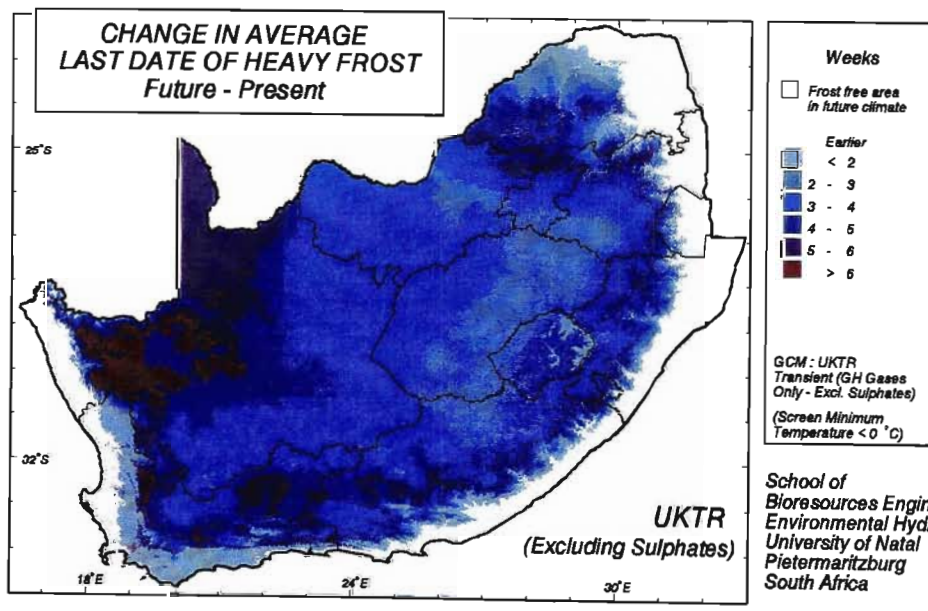


School of
Bioresources Engineering and
Environmental Hydrology
University of Natal
Pietermaritzburg
South Africa

Under a future climate scenario, using minimum temperatures estimated by UKTR-S, frost is predicted to end earlier than at present (Figure 8.10, middle). However, the high Drakensburg will continue to experience frost until late November / early December. On average, heavy frost could end two to five weeks earlier, however, the western parts of the country could expect frost to end up to six weeks earlier (Figure 8.10, bottom).

The statistics calculated using present climatic conditions show that Swaziland is effectively frost free by mid-July, the Northern Province by the end of July, while 80% of the Free State and Eastern Cape have heavy frosts persisting into the second half of September as shown in Table 8.4. However, in a future climate Swaziland and the Northern Province could expect to be mostly frost free by early July, and the Free State and Northern Cape by the end of August.

Table 8.4 Statistics for average last date of heavy frost for present climatic conditions and a future (2X $CO_2$) climate scenario from UKTR-S

| Last Date of Heavy Frost | | | | | | |
|---|---|---|---|---|---|---|
| Province / Country | Date by which at least x% of Province / Country will experience last heavy frost on average | | | | | |
| | 20% | | 50% | | 80% | |
| | Present | Future | Present | Future | Present | Future |
| Northern Province | Early July | Frost Free | 13 July | Early July | 1 August | Early July |
| Mpumalanga | Early July | Frost free | 13 August | 7 July | 2 September | 10 August |
| North-West | 17 August | 23 July | 29 August | 6 August | 2 September | 11 August |
| Northern Cape | 15 August | 8 July | 31 August | 31 July | 14 September | 20 August |
| Gauteng | 15 August | 20 July | 27 August | 3 August | 3 September | 13 August |
| Free State | 5 September | 11 August | 11 September | 20 August | 19 September | 28 August |
| KwaZulu-Natal | Frost Free | Frost Free | 21 July | 5 July | 22 September | 26 July |
| Eastern Cape | 14 July | 12 July | 31 August | 31 July | 24 August | 31 August |
| Western Cape | 11 July | 8 July | 17 August | 16 July | 10 September | 13 August |
| Swaziland | Early July | Frost free | Early July | Frost free | 14 July | 2 July |
| Lesotho | 24 September | 1 September | 14 October | 16 September | * 1 December | 19 November |

* Unreliable: Extrapolated beyond last observed date of 22 November

The patterns of average last date of heavy frost for future climatic conditions using HadCM2-S (Figure 8.11, top left) are very similar to those generated using UKTR-S (Figure 8.10, middle). The average last date for heavy frost does, however, appear to be slightly earlier using output from UKTR-S (Figure 8.10, bottom) compared to those using output from the newer version (Figure 8.11, bottom left). This is particularly evident in the western parts of the study area which experience heavy frost.

Figure 8.11 Average last date of heavy frost: future climate (top left) and the difference in average last date of heavy frost between future and present climates (bottom left) using the future climate scenario from HadCM2-S. Future climate (top right) and the difference in average last date of heavy frost between future and present climates (bottom right) using the future climate scenario from HadCM2+S

By including the effect of sulphate forcing in HadCM2 (Figure 8.11, top right) the average date by which heavy frosts end is not as early as is simulated when using output from the version which excludes sulphate forcing (Figure 8.11, top left). When using output from HadCM2+S a large portion of the study area was estimated to have heavy frosts ending in July under a future climate scenario, particularly on the perimeter of the frost areas, compared to August / September for most of the study area when including the effect of sulphates in the GCM. In both scenarios heavy frosts could persist until December in the high lying areas of Lesotho.

#### 8.1.2.3 Average duration of heavy frost

The average duration of the period of heavy frost is defined by Schulze (1997b) as the number of days between the average first date of heavy frost and the average last date of heavy frost. It should be noted that this duration does not imply that frost occurs on every day.

Although the spatial distribution of frost duration is similar to those of first and last dates of heavy frost, the variability within provinces is much more marked (Schulze, 1997b). At present most of the coastal regions experience a frost duration period of less than 30 days, the interior regions experience a frost period of between 30 and 180 days, while the high lying areas in Lesotho have a period of over 210 days from average start to end of heavy frost (Figure 8.12, top).

## AVERAGE LAST DATE OF HEAVY FROST
### Future Climate

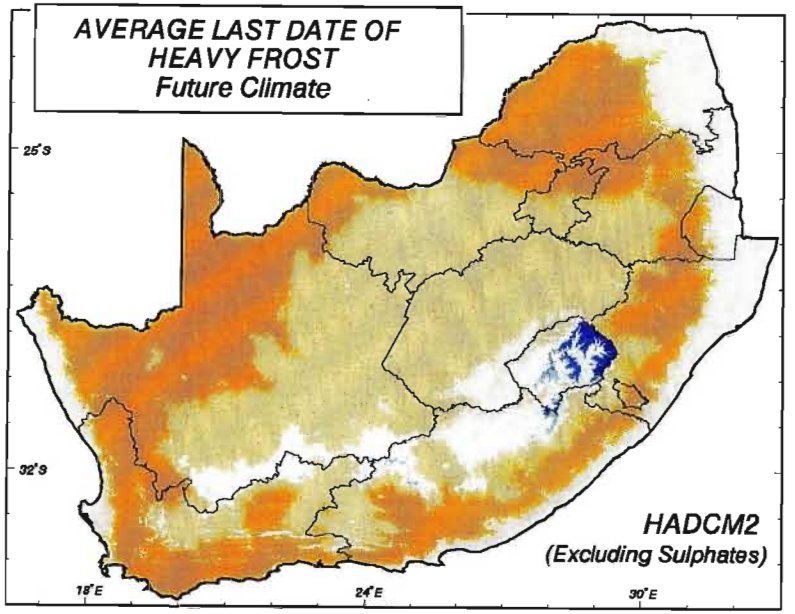


**Month**

- Frost free area
- July
- August
- September
- October
- November
- December

GCM : HadCM2GGa1
Transient (GH Gases Only - Excl. Sulphates)

(Soreen Minimum Temperature < 0 °C)

## AVERAGE LAST DATE OF HEAVY FROST
### Future Climate

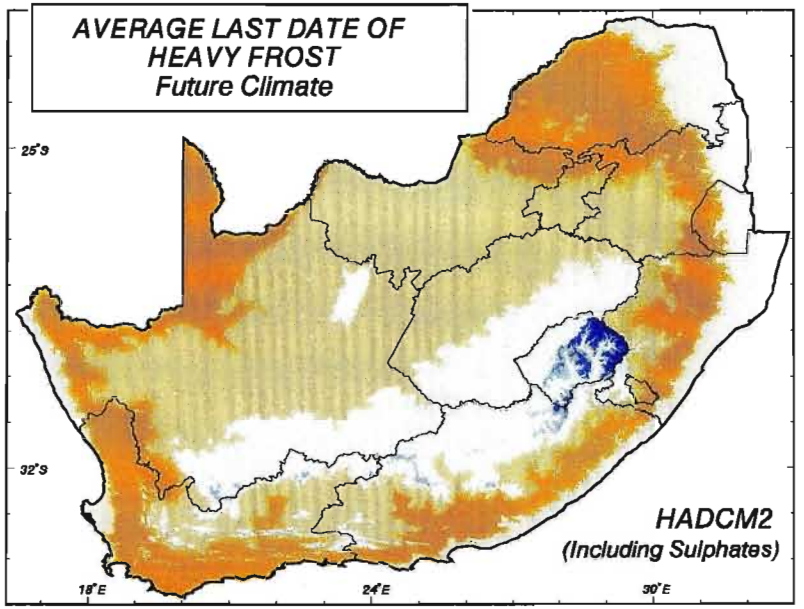


**Month**

- Frost free area
- July
- August
- September
- October
- November
- December

GCM : HadCM2GSa1
Transient (GH Gases & Sulphate Feedback)

(Soreen Minimum Temperature < 0 °C)

## CHANGE IN AVERAGE LAST DATE OF HEAVY FROST
### Future - Present

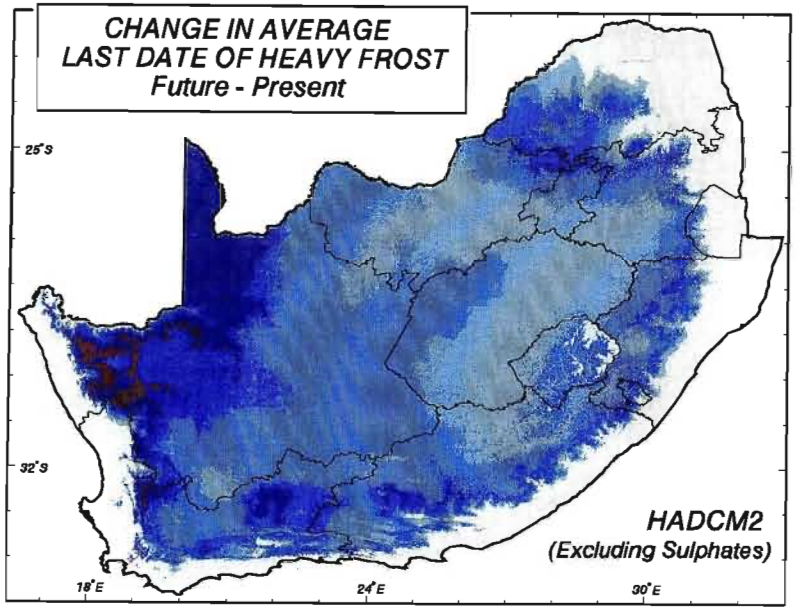


**Weeks**

- Frost free area in future climate

Earlier

- < 2
- 2 - 3
- 3 - 4
- 4 - 5
- 5 - 6
- > 6

GCM : HadCM2GGa1
Transient (GH Gases Only - Excl. Sulphates)

(Soreen Minimum Temperature < 0 °C)

## CHANGE IN AVERAGE LAST DATE OF HEAVY FROST
### Future - Present

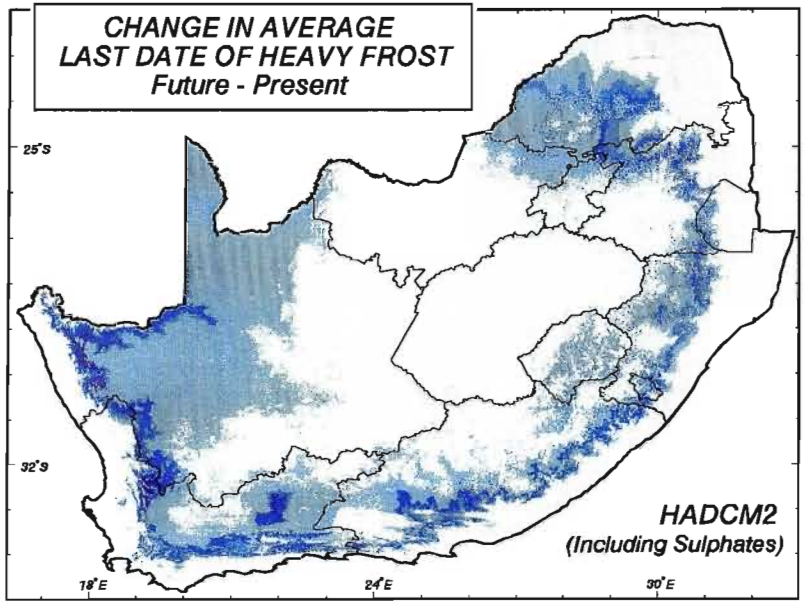


**Weeks**

- Frost free area in future climate

Earlier

- < 2
- 2 - 3
- 3 - 4
- 4 - 5
- 5 - 6
- > 6

GCM : HadCM2GSa1
Transient (GH Gases & Sulphate Feedback)

(Soreen Minimum Temperature < 0 °C)

School of Bioresources Engineering and Environmental Hydrology
University of Natal
Pietermaritzburg
South Africa

Figure 8.12 Average duration of the period of heavy frost (days): for present climate (top), future climate (middle) and the change in the average duration of the period of heavy frost between future and present climates (bottom). Future climate scenario from UKTR-S

Decreases in the duration of the frost period simulated for a future climate are the consequence of higher minimum temperatures as predicted by UKTR-S. In the future, a much larger portion of the study area could expect to experience a frost period of less than 30 days. However, the mountainous areas of Lesotho are still predicted to have a frost season of more than 210 days (Figure 8.12, middle). Figure 8.12 (bottom) illustrates that the coastal areas could expect a reduction of the average duration of the frost period of less than 30 days, the interior by 30 to 75 days and the north-western region could expect reductions in the average frost duration in excess of 75 days.

In addition, the coefficient of variation of average duration of heavy frost is expected to increase in all provinces / countries in a future climate using output from UKTR-S (see present and future CV columns in Table 8.5). This implies that the duration of heavy frost of will be more variable in future compared to the present variability.

Similar results of potential future duration of frost period to those using UKTR-S (Figure 8.12, middle) were obtained using HadCM2-S (Figure 8.13, top left). However, the duration of heavy frost in the western parts of the study area is simulated to be slightly shorter using HadCM2-S (Figure 8.12, bottom and Figure 8.13, bottom left).

Figure 8.13 Average duration of heavy frost: future climate (top left) and the difference in average duration of heavy frost between future and present climates (bottom left) using the future climate scenario from HadCM2-S. Future climate (top right) and the difference in average duration of heavy frost between future and present climates (bottom right) using the future climate scenario from HadCM2+S

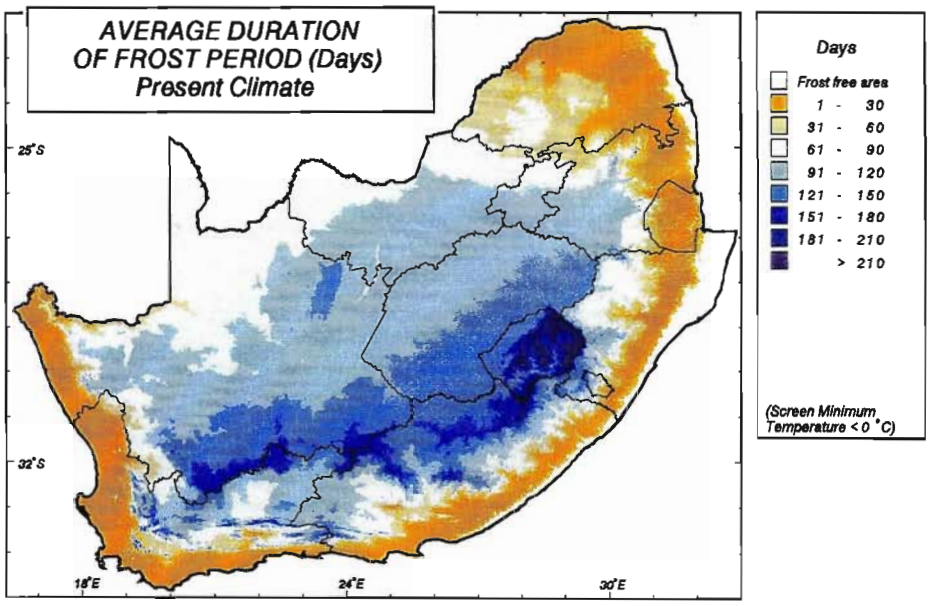


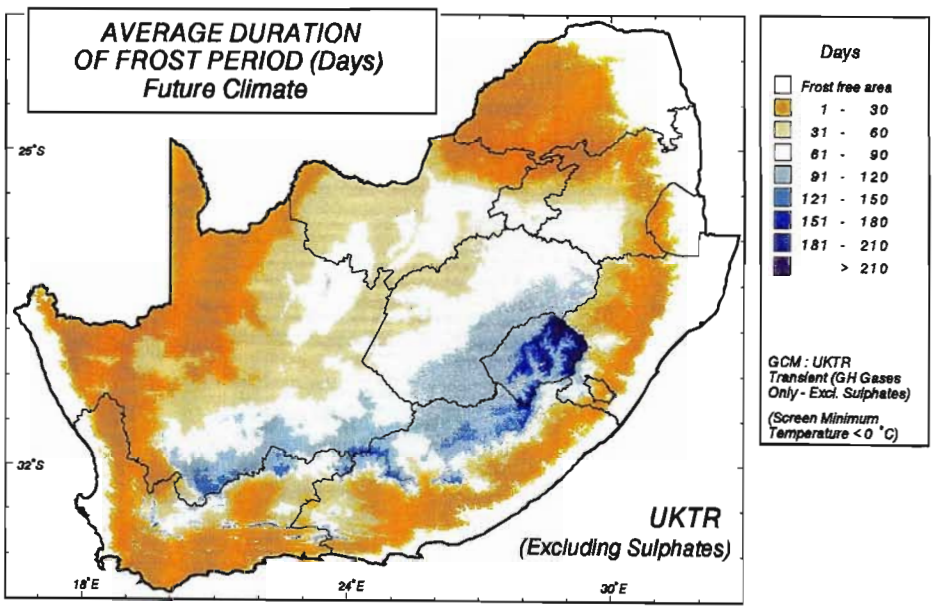


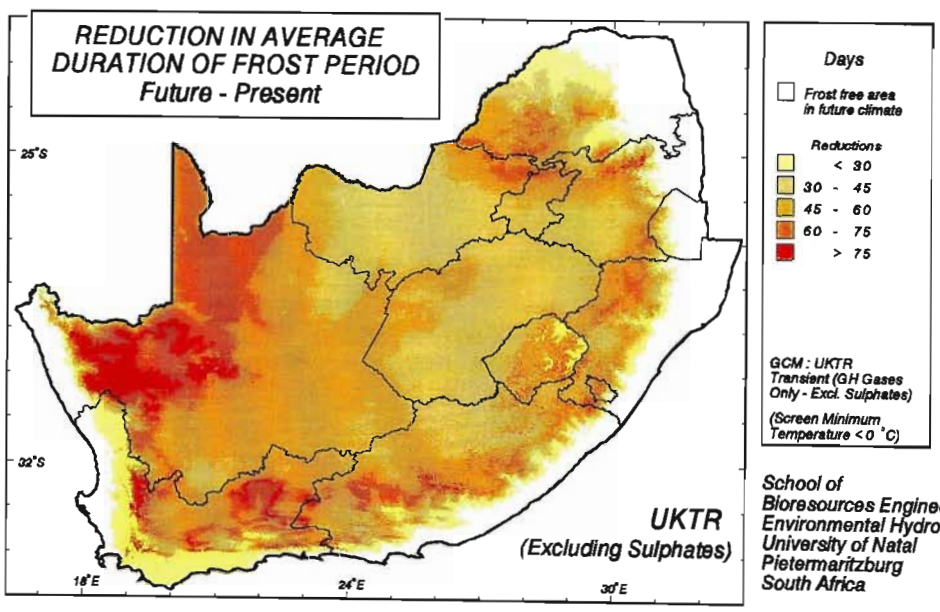


School of
Bioresources Engineering and
Environmental Hydrology
University of Natal
Pietermaritzburg
South Africa

Table 8.5 Statistics for average duration of heavy frost for present climatic conditions and a future (2X $CO_2$) climate scenario from UKTR-S

| Average Duration (days) of Frost Period | | | | | | | | | | | | | | |
|---|---|---|---|---|---|---|---|---|---|---|---|---|---|---|
| Province / Country | Mean Value | | C.V. (%) | | Maximum Value | | Minimum Value | | Exceedence Probability | | | | | |
| | | | | | | | | | 20% | | 50% | | 80% | |
| | Present | Future | Present | Future | Present | Future | Present | Future | Present | Future | Present | Future | Present | Future |
| Northern Province | 26 | 1 | 97 | 324 | 94 | 51 | 0 | 0 | 54 | 1 | 22 | N/A | 1 | 0 |
| Mpumalanga | 62 | 29 | 71 | 108 | 157 | 92 | 0 | 0 | 106 | 64 | 73 | N/A | 1 | 0 |
| North-West | 91 | 47 | 15 | 39 | 118 | 0 | 60 | 78 | 103 | 63 | 95 | 53 | 77 | 30 |
| Northern Cape | 95 | 42 | 35 | 81 | 200 | 0 | 6 | 75 | 122 | 75 | 97 | 41 | 73 | 7 |
| Gauteng | 91 | 46 | 18 | 51 | 117 | 0 | 57 | 68 | 107 | 68 | 96 | 51 | 76 | 27 |
| Free State | 119 | 78 | 11 | 19 | 270 * | 7 | 35 | 93 | 131 | 93 | 118 | 79 | 106 | 62 |
| KwaZulu-Natal | 42 | 16 | 111 | 172 | 270 * | 270 * | 0 | 0 | 84 | 34 | 27 | N/A | 0 | 0 |
| Eastern Cape | 86 | 47 | 64 | 91 | 270 * | 270 * | 0 | 0 | 137 | 94 | 93 | N/A | 13 | 11 |
| Western Cape | 66 | 31 | 76 | 106 | 210 | 173 | 0 | 0 | 114 | 59 | 70 | N/A | 10 | 7 |
| Swaziland | 9 | 1 | 188 | 363 | 87 | 34 | 0 | 0 | 17 | 1 | 1 | N/A | 1 | 0 |
| Lesotho | 195 | 153 | 33 | 50 | 270 * | 270* | 52 | 12 | 270 * | 230 | 173 | 122 | 138 | 98 |

* Unreliable : extrapolated beyond highest observed duration of 260 days



Table 8.6 Statistics for positive chill units (July) for present climatic conditions and a future (2X $CO_2$) climate scenario from UKTR-S

| Positive Chill Units, July | | | | | | | | | | | | | | |
|---|---|---|---|---|---|---|---|---|---|---|---|---|---|---|
| Province / Country | Mean Value | | C.V. (%) | | Maximum Value | | Minimum Value | | Exceedence Probability | | | | | |
| | | | | | | | | | 20% | | 50% | | 80% | |
| | Present | Future | Present | Future | Present | Future | Present | Future | Present | Future | Present | Future | Present | Future |
| Northern Province | N/A * | N/A | N/A | N/A | 333 | 261 | 0 | 0 | N/A | N/A | N/A | N/A | N/A | N/A |
| Mpumalanga | N/A | N/A | N/A | N/A | 350 | 350 | 0 | 0 | N/A | N/A | N/A | N/A | N/A | N/A |
| North-West | 162 | N/A | 27 | N/A | 296 | 223 | 25 | 0 | 202 | N/A | 169 | N/A | 118 | N/A |
| Northern Cape | 213 | N/A | 31 | N/A | 436 | 407 | 0 | 0 | 274 | N/A | 214 | N/A | 154 | N/A |
| Gauteng | 218 | 136 | 17 | 412 | 308 | 237 | 77 | 0 | 246 | 180 | 228 | 188 | 193 | 137 |
| Free State | 245 | 186 | 13 | 89 | 350 | 350 | 183 | 89 | 271 | 228 | 245 | 188 | 216 | 137 |
| KwaZulu-Natal | N/A | N/A | N/A | N/A | 350 | 253 | 0 | 0 | N/A | N/A | N/A | N/A | N/A | N/A |
| Eastern Cape | 207 | N/A | 45 | N/A | 424 | 453 | 0 | 0 | 285 | N/A | 228 | N/A | 132 | N/A |
| Western Cape | 251 | N/A | 29 | N/A | 450 | 450 | 0 | 0 | 314 | N/A | 242 | N/A | 189 | N/A |
| Swaziland | N/A | N/A | N/A | N/A | 302 | 198 | 0 | 0 | N/A | N/A | N/A | N/A | N/A | N/A |
| Lesotho | 291 | 17 | 21 | 82 | 350 | 350 | 120 | 82 | 348 | 350 | 306 | 317 | 259 | 252 |

* N/A denotes the statistics will be meaningless because less than 95% of the province/country has PCUs > 0

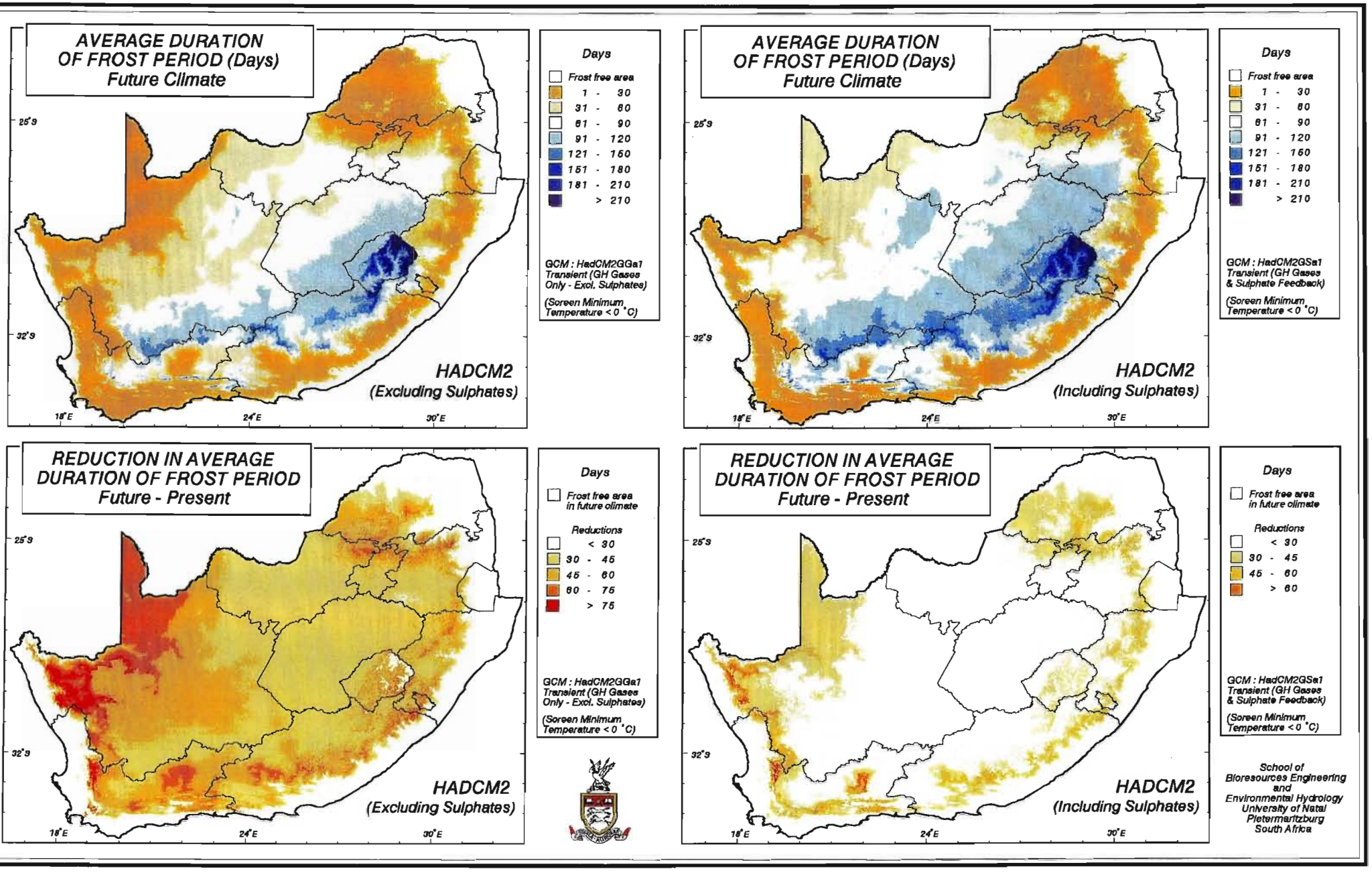
AVERAGE DURATION OF FROST PERIOD (Days) Future Climate
25°S
32°S
18°E
24°E
30°E
HADCM2 (Excluding Sulphates)
Days
Frost free area
1 - 30
31 - 60
61 - 90
91 - 120
121 - 150
151 - 180
181 - 210
> 210
GCM : HadCM2GGa1 Transient (GH Gases Only - Excl. Sulphates)
(Screen Minimum Temperature < 0 °C)
AVERAGE DURATION OF FROST PERIOD (Days) Future Climate
HADCM2 (Including Sulphates)
Days
Frost free area
1 - 30
31 - 60
61 - 90
91 - 120
121 - 150
151 - 180
181 - 210
> 210
GCM : HadCM2GSa1 Transient (GH Gases & Sulphate Feedback)
(Screen Minimum Temperature < 0 °C)
REDUCTION IN AVERAGE DURATION OF FROST PERIOD Future - Present
HADCM2 (Excluding Sulphates)
Days
Frost free area in future climate
Reductions
< 30
30 - 45
45 - 60
60 - 75
> 75
GCM : HadCM2GGa1 Transient (GH Gases Only - Excl. Sulphates)
(Screen Minimum Temperature < 0 °C)
REDUCTION IN AVERAGE DURATION OF FROST PERIOD Future - Present
HADCM2 (Including Sulphates)
Days
Frost free area in future climate
Reductions
< 30
30 - 45
45 - 60
> 60
GCM : HadCM2GSa1 Transient (GH Gases & Sulphate Feedback)
(Screen Minimum Temperature < 0 °C)
School of Bioresources Engineering and Environmental Hydrology
University of Natal
Pietermaritzburg
South Africa

The reductions in heavy frost are not as drastic when the cooling influence of sulphates in the atmosphere is included in HadCM2 (Figure 8.13, top right). However, there is still a significant decrease in areas that are expected to experience heavy frost using a future climate scenario. Reductions in the average duration of heavy frost range from less than 30 days for a large part of the interior of southern Africa to more than 60 days in parts of the western regions of the study area (Figure 8.13, bottom right) when using HadCM2+S. On average, the decreases in frost duration are 20 days more when excluding the effect of sulphates on climate.

### 8.1.3 Potential changes in positive chill units

Certain biennial plants which have a dormant season during winter may require a period of accumulated minimum temperatures below a threshold value in order to stimulate growth, develop leaves, flower or set fruit. Deciduous trees, for example, need a certain period of winter chilling for completion of their seasonal dormancy. The required amount of chilling for completion of the rest period varies between species, cultivars and different locations (Schulze, 1997b).

According to this observation, mathematical relationships have been derived which equate to ranges, or alternatively thresholds, of hourly temperatures to a certain number of hourly chill units (Richardson *et al.*, 1974). The application of chill unit models enables potential growers to, for example

i) predict the time of rest completion and bud break;
ii) determine the time when certain cultural practices (such as sprinkling), envisaged to delay bloom, should begin; or
iii) identify potential growing locations with sufficient chilling for the various cultivars (Schulze, 1977b).

To derive maps of positive chill units (PCUs), the following procedure was adopted by Schulze (1997b). Firstly the hourly values of temperature were determined from daily maximum and minimum temperatures by employing equations developed by Lindsley-Noakes *et al.* (1995). Hourly temperatures derived from these equations were then converted into

PCUs according to intervals suggested by Richardson *et al.* (1974), modified and used by Lindsley-Noakes *et al.* (1995) such that

| | | | | | | |
|---|---|---|---|---|---|---|
| If | 2.4°C | < | $T_t$ | < | 9.1°C, | PCU = 1.0 |
| If | 1.4°C | < | $T_t$ | < | 2.4°C, | PCU = 0.5 |
| If | 9.1°C | < | $T_t$ | < | 12.4°C, | PCU = 0.5 |
| If | 12.4°C | < | $T_t$ | < | 2.4°C, | PCU = 0.0 |
| If | | | $T_t$ | < | 2.4°C, | PCU = 0.0 |
| If | 16.0°C | < | $T_t$ | < | 1.4°C, | PCU = -0.5 |
| If | 18.0°C | < | $T_t$ | | | PCU = -1.0 |

where $T_t$ = temperature (°C) at time t after sunrise, or at time t > 1 hour after sunset, respectively (Schulze, 1997b).

From the hourly PCU calculations, daily PCUs were accumulated, from which monthly and seasonal totals of PCUs could be made. Positive chill unit calculations were performed on data from 325 temperature stations in South Africa, Lesotho and Swaziland, each with a minimum of 10 years' daily maximum and minimum temperature data (Schulze, 1997b). The number of PCUs in the south western Cape is considered to be particularly important as this is the main deciduous fruit growing area of southern Africa.

The potential changes in PCUs with climate change were calculated for May, June, July, August and September as well as the accumulated PCUs for this period. However, only results from the analyses for the month of July and for the accumulated PCUs (May to September) are presented in the following sections. The results from the remaining months are available from the School of BEEH, University of Natal, Pietermaritzburg.

#### 8.1.3.1 Positive chill units for July

The PCUs for present climatic conditions for the month of July for the study region were determined by Schulze (1997b) to range from zero PCUs in the eastern and northern regions to more than 350 PCUs in the south-western Cape (Figure 8.14, top left).

Figure 8.14 Positive chill units (PCUs) for July: for present climate (top left), future climate (bottom left), the shift in climate area (top right) and the change in PCUs for July between future and present climates (bottom right). Future climate scenario from UKTR-S

Using output from UKTR-S the map generated for future PCUs in July shows that most areas could potentially experience large decreases in the number of PCUs compared to present climatic conditions (Figure 8.14, bottom left). There is also a significant decrease in the areas which are expected to experience PCUs in July. These decreases in area occur on the fringe regions of the areas that presently experience PCUs in July (Figure 8.14, top right). The reductions in PCUs in July, in those areas which will experience PCUs in the future, range from less than 50 PCUs in the central parts of the study area to reductions in excess of 200 PCUs in the western regions (Figure 8.14, bottom right). There were, however, gains predicted in and around Lesotho of between 0 and 150 PCUs. The reason for the increase in PCUs in Lesotho in July in future is attributed to an increase in minimum temperatures which were previously too low to qualify as PCUs.

The North-West, Northern Cape, Eastern Cape, Western Cape Provinces presently have PCUs in 95% of the province. However, in future these provinces are expected to have PCUs in July in less than 95% of their area according to climatic output from UKTR-S (see present and future mean values in Table 8.6).

Results of changes in PCUs in July using output from the UKTR-S and HadCM2-S GCMs are very similar (Figures 8.14, bottom left and 8.15, top). There are slightly higher reductions in the number of PCUs in July simulated in some areas when using output from HadCM2-S, however (Figure 8.15, middle).

Figure 8.15 Positive chill units (PCUs) for July: for future climate (top), the change in the positive chill units between future and present climates (middle) and shift in areas experiencing positive chill units (bottom). Future climate scenario from HadCM2-S

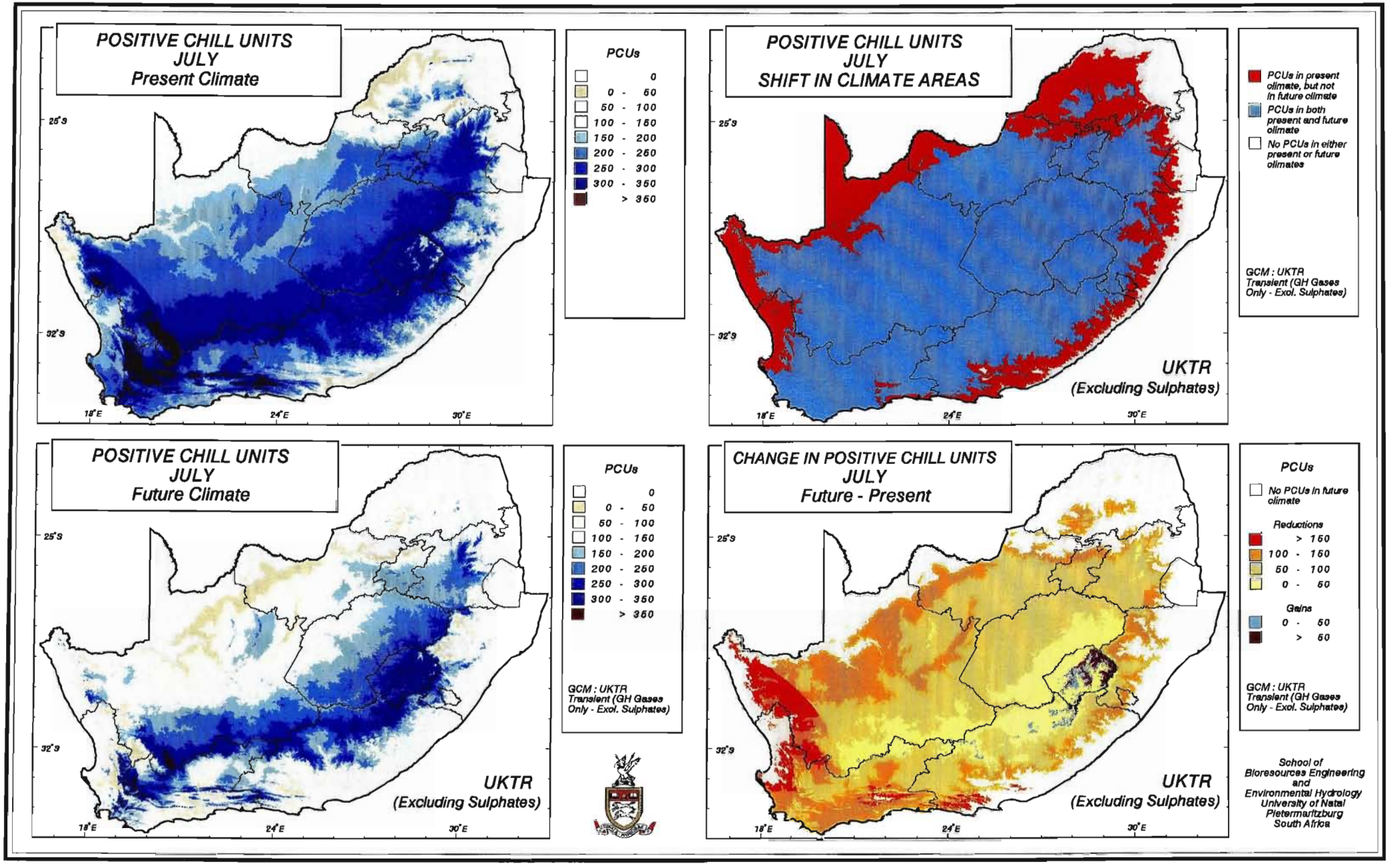
POSITIVE CHILL UNITS
JULY
Present Climate
PCUs
0
0 - 50
50 - 100
100 - 150
150 - 200
200 - 250
250 - 300
300 - 350
> 350
25°S
32°S
18°E
24°E
30°E
POSITIVE CHILL UNITS
JULY
SHIFT IN CLIMATE AREAS
PCUs in present climate, but not in future climate
PCUs in both present and future climate
No PCUs in either present or future climates
GCM : UKTR
Transient (GH Gases Only - Excl. Sulphates)
UKTR
(Excluding Sulphates)
POSITIVE CHILL UNITS
JULY
Future Climate
PCUs
0
0 - 50
50 - 100
100 - 150
150 - 200
200 - 250
250 - 300
300 - 350
> 350
GCM : UKTR
Transient (GH Gases Only - Excl. Sulphates)
UKTR
(Excluding Sulphates)
CHANGE IN POSITIVE CHILL UNITS
JULY
Future - Present
PCUs
No PCUs in future climate
Reductions
> 150
100 - 150
50 - 100
0 - 50
Gains
0 - 50
> 50
GCM : UKTR
Transient (GH Gases Only - Excl. Sulphates)
UKTR
(Excluding Sulphates)
School of Bioresources Engineering and Environmental Hydrology
University of Natal
Pietermaritzburg
South Africa

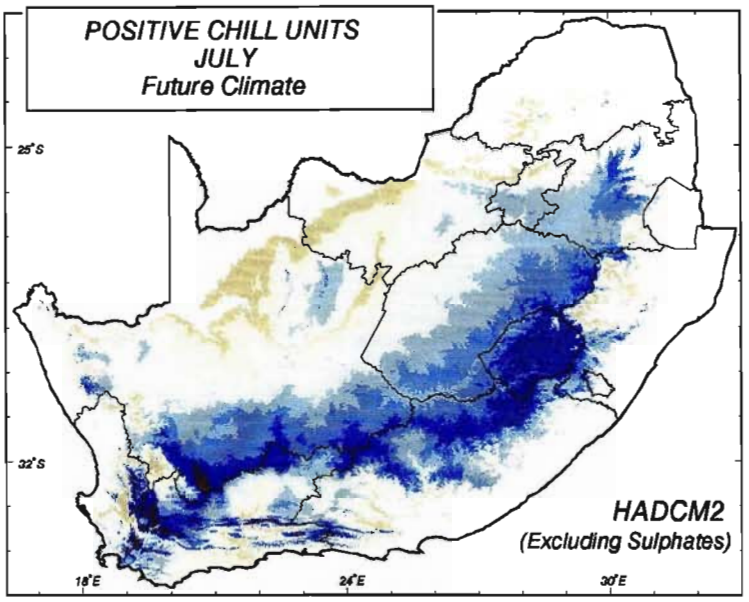


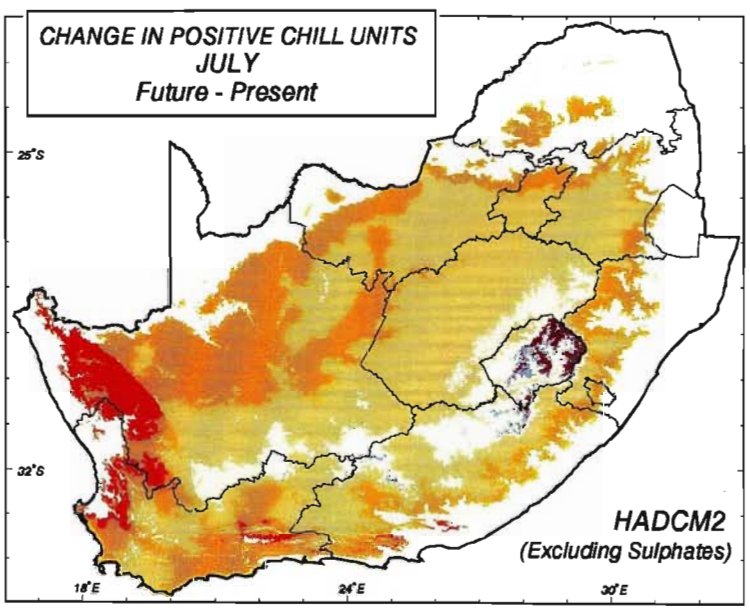


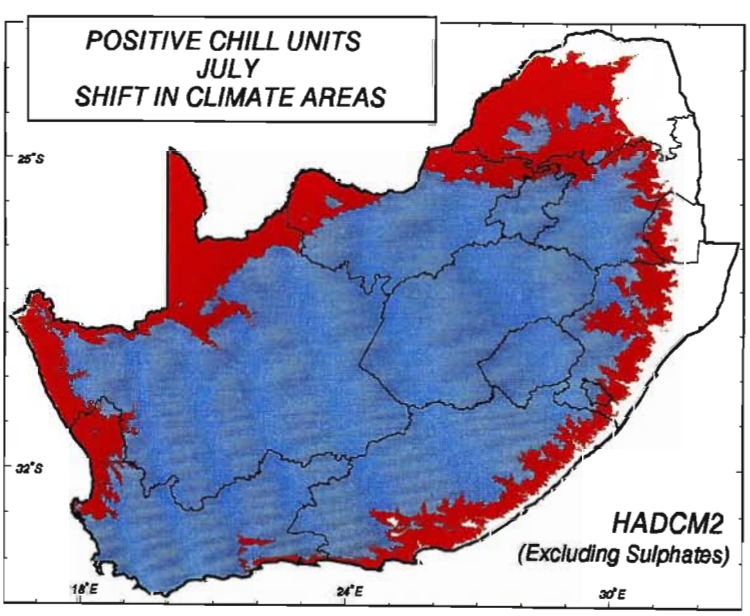


School of
Bioresources Engineering and
Environmental Hydrology
University of Natal
Pietermaritzburg
South Africa

However, when sulphate forcing is included in HadCM2, the differences in the estimates of the potential reductions in PCUs in July are notable. Figure 8.16 (middle) shows that by including sulphate forcing no areas were simulated to have reductions greater than 150 PCUs in July. On average, the reductions in PCUs in July are 50 PCUs higher using the output from HadCM2-S (Figure 8.15, middle) than those using HadCM2+S. By including sulphate forcing in this GCM the decrease in areas experiencing PCUs in July is also not as marked particularly in the northern and western parts of the study area (Figure 8.16, bottom).

Figure 8.16 Positive chill units (PCUs) for July: for future climate (top), the change in the positive chill units between future and present climates (middle) and shift in areas experiencing positive chill units (bottom). Future climate scenario from HadCM2+S

### 8.1.3.2 Accumulated positive chill units for the period May to September

For present climatic conditions the accumulated PCUs of the winter period from May to September range from fewer than 250 PCUs along the fringe areas to more than 1750 PCUs in the south-western parts of the Western Cape (Figure 8.17, top). In a future climate using output from UKTR-S, however, the potential accumulated PCUs for the winter season could decrease significantly (Figure 8.17, middle), with many more areas in the low lying and northern regions of the study area potentially experiencing fewer than 250 accumulated PCUs in this period.

Figure 8.17 Accumulated positive chill units (PCUs) for the period May to September: for present climate (top), future climate (middle) and the change in accumulated PCUs between future and present climates (bottom). Future climate scenario from UKTR-S

In the map of changes to PCUs between the future (UKTR-S output used) and present climates, these decreases range from fewer than 200 accumulated PCUs in the north and west

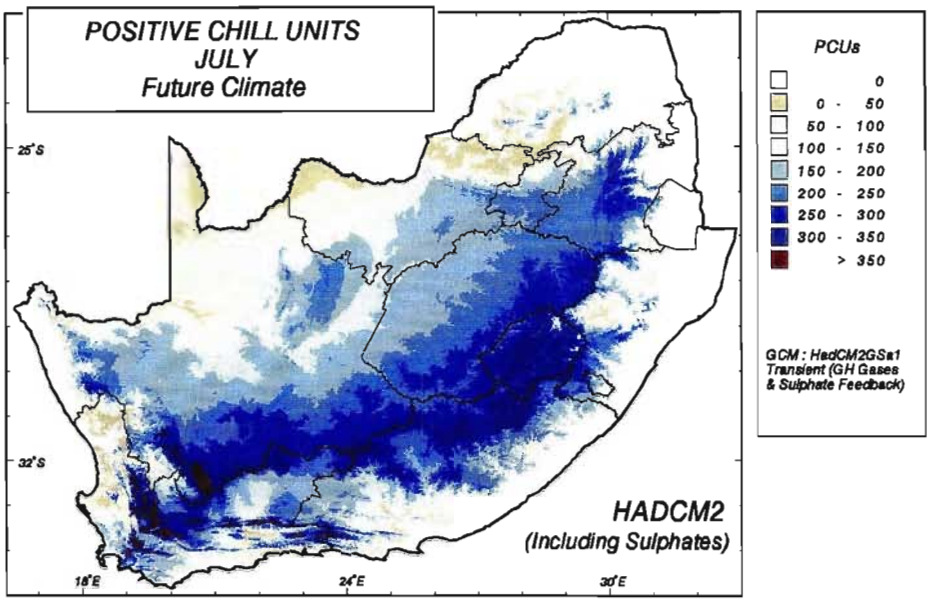


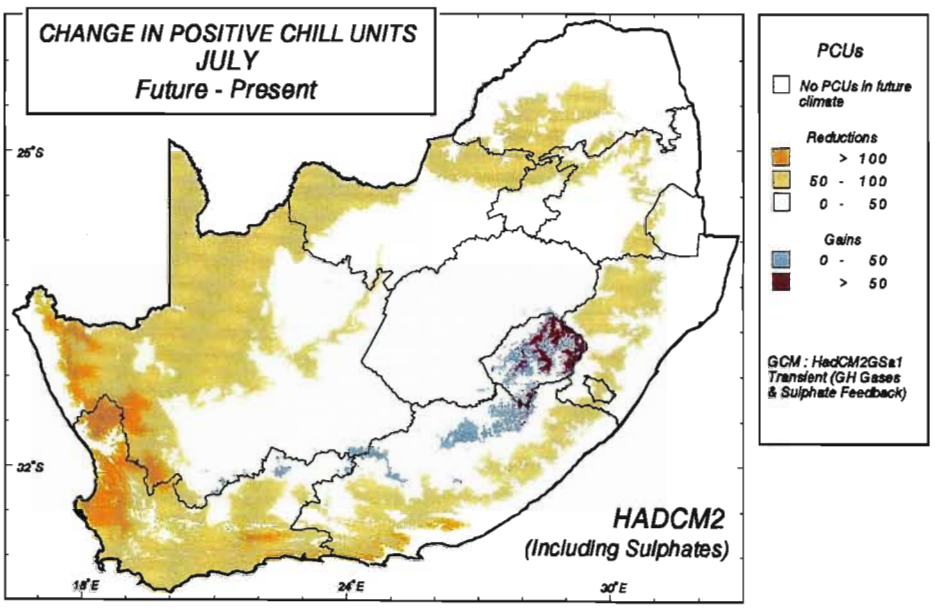


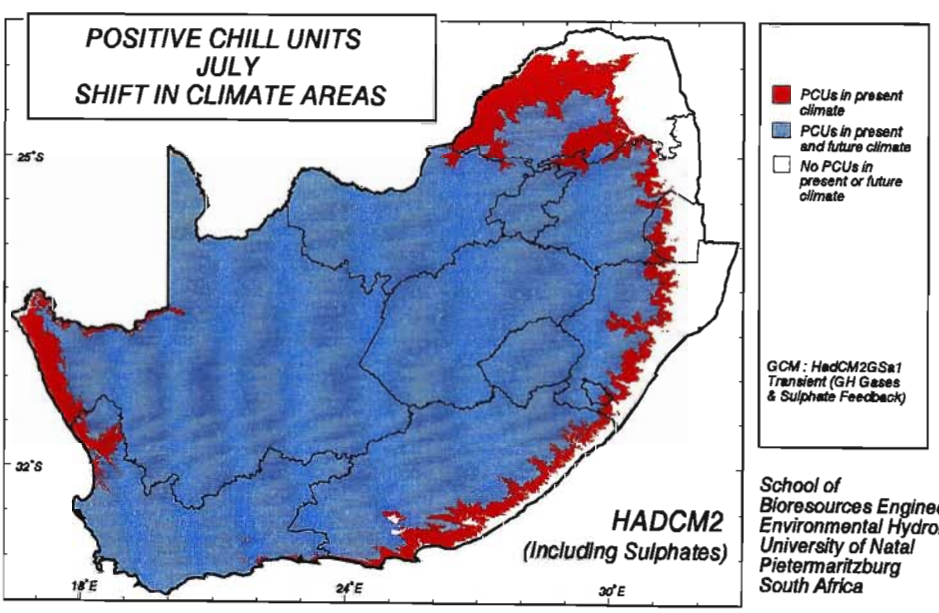


School of
Bioresources Engineering and
Environmental Hydrology
University of Natal
Pietermaritzburg
South Africa

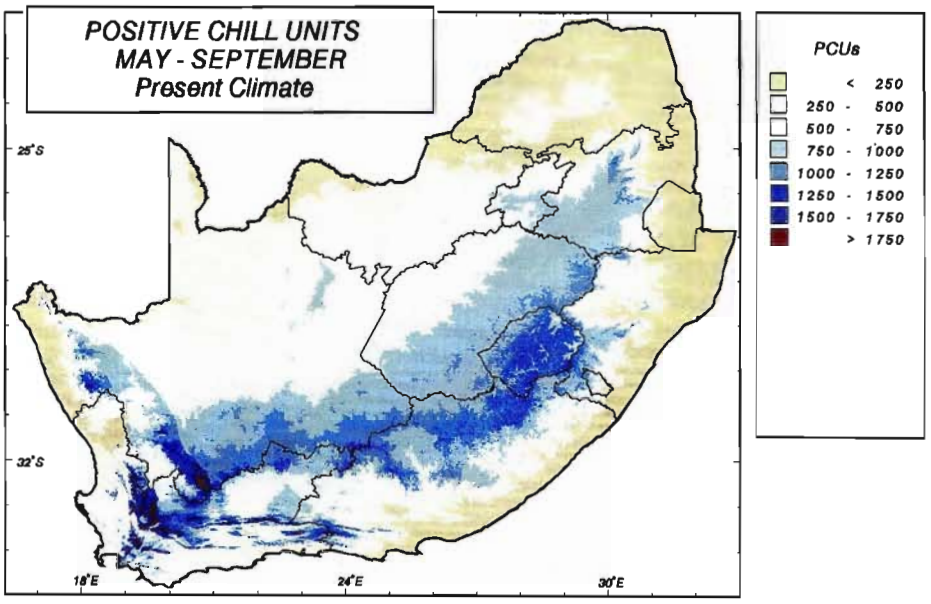


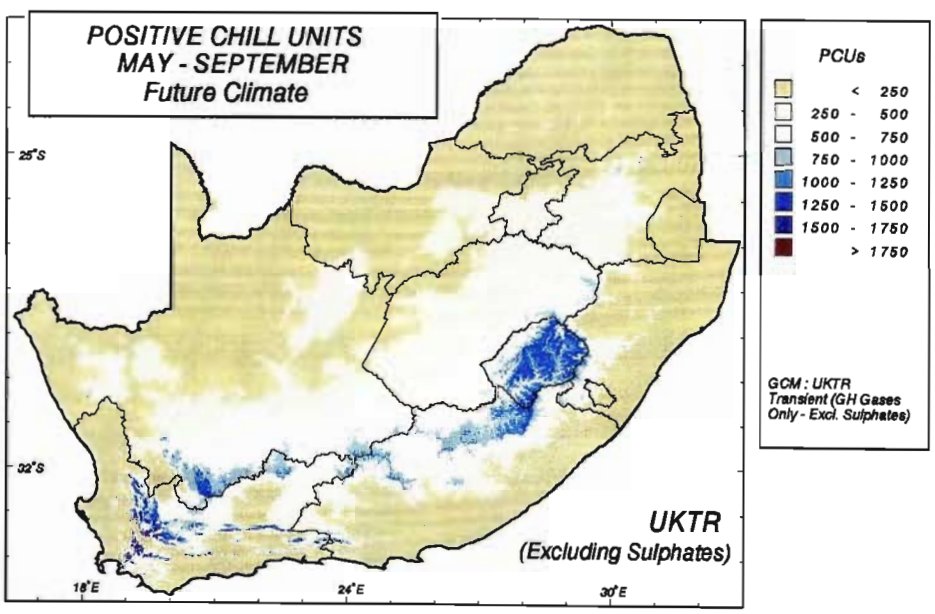


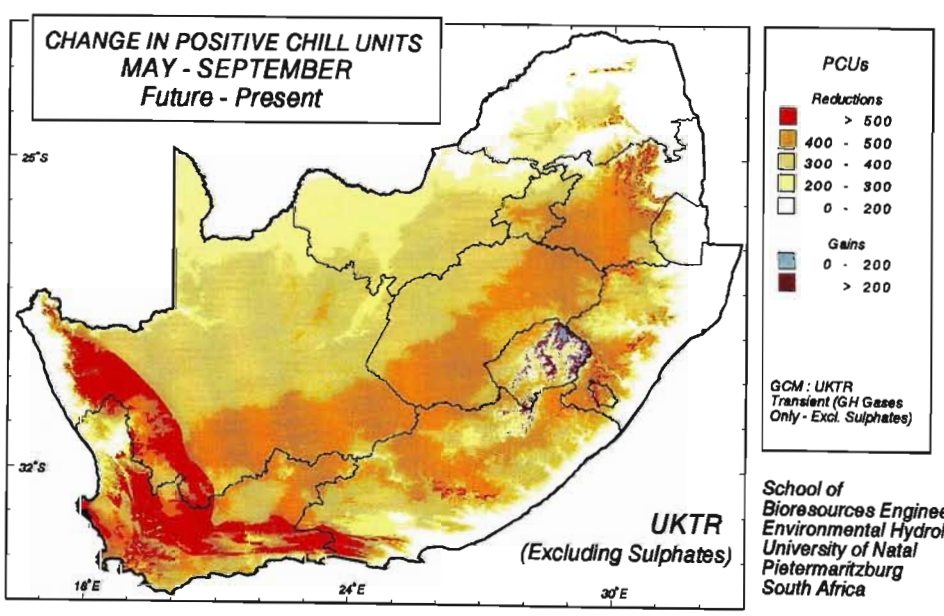


School of
Bioresources Engineering and
Environmental Hydrology
University of Natal
Pietermaritzburg
South Africa

to over 500 PCUs in the western and eastern fringes of the study area (Figure 8.17, bottom). Small gains in excess of 200 accumulated PCUs could be experienced in Lesotho in future. The mean number of accumulated PCUs in Lesotho could increase from 291 at present to 963 in future according to the statistics calculated (see present and future mean values in Table 8.7).

Similarly, large decreases in the number of accumulated (May to September) PCUs were simulated using output from HadCM2-S (Figure 8.18, top left). The patterns of predicted increases in accumulated PCUs for a future climate using HadCM2 (Figure 8.18, bottom left) are very similar to the changes simulated using UKTR-S (Figure 8.17, bottom), with the eastern parts of the study area potentially experiencing reductions in accumulated PCUs in excess of 500. In parts of Lesotho, where gains in PCUs are expected, these gains simulated using output from HadCM2-S (Figure 8.18, bottom left) appear to be lower than the gains expected using output from UKTR-S (Figure 8.17, bottom).

Figure 8.18 Accumulated positive chill units (PCUs) for the period May to September: future climate (top left) and the difference in positive chill units between future and present climates (bottom left) using the future climate scenario from HadCM2-S. Future climate (top right) and the difference in positive chill units between future and present climates (bottom right) using the future climate scenario from HadCM2+S

The reductions in accumulated PCUs are simulated to be less when the sulphate forcing is included in HadCM2 (Figure 8.18, top right) with reductions of more than 300 PCUs in the west of the study area to less than 300 PCUs for most of the rest of southern Africa. Small gains in accumulated PCUs resulting from climate change are possible in Lesotho when using output from HadCM2+S, as shown in Figure 8.18 (bottom right).

### 8.1.4 Potential changes in the duration of moisture growing season

Climate parameters operate in combination with one another, and through the soil, to produce the environment in which the plant has to grow. Through soil moisture, water becomes

Table 8.7 Statistics for accumulated positive chill units for the period May to September for present climate and future (2X $CO_2$) climate scenario from UKTR-S

| Positive Chill Units, Accumulated for period May - September | | | | | | | | | | | | | | |
|---|---|---|---|---|---|---|---|---|---|---|---|---|---|---|
| Province / Country | Mean Value | | CV (%) | | Maximum Value | | Minimum Value | | Exceedence Probability | | | | | |
| | | | | | | | | | 20% | | 50% | | 80% | |
| | Present | Future | Present | Future | Present | Future | Present | Future | Present | Future | Present | Future | Present | Future |
| Northern Province | N/A * | N/A | N/A | N/A | 1031 | 555 | 0 | 0 | N/A | N/A | N/A | N/A | N/A | N/A |
| Mpumalanga | N/A | N/A | N/A | N/A | 1322 | 1101 | 0 | 0 | N/A | N/A | N/A | N/A | N/A | N/A |
| North-West | 421 | N/A | 39 | N/A | 881 | 430 | 48 | 0 | 589 | N/A | 423 | N/A | 249 | N/A |
| Northern Cape | 617 | N/A | 48 | N/A | 1895 | 1706 | 0 | 0 | 877 | N/A | 591 | N/A | 350 | N/A |
| Gauteng | 633 | 264 | 26 | 412 | 930 | 469 | 162 | 0 | 766 | 357 | 691 | 306 | 489 | 165 |
| Free State | 800 | 402 | 19 | 89 | 1402 | 1394 | 483 | 178 | 933 | 541 | 806 | 388 | 648 | 273 |
| KwaZulu-Natal | N/A | N/A | N/A | N/A | 1442 | 1395 | 0 | 0 | N/A | N/A | N/A | N/A | N/A | N/A |
| Eastern Cape | 639 | N/A | 60 | N/A | 1843 | 1676 | 0 | 0 | 1007 | N/A | 645 | N/A | 270 | N/A |
| Western Cape | 758 | N/A | 53 | N/A | 1950 | 1950 | 0 | 0 | 1097 | N/A | 658 | N/A | 425 | N/A |
| Swaziland | N/A | N/A | N/A | N/A | 863 | 394 | 0 | 0 | N/A | N/A | N/A | N/A | N/A | N/A |
| Lesotho | 291 | 963 | 18 | 29 | 1444 | 1413 | 321 | 167 | 1315 | 1220 | 1135 | 1053 | 960 | 659 |

* N/A denotes the statistics will be meaningless because less than 95% of the province/country has PCUs > 0



Table 8.8 Statistics for duration of moisture growing season for present climatic conditions and a future (2X $CO_2$) climate scenario from UKTR-S

| Duration (days) of the Moisture Growing Season | | | | | | | | | | | | | | | | |
|---|---|---|---|---|---|---|---|---|---|---|---|---|---|---|---|---|
| Province / Country | % Suitable area | | Mean Value | | CV (%) | | Maximum Value | | Minimum Value | | Exceedence Probability | | | | | |
| | | | | | | | | | | | 20% | | 50% | | 80% | |
| | Present | Future | Present | Future | Present | Future | Present | Future | Present | Future | Present | Future | Present | Future | Present | Future |
| Northern Province | 71.0 | 65.6 | 113 | 84 | 36 | 54 | 281 | 344 | 0 | 0 | 147 | 124 | 117 | 96 | 81 | 29 |
| Mpumalanga | 90.7 | 99.6 | 177 | 152 | 17 | 25 | 255 | 230 | 0 | 0 | 201 | 179 | 179 | 160 | 160 | 133 |
| North-West | 62.3 | 48.2 | 93 | 53 | 49 | 68 | 364 | 363 | 0 | 0 | 138 | 81 | 101 | 47 | 43 | 20 |
| Northern Cape | 10.8 | 3.2 | 33 | 39 | 84 | 61 | 136 | 122 | 0 | 0 | 54 | 58 | 24 | 38 | 9 | 15 |
| Gauteng | 100.0 | 100.0 | 165 | 145 | 5 | 9 | 198 | 178 | 131 | 16 | 171 | 154 | 166 | 146 | 158 | 137 |
| Free State | 93.5 | 76.0 | 104 | 88 | 63 | 74 | 364 | 359 | 0 | 0 | 177 | 166 | 92 | 59 | 38 | 28 |
| KwaZulu-Natal | 87.7 | 100.0 | 216 | 205 | 18 | 26 | 365 | 365 | 8 | 0 | 235 | 233 | 211 | 194 | 189 | 177 |
| Eastern Cape | 71.0 | 56.9 | 154 | 154 | 60 | 59 | 365 | 365 | 0 | 0 | 234 | 231 | 197 | 197 | 45 | 52 |
| Western Cape | 52.4 | 50.9 | 140 | 119 | 48 | 57 | 365 | 365 | 0 | 0 | 178 | 162 | 132 | 115 | 96 | 62 |
| Swaziland | 77.2 | 100.0 | 200 | 175 | 12 | 19 | 262 | 327 | 10 | 0 | 220 | 196 | 205 | 182 | 183 | 162 |
| Lesotho | 100.0 | 100.0 | 240 | 184 | 10 | 22 | 351 | 276 | 75 | 4 | 222 | 211 | 209 | 192 | 190 | 173 |

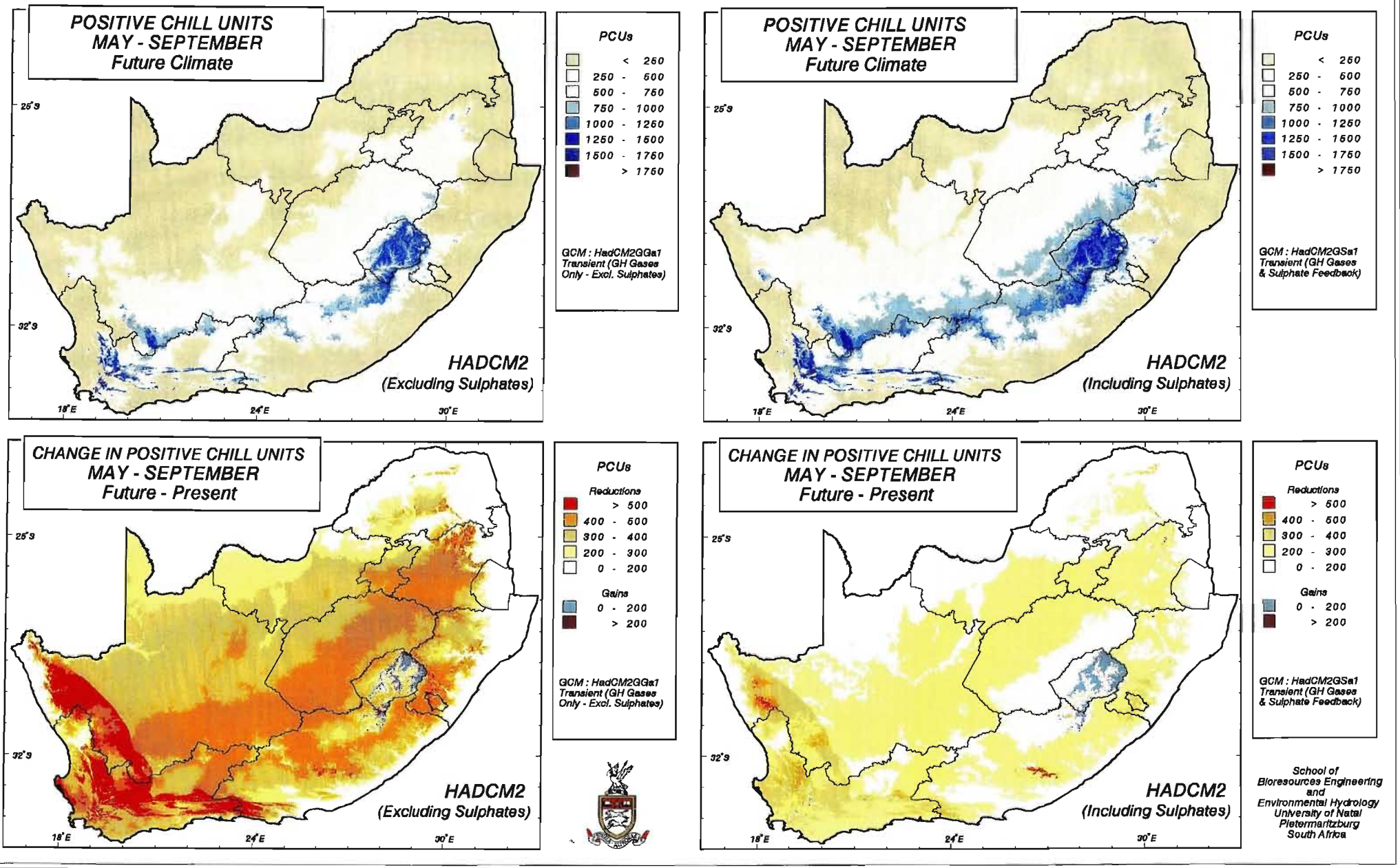
POSITIVE CHILL UNITS
MAY - SEPTEMBER
Future Climate
25°S
32°S
18°E
24°E
30°E
HADCM2
(Excluding Sulphates)
PCUs
< 250
250 - 500
500 - 750
750 - 1000
1000 - 1250
1250 - 1500
1500 - 1750
> 1750
GCM : HadCM2GGa1
Transient (GH Gases
Only - Excl. Sulphates)
POSITIVE CHILL UNITS
MAY - SEPTEMBER
Future Climate
HADCM2
(Including Sulphates)
PCUs
< 250
250 - 500
500 - 750
750 - 1000
1000 - 1250
1250 - 1500
1500 - 1750
> 1750
GCM : HadCM2GSa1
Transient (GH Gases
& Sulphate Feedback)
CHANGE IN POSITIVE CHILL UNITS
MAY - SEPTEMBER
Future - Present
HADCM2
(Excluding Sulphates)
PCUs
Reductions
> 500
400 - 500
300 - 400
200 - 300
0 - 200
Gains
0 - 200
> 200
GCM : HadCM2GGa1
Transient (GH Gases
Only - Excl. Sulphates)
CHANGE IN POSITIVE CHILL UNITS
MAY - SEPTEMBER
Future - Present
HADCM2
(Including Sulphates)
PCUs
Reductions
> 500
400 - 500
300 - 400
200 - 300
0 - 200
Gains
0 - 200
> 200
GCM : HadCM2GSa1
Transient (GH Gases
& Sulphate Feedback)
School of
Bioresources Engineering
and
Environmental Hydrology
University of Natal
Pietermaritzburg
South Africa

available to the plant. Soil water availability is determined by the hydrological budget at a specific locality. For broad agricultural planning purposes the hydrological budget can be expressed in simple interactive terms of averaged climatic variables to give, for example, indices of the average start, end and hence duration of the moisture growing season (Schulze, 1997b).

In order to ascertain when, on average, there is enough water in the soil for sustained plant growth to take place, not only does a certain amount of precipitation have to have occurred, but simultaneously the precipitation must exceed some lower threshold of plant evaporative losses for sustained growth to continue. An average moisture growing season over southern Africa was determined by Schulze (1997b) by adapting a simple water budgeting approach of the FAO (1978), developed originally for agro-ecological zone mapping of Africa. In the FAO (1978) approach adapted for southern Africa, Schulze (1997b) assumed that during the period when

$$P \geq 0.3\ E_r$$

sustained plant growth can take place,

where $P$ = median monthly precipitation (mm) and

$E_r$ = reference potential evaporation for that month which is taken as the mean monthly A-pan equivalent evaporation.

It should be noted that the determination of the duration of the moisture growing season is more complex than merely assuming it to be the difference between the mean start date and mean end date of the growing season. Computations are particularly complex in those provinces which experience (say) a winter rainfall season in part of the province and a summer or all year rainfall season in other parts of the province (Schulze, 1997b). Simulated potential changes of the start and end of the moisture growing season are not presented here, but can be obtained from the School of BEEH, University of Natal, Pietermaritzburg.

The duration of the present moisture growing season as calculated by Schulze (1997b) ranges from an all year season around parts of the coast of KwaZulu-Natal and in parts of the all year

rainfall region of the Eastern and Western Cape provinces, grading through an ever shortening length of the moisture growing season towards the inland (Figure 8.19, top left).

Figure 8.19 Duration of moisture growing season: for present climate (top left), future climate (bottom left), shift in climatically suitable areas (top right) and the change in duration of moisture growing season between future and present climates (bottom right). Future climate scenario from UKTR-S

The simulated duration of the moisture growing season in a future climate as represented by UKTR-S shows that most areas could experience a shortening of the moisture growing season (Figure 8.19, bottom left). Also, there is simulated to be a reduction of areas which will experience a moisture growing season in a future climate (Figure 8.19, top right). These reductions are mostly experienced along the western and northern edges of the present moisture growing season.

Reductions in the duration of the moisture growing season range from less than 50 days in the Western Cape to a reduction of over 150 days in parts of the Eastern Cape (Figure 8.19, bottom right). In most areas the reductions in the duration are less than 100 days. Gains in the duration of the moisture growing season are, however, experienced along the KwaZulu-Natal coast and parts of Lesotho and the Eastern Cape. The greatest gains in duration are along the northern KwaZulu-Natal coast, where up to 50 more days may be expected in the moisture growing season, if the UKTR-S scenario is assumed correct.

The coefficient of variation of moisture growing season is expected to increase in all provinces / countries of the study area in the future, with the exception of the Eastern Cape which was calculated to have a marginally lower coefficient of variation in future (see Table 8.8). Thus, the duration of the moisture growing season is expected to be more variable in most locations in the study area in future.

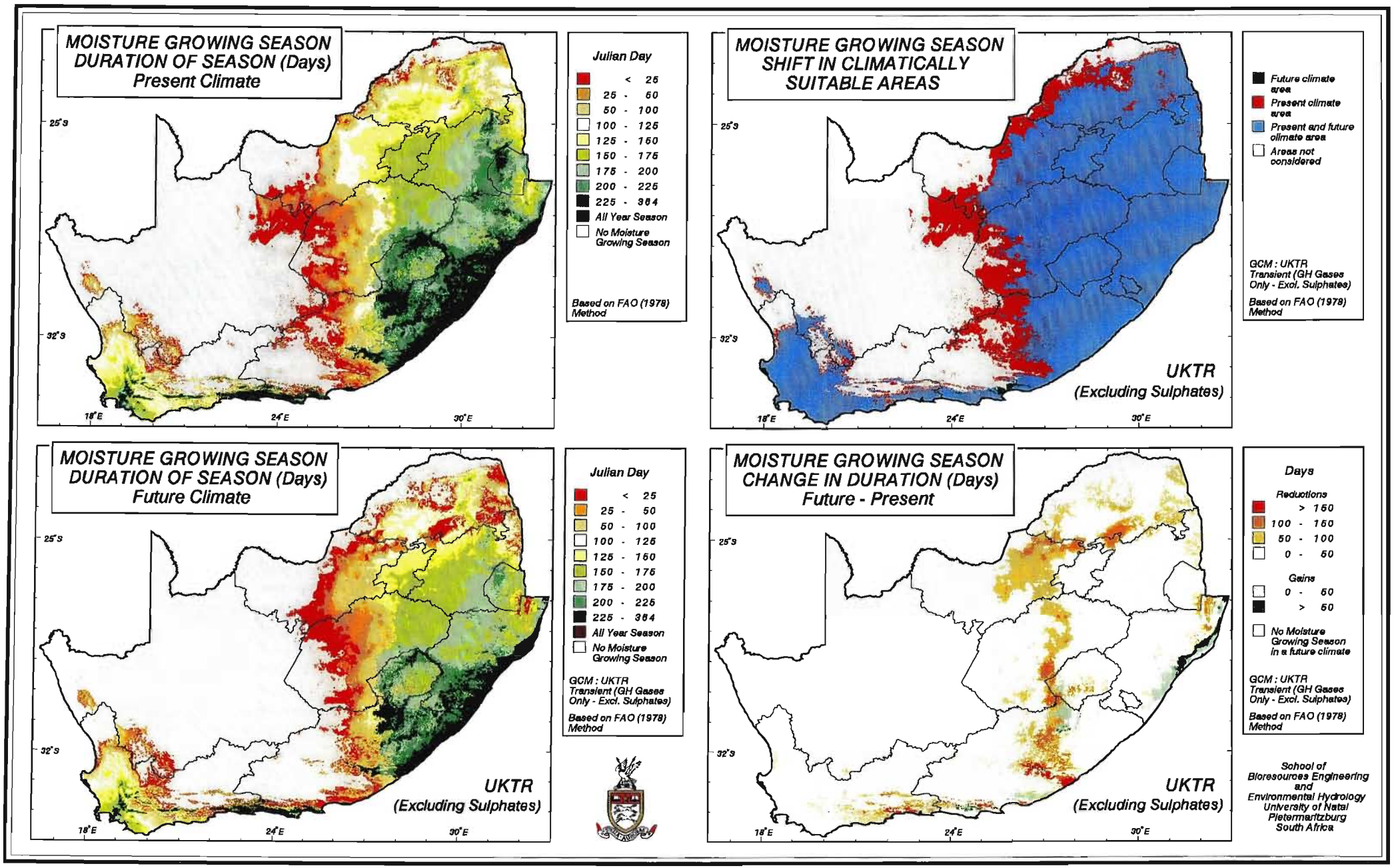
MOISTURE GROWING SEASON
DURATION OF SEASON (Days)
Present Climate
25°S
32°S
18°E
24°E
30°E
Julian Day
< 25
25 - 50
50 - 100
100 - 125
125 - 150
150 - 175
175 - 200
200 - 225
225 - 364
All Year Season
No Moisture Growing Season
Based on FAO (1978) Method
MOISTURE GROWING SEASON
SHIFT IN CLIMATICALLY SUITABLE AREAS
Future climate area
Present climate area
Present and future climate area
Areas not considered
GCM : UKTR Transient (GH Gases Only - Excl. Sulphates)
Based on FAO (1978) Method
UKTR
(Excluding Sulphates)
MOISTURE GROWING SEASON
DURATION OF SEASON (Days)
Future Climate
Julian Day
< 25
25 - 50
50 - 100
100 - 125
125 - 150
150 - 175
175 - 200
200 - 225
225 - 364
All Year Season
No Moisture Growing Season
GCM : UKTR Transient (GH Gases Only - Excl. Sulphates)
Based on FAO (1978) Method
UKTR
(Excluding Sulphates)
MOISTURE GROWING SEASON
CHANGE IN DURATION (Days)
Future - Present
Days
Reductions
> 150
100 - 150
50 - 100
0 - 50
Gains
0 - 50
> 50
No Moisture Growing Season in a future climate
GCM : UKTR Transient (GH Gases Only - Excl. Sulphates)
Based on FAO (1978) Method
UKTR
(Excluding Sulphates)
School of Bioresources Engineering and Environmental Hydrology
University of Natal
Pietermaritzburg
South Africa

As in the case of UKTR-S, reductions in duration of moisture growing season range from greater than 150 days in parts of the Eastern Cape to gains of over 50 days in some of the coastal regions of KwaZulu-Natal when using output from HadCM2-S (Figure 8.20, middle). Differences in the change in the duration between the two versions include 0 - 50 days gains in duration simulated by the newer version of this GCM in the eastern Free State and western Mpumalanga, which were simulated as reductions of 0 - 50 days using output from UKTR-S. A greater reduction in areas which are expected to experience a moisture growing season could be expected when using output from UKTR-S compared to HadCM2-S, particularly in the North-West Province.

Figure 8.20 Duration of moisture growing season: for future climate (top), the change in the duration of moisture growing season between future and present climates (middle) and shift in areas experiencing moisture growing season (bottom). Future climate scenario from HadCM2-S

When future temperatures and precipitation estimates from HadCM2+S are used, there are many more areas with increases in the duration of the moisture growing season (Figure 8.21, top and middle) compared to the results obtained using HadCM2+S. The areas of increases in duration are particularly evident along the KwaZulu-Natal coastline, the Northern Province and the Free State, where the duration of the moisture growing season could increase by more than 50 days.

Figure 8.21 Duration of moisture growing season: for future climate (top), the change in the duration of moisture growing season between future and present climates (middle) and shift in areas experiencing moisture growing season (bottom). Future climate scenario from HadCM2+S

The map of the potential shift in areas which have a moisture growing season (Figure 8.21, bottom) shows potential loss of presently suitable agricultural areas along the western and northern fringes.

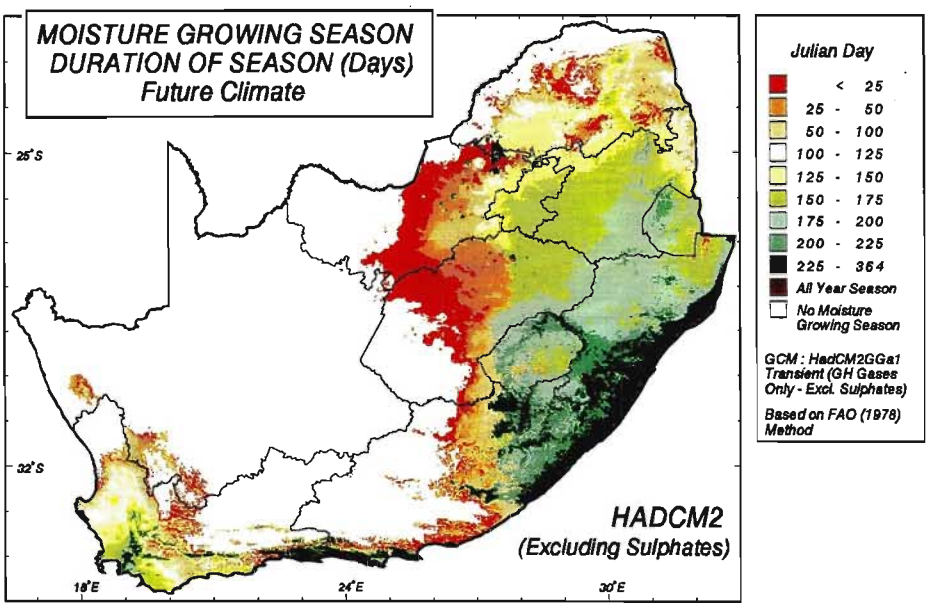


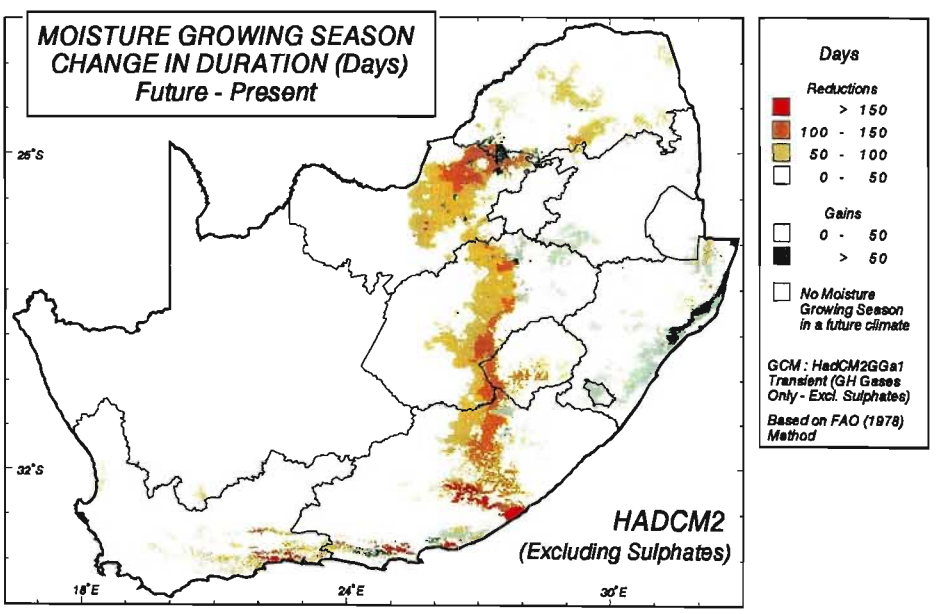


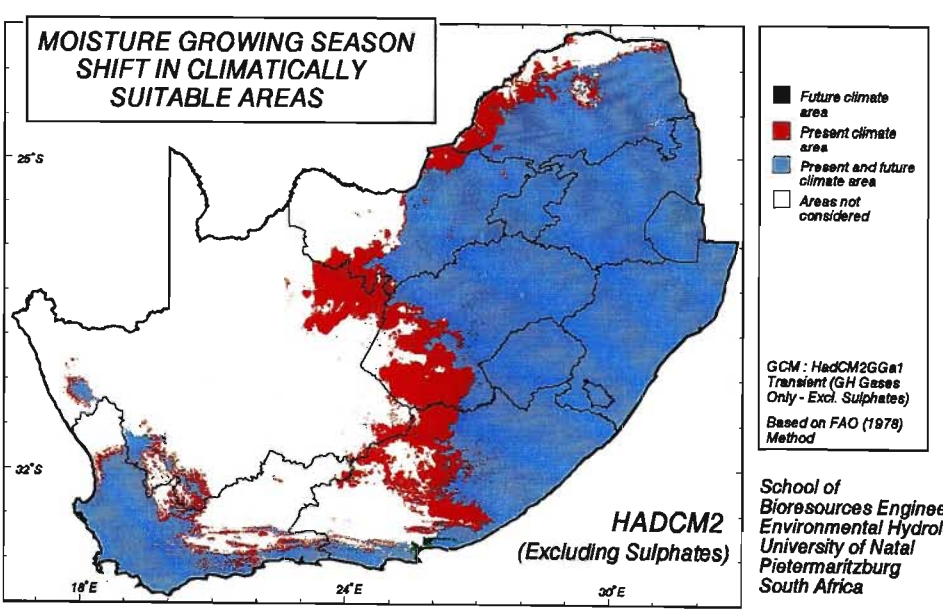


School of
Bioresources Engineering and
Environmental Hydrology
University of Natal
Pietermaritzburg
South Africa

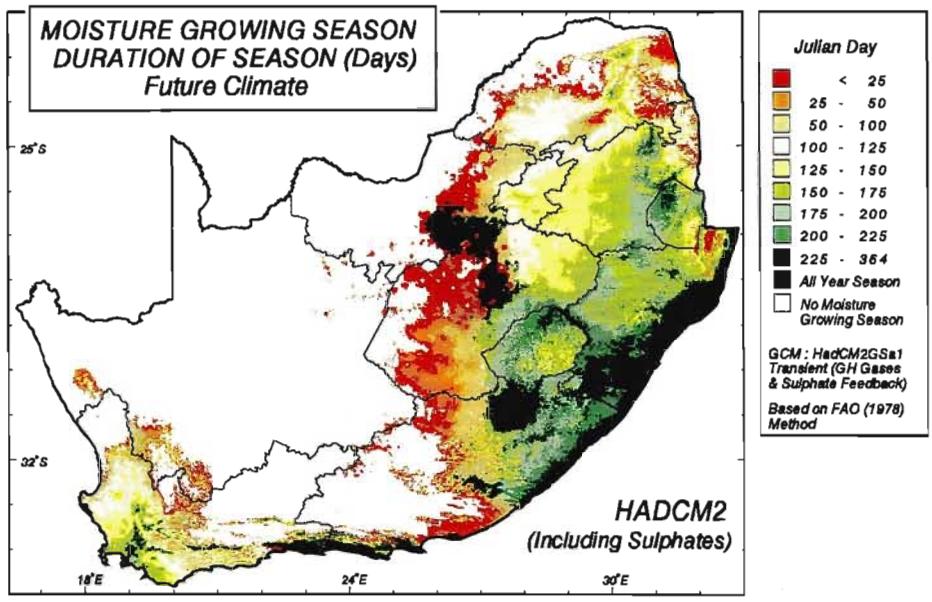


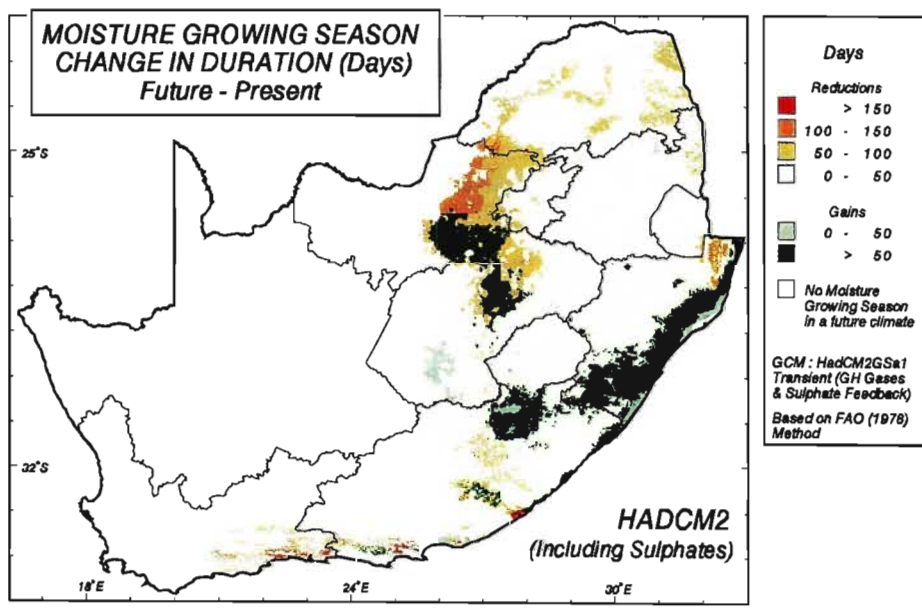


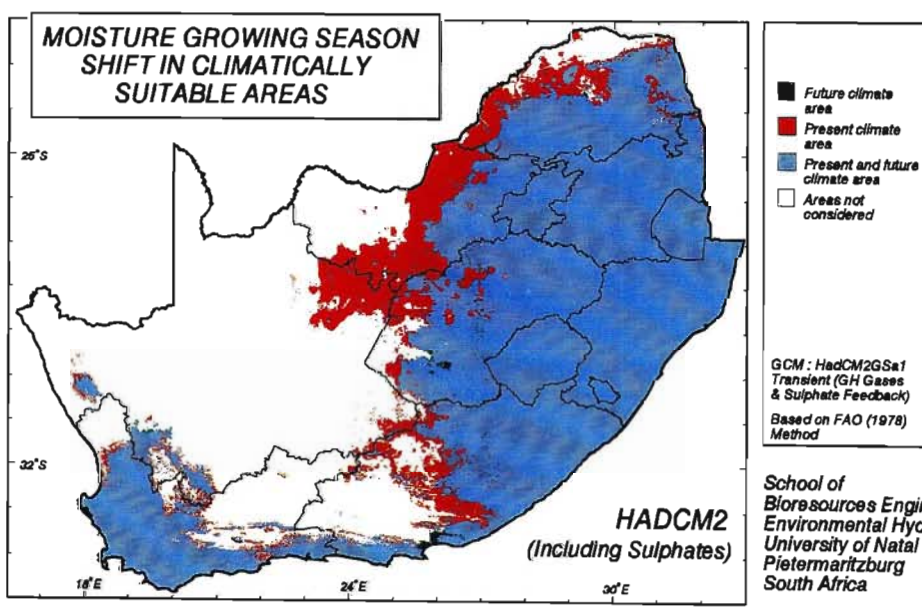


School of
Bioresources Engineering and
Environmental Hydrology
University of Natal
Pietermaritzburg
South Africa

## 8.2 Potential Impacts of Climate Change on Crop, Pasture and Timber Production using Smith's (1994) Climatic Criteria

As mentioned previously, changes in temperature and precipitation are expected to have significant impacts on both crop yields and their distributions of optimum climatic growth areas in southern Africa. To estimate the changes in yields that could be expected with changes in climate crop yield models are usually used. These crop yield models vary in complexity. Some models are simple rule-based and unidirectional climate driven models with yields further modified for variations in soil properties and management level, such as the Smith (1994) models developed for southern Africa. Others are considered to be of intermediate complexity, such as the *ACRU* maize and winter wheat yield submodels which simulate yield by daily soil water budgeting coupled with crop phenology (Schulze, 1997b).

The advantage of using simple crop yield models such as the Smith (1994) models is that the input requirement is relatively simple and easily obtainable. However, the models' estimates are not always accurate because they are not always sufficiently representative of the physical system (Schulze, 1995a). The potential impacts of climate change using future estimates of climate from UKTR-S and HadCM2, both excluding and including sulphate forcing, in conjunction with Smith's (1994) simple climatically determined yield models, were simulated for the following four crops

i) sorghum;
ii) sunflower seed;
iii) groundnut; and
iv) soybean;

as well as for the following two pasture grasses:

i) kikuyu; and
ii) *Eragrostis curvula.*

For the purpose of illustrating the techniques used, only the results obtained for one crop, *viz.* sorghum, and one pasture, *viz.* kikuyu, are presented in this thesis in Sections 8.2.1 and 8.2.2 respectively. However, the results obtained for the other crops and pasture grasses can be obtained from the School of BEEH, University of Natal, Pietermaritzburg.

Commercial afforestation of exotic species covers about 1.3% of the total area of South Africa. The forest products industry is one of the largest and fastest growing sectors of the South African economy. Owing to projected future demand for timber products, it is anticipated that afforestation will expand into previously non-forested and marginal areas in the next 20 - 30 years. Considering the expected growth of these areas and the fact that the climate is predicted to change in forthcoming years, it is important to assess potential changes in mean annual increments of timber and climatically suitable areas of certain commonly planted commercial tree species in southern Africa (Schulze, 1997b).

Potential changes in mean annual increment (MAI) and climatically suitable growing areas of various commercial tree species were assessed for a series of climate change scenarios, *viz.*

i) *Eucalyptus grandis;*
ii) *Pinus patula;*
iii) *Pinus taeda;*
iv) *Pinus elliottii;* and
v) *Acacia mearnsii* (both timber yields and bark yield).

Results for future climatic conditions were generated using output from UKTR-S and HadCM2, both including and excluding sulphate forcing. However, in order to illustrate the techniques used, only the results obtained from the studies of *E. grandis* and *A. mearnsii* (timber) are presented in Sections 8.2.3 and 8.2.4. The maps of potential changes in mean annual increment and climatically suitable areas for the other tree species can be obtained from the School of BEEH, University of Natal, Pietermaritzburg.

### 8.2.1 Potential impact of climate change on sorghum yields

*Sorghum bicolor* is, in comparison with maize, a relatively warm area and drought resistant crop, which can tolerate erratic rainfall and will recover even if wilted for up to 14 days. Sorghum can be cultivated in rainfall regimes ranging from 300 - 1 200 mm in the growing season, however, its optimal rainfall for this period is around 600 mm. It is sensitive to frost and is grown ideally where relative humidities are less than 60%. Sorghum grows in a range of temperatures with optima around 25 °C and a January mean of less than 21 °C. Since flowering takes place 50 - 70 days after planting, rainfall for the stress sensitive third month

should exceed 100 mm. Sorghum grows on a variety of soils, but ideally prefers deep and well drained light to medium textures. The crop tolerates a wide range of drainage conditions, including short periods of waterlogging (Sys *et al.*, 1993; Schulze, 1997b).

Using Smith's (1994) climatic criteria, yields of sorghum were estimated using the effective rainfall for October to March and heat units (base 10 °C) for the same period, with modifications to yield made for soil properties and management levels (Schulze, 1997b). Climatically derived sorghum yields may be adjusted for soil characteristics by various multiplication factors (Smith, 1994, as described in Schulze, 1997b). Using Smith's (1994) climatic criteria only, i.e. without cognisance of the soil properties or level of management, sorghum yield is calculated as

$$Y_{sor} = P_{eom} \times P_{su} \times D_{sh} / 100$$

where $Y_{sor}$ = sorghum yield ($t.ha^{-1}.season^{-1}$)

$P_{eom}$ = effective rainfall fraction for October to March

$= 0.60 + 0.00125 (P_{su} - 480)$ for $400 < P_{su} < 720$

$= 0.90 - 0.00063 (P_{su} - 720)$ for $720 < P_{su} < 960$

$= 0.75 - 0.00125 (P_{su} - 960)$ for $960 < P_{su} < 1\,040$

$= 0.65 - 0.00063 (P_{su} - 1\,040)$ for $1040 < P_{su} < 1\,300$

with $P_{su}$ = accumulated rainfall (mm) for October to March

while $D_{sh}$ = dry matter yield index for sorghum

$= 0.8 + 0.00010 (H_{su} - 1\,200)$ for $1000 < H_{su} < 1\,600$

$= 1.2 + 0.0005 (H_{su} - 1\,600)$ for $1600 < H_{su} < 2\,000$

$= 1.4 - 0.0005 (H_{su} - 2\,000)$ for $2000 < H_{su} < 2\,800$

where $H_{su}$ = accumulated heat units (base 10 °C) in degree days for the period October to March.

Sorghum yields for present climatic conditions were estimated by Schulze (1997b) to range from less than 3 $t.ha^{-1}.season^{-1}$ in the eastern Free State to over 8 $t.ha^{-1}.season^{-1}$ in the east of the study area (Figure 8.22, top left).

| | |
|---|---|
| Figure 8.22 | Sorghum yield ($t.ha^{-1}.season^{-1}$): for present climate (top left), future climate (bottom left), shifts in climatically suitable areas (top right) and changes in yield between future and present climates (bottom right). Future climate scenario from UKTR-S |

Using output from UKTR-S and Smith's (1994) climatic criteria the sorghum yield for a potential future climate was estimated. Being a fairly resilient crop, there is not much change in total area under sorghum in the future (Figure 8.22, bottom left and top right). Mpumalanga, the eastern Free State, Lesotho and southern KwaZulu-Natal are expected to gain new areas which are suitable for cultivation of sorghum in a future climate. However, loses of suitable areas are expected in, *inter alia,* the marginal areas of Swaziland (from 84.5% at present to 47% in future as shown in Table 8.9), north-eastern KwaZulu-Natal and the northern fringes of the present growing areas.

Both increases and decreases in sorghum yield were simulated for a future climate using output from UKTR-S (Figure 8.22, bottom right). Reductions in yield in areas that will be climatically suitable in the future could be over 2 $t.ha^{-1}.season^{-1}$, with the greatest reductions being in the eastern areas of KwaZulu-Natal. Small gains in yield could be expected in the core regions located between the Free State, Mpumalanga and KwaZulu-Natal.

Results using HadCM2-S show similar trends to those obtained using UKTR-S. The most notable difference between the two versions is that more areas could experience reductions in excess of 2 $t.ha^{-1}.season^{-1}$ when using UKTR-S (Figure 8.22, bottom right) compared to results obtained using HadCM2 (Figure 8.23, middle). The shifts in climatically suitable areas are very similar between the two versions (Figure 8.22, top right for UKTR-S and Figure 8.23, bottom for HadCM2-S).

| | |
|---|---|
| Figure 8.23 | Sorghum yield ($t.ha^{-1}.season^{-1}$): for future climate (top), the change in the sorghum yield between future and present climates (middle) and shift in climatically suitable areas (bottom). Future climate scenario from HadCM2-S |

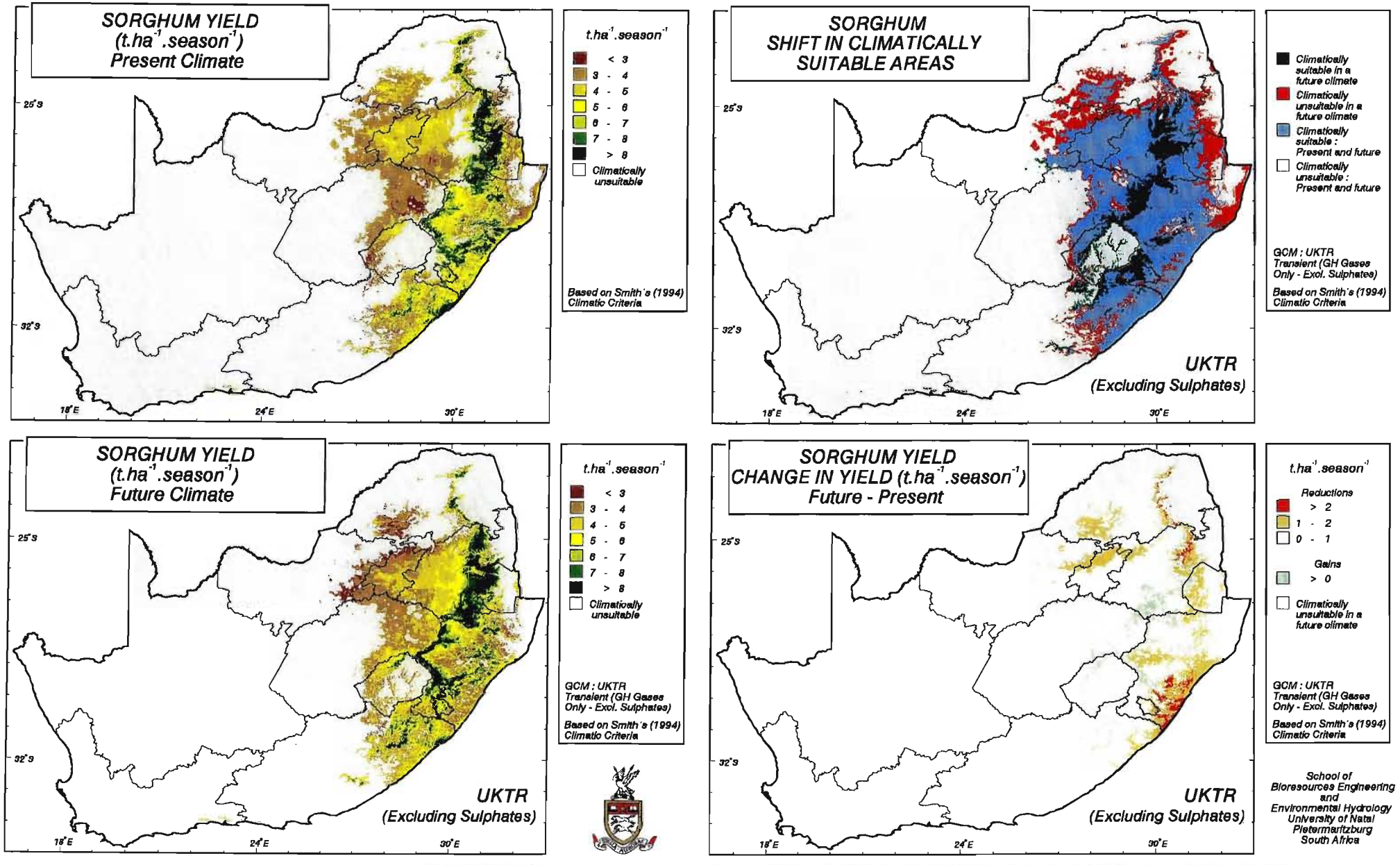
SORGHUM YIELD
(t.ha-1.season-1)
Present Climate
25°S
32°S
18°E
24°E
30°E
t.ha-1.season-1
< 3
3 - 4
4 - 5
5 - 6
6 - 7
7 - 8
> 8
Climatically unsuitable
Based on Smith's (1994) Climatic Criteria
SORGHUM
SHIFT IN CLIMATICALLY
SUITABLE AREAS
UKTR
(Excluding Sulphates)
Climatically suitable in a future climate
Climatically unsuitable in a future climate
Climatically suitable : Present and future
Climatically unsuitable : Present and future
GCM : UKTR
Transient (GH Gases Only - Excl. Sulphates)
Based on Smith's (1994) Climatic Criteria
SORGHUM YIELD
(t.ha-1.season-1)
Future Climate
UKTR
(Excluding Sulphates)
SORGHUM YIELD
CHANGE IN YIELD (t.ha-1.season-1)
Future - Present
Reductions
> 2
1 - 2
0 - 1
Gains
> 0
School of
Bioresources Engineering
and
Environmental Hydrology
University of Natal
Pietermaritzburg
South Africa

Table 8.9 Statistics for sorghum yield for present climatic conditions and a future (2X $CO_2$) climate scenario from UKTR-S

| Sorghum Yield Estimate (t.ha$^{-1}$.season$^{-1}$) | | | | | | | | | | | | | | | | |
|---|---|---|---|---|---|---|---|---|---|---|---|---|---|---|---|---|
| Province / Country | % Suitable Area | | Mean Value | | C.V. (%) | | Maximum Value | | Minimum Value | | Exceedence Probability | | | | | |
| | | | | | | | | | | | 20% | | 50% | | 80% | |
| | Present | Future | Present | Future | Present | Future | Present | Future | Present | Future | Present | Future | Present | Future | Present | Future |
| Northern Province | 26.1 | 11.8 | 4.4 ** | 4.1 | 31.5 | 38.7 | 10.1 | 9.9 | 2.6 | 2.5 | 4.9 | 4.8 | 3.9 | 3.5 | 3.4 | 3.0 |
| Mpumalanga | 65.5 | 5.2 | 5.2 | 5.6 | 35.8 | 29.8 | 10.0 | 10.0 | 2.6 | 2.6 | 7.1 | 7.3 | 4.5 | 5.0 | 3.7 | 4.2 |
| North-West | 16.7 | 8.4 | 3.7 | 3.2 | 11.8 | 10.7 | 6.1 | 5.2 | 2.8 | 2.5 | 3.9 | 3.4 | 3.6 | 3.1 | 3.3 | 2.9 |
| Northern Cape | N/A * | N/A | N/A | N/A | N/A | N/A | N/A | N/A | N/A | N/A | N/A | N/A | N/A | N/A | N/A | N/A |
| Gauteng | 99.9 | 97.1 | 4.5 | 3.9 | 10.1 | 15.0 | 7.6 | 8.0 | 3.2 | 2.5 | 4.8 | 4.4 | 4.5 | 3.9 | 3.9 | 3.4 |
| Free State | 22.2 | 24.9 | 3.4 | 4.1 | 11.5 | 18.7 | 6.1 | 8.8 | 2.5 | 2.7 | 3.7 | 4.5 | 3.4 | 3.9 | 3.9 | 3.6 |
| KwaZulu-Natal | 77.0 | 75.1 | 5.7 | 5.6 | 26.6 | 31.6 | 10.0 | 10.1 | 2.7 | 2.6 | 7.1 | 7.3 | 5.6 | 5.3 | 5.3 | 4.0 |
| Eastern Cape | 23.2 | 23.1 | 5.0 | 5.1 | 29.6 | 28.4 | 9.9 | 9.8 | 2.3 | 2.2 | 6.2 | 6.3 | 4.7 | 4.8 | 4.8 | 3.9 |
| Western Cape | 0.4 | 2.8 | 3.8 | 4.0 | 15.6 | 14.0 | 5.5 | 5.4 | 2.5 | 2.8 | 4.3 | 4.5 | 3.4 | 3.9 | 3.9 | 3.6 |
| Swaziland | 84.5 | 47.0 | 6.1 | 6.8 | 34.6 | 25.6 | 10.0 | 10.0 | 2.6 | 2.6 | 8.4 | 8.4 | 5.9 | 7.0 | 7.0 | 5.0 |
| Lesotho | 22.4 | 33.8 | 3.8 | 4.4 | 23.4 | 29.0 | 0.3 | 9.4 | 2.3 | 2.2 | 4.6 | 5.3 | 3.7 | 4.1 | 4.1 | 3.5 |

* N/A denotes climatically unsuitable at all grid points
** All statistics only for those grid points which qualify as climatically suitable



Table 8.10 Statistics for kikuyu yield for present climatic conditions and a future (2X $CO_2$) climate scenario from UKTR-S

| Kikuyu Yield Estimate (t.ha$^{-1}$.season$^{-1}$) | | | | | | | | | | | | | | | | |
|---|---|---|---|---|---|---|---|---|---|---|---|---|---|---|---|---|
| Province / Country | % Suitable area | | Mean Value | | C.V. (%) | | Maximum Value | | Minimum Value | | Exceedence Probability | | | | | |
| | | | | | | | | | | | 20% | | 50% | | 80% | |
| | Present | Future | Present | Future | Present | Future | Present | Future | Present | Future | Present | Future | Present | Future | Present | Future |
| Northern Province | 42.4 | 19.8 | 6.1 ** | 5.3 | 40.3 | 43.0 | 17.8 | 17.5 | 3.1 | 3.1 | 7.3 | 6.2 | 5.4 | 4.6 | 4.3 | 3.8 |
| Mpumalanga | 91.0 | 79.2 | 9.4 | 8.9 | 35.0 | 34.6 | 18.0 | 17.8 | 3.2 | 3.1 | 12.6 | 11.8 | 8.9 | 8.1 | 6.9 | 6.4 |
| North-West | 35.5 | 21.8 | 5.3 | 4.3 | 17.7 | 15.0 | 11.2 | 8.0 | 3.3 | 3.1 | 6.0 | 48 | 5.1 | 4.1 | 4.5 | 3.7 |
| Northern Cape | N/A | N/A | N/A | N/A | N/A | N/A | N/A | N/A | N/A | N/A | N/A | N/A | N/A | N/A | N/A | N/A |
| Gauteng | 98.6 | 98.6 | 8.2 | 6.1 | 14.2 | 15.5 | 15.1 | 12.4 | 4.8 | 3.5 | 9.0 | 6.7 | 8.3 | 6.1 | 7.2 | 5.3 |
| Free State | 41.2 | 40.4 | 6.6 | 6.0 | 20.1 | 32.7 | 14.4 | 17.4 | 4.2 | 3.2 | 7.4 | 7.0 | 6.5 | 5.6 | 5.4 | 4.3 |
| KwaZulu-Natal | 92.8 | 79.7 | 9.8 | 8.9 | 35.7 | 37.4 | 17.9 | 17.9 | 3.3 | 3.1 | 13.2 | 12.0 | 9.6 | 8.2 | 6.6 | 6.0 |
| Eastern Cape | 32.2 | 29.8 | 8.8 | 7.9 | 34.0 | 34.9 | 17.9 | 17.7 | 3.7 | 3.7 | 11.4 | 9.9 | 8.4 | 7.2 | 6.0 | 5.5 |
| Western Cape | 0.9 | 0.6 | 6.3 | 5.8 | 21.3 | 20.4 | 10.6 | 9.7 | 3.7 | 3.9 | 7.4 | 6.8 | 5.9 | 5.6 | 5.1 | 4.7 |
| Swaziland | 94.8 | 47.1 | 9.5 | 10.5 | 43.7 | 26.6 | 17.9 | 17.3 | 3.1 | 3.8 | 14.1 | 13.1 | 8.6 | 10.9 | 5.5 | 7.7 |
| Lesotho | 39.0 | 57.4 | 7.4 | 7.1 | 27.3 | 35.6 | 14.4 | 17.0 | 3.7 | 3.7 | 9.0 | 8.5 | 6.9 | 6.5 | 5.7 | 5.1 |

* N/A denotes climatically unsuitable at all grid points
** All statistics only for those grid points which qualify as climatically suitable

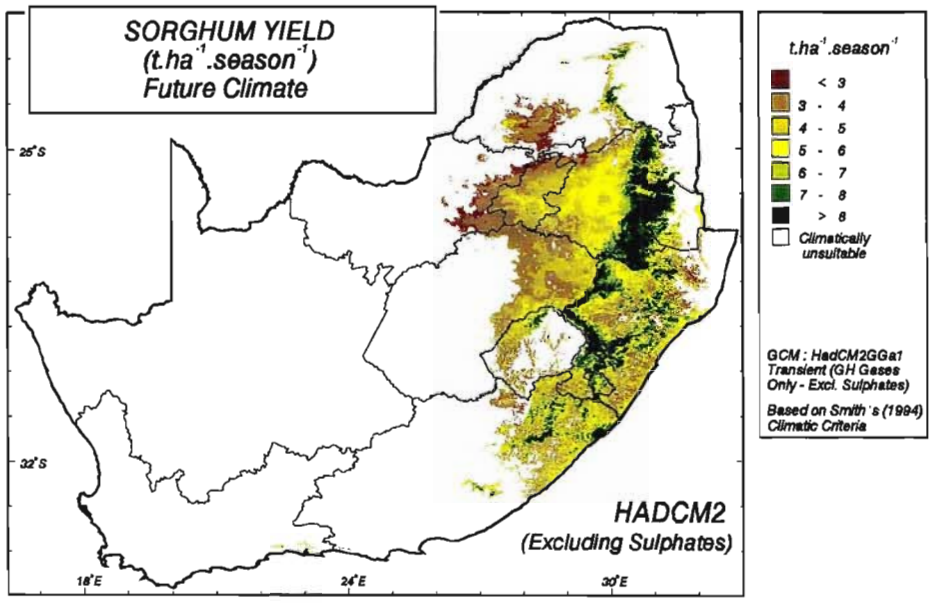


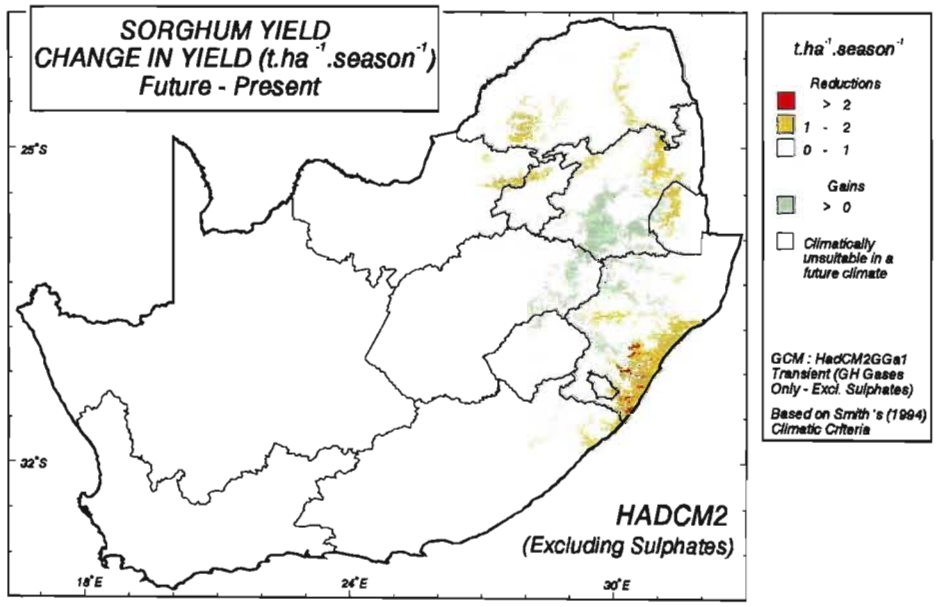


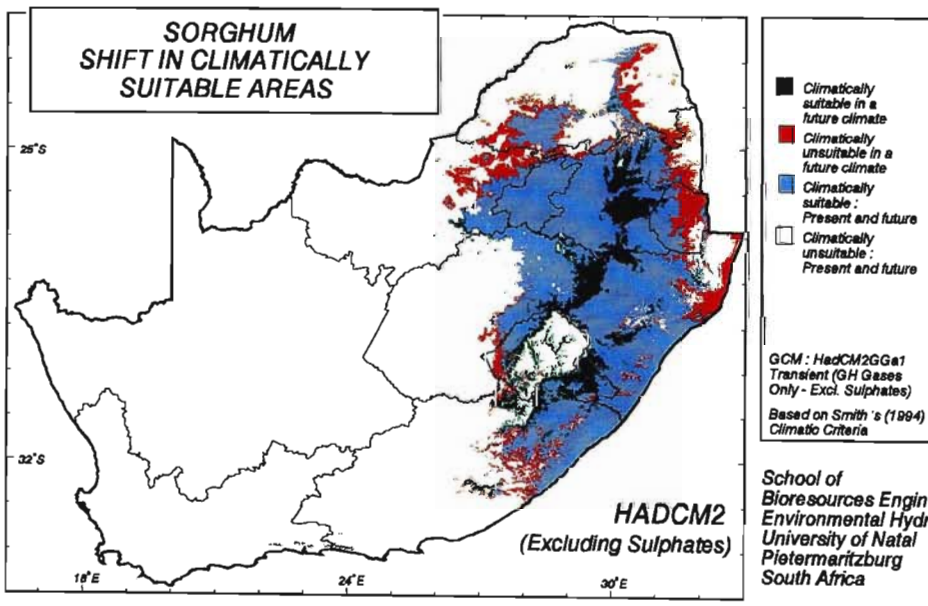


School of
Bioresources Engineering and
Environmental Hydrology
University of Natal
Pietermaritzburg
South Africa

When including the effect of sulphate forcing in HadCM2, fewer areas are expected to experience increases in yield and more areas are potentially climatically unsuitable (Figure 8.24, middle and bottom) compared to the simulations which used output from HadCM2-S (Figure 8.23, middle and bottom). The decrease in climatically suitable areas is particularly evident in the north-western areas, which are climatically suitable for the cultivation of sorghum.

| | |
|---|---|
| Figure 8.24 | Sorghum yield ($t.ha^{-1}.season^{-1}$): for future climate (top), the change in the sorghum yield between future and present climates (middle) and shift in climatically suitable areas (bottom). Future climate scenario from HadCM2+S |

### 8.2.2 Potential impact of climate change on kikuyu yields

Kikuyu (*Pennisetum clandestinum)* is one of the most popular summer (i.e. October to March, in places September to April) pastures grown in southern Africa. It generally thrives best at where the mean annual precipitation is greater than 800 mm, where mean annual temperatures are less than 17 °C and on medium to high fertility, well drained soils (Smith, 1994).

Dry matter yield of kikuyu may be estimated by Smith's (1994) rule based approach using the effective rainfall for the summer months October to March in conjunction with accumulated summer months heat units (base 10 °C), and assuming that base fertilizer levels have been brought up to optimum conditions by addition of phosphates and potassium and that 250 kg nitrogen per ha has been applied (Schulze, 1997b). Considering only the climatic criteria of Smith's (1994) rule based approach for estimating the yield of kikuyu, his tabulated information was expressed in equation form as

$$Y_{kik} = P_{eom} \times P_{su} \times D_{kik} / 100$$

where $Y_{kik}$ = kikuyu yield ($t.ha^{-1}.season^{-1}$)

$P_{eom}$ = effective rainfall fraction for October to March

= $0.60 + 0.00125 (P_{su} - 480)$ for $400 < P_{su} < 720$

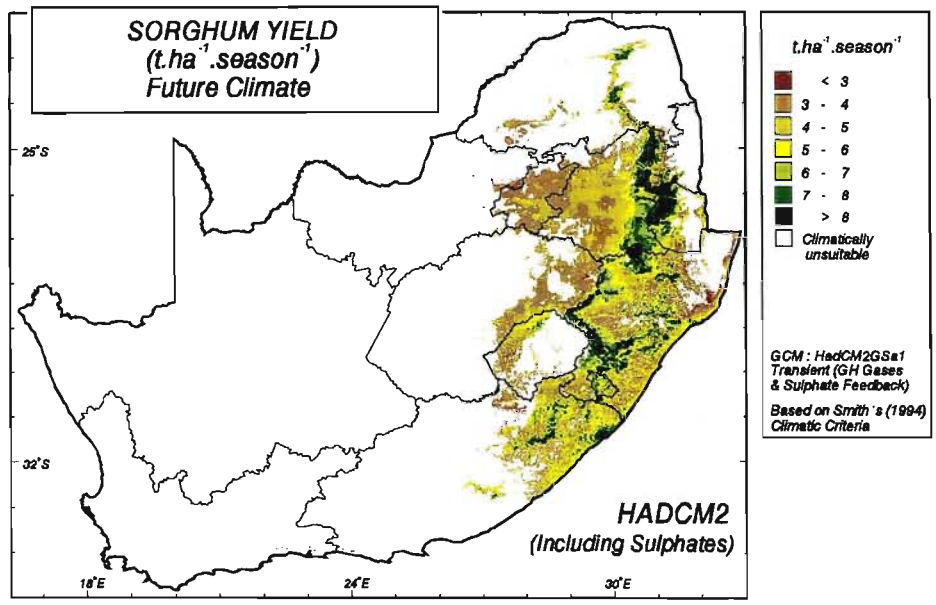


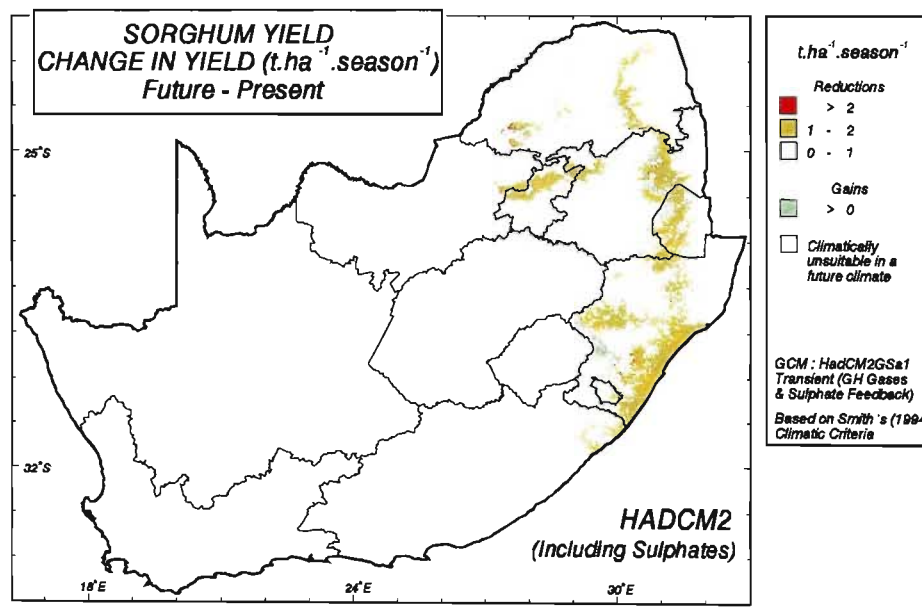


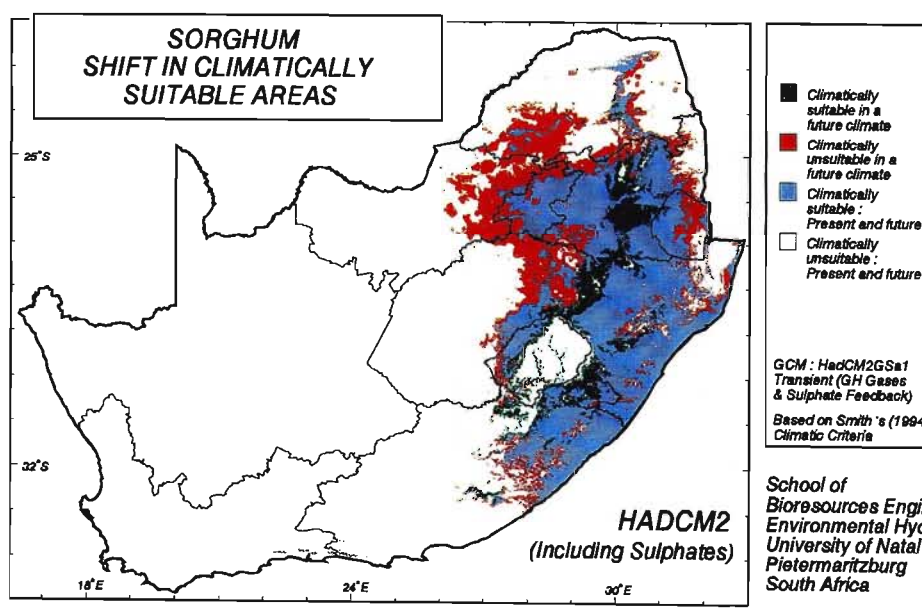


School of
Bioresources Engineering and
Environmental Hydrology
University of Natal
Pietermaritzburg
South Africa

$= 0.90 - 0.00063 (P_{su} - 720)$ for $720 < P_{su} < 960$

$= 0.75 - 0.00125 (P_{su} - 960)$ for $960 < P_{su} < 1\,040$

$= 0.65 - 0.00063 (P_{su} - 1\,040)$ for $1040 < P_{su} < 1\,300$

with $P_{su}$ = accumulated rainfall (mm) for October to March

and $D_{kik}$ = dry matter yield for kikuyu

$= 1.8 + 0.00010 (H_{su} - 1\,000)$ for $1000 < H_{su} < 1\,700$

$= 2.5 + 0.00010 (H_{su} - 1\,700)$ for $1700 < H_{su} < 2\,200$

$= 2.0 - 0.00008 (H_{su} - 2\,200)$ for $2200 < H_{su} < 2\,800$

where $H_{su}$ = accumulated heat units (base 10 °C) in degree days for October to March.

Presently climatically suitable areas for the cultivation of kikuyu are in the eastern half of the study area where yields are estimated to range from less than 4 $t.ha^{-1}.season^{-1}$ to more than 14 $t.ha^{-1}.season^{-1}$. These yields shown in Figure 8.25 (top left) were calculated by Schulze (1997b) using Smith's (1994) climatic criteria.

Figure 8.25 Kikuyu yield ($t.ha^{-1}.season^{-1}$): for present climate (top left), future climate (bottom left), shifts in climatically suitable areas (top right) and changes in yield between future and present climates (bottom right). Future climate scenario from UKTR-S

Although there is not expected to be a very large loss in climatically suitable areas for kikuyu cultivation in the future (Figure 8.25, top right), considerable reductions in yield are expected (Figure 8.25, bottom right) using output from the UKTR-S. Most of these decreases in climatically suitable areas are expected along the fringes of the areas presently suitable for cultivation, particularly along the northern and eastern fringes where it becomes too hot for the cultivation of kikuyu. A 50% decrease in climatically suitable area from present to future climate was estimated for Swaziland (see Table 8.10). Some parts of Lesotho, however, could become climatically suitable for kikuyu cultivation in a future climate, if the simulation of future climatic conditions are assumed correct.

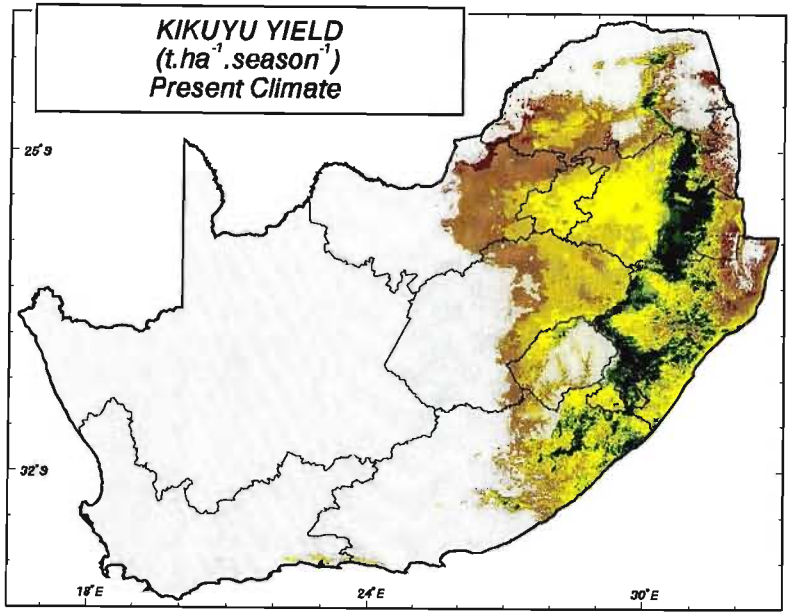


t.ha$^{-1}$.season$^{-1}$

- < 4
- 4 - 6
- 6 - 8
- 8 - 10
- 10 - 12
- 12 - 14
- > 14
- Climatically unsuitable

Based on Smith's (1994) Climatic Criteria

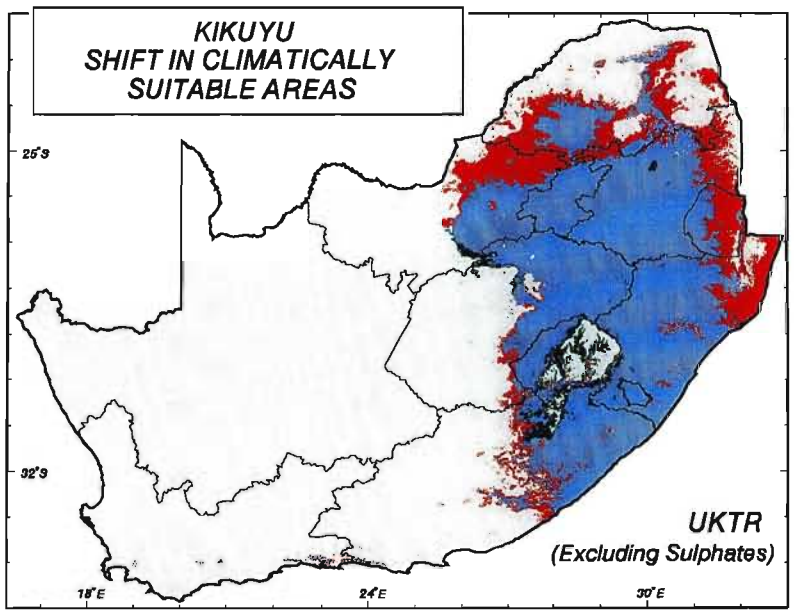


- Climatically suitable in a future climate
- Climatically unsuitable in a future climate
- Climatically suitable : Present and future
- Climatically unsuitable : Present and future

GCM : UKTR Transient (GH Gases Only - Excl. Sulphates)

Based on Smith's (1994) Climatic Criteria

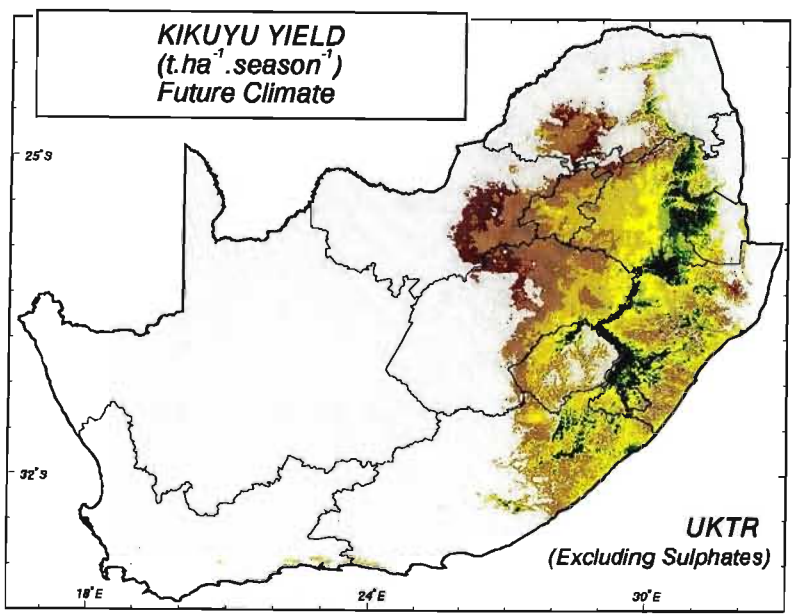


t.ha$^{-1}$.season$^{-1}$

- < 4
- 4 - 6
- 6 - 8
- 8 - 10
- 10 - 12
- 12 - 14
- > 14
- Climatically unsuitable

GCM : UKTR Transient (GH Gases Only - Excl. Sulphates)

Based on Smith's (1994) Climatic Criteria

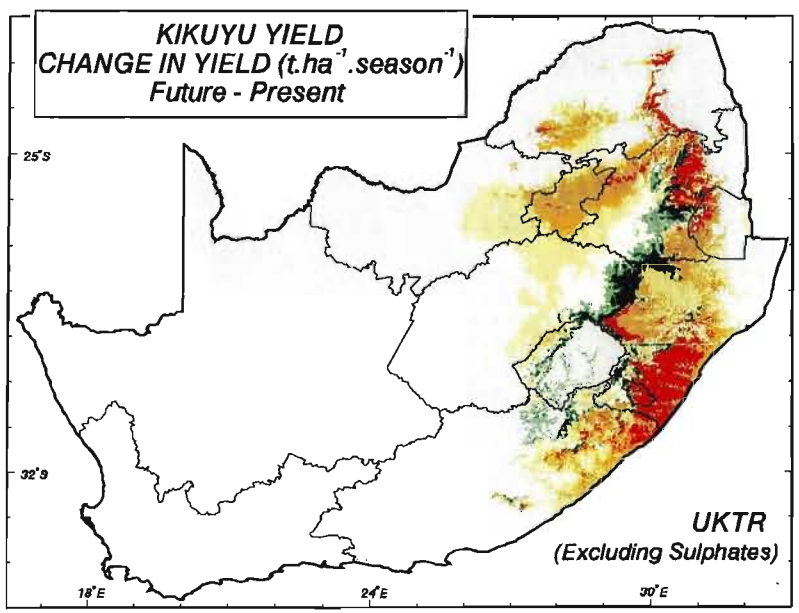


t.ha$^{-1}$.season$^{-1}$

Reductions
- > 3
- 2 - 3
- 1 - 2
- 0 - 1

Gains
- 0 - 1
- > 1

- Climatically unsuitable in a future climate

GCM : UKTR Transient (GH Gases Only - Excl. Sulphates)

Based on Smith's (1994) Climatic Criteria

School of Bioresources Engineering and Environmental Hydrology
University of Natal
Pietermaritzburg
South Africa

Most areas are simulated to have a decrease in kikuyu yield using the UKTR-S future climate scenario, with reductions ranging from less than 1 $t.ha^{-1}.season^{-1}$ in the optimal growth regions to a more than 3 $t.ha^{-1}.season^{-1}$ along the southern KwaZulu-Natal coastline (Figure 8.25, bottom right). Some increases in kikuyu yields, of approximately 1 $t.ha^{-1}.season^{-1}$, could be expected in eastern Free State and central Mpumalanga, however.

The shift in climatically suitable areas for the cultivation of kikuyu using output from HadCM2-S (Figure 8.26, bottom) is very similar to results using output from UKTR-S (Figure 8.25, top right). There are, however, differences between the two versions in the change in yield with a future climate. Results using output from UKTR-S (Figure 8.25, bottom right) show higher reductions in yield than those using output from HadCM2+S, particularly in southern KwaZulu-Natal.

Figure 8.26 Kikuyu yield ($t.ha^{-1}.season^{-1}$): for future climate (top), the change in the kikuyu yield between future and present climates (middle) and shift in climatically suitable areas (bottom). Future climate scenario from HadCM2-S

Gains in kikuyu yield are simulated to not be as great when including the influence of sulphate forcing in HadCM2 (Figure 8.27, middle). In addition, more areas could experience reductions in excess of 3 $t.ha^{-1}.season^{-1}$ when including sulphate forcing. There are expected to be greater decreases in climatically suitable areas when using output from HadCM2-S , especially in the western parts of the climatically suitable areas (Figure 8.27, bottom).

Figure 8.27 Kikuyu yield ($t.ha^{-1}.season^{-1}$): for future climate (top), the change in the kikuyu yield between future and present climates (middle) and shift in climatically suitable areas (bottom). Future climate scenario from HadCM2+S

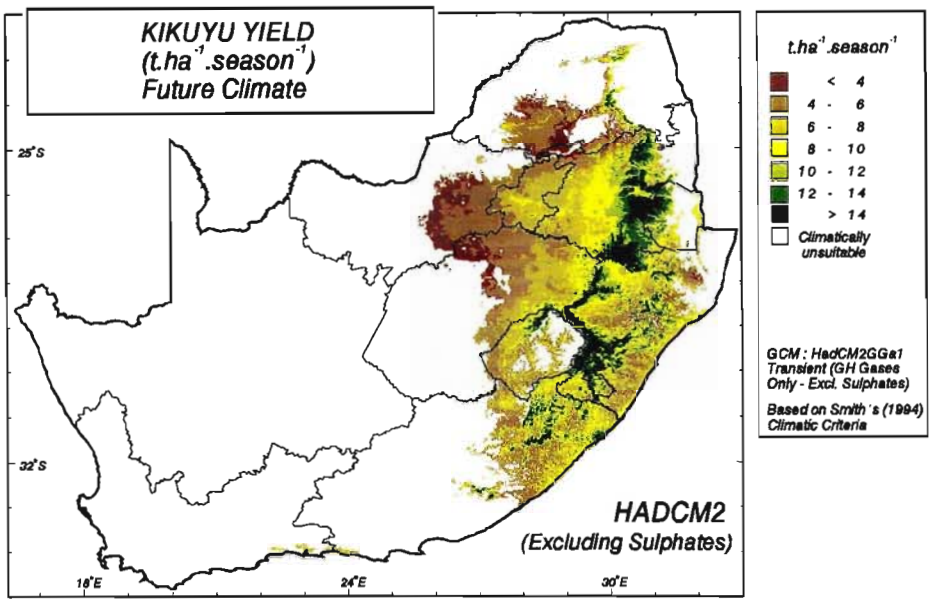


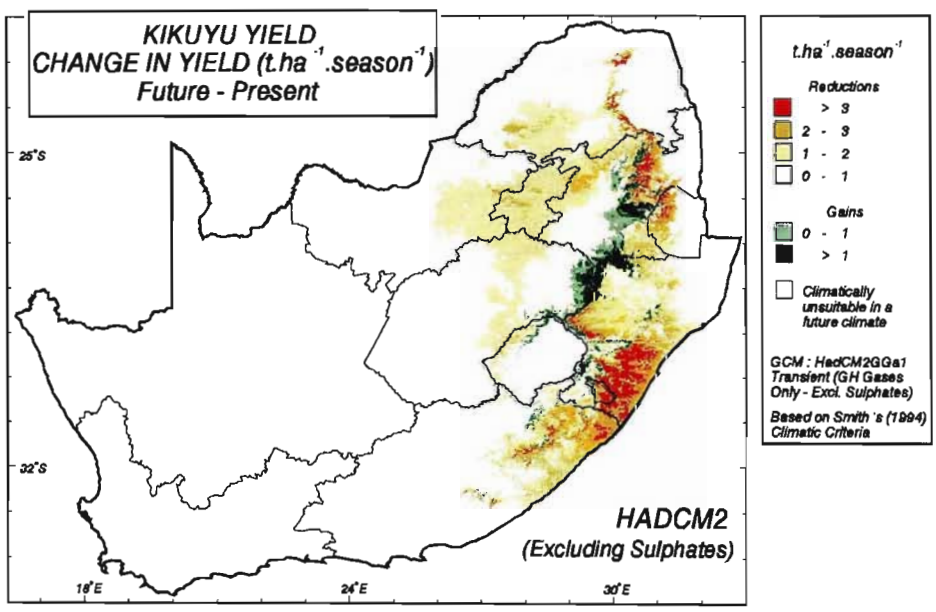


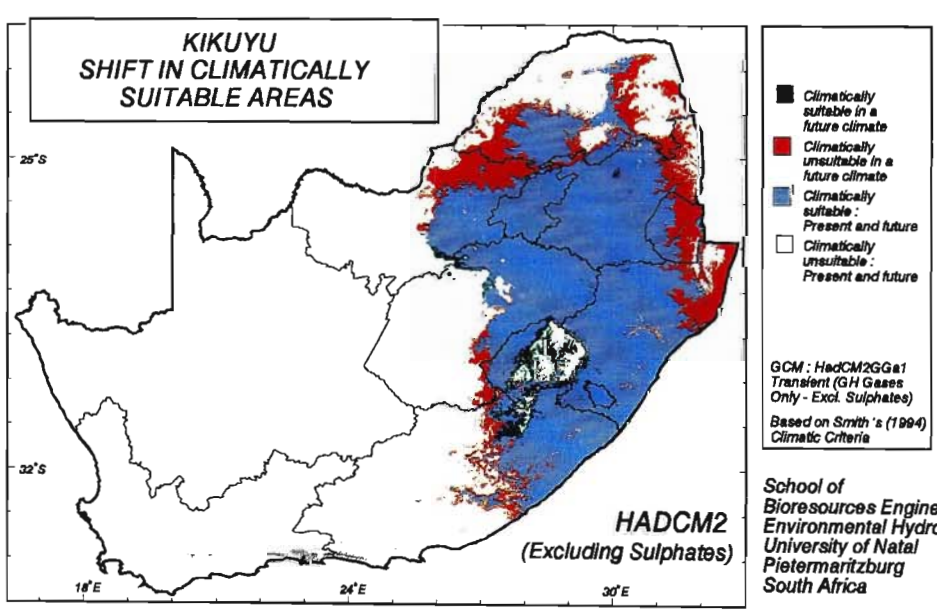


School of
Bioresources Engineering and
Environmental Hydrology
University of Natal
Pietermaritzburg
South Africa

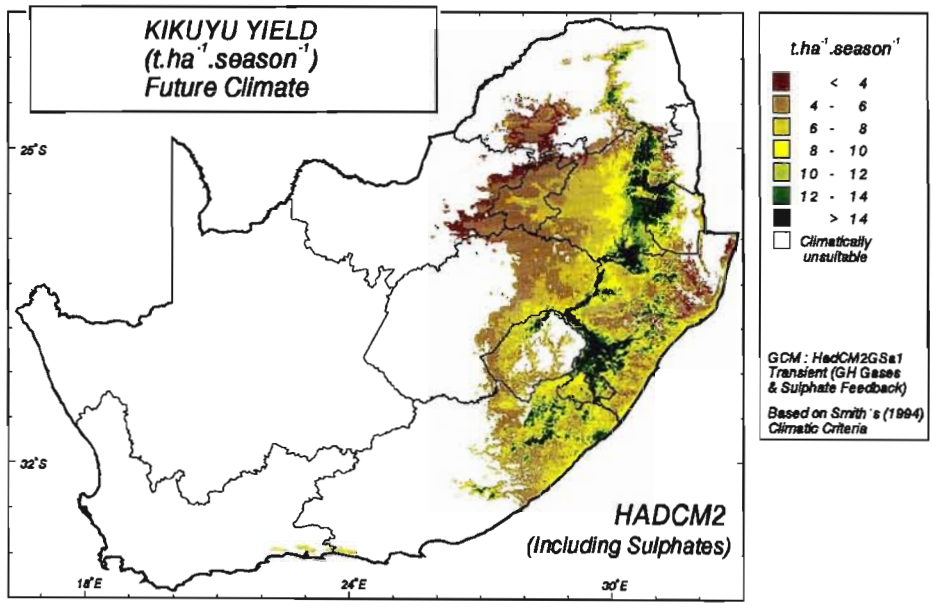


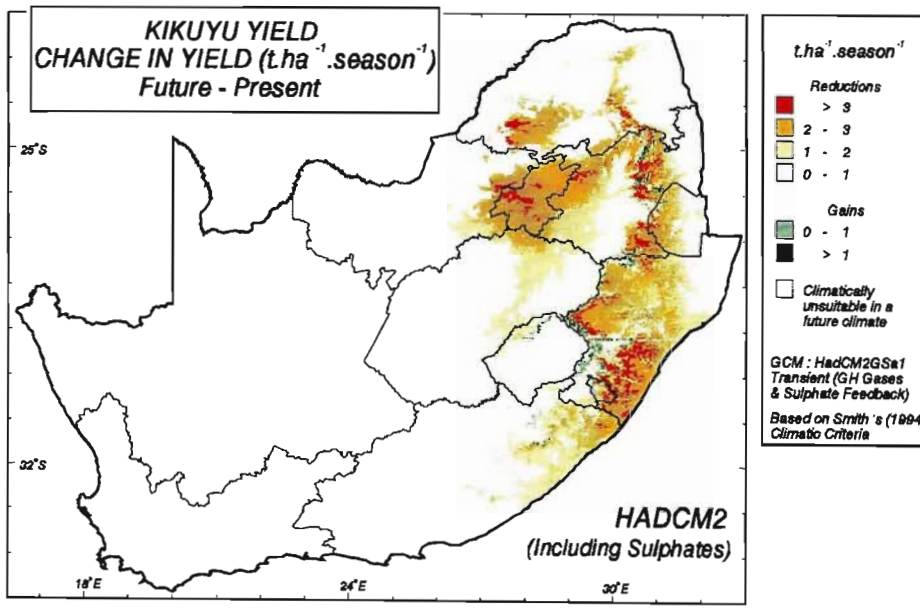


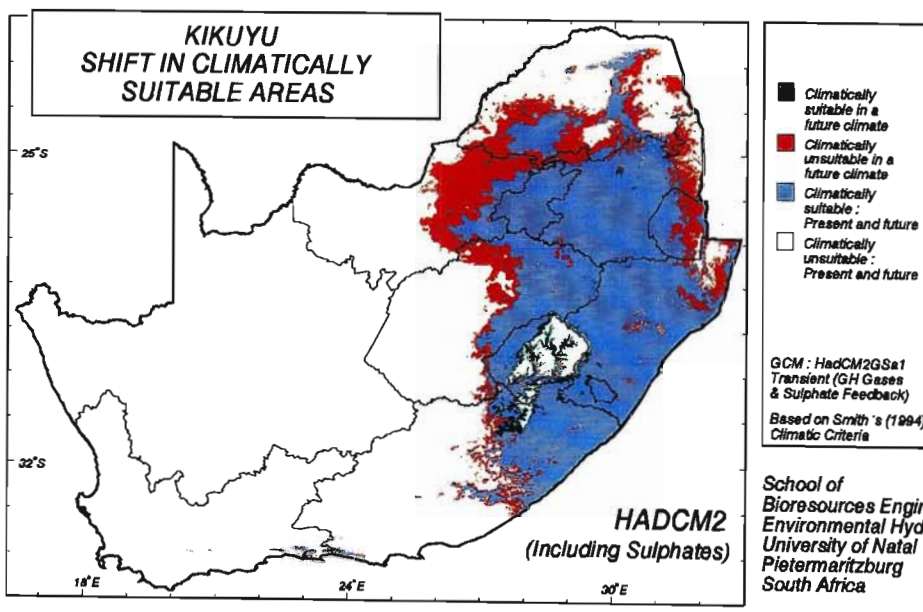


School of
Bioresources Engineering and
Environmental Hydrology
University of Natal
Pietermaritzburg
South Africa

### 8.2.3 Potential changes in mean annual increment and climatically suitable areas for *Eucalyptus grandis*

Eucalypts make up 41% of the 1.33 million ha under commercial tree plantations of South Africa, and of the eucalypt plantings about 75% is established to *Eucalyptus grandis* (Herbert, 1992). Eucalypt plantations in southern Africa, with rotation lengths varying from 6 - 12 years, have mean annual increments (MAIs) ranging from 4 - 35 $t.ha^{-1}$ (Herbert, 1992), while the average MAI in South Africa is about 12 $t.ha^{-1}$. A mean annual increment of about 10 $t.ha^{-1}$ is considered profitable (Schönau and Stubbings, 1987).

The species requires well drained dystrophic soils with a minimum effective rooting depth of 0.6 m for soils with > 35% clays, to 0.8 m with < 25% clays (Smith, 1994). Using Smith's (1994) rule-based approach for estimating mean annual increments of *Eucalyptus grandis* and considering only his climatic criteria and not soil or management factors, the tabulated information he provided on mean annual increment was expressed by Schulze (1997b) in equation form as

$$MAI_{Eg} = P_{Eg} \times T_{Eg}$$

where $MAI_{Eg}$ = mean annual increment of *Eucalyptus grandis* ($t.ha^{-1}$)

$P_{Eg}$ = basic rainfall related mean annual increment of *Eucalyptus grandis*

= 12 + 0.04 (mean annual precipitation - 800)

$T_{Eg}$ = temperature adjustment for mean annual increment of *Eucalyptus grandis*

= 0.7 + 0.10 (mean annual temperature - 14)

for mean annual temperature < 16 °C

= 0.9 + 0.05 (mean annual temperature - 16)

for mean annual temperature ≥ 16 °C.

At present the mean annual increment for *Eucalyptus grandis* ranges from less than 18 $t.ha^{-1}$ in southern Mpumalanga to more than 30 $t.ha^{-1}$ along the KwaZulu-Natal coast and other core regions of the present climatically suitable areas, as shown in Figure 8.28 (top left).

Figure 8.28 Mean annual increment of *Eucalyptus grandis* ($t.ha^{-1}$): for present climate (top left), future climate (bottom left), shifts in climatically suitable areas (top right) and changes in yield between future and present climates (bottom right). Future climate scenario from UKTR-S

The majority of areas considered climatically suitable for *Eucalyptus grandis* are expected to be lost in the future as shown in Figure 8.28 (top right) and reflected in the statistics calculated for percentage suitable area (Table 8.11). The climatically suitable areas that could be lost are the coastal regions of KwaZulu-Natal, the Eastern Cape and the marginal lands on the fringes of the presently suitable areas. New growth areas are, however, projected to be located in the Drakensberg range in KwaZulu-Natal. In areas that are expected to still be climatically suitable in the future, there could be up to a 8 $t.ha^{-1}$ reduction in mean annual increment, with very few areas showing any gains in yield (Figure 8.28, bottom right).

Very similar estimates of future MAI, changes in MAI and shifts in climatically suitable areas of *Eucalyptus grandis* are obtained using HadCM2 (Figure 8.29) compared to UKTR-S (Figure 8.28).

Figure 8.29 Mean annual increment of *Eucalyptus grandis* ($t.ha^{-1}$): for future climate (top), the change in the mean annual increment of *Eucalyptus grandis* between future and present climates (middle) and shift in climatically suitable areas (bottom). Future climate scenario from HadCM2-S

In simulations which used output from HadCM2 which included the cooling effect of sulphates in the atmosphere, some areas that become climatically unsuitable when excluding sulphates, e.g. the KwaZulu-Natal coastline (Figure 8.30, bottom), remain climatically suitable. However, reductions of over 8 $t.ha^{-1}$ are simulated in these areas (Figure 8.30, middle).

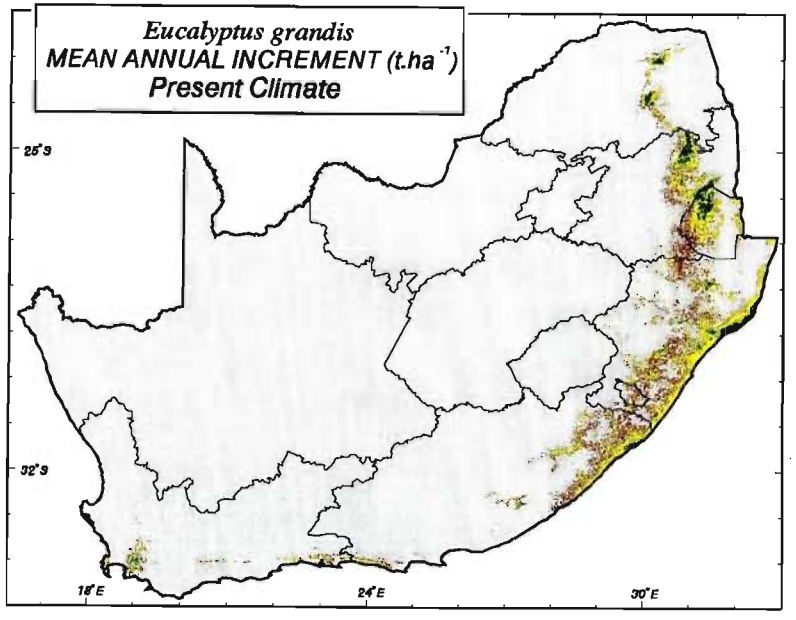


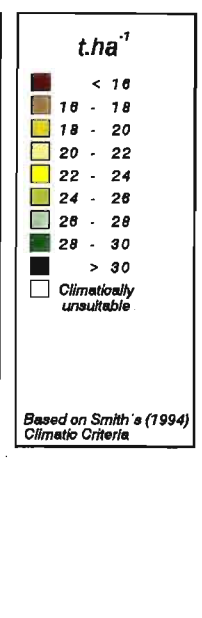


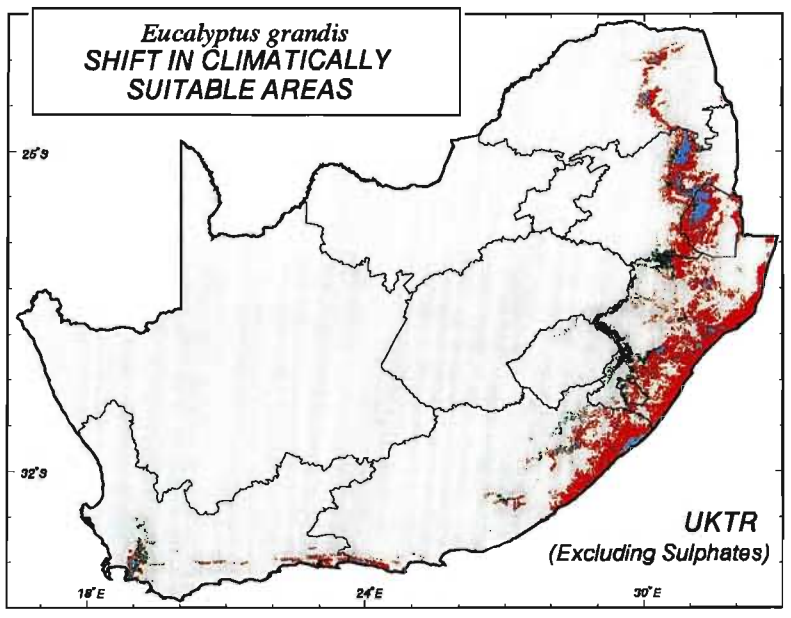


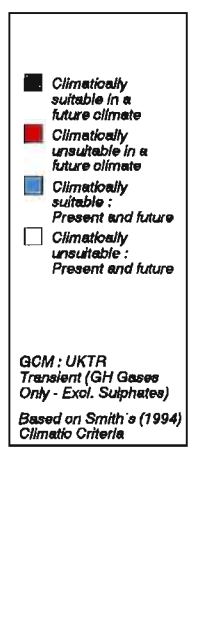


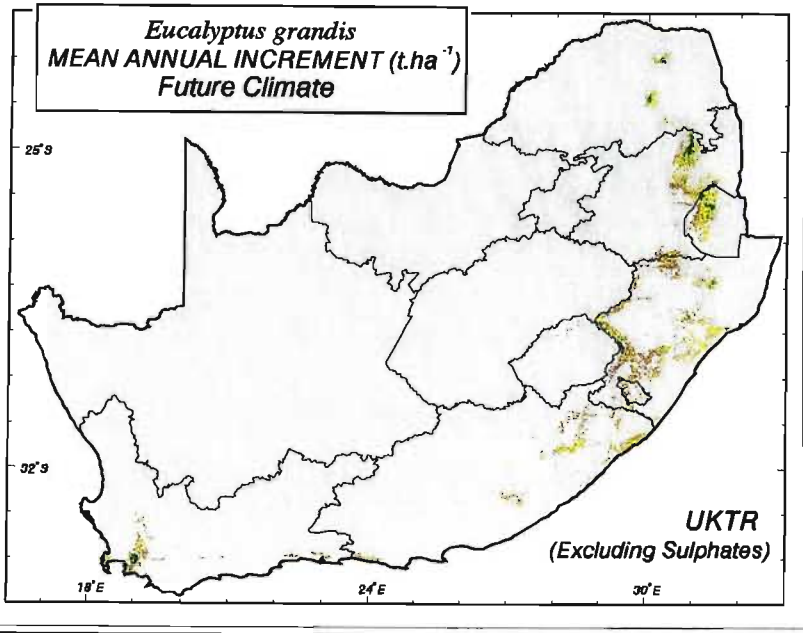


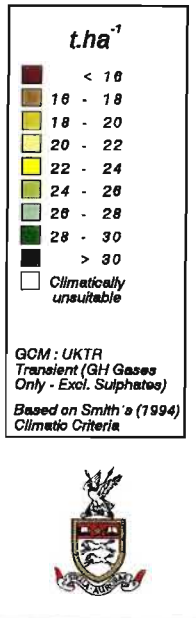




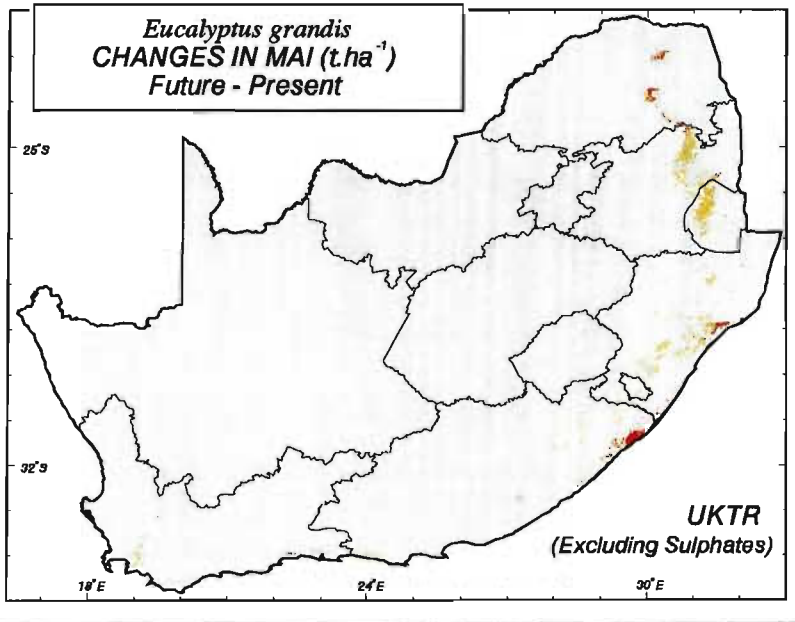


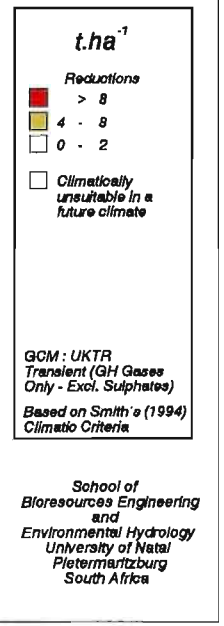


School of
Bioresources Engineering
and
Environmental Hydrology
University of Natal
Pietermaritzburg
South Africa

Table 8.11 Statistics for mean annual increment of *Eucalyptus grandis* for present climatic conditions and a future (2X $CO_2$) climate scenario from UKTR-S

| ***Eucalyptus grandis* Mean Annual Increment Estimate ($t.ha^{-1}$)** | | | | | | | | | | | | | | | | |
|---|---|---|---|---|---|---|---|---|---|---|---|---|---|---|---|---|
| Province / Country | % Suitable area | | Mean Value | | CV (%) | | Maximum Value | | Minimum Value | | Exceedence Probability | | | | | |
| | | | | | | | | | | | 20% | | 50% | | 80% | |
| | Present | Future | Present | Future | Present | Future | Present | Future | Present | Future | Present | Future | Present | Future | Present | Future |
| Northern Province | 2.9 | 0.8 | 22.4 ** | 23.6 | 33.0 | 28.7 | 58.8 | 52.8 | 10.8 | 14.7 | 27.8 | 28.0 | 20.3 | 21.5 | 16.4 | 18.3 |
| Mpumalanga | 13.0 | 6.4 | 21.1 | 21.4 | 32.3 | 27.4 | 53.1 | 48.5 | 10.3 | 11.9 | 26.2 | 25.8 | 19.1 | 19.8 | 15.4 | 16.6 |
| North-West | N/A * | N/A | N/A | N/A | N/A | N/A | N/A | N/A | N/A | N/A | N/A | N/A | N/A | N/A | N/A | N/A |
| Northern Cape | N/A | N/A | N/A | N/A | N/A | N/A | N/A | N/A | N/A | N/A | N/A | N/A | N/A | N/A | N/A | N/A |
| Gauteng | N/A | NA | N/A | N/A | N/A | N/A | N/A | N/A | N/A | N/A | N/A | N/A | N/A | N/A | N/A | N/A |
| Free State | N/A | N/A | N/A | N/A | N/A | N/A | N/A | N/A | N/A | N/A | N/A | N/A | N/A | N/A | N/A | N/A |
| KwaZulu-Natal | 28.3 | 6.6 | 20.5 | 18.8 | 27.5 | 23.9 | 45.8 | 45.5 | 11.1 | 10.2 | 24.4 | 21.2 | 19.2 | 17.8 | 15.8 | 15.5 |
| Eastern Cape | 8.6 | 2.4 | 18.6 | 18.2 | 24.7 | 18.6 | 44.3 | 38.6 | 11.2 | 11.8 | 22.1 | 20.7 | 17.4 | 17.5 | 14.7 | 15.4 |
| Western Cape | 2.1 | 1.3 | 18.3 | 19.8 | 29.9 | 37.2 | 53.6 | 51.1 | 10.2 | 10.4 | 21.3 | 23.5 | 17.0 | 17.5 | 14.3 | 14.6 |
| Swaziland | 44.1 | 17.2 | 21.7 | 21.9 | 26.3 | 21.3 | 48.7 | 42.0 | 13.4 | 14.3 | 26.5 | 25.8 | 20.3 | 21.1 | 16.7 | 17.7 |
| Lesotho | N/A | 0.1 | N/A | 14.2 | N/A | 11.8 | N/A | 17.9 | N/A | 11.9 | N/A | 15.4 | N/A | 14.3 | N/A | 12.6 |

* N/A denotes climatically unsuitable at all grid points

** All statistics only for those grid points which qualify as climatically suitable



Table 8.12 Statistics for mean annual increment of *Acacia mearnsii* for present climatic conditions and a future (2X $CO_2$) climate scenario from UKTR-S

| ***Acacia mearnsii* Mean Annual Increment Estimate of Timber ($t.ha^{-1}$)** | | | | | | | | | | | | | | | | |
|---|---|---|---|---|---|---|---|---|---|---|---|---|---|---|---|---|
| Province / Country | % Suitable area | | Mean Value | | CV (%) | | Maximum Value | | Minimum Value | | Exceedence Probability | | | | | |
| | | | | | | | | | | | 20% | | 50% | | 80% | |
| | Present | Future | Present | Future | Present | Future | Present | Future | Present | Future | Present | Future | Present | Future | Present | Future |
| Northern Province | 1.7 | N/A * | 10.5 ** | N/A | 5.4 | N/A | 12.0 | N/A | 9.1 | N/A | 11.0 | N/A | 10.6 | N/A | 10.0 | N/A |
| Mpumalanga | 8.7 | N/A | 12.1 | N/A | 6.4 | N/A | 12.1 | N/A | 8.6 | N/A | 11.0 | N/A | 10.5 | N/A | 9.9 | N/A |
| North-West | N/A | N/A | N/A | N/A | N/A | N/A | N/A | N/A | N/A | N/A | N/A | N/A | N/A | N/A | N/A | N/A |
| Northern Cape | N/A | N/A | N/A | N/A | N/A | N/A | N/A | N/A | N/A | N/A | N/A | N/A | N/A | N/A | N/A | N/A |
| Gauteng | N/A | N/A | N/A | N/A | N/A | N/A | N/A | N/A | N/A | N/A | N/A | N/A | N/A | N/A | N/A | N/A |
| Free State | N/A | N/A | N/A | N/A | N/A | N/A | N/A | N/A | N/A | N/A | N/A | N/A | N/A | N/A | N/A | N/A |
| KwaZulu-Natal | 28.1 | 2.0 | 9.9 | 9.7 | 8.6 | 5.6 | 12.0 | 11.0 | 7.6 | 9.0 | 107 | 10.0 | 10.0 | 10.0 | 9.0 | 9.0 |
| Eastern Cape | 11.3 | 1.9 | 9.3 | 9.7 | 13.4 | 7.7 | 12.1 | 11.0 | 6.1 | 7.0 | 10.7 | 10.0 | 9.0 | 10.0 | 8.1 | 9.0 |
| Western Cape | 2.6 | 1.6 | 7.8 | 8.4 | 11.2 | 16.2 | 10.4 | 11.0 | 6.0 | 6.0 | 8.8 | 10.0 | 8.0 | 8.0 | 7.1 | 7.0 |
| Swaziland | 20.7 | 0.8 | 10.6 | 9.5 | 6.1 | 5.3 | 12.0 | 10.0 | 8.5 | 9.0 | 11.1 | 10.0 | 10.6 | 10.0 | 10.0 | 9.0 |
| Lesotho | N/A | N/A | N/A | N/A | N/A | N/A | N/A | N/A | N/A | N/A | N/A | N/A | N/A | N/A | N/A | N/A |

* N/A denotes climatically unsuitable at all grid points

** All statistics only for those grid points which qualify as climatically suitable

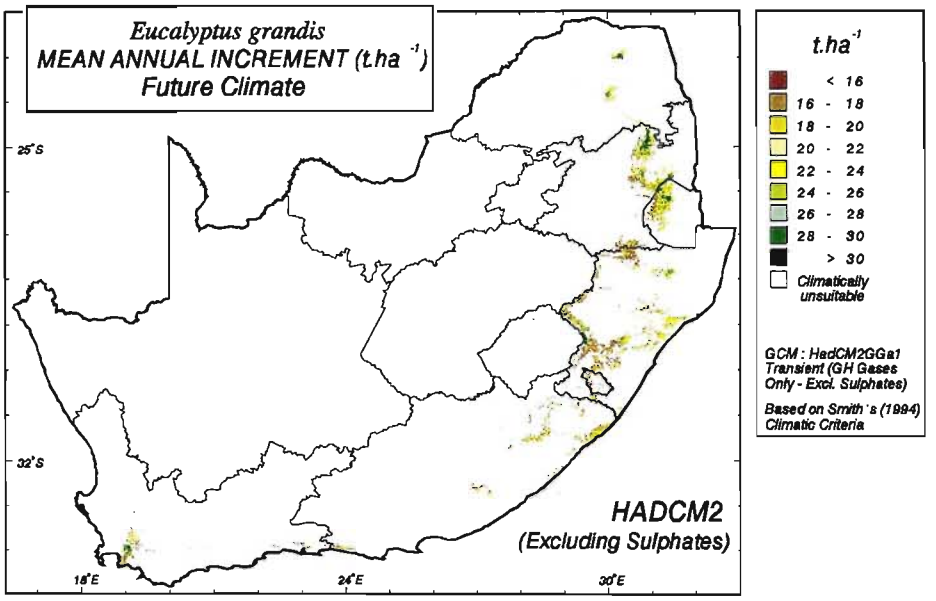


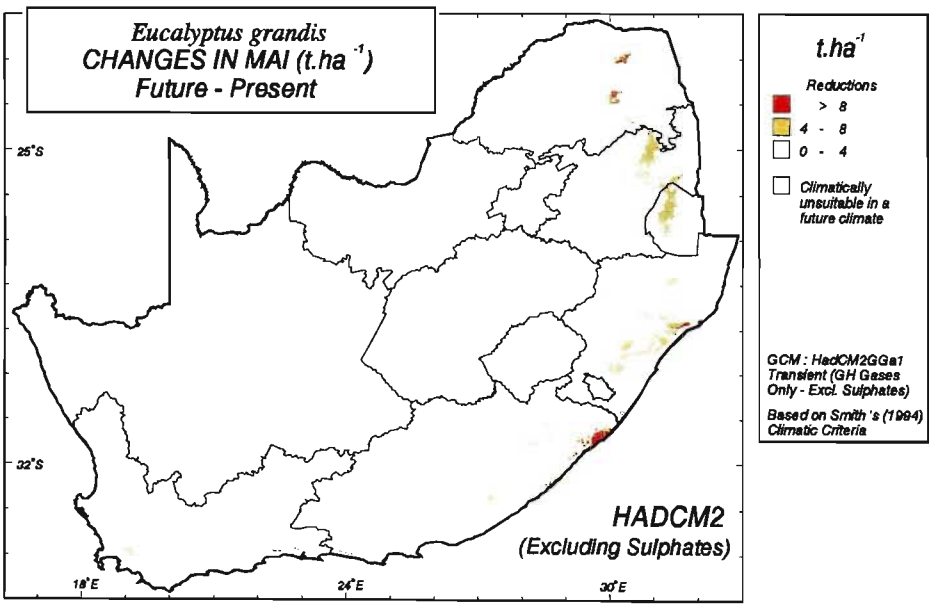


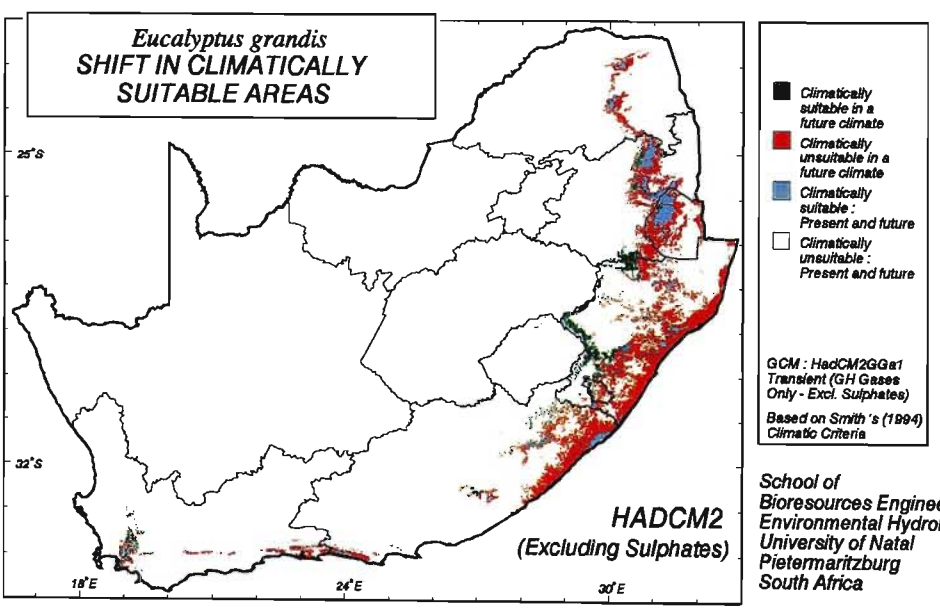


School of
Bioresources Engineering and
Environmental Hydrology
University of Natal
Pietermaritzburg
South Africa

| | |
|---|---|
| Figure 8.30 | Mean annual increment of *Eucalyptus grandis* ($t.ha^{-1}$): for future climate (top), the change in the mean annual increment of *Eucalyptus grandis* between future and present climates (middle) and shift in climatically suitable areas (bottom). Future climate scenario from HadCM2+S |

### 8.2.4 Potential changes in mean annual increment and climatically suitable areas for *Acacia mearnsii* (timber)

Black wattle, a native of south-eastern Australia, has proved to be the most drought resistant of the commercial hardwoods in southern Africa (Herbert, 1993). Requiring only 750 mm MAP for optimum growth in cooler areas (mean annual temperatures < 16°C), increasing to 850 mm in warmer areas, *Acacia mearnsii* is relatively prone to diseases (e.g. bagworm, mirid attacks), the incidence of which increases where it is too wet (mean annual precipitation > 1 200 mm) and when grown on humic topsoils (Schulze, 1997b).

*Acacia mearnsii* covers about 8.2% of the 1.33 million hectare under commercial afforestation in South Africa. Harvested for both its bark and its timber with an 8 - 9 year rotation in high potential areas, increasing to 11 years in less productive areas, black wattle can grow on certain soils with an effective rooting depth of only 0.3 m (Schulze, 1997b).

Using Smith's (1994) rule based approach for estimating the mean annual increment of *Acacia mearnsii* and considering only climatic criteria and not soil or management factors, the equation used by Schulze (1997a) was expressed as

$$MAI_{Amt} = P_{Amt} \times T_{Amt}$$

where $MAI_{Amt}$ = mean annual increment of *Acacia mearnsii* (timber, $t.ha^{-1}$)

$P_{Amt}$ = basic rainfall related MAI of *Acacia mearnsii* (timber)
= 9.75 + 0.0025 (mean annual precipitation - 700)

$P_{Amt}$ = temperature adjustment for MAI of *Acacia mearnsii* (timber)

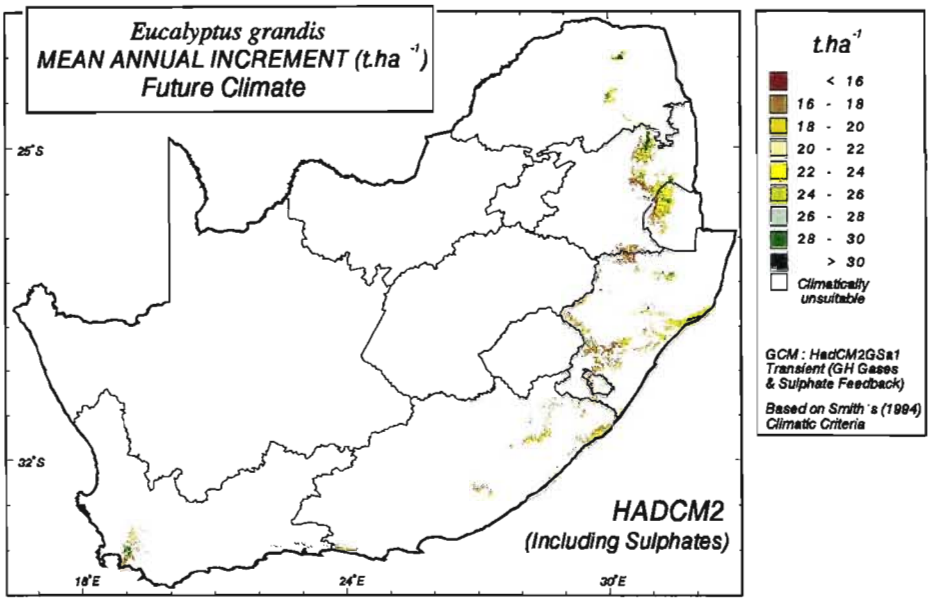


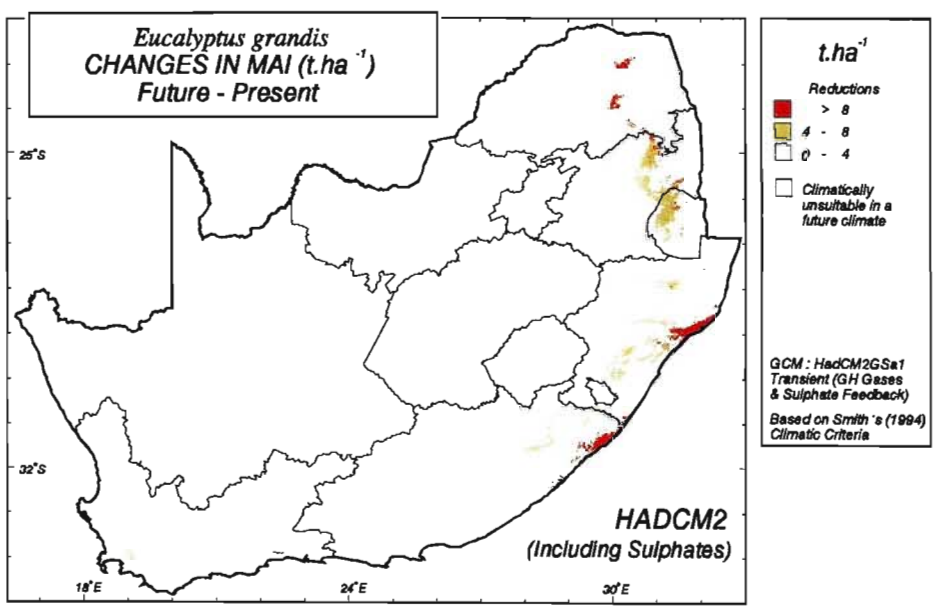


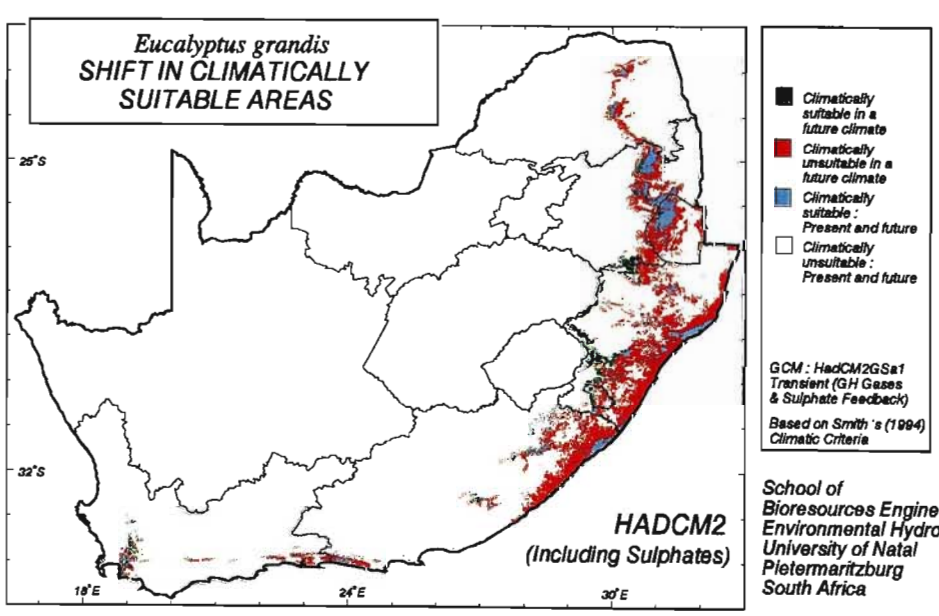


School of
Bioresources Engineering and
Environmental Hydrology
University of Natal
Pietermaritzburg
South Africa

= 0.7 + 0.1 (mean annual temperature - 15) for mean annual temperature < 17 °C

= 0.9 + 0.2 (mean annual temperature - 17) for 17 °C < mean annual temperature < 18 °C

= 1.1 - 0.1 (mean annual temperature - 18) for mean annual temperature > 18 °C.

Mean annual increments of *Acacia mearnsii* for present climatic conditions were estimated by Schulze (1997b) to range from less than 7 $t.ha^{-1}$ in the more southern and western reaches of the climatically suitable areas at present to over 11 $t.ha^{-1}$ along the eastern fringes (Figure 8.31, top left).

Figure 8.31 Mean annual increment of *Acacia mearnsii* ($t.ha^{-1}$): for present climate (top left), future climate (bottom left), shifts in climatically suitable areas (top right) and changes in yield between future and present climates (bottom right). Future climate scenario from UKTR-S

There is expected to be an almost complete loss of climatically suitable areas for the commercial cultivation of *Acacia mearnsii* for a future climate scenario from the UKTR-S (Figure 8.31, bottom left and top right). This is particularly evident in the northern regions of Mpumalanga and Northern Province, where *Acacia mearnsii* is expected to be climatically unsuitable in future (see percentage suitable area columns in Table 8.12). No notable reductions or gains where simulated for *Acacia mearnsii* timber in a future climate using output from UKTR-S (Figure 8.31, bottom right).

Similar results to those generated using UKTR-S are obtained using HadCM2-S. Although the decreases in climatically suitable areas are very similar (Figure 8.31, top right and Figure 8.32, bottom), there are differences in the decreases in yield between the two versions. The simulation using a future climate scenario from UKTR-S gives a higher reduction in yield (Figure 8.31, bottom left) than that of HadCM2-S (Figure 8.32, middle).

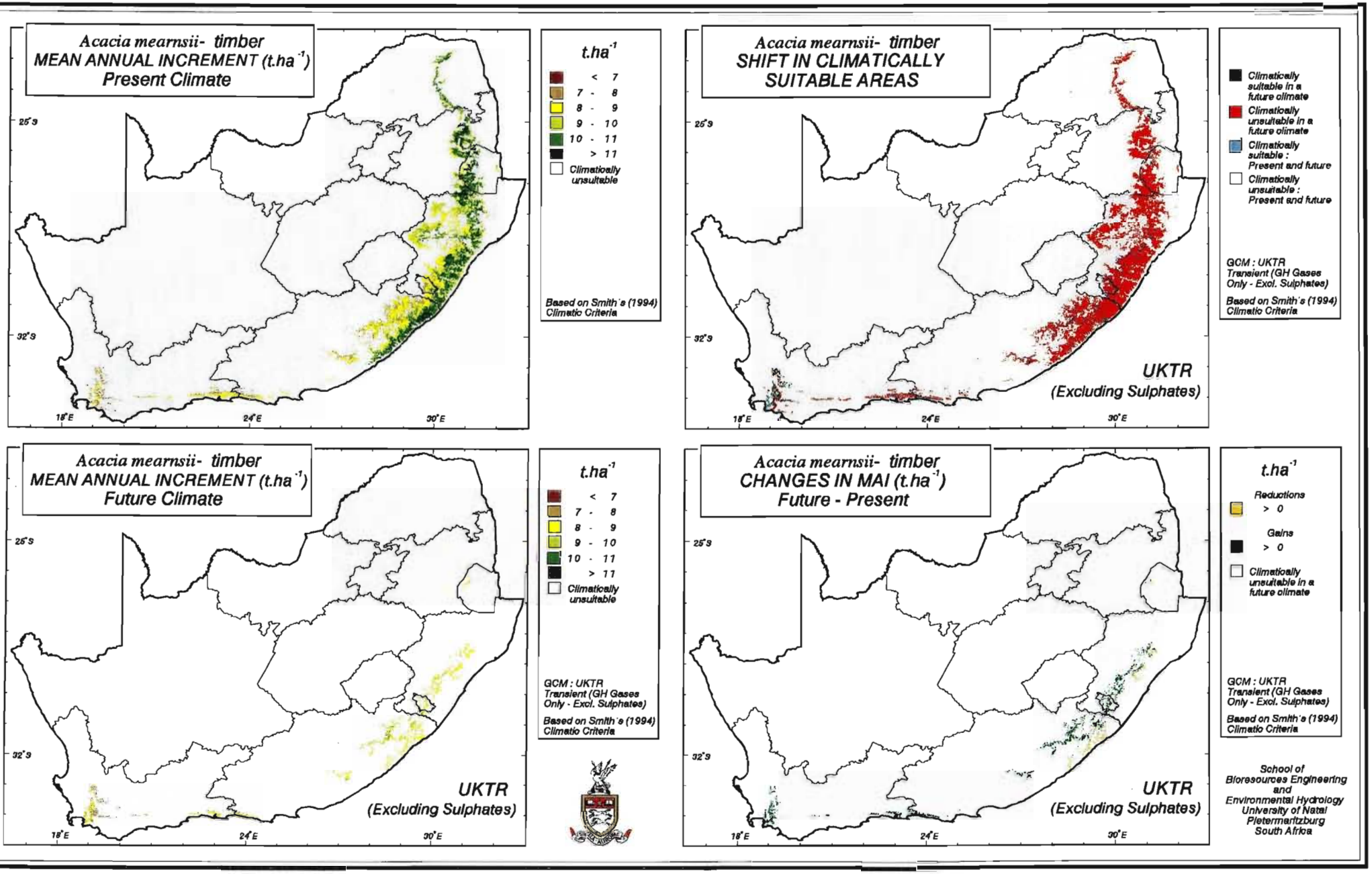
Acacia mearnsii- timber
MEAN ANNUAL INCREMENT (t.ha-1)
Present Climate
t.ha-1
< 7
7 - 8
8 - 9
9 - 10
10 - 11
> 11
Climatically unsuitable
Based on Smith's (1994) Climatic Criteria
25°S
32°S
18°E
24°E
30°E
Acacia mearnsii- timber
SHIFT IN CLIMATICALLY SUITABLE AREAS
Climatically suitable in a future climate
Climatically unsuitable in a future climate
Climatically suitable : Present and future
Climatically unsuitable : Present and future
GCM : UKTR
Transient (GH Gases Only - Excl. Sulphates)
Based on Smith's (1994) Climatic Criteria
UKTR
(Excluding Sulphates)
Acacia mearnsii- timber
MEAN ANNUAL INCREMENT (t.ha-1)
Future Climate
t.ha-1
< 7
7 - 8
8 - 9
9 - 10
10 - 11
> 11
Climatically unsuitable
GCM : UKTR
Transient (GH Gases Only - Excl. Sulphates)
Based on Smith's (1994) Climatic Criteria
UKTR
(Excluding Sulphates)
Acacia mearnsii- timber
CHANGES IN MAI (t.ha-1)
Future - Present
t.ha-1
Reductions
> 0
Gains
> 0
Climatically unsuitable in a future climate
GCM : UKTR
Transient (GH Gases Only - Excl. Sulphates)
Based on Smith's (1994) Climatic Criteria
UKTR
(Excluding Sulphates)
School of Bioresources Engineering and Environmental Hydrology
University of Natal
Pietermaritzburg
South Africa

| | |
|---|---|
| Figure 8.32 | Mean annual increment of *Acacia mearnsii* ($t.ha^{-1}$): for future climate (top), change in the mean annual increment of *Acacia mearnsii* between future and present climates (middle) and shift in climatically suitable areas (bottom). Future climate scenario from HadCM2-S |

Although large areas of land that were previously suitable for the cultivation of *Acacia mearnsii* could become climatically unsuitable in a future climate determined from output of HadCM2+S (Figure 8.33, bottom), the loss of area is not as great as that from the simulations using HadCM2-S (Figure 8.32, bottom).

| | |
|---|---|
| Figure 8.33 | Mean annual increment of *Acacia mearnsii* ($t.ha^{-1}$): for future climate (top), change in the mean annual increment of *Acacia mearnsii* between future and present climates (middle) and shift in climatically suitable areas (bottom). Future climate scenario from HadCM2+S |

## 8.3 Potential Changes in Crop Yields and Distributions of Optimum Growth Areas Using Models of Intermediate Complexity

Some crop yield models are considered to be of intermediate complexity such as the *ACRU* maize and winter wheat yield submodels imbedded in *ACRU*. The maize yield submodel, for example, simulates maize yields by daily soil water budgeting coupled with crop phenology and includes certain feedbacks in its routines (Schulze, 1997a). Potential changes in maize yield resulting from climate change were simulated using this model and the results are presented in Sections 8.3.1 to 8.3.5. In addition, potential changes in winter wheat yield resulting from climate change were simulated using the *ACRU* winter wheat yield submodel, with results as presented in Sections 8.3.6 and 8.3.7 (cf. Figure 8.2).

The crop yield assessments in this chapter were carried out using monthly temperatures, however, daily temperatures estimates for each Quaternary Catchment became available towards the end of this study. The phenology-based maize and winter wheat submodels of

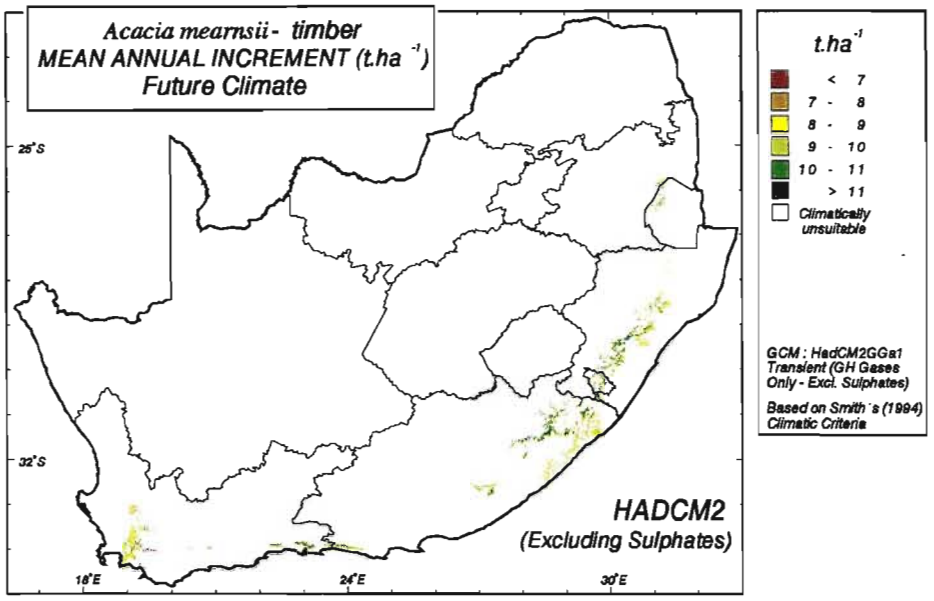


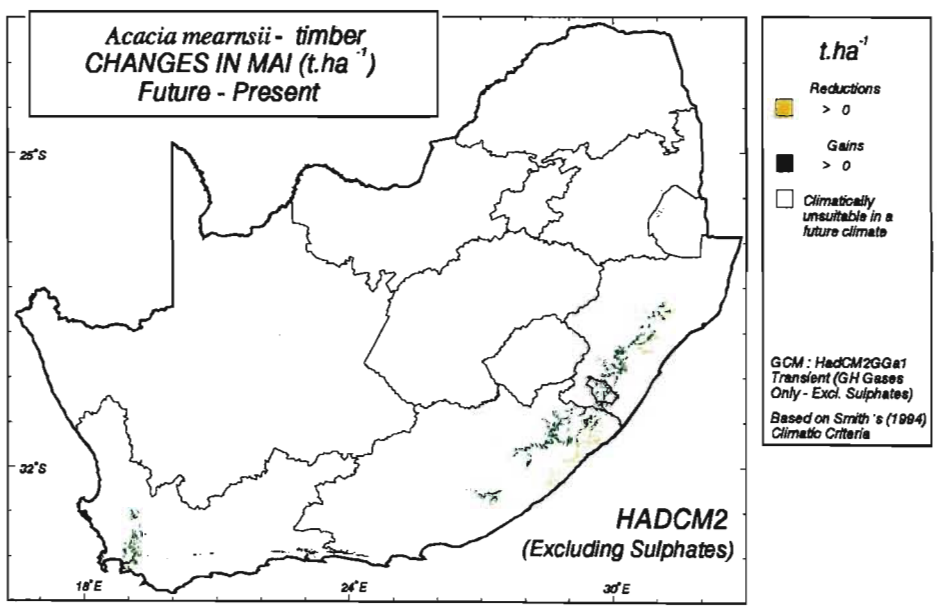


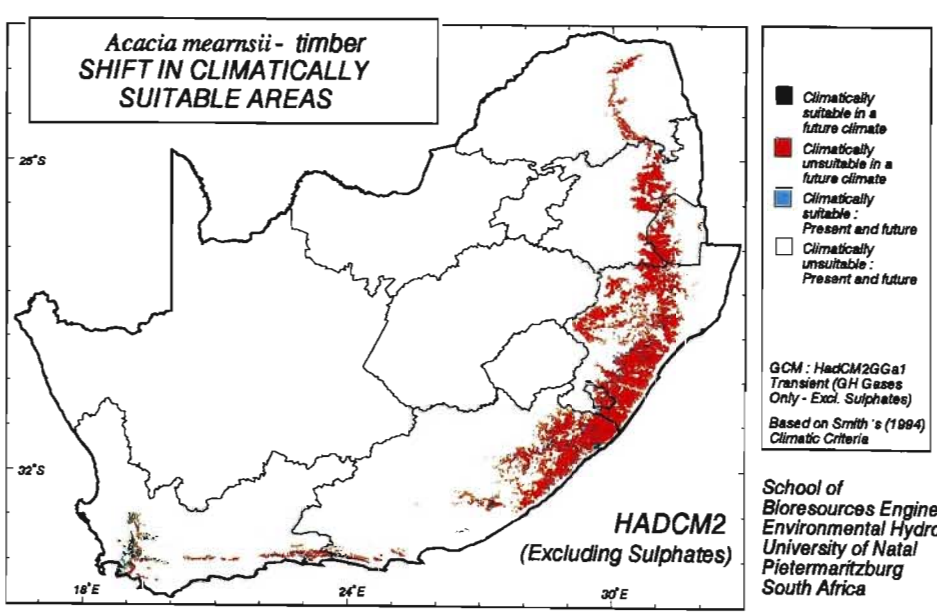


School of
Bioresources Engineering and
Environmental Hydrology
University of Natal
Pietermaritzburg
South Africa

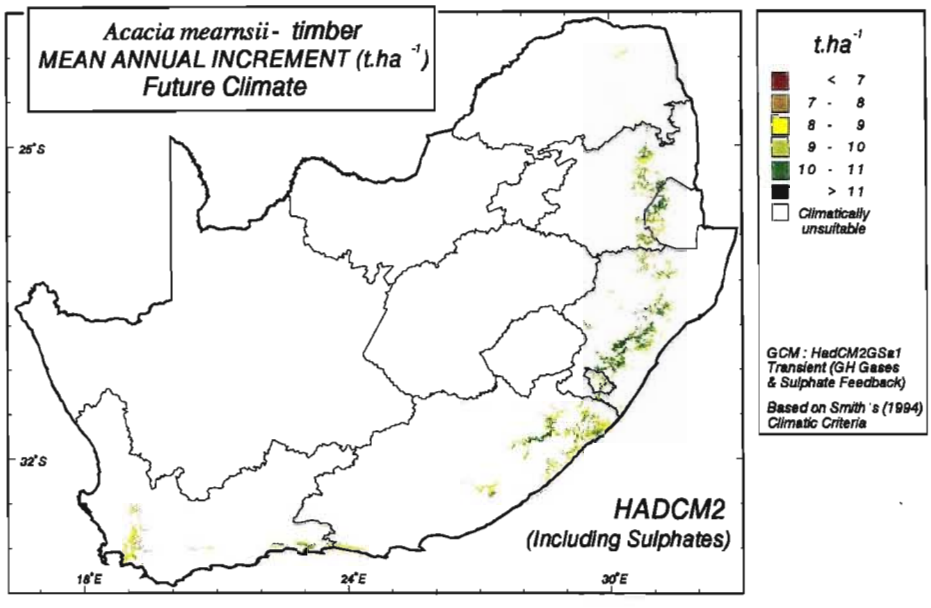


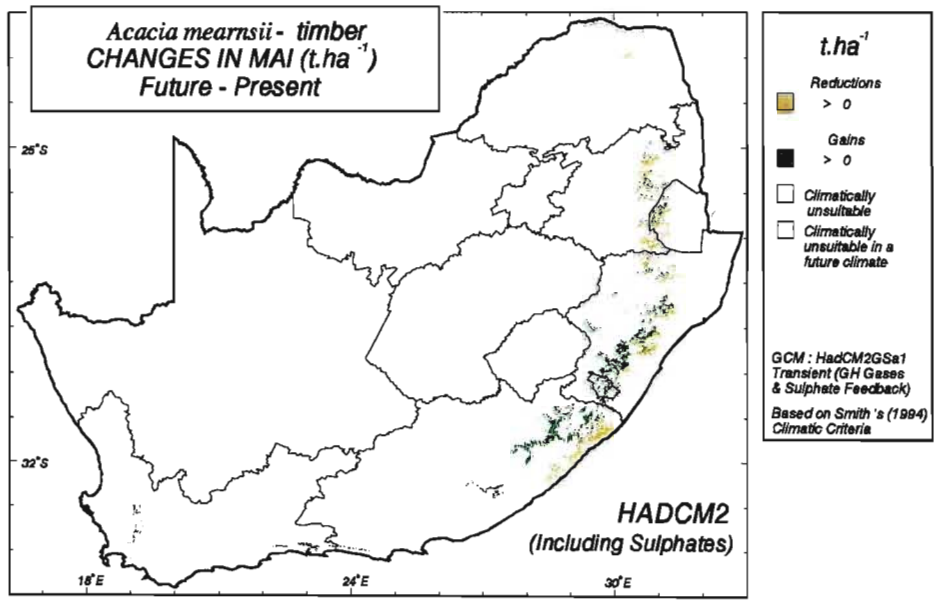


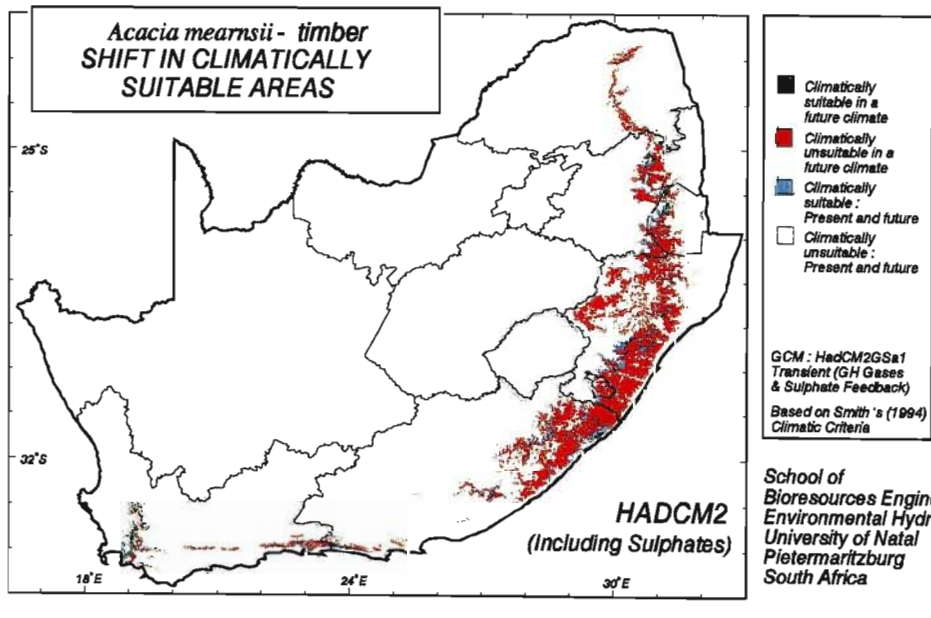


School of
Bioresources Engineering and
Environmental Hydrology
University of Natal
Pietermaritzburg
South Africa

*ACRU* are sensitive to daily, seasonal and inter-annual changes in temperature. Therefore, a comparative study was carried out to compare the use of monthly and daily temperature input into the *ACRU* model when simulating potential maize yields under a present climate scenario. The results of potential changes in maize yield resulting from climate change and the threshold analysis presented in Section 8.3.5 were, however, carried out using monthly temperature input to be consistent with the other climate impact assessments conducted on agricultural crops in this thesis.

### 8.3.1 The *ACRU* maize yield submodel

Maize (*Zea mais*) is the staple crop of southern Africa and of the 10 million ha under cultivation in South Africa, it accounts for 36% by area. Maize optimally requires 500 - 1 000 mm rainfall in the October to March growing season, but short season varieties can give reasonable yields with as little as 300 mm of well distributed rainfall. Maize thrives in hot, frost free climates, with minimum temperatures ideally between 12 - 24 °C and maxima between 26 - 29 °C. For germination, the optimum mean daily temperature is 18 - 21 °C. This crop also prefers well drained deep loams (Schulze, 1997b).

The crop is most sensitive to soil moisture stress from the beginning of flowering to the end of grain formation and during tasseling each day with moisture stress can reduce final yield by up to 8%. Maize is also sensitive to humid conditions (Sys *et al.*, 1993; Schulze, 1997b). The maize yield model imbedded in the *ACRU* agrohydrological modelling system (Domleo, 1990; Schulze, 1995a) is a generic phenologically-based (i.e. growth stage) submodel developed around concepts proposed by Hanks (1974). It phenological switches are driven by thermal time, i.e. by degree days (cf. Section 8.1.1). The maize yield submodel has been tested extensively under South African conditions (Schulze, 1995a; Schulze, 1997b). For this study maize is assumed to be planted on 15 November and have a maximum growing season length of 150 days unless maturity is reached before that, dependent on temperature (cf. Chapter 7, Section 7.3.5).

The maize yield estimate is controlled by transpiration ratios, with different sensitivities to yield reduction in its three phenological stages, such that

$$Y_m = Y_{pm} (E_{t1} / E_{tm1})^{\alpha m1} (E_{t2} / E_{tm2})^{\alpha m2} (E_{t3} / E_{tm3})^{\alpha m3}$$

where $Y_m$ = maize grain yield ($t.ha^{-1}.season^{-1}$)

$Y_{pm}$ = potential maize grain yield ($t.ha^{-1}$) for the season, obtained from local information, or input as a default value of 9 $t.ha^{-1}$

$E_{ti}$ = accumulated actual crop transpiration (mm) for a given growth stage, *i*, from all horizons

$E_{tmi}$ = accumulated maximum (i.e. potential) transpiration (mm) for a given growth stage, *i*, from all soil horizons

$\alpha_{mi}$ = exponent to allow for different weighting of the influence of soil water stress on maize in growth stage *i*

1 = growth stage $i = 1$: emergence to flower initiation

2 = growth stage $i = 2$: flowering stage

3 = growth stage $i = 3$: end of flowering stage to maturity.

The commencement of the growth stages are determined using degree days (cf. Section 8.1.1). The effective heat units for maize, between upper and lower threshold daily mean temperatures (10 °C and 30 °C respectively) are accumulated from date of planting and are used to delimit onset and end of growth stages. Default values were used in this study for various states of phenological development as given in Table 8.13 (Domleo, 1990; Schulze *et al.*, 1995d).

Table 8.13 Typical values of phenological states of maize related to accumulated growing degree days after planting (Domleo, 1990; Schulze *et al.*, 1995d)

| Phenological State | Growing Degree Days |
|---|---|
| Emergence | 150 |
| Onset of Flowering | 700 |
| End of Flowering | 1150 |
| Maturity | 1700 |

When modelling future maize yield with the *ACRU* model two scenarios were considered, *viz.*, the inclusion and the exclusion of the so-called fertilization effect, i.e. the suppression of plant transpiration due to increases in $CO_2$ concentrations, in order to compare the sensitivity of a possible transpiration suppression on yield (cf. Chapter 2, Section 2.3.1.1). Furthermore, a simple economic analysis was carried out to ascertain potential changes in the profitability of dryland maize production when either including or excluding potential transpiration suppression owing to increased concentrations of $CO_2$.

Carbon dioxide is expected to have significant effects on crop yield due to altered transpiration rates. Transpiration rates are predicted to be suppressed in a future climate with higher $CO_2$ concentrations due to the partial closure of stomata by the plant (cf. Chapter 2, Section 2.3.1.1). Results from the IBSNAT crop growth models (developed by the US Agency for International Development's International Benchmark Sites Network for Agrotechnology Transfer) demonstrated that the direct effects of an increase in $CO_2$ concentrations was an improvement in crop yields and water use efficiency (IBSNAT, 1989; Parry *et al.*, 1999).

C4 plants are expected to show more marked transpiration suppression than C3 plants. Thus, as maize is classified as having a C4 photosynthetic pathway, this crop is expected to show a decrease in plant water use in a future climate compared to the present climate which could partially offset any adverse effects of climate change (Bouten and Goudriaan, 1994). Maximum transpiration suppression rates in *ACRU* are set at 22% for C4 plants such as maize in a future climate (cf. Chapter 4, Section 4.4.2.1).

### 8.3.2 Sensitivity of simulated maize yield to temperature resolution: monthly vs daily temperature input

Maximum and minimum temperatures can either be input on a monthly or daily basis into the *ACRU* model. If monthly temperatures are input then daily temperatures are generated using an harmonic analysis within the *ACRU* model. However, by using monthly temperature any input inter-seasonal fluctuations in temperature, which could have significant influences on maize yields from year to year, are not accounted for.

As daily temperature estimates for each Quaternary Catchment became available towards the end of this study, a comparison of maize yield under present climate conditions simulated using the *ACRU* maize submodel with both monthly and daily temperature input was undertaken in order to assess the sensitivity of maize yield to the level of temperature input.

Median maize yield under present climatic conditions was estimated using the *ACRU* maize yield submodel for southern Africa with temperatures firstly input on a monthly basis (Figure 8.34, top) and secondly on a daily basis for the period 1951 - 1993 (Figure 8.34, middle). Areas in the study region where the mean annual rainfall is less than 300 mm are assumed to be climatically unsuitable for maize production and are coloured grey on the maps.

Figure 8.34 Median maize yields ($t.ha^{-1}.season^{-1}$) using monthly temperature inputs (top), using daily temperature inputs (middle) and per cent change in median maize yield using monthly and daily temperature inputs compared to monthly temperature inputs (bottom). Present climate scenario

When using monthly temperature input the median maize yields range from less than 1.5 $t.ha^{-1}.season^{-1}$ in the south-western Cape and central parts of the study area to more than 4.5 $t.ha^{-1}.season^{-1}$ in southern KwaZulu-Natal, parts of the Eastern Cape, Lesotho, Swaziland and Mpumalanga. On the whole the maize yields were simulated to decrease from the eastern to the western half of the study area under present climatic conditions (Figure 8.34, top).

Although the maps of median maize yield for present climatic conditions generated using monthly (Figure 8.34, top) and daily temperatures (Figure 8.34, middle) appear similar, when the map of difference in maize yield is analysed (Figure 8.34, bottom) the differences become more apparent.

Most areas only incur less than a 5% higher or lower estimate in yield between the two levels of temperature input. However, some parts of the study area, such as Lesotho, were simulated to have 15% more yield using the daily temperatures as opposed to monthly temperatures as input. High-lying areas in Mpumalanga, Swaziland and the Northern Province were simulated to have 5% higher yields using monthly temperatures rather than daily maximum and

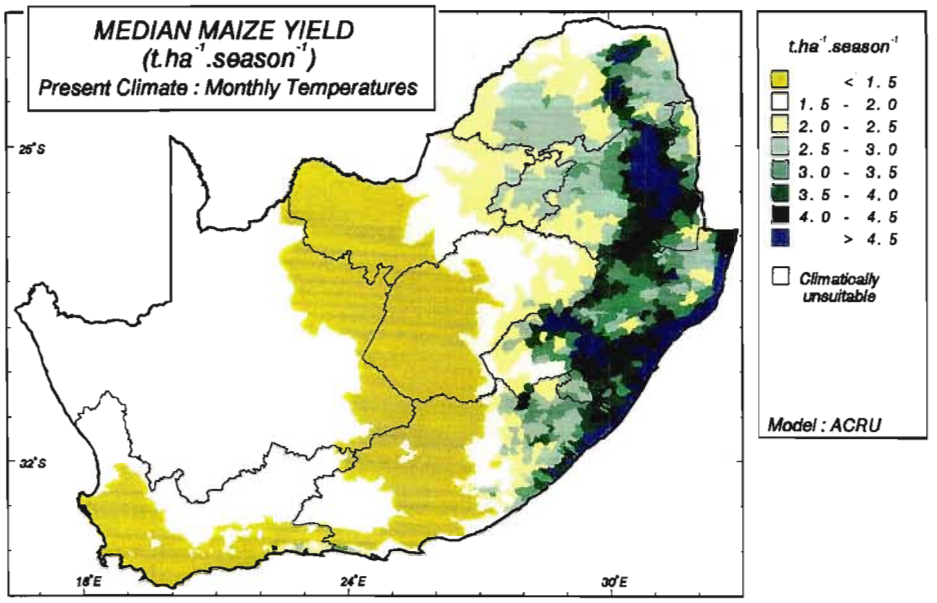


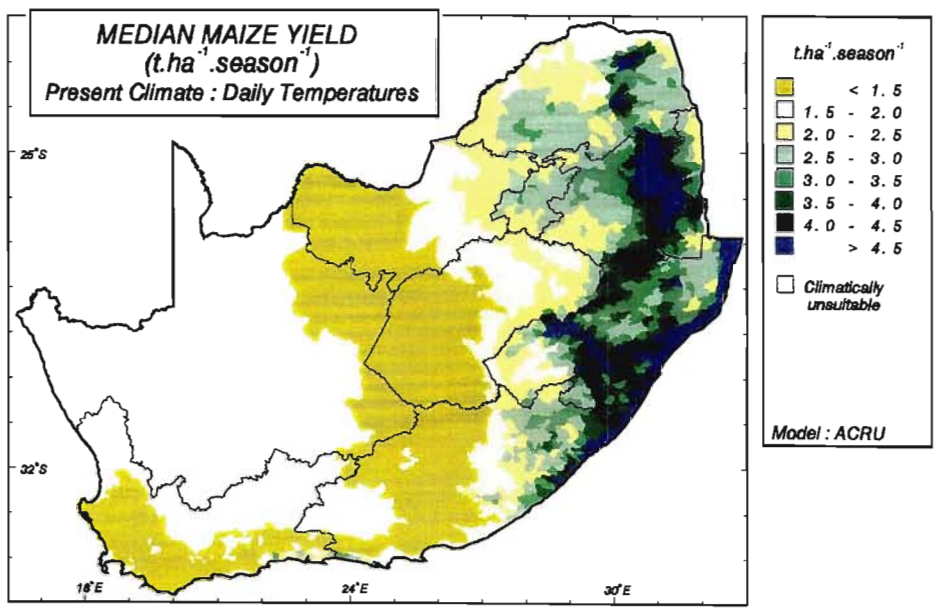


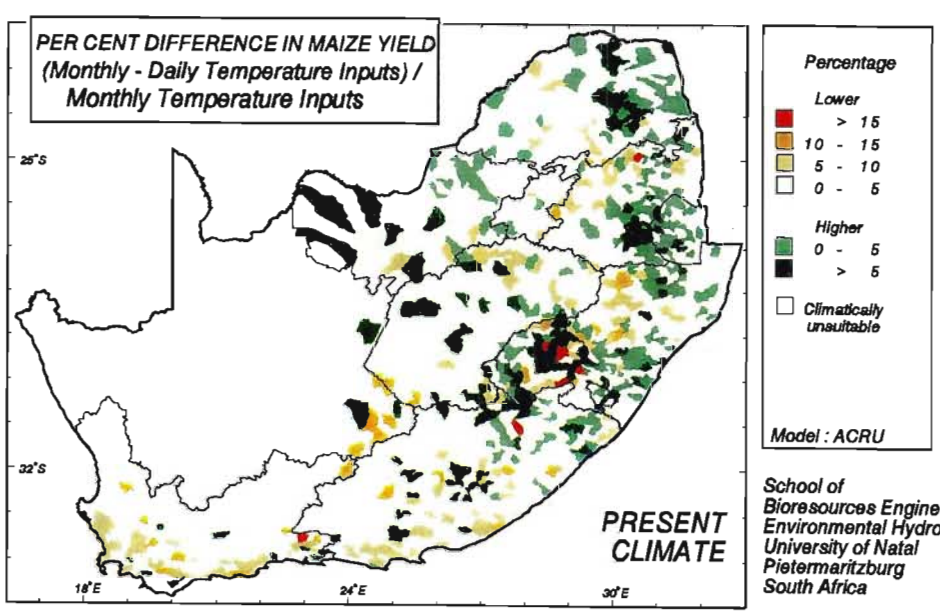


School of
Bioresources Engineering and
Environmental Hydrology
University of Natal
Pietermaritzburg
South Africa

minimum temperatures. This difference in median maize yields could be accounted for by the higher variability found in the daily temperature data set which, particularly in the case of low temperatures, could result in a higher stress on the maize plants resulting in lower yields being estimated with daily temperature input (Figure 8.34, bottom).

### 8.3.3 Potential impacts of climate change on maize yield

Using future climate estimates from the HadCM2 GCM, both including and excluding sulphates, and the *ACRU* maize yield submodel, changes in maize yield resulting from climate change were simulated both including and excluding the effects of $CO_2$ transpiration suppression. For consistency with the rest of the agriculture climate impact assessments, maximum and minimum temperatures were input on a monthly basis.

The first simulation used output from HadCM2-S and $CO_2$ transpiration suppression was not considered. Using this future climate scenario most areas that are considered climatically suitable for the cultivation of maize are expected to have reductions in median maize yield, with only a small number of catchments simulated to have relatively minor increases in yield (Figure 8.35, middle). These reductions ranged from less than 1 $t.ha^{-1}.season^{-1}$ for large parts of the study area to more than 3 $t.ha^{-1}.season^{-1}$ in northern Lesotho. Reductions of between 1 and 2 $t.ha^{-1}.season^{-1}$ could be expected for large parts of southern KwaZulu-Natal. There is expected to be an increase in climatically unsuitable areas under a future climate scenario (coloured in grey on Figure 8.35, middle) as more areas are expected to experience a mean annual rainfall of less than 300 mm in future according to climate output from HadCM2-S, compared to present climate conditions (Figure 8.35, top).

Figure 8.35 Median maize yields ($t.ha^{-1}.season^{-1}$): changes in yield between future and present climates (top left) and per cent change in yield (bottom left) using the future climate scenario from HadCM2-S. Changes in yield between future and present climates (top right) and per cent change in yield (bottom right) using the future climate scenario from HadCM2+S. Carbon dioxide induced transpiration suppression not considered

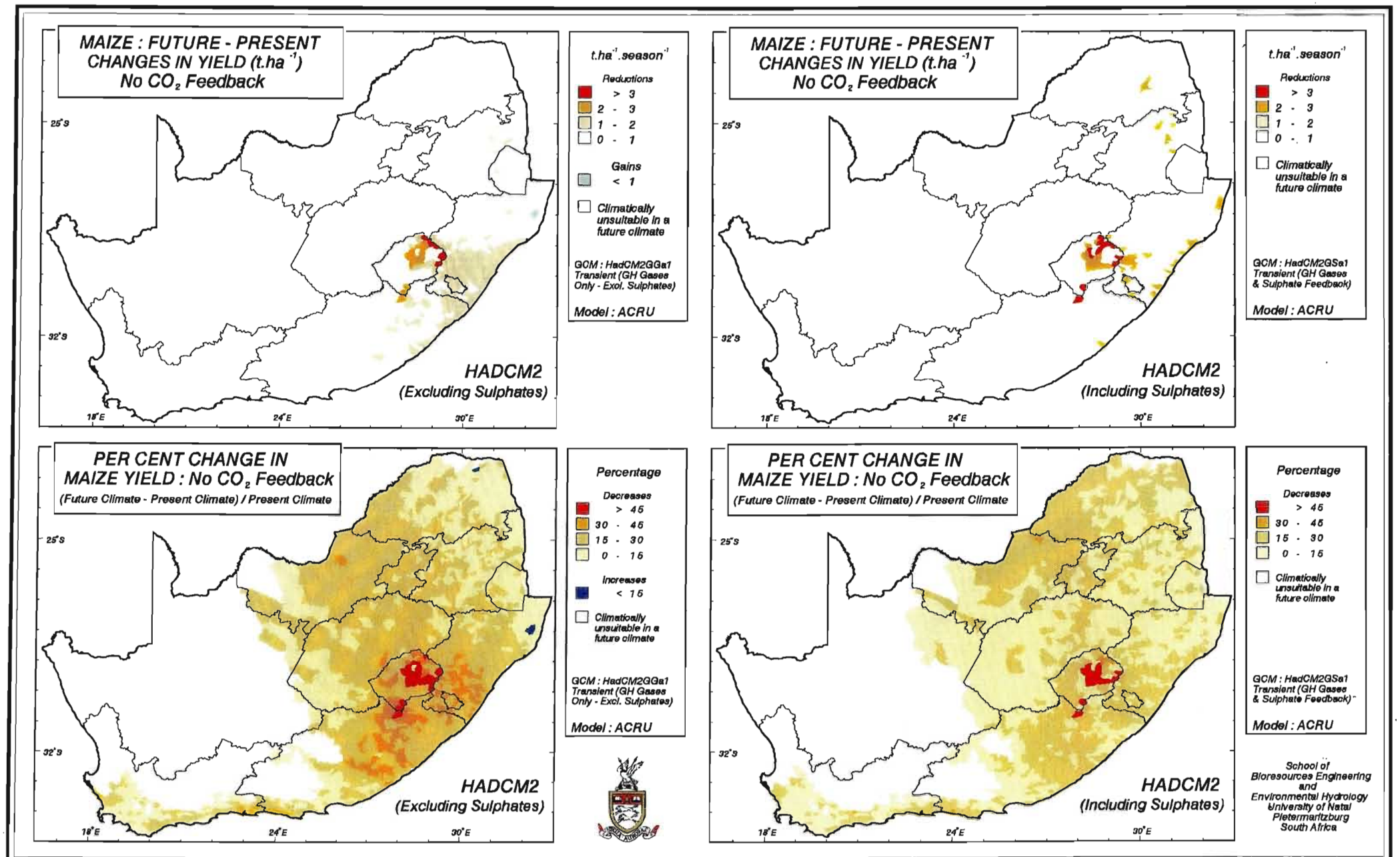
MAIZE : FUTURE - PRESENT
CHANGES IN YIELD (t.ha -1)
No CO2 Feedback
25°S
32°S
18°E
24°E
30°E
HADCM2
(Excluding Sulphates)
t.ha-1.season-1
Reductions
> 3
2 - 3
1 - 2
0 - 1
Gains
< 1
Climatically unsuitable in a future climate
GCM : HadCM2GGa1 Transient (GH Gases Only - Excl. Sulphates)
Model : ACRU
MAIZE : FUTURE - PRESENT
CHANGES IN YIELD (t.ha -1)
No CO2 Feedback
HADCM2
(Including Sulphates)
t.ha-1.season-1
Reductions
> 3
2 - 3
1 - 2
0 - 1
Climatically unsuitable in a future climate
GCM : HadCM2GSa1 Transient (GH Gases & Sulphate Feedback)
Model : ACRU
PER CENT CHANGE IN
MAIZE YIELD : No CO2 Feedback
(Future Climate - Present Climate) / Present Climate
HADCM2
(Excluding Sulphates)
Percentage
Decreases
> 45
30 - 45
15 - 30
0 - 15
Increases
< 15
Climatically unsuitable in a future climate
GCM : HadCM2GGa1 Transient (GH Gases Only - Excl. Sulphates)
Model : ACRU
PER CENT CHANGE IN
MAIZE YIELD : No CO2 Feedback
(Future Climate - Present Climate) / Present Climate
HADCM2
(Including Sulphates)
Percentage
Decreases
> 45
30 - 45
15 - 30
0 - 15
Climatically unsuitable in a future climate
GCM : HadCM2GSa1 Transient (GH Gases & Sulphate Feedback)
Model : ACRU
School of Bioresources Engineering and Environmental Hydrology
University of Natal
Pietermaritzburg
South Africa

These decreases in maize yield equate to a 15 to 30% decrease in yields simulated under present climatic conditions for large parts of the climatically suitable areas (Figure 8.35, bottom left). In southern KwaZulu-Natal there is simulated to be between a 30 and 45% decrease in maize yield resulting from climate change using the future scenario from HadCM2-S. The largest decreases are simulated in parts of Lesotho, where the yields could decrease to 55% of present maize yields.

When the influence of sulphate forcing is included in HadCM2, and the effect of $CO_2$ transpiration suppression remains excluded from the *ACRU* model, the reductions in median maize yield with a future climate are not as large (Figure 8.35, top right). Most of the areas that remain climatically suitable in a future climate are simulated to experience decreases in maize yield of less than 1 $t.ha^{-1}.season^{-1}$ using output from HadCM2+S. However, decreases in excess of 45% of yields under present climatic conditions are simulated for parts of Lesotho (Figure 8.35, bottom right).

Considerably different results are obtained when the effect of transpiration suppression resulting from increased atmospheric $CO_2$ concentrations is included in the simulations from HadCM2-S. Most of the climatically suitable areas are simulated to show gains in median maize yield (Figure 8.36, top left), with some catchments in northern KwaZulu-Natal simulated to experience gains in yield in excess of 2 $t.ha^{-1}.season^{-1}$. There are, however, small reductions in yield possible in Lesotho and catchments in the west and south of the climatically suitable areas using this climate scenario. These changes in yield equate to more than a 30% increase in maize yield from present climatic conditions in parts of the Northern Province, Mpumalanga and KwaZulu-Natal (Figure 8.39, bottom left) and less than a 15% decrease in the catchments located in the western parts of the climatically suitable areas.

Figure 8.36 Median maize yields ($t.ha^{-1}.season^{-1}$): changes in yield between future and present climates (top left) and per cent change in yield (bottom left) using the future climate scenario from HadCM2-S. Changes in yield between future and present climates (top right) and per cent change in yield (bottom right) using the future climate scenario from HadCM2+S. Carbon dioxide induced transpiration suppression is considered

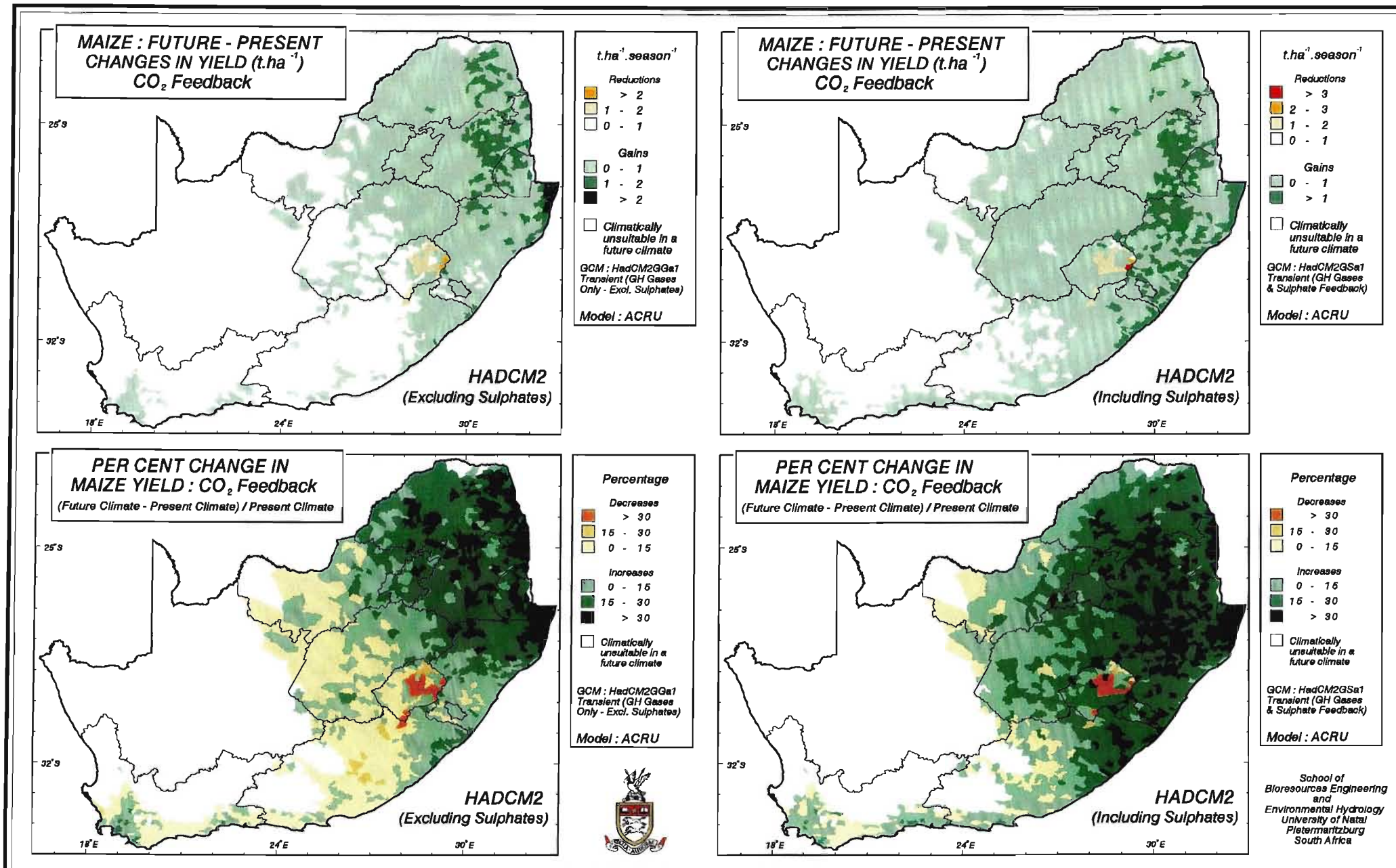
MAIZE : FUTURE - PRESENT
CHANGES IN YIELD (t.ha -1)
CO2 Feedback
25°S
32°S
18°E
24°E
30°E
HADCM2
(Excluding Sulphates)
t.ha-1.season-1
Reductions
> 2
1 - 2
0 - 1
Gains
0 - 1
1 - 2
> 2
Climatically unsuitable in a future climate
GCM : HadCM2GGa1 Transient (GH Gases Only - Excl. Sulphates)
Model : ACRU
MAIZE : FUTURE - PRESENT
CHANGES IN YIELD (t.ha -1)
CO2 Feedback
HADCM2
(Including Sulphates)
Reductions
> 3
2 - 3
1 - 2
0 - 1
Gains
0 - 1
> 1
Climatically unsuitable in a future climate
GCM : HadCM2GSa1 Transient (GH Gases & Sulphate Feedback)
Model : ACRU
PER CENT CHANGE IN
MAIZE YIELD : CO2 Feedback
(Future Climate - Present Climate) / Present Climate
HADCM2
(Excluding Sulphates)
Percentage
Decreases
> 30
15 - 30
0 - 15
Increases
0 - 15
15 - 30
> 30
Climatically unsuitable in a future climate
GCM : HadCM2GGa1 Transient (GH Gases Only - Excl. Sulphates)
Model : ACRU
PER CENT CHANGE IN
MAIZE YIELD : CO2 Feedback
(Future Climate - Present Climate) / Present Climate
HADCM2
(Including Sulphates)
Percentage
Decreases
> 30
15 - 30
0 - 15
Increases
0 - 15
15 - 30
> 30
Climatically unsuitable in a future climate
GCM : HadCM2GSa1 Transient (GH Gases & Sulphate Feedback)
Model : ACRU
School of
Bioresources Engineering
and
Environmental Hydrology
University of Natal
Pietermaritzburg
South Africa

When a future climate scenario from HaCM2+S is used, more of the climatically suitable areas are simulated to have gains in maize yield, with KwaZulu-Natal possibly having the highest gains in yield (Figure 8.36, top right). Many catchments in KwaZulu-Natal could have a 30% increase in maize yield from present climatic conditions (Figure 8.36, bottom right).

From these results is can be concluded than $CO_2$ feedback could offset the adverse effects of climate change on maize yield in some areas of southern Africa.

### 8.3.4 Potential economic impact of climate change on maize yield

For the purpose of this study the breakeven production for commercially planted dryland maize was set in *ACRU* at 3 $t.ha^{-1}$ and the selling price was set at R750 per tonne of grain (Ortmann, 1999, pers. comm.). This is a general figure for commercial production in South Africa. It varies regionally with topography, fertiliser usage, labour costs and land prices. The analysis does not apply to subsistence farming.

Two simulations were performed using *ACRU*, *viz.* including and excluding the effects of $CO_2$ transpiration suppression. In both cases monthly means of daily maximum and minimum temperatures were used. Present net profits were simulated using the *ACRU* maize yield model to range from losses in excess of R1 000 per hectare for most of the western parts of the climatically suitable areas, to profits in excess of R2 000 per hectare in parts of Mpumalanga, KwaZulu-Natal and Lesotho (Figure 8.37, top).

Figure 8.37 Gross profit of maize ($R.ha^{-1}$): for present climatic conditions (top), changes in profit between future and present climates using the future climate scenario from HadCM2-S (middle) and changes in profit between future and present climates using the future climate scenario from HadCM2+S (bottom). Carbon dioxide induced transpiration suppression not considered

Significant losses in profit were simulated by *ACRU* using changes in climate from HadCM2-S and excluding the effects of $CO_2$ feedbacks from the *ACRU* maize yield model (Figure 8.37,

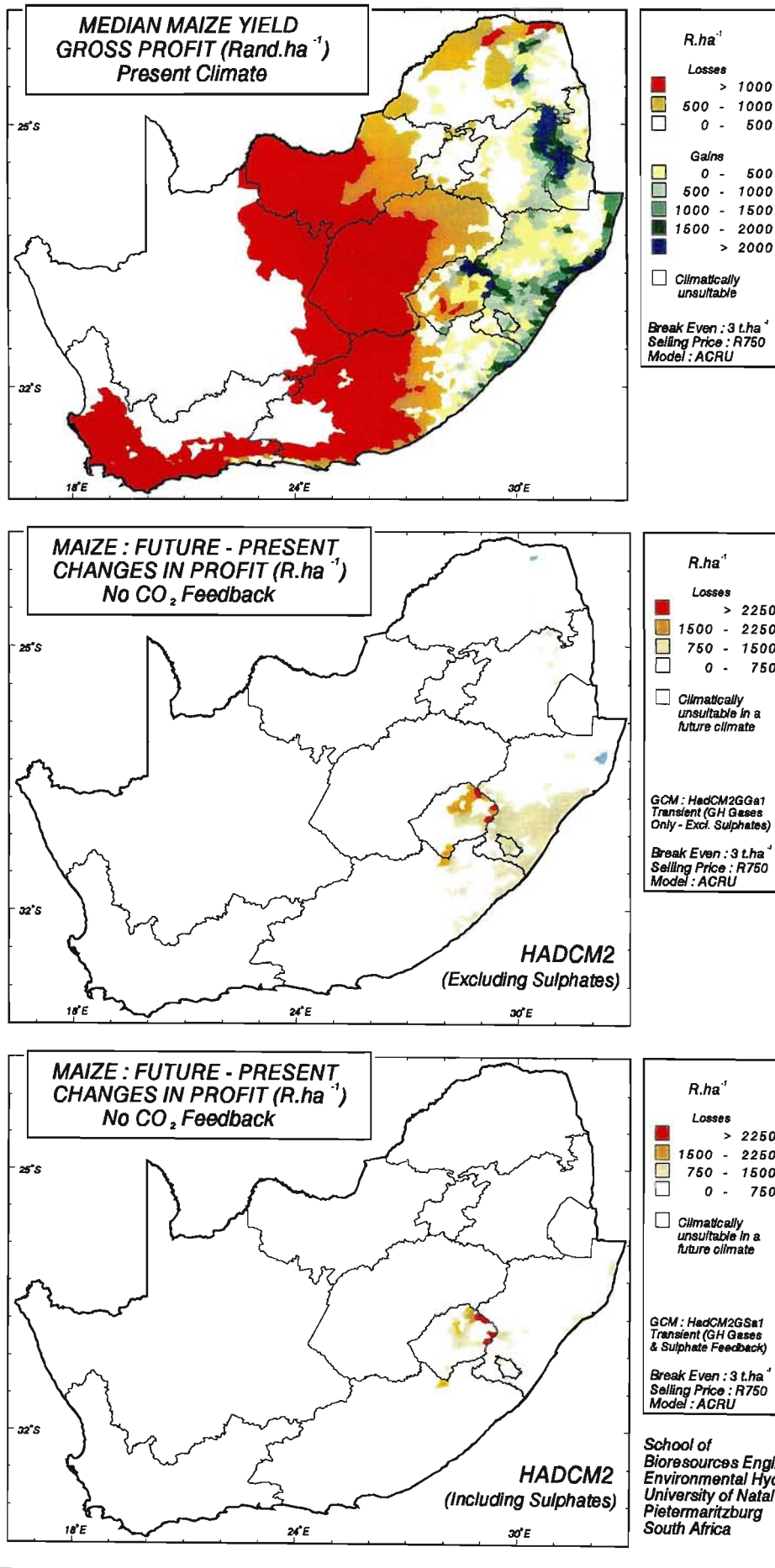


*School of*
*Bioresources Engineering and*
*Environmental Hydrology*
*University of Natal*
*Pietermaritzburg*
*South Africa*

middle). These losses ranged from less than R750 per hectare in the central parts of the study area to more than R2 250 per hectare in Lesotho.

The entire study area was simulated to experience reductions in profit compared to present climatic conditions (Figure 8.37, bottom) when using HadCM2+S and $CO_2$ transpiration suppression being excluded. However, the reductions were not as large as those simulated using this GCM when excluding sulphate forcing. Most areas that remain climatically suitable for the cultivation of maize could, assuming the HadCM2+S future climate scenario, experience losses less than R750 per hectare. However, isolated parts of Lesotho could expect losses in excess of R2 250 per hectare in a future climate if maize were to be grown there under commercial conditions.

The changes in profit resulting from climate change using output from HadCM2-S were estimated using *ACRU*, this time with the $CO_2$ fertilization feedbacks included in the simulation (Figure 8.38, middle). Most areas were estimated to have gains in profit using this scenario, with most areas possibly experience gains of less than R750 per hectare. The largest gains, of more than R1 500 per hectare, were simulated to occur in the north of KwaZulu-Natal.

Figure 8.38 Gross profit of maize ($R.ha^{-1}$): for present climatic conditions (top), changes in profit between future and present climates using the future climate scenario from HadCM2-S (middle) and changes in profit between future and present climates using the future climate scenario from HadCM2+S (bottom). Carbon dioxide induced transpiration suppression is considered

An increase in the number of catchments which could experience gains in profit in excess of R750 per hectare is simulated when sulphate forcing is included in HadCM2 (Figure 8.38, bottom). These catchments are primarily located in KwaZulu-Natal, Mpumalanga and Swaziland.

Thus, the incorporation of predicted $CO_2$ transpiration suppression effects in climate impacts assessment of agriculture has a significant effect on the predictions of crop yield in a future

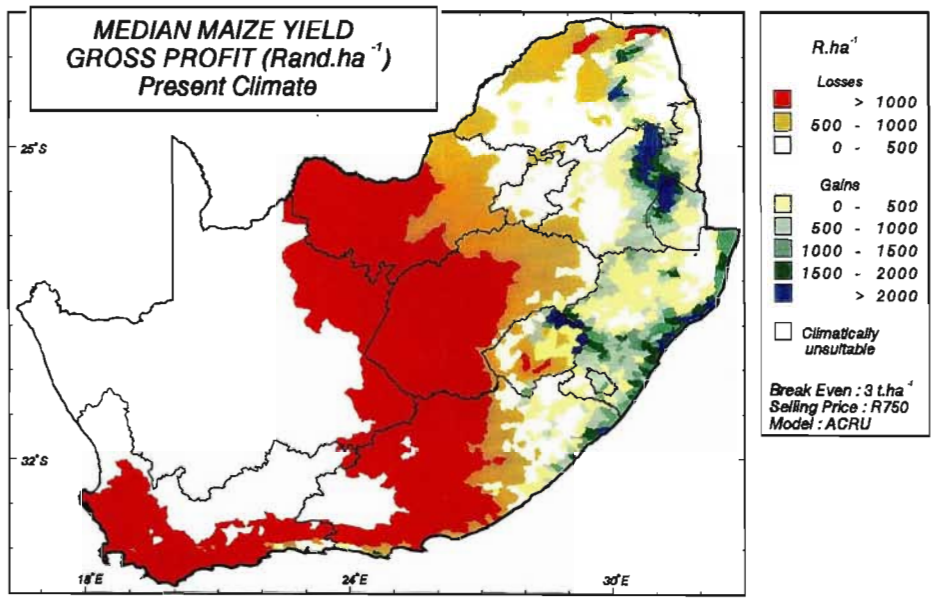


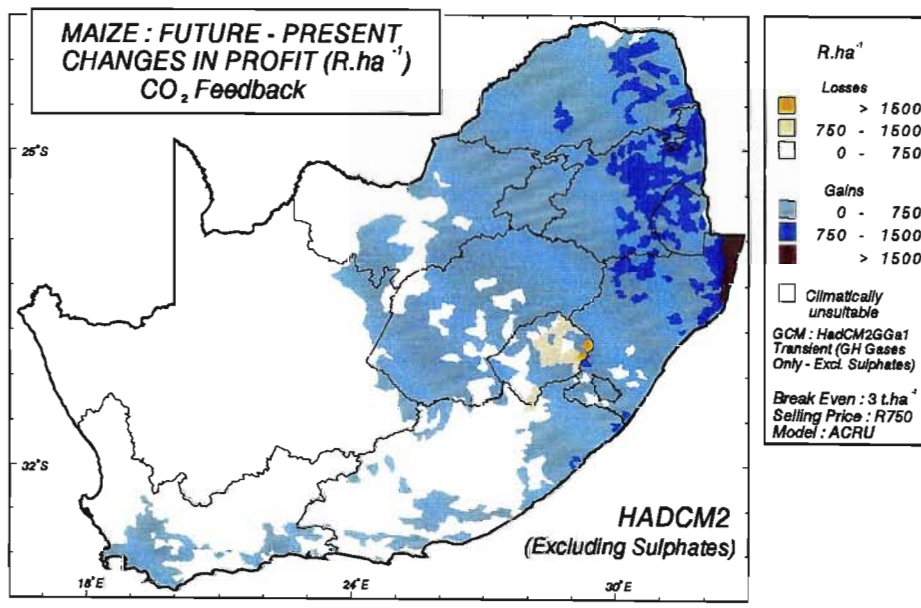


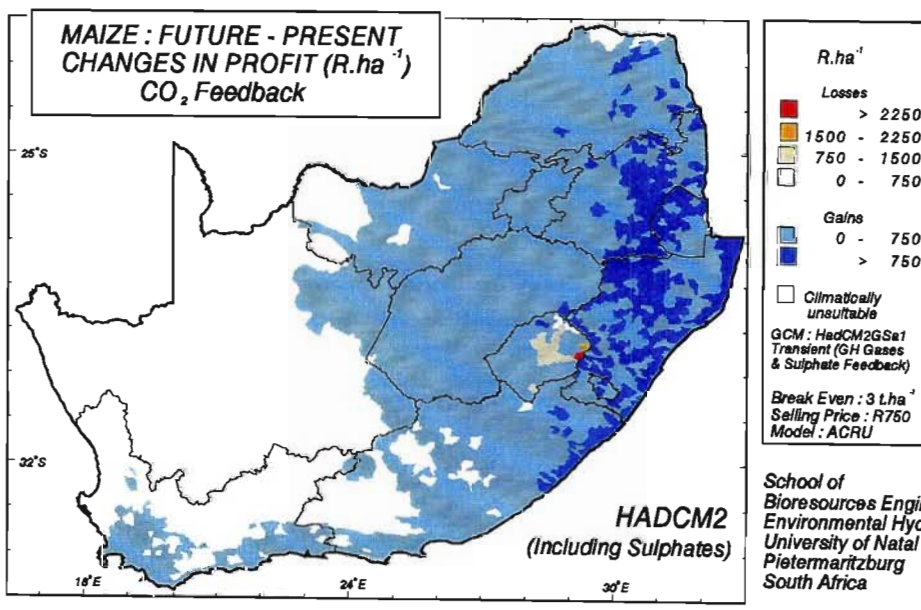


*School of*
*Bioresources Engineering and*
*Environmental Hydrology*
*University of Natal*
*Pietermaritzburg*
*South Africa*

climate and, therefore, a subsequent effect on estimations of potential changes in gross profit in the study area. In addition, there are significant differences simulated when including and excluding sulphate feedbacks in the HadCM2. The yields simulated using output from HadCM2+S are generally higher than when using output from HadCM2-S.

### 8.3.5 Threshold analysis of median maize yield

If a 10% increase or decrease in median annual maize yield is considered a significant change in yield then, using the threshold analysis described in Section 3.4.4 of Chapter 3 and using HadCM2+S in the *ACRU* model, produces the following result.

The year by which each Quaternary Catchment was simulated to experience a 10% decrease or increase in median annual maize yield was estimated as shown in Figure 8.39. Most areas that experience an increase in maize yield are simulated to show a 10% increase only by 2060 (the effective doubling of $CO_2$ scenario for HadCM2). Only a small number of catchments are shown to potentially have a 10% increase in median maize yield before 2060, but there does not seem to be any pattern to the dates of projected increase in yield. The areas simulated to show a decrease in maize yield, however, could show a 10% decrease before 2030.

| | |
|---|---|
| Figure 8.39 | Threshold analysis of median annual maize yield showing the year by which a 10% change in yield is simulated to occur. Future climate scenario from HadCM2+S |

From the threshold analysis of maize yield it can be concluded that maize has a relatively high tolerance to climate change.

### 8.3.6 Potential impacts of climate change on winter wheat yield using the *ACRU* winter wheat yield submodel

Wheat is a cool season crop, however, the young plants could be harmed by mean temperatures dropping below 5 °C (Smith, 1994). Mean daily temperatures for optimum growth vary between 15 and 20 °C (Doorenbos and Kassam, 1979). Winter wheat yields are

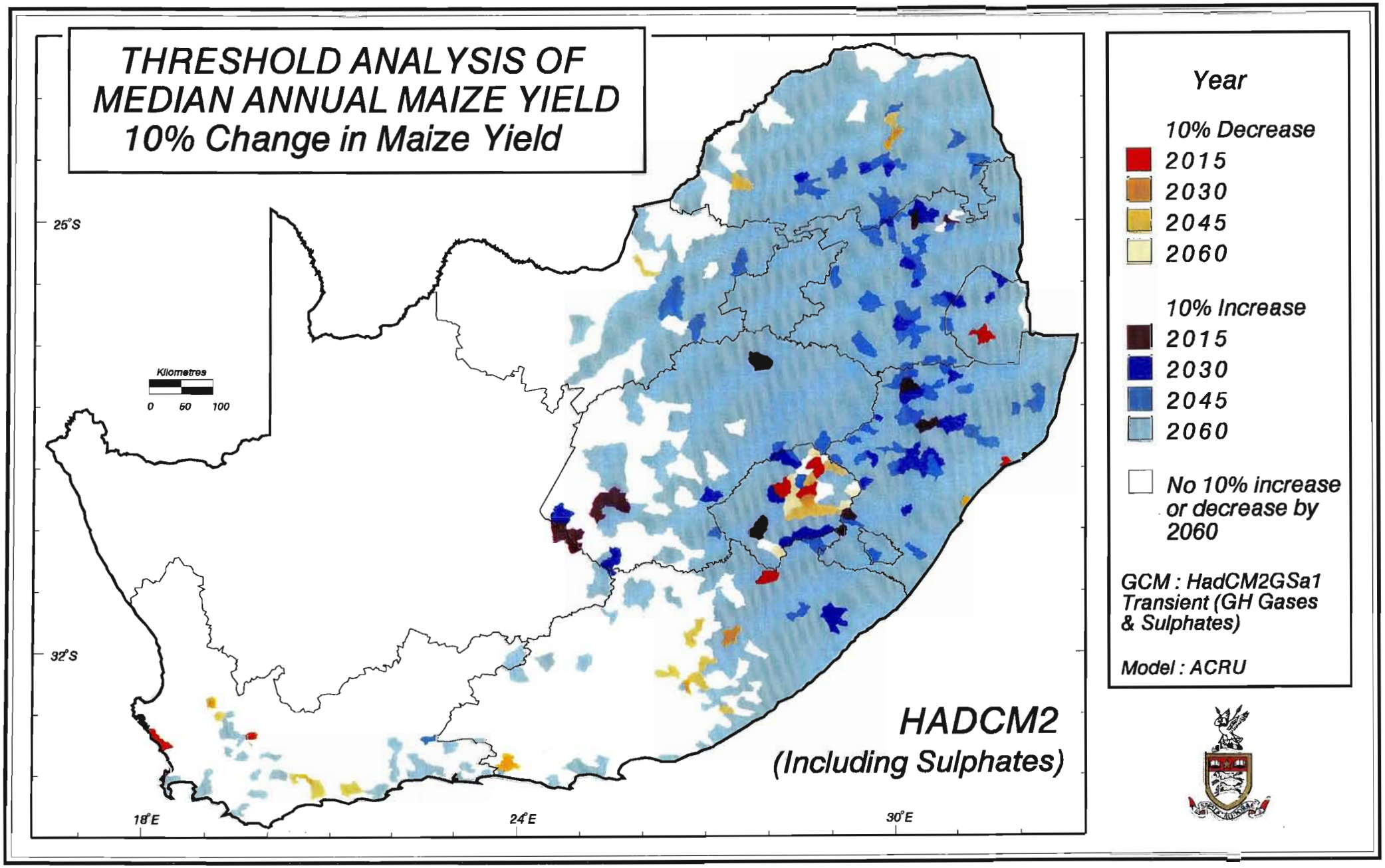
THRESHOLD ANALYSIS OF
MEDIAN ANNUAL MAIZE YIELD
10% Change in Maize Yield
25°S
32°S
18°E
24°E
30°E
Kilometres
0 50 100
HADCM2
(Including Sulphates)
Year
10% Decrease
2015
2030
2045
2060
10% Increase
2015
2030
2045
2060
No 10% increase or decrease by 2060
GCM : HadCM2GSa1 Transient (GH Gases & Sulphates)
Model : ACRU

also affected by high temperatures and high relative humidity and for this reason cannot be grown in much of the KwaZulu-Natal coastal region, for example. Owing to the complexity of factors contributing to the suitability of winter wheat for cultivation, the whole study area has been considered in this analysis and the climatically unsuitable areas have not been eliminated. The primary cultivation regions are the southern Free State, Western Cape and western coastline of South Africa and, therefore, particular attention will be paid to these regions in this analysis.

Potential changes in winter wheat are simulated using HadCM2-S and HadCM2+S and $CO_2$ induced transpiration suppression of 15% is included with wheat being a C3 plant. The modified version of the winter wheat model, in which the various phenological stages are activated by growing degree days and $CO_2$ induced transpiration suppression is included, is used for these assessments. The estimation of winter wheat yields using the winter wheat submodel in *ACRU* is described in Chapter 4, Section 4.5. An economic analysis has been carried out to assess potential changes in profits and losses from the cultivation of winter wheat resulting from climate change.

The median winter wheat yields for present climatic conditions range from less than 1 $t.ha^{-1}.season^{-1}$ in the far north of the study area to more than 5 $t.ha^{-1}.season^{-1}$ in catchments predominantly located in the Western Cape, Northern Cape and Free State Provinces (Figure 8.40, top).

Figure 8.40 Median winter wheat yields ($t.ha^{-1}.season^{-1}$) for present climate (top) and gross profit of winter wheat ($R.ha^{-1}$) for present climate (bottom). Carbon dioxide induced transpiration suppression is considered

For the purpose of this study the breakeven production for commercially planted dryland winter wheat was set in *ACRU* at 1 $t.ha^{-1}$ and the selling price was set at R900 per tonne of grain (Darroch, 2000, pers. comm.). As in the case of profits for maize this is a general figure for commercial production in South Africa. Under present climatic conditions profits are simulated to be made in most parts of the study area, with profits in excess of R2 000 per hectare simulated in the primary growing areas (Figure 8.40, bottom).

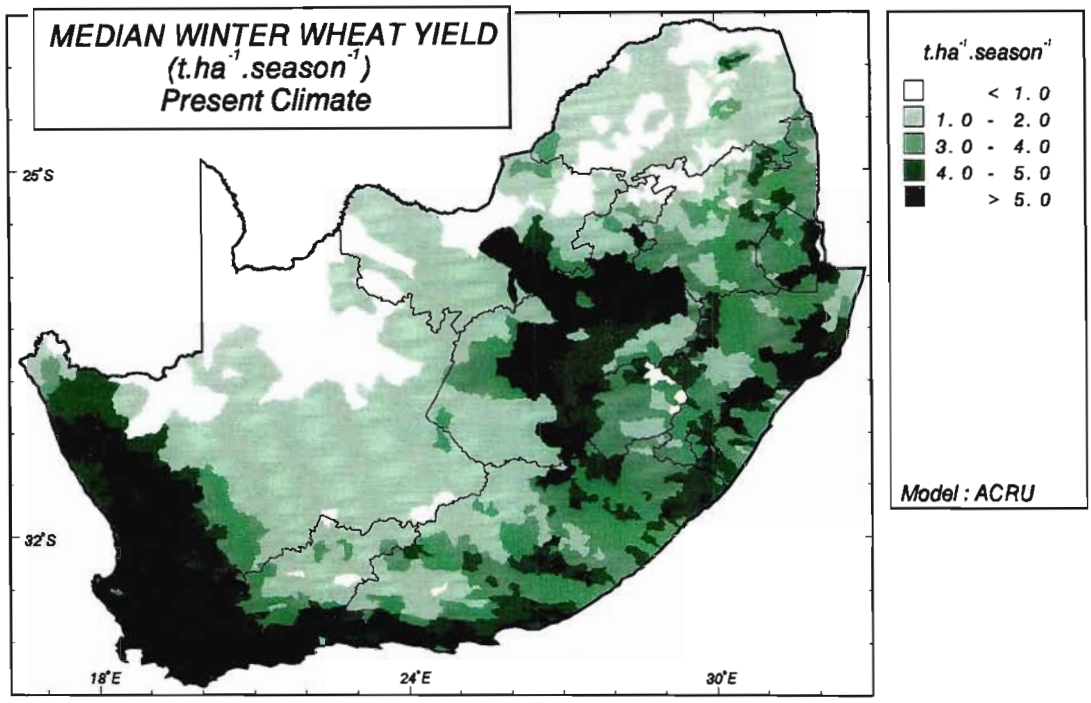
MEDIAN WINTER WHEAT YIELD
(t.ha-1.season-1)
Present Climate
25°S
32°S
18°E
24°E
30°E
t.ha-1.season-1
< 1.0
1.0 - 2.0
3.0 - 4.0
4.0 - 5.0
> 5.0
Model : ACRU

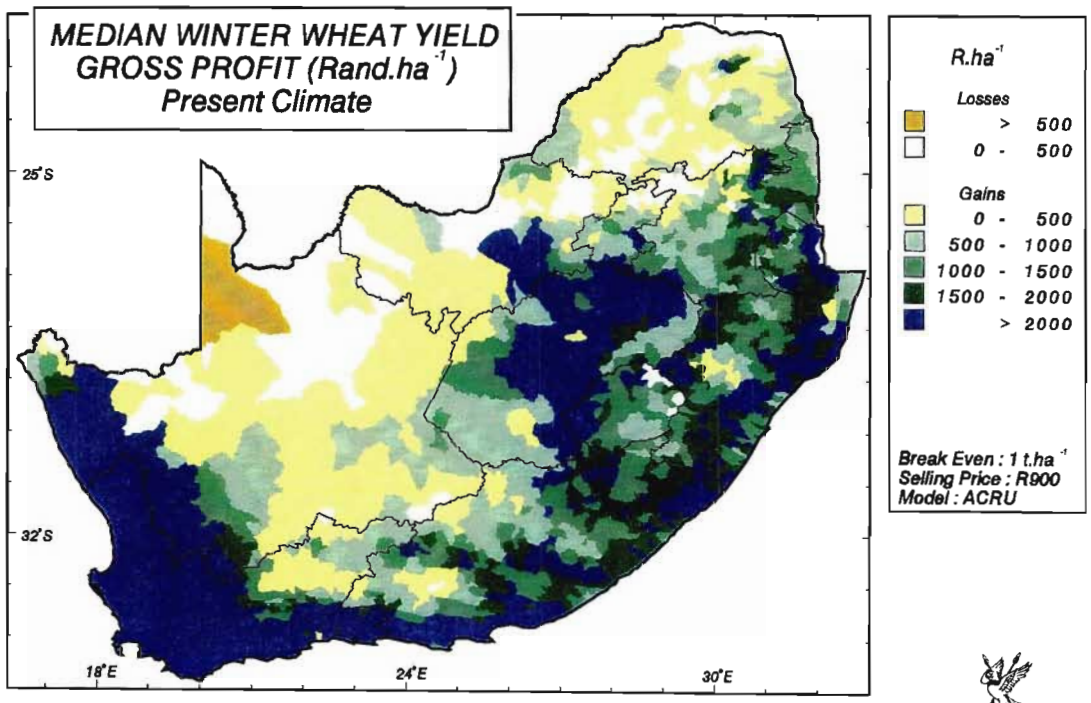
MEDIAN WINTER WHEAT YIELD
GROSS PROFIT (Rand.ha-1)
Present Climate
25°S
32°S
18°E
24°E
30°E
R.ha-1
Losses
> 500
0 - 500
Gains
0 - 500
500 - 1000
1000 - 1500
1500 - 2000
> 2000
Break Even : 1 t.ha-1
Selling Price : R900
Model : ACRU

Most parts of the climatically suitable areas are simulated to have decreases in winter wheat yield under a future climate scenario from HadCM2-S (Figure 8.41, top left). Of particular significance are the decreases in winter wheat yield simulated in the Western Cape Province. These decreases could be attributed to the decrease in rainfall simulated by this GCM in that area in winter which is the rainy season (cf. Figure 6.8). Small gains in winter wheat yield are, however, simulated in the north of the study area. When these changes in yield are expressed as a percentage of differences in yield between the two climate scenarios over present climate yields, the decreases in winter wheat yield range from less than 40% in many areas to over 40% in many catchments in the Northern Cape, Western Cape and Eastern Cape Provinces (Figure 8.41, bottom left). The gains in winter wheat yield resulting from climate change are simulated to be between 0 and 60% assuming the scenario from HadCM2-S to be correct.

Figure 8.41 Median winter wheat yields ($t.ha^{-1}.season^{-1}$): changes in yield between future and present climates (top left) and per cent change in yield (bottom left) using the future climate scenario from HadCM2-S. Changes in yield between future and present climates (top right) and per cent change in yield (bottom right) using the future climate scenario from HadCM2+S. Carbon dioxide induced transpiration suppression is considered

Similar increases and decreases in winter wheat yield as those simulated using HadCM2-S are simulated when using output from HadCM2+S and including $CO_2$ transpiration suppression feedbacks (Figure 8.41, top right). However, fewer catchments are simulated to have increases in yield. The percentage decreases in the Western Cape and Northern Cape Provinces are lower when using the scenario from HadCM2+S compared to those using output from HadCM2-S (Figure 8.41, bottom right).

A study into the sensitivity of winter wheat production in Denmark to changes in climate showed that winter wheat yields decreased with increased temperatures and decreased with decreased precipitation. This was the combination of climate changes simulated to occur by HadCM2 in the western parts of the study area (Olesen *et al.*, 2000).

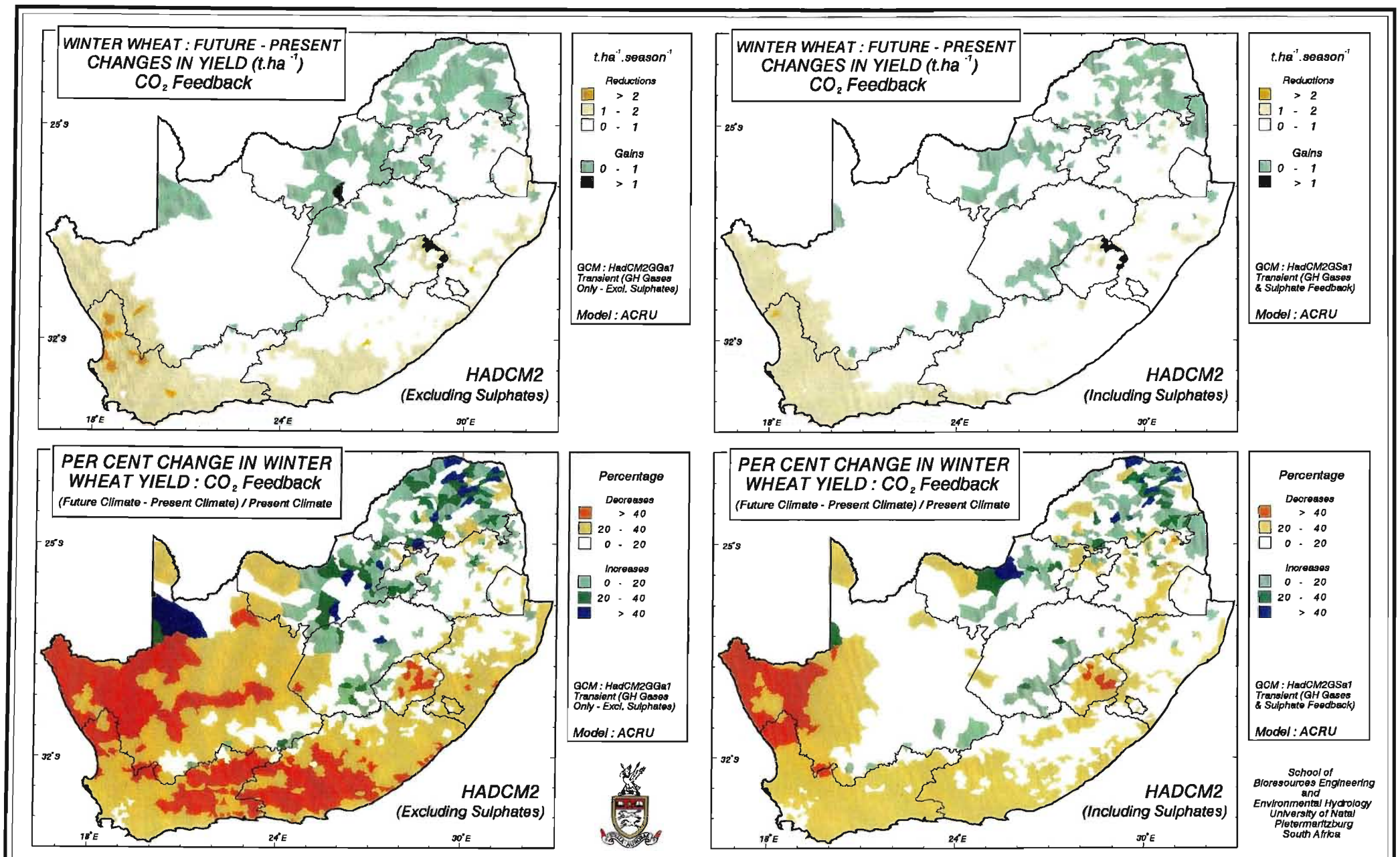
WINTER WHEAT : FUTURE - PRESENT
CHANGES IN YIELD (t.ha -1)
CO2 Feedback
25°S
32°S
18°E
24°E
30°E
HADCM2
(Excluding Sulphates)
t.ha-1.season-1
Reductions
> 2
1 - 2
0 - 1
Gains
0 - 1
> 1
GCM : HadCM2GGa1
Transient (GH Gases
Only - Excl. Sulphates)
Model : ACRU
WINTER WHEAT : FUTURE - PRESENT
CHANGES IN YIELD (t.ha -1)
CO2 Feedback
HADCM2
(Including Sulphates)
t.ha-1.season-1
Reductions
> 2
1 - 2
0 - 1
Gains
0 - 1
> 1
GCM : HadCM2GSa1
Transient (GH Gases
& Sulphate Feedback)
Model : ACRU
PER CENT CHANGE IN WINTER
WHEAT YIELD : CO2 Feedback
(Future Climate - Present Climate) / Present Climate
HADCM2
(Excluding Sulphates)
Percentage
Decreases
> 40
20 - 40
0 - 20
Increases
0 - 20
20 - 40
> 40
GCM : HadCM2GGa1
Transient (GH Gases
Only - Excl. Sulphates)
Model : ACRU
PER CENT CHANGE IN WINTER
WHEAT YIELD : CO2 Feedback
(Future Climate - Present Climate) / Present Climate
HADCM2
(Including Sulphates)
Percentage
Decreases
> 40
20 - 40
0 - 20
Increases
0 - 20
20 - 40
> 40
GCM : HadCM2GSa1
Transient (GH Gases
& Sulphate Feedback)
Model : ACRU
School of
Bioresources Engineering
and
Environmental Hydrology
University of Natal
Pietermaritzburg
South Africa

### 8.3.7 Potential economic impact of climate change on winter wheat yield

These simulated changes in winter wheat yield result in potential changes in profit in the study area. Most areas are simulated to experience losses in a future climate scenario from HadCM2-S and including $CO_2$ transpiration feedbacks (Figure 8.42, top). In the primary growing areas there is simulated to be losses of between R900 and R1 800 per hectare in the Western Cape, for example, resulting from decreases in winter wheat yield in these areas. However, there are increases in profit of less than R900 per hectare simulated in some parts of the Free State Province using output from HadCM2-S. A similar pattern of profits and losses results when using output from HadCM2+S as input into the *ACRU* model (Figure 8.42, bottom).

| | |
|---|---|
| Figure 8.42 | Gross profit of winter wheat ($R.ha^{-1}$): changes in profit between future and present climates using the future climate scenario from HadCM2-S (top) and changes in profit between future and present climates using the future climate scenario from HadCM2+S (bottom). Carbon dioxide induced transpiration suppression is considered |

## 8.4 Potential Impacts of Climate Change on Plant Pest Life Cycles: Codling Moth

It has already been stated previously in the section on heat units (cf. Section 8.1.1) that the growth and development of many organisms is dependent on temperature. The spatial distribution of disease vectors, pests and, similarly, species used in biological control of exotic pests is thus also temperature dependent (Schulze, 1997b).

Zalom *et al.* (1983) illustrate that successive stages of development of organisms decrease progressively with higher temperatures, often until temperatures become too high and growth is then affected negatively. Specific species thus frequently have defined lower and upper thresholds of temperature between which development takes place, with rates of development to complete a life cycle dependent on accumulated heat units. Life cycles are thus measured by physiological time rather than by calendar time (Zalom *et al.*, 1983).

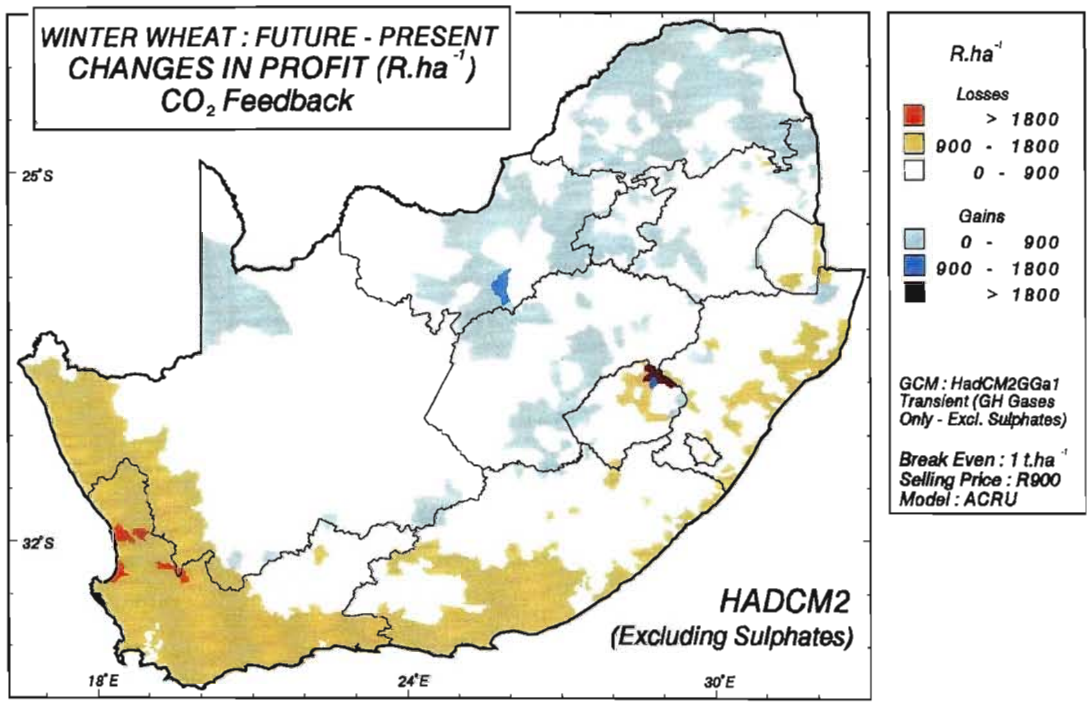
WINTER WHEAT : FUTURE - PRESENT
CHANGES IN PROFIT (R.ha-1)
CO2 Feedback
25°S
32°S
18°E
24°E
30°E
HADCM2
(Excluding Sulphates)
R.ha-1
Losses
> 1800
900 - 1800
0 - 900
Gains
0 - 900
900 - 1800
> 1800
GCM : HadCM2GGa1
Transient (GH Gases
Only - Excl. Sulphates)
Break Even : 1 t.ha-1
Selling Price : R900
Model : ACRU

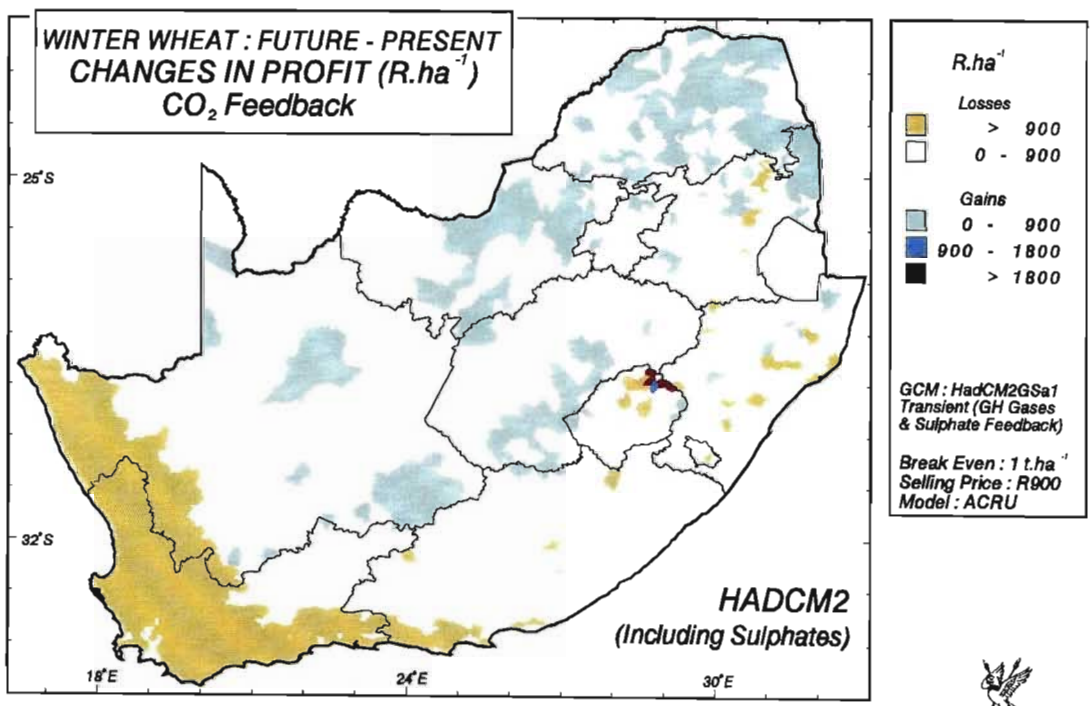
WINTER WHEAT : FUTURE - PRESENT
CHANGES IN PROFIT (R.ha-1)
CO2 Feedback
25°S
32°S
18°E
24°E
30°E
HADCM2
(Including Sulphates)
R.ha-1
Losses
> 900
0 - 900
Gains
0 - 900
900 - 1800
> 1800
GCM : HadCM2GSa1
Transient (GH Gases
& Sulphate Feedback)
Break Even : 1 t.ha-1
Selling Price : R900
Model : ACRU

Lower and upper temperature (°C) thresholds and accumulated degree days for one life cycle of three selected agricultural pests are, respectively

| | | | | |
|---|---|---|---|---|
| i) | Codling moth | 11.1 °C, | 34.4 °C, | 603 °days |
| ii) | Oriental fruit moth | 7.2 °C, | 32.2 °C, | 535 °days |
| iii) | Egyptian alfalfa weevil | 7.2 °C, | none, | 444 °days. |

Such information is important for better pest control, because if the stages of pest life cycles can be predicted, then conflict between cultural practices (such as the application of irrigation) and pest control (such as spraying) can be minimised (Zalom *et al.*, 1983; Schulze, 1997b).

Assuming that codling moth could breed throughout southern Africa and no factors than accumulated ° days were to affect their life cycle development, the present number of life cycles per annum was computed by Schulze (1997b) and shown in Figure 8.43 (top). The highest number of life cycles was simulated in the north and east, with lower number of life cycles in the cooler regions of the study area.

Figure 8.43 Life cycles of codling moth: for present climate (top), future climate (middle) and change in number of life cycles from present to future climates (bottom). Future climate scenario from UKTR-S

Under a future temperature regime, such as that represented by UKTR-S, the likely numbers of life cycles of codling moth are set to increase markedly (Figure 8.43, middle). The northern parts of the study region, such as the North-West and Northern Cape Provinces, could expect a possible additional two life cycles per annum in a warmer future (see Table 8.14). Lesotho and the surrounding areas should not experience significant changes in the number of life cycles of codling moth in the future (Figure 8.43, bottom).

A similar pattern of increases in life cycles is noted in Figure 8.44 (top left and bottom left) which was generated using output from HadCM2-S. The increases in the number of life cycles of the codling moth are not as large when output from HadCM2+S is used (Figure 8.44, top right and bottom right). The greatest gains in number of life cycles are again located in

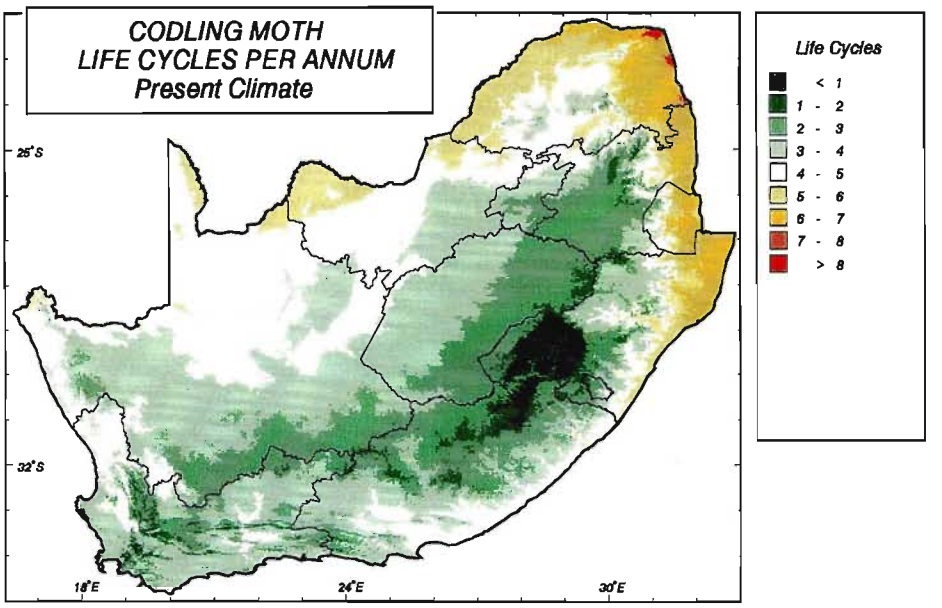


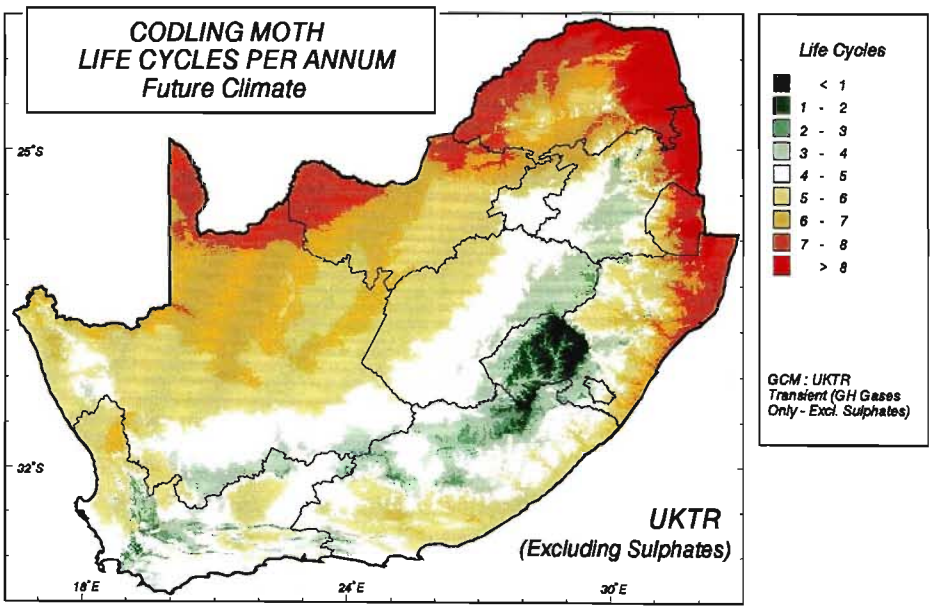


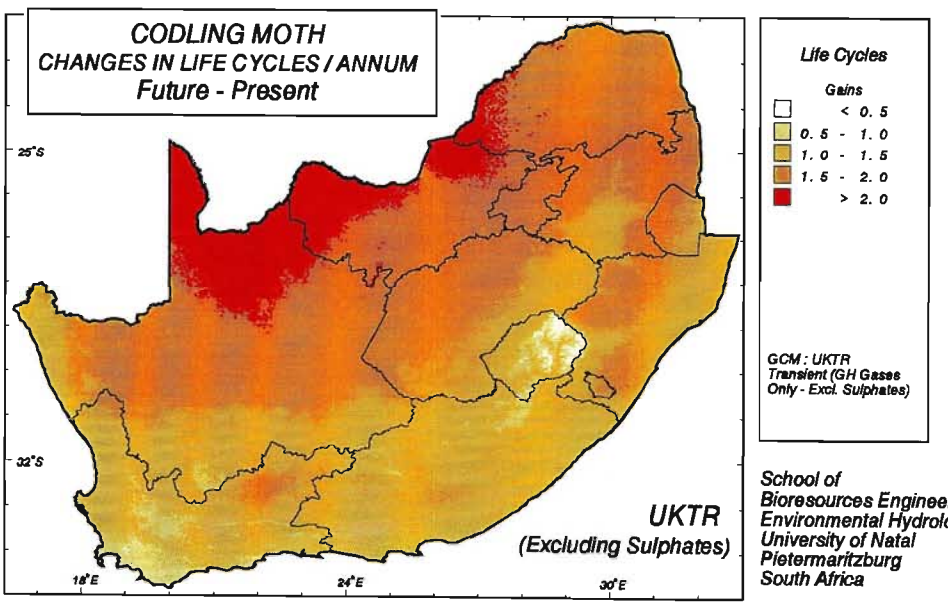


School of
Bioresources Engineering and
Environmental Hydrology
University of Natal
Pietermaritzburg
South Africa

Table 8.14 Statistics for life cycles of codling moth for present climatic conditions and a future (2X $CO_2$) climate scenario from UKTR-S

| Codling Moth (Life Cycles per Annum) | | | | | | | | | | | | | | |
|---|---|---|---|---|---|---|---|---|---|---|---|---|---|---|
| Province / Country | Mean Value | | C.V. (%) | | Maximum Value | | Minimum Value | | Exceedence Probability | | | | | |
| | | | | | | | | | 20% | | 50% | | 80% | |
| | Present | Future | Present | Future | Present | Future | Present | Future | Present | Future | Present | Future | Present | Future |
| Northern Province | 5.4 | 7.3 | 18.5 | 13.5 | 7.7 | 0.5 | 2.0 | 3.6 | 6.3 | 8.1 | 5.4 | 7.4 | 4.5 | 6.4 |
| Mpumalanga | 3.7 | 5.3 | 40.4 | 29.2 | 7.2 | 8.9 | 0.2 | 1.3 | 5.1 | 6.8 | 3.1 | 4.8 | 2.5 | 4.0 |
| North-West | 4.5 | 6.5 | 13.1 | 11.1 | 6.1 | 0.2 | 2.9 | 4.7 | 5.1 | 7.2 | 4.5 | 6.5 | 3.9 | 5.8 |
| Northern Cape | 4.0 | 5.7 | 17.8 | 16.8 | 6.9 | 8.4 | 1.0 | 1.8 | 4.6 | 6.6 | 4.0 | 5.7 | 3.3 | 4.8 |
| Gauteng | 3.4 | 5.1 | 13.8 | 10.7 | 5.0 | 6.8 | 2.6 | 4.2 | 3.7 | 5.6 | 3.3 | 5.0 | 3.0 | 4.7 |
| Free State | 3.1 | 4.7 | 18.3 | 15.3 | 4.2 | 6.1 | 0.0 | 0.0 | 3.7 | 5.4 | 3.1 | 4.7 | 2.6 | 4.1 |
| KwaZulu-Natal | 4.3 | 5.8 | 34.5 | 25.3 | 7.0 | 8.4 | 0.0 | 0.0 | 5.8 | 7.3 | 4.1 | 5.6 | 3.0 | 4.5 |
| Eastern Cape | 3.2 | 4.5 | 27.6 | 21.1 | 5.4 | 6.7 | 0.0 | 0.2 | 4.0 | 5.3 | 3.2 | 4.6 | 2.5 | 3.8 |
| Western Cape | 3.4 | 4.6 | 21.7 | 18.9 | 5.6 | 6.7 | 0.4 | 0.8 | 4.0 | 5.4 | 3.4 | 4.7 | 2.8 | 3.9 |
| Swaziland | 5.4 | 7.0 | 20.0 | 15.0 | 7.1 | 8.6 | 2.2 | 3.9 | 6.4 | 7.9 | 5.8 | 7.3 | 4.4 | 6.0 |
| Lesotho | 1.2 | 2.1 | 77.6 | 60.4 | 3.5 | 5.1 | 0.0 | 0.0 | 2.2 | 5.1 | 1.0 | 2.1 | 0.1 | 0.7 |

the northern parts of southern Africa, however, only one extra life cycle per year is simulated in these regions.

Figure 8.44 Life cycles of codling moth: for future climate (top left) and the change in life cycles between future and present climates (bottom left) using the future climate scenario from HadCM2-S. Future climate (top right) and the change in life cycles between future and present climates (bottom right) using the future climate scenario from HadCM2+S

All else remaining the same, such temperature increases could have severe consequences for pest control in a possible future climate.

* * * * * * *

This chapter has illustrated how the refinements to modelling tools may be used to simulate changes in crop yield, pasture production, timber mean annual increment and pest life cycles under conditions of a changed climate. Both simple crop models, such as those based on Smith's (1994) climatic criteria, and more complex phenologically driven models which can account dynamically for temperature and rainfall changes on crop development as well as for $CO_2$ feedbacks on transpiration suppression and duration of growing season, such as the *ACRU* maize and winter wheat yield submodels, were used in conjunction with downscaled GCM output for 2X $CO_2$ scenarios and spatial databases.

Results from simulations with did not included $CO_2$ induced transpiration suppression point to general decreases in yields of crops, pastures and timber production as well as a decreases in climatically suitable areas for most of the crops studies within the study area. The exception seemed to be in Lesotho where an increase in yield was often found, as well as an increase in climatically suitable areas. However, when $CO_2$ transpiration supersession was included in the model, such as in the maize and winter wheat simulations, the adverse effects of climate change were offset to varying degrees with many areas simulated to have increases in crop yield under a future climate scenario.

## CODLING MOTH
## LIFE CYCLES PER ANNUM
### Future Climate

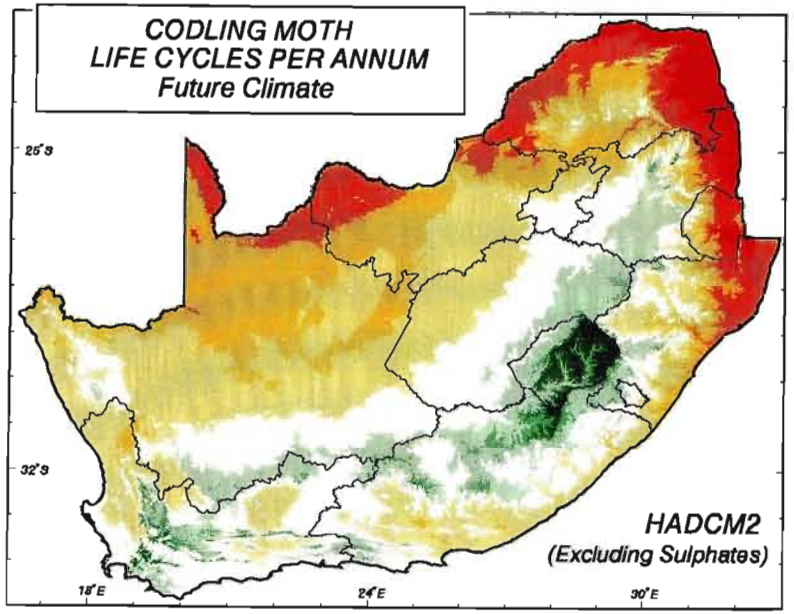


Life Cycles
- < 1
- 1 - 2
- 2 - 3
- 3 - 4
- 4 - 5
- 5 - 6
- 6 - 7
- 7 - 8
- > 8

GCM : HadCM2GGa1
Transient (GH Gases
Only - Excl. Sulphates)

## CODLING MOTH
## LIFE CYCLES PER ANNUM
### Future Climate

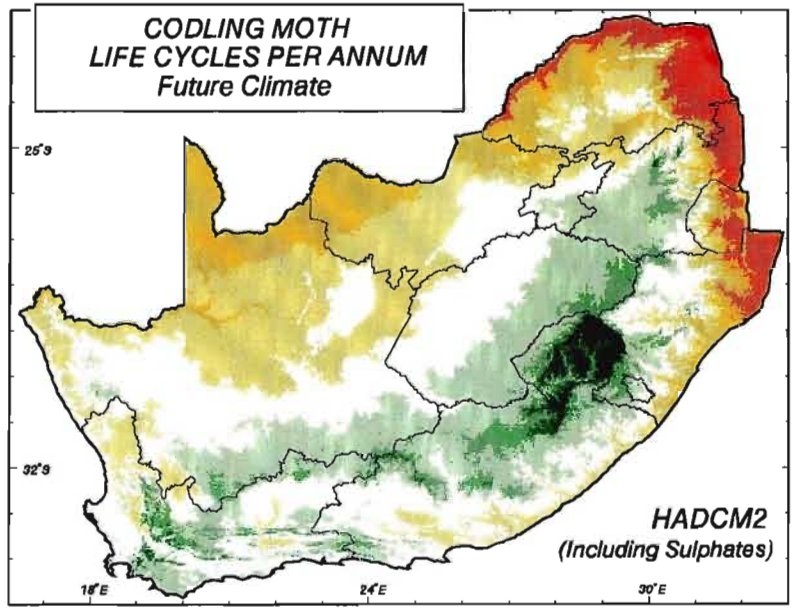


Life Cycles
- < 1
- 1 - 2
- 2 - 3
- 3 - 4
- 4 - 5
- 5 - 6
- 6 - 7
- 7 - 8
- > 8

GCM : HadCM2GSa1
Transient (GH Gases
& Sulphate Feedback)

## CODLING MOTH
## CHANGES IN LIFE CYCLES / ANNUM
### Future - Present

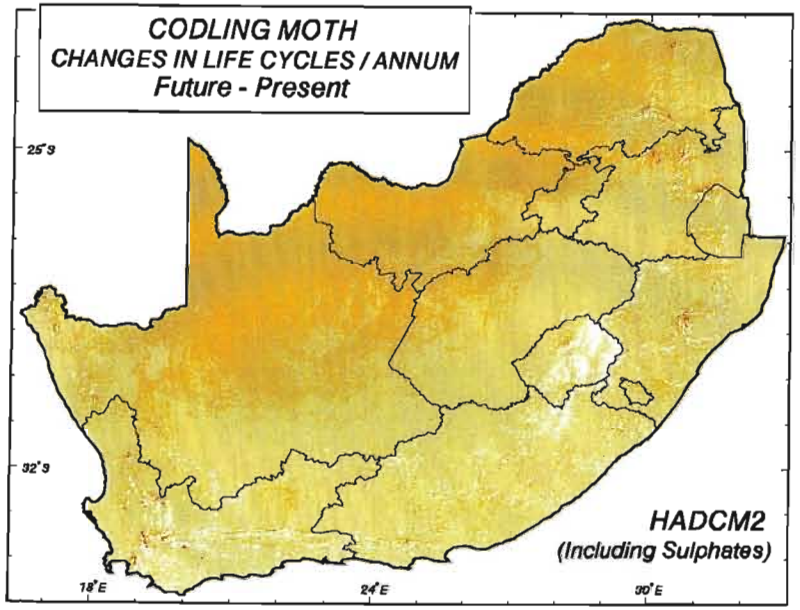


Life Cycles
Gains
- < 0.5
- 0.5 - 1.0
- 1.0 - 1.5
- > 1.5

GCM : HadCM2GSa1
Transient (GH Gases
& Sulphate Feedback)

## CODLING MOTH
## CHANGES IN LIFE CYCLES / ANNUM
### Future - Present

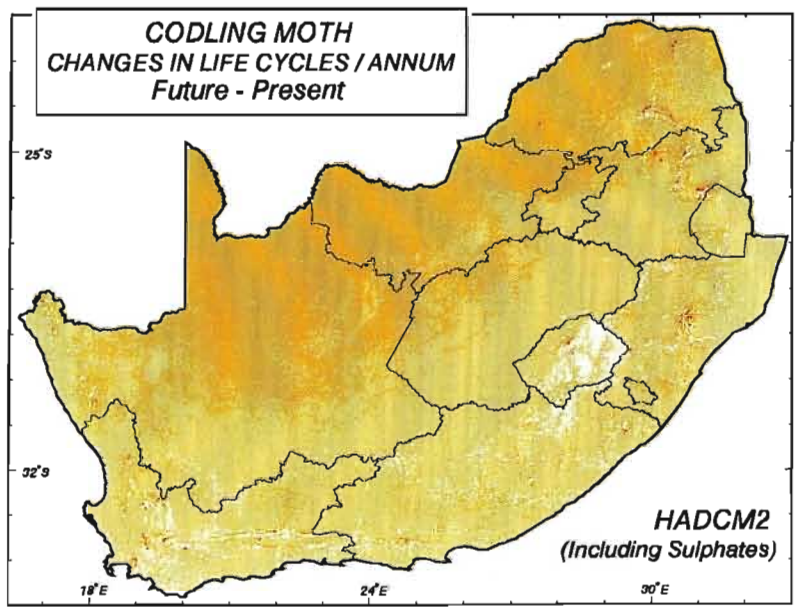


Life Cycles
Gains
- < 0.5
- 0.5 - 1.0
- 1.0 - 1.5
- > 1.5

GCM : HadCM2GSa1
Transient (GH Gases
& Sulphate Feedback)

School of
Bioresources Engineering
and
Environmental Hydrology
University of Natal
Pietermaritzburg
South Africa

The assessment of potential changes in the life cycles of the codling moth showed a potential increase in the number of life cycles of this agricultural pest resulting from climate change which, if indicative of the potential changes in most crop pests life cycles, could have significant implications for agriculture in the study area.

In the next chapter the model and database refinements developed are used to illustrate potential changes in water resources in southern Africa using the *ACRU* model at the scale of Quaternary Catchments.

# 9. APPLICATION OF TECHNIQUES TO ASSESS POTENTIAL IMPACTS OF CLIMATE CHANGE ON WATER RESOURCES IN SOUTHERN AFRICA

Although climate change is expected to affect many sectors of the natural and man-made sectors of our environment (Ringius *et al.*, 1996), water is considered to be the most critical factor associated with climate change impacts and adaptability. Water is becoming an increasingly scarce resource in many parts of the developing world, mostly as a consequence of demands made by increasing populations (MacIver, 1998; Stakhiv, 1998). Water is considered a limiting resource for development in southern Africa and changes in the water resources of this area could have major implications for the economy of the region (Shackleton *et al.*, 1996; Basson, 1997).

The climate impact assessments results obtained using the *ACRU* modelling system were for the 1946 Quaternary Catchments covering southern Africa, with the hydrology of the Quaternary Catchments simulated as both individual and hydrologically interlinked cascading catchments (cf. Chapter 7, Sections 7.6 and 7.7).

In this chapter the results from the application of the techniques developed for water resources impacts assessments are divided into six main sections, as displayed in Figure 9.1. The first objective in the assessment of the potential impact of climate change on the water resources of southern Africa was to compare potential impacts of key hydrological responses using four GCMs, *viz.* the CSM (1998), Genesis (1998), HadCM2 which excludes sulphate feedbacks (HadCM2-S) and HadCM2 which includes sulphates (HadCM2+S) GCMs.

The results from the simulations using the four selected GCMs, of changes in runoff, percolation into the vadose zone and an example of a hydrological response resulting from irrigation in a Quaternary Catchment, *viz.* stormflow from irrigated areas, are presented in Section 9.1.

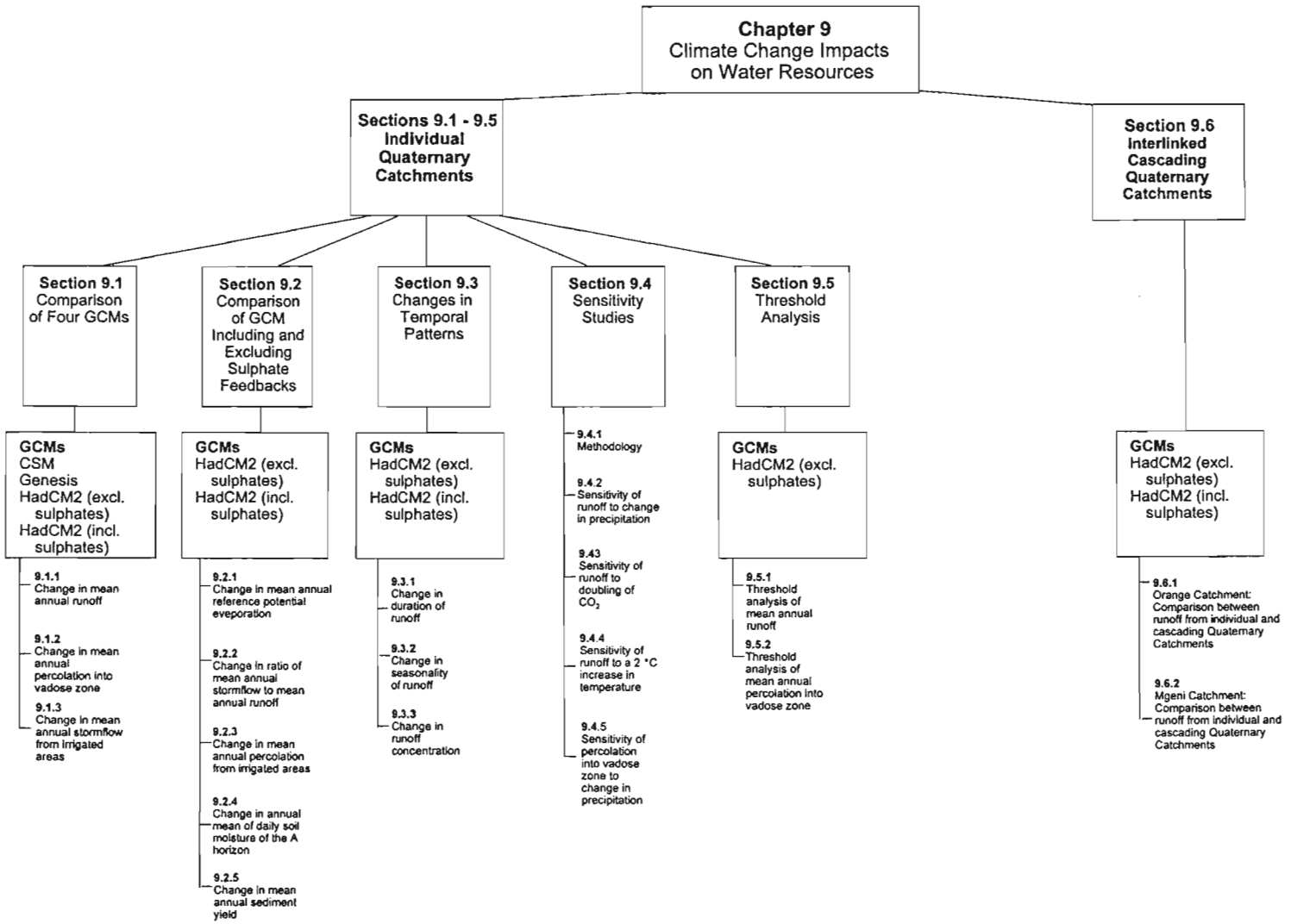


Figure 9.1 Layout plan of Chapter 9: Application of techniques to assess impacts of climate change on agriculture in southern Africa

Further simulations of potential changes in hydrological responses resulting from climate change were carried out, however, only output from HadCM2 was used. The HadCM2 GCM was selected as both maximum and minimum temperatures were provided as well as output from simulations which both included and excluded sulphate forcing. By using this GCM a comparison could be made of the difference in results obtained by including or excluding sulphate feedback. The hydrological responses simulated were the ratio of stormflow to total runoff ratio, percolation from irrigated areas, soil moisture of the A horizon and sediment yield. The water resources assessments using only HadCM2, both including and excluding sulphates, are presented in Section 9.2.

The aforementioned results indicate potential changes in the spatial patterns of hydrological responses, however, they do not give an indication of the temporal changes that might occur. Thus, the next objective was to carry out an assessment of potential changes in the temporal patterns of runoff in the study area. Potential changes in the duration, seasonality and concentration of runoff are provided in Section 9.3.

Runoff and percolation into the vadose zone are hypothesised to be sensitive to changes in climate, in particular to changes in precipitation. Sensitivity analyses were performed on individual Quaternary Catchments in southern Africa to assess the sensitivity of runoff to changes in precipitation, temperature and atmospheric $CO_2$ concentrations, as well as the sensitivity of percolation to a change in precipitation to the vadose zone in Sections 9.4. Threshold analyses were carried out on runoff and percolation to the vadose zone to ascertain when a significant increase or decrease in these hydrological responses might occur. The results from the threshold analyses are presented in Section 9.5.

The results from the first five sections were obtained by simulating hydrological responses from individual Quaternary Catchments which do not take upstream contributions into account. In reality, however, runoff from one Quaternary Catchment flows to its downstream catchment. Therefore, to assess potential changes in accumulated runoff, two case studies on large catchments in southern Africa were carried out. Potential changes in runoff from both individual Quaternary Catchments and from interlinked cascading Quaternary Catchments in these two catchments resulting from climate change as output by HadCM2 were simulated and the results are presented in Section 9.6.

## 9.1 Comparison of Potential Impacts of Climate Change on Hydrological Responses of Individual Quaternary Catchments Simulated Using Four GCMs

An *ACRU* input menu for each Quaternary Catchment was created which contained information (e.g. climate, soils, land cover) pertaining to that Quaternary Catchment (cf. Chapter 7, Section 7.6). The land use was assumed to be veld in fair hydrological condition. In addition, no anthropogenic perturbations such as abstractions from rivers or reservoirs, or inter-basin transfers were considered. Hydrological responses from these catchments were then simulated using *ACRU* with 45 years of daily climate data for

i) present climatic conditions; and

ii) perturbed future climatic conditions, using estimates of temperature and rainfall from the four GCMs (CSM (1998), Genesis (1998), HadCM2 both including and excluding sulphate forcing) for a 2X $CO_2$ climate scenario.

Maps for the southern African study region were generated representing both absolute differences between future and present hydrological responses (future - present) and the relative change in output (future / present). The absolute and relative changes in mean annual runoff, percolation into the vadose zone and stormflow from irrigated areas resulting from climate change were calculated using the four selected GCMs.

### 9.1.1 Simulated changes in mean annual runoff

The map of present mean annual runoff (MAR) as simulated by the *ACRU* model (Figure 9.2) shows that the western half of the study area (with the exception of the south-western region) experiences much less runoff than the eastern part of the study area. Any decreases in runoff for a 2X $CO_2$ scenario are assumed to have negative effects on the water resources of an area and vice versa.

Figure 9.2 Mean annual simulated runoff (mm) for present climatic conditions

Figure 9.3 depicts the absolute changes in runoff as simulated by *ACRU* using the temperature and precipitation changes simulated the four selected GCMs. Areas coloured in shades from

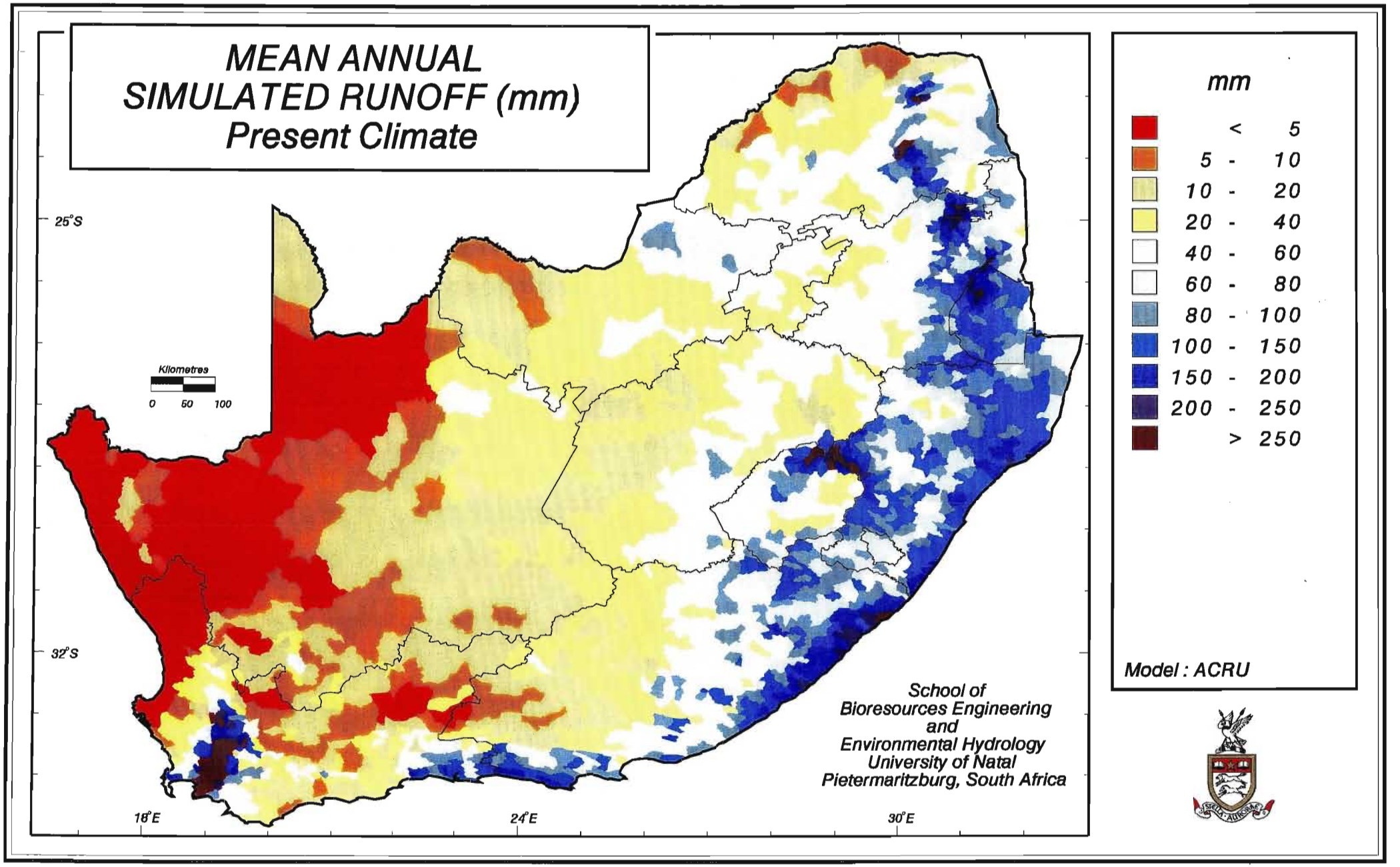
MEAN ANNUAL
SIMULATED RUNOFF (mm)
Present Climate
25°S
32°S
16°E
24°E
30°E
Kilometres
0 50 100
mm
< 5
5 - 10
10 - 20
20 - 40
40 - 60
60 - 80
80 - 100
100 - 150
150 - 200
200 - 250
> 250
Model : ACRU
School of
Bioresources Engineering
and
Environmental Hydrology
University of Natal
Pietermaritzburg, South Africa

cream to red indicate regions where runoff is predicted to decrease in predicted future climates, while shades of blues identify regions where runoff is simulated to increase with a 2X $CO_2$ climate scenario.

| Figure 9.3 | Simulated absolute changes in mean annual runoff (mm) using the future climate scenarios from the four selected GCMs |
|---|---|

With CSM (1998) output a small increase of MAR between 0 and 15 mm is predicted for most regions in the study area (Figure 9.3, top left). There are, however, slight decreases of MAR predicted using this GCM in the north and increases in excess of 45 mm along the eastern seaboard in the Eastern Cape Province. Using Genesis (1998), increases in MAR for the entire study area are simulated with *ACRU*, with large increases in excess of 150 mm predicted along the eastern coastline and parts of the high-lying Drakensberg mountains (Figure 9.3, bottom left).

Using the climate output from the two scenarios of HadCM2, on the other hand, the *ACRU* model predicts slight decreases in MAR of less than 15 mm for most of the study region (Figure 9.3, top and bottom right). There are, however, significant decreases in MAR (greater than 150 mm) predicted from future climates generated by these GCMs in the south-west of the study area and in the north of Lesotho. Small increases in MAR could be expected along the eastern coastline according to these GCMs. Output from HadCM2+S (Figure 9.3, bottom right) appears to produce more areas with increases in runoff than output from HadCM2 where sulphate forcing is excluded.

Figure 9.4 depicts the simulated relative change in MAR as a ratio of the future runoff to present runoff, using the climate as predicted by the four selected GCMs together with the *ACRU* model. Areas of predicted relative decreases in MAR are shown in shades of light brown to red while to areas of simulated increases are shown in blue. The cream areas indicate those regions where the GCMs' climate output, when used in *ACRU,* simulated no significant relative changes in MAR (i.e. within the range of a 10% increase to a 10% decrease).

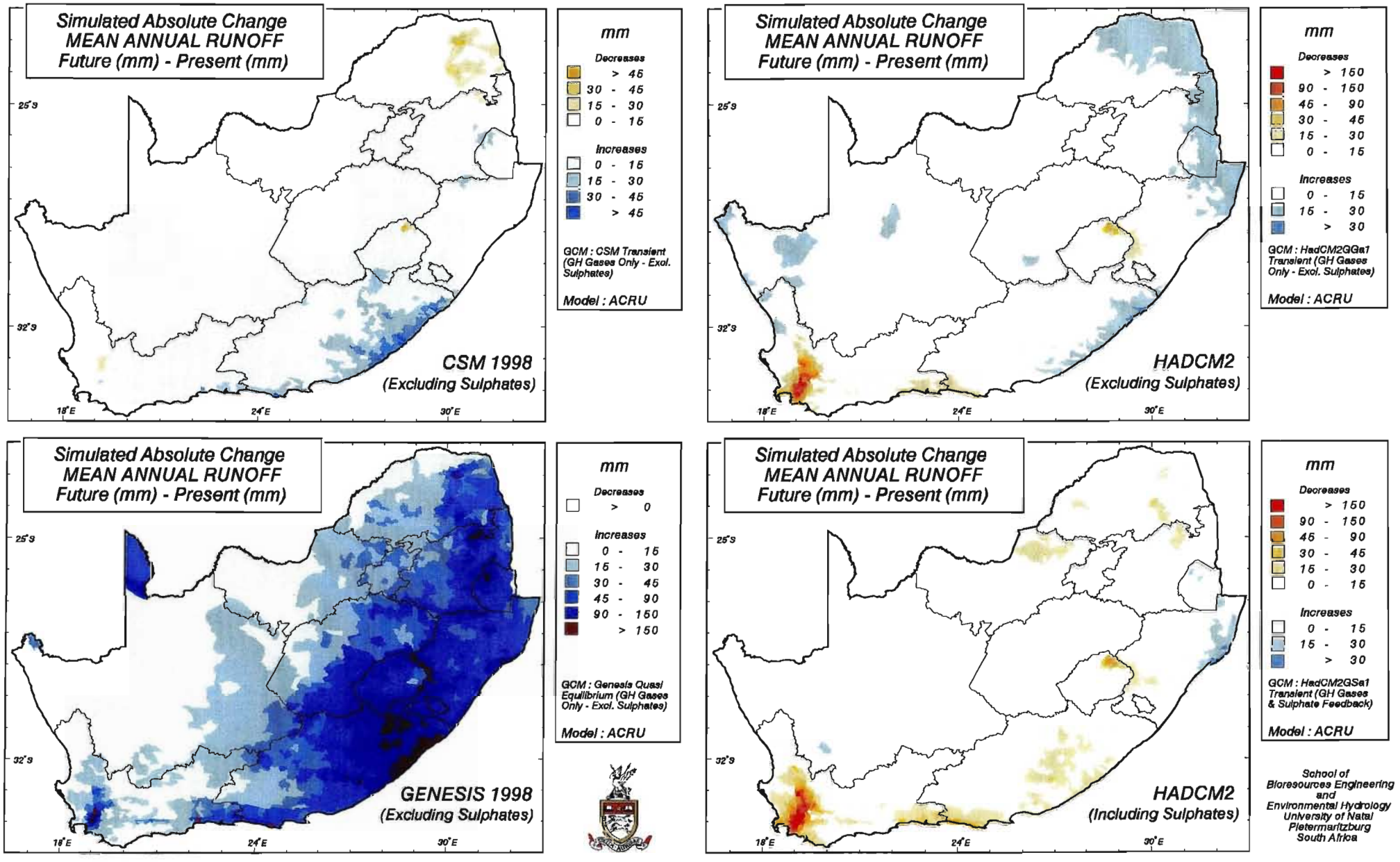
Simulated Absolute Change
MEAN ANNUAL RUNOFF
Future (mm) - Present (mm)
25°S
32°S
18°E
24°E
30°E
CSM 1998
(Excluding Sulphates)
mm
Decreases
> 45
30 - 45
15 - 30
0 - 15
Increases
0 - 15
15 - 30
30 - 45
> 45
GCM : CSM Transient (GH Gases Only - Excl. Sulphates)
Model : ACRU
Simulated Absolute Change
MEAN ANNUAL RUNOFF
Future (mm) - Present (mm)
HADCM2
(Excluding Sulphates)
mm
Decreases
> 150
90 - 150
45 - 90
30 - 45
15 - 30
0 - 15
Increases
0 - 15
15 - 30
> 30
GCM : HadCM2GGa1 Transient (GH Gases Only - Excl. Sulphates)
Model : ACRU
Simulated Absolute Change
MEAN ANNUAL RUNOFF
Future (mm) - Present (mm)
GENESIS 1998
(Excluding Sulphates)
mm
Decreases
> 0
Increases
0 - 15
15 - 30
30 - 45
45 - 90
90 - 150
> 150
GCM : Genesis Quasi Equilibrium (GH Gases Only - Excl. Sulphates)
Model : ACRU
Simulated Absolute Change
MEAN ANNUAL RUNOFF
Future (mm) - Present (mm)
HADCM2
(Including Sulphates)
mm
Decreases
> 150
90 - 150
45 - 90
30 - 45
15 - 30
0 - 15
Increases
0 - 15
15 - 30
> 30
GCM : HadCM2GSa1 Transient (GH Gases & Sulphate Feedback)
Model : ACRU
School of
Bioresources Engineering
and
Environmental Hydrology
University of Natal
Pietermaritzburg
South Africa

Figure 9.4 Simulated relative changes in mean annual runoff using the future climate scenarios from the four selected GCMs

Even though the future climate from CSM (1998) does not translate into any significant increases in absolute MAR along the west coast, the relative change in MAR in the area, as simulated by *ACRU*, is significant (Figure 9.4, top left). Using output from this GCM in *ACRU*, the northern regions of the study area could expect a small decrease in relative MAR. The map generated using output from Genesis (1998) shows a large portion of the central study region to have between two and six times more runoff simulated by *ACRU* for a 2X $CO_2$ scenario (Figure 9.4, bottom left).

The future climate scenario of HadCM2-S produces predictions of significant decreases, to only 30% of the present simulated MAR, in some regions of the western part of the study area (Figure 9.4, top right). The same GCM, but including sulphates, however, generates a more conservative change in MAR for 2X $CO_2$ climatic conditions. This GCM predicts climates which produce significant increases (> two times) in simulated MAR with the *ACRU* model compared to the present runoff along parts the western coast in close proximity to areas with could experience less than 30% of their present MAR.

### 9.1.2 Simulated changes in percolation into the vadose zone

Water supply from precipitation, streamflow or groundwater may be impacted by climate change (IPCC, 1996a). Therefore, climate change may affect regions that are solely or highly dependent on groundwater for water supply (Conley, 1996). Groundwater supplies have to be replenished, i.e. recharged, periodically. Percolation rates may decrease or increase depending on the climate change scenario considered. In this study saturated drainage out of the bottom of the soil's B horizon into the vadose, i.e. intermediate, zone was simulated using the *ACRU* model. This saturated drainage is an index of percolation through the soil profile and is assumed to eventually percolate into the groundwater store. In these simulations drainage into the vadose zone excludes channel transmission losses and drainage from irrigated areas of the catchment.

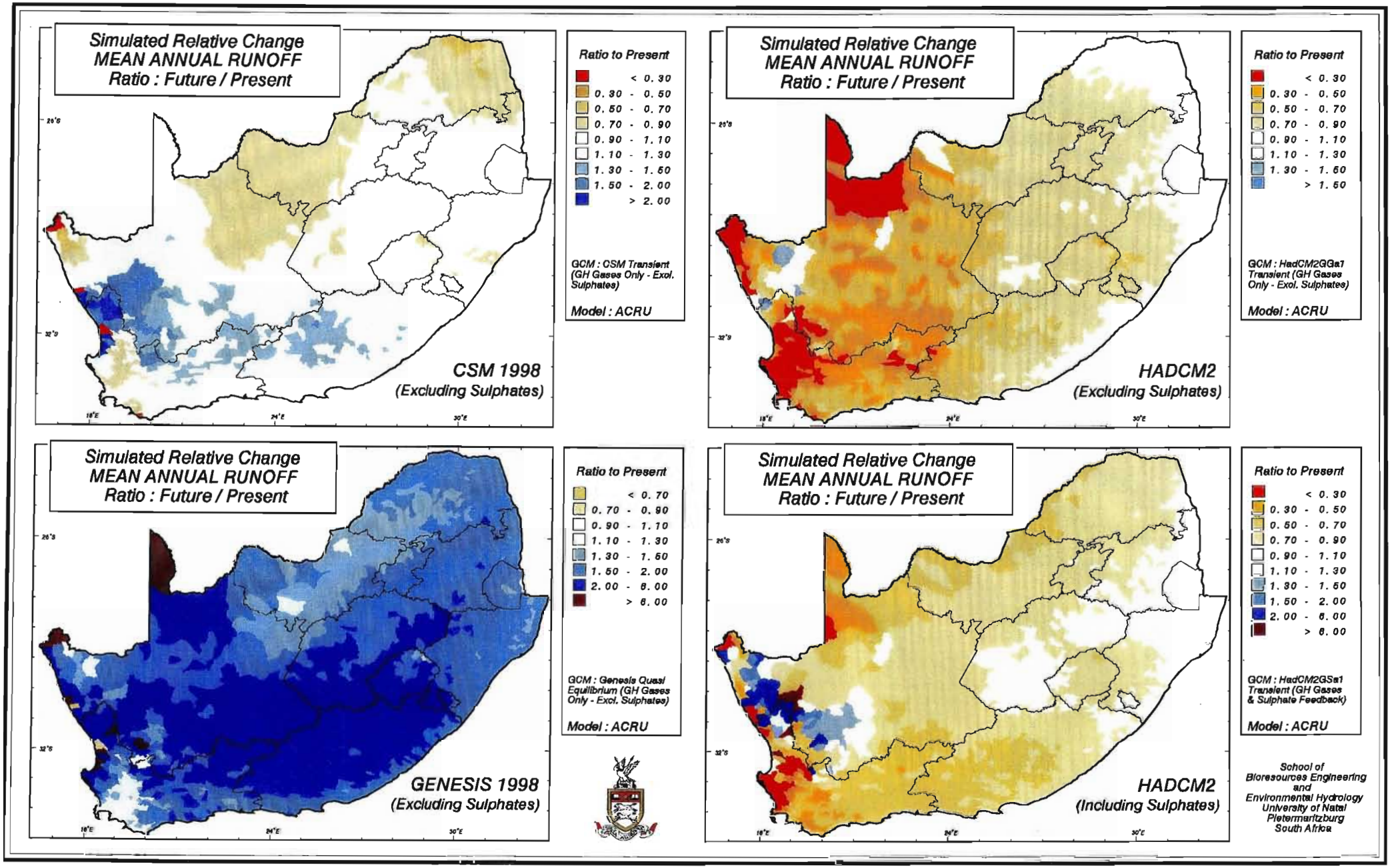
Simulated Relative Change
MEAN ANNUAL RUNOFF
Ratio : Future / Present
Ratio to Present
< 0.30
0.30 - 0.50
0.50 - 0.70
0.70 - 0.90
0.90 - 1.10
1.10 - 1.30
1.30 - 1.50
1.50 - 2.00
> 2.00
GCM : CSM Transient (GH Gases Only - Excl. Sulphates)
Model : ACRU
CSM 1998
(Excluding Sulphates)
Simulated Relative Change
MEAN ANNUAL RUNOFF
Ratio : Future / Present
Ratio to Present
< 0.30
0.30 - 0.50
0.50 - 0.70
0.70 - 0.90
0.90 - 1.10
1.10 - 1.30
1.30 - 1.50
> 1.50
GCM : HadCM2GGa1 Transient (GH Gases Only - Excl. Sulphates)
Model : ACRU
HADCM2
(Excluding Sulphates)
Simulated Relative Change
MEAN ANNUAL RUNOFF
Ratio : Future / Present
Ratio to Present
< 0.70
0.70 - 0.90
0.90 - 1.10
1.10 - 1.30
1.30 - 1.50
1.50 - 2.00
2.00 - 6.00
> 6.00
GCM : Genesis Quasi Equilibrium (GH Gases Only - Excl. Sulphates)
Model : ACRU
GENESIS 1998
(Excluding Sulphates)
Simulated Relative Change
MEAN ANNUAL RUNOFF
Ratio : Future / Present
Ratio to Present
< 0.30
0.30 - 0.50
0.50 - 0.70
0.70 - 0.90
0.90 - 1.10
1.10 - 1.30
1.30 - 1.50
1.50 - 2.00
2.00 - 6.00
> 6.00
GCM : HadCM2GSa1 Transient (GH Gases & Sulphate Feedback)
Model : ACRU
HADCM2
(Including Sulphates)
School of
Bioresources Engineering
and
Environmental Hydrology
University of Natal
Pietermaritzburg
South Africa

Areas with a high soil moisture content in the B horizon generally exhibit high rates of percolation into the vadose zone. Low rates of percolation are evident in the arid and semi-arid interior of southern Africa. Most of the study region receives less than 5 mm percolation into the vadose zone under present climatic conditions (Figure 9.5). Parts of the Western Cape Province, however, receive more than 80 mm percolation per annum.

| | |
|---|---|
| Figure 9.5 | Mean annual simulated percolation (mm) into the vadose zone for present climatic conditions |

When percolation into the vadose zone is simulated by the *ACRU* model, future climates from all four selected GCMs generate a 0 to 10 mm increase in mean annual percolation for most of the study region (Figure 9.6). As was the case in the simulations of absolute changes in MAR in Figure 9.3, future climate scenarios from HadCM2 produce decreases in percolation into the vadose zone in the south-west of the study area and north of Lesotho (Figure 9.6, top right and bottom right). When using CSM (1998) output in *ACRU*, small decreases in these regions are simulated. Using output from Genesis (1998), on the other hand, produces changes in precipitation from which *ACRU* simulates large increases (in excess of 40 mm) in mean annual percolation in the eastern parts of the study area.

| | |
|---|---|
| Figure 9.6 | Simulated absolute changes in mean annual percolation into the vadose zone (mm) using the future climate scenarios from the four selected GCMs |

CSM (1998) future climate generates significant relative decreases in simulated percolation (Figure 9.7, top left). According to the future climate scenario from this GCM a large portion of the study area is likely to receive only 5% of present percolation to the vadose zone. Relative increases are, however, expected along the eastern coastline and other isolated areas. Climate output from HadCM2+S also generates large relative decreases in percolation (Figure 9.7, bottom right).

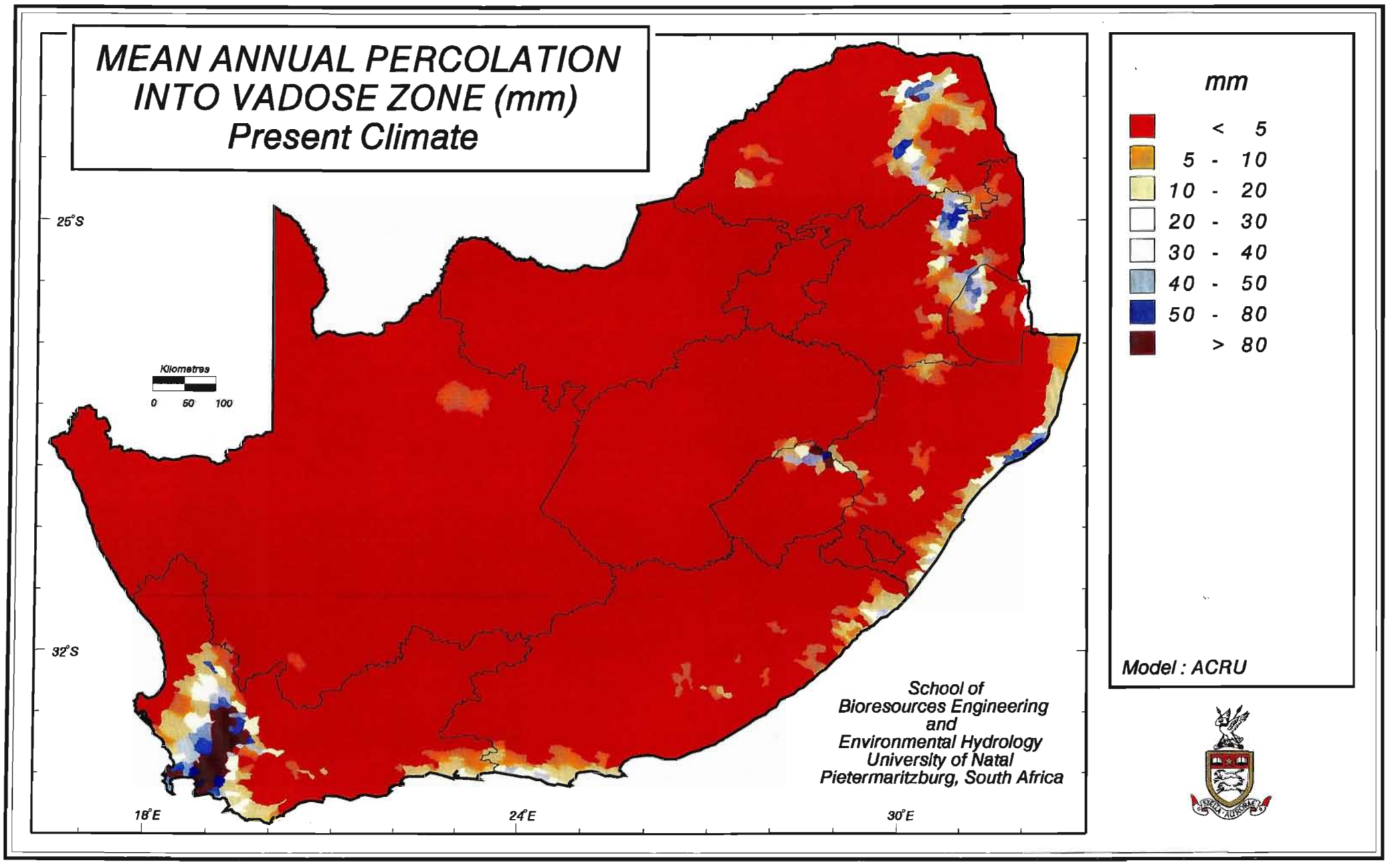
MEAN ANNUAL PERCOLATION INTO VADOSE ZONE (mm)
Present Climate
25°S
32°S
18°E
24°E
30°E
Kilometres
0 50 100
mm
< 5
5 - 10
10 - 20
20 - 30
30 - 40
40 - 50
50 - 80
> 80
Model : ACRU
School of
Bioresources Engineering
and
Environmental Hydrology
University of Natal
Pietermaritzburg, South Africa

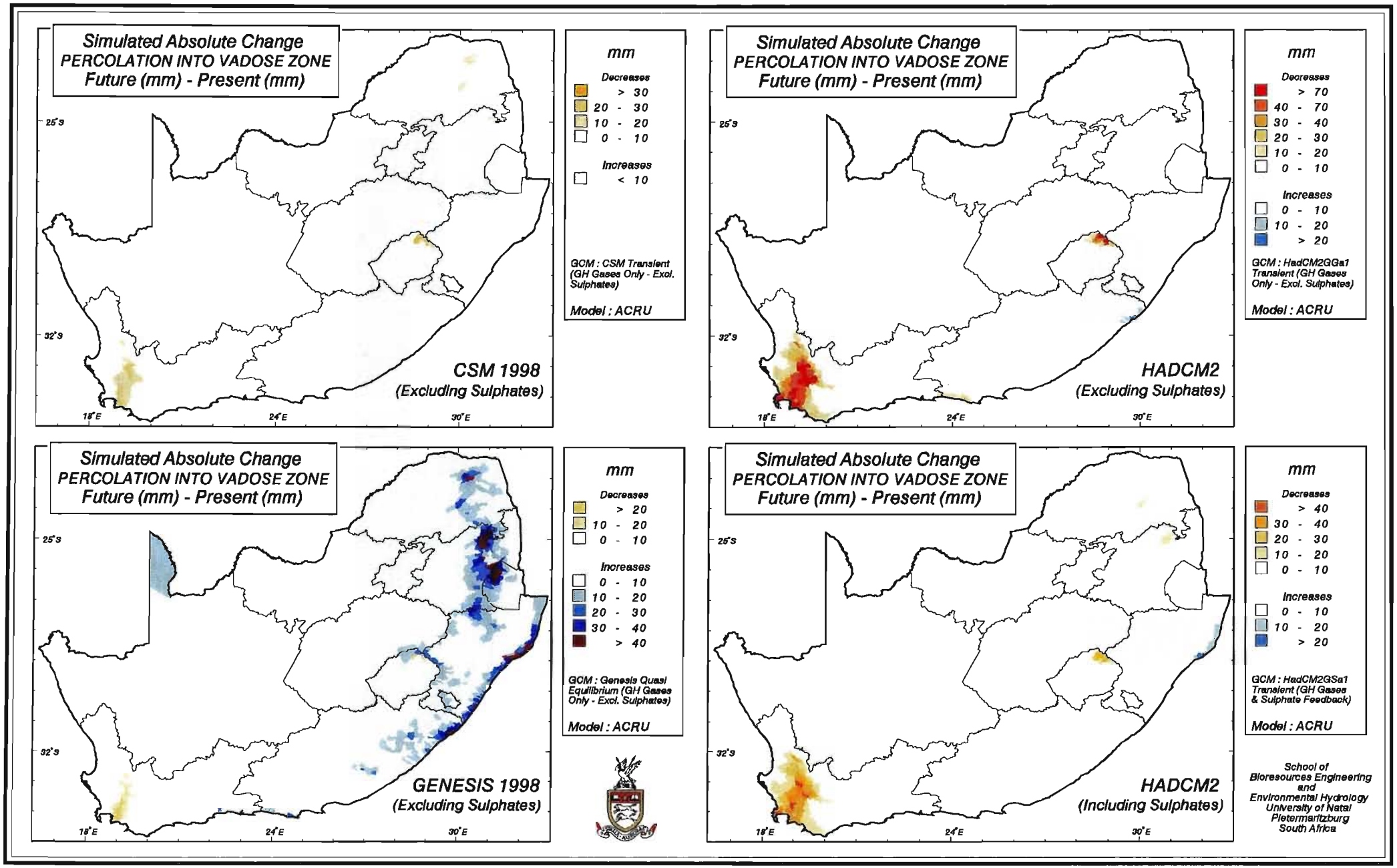
Simulated Absolute Change
PERCOLATION INTO VADOSE ZONE
Future (mm) - Present (mm)
25°S
32°S
18°E
24°E
30°E
CSM 1998
(Excluding Sulphates)
mm
Decreases
> 30
20 - 30
10 - 20
0 - 10
Increases
< 10
GCM : CSM Transient (GH Gases Only - Excl. Sulphates)
Model : ACRU
Simulated Absolute Change
PERCOLATION INTO VADOSE ZONE
Future (mm) - Present (mm)
HADCM2
(Excluding Sulphates)
mm
Decreases
> 70
40 - 70
30 - 40
20 - 30
10 - 20
0 - 10
Increases
0 - 10
10 - 20
> 20
GCM : HadCM2GGa1 Transient (GH Gases Only - Excl. Sulphates)
Model : ACRU
Simulated Absolute Change
PERCOLATION INTO VADOSE ZONE
Future (mm) - Present (mm)
GENESIS 1998
(Excluding Sulphates)
mm
Decreases
> 20
10 - 20
0 - 10
Increases
0 - 10
10 - 20
20 - 30
30 - 40
> 40
GCM : Genesis Quasi Equilibrium (GH Gases Only - Excl. Sulphates)
Model : ACRU
Simulated Absolute Change
PERCOLATION INTO VADOSE ZONE
Future (mm) - Present (mm)
HADCM2
(Including Sulphates)
mm
Decreases
> 40
30 - 40
20 - 30
10 - 20
0 - 10
Increases
0 - 10
10 - 20
> 20
GCM : HadCM2GSa1 Transient (GH Gases & Sulphate Feedback)
Model : ACRU
School of Bioresources Engineering and Environmental Hydrology
University of Natal
Pietermaritzburg
South Africa

| Figure 9.7 | Simulated relative changes in mean annual percolation into the vadose zone using the future climate scenarios from the four selected GCMs |
|---|---|

HadCM2-S produces a future climate from which the *ACRU* model predicts that most regions could expect within a 20% decrease or increase in percolation (Figure 9.7, top right). There are some areas that could expect five times more percolation than they do now, but there does not seem to be any pattern in the location of these areas. The south-western area could expect significant decreases in percolation according to this GCM's predictions for a 2X $CO_2$ climate. As would be expected, Genesis' (1998) future climate produces large relative increases in percolation through the soil profile for large portions of the study area (Figure 9.7, bottom left).

### 9.1.3 Simulated changes in stormflow from irrigated areas

*ACRU* contains routines which can simulate irrigation water requirements for a range of crops under a variety of soil conditions and different modes of applying, i.e. scheduling, the irrigated water. Output from irrigation routines also contain estimates of the amount of stormflow and deep percolation generated from irrigated areas. For the irrigation simulations which follow it was assumed that both a summer and winter crop were irrigated on a 0.8 m deep sandy loam soil and that there were no constraints to the supply of water that was available. The assumption was made that water was applied at an 80% efficiency to fill the soil profile to its drained upper limit on demand once the crop had depleted the plant available water to 50% (cf. Chapter 7, Section 7.3.2.3).

Mean annual stormflow from irrigated areas is an index of management of irrigation water application, with high values indicating, *inter alia*, that a different mode of application (e.g. deficit irrigation) might yield lower stormflow losses, which deplete the field of topsoil and natural / artificial nutrients. Under present climatic conditions mean annual stormflow from irrigated areas ranges from only 5 mm in the western parts of the study area where irrigation is usually the major source of water to crops to over 250 mm along the eastern seaboard and in the south-western regions where irrigation is often only supplementary to rainfall in the rainy season (Figure 9.8).

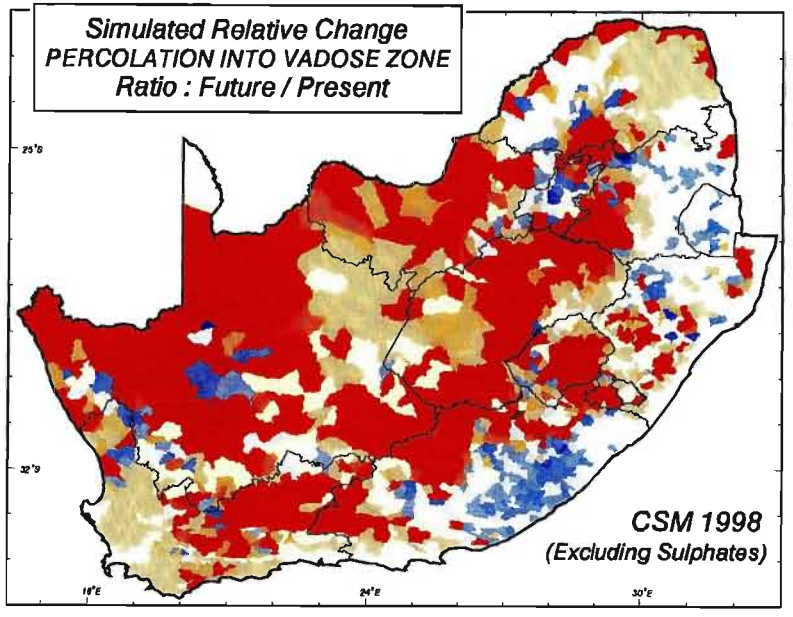


Ratio to Present

| | |
|---|---|
| < | 0.05 |
| 0.05 - | 0.10 |
| 0.10 - | 0.20 |
| 0.20 - | 0.40 |
| 0.40 - | 0.80 |
| 0.80 - | 1.20 |
| 1.20 - | 1.60 |
| 1.60 - | 2.00 |
| 2.00 - | 5.00 |
| 5.00 - | 10.00 |
| > | 10.00 |

GCM : CSM Transient (GH Gases Only - Exol. Sulphates)

Model : ACRU

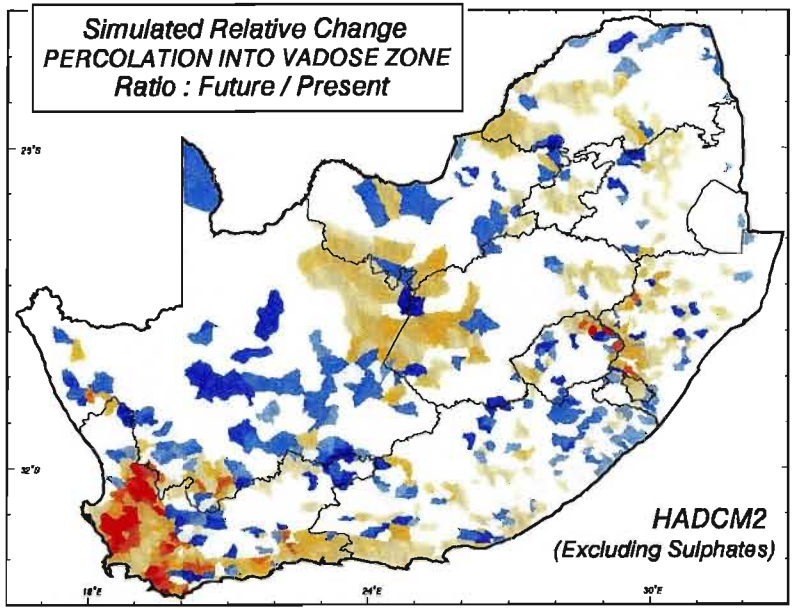


Ratio to Present

| | |
|---|---|
| < | 0.05 |
| 0.05 - | 0.10 |
| 0.10 - | 0.20 |
| 0.20 - | 0.40 |
| 0.40 - | 0.80 |
| 0.80 - | 1.20 |
| 1.20 - | 1.60 |
| 1.60 - | 2.00 |
| 2.00 - | 5.00 |
| > | 5.00 |

GCM : HadCM2GGa1 Transient (GH Gases Only - Exol. Sulphates)

Model : ACRU

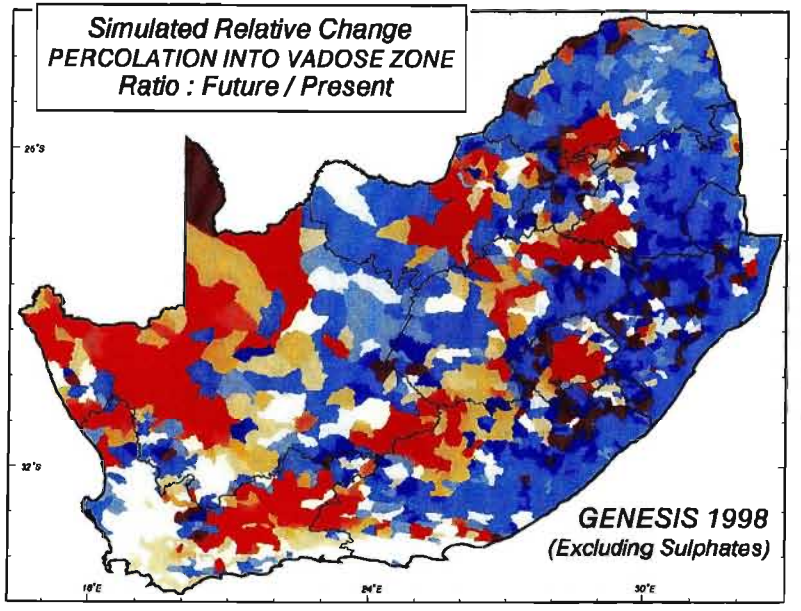


Ratio to Present

| | |
|---|---|
| < | 0.05 |
| 0.05 - | 0.10 |
| 0.10 - | 0.20 |
| 0.20 - | 0.40 |
| 0.40 - | 0.80 |
| 0.80 - | 1.20 |
| 1.20 - | 1.60 |
| 1.60 - | 2.00 |
| 2.00 - | 5.00 |
| 5.00 - | 10.00 |
| > | 10.00 |

GCM : Genesis Quasi Equilibrium (GH Gases Only - Exol. Sulphates)

Model : ACRU

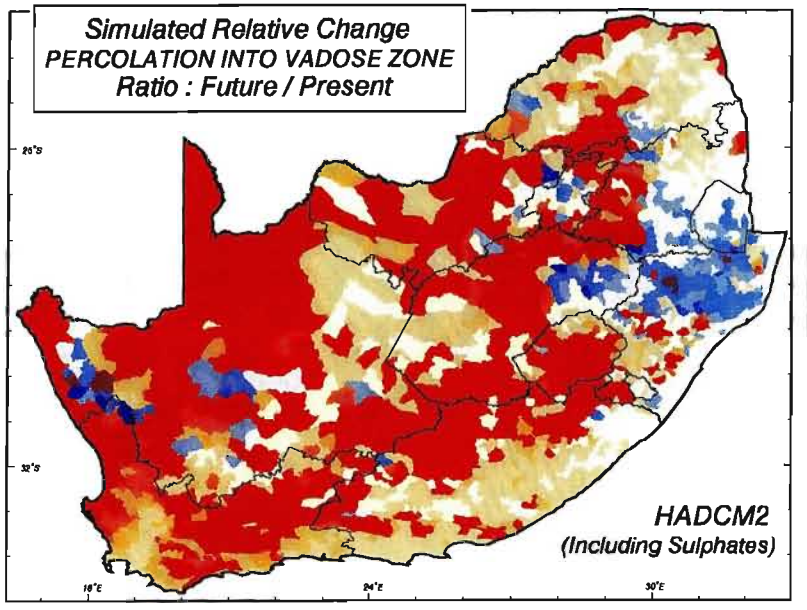


Ratio to Present

| | |
|---|---|
| < | 0.05 |
| 0.05 - | 0.10 |
| 0.10 - | 0.20 |
| 0.20 - | 0.40 |
| 0.40 - | 0.80 |
| 0.80 - | 1.20 |
| 1.20 - | 1.60 |
| 1.60 - | 2.00 |
| 2.00 - | 5.00 |
| 5.00 - | 10.00 |
| > | 10.00 |

GCM : HadCM2GSa1 Transient (GH Gases & Sulphate Feedback)

Model : ACRU

School of
Bioresources Engineering
and
Environmental Hydrology
University of Natal
Pietermaritzburg
South Africa

| Figure 9.8 | Mean annual simulated stormflow from irrigated areas (mm) for present climatic conditions |
|---|---|

From CSM (1998) output, *ACRU* predicts that more than half of the study area can expect an absolute increase in stormflow from irrigated areas in most areas (Figure 9.9, top left), with the greatest increases, in excess of 30 mm, on the Eastern Cape coastline. The northern areas could in future experience decreases in stormflow from irrigated areas according to output from this GCM.

| Figure 9.9 | Simulated absolute changes in mean annual stormflow from irrigated areas (mm) using the future climate scenarios from the four selected GCMs |
|---|---|

As in the other hydrological responses, a future climate predicted by Genesis (1998) again produces large increases in this *ACRU* generated hydrological response, with some areas of the Eastern Cape simulated to yield a more than 90 mm increase in stormflow from irrigated areas (Figure 9.9, bottom left). The patterns of stormflow from irrigation predicted by *ACRU* when using HadCM2's climate output (Figure 9.9, top right and bottom right) are similar to the increases and decreases reflected in the runoff maps (Figure 9.3, top right and bottom right).

CSM (1998) future climate used in *ACRU* generates a range of relative irrigation stormflow changes, from a 30% decrease to a 30% increase (Figure 9.10, top left). From HadCM2-S output and *ACRU*, however, estimates are produced indicating that some regions in the north and west that could expect 70% less stormflow from irrigated areas than at present (Figure 9.10, top right).

| Figure 9.10 | Simulated relative changes in mean annual stormflow from irrigated areas using the future climate scenarios from the four selected GCMs |
|---|---|

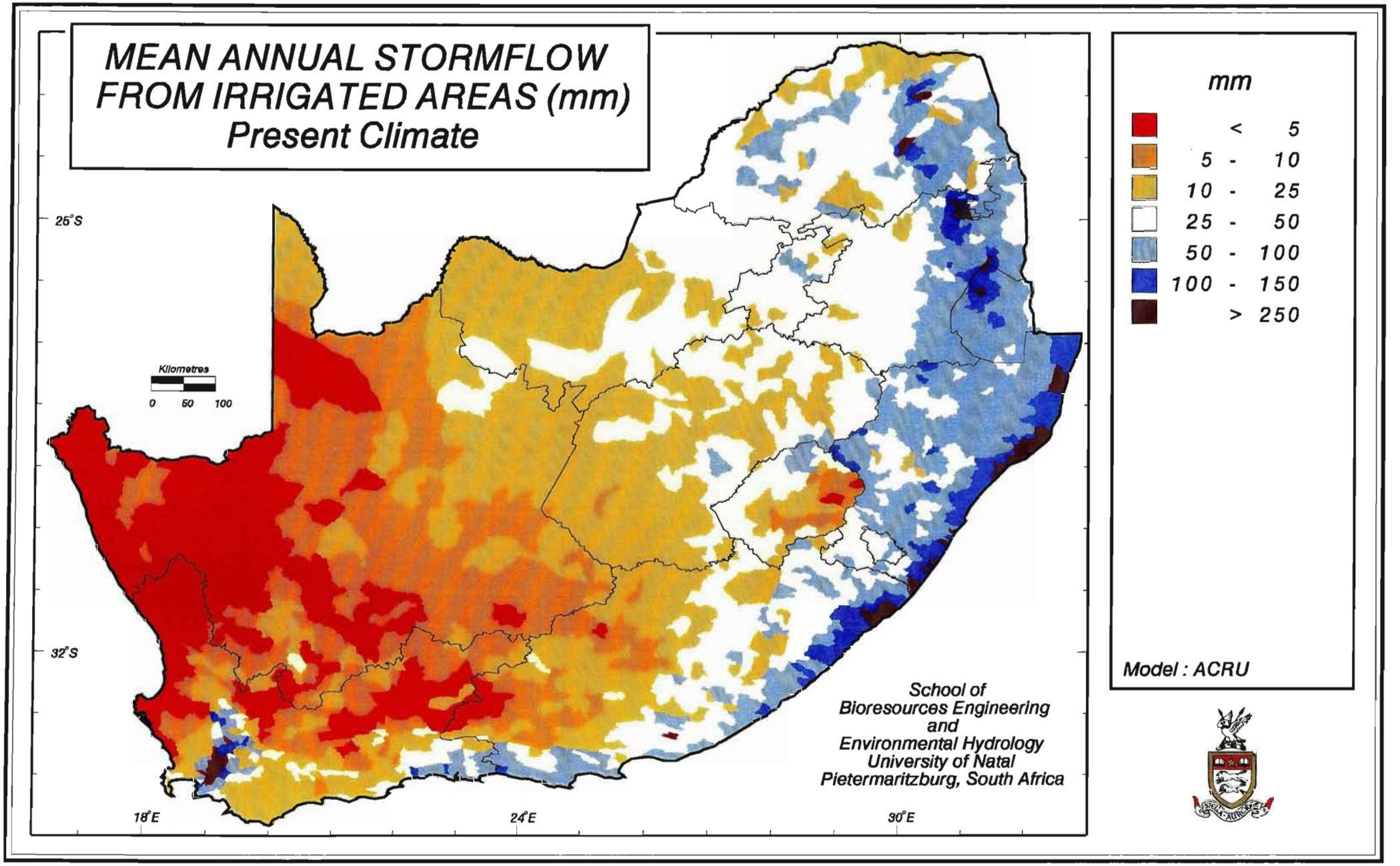
MEAN ANNUAL STORMFLOW
FROM IRRIGATED AREAS (mm)
Present Climate
25°S
32°S
18°E
24°E
30°E
Kilometres
0 50 100
mm
< 5
5 - 10
10 - 25
25 - 50
50 - 100
100 - 150
> 250
Model : ACRU
School of
Bioresources Engineering
and
Environmental Hydrology
University of Natal
Pietermaritzburg, South Africa

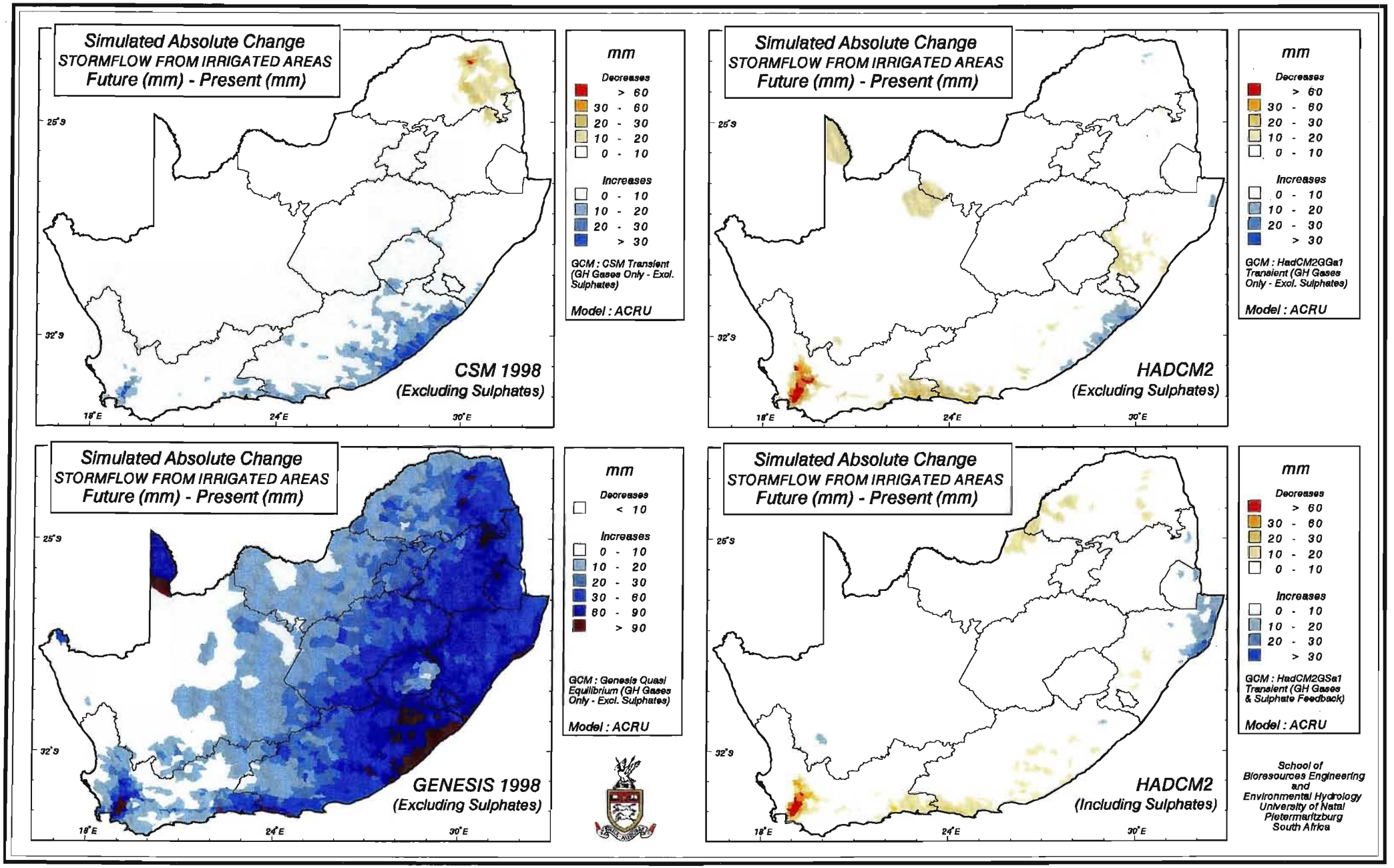
Simulated Absolute Change
STORMFLOW FROM IRRIGATED AREAS
Future (mm) - Present (mm)
25°S
32°S
18°E
24°E
30°E
CSM 1998
(Excluding Sulphates)
mm
Decreases
> 60
30 - 60
20 - 30
10 - 20
0 - 10
Increases
0 - 10
10 - 20
20 - 30
> 30
GCM : CSM Transient (GH Gases Only - Excl. Sulphates)
Model : ACRU
Simulated Absolute Change
STORMFLOW FROM IRRIGATED AREAS
Future (mm) - Present (mm)
HADCM2
(Excluding Sulphates)
mm
Decreases
> 60
30 - 60
20 - 30
10 - 20
0 - 10
Increases
0 - 10
10 - 20
20 - 30
> 30
GCM : HadCM2GGa1 Transient (GH Gases Only - Excl. Sulphates)
Model : ACRU
Simulated Absolute Change
STORMFLOW FROM IRRIGATED AREAS
Future (mm) - Present (mm)
GENESIS 1998
(Excluding Sulphates)
mm
Decreases
< 10
Increases
0 - 10
10 - 20
20 - 30
30 - 60
60 - 90
> 90
GCM : Genesis Quasi Equilibrium (GH Gases Only - Excl. Sulphates)
Model : ACRU
Simulated Absolute Change
STORMFLOW FROM IRRIGATED AREAS
Future (mm) - Present (mm)
HADCM2
(Including Sulphates)
mm
Decreases
> 60
30 - 60
20 - 30
10 - 20
0 - 10
Increases
0 - 10
10 - 20
20 - 30
> 30
GCM : HadCM2GSa1 Transient (GH Gases & Sulphate Feedback)
Model : ACRU
School of Bioresources Engineering and Environmental Hydrology
University of Natal
Pietermaritzburg
South Africa

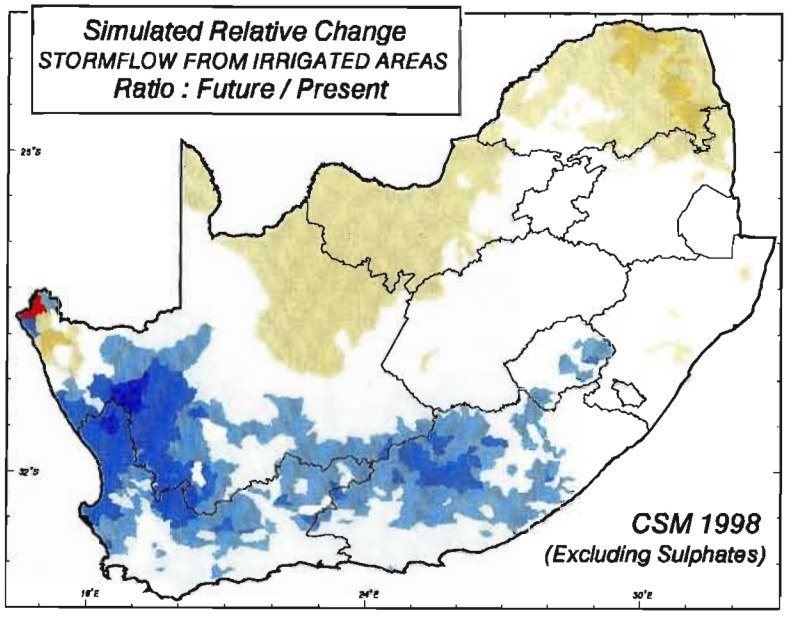


Ratio to Present

| | |
|---|---|
| 0.0 - | 0.3 |
| 0.3 - | 0.5 |
| 0.5 - | 0.7 |
| 0.7 - | 0.9 |
| 0.9 - | 1.1 |
| 1.1 - | 1.3 |
| 1.3 - | 1.5 |
| 1.5 - | 3.0 |
| 3.0 - | 6.0 |
| > | 6.0 |

GCM : CSM Transient (GH Gases Only - Excl. Sulphates)

Model : ACRU

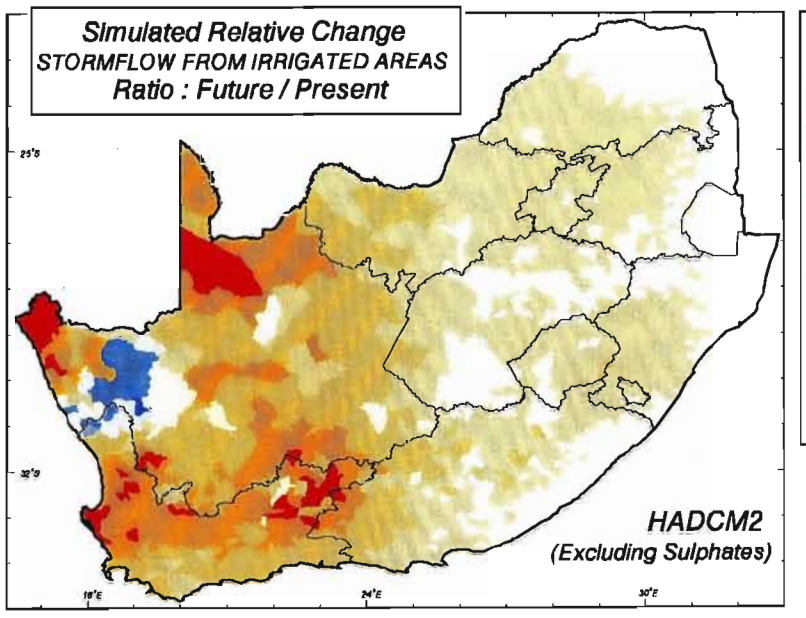


Ratio to Present

| | |
|---|---|
| 0.0 - | 0.3 |
| 0.3 - | 0.5 |
| 0.5 - | 0.7 |
| 0.7 - | 0.9 |
| 0.9 - | 1.1 |
| 1.1 - | 1.3 |
| 1.3 - | 1.5 |
| 1.5 - | 3.0 |
| > | 3.0 |

GCM : HadCM2GGa1 Transient (GH Gases Only - Excl. Sulphates)

Model : ACRU

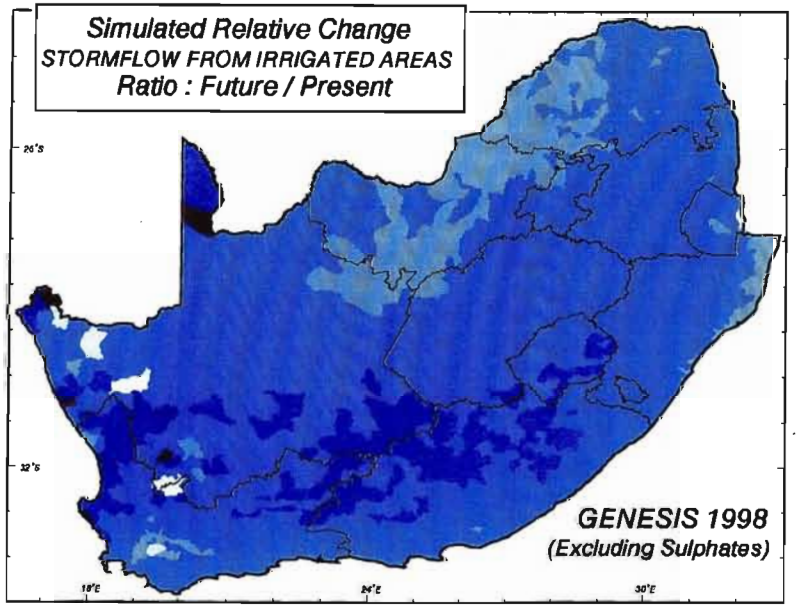


Ratio to Present

| | |
|---|---|
| < | 1.1 |
| 1.1 - | 1.3 |
| 1.3 - | 1.5 |
| 1.5 - | 3.0 |
| 3.0 - | 6.0 |
| 6.0 - | 12.0 |
| > | 12.0 |

GCM : Genesis Quasi Equilibrium (GH Gases Only - Excl. Sulphates)

Model : ACRU

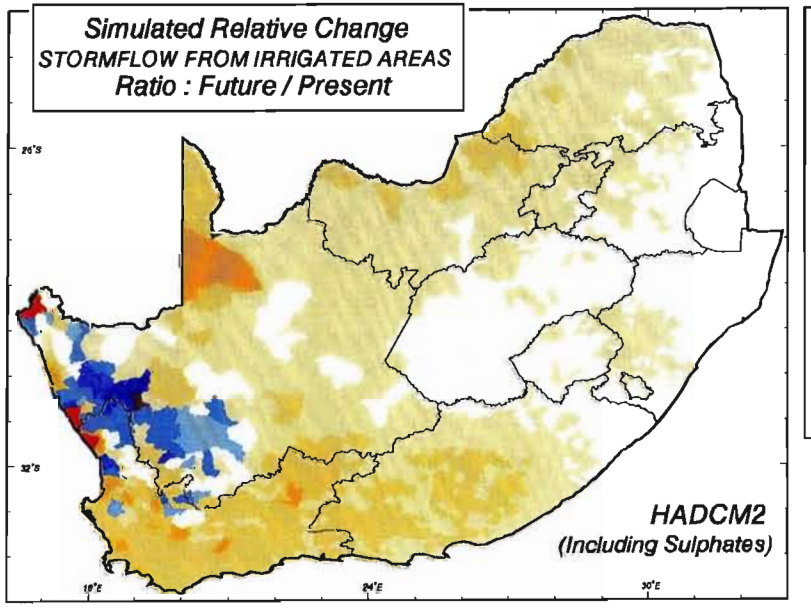


Ratio to Present

| | |
|---|---|
| 0.0 - | 0.3 |
| 0.3 - | 0.5 |
| 0.5 - | 0.7 |
| 0.7 - | 0.9 |
| 0.9 - | 1.1 |
| 1.1 - | 1.3 |
| 1.3 - | 1.5 |
| 1.5 - | 3.0 |
| 3.0 - | 6.0 |
| 6.0 - | 12.0 |
| > | 12.0 |

GCM : HadCM2GSa1 Transient (GH Gases & Sulphate Feedback)

Model : ACRU

School of
Bioresources Engineering
and
Environmental Hydrology
University of Natal
Pietermaritzburg
South Africa

The future climate of HadCM2+S (Figure 9.10, bottom right) produces irrigation stormflows with *ACRU* displaying a similar pattern as that generated using output from HadCM2-S. However, the decreases in stormflow are not as high. As with the other hydrological responses, output from Genesis (1998) generates large increases in stormflow from irrigated areas (Figure 9.10, bottom left).

From the results obtained in Section 9.1 it is evident that simulations which used Genesis (1998) for scenarios of future climate displays notable differences to the results obtained using the other three GCMs. This GCM is a quasi-equilibrium GCM compared to the other three GCMs, which are transient. This could be one reason for the discrepancies. From the results obtained it is felt that this GCM should not be used in subsequent simulations in this thesis.

## 9.2 Comparison of Potential Impacts of Climate Change on Hydrological Responses using HadCM2, Both Including and Excluding Sulphate Forcing

For the remaining impact assessments of climate change on hydrological responses, only the HadCM2 GCM, both including and excluding sulphate forcing, was used. The HadCM2 GCM was selected because both maximum and minimum temperatures are output and simulations which both included and excluded the effect of sulphate forcing in the atmosphere could be undertaken to assess the impact of sulphate feedback on hydrological responses in the study area.

### 9.2.1 Simulated changes in mean annual reference potential evaporation

A hydrological simulation model such as *ACRU* requires an input of potential evaporation as one of its important driver variables (Schulze and Kunz, 1995). For this study the Linacre (1991) equation was selected (cf. Section 7.6 of Chapter 7) as the reference for potential evaporation, $E_r$ , as it was derived using the principles of the physically based Penman equation yet it uses only maximum and minimum temperatures (to estimate solar radiation and vapour pressure deficit), together with latitude (to modulate the radiation component for day length) and altitude (which influences the psychrometric constant, net radiation and vapour pressure). The present mean annual reference potential evaporation for the study area ranges

from less than 1 400 mm along the western coastline to greater than 2 600 mm in the north-central region (Figure 9.11, top).

| | |
|---|---|
| Figure 9.11 | Mean annual potential evaporation (mm) for present climatic conditions (top), ratio of mean annual stormflow to mean annual total runoff as simulated for present climatic conditions (middle) and mean annual percolation from irrigated areas (mm) for present climatic conditions (bottom) |

HadCM2-S predicts changes in temperature which, when applied in the Linacre equation for $E_r$ , result in an increase in mean annual evaporation of between 250 and 650 mm. The highest increases in mean annual potential evaporation could be expected in the northern central regions and the smallest increases in the south-west, according to temperatures changes predicted by this GCM (Figure 9.12, top left). The increase in mean annual evaporation in the north equates to a 25% increase in mean annual evaporation in that area compared to a 15% increase in the south-west of the study area when using the Linacre equation to determine reference for potential evaporation (Figure 9.12, top right).

| | |
|---|---|
| Figure 9.12 | Mean annual potential evaporation using the Linacre (1991) equation (mm): simulated absolute changes (top left) and simulated relative changes (top right) using the future climate scenario from HadCM2-S; simulated absolute changes (bottom left) and simulated relative changes (bottom right) using the future climate scenario from HadCM2+S |

Increases in mean annual potential evaporation were also obtained using the Linacre (1991) equation and changes in temperature from HadCM2 but including sulphate feedback (Figure 9.12, bottom left). These increases, however, were not as large as those obtained using this GCM but excluding sulphates (cf. Figure 9.12, top left). The increases range from less than 250 mm along the southern African coastline to over 350 mm in the northern central regions. On average the increases in potential evaporation were found to be 200 mm higher when sulphate forcing is excluded from the HadCM2 simulations. In relative terms these increases

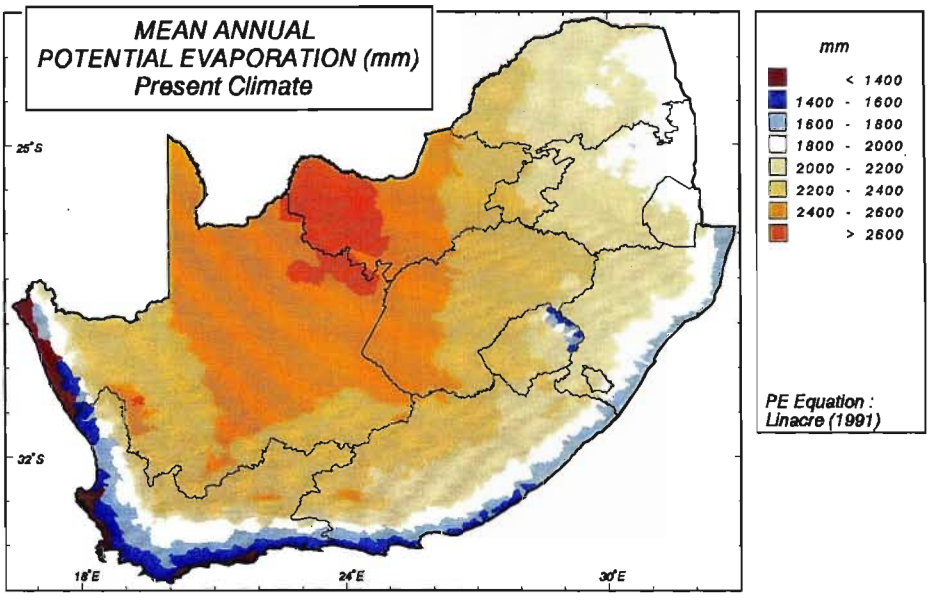


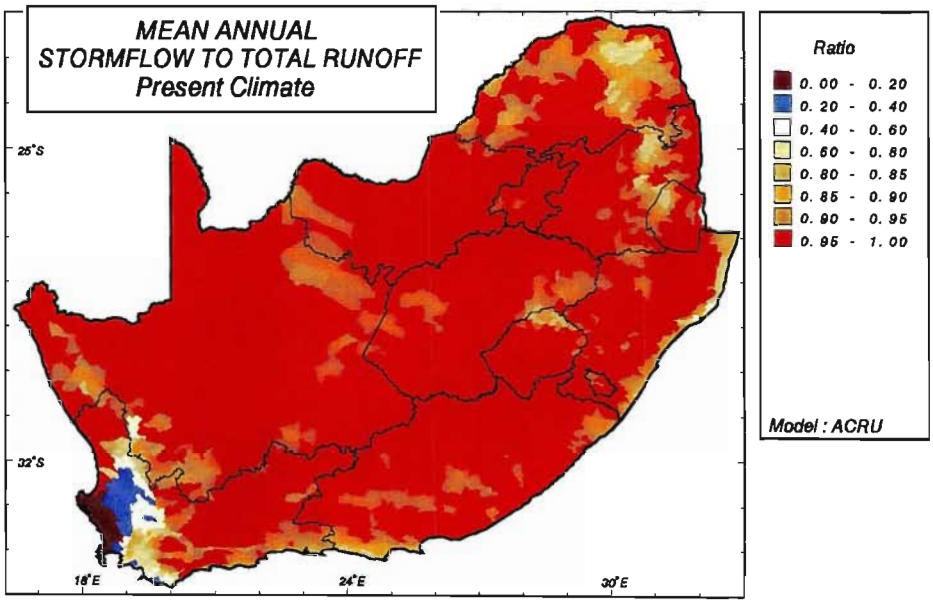


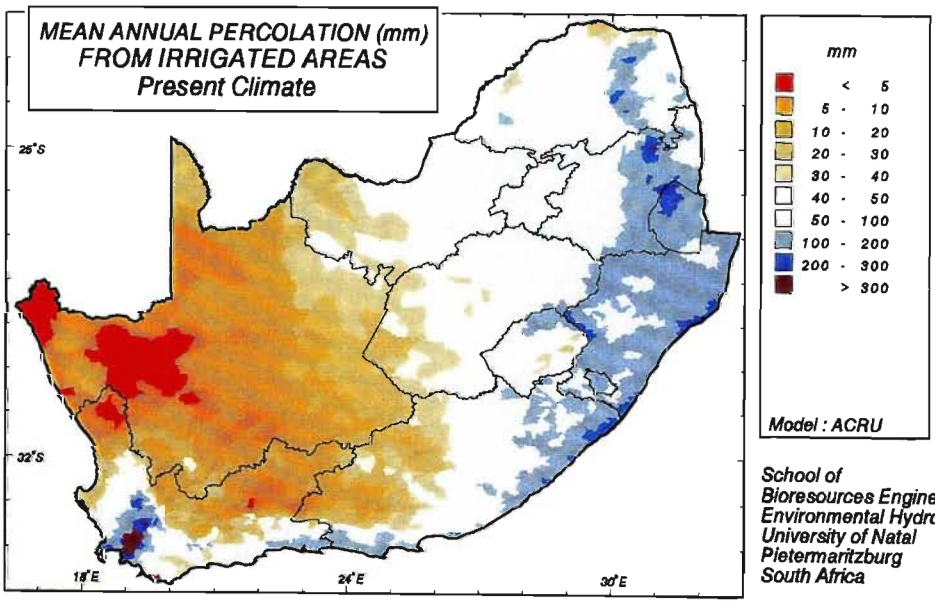


School of
Bioresources Engineering and
Environmental Hydrology
University of Natal
Pietermaritzburg
South Africa

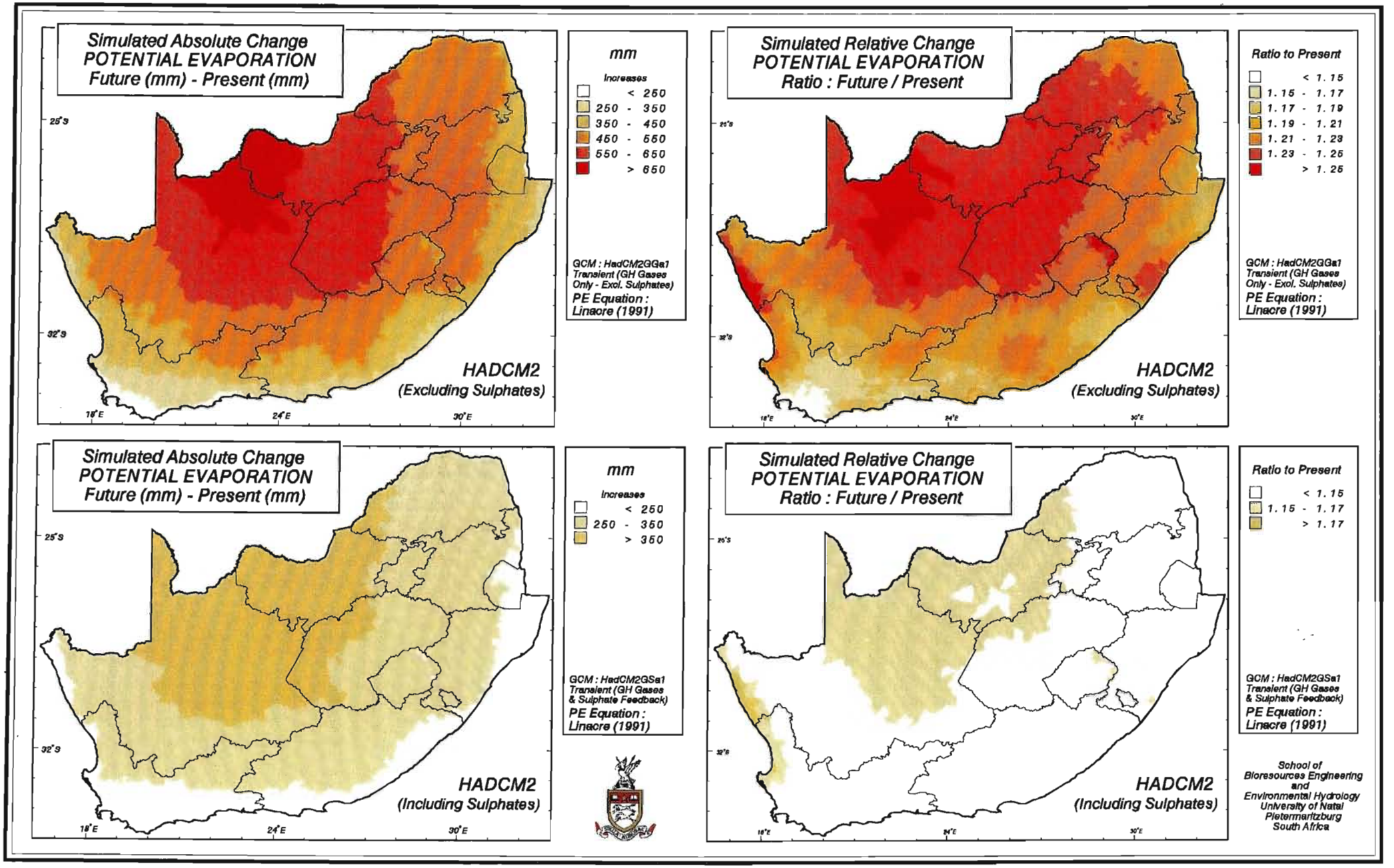
Simulated Absolute Change
POTENTIAL EVAPORATION
Future (mm) - Present (mm)
25°S
32°S
18°E
24°E
30°E
HADCM2
(Excluding Sulphates)
mm
Increases
< 250
250 - 350
350 - 450
450 - 550
550 - 650
> 650
GCM : HadCM2GGa1
Transient (GH Gases
Only - Excl. Sulphates)
PE Equation :
Linacre (1991)
Simulated Relative Change
POTENTIAL EVAPORATION
Ratio : Future / Present
HADCM2
(Excluding Sulphates)
Ratio to Present
< 1.15
1.15 - 1.17
1.17 - 1.19
1.19 - 1.21
1.21 - 1.23
1.23 - 1.25
> 1.25
GCM : HadCM2GGa1
Transient (GH Gases
Only - Excl. Sulphates)
PE Equation :
Linacre (1991)
Simulated Absolute Change
POTENTIAL EVAPORATION
Future (mm) - Present (mm)
HADCM2
(Including Sulphates)
mm
Increases
< 250
250 - 350
> 350
GCM : HadCM2GSa1
Transient (GH Gases
& Sulphate Feedback)
PE Equation :
Linacre (1991)
Simulated Relative Change
POTENTIAL EVAPORATION
Ratio : Future / Present
HADCM2
(Including Sulphates)
Ratio to Present
< 1.15
1.15 - 1.17
> 1.17
GCM : HadCM2GSa1
Transient (GH Gases
& Sulphate Feedback)
PE Equation :
Linacre (1991)
School of
Bioresources Engineering
and
Environmental Hydrology
University of Natal
Pietermaritzburg
South Africa

in mean potential evaporation equate to an increase of less than 15% for most of the study area, with the northern central area potentially experiencing more than 17% more evaporation than at present (Figure 9.12, bottom right).

The simulated increases in evaporation using the Linacre (1991) equation are higher than would have been estimated using a 3% increase in evaporation per degree increase in temperature which is often used in other studies (Kunz, 1993). The Linacre (1991) equation was, however, selected as not enough information was available to utilise the Penman equation and by using the Linacre (1991) equation the temperature inputs that were available could be optimised.

### 9.2.2 Simulated changes in the ratio of mean annual stormflow to mean annual runoff

In *ACRU* the generated runoff comprises of both baseflow and stormflow, with the stormflow component being the water which is generated on or near the surface of the catchment from a rainfall event, to contribute to flow in the streams within that catchment (Schulze *et al.*, 1995b). The ratio of stormflow to total runoff thus indicates that proportion of the runoff that feeds the streams as stormflow. It is an important index of, for example, the potential for sediment yield to be produced (cf. Section 7.3.2.4 in Chapter 7).

For present climatic conditions the *ACRU* model, as configured for this particular study assuming a land cover of grassland in fair hydrological condition, simulates that most of the MAR of the study area is made up of stormflow (Figure 9.11, middle). The exception is the south-western Cape where stormflow constitutes less than 40% of the runoff generated.

The absolute change in the ratio of stormflow to total runoff was firstly calculated using the climatic output from HadCM2-S (Figure 9.13, top left). For a large proportion of the study area, only a small increase or decrease in this ratio was simulated with the *ACRU* model. The exception was in the south-western Cape where HadCM2-S predicted a 15 - 25% decrease in winter rainfall (cf. Figure 6.8, top right). This could imply a reduction in the baseflow component of runoff, hence the increase in the ratio of stormflow to total runoff. In the south-western region of the study area the ratio of mean annual stormflow as a portion of MAR is simulated to increase by 0.3 to 0.7.

Figure 9.13 Ratio of mean annual stormflow to mean annual total runoff: simulated absolute changes (top left) and relative changes (top right) using the future climate scenario from HadCM2-S; simulated absolute changes (bottom left) and relative changes (bottom right) using the future climate scenario from HadCM2+S

Most of southern Africa is simulated to show little relative change in the ratio of mean annual stormflow to MAR (coloured cream on Figure 9.13, top right). However, for many catchments in the south-western Cape a three to five fold increase in stormflow as a portion of runoff is simulated using the climatic output from HadCM2-S for the same reasons as described in previous paragraph. In a few catchments this ratio could increase to as much as eight fold (coloured purple on Figure 9.13, top right).

When output from HadCM2+S is used, the south-western Cape again shows the greatest changes in the ratio of stormflow to runoff (Figure 9.13, bottom left). Most other areas are simulated to have a small change in this ratio. When these results are expressed as a ratio of the future ratio of stormflow to runoff over the present ratio of stormflow to runoff, a significant increase in stormflow as a portion of runoff is simulated in the Western Cape. In some parts of the Western Cape there is simulated to be a three to six fold increase in the amount of stormflow compared to total runoff using output from HadCM2+S (Figure 9.13, bottom right).

### 9.2.3 Simulated changes in mean annual percolation from irrigated areas

Areas under irrigation on occasion generate deep percolation water which drains out beneath the active root zone. This occurs when overirrigation has taken place or when soil water in the root zone is displaced downwards by rain falling on wet (e.g. recently irrigated) soil. Under present climatic conditions the mean annual percolation from irrigation ranges from 5 mm in the north-west to more than 300 mm in the south-west (Figure 9.11, bottom).

The *ACRU* model simulates small increases in mean annual percolation from irrigation (of between 0 and 10 mm) along parts of the eastern coastline from the changes in climate

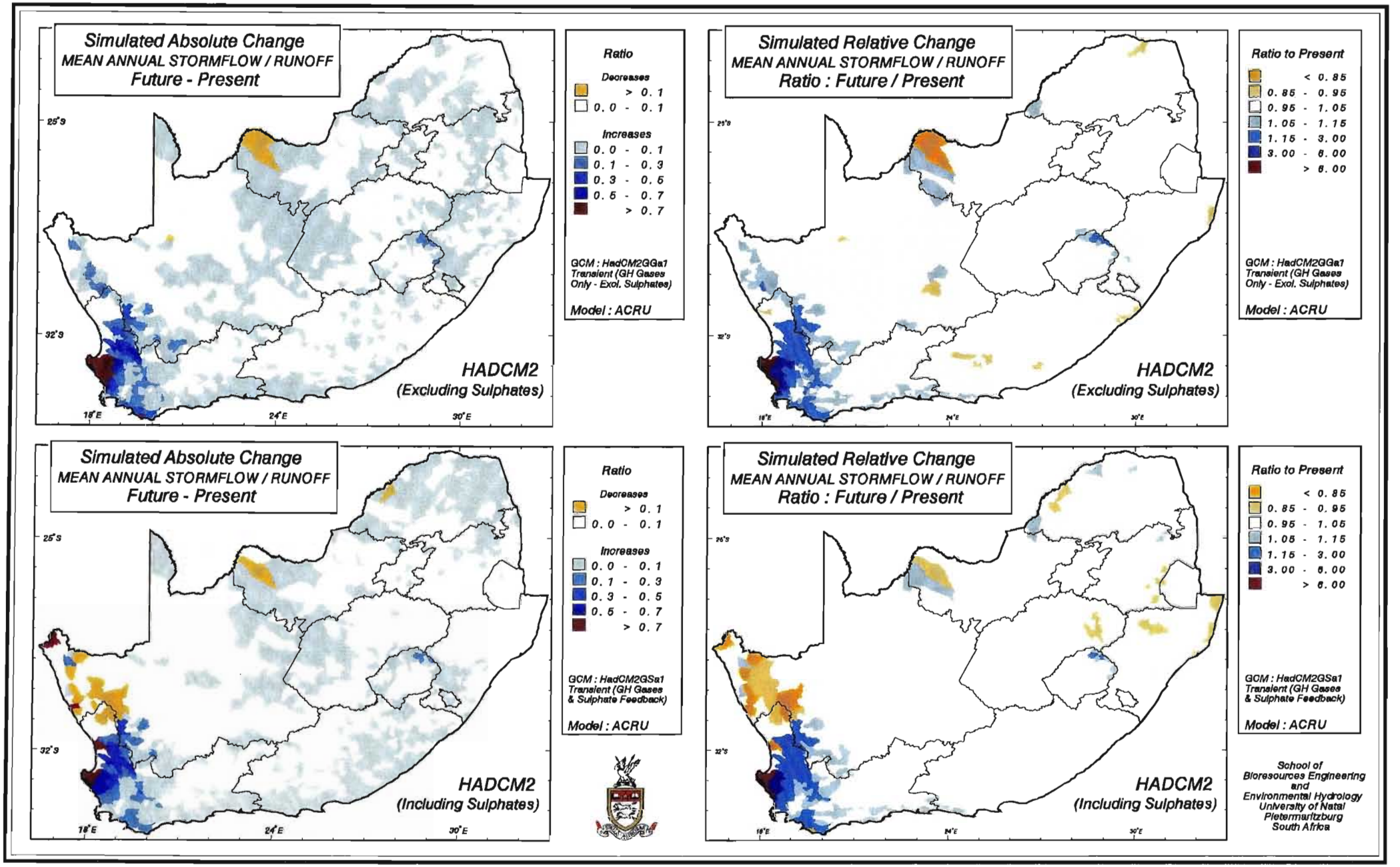
Simulated Absolute Change
MEAN ANNUAL STORMFLOW / RUNOFF
Future - Present
25°S
32°S
18°E
24°E
30°E
HADCM2
(Excluding Sulphates)
Ratio
Decreases
> 0.1
0.0 - 0.1
Increases
0.0 - 0.1
0.1 - 0.3
0.3 - 0.5
0.5 - 0.7
> 0.7
GCM : HadCM2GGa1
Transient (GH Gases
Only - Excl. Sulphates)
Model : ACRU
Simulated Relative Change
MEAN ANNUAL STORMFLOW / RUNOFF
Ratio : Future / Present
HADCM2
(Excluding Sulphates)
Ratio to Present
< 0.85
0.85 - 0.95
0.95 - 1.05
1.05 - 1.15
1.15 - 3.00
3.00 - 6.00
> 6.00
GCM : HadCM2GGa1
Transient (GH Gases
Only - Excl. Sulphates)
Model : ACRU
Simulated Absolute Change
MEAN ANNUAL STORMFLOW / RUNOFF
Future - Present
HADCM2
(Including Sulphates)
Ratio
Decreases
> 0.1
0.0 - 0.1
Increases
0.0 - 0.1
0.1 - 0.3
0.3 - 0.5
0.5 - 0.7
> 0.7
GCM : HadCM2GSa1
Transient (GH Gases
& Sulphate Feedback)
Model : ACRU
Simulated Relative Change
MEAN ANNUAL STORMFLOW / RUNOFF
Ratio : Future / Present
HADCM2
(Including Sulphates)
Ratio to Present
< 0.85
0.85 - 0.95
0.95 - 1.05
1.05 - 1.15
1.15 - 3.00
3.00 - 6.00
> 6.00
GCM : HadCM2GSa1
Transient (GH Gases
& Sulphate Feedback)
Model : ACRU
School of
Bioresources Engineering
and
Environmental Hydrology
University of Natal
Pietermaritzburg
South Africa

predicted by HadCM2-S. Most areas could expect decreases in mean annual percolation from irrigated areas in the future, however, the largest decreases could be expected in the south-west, according to output from this GCM (Figure 9.14, top left).

Figure 9.14 Mean annual percolation from irrigated areas (mm): simulated absolute changes (top left) and relative changes in mean annual percolation from irrigated areas (top right) using the future climate scenario from HadCM2-S; simulated absolute changes (bottom left) and relative changes in mean annual percolation from irrigated areas (bottom right) using the future climate scenario from HadCM2+S

The map of relative changes in mean annual percolation from irrigation shows that the absolute increases shown in Figure 9.14 (top right) are not significant in relative terms. Most parts of the study area could experience a 10 - 30% reduction in mean annual percolation from irrigation (0.7 - 0.9 ratio to present) in the future using climatic output from HadCM2-S and the irrigation routines of the *ACRU* model.

A large number of catchments in the study area were simulated to experience small decreases in mean annual percolation from irrigation when changes in climate were taken from HadCM2+S. There were, however, increases in percolation from irrigation in excess of 10 mm simulated by *ACRU* in the northern coastal parts of KwaZulu-Natal (Figure 9.14, bottom left). However, in relative terms these increases in percolation from irrigation in KwaZulu-Natal are not significant, equating to less than a 10% increase. Most parts of the study area are simulated to have between a 10% and 30% reduction in mean annual increases in percolation from irrigation if the scenario of sulphate forcing is assumed correct (Figure 9.14, bottom right).

### 9.2.4 Simulated changes in annual mean of daily soil moisture of the A horizon

Soil moisture content in the A and B horizon influences a range of hydrological responses. Generally, soil moisture content in the A horizon influences the rate of evaporation from the soil surface, stormflow generation and the amount of saturated drainage from the A horizon

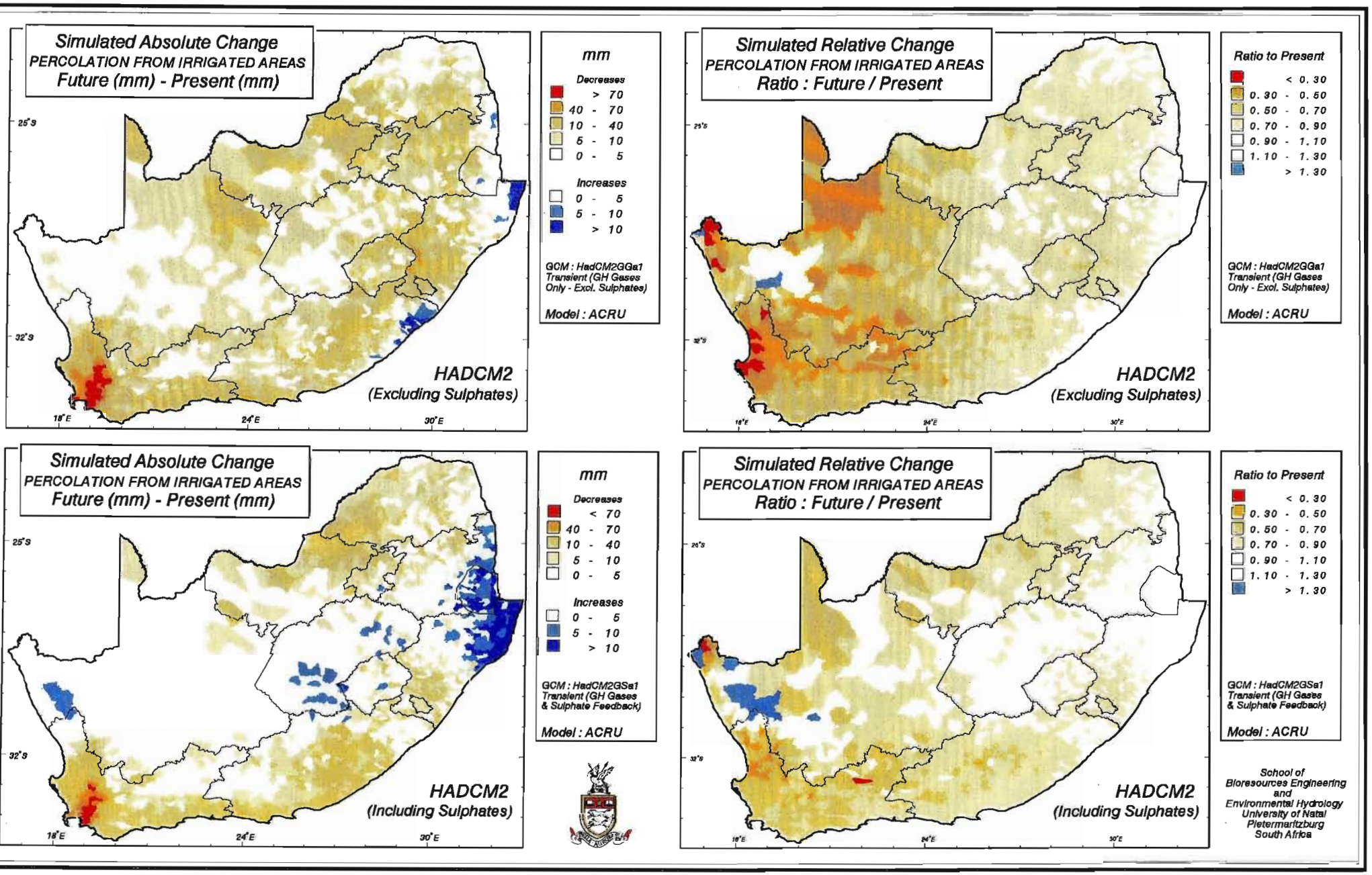
Simulated Absolute Change
PERCOLATION FROM IRRIGATED AREAS
Future (mm) - Present (mm)
25°S
32°S
18°E
24°E
30°E
HADCM2
(Excluding Sulphates)
mm
Decreases
> 70
40 - 70
10 - 40
5 - 10
0 - 5
Increases
0 - 5
5 - 10
> 10
GCM : HadCM2GGa1
Transient (GH Gases
Only - Excl. Sulphates)
Model : ACRU
Simulated Relative Change
PERCOLATION FROM IRRIGATED AREAS
Ratio : Future / Present
HADCM2
(Excluding Sulphates)
Ratio to Present
< 0.30
0.30 - 0.50
0.50 - 0.70
0.70 - 0.90
0.90 - 1.10
1.10 - 1.30
> 1.30
GCM : HadCM2GGa1
Transient (GH Gases
Only - Excl. Sulphates)
Model : ACRU
Simulated Absolute Change
PERCOLATION FROM IRRIGATED AREAS
Future (mm) - Present (mm)
HADCM2
(Including Sulphates)
mm
Decreases
< 70
40 - 70
10 - 40
5 - 10
0 - 5
Increases
0 - 5
5 - 10
> 10
GCM : HadCM2GSa1
Transient (GH Gases
& Sulphate Feedback)
Model : ACRU
Simulated Relative Change
PERCOLATION FROM IRRIGATED AREAS
Ratio : Future / Present
HADCM2
(Including Sulphates)
Ratio to Present
< 0.30
0.30 - 0.50
0.50 - 0.70
0.70 - 0.90
0.90 - 1.10
1.10 - 1.30
> 1.30
GCM : HadCM2GSa1
Transient (GH Gases
& Sulphate Feedback)
Model : ACRU
School of
Bioresources Engineering
and
Environmental Hydrology
University of Natal
Pietermaritzburg
South Africa

to the B horizon. Consequently, climate change effects on soil moisture content may be significant to those and other hydrological responses.

The soil moisture content of a soil horizon is dependent, *inter alia*, on the thickness of the respective horizon, its texture (and hence the permanent wilting point, drained upper limit and porosity) and the interplay of the local climatic regime and vegetative cover. The annual mean of daily soil moisture in the A horizon under present climatic conditions is illustrated in Figure 9.15 (top). The arid and semi-arid areas of the interior have a annual mean of daily soil moisture in the A horizon of less than 25 mm, in contrast to the higher rainfall areas to the north and east of the region, which have a annual mean of daily soil moisture in the A horizon ranging from 45 mm to greater than 55 mm.

Figure 9.15 Annual mean of daily soil moisture content in the A horizon (mm) for present climatic conditions (top) and mean annual sediment yield ($t.ha^{-1}$) for present climatic conditions (bottom)

Figure 9.16 (top left) illustrates the simulated absolute changes in annual means of daily soil moisture in the A horizon using HadCM2-S. Decreases in annual mean of daily soil moisture in the A horizon for the south-western parts of the study region could be attributed to the projected decreases in mean annual precipitation over that region in winter (cf. Figure 6.8, top right), coupled with an increase in temperature and hence reference evaporation.

Figure 9.16 Annual mean of daily soil moisture content in the A horizon (mm): simulated absolute changes (top left) and relative changes (top right) using the future climate scenario from HadCM2-S; simulated absolute changes (bottom left) and relative changes (bottom right) using the future climate scenario from HadCM2+S

The simulated relative changes in annual mean of daily soil moisture in the A horizon using this GCM show a similar pattern to the absolute changes, with the south-western Cape

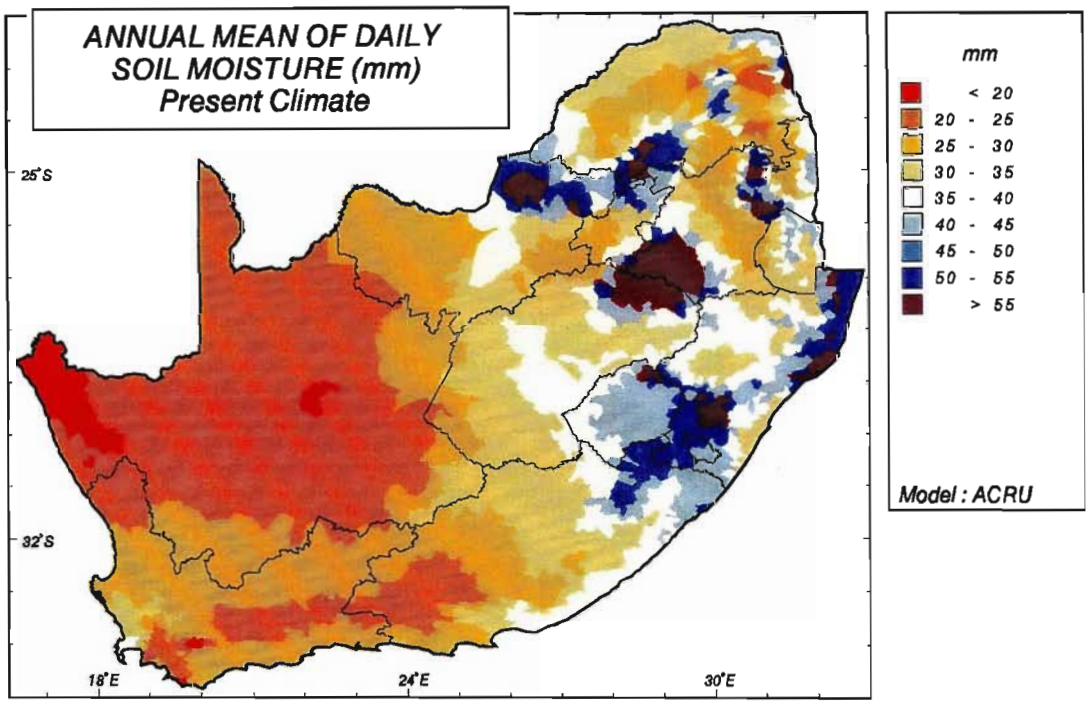
ANNUAL MEAN OF DAILY
SOIL MOISTURE (mm)
Present Climate
25°S
32°S
18°E
24°E
30°E
mm
< 20
20 - 25
25 - 30
30 - 35
35 - 40
40 - 45
45 - 50
50 - 55
> 55
Model : ACRU

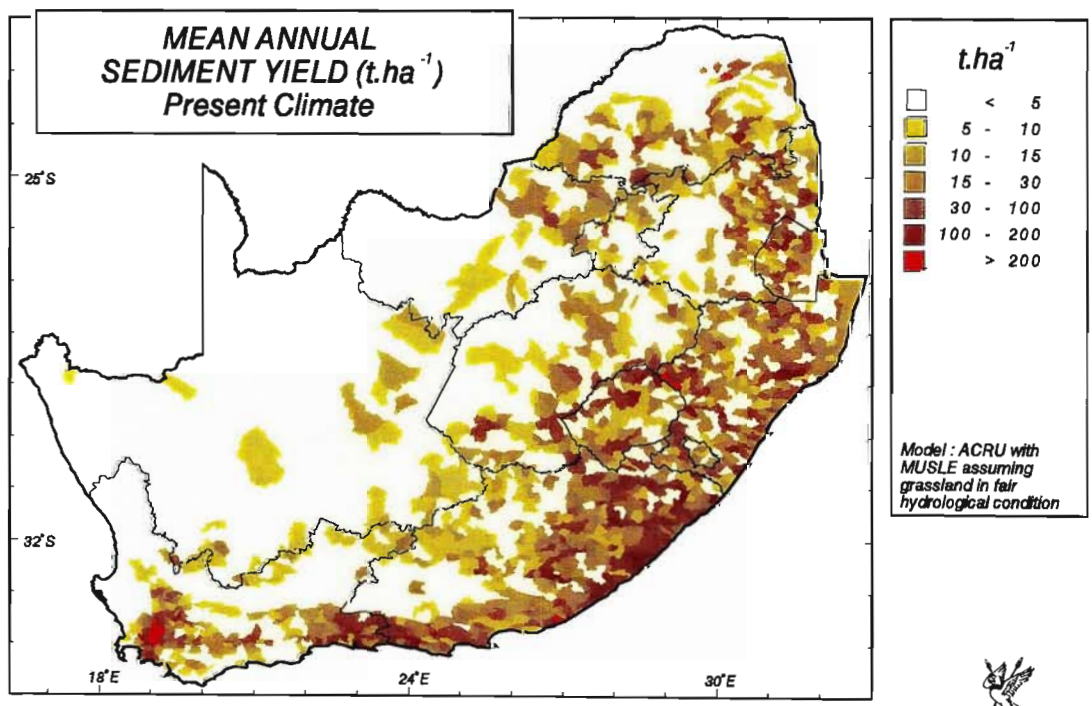
MEAN ANNUAL
SEDIMENT YIELD (t.ha-1)
Present Climate
25°S
32°S
18°E
24°E
30°E
t.ha-1
< 5
5 - 10
10 - 15
15 - 30
30 - 100
100 - 200
> 200
Model : ACRU with
MUSLE assuming
grassland in fair
hydrological condition

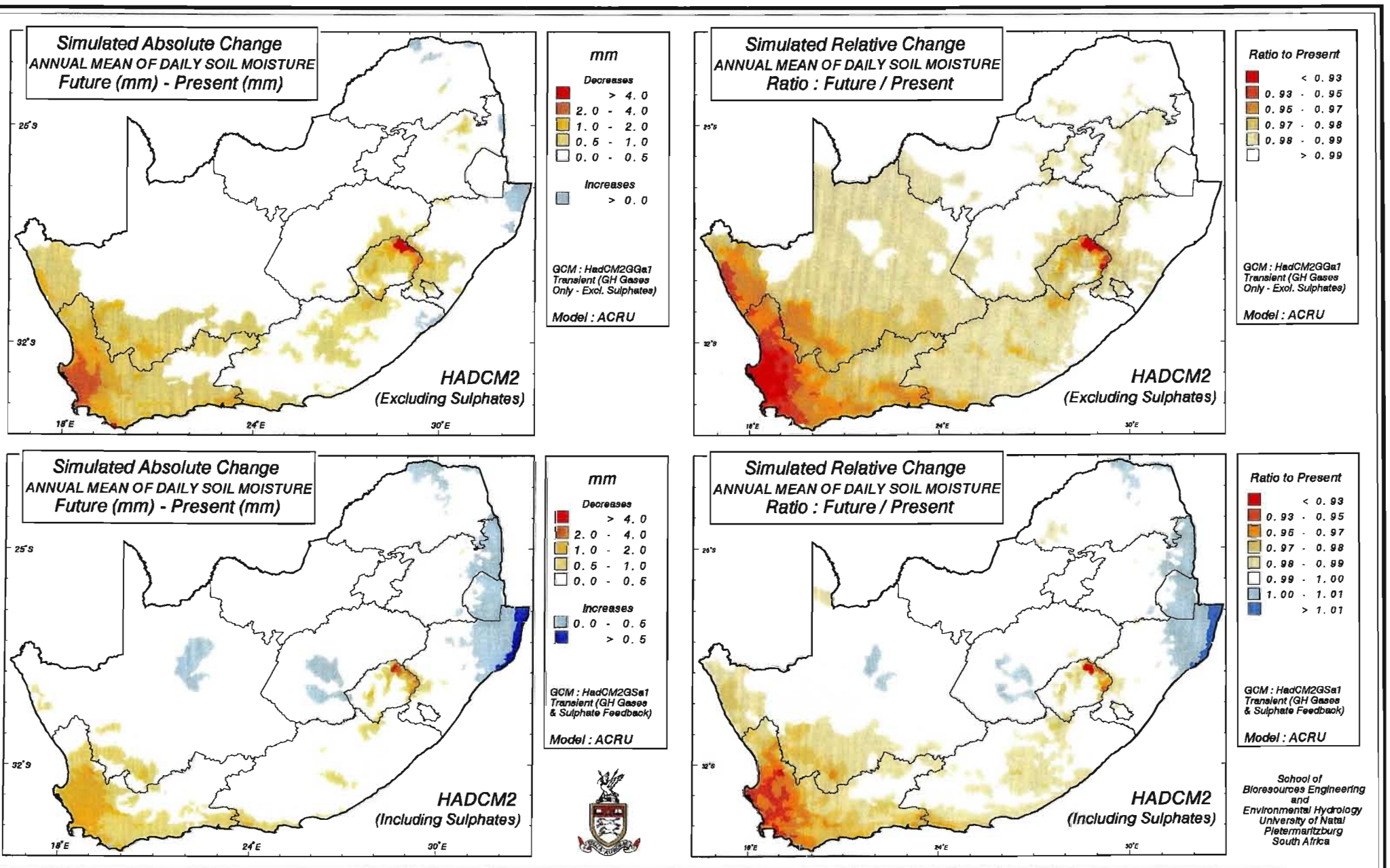
Simulated Absolute Change
ANNUAL MEAN OF DAILY SOIL MOISTURE
Future (mm) - Present (mm)
25°S
32°S
18°E
24°E
30°E
HADCM2
(Excluding Sulphates)
mm
Decreases
> 4.0
2.0 - 4.0
1.0 - 2.0
0.5 - 1.0
0.0 - 0.5
Increases
> 0.0
GCM : HadCM2GGa1
Transient (GH Gases
Only - Excl. Sulphates)
Model : ACRU
Simulated Relative Change
ANNUAL MEAN OF DAILY SOIL MOISTURE
Ratio : Future / Present
HADCM2
(Excluding Sulphates)
Ratio to Present
< 0.93
0.93 - 0.95
0.95 - 0.97
0.97 - 0.98
0.98 - 0.99
> 0.99
GCM : HadCM2GGa1
Transient (GH Gases
Only - Excl. Sulphates)
Model : ACRU
Simulated Absolute Change
ANNUAL MEAN OF DAILY SOIL MOISTURE
Future (mm) - Present (mm)
HADCM2
(Including Sulphates)
mm
Decreases
> 4.0
2.0 - 4.0
1.0 - 2.0
0.5 - 1.0
0.0 - 0.5
Increases
0.0 - 0.5
> 0.5
GCM : HadCM2GSa1
Transient (GH Gases
& Sulphate Feedback)
Model : ACRU
Simulated Relative Change
ANNUAL MEAN OF DAILY SOIL MOISTURE
Ratio : Future / Present
HADCM2
(Including Sulphates)
Ratio to Present
< 0.93
0.93 - 0.95
0.95 - 0.97
0.97 - 0.98
0.98 - 0.99
0.99 - 1.00
1.00 - 1.01
> 1.01
GCM : HadCM2GSa1
Transient (GH Gases
& Sulphate Feedback)
Model : ACRU
School of
Bioresources Engineering
and
Environmental Hydrology
University of Natal
Pietermaritzburg
South Africa

simulated to have a 7% decrease in annual mean of daily soil moisture in the A horizon (0.93 of present) in the future (Figure 9.16, top right).

By including sulphate forcing in HadCM2 most catchments in the study were simulated to show less than a 0.5 mm reduction in annual mean of daily soil moisture (Figure 9.16, bottom left). Compared to the results obtained using output from HadCM2-S the decreases in soil moisture in the south-western Cape simulated using HadCM2+S are not as great and increases in soil moisture in KwaZulu-Natal could exceed 0.5 mm. In both scenarios decreases in annual mean of daily soil moisture in excess of 2 mm were simulated.

In relative terms this corresponds to 7% decrease in soil moisture in a few catchments in Lesotho and a 2 - 5% decrease in the south-western Cape using output from HadCM2+S (Figure 9.16, bottom right). The increases of 0.5 mm in northern KwaZulu-Natal only equates to a 1% increase in soil moisture.

### 9.2.5 Simulated changes in mean annual sediment yield

Sediment yield in the *ACRU* model is generated on an event-by-event basis using the Modified Universal Soil Loss Equation (Williams, 1975) which requires, on a daily basis, input of stormflow and peak discharge, and on a monthly basis a crop cover factor and in a once off basis erosion-related input on slope, soil and management practice (cf. Chapter 7, Section 7.3.2.4).

The mean annual sediment yield generated by the *ACRU* model on a Quaternary Catchment basis assuming land cover throughout to be grassland in fair hydrological condition is less than 5 $t.ha^{-1}$ for present climatic conditions for large portions of the study area, as illustrated in Figure 9.15 (bottom). Along the eastern seaboard sediment yields range from approximately 10 $t.ha^{-1}$ to 200 $t.ha^{-1}$.

Using output from HadCM2-S, the increases in sediment yield simulated for the study area, of between 0 and 5 $t.ha^{-1}$, are along parts of the eastern coastline and in the north-eastern regions (Figure 9.17, top left). The majority of the remainder of the study area is simulated by *ACRU* to experience decreases in mean annual sediment yield of between 0 and 2 $t.ha^{-1}$

compared to sediment yields simulated under present climatic conditions. However, the southern and south-western regions of the study area as well as the high lying regions of Lesotho could experience more than 20 $t.ha^{-1}$ less mean annual sediment yield than at present.

Figure 9.17 Mean annual sediment yield ($t.ha^{-1}$) assuming veld in fair hydrological condition: simulated absolute changes (top left) and relative changes (top right) using the future climate scenario from HadCM2-S; simulated absolute changes (bottom left) and relative changes (bottom right) using the future climate scenario from HadCM2+S

In relative terms this equates to a 10 to 30% simulated increase in sediment yield in the eastern and northern parts and decreases in excess of 70% compared to the present sediment yield for some scattered areas in the west of the study region (Figure 9.17, top right) when using output from HadCM2-S.

The simulated change in mean annual sediment yield is different when using the 2X $CO_2$ scenario of HadCM2+S as shown in Figure 9.17 (bottom left) compared to that which excluded sulphate forcing (Figure 9.17, top left). Using changes in climate from the scenario which included sulphate forcing, *ACRU* simulated larger increases in sediment yield in KwaZulu-Natal for example. However, decreases in sediment yield were simulated along the northern Eastern Cape coast using the HadCM2+S scenario, compared to increases in excess of 10 $t.ha^{-1}$ using the no sulphates scenario.

In relative terms this equates to a 50% increase in sediment yield in the western parts of the study area in a future climate simulated by HadCM2+S. However, a large part of the study area is simulated to have between a 10 and 30% decrease in mean annual sediment yield in a future climate (Figure 9.17, bottom right).

By including sulphate forcing in the GCM simulations of climate (Figure 9.17, bottom left), there appears to be a greater number of catchments which have an increase in simulated sediment yield compared to the results obtained using the scenario which excluded sulphate

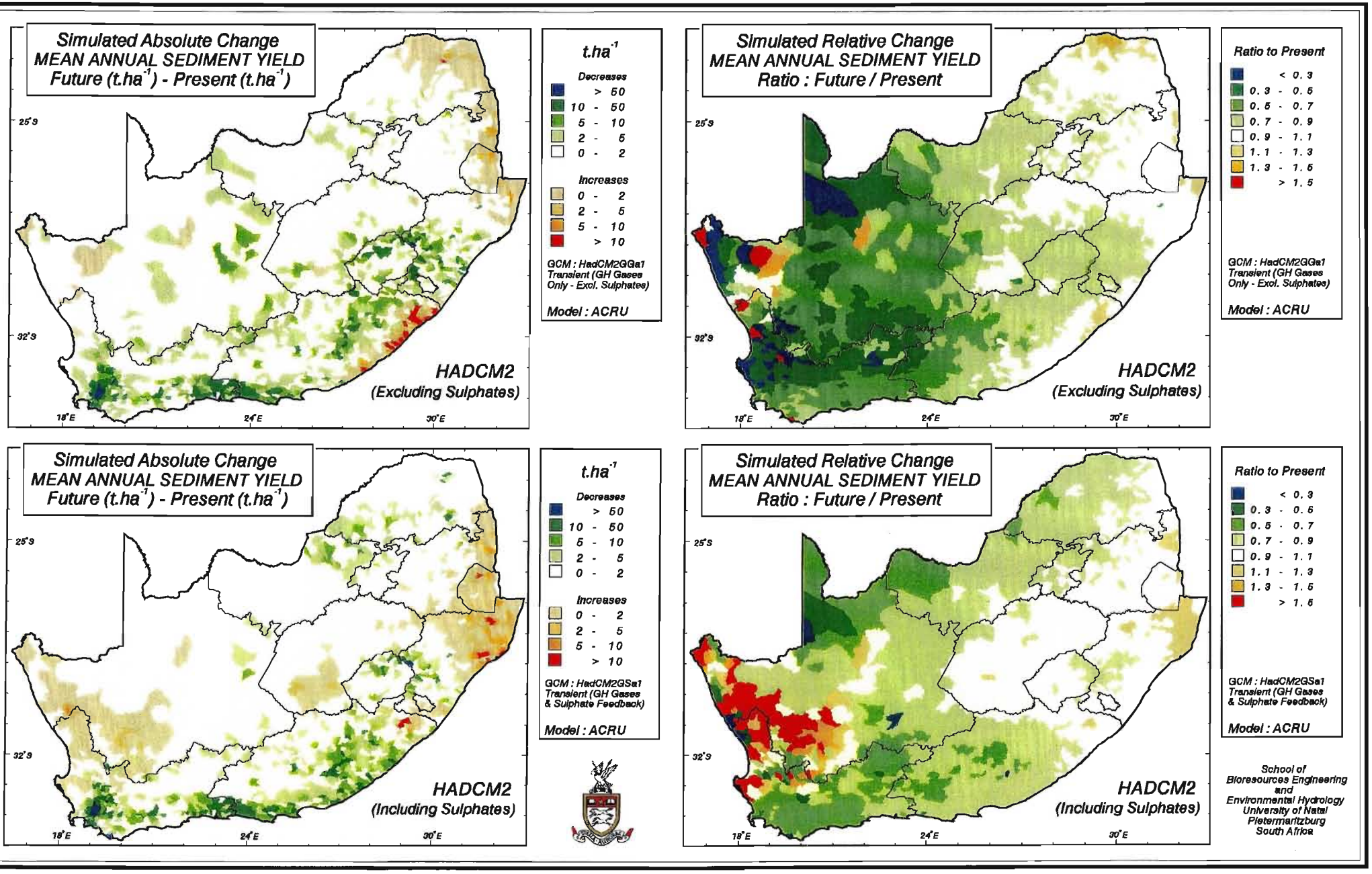
Simulated Absolute Change
MEAN ANNUAL SEDIMENT YIELD
Future (t.ha-1) - Present (t.ha-1)
25°S
32°S
18°E
24°E
30°E
HADCM2
(Excluding Sulphates)
t.ha-1
Decreases
> 50
10 - 50
5 - 10
2 - 5
0 - 2
Increases
0 - 2
2 - 5
5 - 10
> 10
GCM : HadCM2GGa1
Transient (GH Gases
Only - Excl. Sulphates)
Model : ACRU
Simulated Relative Change
MEAN ANNUAL SEDIMENT YIELD
Ratio : Future / Present
Ratio to Present
< 0.3
0.3 - 0.5
0.5 - 0.7
0.7 - 0.9
0.9 - 1.1
1.1 - 1.3
1.3 - 1.5
> 1.5
GCM : HadCM2GGa1
Transient (GH Gases
Only - Excl. Sulphates)
Model : ACRU
Simulated Absolute Change
MEAN ANNUAL SEDIMENT YIELD
Future (t.ha-1) - Present (t.ha-1)
HADCM2
(Including Sulphates)
t.ha-1
Decreases
> 50
10 - 50
5 - 10
2 - 5
0 - 2
Increases
0 - 2
2 - 5
5 - 10
> 10
GCM : HadCM2GSa1
Transient (GH Gases
& Sulphate Feedback)
Model : ACRU
Simulated Relative Change
MEAN ANNUAL SEDIMENT YIELD
Ratio : Future / Present
HADCM2
(Including Sulphates)
Ratio to Present
< 0.3
0.3 - 0.5
0.5 - 0.7
0.7 - 0.9
0.9 - 1.1
1.1 - 1.3
1.3 - 1.5
> 1.5
GCM : HadCM2GSa1
Transient (GH Gases
& Sulphate Feedback)
Model : ACRU
School of
Bioresources Engineering
and
Environmental Hydrology
University of Natal
Pietermaritzburg
South Africa

forcing (Figure 9.17, top left). This could be attributed to higher precipitation amounts simulated by HadCM2+S.

In this comparison of the potential impact of climate change on the simulations of hydrological responses by including and excluding sulphate forcing, it can be concluded that when using HadCM2+S, the higher precipitation amounts result in higher soil moisture contents, greater simulated percolation from irrigated areas and higher sediment yields while the lower temperatures result in lower potential evaporation rates compared to the scenario which excluded sulphate forcing.

## 9.3 Potential Changes in Temporal Runoff Patterns

The mapped potential changes to mean annual runoff across southern Africa resulting from climate change have been presented in a previous section (cf. Figure 9.4). These maps give an indication of the spatial patterns of changes in runoff, i.e. *where* in southern Africa increases or decreases in runoff could occur. However, these maps do not give any indication as to *when*, during the year, these changes in runoff might be expected, whether there is a simulated change in the number of months experiencing runoff or in the concentration of the runoff during the year. Therefore, potential changes in the number of months experiencing flows in a year of median hydrological responses, as well as, the seasonality and concentration of runoff in the study area were determined. The median value, or 50th percentile, is the middle value when a data series is ranked from highest to lowest. In hydrology mean values are frequently skewed by extreme events such as a few large floods that may have occurred. Thus, the median value is preferable to use as a statistic of the expected magnitude of runoff in certain instances.

### 9.3.1 Potential changes in duration of runoff

Runoff does not occur in every month of the year in certain catchments, particularly those in the dry north-western parts of southern Africa. It is expected that the number of months experiencing runoff in a year with median flow could change with changes in climate. Output from HadCM2, both excluding and including sulphates, was used to determine the potential

changes in the duration of runoff in southern Africa by calculating the number of months experiencing flows during a year of median flows.

Under present climatic conditions most Quaternary Catchments in the east of the study area experience flows throughout the year in a median year (coloured in purple in the top map in Figure 9.18). The major exception is the far north of South Africa which generally has between one and eight months of runoff. The south-western and southern coastal areas also experience long durations of runoff during the year under present climatic conditions. The driest parts of the study area, for example in the north-west, in many cases have no months recording runoff amounts at the 50th percentile (coloured in red in Figure 9.18, top). In general, the duration of runoff increases from west to east in the study area.

Figure 9.18 Number of months, in a median year, experiencing runoff under present climatic conditions (top), two months with highest consecutive flow under present climatic conditions (middle) and number of months over which 50% of flow occurs under present climatic conditions (bottom)

Using output from HadCM2+S many more catchments in the west of the study area are simulated to have no runoff under median conditions (Figure 9.19, top left). The reductions in the number of months of median flow in this western half of the study area range from greater than six months in the Western Cape Province to less than three months in the more centrally located catchments as shown in Figure 9.19 (bottom left). Assuming this GCM scenario to be correct, the duration of runoff in the eastern half of the study area will either remain unchanged with flow throughout the year, or in a few catchments there could be a increase in the runoff duration of a few months.

Figure 9.19 Number of months experiencing runoff: for future climatic conditions (top left) and change in number of months experiencing runoff (bottom left) using the future climate scenario from HadCM2-S; for future climatic conditions (top right) and change in number of months experiencing runoff (bottom right) using the future climate scenario from HadCM2+S

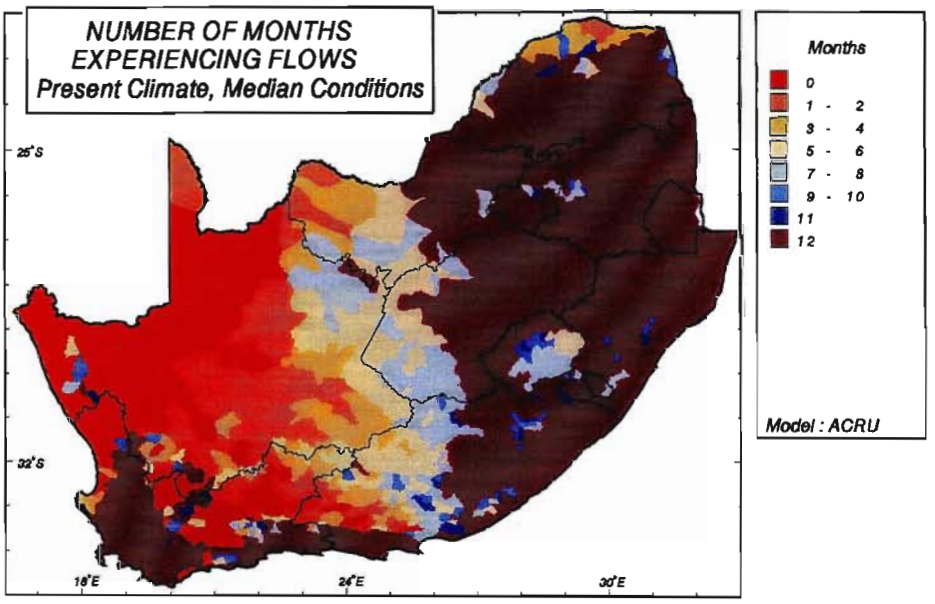


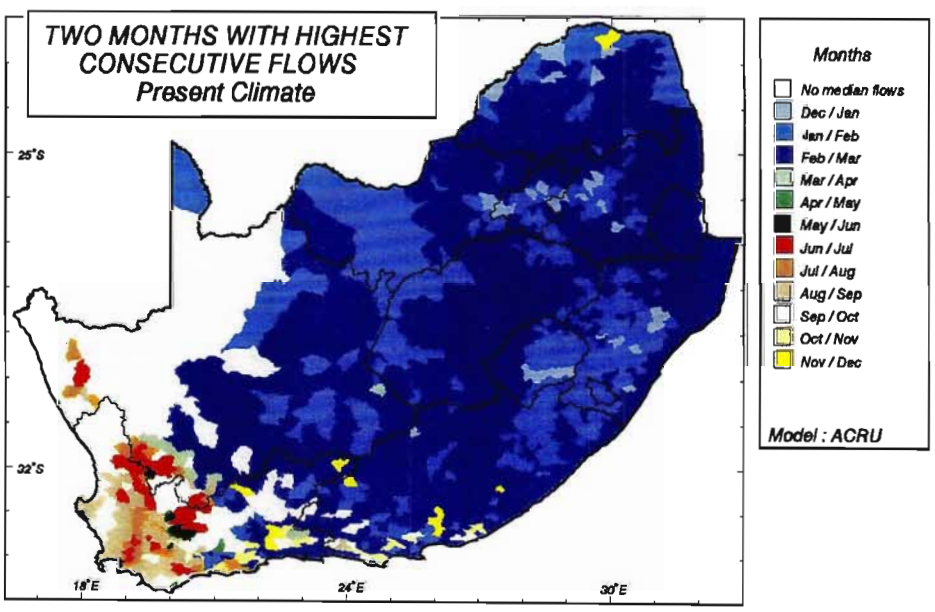


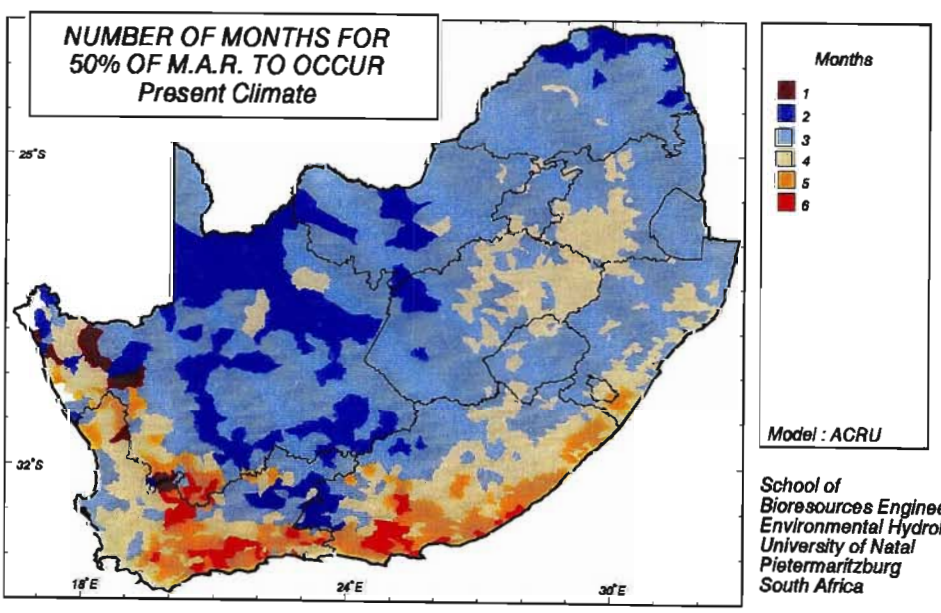


School of
Bioresources Engineering and
Environmental Hydrology
University of Natal
Pietermaritzburg
South Africa

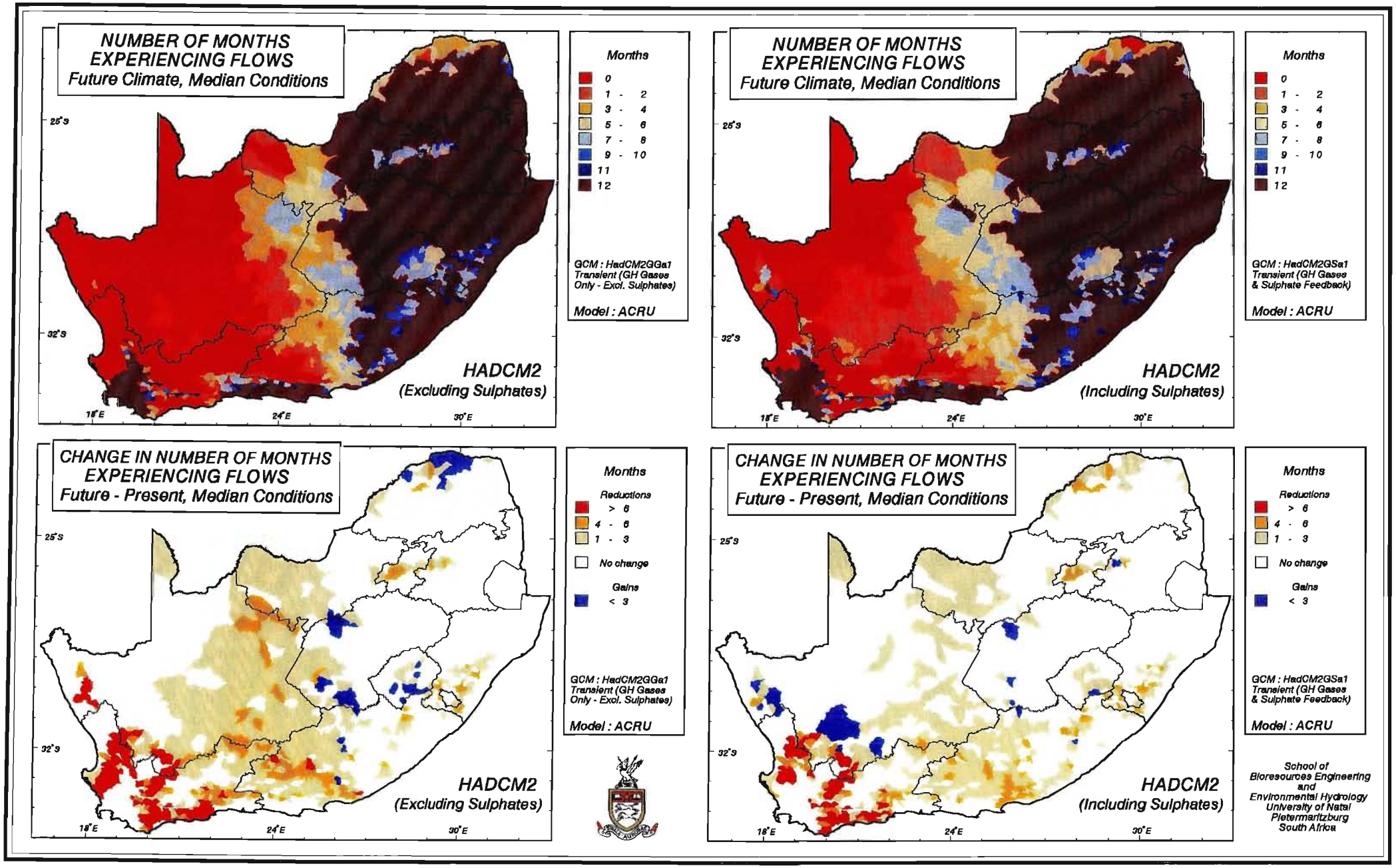
NUMBER OF MONTHS EXPERIENCING FLOWS
Future Climate, Median Conditions
25°S
32°S
18°E
24°E
30°E
HADCM2
(Excluding Sulphates)
Months
0
1 - 2
3 - 4
5 - 6
7 - 8
9 - 10
11
12
GCM : HadCM2GGa1
Transient (GH Gases
Only - Excl. Sulphates)
Model : ACRU
NUMBER OF MONTHS EXPERIENCING FLOWS
Future Climate, Median Conditions
HADCM2
(Including Sulphates)
GCM : HadCM2GSa1
Transient (GH Gases
& Sulphate Feedback)
Model : ACRU
CHANGE IN NUMBER OF MONTHS EXPERIENCING FLOWS
Future - Present, Median Conditions
Reductions
> 6
4 - 6
1 - 3
No change
Gains
< 3
HADCM2
(Excluding Sulphates)
CHANGE IN NUMBER OF MONTHS EXPERIENCING FLOWS
Future - Present, Median Conditions
HADCM2
(Including Sulphates)
School of
Bioresources Engineering
and
Environmental Hydrology
University of Natal
Pietermaritzburg
South Africa

The decreases in runoff duration are not as large when output from HadCM2+S is used (Figure 9.19, top right). The greatest decreases in duration are again simulated in the Western Cape Province, however, most the study area shows little change in runoff duration using this GCM scenario (Figure 9.19, bottom right).

### 9.3.2 Potential changes in seasonality of runoff

Plotting the two months with highest consecutive flows gives an indication of the seasonality of the runoff in each catchment. The map of seasonality based on median monthly flows for present climatic conditions (Figure 9.18, middle) shows that most catchments in southern Africa have the majority of the runoff in either January / February or February / March. The western Cape does, however, have a winter runoff season, with the two months of highest consecutive flows being mostly between June and August.

Some catchments, particularly in Lesotho and the Eastern Cape Province, were simulated to have a shift in seasonality of runoff from January / February under present climatic conditions to November / December (Figure 9, 20,top) using a future climate scenario from HadCM2-S. On the whole there is no simulated change in seasonality for most catchments in southern Africa with climate change. This is also the case when using output from HadCM2+S, as shown in Figure 9. 20 (bottom). The greatest shifts in seasonality are potentially going to occur in the Western Cape Province where the consecutive months with highest runoffs could occur two months earlier than at present.

| | |
|---|---|
| Figure 9.20 | Two consecutive months with highest flows: for future climatic conditions using the future climate scenario from HadCM2-S (top) and for future climatic conditions using the future climate scenario from HadCM2+S (bottom) |

### 9.3.3 Potential changes in concentration of runoff

The index of the concentration of runoff was determined by calculating the number of months needed to for 50% of the mean annual flow to occur. The higher the number of months

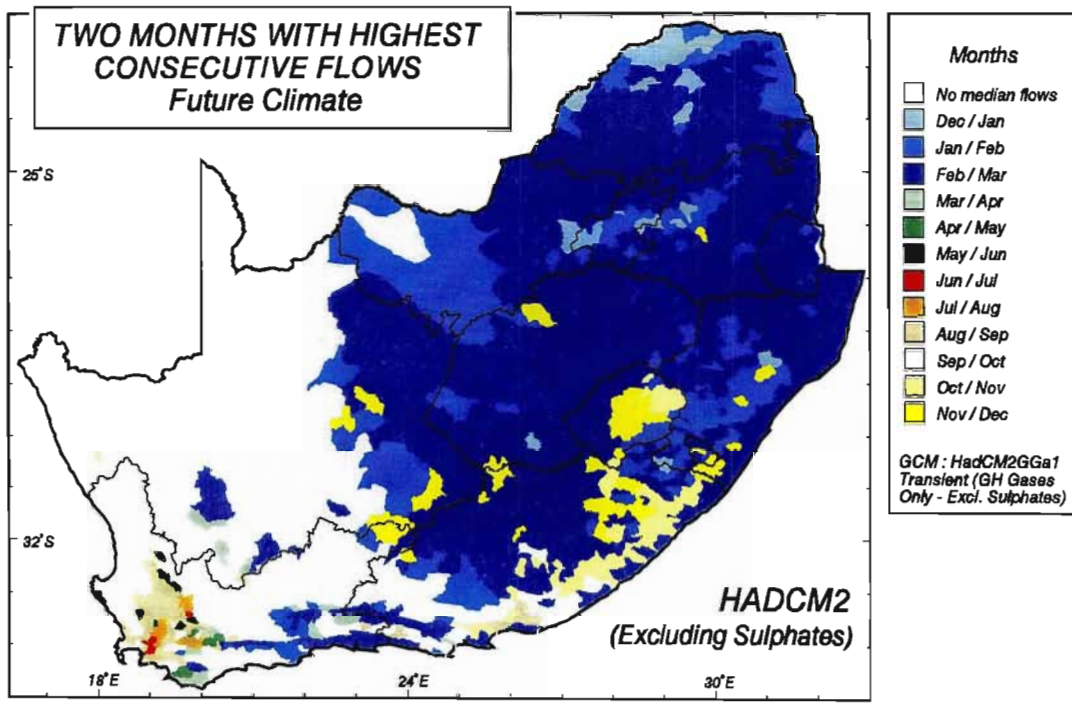
TWO MONTHS WITH HIGHEST CONSECUTIVE FLOWS
Future Climate
25°S
32°S
18°E
24°E
30°E
HADCM2
(Excluding Sulphates)
Months
No median flows
Dec / Jan
Jan / Feb
Feb / Mar
Mar / Apr
Apr / May
May / Jun
Jun / Jul
Jul / Aug
Aug / Sep
Sep / Oct
Oct / Nov
Nov / Dec
GCM : HadCM2GGa1
Transient (GH Gases
Only - Excl. Sulphates)

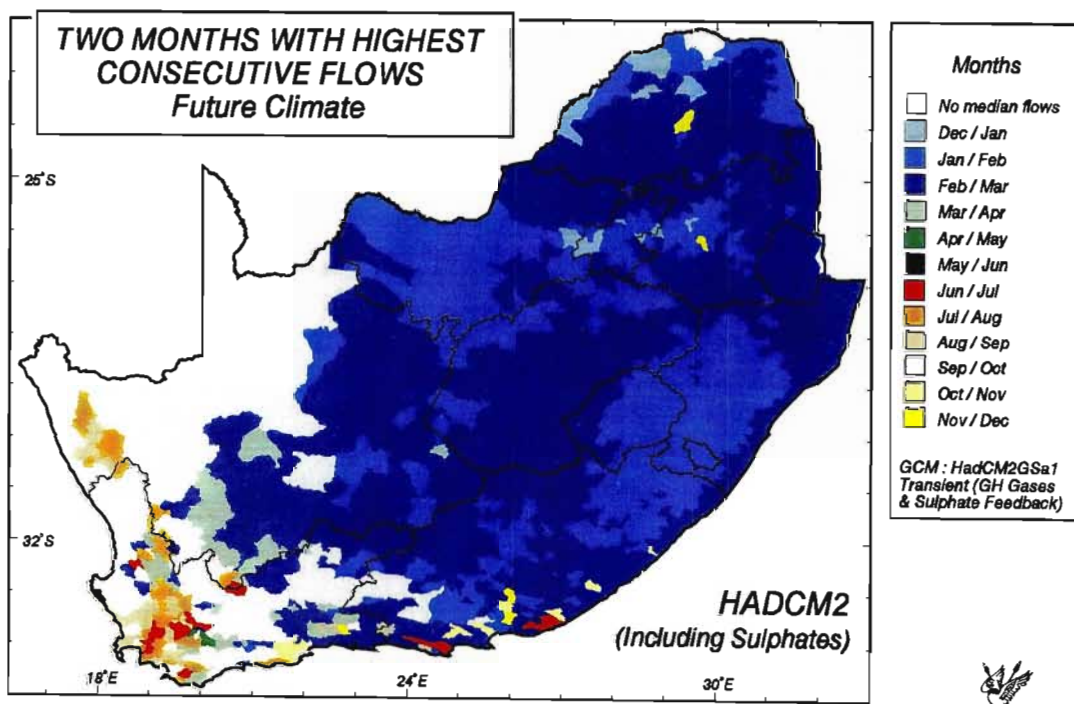
TWO MONTHS WITH HIGHEST CONSECUTIVE FLOWS
Future Climate
25°S
32°S
18°E
24°E
30°E
HADCM2
(Including Sulphates)
Months
No median flows
Dec / Jan
Jan / Feb
Feb / Mar
Mar / Apr
Apr / May
May / Jun
Jun / Jul
Jul / Aug
Aug / Sep
Sep / Oct
Oct / Nov
Nov / Dec
GCM : HadCM2GSa1
Transient (GH Gases
& Sulphate Feedback)

needed for 50% of flow to occur, the lower the concentration of the runoff in the study area.

Under present climatic conditions the lowest concentrations of runoff were determined to occur along the coastal areas, particularly in the southern regions, in northern Free State and southern Mpumalanga (Figure 9.18, bottom). Most catchments in the study area have 50% of the mean runoff occurring in only two to three months of the year.

Using output from HadCM2-S, the number of months needed to record 50% of the mean annual runoff was determined from *ACRU* simulations (Figure 9.21, top left). The concentration of runoff was simulated to change in a future climate with particularly notable differences in the western and more southern parts of the study area where the concentration of runoff could increase, as is shown by the decrease in the number of months in Figure 9.21 (bottom left). The number of months required for 50% of the mean annual runoff to occur may, however, increase in the central parts of the study area resulting in a decrease in runoff concentrations in these areas.

Figure 9.21 Number of months over which 50% of mean annual flows occur: for future climatic conditions (top left) and shift in number of months over which 50% of flow occurs (bottom left) using the future climate scenario from HadCM2-S; for future climatic conditions (top right) and shift in number of months over which 50% of flow occurs (bottom right) using the future climate scenario from HadCM2+S

In comparison, a significant increase in runoff concentration was shown in the western parts of the study area in the Figure 9.21 (top right and bottom right) when including sulphate aerosols in the HadCM2 simulations. In this map many catchments in the west need only one month to attain 50% of their mean annual runoff under this future climate scenario. Scattered catchments in the eastern half of southern Africa were simulated to require an additional month to reach 50% of the mean annual runoff (Figure 9.21, bottom right), implying a decrease in runoff concentration.

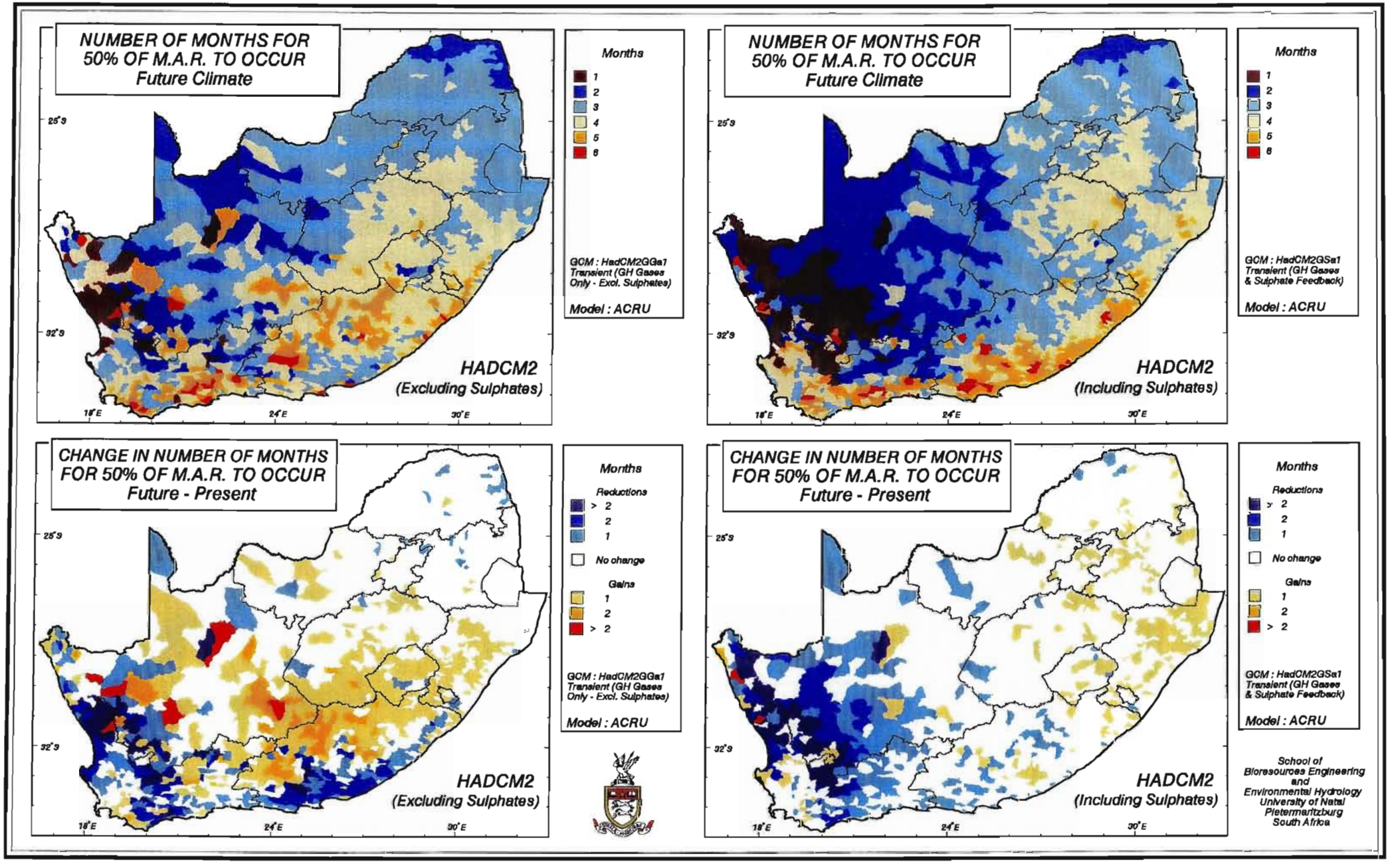
NUMBER OF MONTHS FOR 50% OF M.A.R. TO OCCUR Future Climate
25°S
32°S
18°E
24°E
30°E
HADCM2 (Excluding Sulphates)
Months
1
2
3
4
5
6
GCM : HadCM2GGa1 Transient (GH Gases Only - Excl. Sulphates)
Model : ACRU
NUMBER OF MONTHS FOR 50% OF M.A.R. TO OCCUR Future Climate
HADCM2 (Including Sulphates)
Months
1
2
3
4
5
6
GCM : HadCM2GSa1 Transient (GH Gases & Sulphate Feedback)
Model : ACRU
CHANGE IN NUMBER OF MONTHS FOR 50% OF M.A.R. TO OCCUR Future - Present
HADCM2 (Excluding Sulphates)
Months
Reductions
> 2
2
1
No change
Gains
1
2
> 2
GCM : HadCM2GGa1 Transient (GH Gases Only - Excl. Sulphates)
Model : ACRU
CHANGE IN NUMBER OF MONTHS FOR 50% OF M.A.R. TO OCCUR Future - Present
HADCM2 (Including Sulphates)
Months
Reductions
> 2
2
1
No change
Gains
1
2
> 2
GCM : HadCM2GSa1 Transient (GH Gases & Sulphate Feedback)
Model : ACRU
School of Bioresources Engineering and Environmental Hydrology University of Natal Pietermaritzburg South Africa

From this study of changes in temporal runoff patterns it is concluded that there is simulated to be a decrease in the duration of runoff, a shift in the seasonality of runoff and an increase in the concentration of runoff in a 2X $C0_2$ scenario. These changes could have significant implications for water users and managers in southern Africa.

## 9.4 Sensitivity Studies

The primary forcing function of greenhouse gas induced climate change is represented by effective changes in atmospheric $CO_2$ concentrations ($\Delta CO_2$), which in turn trigger secondary forcing functions such as changes in temperature ($\Delta T$) and changes in precipitation ($\Delta P$).

In an hydrological context, increases in levels of ambient $CO_2$ can result in a fertilisation effect on the photosynthetic process, with associated increases in plant stomatal resistances which, hydrologically, imply reductions in transpiration with consequences and implications in the soil moisture regime and hence runoff generation (cf. Chapter 2, Section 2.3.1.1).

Changes in temperature, on the other hand, are an important determinant of potential evaporation, which in turn drives the actual evaporation and hence controls soil moisture and runoff processes. Temperature, furthermore, activates the potential rate of plants' seasonal growth cycles through the concept of thermal time, or growing degree days (cf. Section 8.1 in Chapter 8).

The most important climatic variable in hydrology is, however, rainfall. Permutations of wet and dry day rainfall sequences and antecedent catchment wetness conditions are all crucial to the impact which magnitudes and intensities of episodic rainfall events have on the generation of the main component of runoff, *viz.* stormflow and baseflow through recharge of groundwater.

### 9.4.1 Methodology used for sensitivity analysis

Hydrological sensitivity analyses can be performed by operating a simulation model, such as *ACRU*, on a particular catchment under analysis and then incrementally perturbing one

component at a time of the historical input data (e.g. precipitation or temperature) within the range of climatic conditions likely to occur in a region. Through such an analysis, information can be gained on the sensitivity of the outputs to changes in the inputs.

The following methodology was used to assess the sensitivity of selected hydrological responses in southern Africa to changes in precipitation amounts, with present temperature and $CO_2$ concentrations held constant:

i) Following a baseline run in which hydrological responses were assessed for present (baseline) precipitation, precipitation was first increased by 10% from its baseline value for each rainfall event, and then decreased by 10% from the present, in each case noting the changes in hydrological responses. The choice of using a 10% increase and decrease in precipitation rather than, say, a 20% change was that a 10% change is within the general range given by the four selected GCMs in the rainy season (cf. Chapter 6, Section 6.5.2.3).

ii) Model output variables, e.g. runoff and percolation of soil water into the vadose zone, from the three possible precipitation regimes (+10%,0%, -10%) were used in an equation developed by Wigley and Jones (1985) for estimation the sensitivity of the variable to changes in precipitation. The equation for the sensitivity analyses takes the form

$$I_s = \frac{[X_{1.1} - X_{0.9}]}{X_{1.0}} \Big/ \frac{[P_{1.1} - P_{0.9}]}{P_{1.0}}$$

where
- $I_s$ = index of sensitivity of that variable
- $X$ = value of the hydrological response variable, e.g. runoff, from a sensitivity simulation
- $P$ = value of precipitation used in the sensitivity analyses
- 1.1, 1.0, 0.9 = subscripts referring to the range of perturbations of possible future precipitation regimes, where 1.1 is a 10% increase, 1.0 is the baseline and 0.9 is a 10% decrease in precipitation.

An $I_s$ value of 2 would indicate that the hydrological variable changes by a factor of 2 compared with an equivalent change in precipitation while an $I_s$ value of 0.5 would imply

relative insensitivity of that variable to a change in precipitation, its change would be half that of a change in the driving variable.

Some areas in southern Africa may be more sensitive than others to the individual hydrological drivers of climate change, *viz.* $\Delta CO_2$, $\Delta T$ and $\Delta P$. Figure 9.22 illustrates the relative sensitivities of mean annual runoff to changes in $CO_2$ (from 360 - 560 ppmv), temperature (assumed to be a uniform increase of 2 °C over southern Africa) and precipitation (changed through -10% to +10% of the present precipitation). In each case the other two variables were held constant at present levels when running *ACRU*.

Figure 9.22 Sensitivities of changes in $CO_2$ (top), temperature (middle) and rainfall (bottom) on simulated mean annual runoff

### 9.4.2 Sensitivity of runoff to changes in precipitation

Figure 9.22 (top) illustrates that runoff is very sensitive to changes in precipitation. Areas with a sensitivity index of 2 - 4 are already considered highly sensitive to a change in precipitation with runoff doubling to quadrupling for every unit change in precipitation, whilst those areas with a sensitivity index greater than four are considered to be those areas most sensitive to a change in precipitation. Mean annual runoff (MAR) along the eastern coast is relatively less sensitive to changes in precipitation, primarily because the rain falls in the hot summer months, often as interspersed thunderstorms, giving the soil the opportunity to start drying out between rainfall events.

The areas most sensitive to a change in precipitation are in the winter rainfall region where a small change in precipitation will have a large effect on the runoff response because evaporative losses to transpiration are low in winter and antecedent soil moisture conditions often remain high between rainfall events, which often also occur on consecutive day of frontal activity.

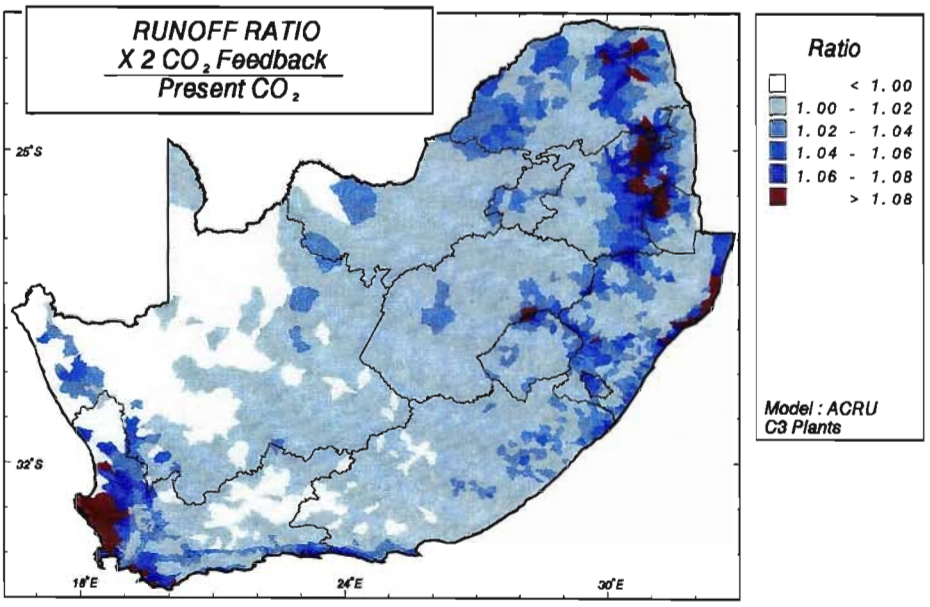


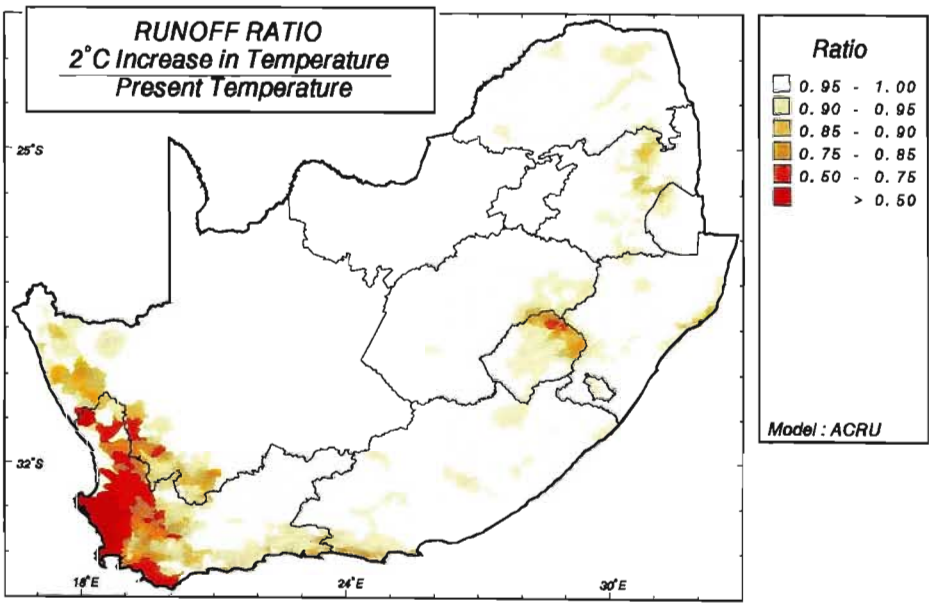


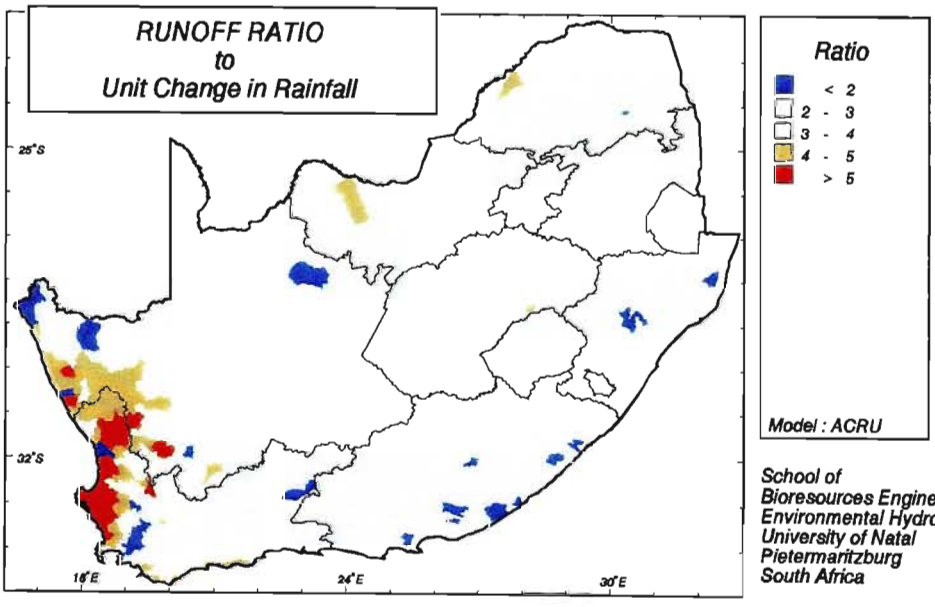


School of
Bioresources Engineering and
Environmental Hydrology
University of Natal
Pietermaritzburg
South Africa

### 9.4.3 Sensitivity of runoff to an effective doubling in atmospheric carbon dioxide concentrations

When the $CO_2$ fertilisation effect is activated in *ACRU* to account for an assumed effective doubling of atmospheric $CO_2$, the resultant suppression of transpiration reduces the drying out of soil, particularly for vegetation with a high water use coefficient in which transpiration dominates the evapotranspiration process. Consequently, soil moisture remains at a higher level and runoff is expected to increase. With relatively low water use coefficients over most of southern Africa, however, the effect of the $CO_2$ induced transpiration suppression in not as pronounced as would be expected. This is illustrated in Figure 9.22 (middle), where over most of southern Africa only a 2% increase in MAR is simulated. The exceptions are the southern regions of the Western Cape Province and scattered areas in the north and along the eastern seaboard where increases in MAR of more than 8% are simulated by *ACRU*. The doubling of $CO_2$ by itself is thus relatively insensitive from a hydrological perspective.

### 9.4.4 Sensitivity of runoff to a 2 °C increase in temperature

An increase in temperature results in both an increase in reference potential evaporation (cf. Figure 9.12) as well as an increase in the potential water use coefficient (cf. Figures 4.3, 4.4, 4.5 and 4.6), both of which are hypothesised to reduce the antecedent moisture content of soil, and hence runoff. Figure 9.22 (bottom) shows, however, that the effect of a 2 °C increase in temperature, by itself, is a relatively insensitive one in regard to hydrological responses, with only a 5% decrease in MAR evident over most of southern Africa. What is significant, however, is the high sensitivity of temperature in the high altitude areas of Lesotho and the southern Western Cape, where the 2 °C increase appears enough to exceed a temperature threshold above which evaporation responds rapidly.

### 9.4.5 Sensitivity of percolation into vadose zone to changes in precipitation

Mean annual percolation through the soil profile into the vadose zone is extremely sensitive to changes in precipitation. This is illustrated in Figure 9.23, where a large portion of southern Africa displays a sensitive index of greater than five. In absolute values percolation rates are very low, consequently a change in precipitation has a large relative effect on

percolation. Those areas less sensitive to a precipitation change include the more arid and semi-arid regions of the interior. Percolation in these areas is negligible and thus remains unaffected by a change in already low amounts of precipitation.

Figure 9.23 Sensitivity of percolation into the vadose zone to changes in precipitation

## 9.5 Threshold Analysis

If a 10% increase or decrease in mean annual runoff or mean annual percolation into the vadose zone is considered a significant change in hydrological response from a water resources perspective, then the threshold analysis, described in Section 7.4.3 of Chapter 7 and using HadCM2-S in the *ACRU* model produces the results described into the following sections.

### 9.5.1 Threshold analysis of mean annual runoff

The year by which each Quaternary Catchment was simulated to experience a 10% decrease or increase in MAR was estimated. The western half of the study area may already experience a 10% simulated decrease in MAR by the year 2015 (Figure 9.24, top). This corresponds to a $^1/_4$ change in HadCM2 climate output. Moving from the western half of the study area towards the eastern coastline, the year by which a 10% decrease occurs is progressively later, with the central northern regions only expected to experience a 10% decrease in MAR by 2060, when climatic conditions are considered equivalent to those of a 2X $CO_2$ atmosphere.

Figure 9.24 Threshold analysis of mean annual runoff, showing the year by which a 10% change in runoff is simulated to occur (top) and threshold analysis of mean annual percolation of soil water into the vadose zone, showing the year by which a 10% change in percolation is simulated to occur (bottom). Future climate scenario from HadCM2-S

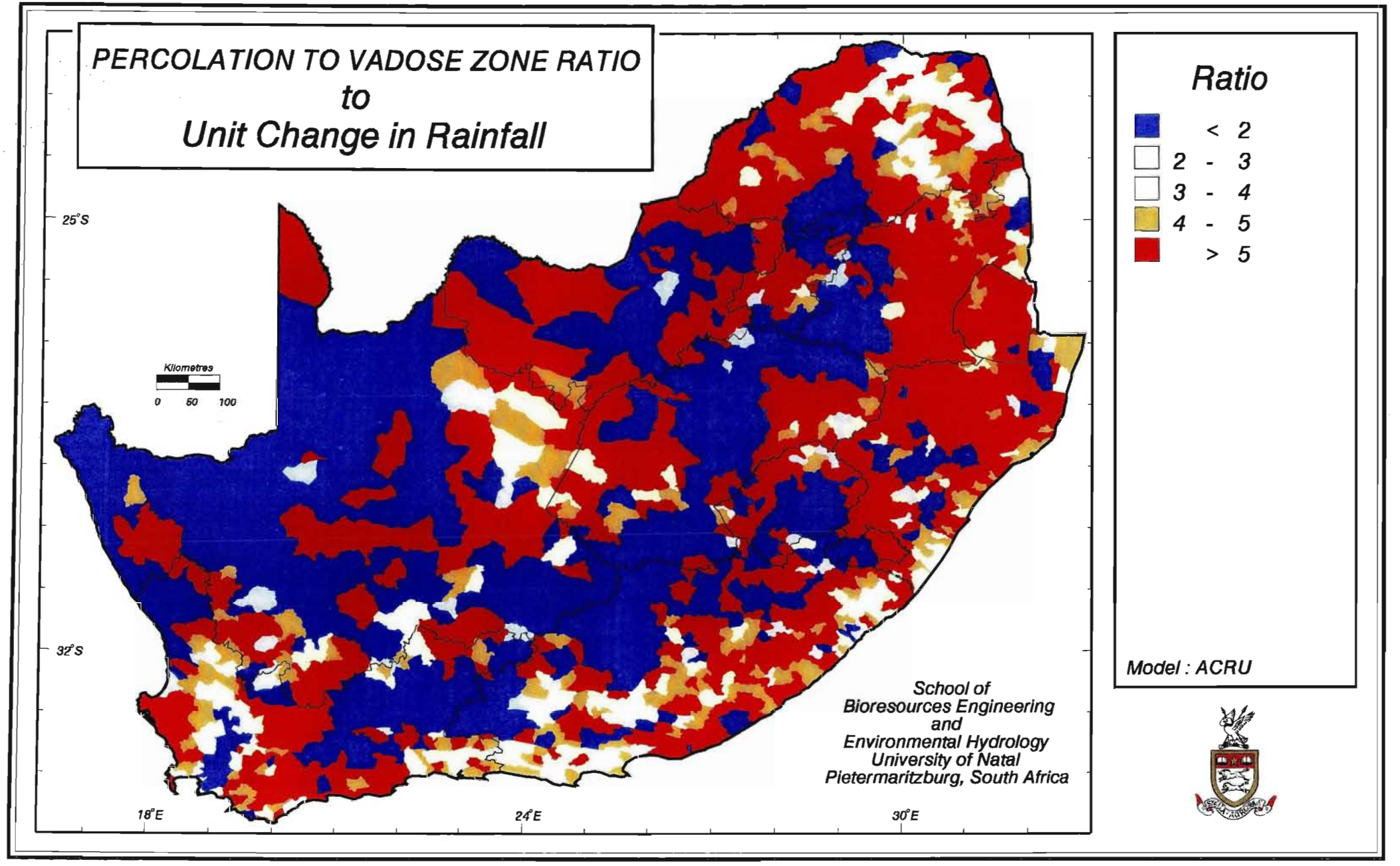
PERCOLATION TO VADOSE ZONE RATIO
to
Unit Change in Rainfall
25°S
32°S
18°E
24°E
30°E
Kilometres
0 50 100
Ratio
< 2
2 - 3
3 - 4
4 - 5
> 5
Model : ACRU
School of
Bioresources Engineering
and
Environmental Hydrology
University of Natal
Pietermaritzburg, South Africa

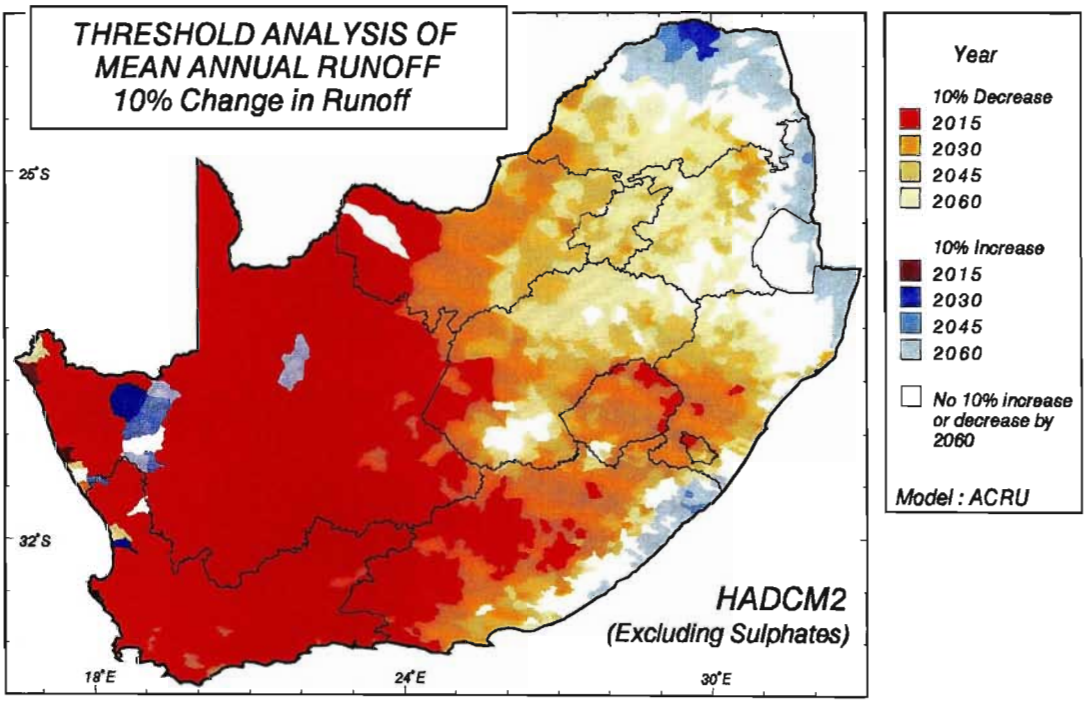
THRESHOLD ANALYSIS OF
MEAN ANNUAL RUNOFF
10% Change in Runoff
25°S
32°S
18°E
24°E
30°E
HADCM2
(Excluding Sulphates)
Year
10% Decrease
2015
2030
2045
2060
10% Increase
2015
2030
2045
2060
No 10% increase or decrease by 2060
Model : ACRU

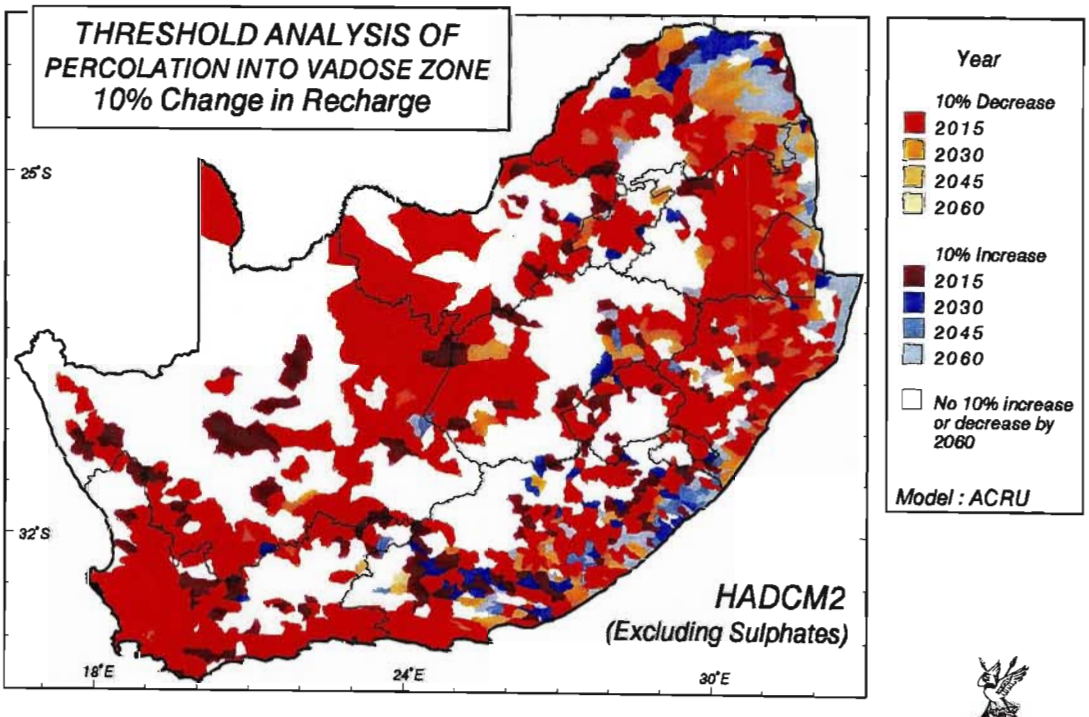
THRESHOLD ANALYSIS OF
PERCOLATION INTO VADOSE ZONE
10% Change in Recharge
25°S
32°S
18°E
24°E
30°E
HADCM2
(Excluding Sulphates)
Year
10% Decrease
2015
2030
2045
2060
10% Increase
2015
2030
2045
2060
No 10% increase or decrease by 2060
Model : ACRU

The northern and eastern regions of the study area experience increases in runoff in the future climate as simulated by *ACRU* using output from HadCM2-S. The areas that experience a 10% increase in runoff generally experience this increase only after 2030. There are, however, a number of Quaternary Catchments on the west coast which could experience a 10% increase in runoff by 2015 already.

### 9.5.2 Threshold analysis of mean annual percolation of soil water into the vadose zone

A more patchy image results from the threshold analysis of mean annual percolation into the vadose zone (Figure 9.24, bottom). The regions which experience a 10% decrease in mean annual percolation mostly experience this decrease by 2015 already, when only $^1/_4$ of a 2X $CO_2$ climate change scenario is hypothesised to have occurred. There are also a number of Quaternary Catchments which show a 10% increase in percolation by 2015, however, there does not appear to be any pattern to the changes using output from HadCM2-S. The 10% threshold response to percolation thus generally appears much earlier than that for runoff.

## 9.6 Case Studies of Hydrological Responses to Climate Change on Selected Large Catchments Assuming Baseline Conditions

The river basin is frequently viewed as the ideal unit by which to address water resource issues comprehensively. Assessing the potential impacts of climate change at the level of the river basin is a logical way of regionalising such an assessment because both water supply and water quality issues, for example, typically use catchments divides as the physical boundaries for analysis (Yarnal, 1998).

Two large catchments were selected to assess the impact of potential changes in climate at the river basin, or catchment, scale. These were the Orange River Catchment located in the north-west of the study area and the Mgeni River Catchment found in the eastern part of the study area. The simulated changes in MAR resulting from climate change from individual and cascading Quaternary Catchments for these two large catchments were determined using climatic output from HadCM2, both excluding and including sulphates.

### 9.6.1 The Orange Catchment: Comparison between runoff from individual and interlinked cascading Quaternary Catchments

The Orange River Catchment is a large catchment located in the north-west of the study area. The catchment covers 607 052 $km^2$ and comprises 481 Quaternary Catchments making up Primary Catchments C and D (coloured cream and light grey in Figure 5.2).

Under present climatic conditions simulated MAR from individual Quaternary Catchments in the Orange Catchment ranges from less than 5 mm in the northern and western regions to over 250 mm in the eastern parts of the catchment in the source areas of Lesotho (Figure 9.25, top).

Figure 9.25 Mean annual runoff (mm) from individual Quaternary Catchments in the Orange Catchment: present climatic conditions (top) and mean annual accumulated runoff ($m^3$ x $10^6$) for cascading Quaternary Catchments in the Orange Catchment under present climatic conditions (bottom) and assuming veld in fair hydrological condition

The *ACRU* simulations to determine accumulated runoff from interlinked Quaternary Catchments were carried out in distributed catchment mode to enable the calculation of accumulated flows at the exit of each Quaternary Catchment (cf. Chapter 7, Section 7.7).

As the streamflows from individual Quaternary Catchments cascade into their respective downstream Quaternary Catchments, the simulated volumes of accumulated runoff were simulated using *ACRU* to increase from 50 x $10^6$ $m^3$ to 20 000 x $10^6$ $m^3$ at the mouth of the catchment (coloured in purple) under present climatic conditions (Figure 9.25, bottom).

The climatic output from HadCM2-S was used to simulate changes in MAR from each Quaternary Catchment in the Orange Catchment with *ACRU*. The absolute changes in MAR from individual Quaternary Catchments using output from this GCM show decreases in MAR of between 0 and 45 mm and small increases of less than 30 mm in a future climate (Figure 9.26, top left). Most Quaternary Catchments in this catchment are expected to have a 0 - 15

# Mean Annual Runoff : Orange Catchment

**Present Climate**

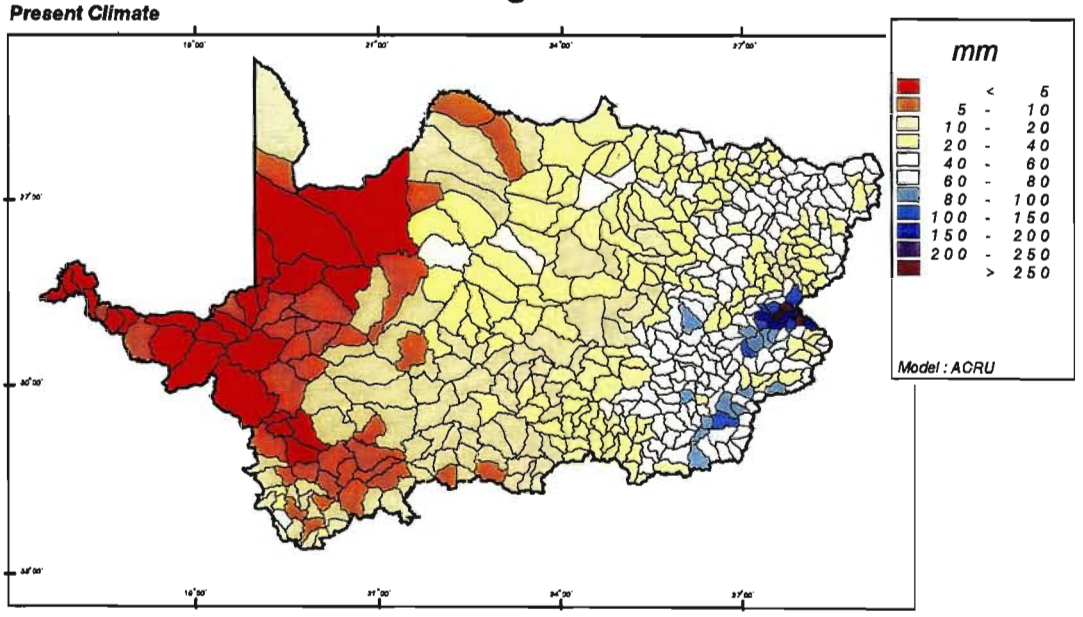


# Mean Annual Accumulated Runoff : Orange Catchment

**Present Climate**

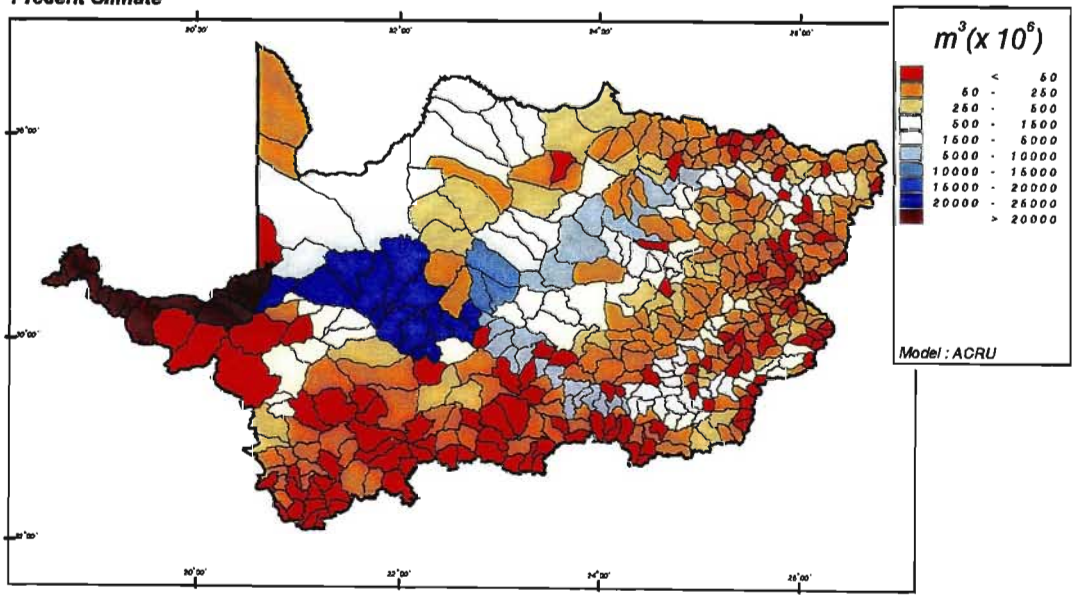

mm reduction in MAR in a future climate. The highest reductions in MAR are simulated in the eastern parts of the catchment in northern Lesotho.

| | |
|---|---|
| Figure 9.26 | Mean annual runoff (mm) from individual catchments in the Orange Catchment: simulated absolute changes (top left) and relative changes in mean annual runoff (bottom left) using the future climate scenario from HadCM2-S; simulated absolute changes (top right) and relative changes in mean annual runoff (bottom right) using the future climate scenario from HadCM2+S |

The relative changes in MAR for this catchment using HadCM2-S were calculated as the ratio of future MAR over present MAR. Even though the simulated absolute changes in MAR in this catchment are quite small, using the 2X $CO_2$ output from HadCM2-S, these changes in the northern and western areas equate to more than a 70% decrease in MAR (Figure 9.26, bottom left). A few isolated Quaternary Catchments are expected to have a 30% increase in MAR, however, most Quaternary Catchments are simulated to have between a 30 and 70% reduction in MAR.

In comparison when using input from HadCM2+S more Quaternary Catchments are simulated to have increases in MAR in a future climate scenario, however, most catchments have between a 0 and 15 mm decrease in MAR resulting from climate change (Figure 9.26, top right). In relative terms this equates to less than a 30% decrease in MAR in most Quaternaries assuming the future climate scenario from HadCM2-S (Figure 9.26, bottom right).

Many of the source Quaternary Catchments are simulated using the *ACRU* model and output from HadCM2-S to have less than a 100 x $10^6$ $m^3$ decrease in mean annual accumulated for a future climate scenario (Figure 9.27, top left). The mouth of the river, however, is simulated to experience more than a 4 000 x $10^6$ $m^3$ decrease in mean annual accumulated runoff in a future climate. Small increases in accumulated runoff are simulated in some of the source catchments in the east of the Orange Catchment, however, these are relatively insignificant compared to the large decreases simulated at the mouth of the river.

## Change in Mean Annual Runoff : Orange Catchment

Future - Present Climate

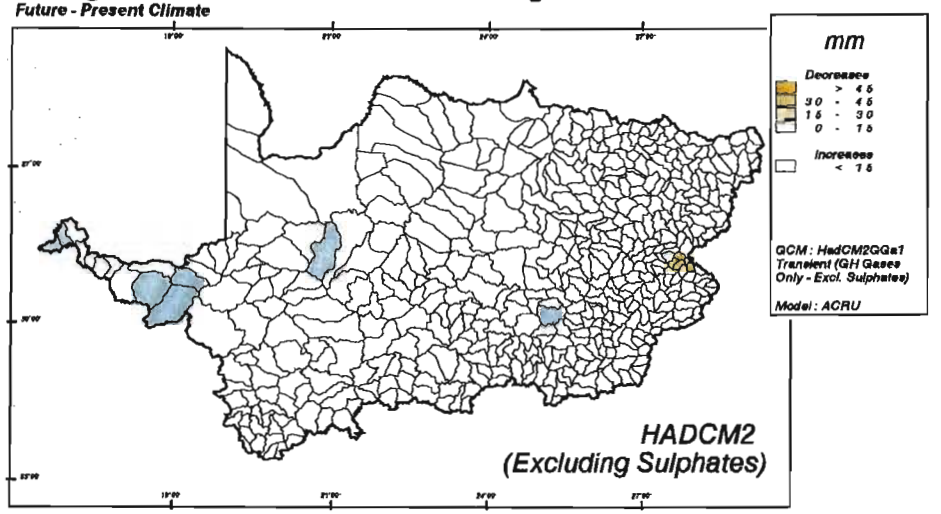


## Change in Mean Annual Runoff : Orange Catchment

Future - Present Climate

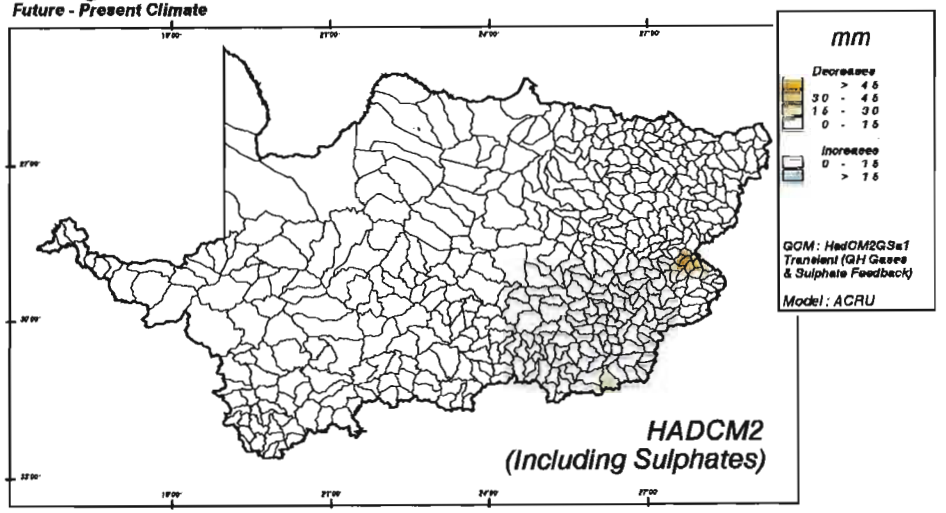


## Ratio of Mean Annual Runoff : Orange Catchment

Future / Present Climate

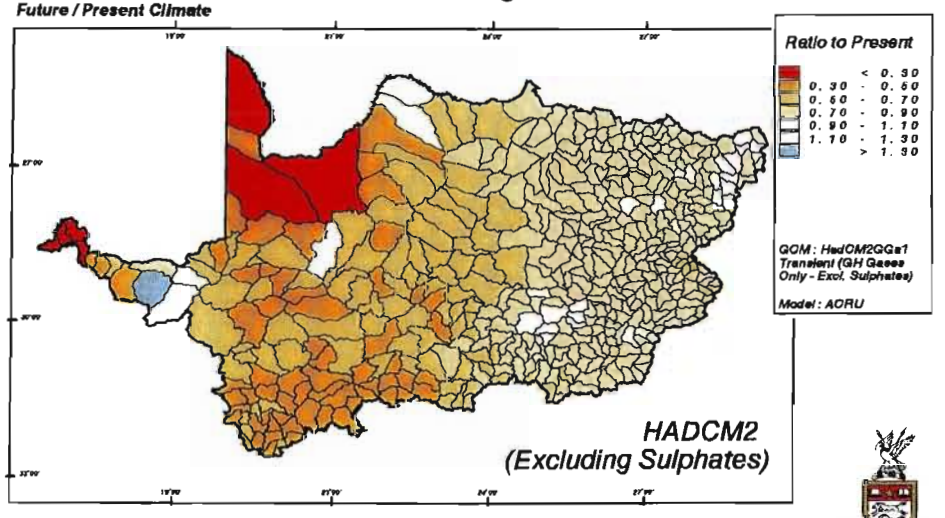


## Ratio of Mean Annual Runoff : Orange Catchment

Future / Present Climate

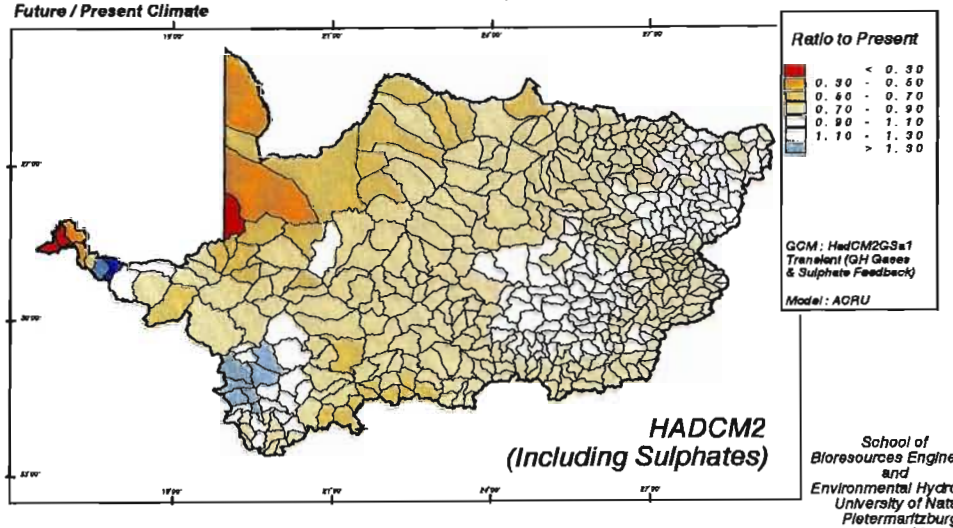


School of
Bioresources Engineering
and
Environmental Hydrology
University of Natal
Pietermaritzburg
South Africa

Figure 9.27 Mean annual accumulated runoff ($m^3$ x $10^6$) from cascading catchments in the Orange Catchment: simulated absolute changes (top left) and relative changes in mean annual accumulated runoff (bottom left) using the future climate scenario from HadCM2-S; simulated absolute changes (top right) and relative changes in mean annual accumulated runoff (bottom right) using the future climate scenario from HadCM2+S

In relative terms these decreases equate to a 15 - 25% decrease in accumulated runoff exiting the Orange River from all the contributing Quaternary Catchments (Figure 9.27, bottom left). The largest relative decreases are simulated to occur in the northern and southern Quaternary Catchments where in some catchments decreases in excess of 45% of present accumulated runoff could occur.

When using output from HadCM2+S, decreases in excess of 2 000 x $10^6$ $m^3$ accumulated runoff resulting from climate change are simulated at the outlet of the Orange River (Figure 9.27, top right). More catchments in the source areas are simulated to have small increases in accumulated runoff in a 2X $CO_2$ scenario. The relative differences in accumulated runoff equate to a 5 to 10% decrease in mean annual accumulated runoff at the mouth of the Orange River as shown in Figure 9.27 (bottom right). The catchments simulated to have increases in mean annual accumulate runoff were calculated to have a 5% increase in accumulated runoff when using a future climate scenario from HadCM2+S.

### 9.6.2 The Mgeni Catchment: Comparison between runoff from individual and interlinked cascading Quaternary Catchments

The Mgeni Catchment is a much smaller catchment than the Orange, covering 4469 $km^2$ and comprising only 12 Quaternary Catchments. The present MAR of the Mgeni Catchment simulated using *ACRU* for each Quaternary Catchment and assuming veld in fair hydrological condition ranges from less than 70 mm to more than 140 mm as illustrated in Figure 9.28 (top). Under present climatic conditions the mean annual accumulated runoff in the Mgeni Catchment ranges from less than 30 x $10^6$ $m^3$ at the source to more than 420 x $10^6$ $m^3$ at the mouth of the catchment (Figure 9.28, bottom).

## Change in Mean Annual Accumulated Runoff : Orange Catchment

Future - Present Climate

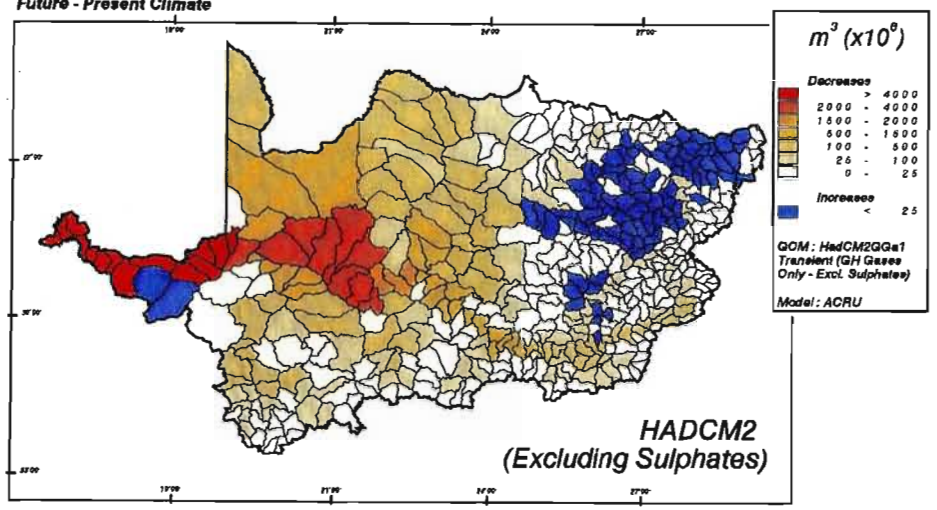


## Change in Mean Annual Accumulated Runoff : Orange Catchment

Future - Present Climate

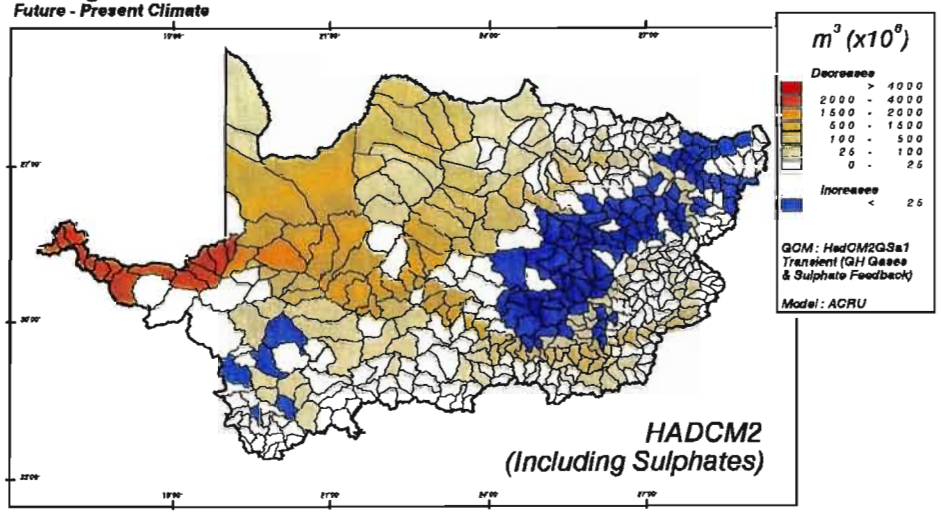


## Ratio of Mean Annual Accumulated Runoff : Orange Catchment

Future / Present Climate

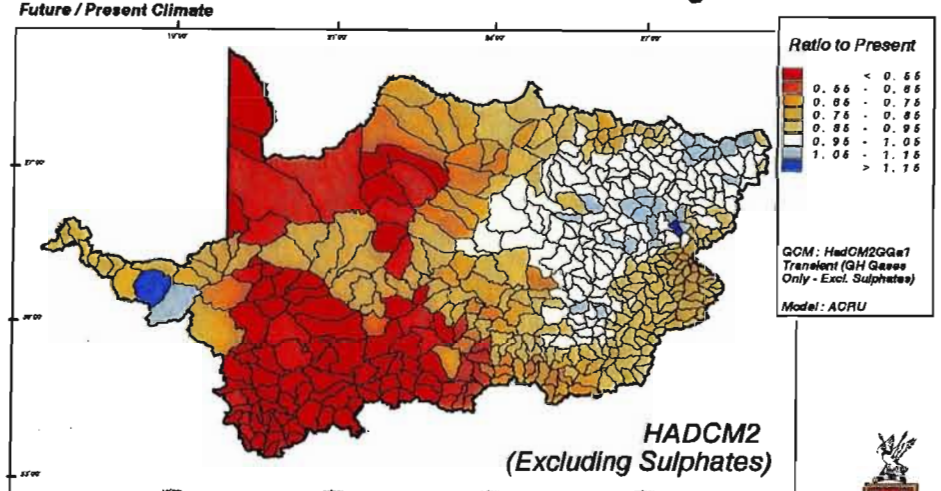


## Ratio of Mean Annual Accumulated Runoff : Orange Catchment

Future / Present Climate

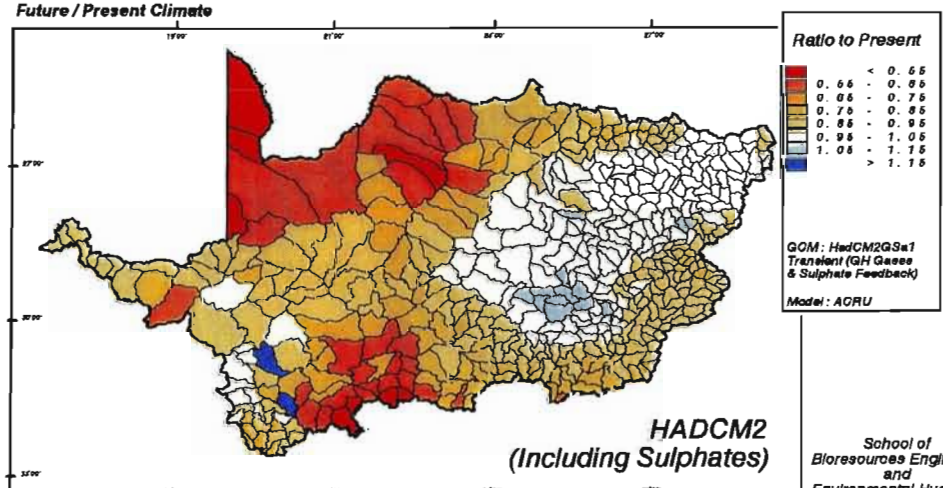


School of
Bioresources Engineering
and
Environmental Hydrology
University of Natal
Pietermaritzburg
South Africa

Figure 9.28 Mean annual runoff (mm) from individual Quaternary Catchments in the Mgeni Catchment under present climatic conditions (top) and mean annual accumulated runoff ($m^3$ x $10^6$) for cascading Quaternary Catchments in the Mgeni Catchment under present climatic conditions (bottom) and assuming veld in fair hydrological condition

The simulated absolute change in runoff, using future climatic conditions from HadCM2-S, shows a 0 - 15 mm reduction in MAR in the eastern half of the catchment and a 15 - 25 mm reduction in MAR in the western half of the catchment (Figure 9.29, top left). The ratio of future over present MAR shows a 15 to 30% reduction in MAR in the western Quaternary Catchments and less than a 15% reduction in MAR in the eastern Quaternary Catchments when using output from HadCM2-S (Figure 9.29, bottom left).

Figure 9.29 Mean annual runoff (mm) from individual Quaternary Catchments in the Mgeni Catchment: simulated absolute changes (top left) and relative changes in mean annual runoff (bottom left) using the future climate scenario from HadCM2-S; simulated absolute changes (top right) and relative changes in mean annual runoff (bottom right) using the future climate scenario from HadCM2+S

The reductions in MAR simulated using the *ACRU* model are not as great when perturbing baseline climate with output from HadCM2+S (Figure 9.29, top right). The source catchments of the Mgeni were simulated to have a 15 mm decrease in MAR and the central Quaternary Catchments only a 5 mm decrease in runoff. This equates to a 20% decrease in MAR in the western Quaternary Catchments and less than a 5% decrease in the eastern catchments near the mouth of the river as shown in Figure 9.29 (bottom right).

When the runoff of the Mgeni River was simulated using the distributed mode in *ACRU* for accumulated flows, more than a 75 x $10^6$ $m^3$ reduction in mean annual accumulated runoff was simulated at the mouth of the catchment using future climate from HadCM2-S (Figure 9.30, top left). However, smaller decreases in mean annual accumulated runoff of less than 10 x

## Mean Annual Runoff : Mgeni Catchment

**Present Climate**

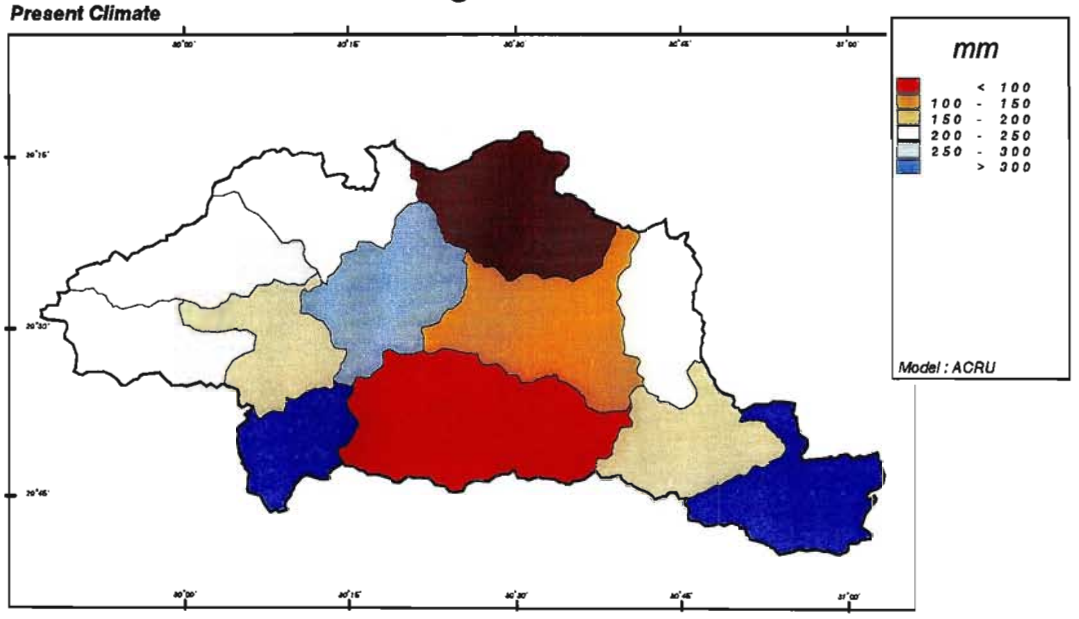


## Mean Annual Accumulated Runoff : Mgeni Catchment

**Present Climate**

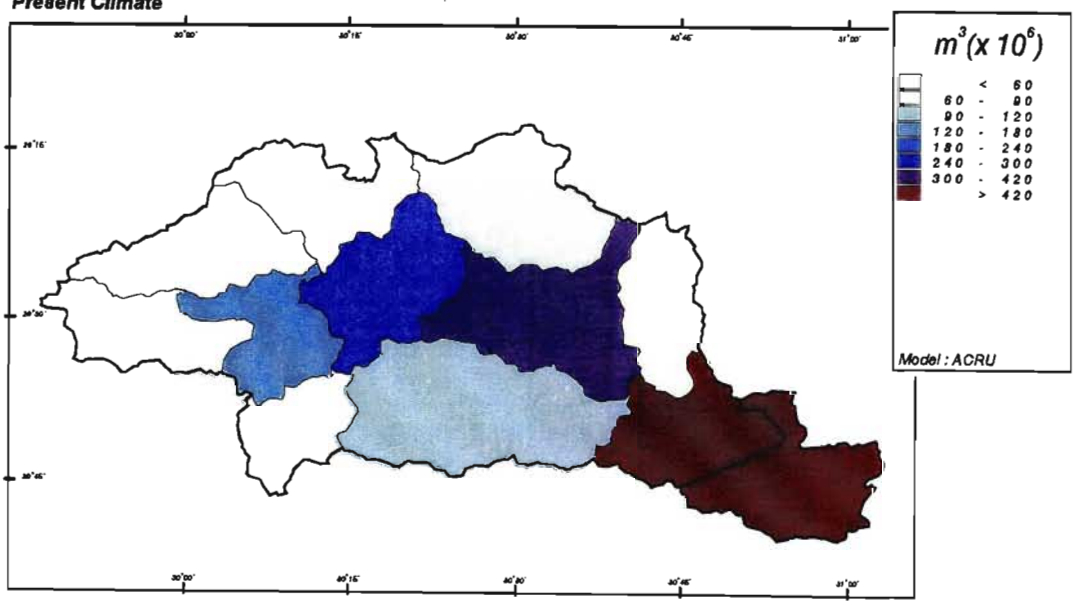

## Change in Mean Annual Runoff : Mgeni Catchment

Future - Present Climate

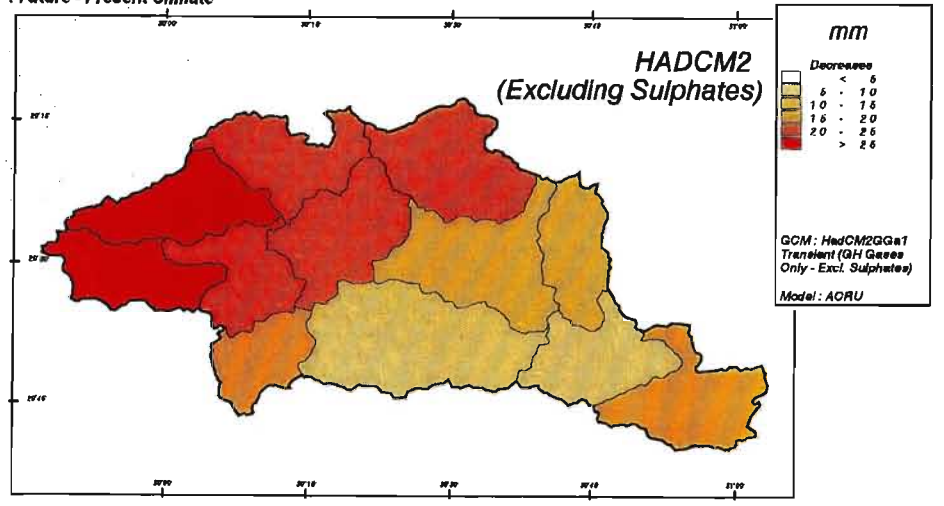


## Change in Mean Annual Runoff : Mgeni Catchment

Future - Present Climate

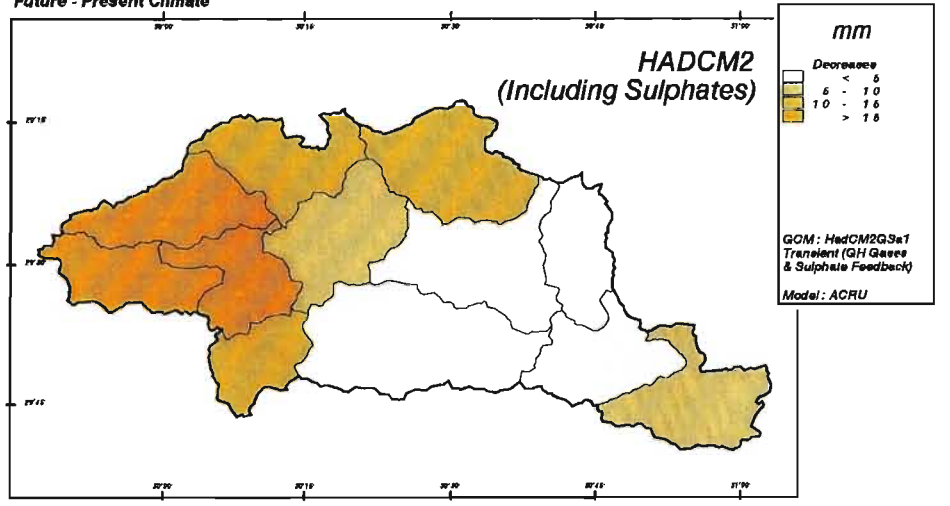


## Ratio of Mean Annual Runoff : Mgeni Catchment

Future / Present Climate

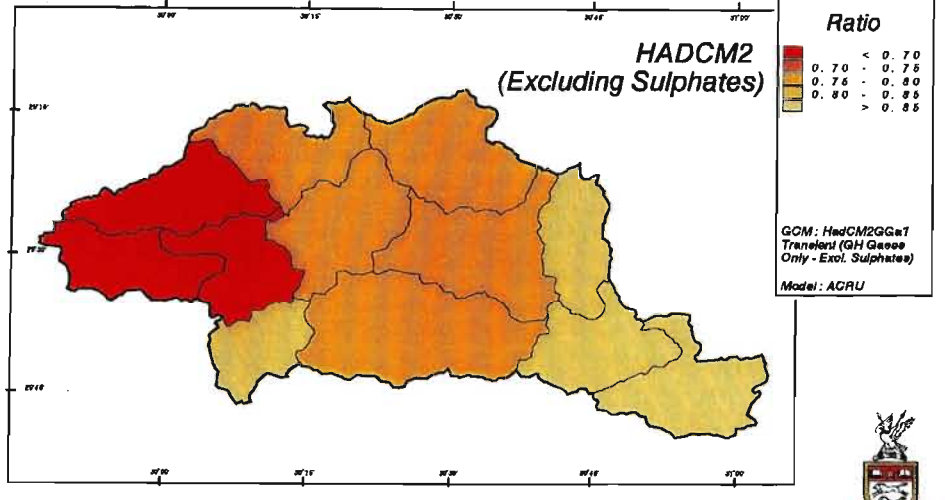


## Ratio of Mean Annual Runoff : Mgeni Catchment

Future / Present Climate

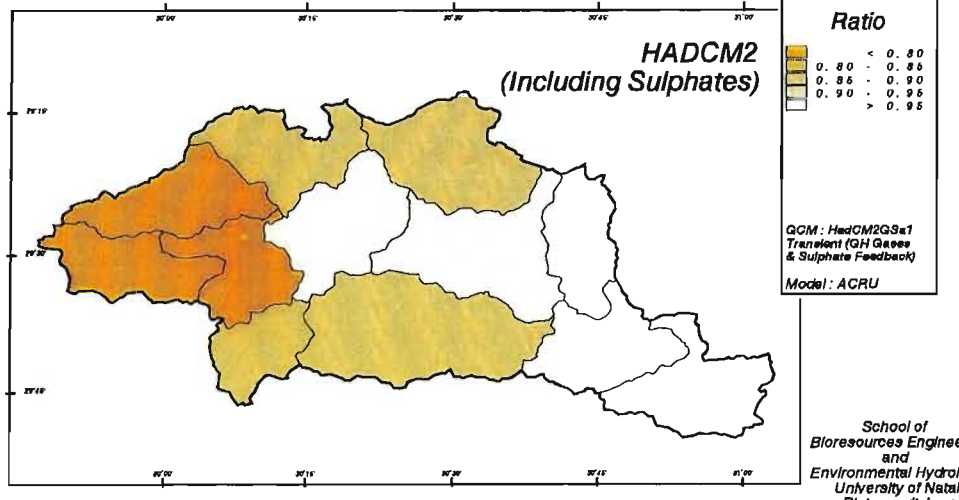


School of
Bioresources Engineering
and
Environmental Hydrology
University of Natal
Pietermaritzburg
South Africa

$10^6$ $m^3$ were simulated in other Quaternary Catchments. The largest relative decreases were simulated in the source catchments where the mean annual accumulated runoff was simulated to decrease by more than 28% from that under present climatic conditions (Figure 9.30, bottom left).

| | |
|---|---|
| Figure 9.30 | Mean annual accumulated runoff ($m^3$ x $10^6$) from cascading catchments in the Mgeni Catchment: simulated absolute changes (top left) and relative changes in mean annual accumulated runoff (bottom left) using the future climate scenario from HadCM2-S; simulated absolute changes (top right) and relative changes in mean annual accumulated runoff (bottom right) using the future climate scenario from HadCM2+S |

The map of changes in mean annual accumulated runoff simulated using HadCM2+S shows similar decreases in mean annual accumulated runoff (Figure 9.30, top right) to that generated using output from HadCM2-S (Figure 9.30, top left). However, the decreases are not as large and range from a 30% in the source catchments to less than a 16% decrease in mean annual accumulated runoff at the mouth (Figure 9.30, bottom right).

* * * * * * *

This chapter has presented the results from the water resources impact assessment of the potential effect of climate change. Potential absolute and relative changes in mean annual runoff, percolation into the vadose zone and stormflow from irrigation were determined using *ACRU* and the output from the four selected GCMs. Decreases in runoff are simulated using output from the HadCM2 GCMs for most parts of southern Africa. Using future climate scenarios from CSM (1998) and Genesis (1998), however, increases in runoff are generally simulated. Similar directions of change are simulated for stormflow from irrigated area. The uncertainty in the four selected GCMs is reflected in the range of results obtained for this component of the study. From the results obtained Genesis (1998) was excluded for subsequent simulations.

## Change in Mean Annual Accumulated Runoff : Mgeni Catchment

*Future - Present Climate*

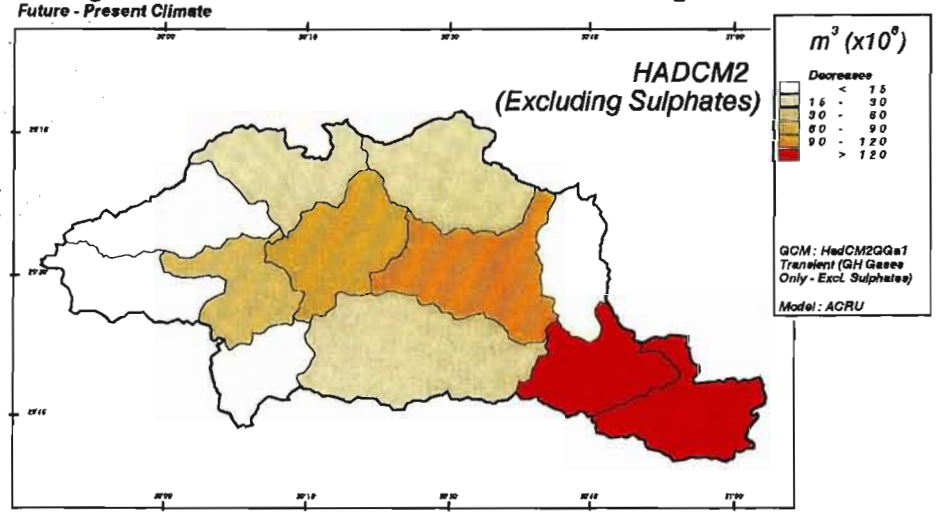


## Change in Mean Annual Accumulated Runoff : Mgeni Catchment

*Future - Present Climate*

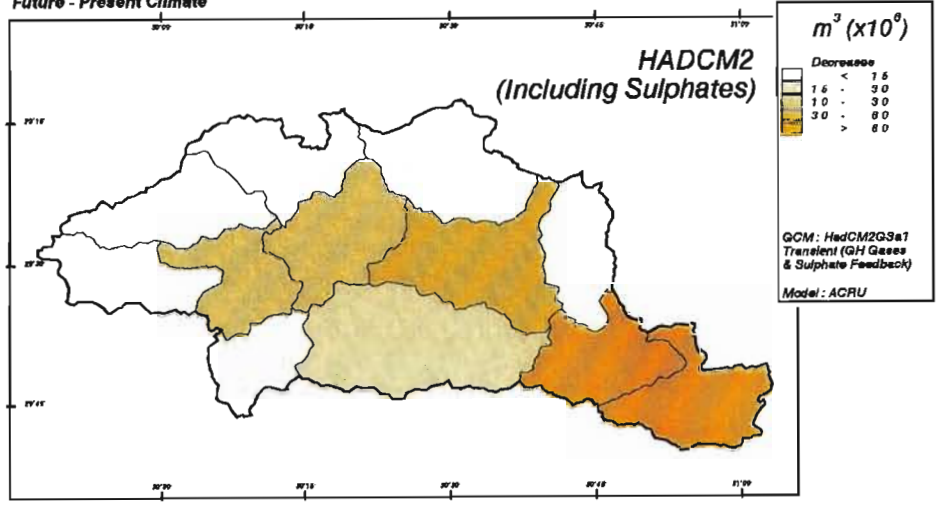


## Ratio of Mean Annual Accumulated Runoff : Mgeni Catchment

*Future / Present Climate*

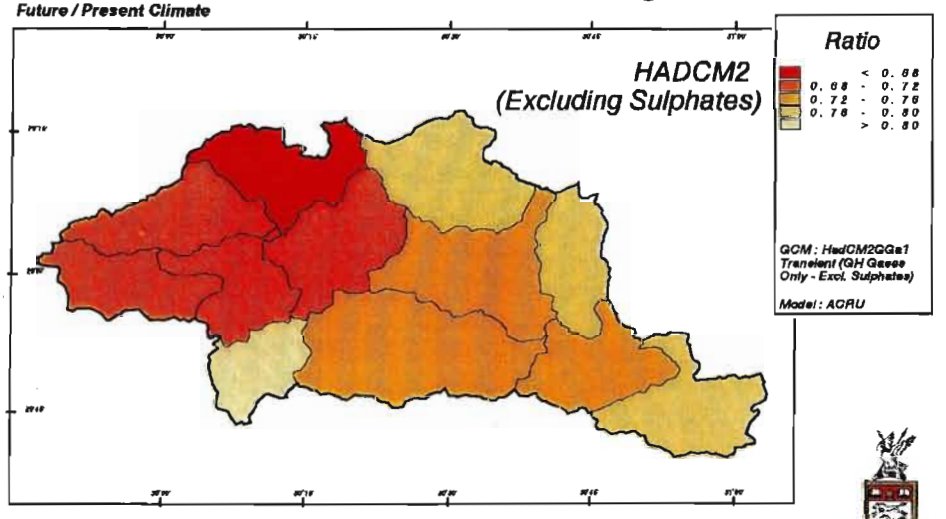


## Ratio of Mean Annual Accumulated Runoff : Mgeni Catchment

*Future / Present Climate*

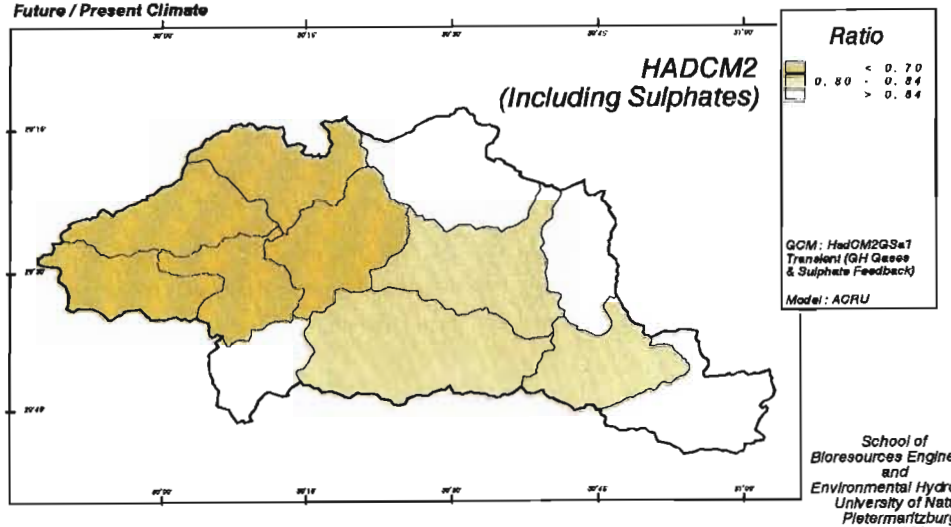



School of
Bioresources Engineering
and
Environmental Hydrology
University of Natal
Pietermaritzburg
South Africa

Significant differences in hydrological response were simulated when including or excluding sulphate feedbacks in the HadCM2 GCM. Sulphate aerosols have a cooling effect in the atmosphere and increases in rainfall is simulated using output from this GCM. These changes result in less evaporation, higher soil water contents, higher sediment yields and greater percolation from irrigated areas being simulated compared to simulations using HadCM2-S.

Potential changes in water resources are expected both spatially and temporally from climate change. From the study of potential changes of the temporal distribution of runoff, using output from HadCM2, it was concluded that a possible decrease in runoff duration during the year could be expected. In addition, there is simulated to be a shift in the seasonality of monthly runoff, with the greatest shifts potentially occurring in the Western Cape. The is also simulated to be an increase in the concentration of runoff in the study area.

The sensitivity studies indicated that percolation into the vadose zone is particularly sensitive to a change in rainfall and that runoff is also highly sensitive to a change in rainfall. From the threshold analysis of runoff it was concluded that the western half of the study may experience a 10% decrease in runoff by 2015 already, with date by which this decrease occurs moving progressively later from west to east across southern Africa.

Two case studies were performed to assess the potential impact of climate change on accumulated runoff on large catchments in the study area, *viz.* the Orange and Mgeni Catchments. Significant decreases in mean annual runoff from individual catchments, as well as accumulated mean annual runoff were simulated under both HadCM2 excluding and included sulphate scenarios for a future climate scenario in the selected catchments.

A more detailed study of the Mgeni Catchment was carried out to assess potential changes in water demand and supply with climate change as well as the impact of present land use on baseline conditions in an operational catchment. The results from that study are presented in the following chapter.

# 10. POTENTIAL IMPACTS OF CLIMATE CHANGE ON THE WATER RESOURCES OF THE MGENI CATCHMENT, KWAZULU-NATAL, SOUTH AFRICA

Thus far, throughout this thesis, land cover has been kept as a constant, *viz.* grassland in fair hydrological condition, and therefore the impacts that have been assessed have been solely that of climate change. However, in operational catchments an added complexity is that land cover. Land cover is often severely perturbed (e.g. agriculture, urban areas, irrigation water transfers and return flows) and therefore it is difficult to isolate what is, in fact, impact of land use and what is impact of climate change. In this chapter such an operational catchment's responses to climate change and change in land use are assessed and an evaluation of individual and combined effects is made.

A brief background to the Mgeni Catchment is given in Section 10.1. This is followed in Section 10.2 by an assessment of the potential impacts of climate change on runoff and sediment yield assuming baseline land cover conditions of Acocks' Veld Types (Acocks, 1988). In this chapter output for a future climate scenario was obtained from the HadCM2 GCM including sulphate feedback (HadCM2+S).

The impact of land use change on the water resources of the Mgeni Catchment was determined (Section 10.3). In Section 10.4 a comparison of the impact of climate change versus that of land use change on baseline conditions is presented. Assuming present land use, the potential impact of climate change on this catchment is determined to assess potential changes in runoff from individual catchments, accumulated runoff and sediment yield, with the later used as an indicator of water quality in the catchment (Section 10.5).

Midmar Dam primarily supplies water to Pietermaritzburg, Durban and the surrounding areas. To assess potential changes in water demand and supply in the Mgeni Catchment resulting from climate change, alterations in the runoff contribution from one of the Quaternary Catchments which feeds Midmar Dam are simulated (Section 10.6). Lastly in Section 10.7,

potential changes in the monthly accumulated runoff from this contributing Quaternary Catchments which feeds Midmar Dam are simulated using *ACRU*.

## 10.1 Background to the Mgeni Catchment

The Mgeni Catchment is located in the KwaZulu-Natal Province on the eastern coastline of South Africa (Figure 10.1) and covers an area of 4 387 km$^2$. There are five large dams in the catchment, *viz*. Midmar, Albert Falls, Nagle, Henley and Inanda Dams. The Mgeni Catchment supplies approximately 45% of the water requirements of the KwaZulu-Natal Province and it a vital source of water for two large urban centres, *viz*. Durban and Pietermaritzburg (Kienzle *et al.*, 1997). This area has a variable rainfall averaging around 900 - 1000 mm per annum (Kienzle *et al.*, 1997; Schulze, 1997b).

Figure 10.1 Overview and location of the Mgeni Catchment in KwaZulu-Natal, South Africa

The Mgeni Catchment has been divided into 145 subcatchments as shown in Figure 10.2, however, in this study *ACRU* simulations are carried out upstream of Inanda Dam, *viz*. from Subcatchment 1 to Subcatchment 137.

Figure 10.2 Division of the Mgeni Catchment into subcatchments

All results presented in this chapter were obtained from *ACRU* simulations carried for the period 1960 to 1993 using the *ACRU* input menus for this catchment prepared by the School of BEEH (Kienzle *et al.*, 1997, Schulze and Nortje, 2000, pers. comm.).

Monthly means of daily maximum and minimum temperatures for each of the 137 subcatchments were generated from daily temperatures (cf. Section 5.3 of Chapter 5) for the period 1960 to 1993. In addition, instead of using the A-pan equivalent values initially input

# Mgeni Catchment Overview

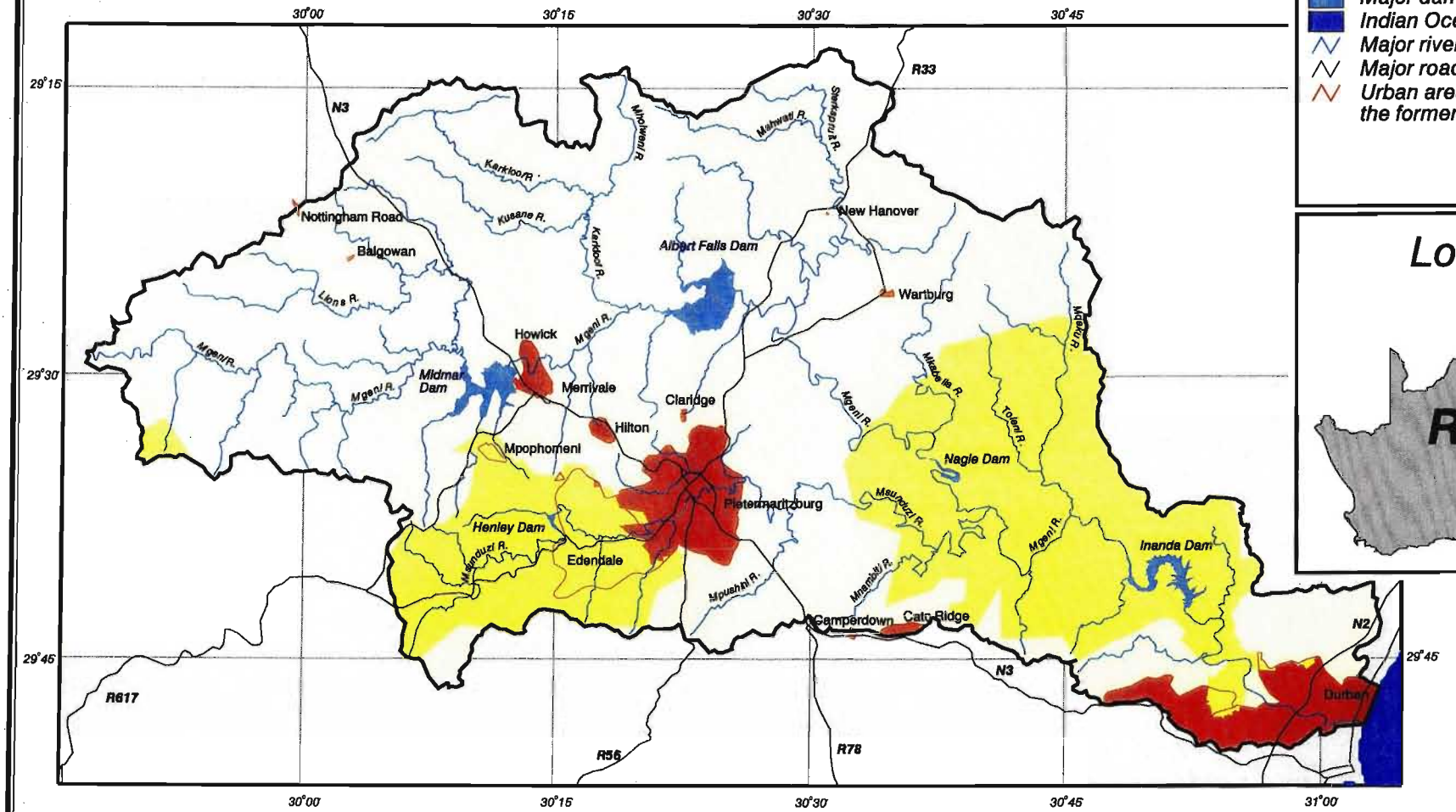


## Legend

- Former KwaZulu areas
- Formal urban areas
- Major dams
- Indian Ocean
- Major rivers
- Major roads
- Urban areas of the former KwaZulu

## Location


Kilometre

0 5 10 15 20 25

Gauss Conformal Projection (31°)

# Mgeni Catchment
## Monitoring Network and ACRU Subcatchments

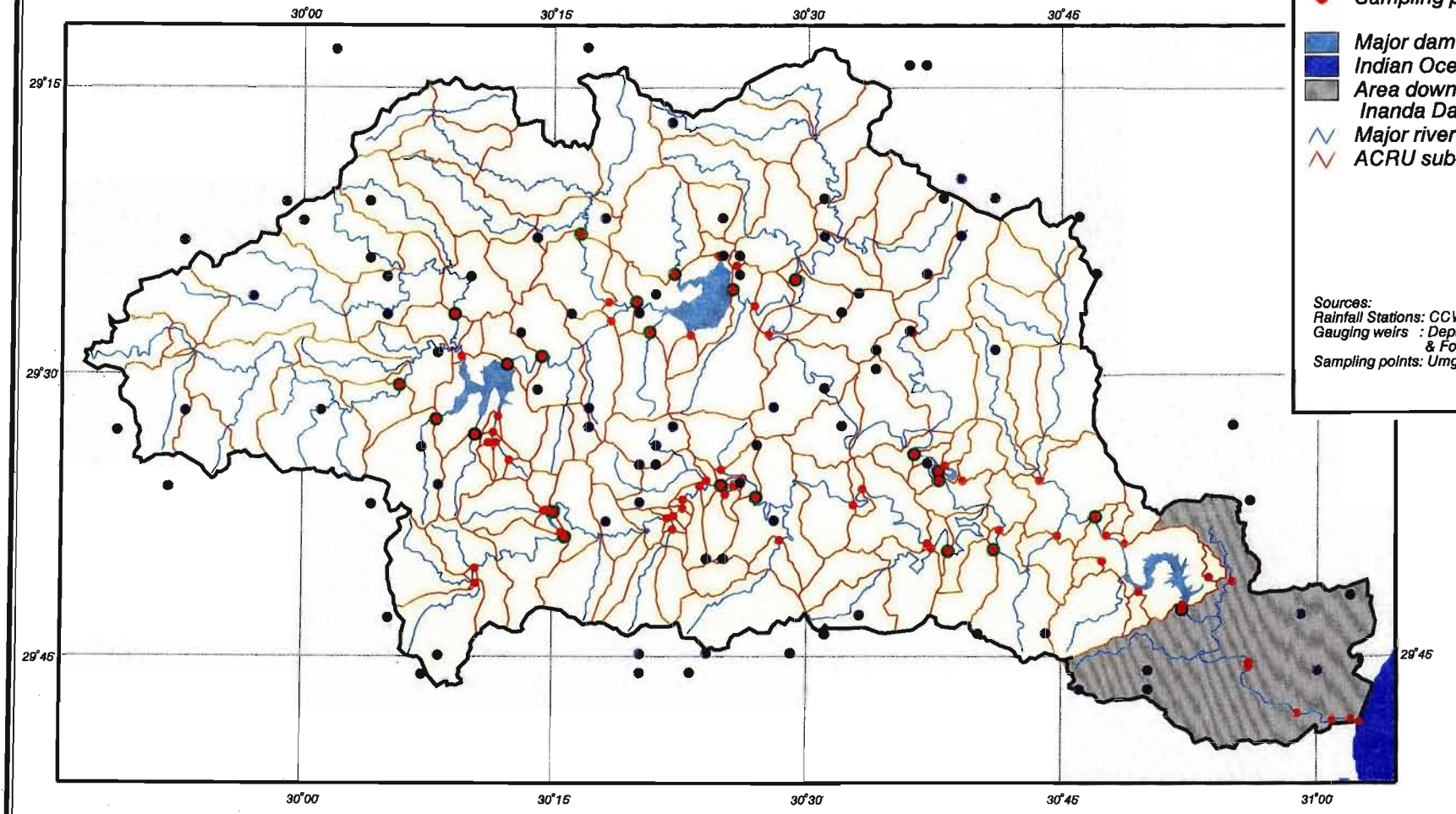


### Legend

- Rainfall station
- Gauging weir
- Sampling point
- Major dams
- Indian Ocean
- Area downstream of Inanda Dam
- Major rivers
- ACRU subcatchments

Sources:
Rainfall Stations: CCWR (1994)
Gauging weirs : Department of Water Affairs & Forestry (1994)
Sampling points: Umgeni Water (1993)

into the menu, evaporation was calculated using the Linacre (1991) equation using monthly temperature input (cf. Chapter 7, Section 7.6) so as to enable a realistic correction to be made for increased potential evaporation for a 2X $CO_2$ scenario.

All future climate scenarios of temperature and precipitation were obtained from the HadCM2+S. The differences in temperature and ratio change in precipitation between future and present climatic conditions for each of the 137 subcatchments were determined by assigning the simulated change in climate of the Quaternary Catchment they are located in.

Under present climatic conditions the monthly means of daily maximum temperatures in the Mgeni Catchment as a whole range from 16.4 °C in June to 27.9 °C in February. For a future climate scenario the temperatures are simulated to range from 18.0 °C in June to 29.5 °C in February. The average maximum monthly temperatures in the Mgeni Catchment are simulated by HadCM2+S to increase by between 1.4 and 2.1 °C in a future climate scenario.

The spatially averaged monthly means of minimum temperatures, on the other hand, range from 3.2 °C in June to 19.3 °C in January under present climatic conditions and are projected to range from 5.0 °C in June to 20.9 °C in February in a future climate scenario using output from HadCM2+S. An increase in average minimum monthly temperatures of between 1.1 and 2.1 °C is simulated by this GCM for the Mgeni Catchment.

The generalised soil description for the Mgeni Catchment is that of a deep, sandy clay loam. However, detailed information on soil horizon thickness, critical soil water contents and saturated soil water redistribution rates for each of the 137 subcatchments are input in the *ACRU* input menu. This information was obtained from the Institute of Soil, Climate and Water.

The first objective of this component of the study was to assess the potential impact of climate change on Mgeni Catchment assuming baseline land cover conditions. The results from this assessment are presented in the following section.

## 10.2 Assessment of Potential Impact of Climate Change on Water Resources Assuming Baseline Land Cover Conditions

In order to assess the potential impact of climate change on the water resources of the Mgeni Catchments, Acocks' 1988 Veld Types (Acocks, 1988) were used to represent baseline land cover conditions. These Veld Types are shown in Figure 10.3. It is assumed under baseline land cover conditions that no dams exist, nor are there any water transfers or abstractions.

| Figure 10.3 | Distribution of Acocks' Veld Types in the Mgeni Catchment (Acocks, 1988) |
|---|---|

Potential changes in mean annual runoff from individual subcatchments, mean annual accumulated runoff and mean annual sediment yield resulting from changes in climate were determined. It is assumed that the spatial distribution of the Acocks' Veld Types will not change under a future climate scenario.

### 10.2.1 Potential impacts of climate change on mean annual runoff

The present climate mean annual runoff (MAR) from individual subcatchments in the Mgeni Catchment, assuming Acocks' Veld Types, ranges from 100 mm from the more eastern and southern subcatchments to over 360 mm in the far northern subcatchments (Figure 10.4, top). Therefore, runoff is primarily generated in western and northern subcatchments. Using a future climate scenario from HadCM2+S, more subcatchments are simulated to generate less than 100 mm MAR (Figure 10.4, middle). Decreases in MAR are also simulated in the northern parts of the Mgeni Catchment, which could have significant implications on the accumulated runoff totals, as this area is a primary contributor to runoff in the Catchment under present climatic conditions.

# Mgeni Catchment
# Baseline Land Cover (Acocks' Veld Types)

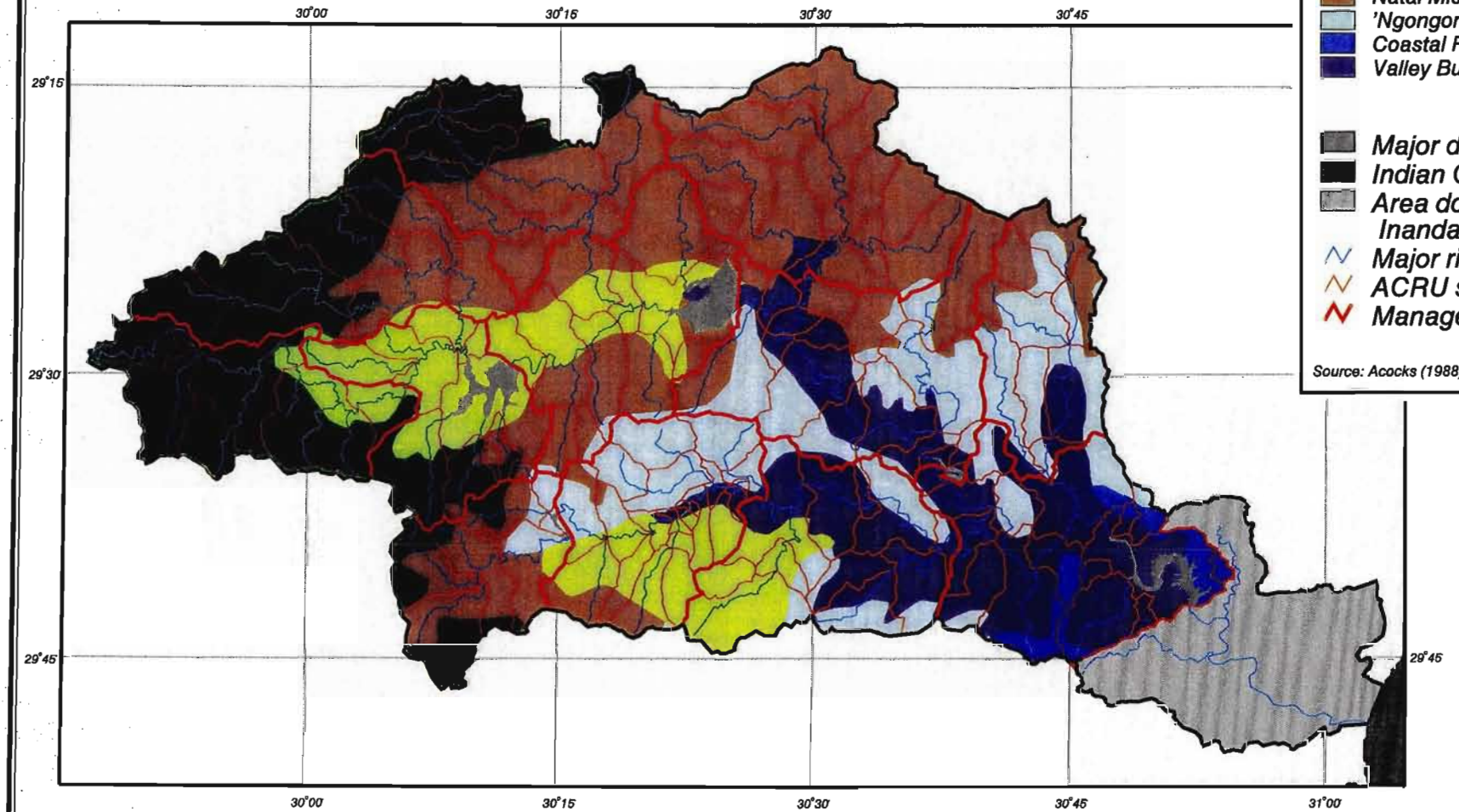


Highland & Dohne Sourveld
Southern Tall Grassveld
Natal Mist Belt, 'Ngongoni Veld
'Ngongoni Veld - Zululand
Coastal Forest & Thornveld
Valley Bushveld

Major dams
Indian Ocean
Area downstream of Inanda Dam
Major rivers
ACRU subcatchments
Management Catchments

Source: Acocks (1988)

Kilometre
0 5 10 15 20 25

Gauss Conformal Projection (31°)

Figure 10.4 Mean annual runoff (mm) of the Mgeni Catchment assuming Acocks' Veld Types: Present climate (top), future climate (middle) and percentage changes in mean annual runoff compared to the present climate (bottom). Future climate scenario from HadCM2+S

The greatest decreases in MAR resulting from climate change, in excess of 100 mm, are simulated in the north-west of the catchment. These decreases in MAR equate to a 20 to 30% decrease of the simulated runoff from Acocks' Veld Types under a present climate scenario (Figure 10.4, bottom). The majority of the Mgeni Catchment is simulated to experience a 0 to 20% decrease in MAR from present climatic conditions for baseline land cover. Only one subcatchment was simulated to have an increase in MAR, however, this increase was found to be less than 10% of present MAR.

### 10.2.2 Potential impacts of climate change on mean annual accumulated runoff

There are 12 Management Areas (essentially Quaternary Catchments) within the Mgeni Catchment as shown in Figure 10.5.

Figure 10.5 The 12 Management Areas in the Mgeni Catchment (Kienzle *et al.*, 1997)

The flow configuration of the 12 Management Areas is shown in Figure 10.6. In order to determine accumulative flows in the Mgeni Catchment, the flow configuration of the 137 subcatchments used in this study needed to be determined and this configuration is given in Figure 10.7.

Under a present climate scenario and assuming Acocks' Veld Types as baseline land cover, the mean annual accumulated runoff ranges from 25 x $10^6$ $m^3$ in the source catchments (shaded red in Figure 10.8, top) to more than 600 x $10^6$ $m^3$ at Inanda Dam in the east.

## Mean Annual Runoff : Acocks' Veld Types

**Mgeni Catchment : Present Climate**

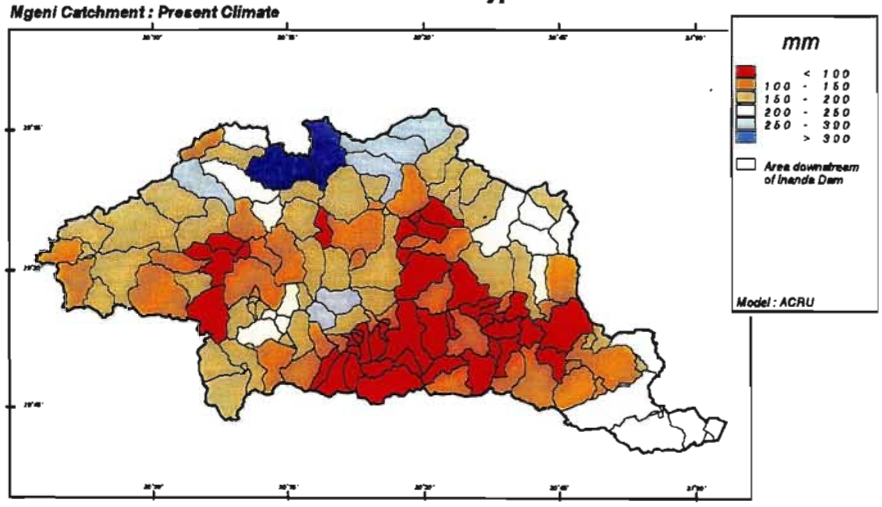


## Mean Annual Runoff : Acocks' Veld Types

**Mgeni Catchment : Future Climate**

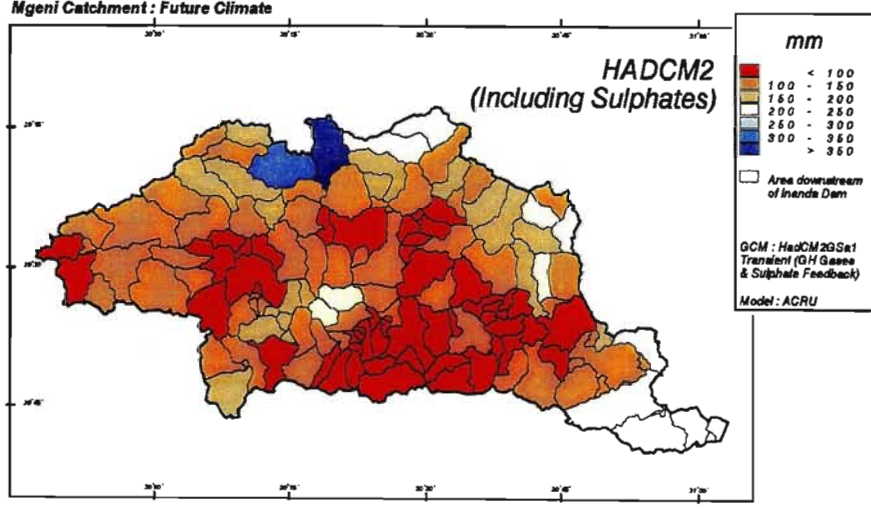


## Impact of Climate Change on Mean Annual Runoff : Acocks' Veld Types

**Mgeni Catchment : (Future Climate - Present Climate) / Present Climate**

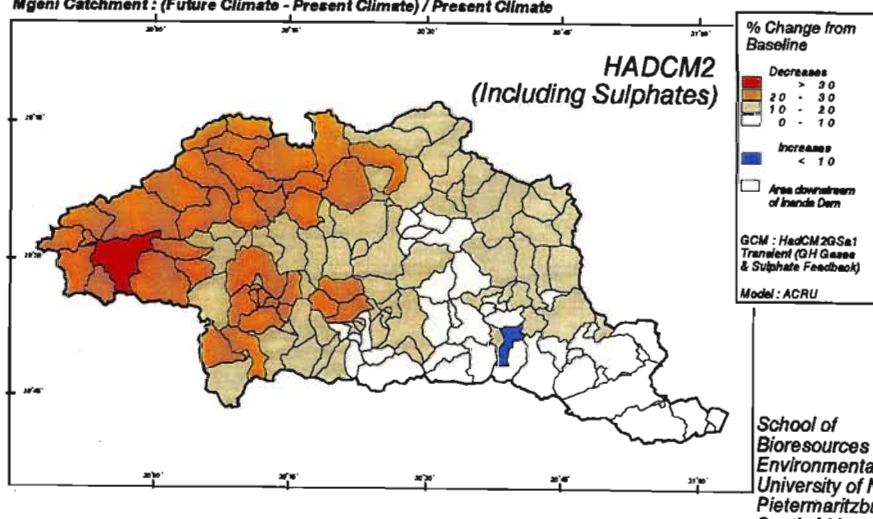


*School of*
*Bioresources Engineering and*
*Environmental Hydrology*
*University of Natal*
*Pietermaritzburg*
*South Africa*

# Mgeni Catchment
# Management Subcatchments

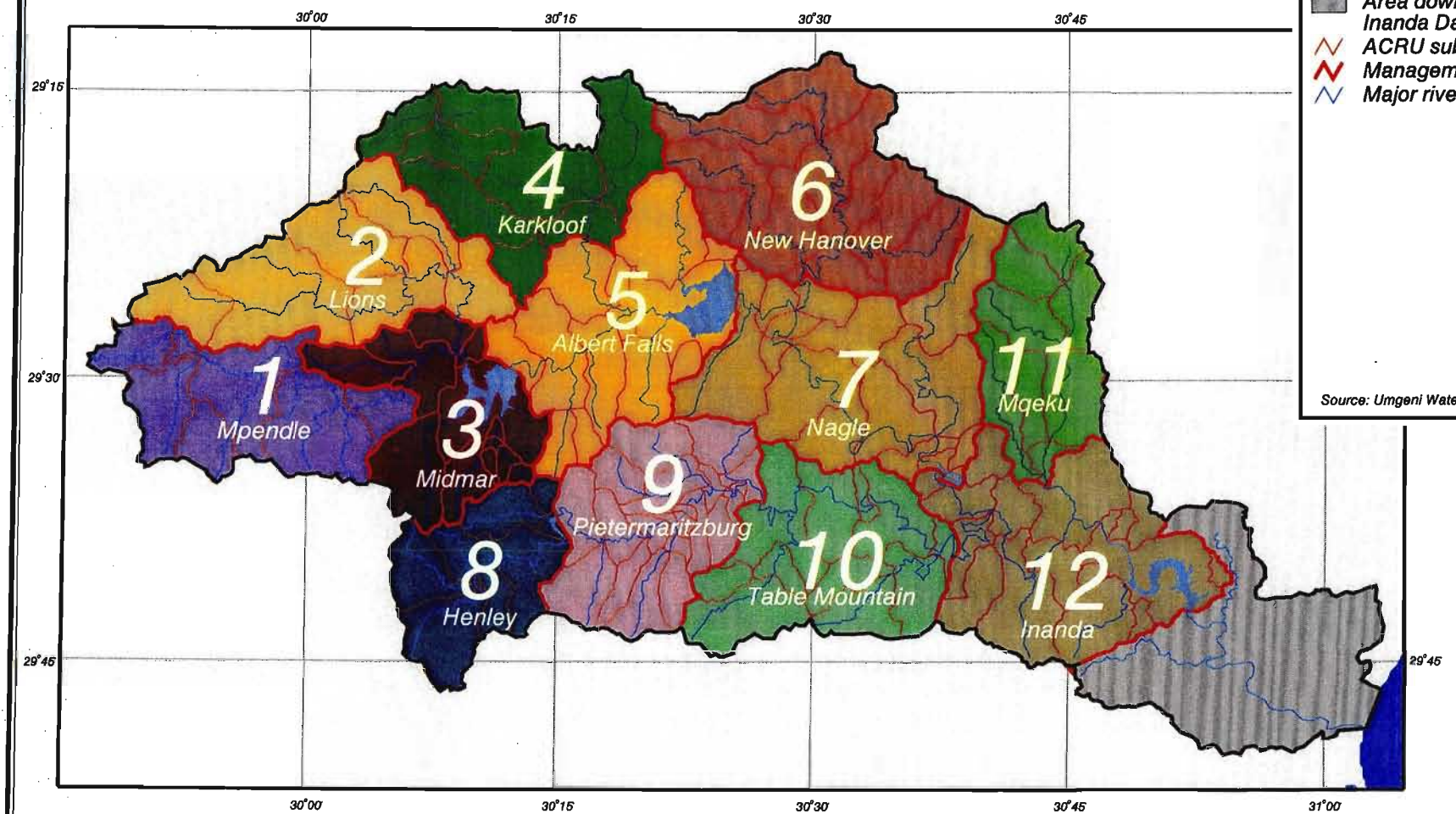


## Legend

- Major dams
- Indian Ocean
- Area downstream of Inanda Dam
- ACRU subcatchments
- Management subcatchments
- Major rivers

Source: Umgeni Water (1994)

Kilometre

0 5 10 15 20 25

Gauss Conformal Projection (31°)

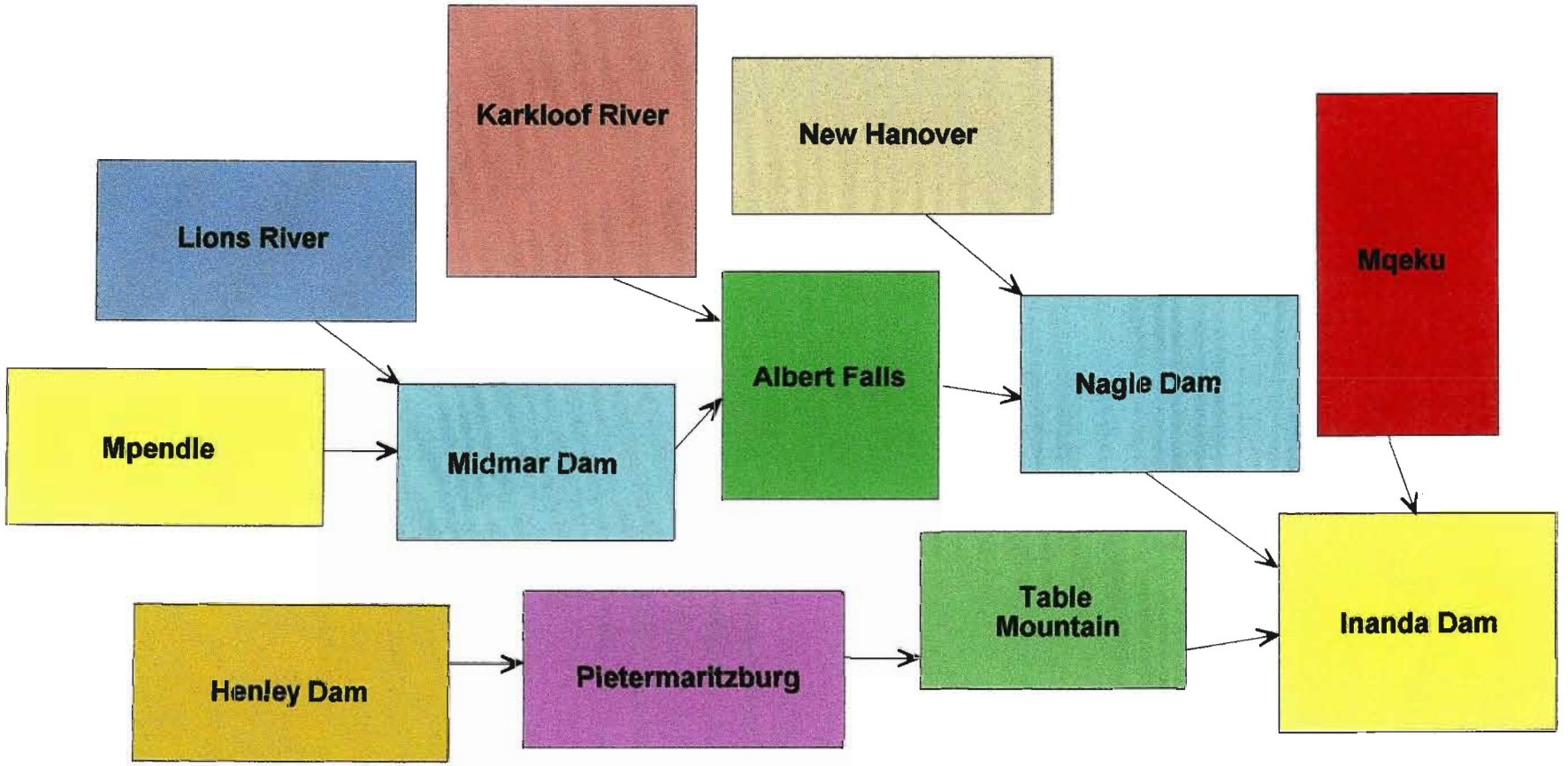


Figure 10.6 The configuration of the 12 Management Areas of the Mgeni Catchment

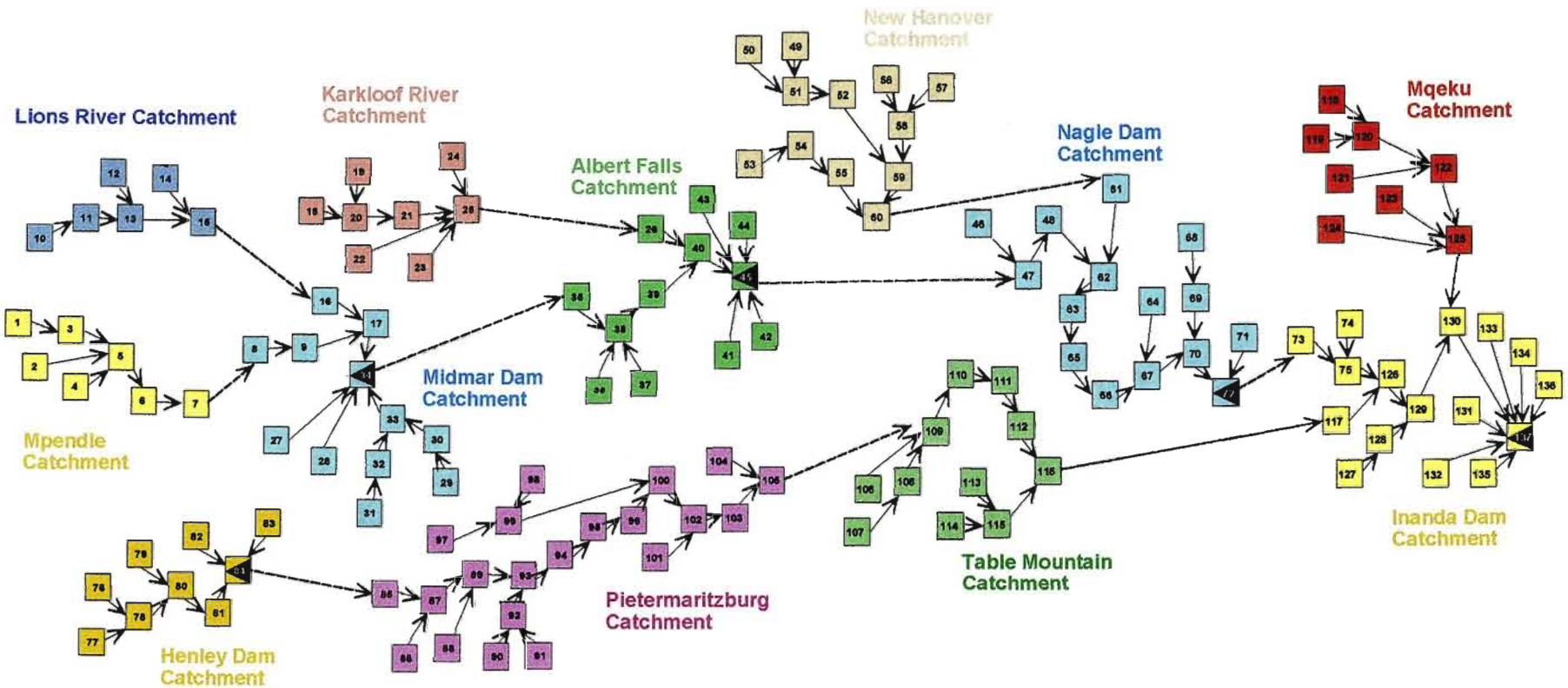


Figure 10.7 The configuration of the 137 subcatchments in the 12 Management Areas of the Mgeni Catchment

Figure 10.8 Mean annual accumulated runoff ($m^3$ x $10^6$) of the Mgeni Catchment assuming baseline land cover conditions represented by Acocks' Veld Types: Present climate (top), future climate (middle) and percentage changes in mean annual accumulated runoff compared to present climate (bottom). Future climate scenario from HadCM2+S

However, using a 2X $CO_2$ scenario from HadCM2+S, the mean annual accumulated runoff could decrease to 500 x $10^6$ $m^3$ at Inanda Dam (Figure 10.8, middle). In addition, many more subcatchments were simulated to have mean annual accumulated runoff less than 25 x $10^6$ $m^3$. Assuming baseline land cover represented by Acocks' Veld Types the most significant differences are in the western source catchments. A more than 20% decrease from present mean annual accumulated runoff results from climate change simulations (Figure 10.8, bottom). At the outlet of Inanda Dam the mean annual accumulated runoff is simulated to decrease to 85 - 90% of present values.

### 10.2.3 Potential impacts of climate change on mean annual sediment yield

Sediment yield in the Mgeni catchment is determined for each subcatchment individually using the MUSLE equation (cf. Section 8.3.2.5 in Chapter 8). The mean annual sediment yields for present and future climate scenarios, assuming Acocks' Veld Types and a future climate scenario from HadCM2+S, are very similar (Figures 10.9, top and middle). The decreases in sediment yield simulated are less than 1 $t.ha^{-1}$ for the entire catchment and only a few subcatchments are simulated to have small increases in mean annual sediment yield resulting from climate change. Using Acocks' Veld Types most subcatchments are simulated in a future climate to have less than a 20% decrease in mean annual sediment yield simulated under present climatic conditions (Figure 10.9, bottom).

## Mean Annual Accumulated Runoff : Acocks' Veld Types

**Mgeni Catchment : Present Climate**

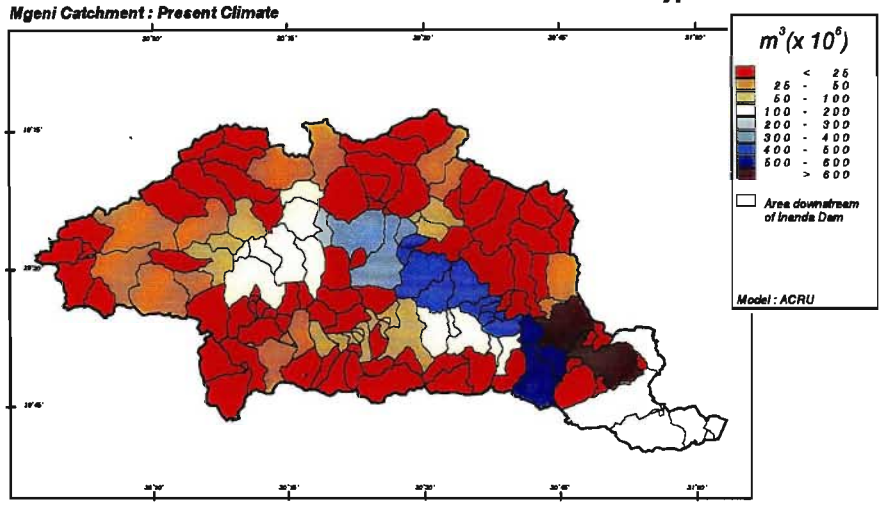


## Mean Annual Accumulated Runoff : Acocks' Veld Types

**Mgeni Catchment : Future Climate**

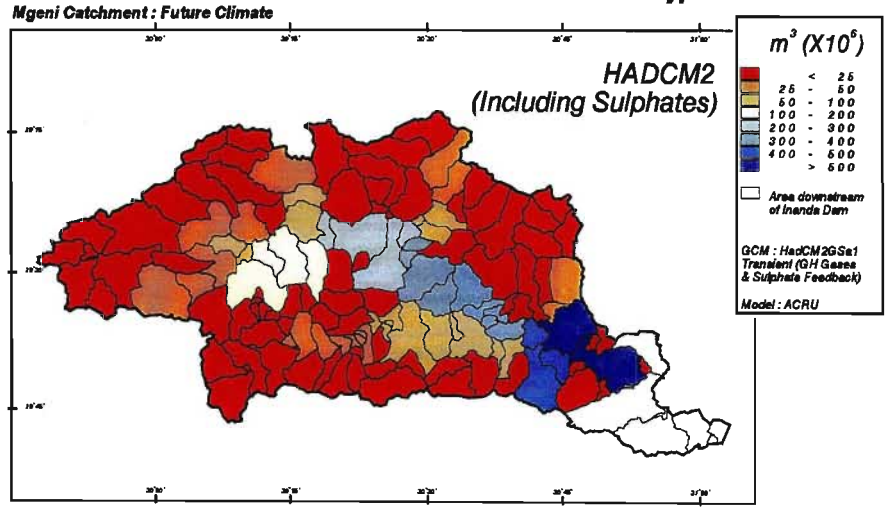


## Impact of Climate Change on Mean Annual Accumulated Runoff : Acocks' Veld Types

**Mgeni Catchment : (Future Climate - Present Climate) / Present Climate**

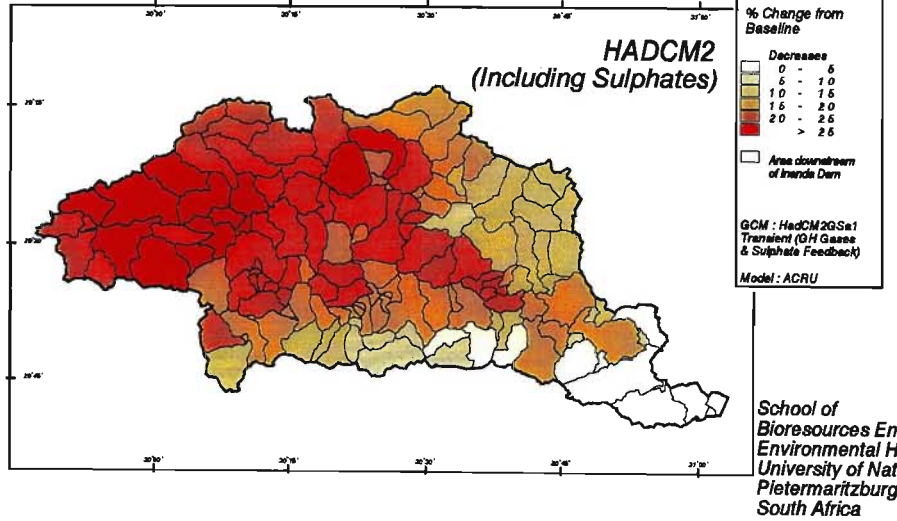



*School of*
*Bioresources Engineering and*
*Environmental Hydrology*
*University of Natal*
*Pietermaritzburg*
*South Africa*

Figure 10.9 Mean annual sediment yield ($t.ha^{-1}$) from the Mgeni Catchment assuming baseline land cover conditions represented by Acocks' Veld Types: Present climate (top), future climate (middle) and percentage changes in mean annual sediment yield from present climate (bottom). Future climate scenario from HadCM2+S

## 10.3 Assessment of Impact of Present Land Use on Water Resources

The *ACRU* input menu for the Mgeni Catchment for present land use was initially established by Kienzle *et al.* (1997) and was subsequently updated and checked by Schulze and Nortje (2000, pers. comm.). The same 137 subcatchments as used in Section 10.2 were used for the simulations of the impact of present land use. The information on land use of the Mgeni Catchment to represent present conditions and correspond with the period of present climate (1960 - 1993) was obtained from the 1986 SPOT Satellite Imagery (Figure 10.10). The *ACRU* input menu for present land use in the catchment includes irrigation abstractions, dams, agriculture and forestry. Information on the 1 138 farm dams contained in the *ACRU* input menu includes location, surface area at full capacity, wall length, axis length, basin slope, dam shape, storage capacity, area / capacity relationships and abstractions (Kienzle *et al.*, 1997).

Figure 10.10 Present land use in the Mgeni Catchment, KwaZulu-Natal, South Africa (Kienzle *et al.*, 1997)

Under the scenario of present land use irrigation takes place throughout of the year in this catchment. It is assumed that from October to March supplementary irrigation water is applied based on crop water demand to refill the soil profile to the drained upper limit, once plant available water is depleted to 50%. While for the rest of the year a fixed amount per fixed cycle of irrigation water is applied. In the months where a fixed irrigation cycle is used, 21 mm is applied every 7 days unless a threshold rainfall had occurred during the cycle.

## Mean Annual Sediment Yield : Acocks' Veld Types

**Mgeni Catchment : Present Climate**

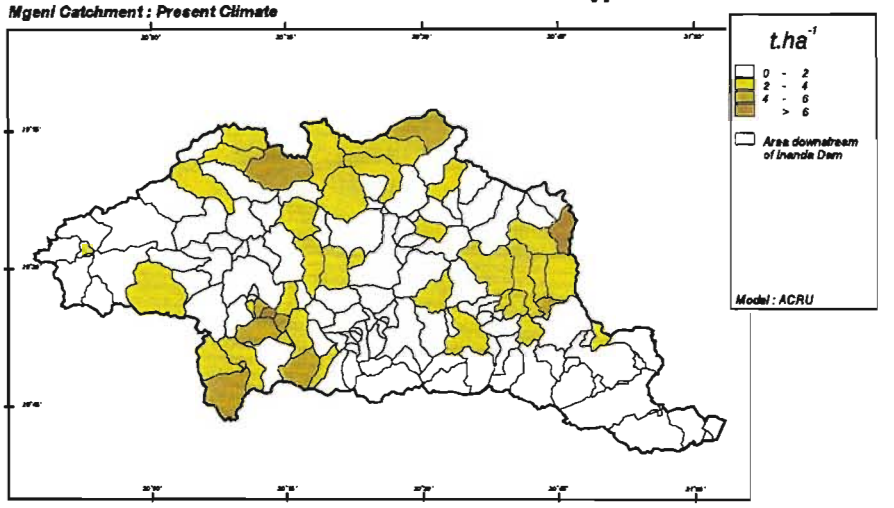


## Mean Annual Sediment Yield : Acocks' Veld Types

**Mgeni Catchment : Future Climate**

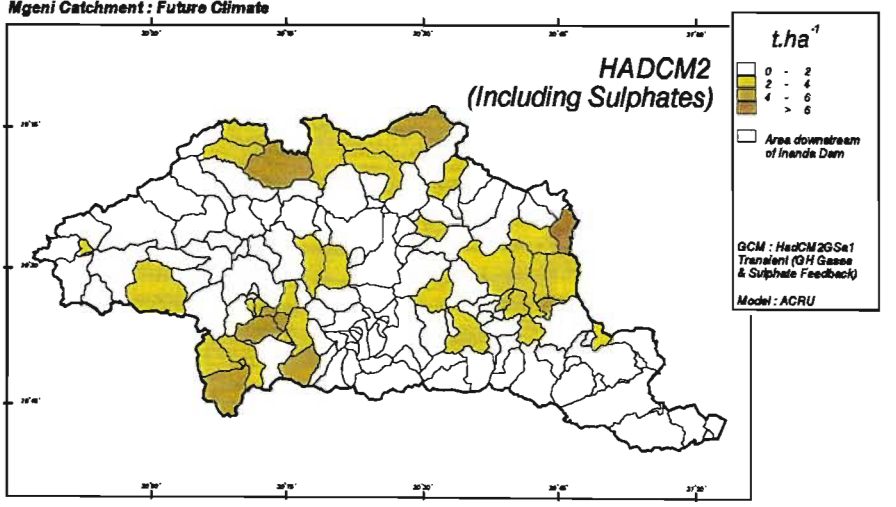


## Impact of Climate Change on Mean Annual Sediment Yield : Acocks' Veld Types

**Mgeni Catchment : (Future Climate - Present Climate) / Present Climate**

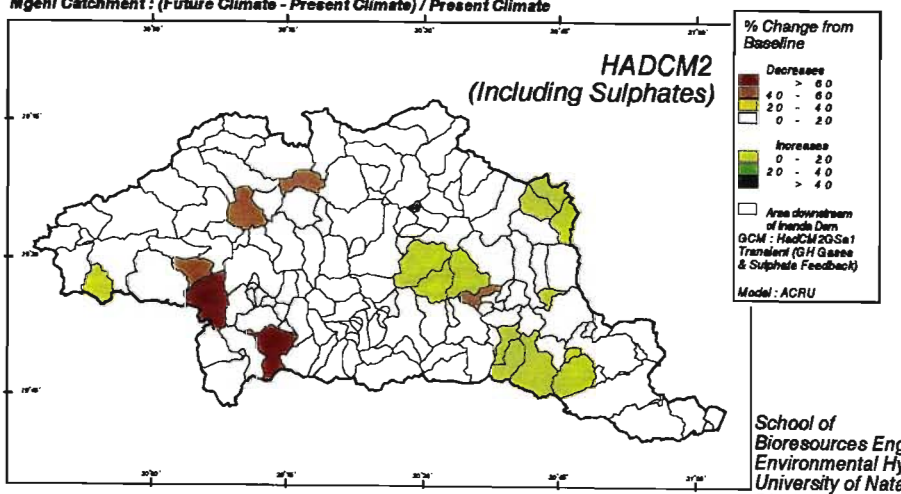


*School of*
*Bioresources Engineering and*
*Environmental Hydrology*
*University of Natal*
*Pietermaritzburg*
*South Africa*

# Mgeni Catchment
# Land Cover (Satellite Imagery, 1986)

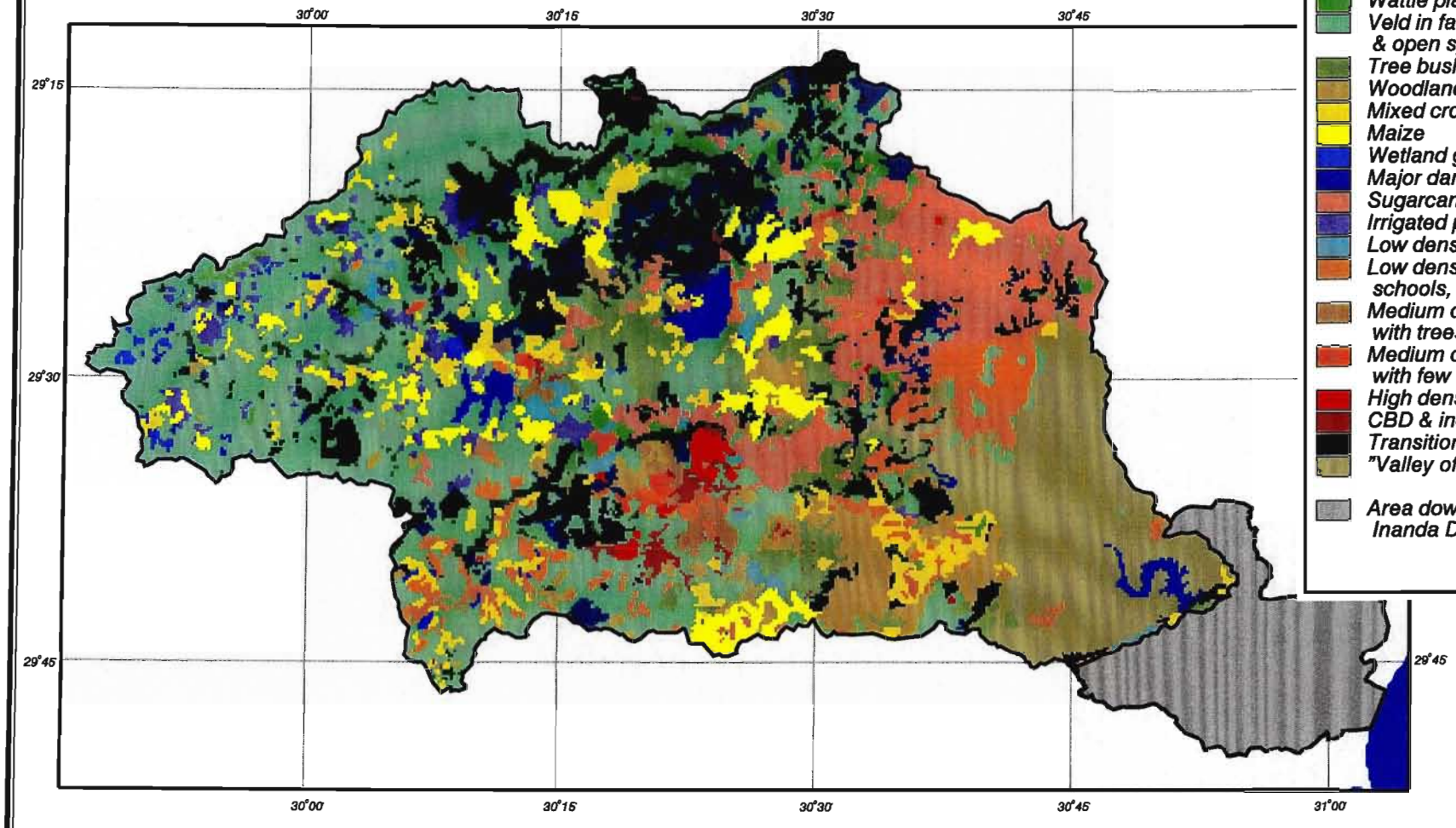


## Legend

- Indigenous forest
- Eucalypt plantation
- Pine plantation
- Wattle plantation
- Veld in fair condition & open spaces
- Tree bush savanna
- Woodland
- Mixed crops
- Maize
- Wetland grasses
- Major dams
- Sugarcane
- Irrigated pastures & crops
- Low density smallholdings
- Low density residential, schools, parks, etc.
- Medium density residential, with trees
- Medium density residential, with few trees
- High density residential
- CBD & industrial
- Transitional housing
- "Valley of a 1000 Hills"
- Area downstream of Inanda Dam

Kilometre

0 5 10 15 20 25

Gauss Conformal Projection (31°)

Irrigation is either supplied from a dam in the catchment or from a river, depending on the actual situation within the subcatchment.

The streamflow values from six of the 12 Management Areas were verified against observed data by Kienzle *et al.* (1997). The verification studies of monthly totals of daily simulated and observed streamflows gave coefficients of determination ($r^2$) above 78% and with four exceeding 84%. In addition, the month-by-month comparisons of simulated versus observed median streamflows show a very good correspondence. "From these highly successful verification studies it may be concluded that the *ACRU* model can be used with confidence to simulate hydrological responses in the Mgeni Catchment" (Kienzle *et al.*, 1997; pg 18).

### 10.3.1 Impacts of present land use on mean annual runoff

Assuming present land use, the mean annual runoff in the catchment ranges from less than 100 mm, with most of these subcatchments located in the Nagle Dam, Table Mountain and New Hanover Management Areas, to over 250 mm in a number of subcatchments (Figure 10.11, top left).

Figure 10.11 Mean annual runoff (mm) of the Mgeni Catchment assuming present land use (top left) and percentage changes in mean annual runoff compared to the baseline land cover represented by Acocks' Veld Types (bottom left). Mean annual accumulated runoff ($m^3 \times 10^6$) assuming present land use (top right) and percentage changes in mean annual accumulated runoff compared to baseline land cover (bottom right). Present climate scenario

Both increases and decreases in MAR are simulated when comparing the MAR from present land use to that from baseline conditions represented by Acocks' Veld Types (Figure 10.11, bottom left). The greatest decreases (over 70% of present MAR) are simulated in the northern subcatchments located mainly in the Karkloof and New Hanover Management Areas (cf. Figure 10.5). The Karkloof Area is planted to commercial forests, whereas the New Hanover Area is also an agricultural region where sugarcane is planted. The planting of commercially

## Mean Annual Runoff : Present Land use

**Mgeni Catchment : Present Climate**

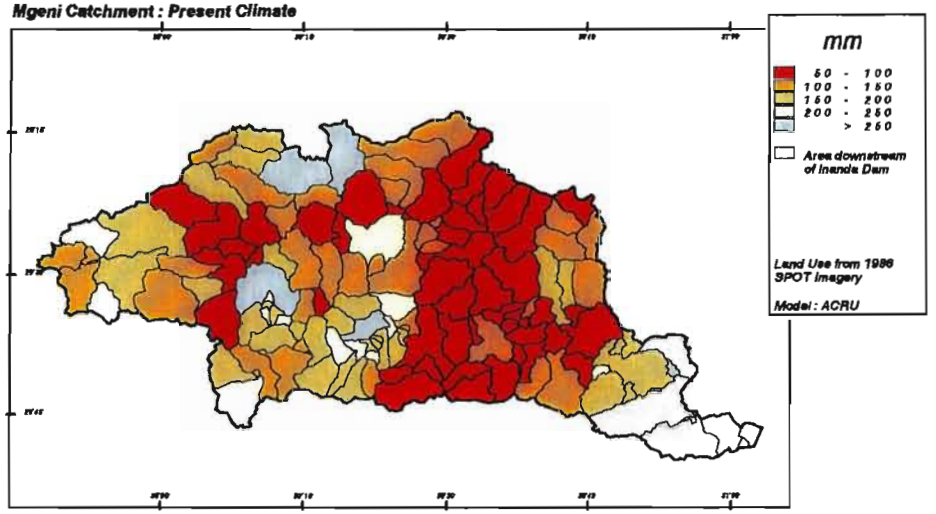


## Mean Annual Accumulated Runoff : Present Land Use

**Mgeni Catchment : Present Climate**

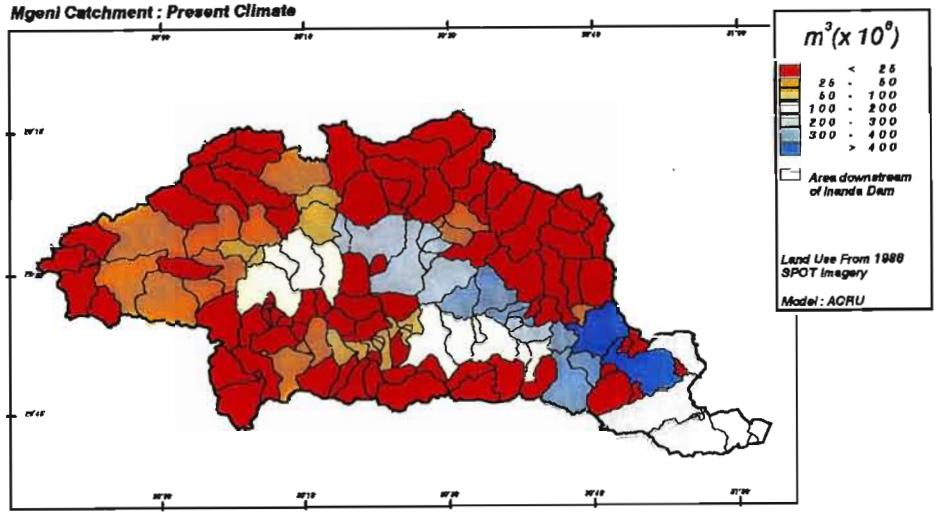


## Impact of Present Land Use on Mean Annual Runoff

**Mgeni Catchment : (MAR Present LU - MAR Baseline LU) / MAR Baseline LU**

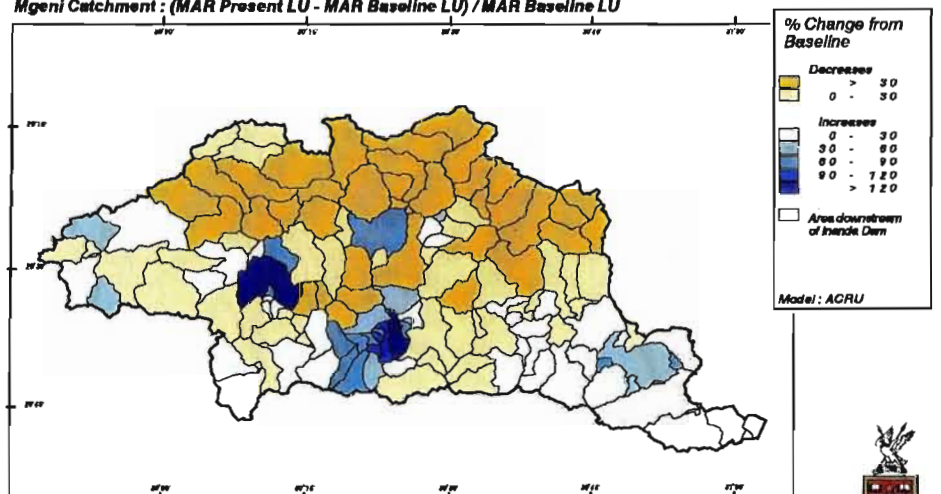


## Impact of Present Land Use on Mean Annual Accumulated Runoff

**Mgeni Catchment : (Accum. R Present LU - Accum. R Baseline LU) / Accum. R Baseline LU**

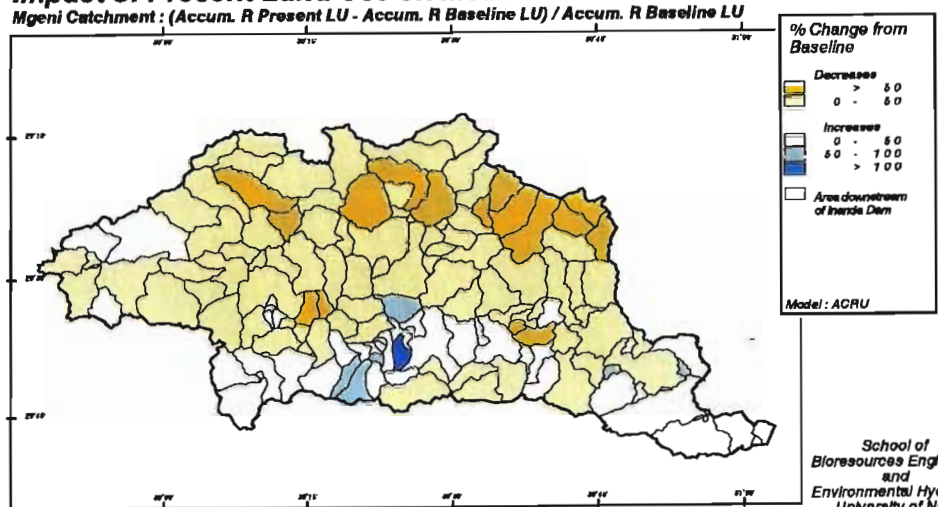


School of Bioresources Engineering and Environmental Hydrology
University of Natal
Pietermaritzburg
South Africa

cultivated trees is known to result in a decrease in MAR from baseline conditions (Schulze, 1995a).

The most significant increases in MAR with land use change are simulated to occur in the southern and eastern parts of the Mgeni Catchment. Increases in MAR from baseline conditions in excess of 90% of present MAR are simulated for the Pietermaritzburg Management Area (cf. Figures 10.5). This is the location of a large urban centre where the many impervious areas result in increases in runoff. Increases in MAR towards the mouth of the catchment in the Valley of a Thousand Hills (cf. Figure 10.5) are also simulated and this rural residential area with a population density of more than 200 inhabitants per $km^2$ and is heavily overgrazed (Kienzle *et al.*, 1997).

### 10.3.2 Impacts of present land use on mean annual accumulated runoff

Using present land use conditions the mean annual accumulated runoff in the Mgeni Catchment ranges from less than 25 x $10^6$ $m^3$ in the source catchments to more than 400 x $10^6$ $m^3$ at Inanda Dam (Figure 10.11, top right). There are significant decreases in mean annual accumulated runoff simulated for present land use conditions (Figure 10.11, bottom right) in comparison to those from the baseline run. The northern two-thirds of the catchment is simulated to have between a 0 and 50% decrease in present accumulated runoff as a result of changes in land use. On the other hand, in the Pietermaritzburg area there is a more than doubling of present accumulated runoff under present land use compared to that from baseline conditions.

### 10.3.3 Impacts of present land use on mean annual sediment yield

The present climate mean annual sediment yield, assuming present land use, ranges from less than 2 $t.ha^{-1}$ in many subcatchments to over 12 $t.ha^{-1}$ in the Valley of a Thousand Hills, which is a highly degraded area as a consequence primarily of overgrazing (Figure 10.12, top). High sediment yields are also simulated in the Edendale area near Pietermaritzburg in the south-east of the Mgeni Catchment where many informal settlements are located.

Figure 10.12 Mean annual sediment yield ($t.ha^{-1}$) of the Mgeni Catchment assuming present land use (top) and percentage changes in mean annual runoff compared to baseline land cover represented by Acocks' Veld Types (bottom). Present climate scenario

Thus, the impacts of present land use on baseline land cover conditions are significant, with increases in sediment yield up to greater than 600% of baseline sediment yields in the urbanised / degraded eastern subcatchments, while decreases in sediment yield in excess of 75% occur in the heavily forested subcatchments (Figure 10.12, bottom). However, the decreases in mean annual sediment yield are not as large as the increases, with most of these subcatchments having increases of between 0 and 75% of baseline sediment yield.

## 10.4 Comparison of the Potential Impacts of Climate Change Versus Impacts of Present Land Use on Baseline Water Resources

From the previous sections, therefore, climate change is simulated to result in changes in MAR of between a 30% decrease and 10% increase from baseline land cover conditions, whereas, when present land use is compared to baseline land cover conditions the change in simulated MAR ranges from a 30% decrease to over 120% increase. Thus, present land use appears to have more of an impact on baseline MAR than climate change.

In the case of sediment yield, *ACRU* simulations using a future climate scenario from HadCM2+S, result in a 0 - 20% decrease in baseline sediment yield with climate change for most parts of the Mgeni Catchment. However, some subcatchments are simulated to have more than a 40% increase or decrease in baseline sediment yield resulting from climate change. The impact of present land use is, however, particularly dramatic in the sediment yield simulations. Poor land use management in the Pietermaritzburg surrounds and the Valley of a Thousand Hills area results in large (> 600%) increases in mean annual sediment yields compared to those simulated for baseline land cover. There are also decreases in

## Mean Annual Sediment Yield : Present Land Use

**Mgeni Catchment : Present Climate**

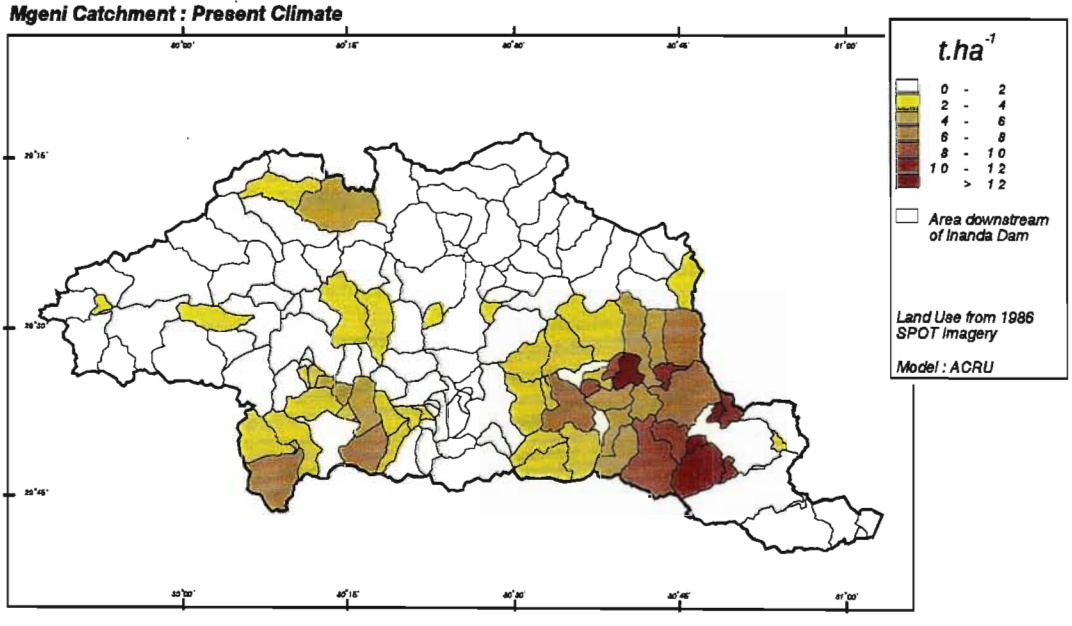


## Impact of Present Land Use on Mean Annual Sediment Yield

**Mgeni Catchment : (Present Land Use - Acocks' Veld Types) / Acocks' Veld Types**

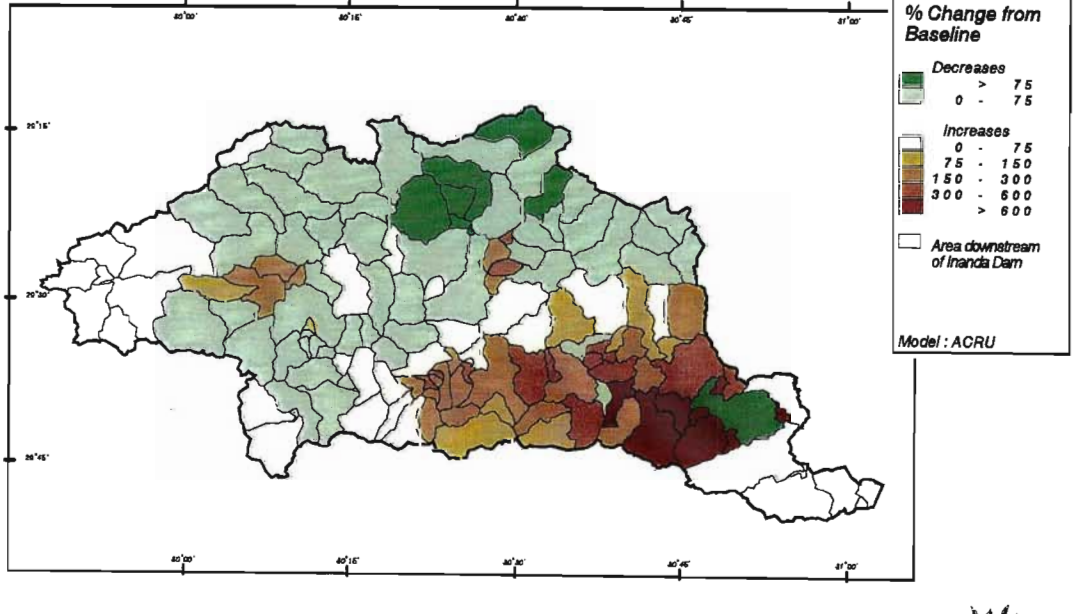

sediment yield simulated mainly in the north of the catchment which are largely under sugarcane and commercial forest plantations.

The next objective was to assess the potential impact of climate change on water resources under present land use in the Mgeni Catchment, as discussed in the following section.

## 10.5 Assessment of Potential Impacts of Climate Change on Water Resources Assuming Present Land Uses

From the previous sections it is evident that land use change has had a greater impact on the hydrology of the Mgeni Catchment than potential climate change. However, the impact of climate change on water demand and supply or sediment yield, and therefore water quality, under present land use conditions may be nevertheless significant.

### 10.5.1 Potential changes in mean annual runoff from present land uses with climate change

Most subcatchments are simulated to have less than 100 mm MAR under present land uses together with a future climate scenario from HadCM2+S (Figure 10.13, top left). Most subcatchments are simulated to have between a 10 and 30% decrease in MAR in a future climate (Figure 10.13, bottom left).

| | |
|---|---|
| Figure 10.13 | Mean annual runoff (mm) in the Mgeni Catchment assuming present land uses: future climate scenario (top left) and percentage changes in mean annual runoff compared to present climate (bottom left). Mean annual accumulated runoff ($m^3$ x $10^6$) for a future climate scenario (top right) and percentage changes in mean annual accumulated runoff compared to present climate (bottom right). Future climate scenario from HadCM2+S |

## Mean Annual Runoff : Present Land use

**Mgeni Catchment : Future Climate**

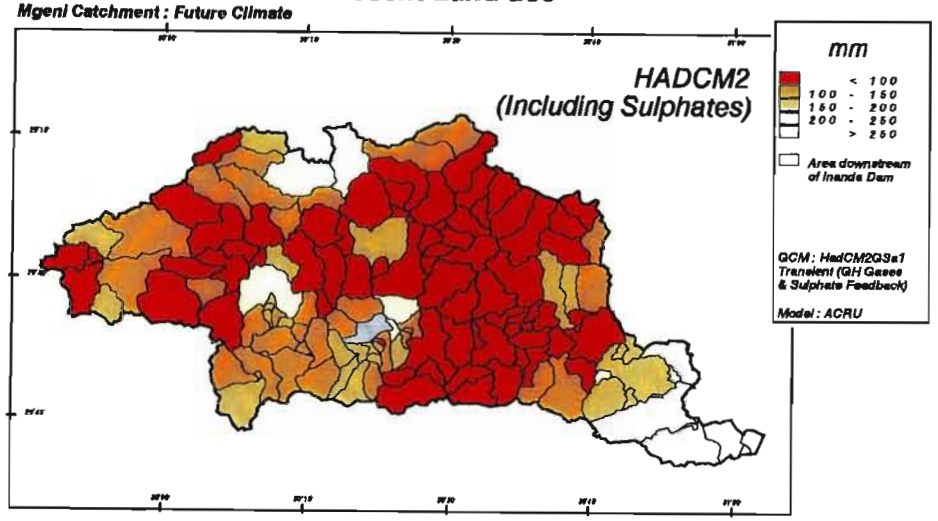


## Mean Annual Accumulated Runoff : Present Land Use

**Mgeni Catchment : Future Climate**

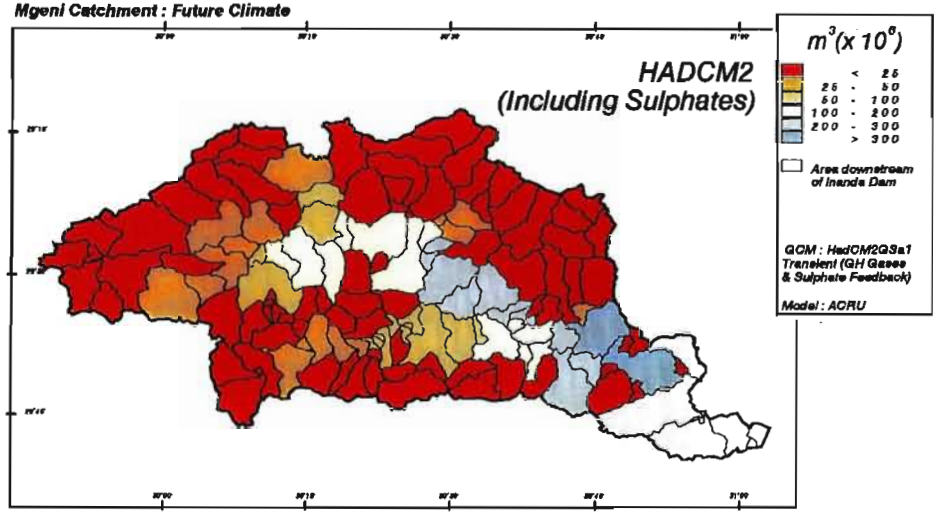


## Impact of Climate Change on Mean Annual Runoff : Present Land Use

**Mgeni Catchment : (Future Climate - Present Climate) / Present Climate**

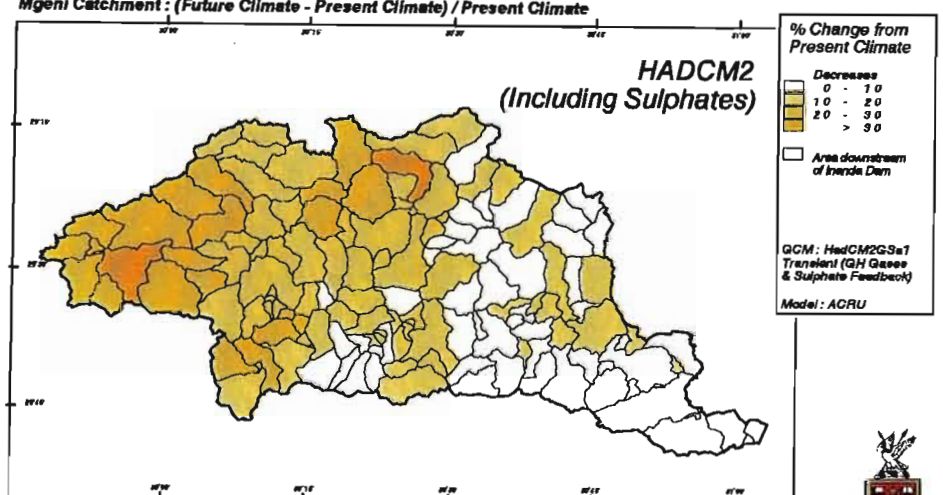


## Impact of Climate Change on Mean Annual Accumulated Runoff : Present Land Use

**Mgeni Catchment : (Future Climate - Present Climate) / Present Climate**

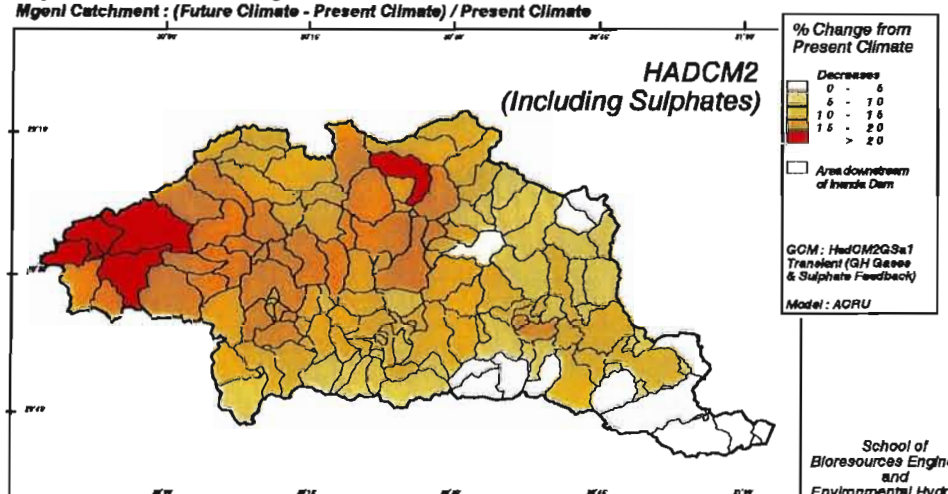



School of
Bioresources Engineering
and
Environmental Hydrology
University of Natal
Pietermaritzburg
South Africa

### 10.5.2 Potential changes in mean annual accumulated runoff with climate change

All subcatchments in the Mgeni Catchment are simulated to have decreases in mean annual accumulated runoff in a future climate (Figures 10.13, top right and bottom right). The largest decreases, of more than 20% of MAR, are simulated in source catchments located in the Lions River Management Area (cf. Figure 10.5).

There are no significant differences in mean annual accumulated runoff along the main stem of the Mgeni Catchment resulting from climate change (cf. Figure 10.13, bottom right) and this is because of the normal flow releases from the various large dams located along the main river stem which dampen the impact of climate change on accumulated runoff downstream of the dam.

### 10.5.3 Potential changes in mean annual sediment yield with climate change

Many subcatchments are simulated to have less than 1 $t.ha^{-1}$ of sediment exiting the subcatchment under a future climate scenario from HadCM2+S. The highest sediment yields are simulated to occur at the subcatchments near Inanda Dam under a future climate scenario (Figure 10.14, top).

Figure 10.14 Mean annual sediment yield ($t.ha^{-1}$) in the Mgeni Catchment assuming present land uses: future climate scenario (top) and percentage changes in mean annual sediment yield compared to present climate (bottom). Future climate scenario from HadCM2+S

Most subcatchments show a 0 - 30% decrease from present sediment yield in a future climate (Figure 10.14, bottom), with some subcatchments simulated to have a 90% decrease in present sediment yield. There are, however, subcatchments which could have increases in mean annual sediment yield under a future climate scenario, but these decreases are relatively small (30% more sediment yield than under present climatic conditions). These reductions in sediment yield could have a positive impact on water quality in the Mgeni Catchment both in

## Mean Annual Sediment Yield : Present Land Use

**Mgeni Catchment : Future Climate**

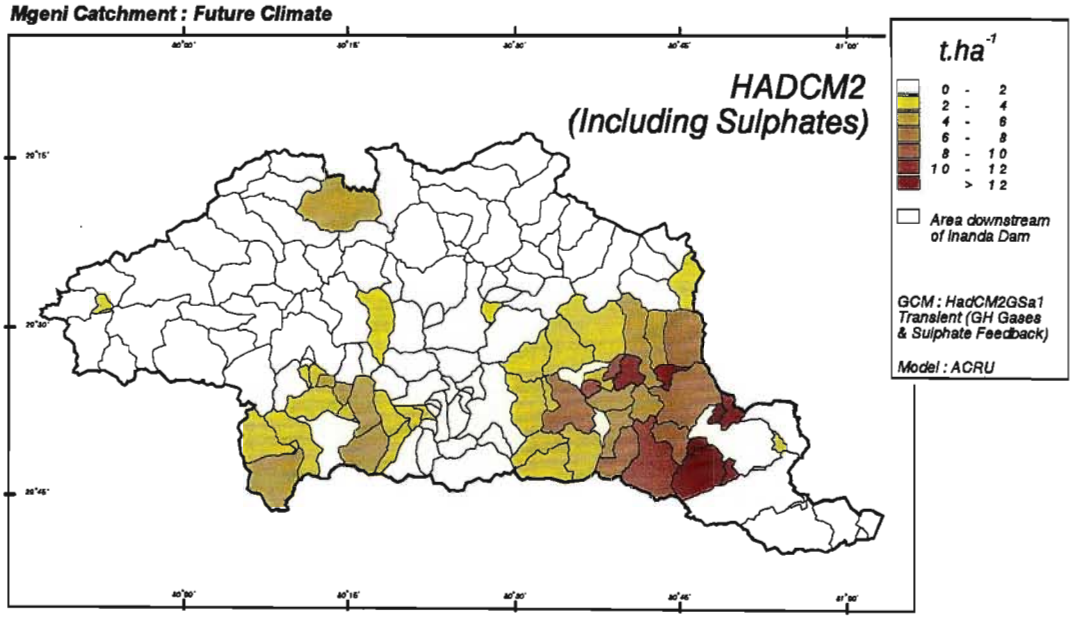


## Impact of Climate Change on Mean Annual Sediment Yield : Present Land Use

**Mgeni Catchment : (Future Climate - Present Climate) / Present Climate**

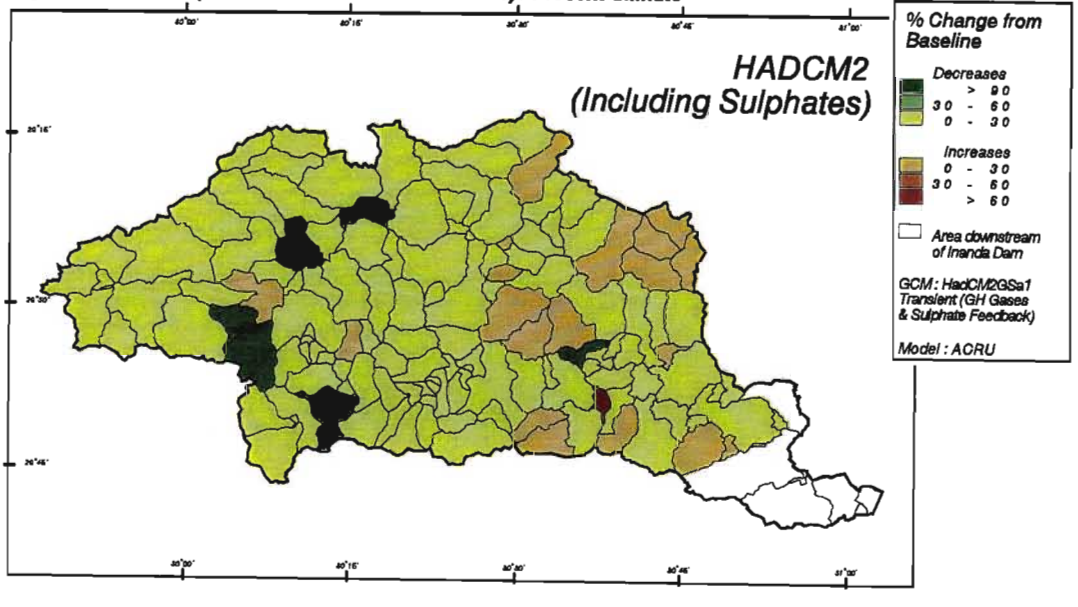

terms of a decrease in suspended sediment as well as improving the biological status of the water supply as the soil particles can carry phosphorus and pathogens which are indicated by the presence of *E.coli* (Kienzle *et al.*, 1997).

## 10.6 Potential Changes in Water Demand and Supply with Climate Change

Climate change could result in changes in water demand both intra-annually and spatially. Changes in water supply in turn affect water consumption, ecosystems and dam operations. Adaptation to changes in water demand and supply as well as non-climatic influences on water resources need to be factored into a study of potential changes in water supply and demand (Shiklomanov, 1999).

In some developed countries water consumption is decreasing through more efficient water use. However, this is not generally the case is most developing countries where water demand is growing primarily through expanding population, thereby increasing the vulnerability to climate variability (Shiklomanov, 1999). Population growth and industrial development in the Mgeni Catchment are expected to increase water demand from 250 million $m^3$ per annum in 1996 to between 375 and 500 million $m^3$ per annum in 2010, depending on the demographic scenario used (DWAF, 1998).

To assess potential changes in water supply from Midmar Dam, the accumulated runoff from the Lions River Management Area (cf. Figure 10.7), *viz.* Subcatchments 1 through to 15, which contributes to the water stored in Midmar Dam, were assessed. Significant decreases in accumulated runoff from these 15 contributing subcatchments resulting from climate change are simulated (Figure 10.15). The simulations from *ACRU* indicate that, apart from one or two exceptions, the accumulated runoff in the high flow months is significantly lower. In addition, the recession of the hydrograph starts earlier and baseflows in low flow months are lower.

If water demand from the agricultural and industrial users, as well as an increasing urban population, increases in future then these decreases in runoff could have significant

implications for users of water supply from the Midmar Dam which supplies water to both the Pietermaritzburg and Durban metropolitan areas as well as the surrounding areas.

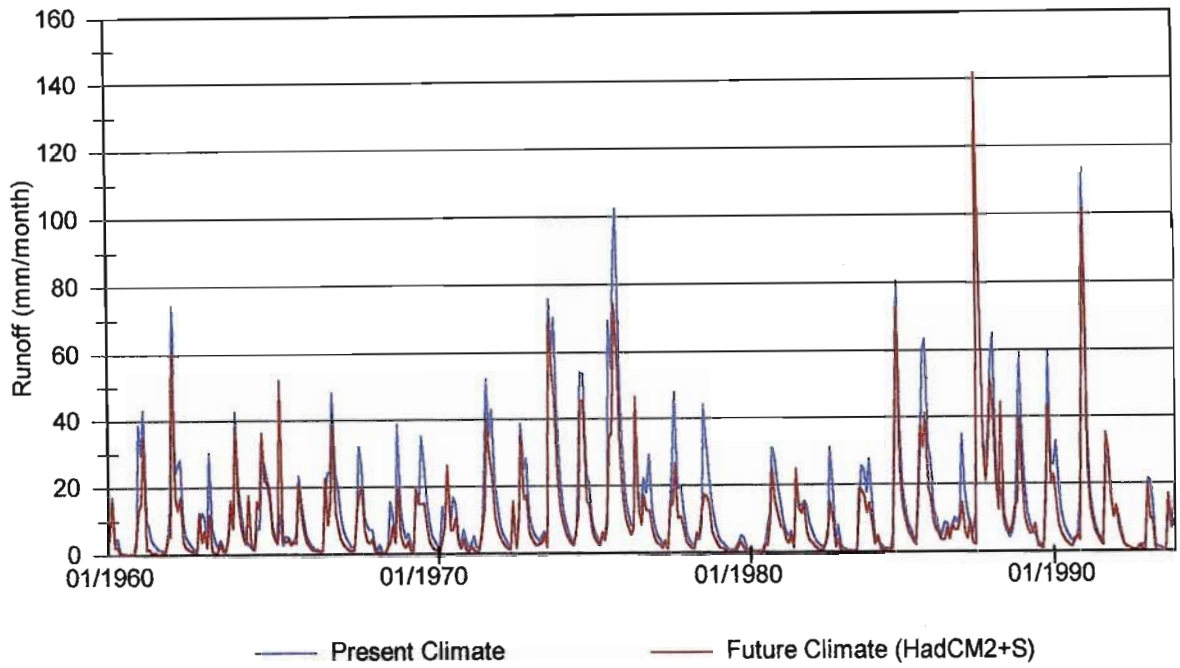


Figure 10.15 Time series of monthly totals of daily runoff (mm) at Subcatchment 15 of the Mgeni Catchment for present and future climatic conditions (GCM: HadCM2+S)

## 10.7 Potential Changes in Mean Monthly Accumulated Runoff

Potential changes in mean monthly accumulated runoff at Subcatchment 15 were assessed to evaluate when these changes in runoff are simulated to occur during the year. Most months are simulated to have decreases in accumulated runoff with the HadCM2+S GCM future climate scenario with the exceptions being June, September and November (Figure 10.16). The largest decreases in accumulated runoff are simulated to occur in the high flow months, with a 24% decrease simulated in January, for example.

Runoff occurring in the high flows months is generally stored in Midmar Dam for release in the low flow months of the year. If large decreases in runoff occur in these high flow months

under a future climate scenario then this could have significant implications for storage levels of Midmar Dam, which could affect water supply in the low flow months.

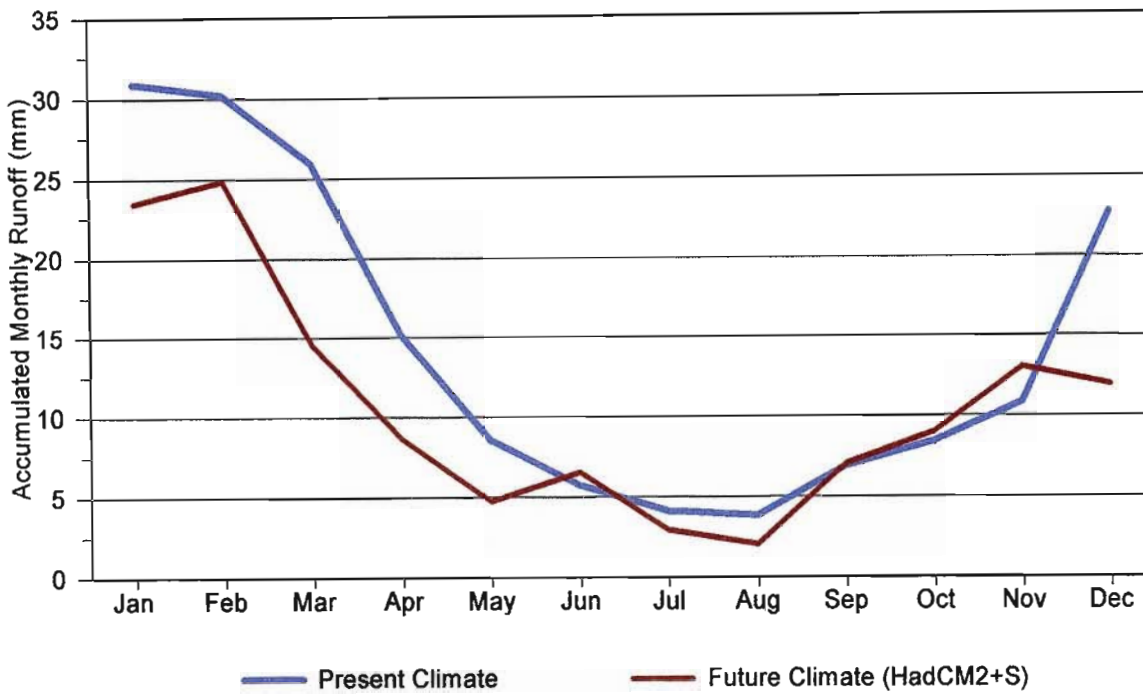


Figure 10.16 Average accumulated monthly runoff (mm) at Subcatchment 15 of the Mgeni Catchment for present and future climatic conditions (GCM: HadCM2+S)

* * * * * * *

The relative impacts of climate change versus land use change were assessed using the Mgeni Catchment as a case study. For the assessment of relative impacts of present land use on baseline land cover conditions, and climate change on baseline land cover conditions, it was found that land use change has a greater impact on runoff and sediment yield in the catchment than climate change. By modifying the land cover from Acocks' Veld Types to the present land uses which included large urban areas on the one hand and significant areas under intensive agriculture and commercial forestry on the other, there are both increases and decreases in the runoff from the Catchment. In addition, large increases in sediment yield were simulated between baseline land cover conditions and present land use, especially in degraded areas.

The analyses of potential impacts of climate change on present land use showed a potential decrease in runoff from the Mgeni Catchment. The highest decreases in mean annual accumulated flow were simulated in the source catchments. Smaller decreases of between 10 and 20% from present accumulated runoff was simulated along the main stem of the Mgeni River owing to the moderating effects of the major dams which have been constructed on the river. In general, sediment yields were simulated to decrease under a future climate scenario from HadCM2+S.

There is expected to be an increase in water demand in the future in the Mgeni Catchment and from the study of potential changes in water supply from Midmar Dam it was concluded that decreases in accumulated runoff simulated upstream of Midmar Dam could result in water supply problems under a future climate scenario.

A range of uncertainties exists in climate impact assessment, from uncertainties in the scenarios from the GCMs to the models used in climate impact assessments. Cognisance has to be taken of these uncertainties in climate change assessments as discussed in the following chapter.

# 11. UNCERTAINTIES IN CLIMATE IMPACT ASSESSMENTS

Even under a stationary climate the impacts of non-climate factors such as population growth and technological advances on land use and hydrology already represent areas of uncertainty. These uncertainties are further compounded when predictions of potential changes in water resources are made for a future climate scenario and are becoming increasingly important as the water resources sector begins to consider climate change in water resources management decisions and water resources planning.

Pittock and Jones (2000) suggest that managers in Australia perceive the uncertainty in climate impacts assessments to be too high, that adaptation (cf. Chapter 12) can cope with the changes that occur and that market reform has sufficient adaptive capacity to cope with climate change. Thus, the question arises as to where the uncertainties in climate impact assessment originate from.

The various sources of uncertainty in climate impact assessments are outlined in Section 11.1. The issue of how to convey the uncertainty inherent in these assessments to stakeholders is addressed in Section 11.2 and techniques of dealing with uncertainty in these assessments are discussed in Section 11.3.

## 11.1 Sources of Uncertainties in Climate Impact Assessments

Broadly, uncertainties in climate impact assessments arise from unknowable knowledge and incomplete knowledge (Arnell, 1999; Hulme and Carter, 1999; New and Hulme, 1999). Unknowable knowledge refers to knowledge that cannot be described in terms of "objectively testable probability distributions". It arises from the inability to determine the reactions of future society and the climate system. Incomplete knowledge arises from model design (either from the climate or impact model) through incomplete understanding of biophysical processes (Gyalistras, 1999; Hulme and Carter, 1999; New and Hulme, 1999). Gyalistras (1999)

represents this concept in Figure 11.1. The two large arrows represent the two possible strategies of dealing with uncertainty.

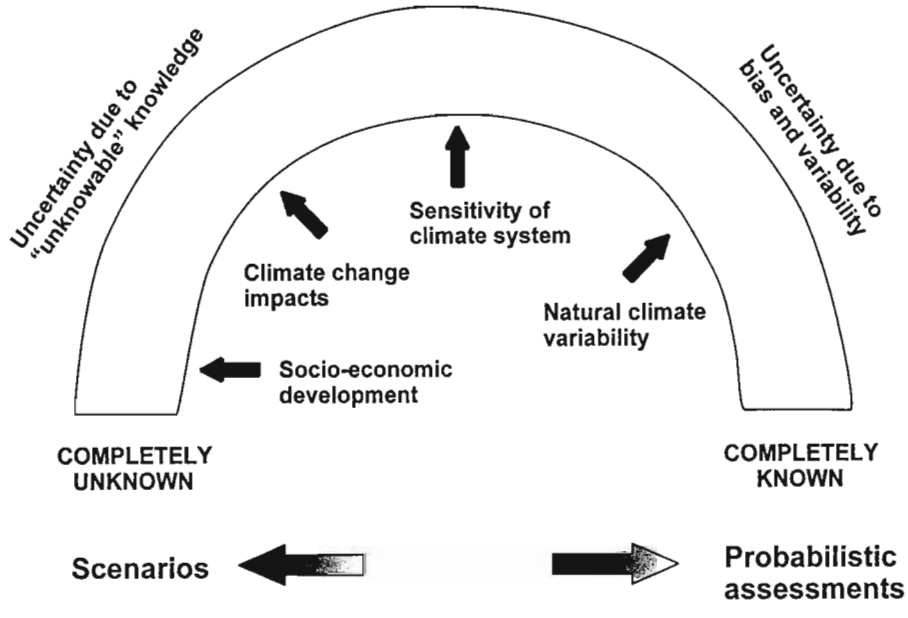


Figure 11.1 Spectrum of uncertainties related to climate impact studies showing a gradual transition from statistically quantifiable uncertainty (right hand side of spectrum) to "unknowable" knowledge (Gyalistras, 1999)

Uncertainties in climate impact assessments can arise from a variety of sources. These sources include

i) the emissions scenarios which are used to force the GCMs;

ii) the climate forcing used in the GCM;

iii) the output from the GCM as well as the climate reference period used in the climate impacts assessment (Bergström *et al.*, 2000);

iv) natural climate variability;

v) the downscaling on the GCM to a regional scale either through a statistical, dynamical or other method (Schulze, 2000b);

vi) the model used to carry out the climate impact assessment, which includes the quality of the data used as input to the model (Bergström *et al.*, 2000);

vii) the impacts assessment itself which could be a single or multitude of results; and

viii) adaptation to climate change impacts.

These uncertainties can be represented diagrammatically (Figure 11.2) as suggested by Viner (2000b).

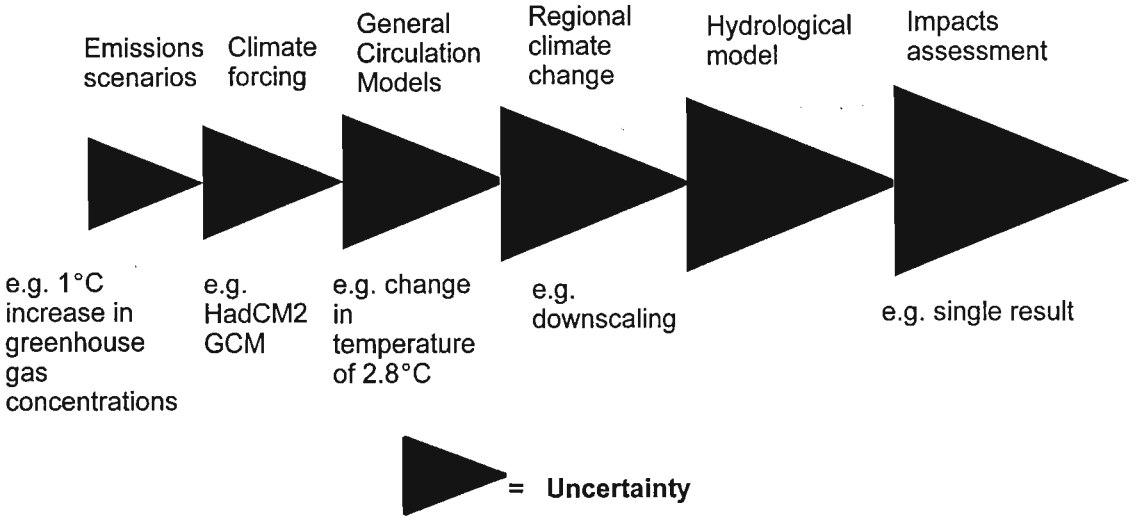


Figure 11.2 Uncertainties in climate impact assessments (after Viner, 2000b)

However, according to Viner (2000b), these uncertainties do not increase slightly as each stage of the assessment as shown in Figure 11.2, but in reality the uncertainties are compounded and show more of an exponential growth with time, as displayed in Figure 11.3.

Each of these sources of uncertainty in climate impact assessment will be analysed in more detail in the following sections.

### 11.1.1 Uncertainties derived from the emissions scenarios

Rates of emissions of greenhouse gases are influenced by economic activity, population growth and technology. Future emission levels of both greenhouse gases and aerosols fall into the category of unknowable knowledge as the rates of change of these factors are uncertain (Jones, 2000). Each emissions scenario implies different levels of atmospheric composition and hence radiative forcing and a range of possible emissions scenarios are used in GCMs (Carter, 1998; New and Hulme, 1999). Most transient climate change experiments conducted with GCMs use a greenhouse gas forcing scenario of 1% per annum increase in equivalent greenhouse gas concentration. This scenario approximates the IS92a emissions scenario

(Leggett *et al.*, 1992). Although this scenario is commonly used in GCMs, future greenhouse gas forcing is highly uncertain and in reality these growth rates could range from less than 0.5% to greater than 1% per annum (Hulme and Carter, 1999).

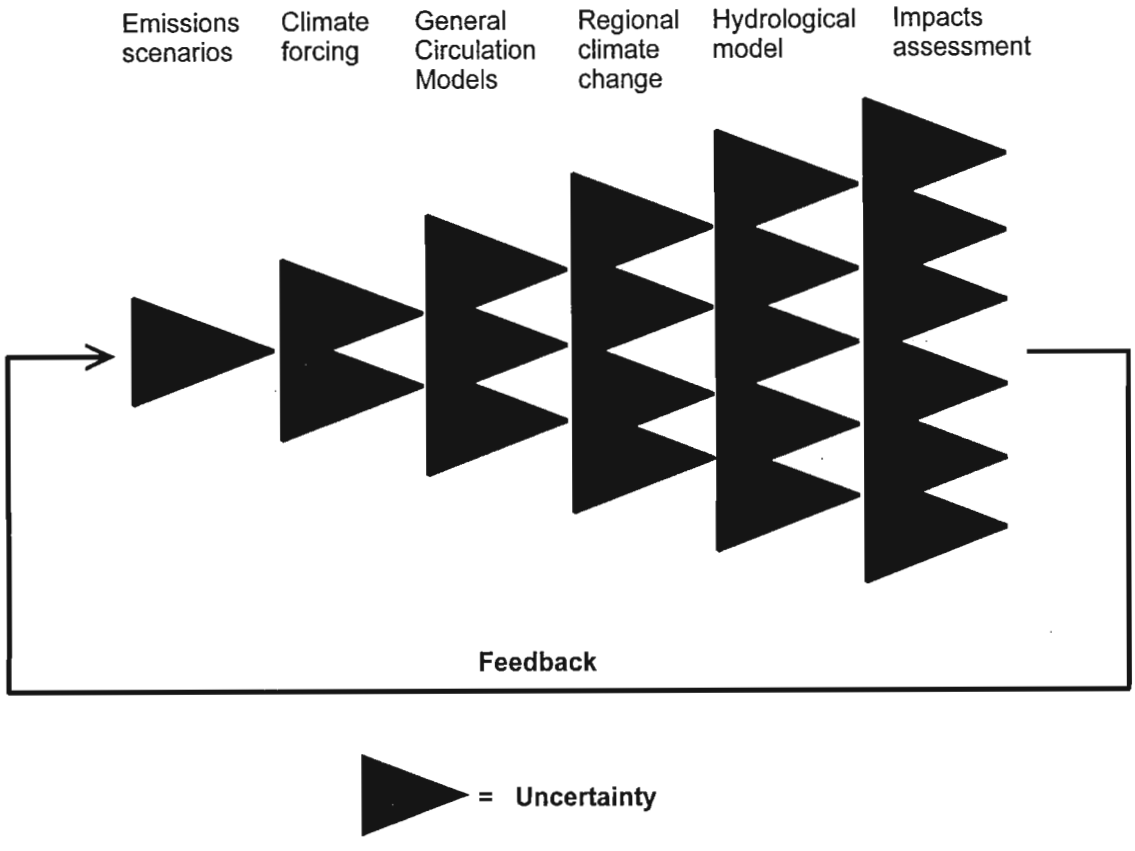


Figure 11.3 Uncertainties in climate impact assessments showing an exponential accumulation (after Viner, 2000b)

### 11.1.2 Uncertainties arising from the climate forcing used

Different results can be obtained from the GCM even when using the same data set; this adds to the uncertainty in the GCMs (Bonell *et al.*, 1999). By carrying out ensemble simulations a wider range of possible future climates is generated and thus a wider range of future impacts is also created. According to Hulme and Carter (1999), this source of uncertainty is additional to that introduced by different forcing scenarios and different climate models and is inherent in all projections of future climate by GCMs.

### 11.1.3 Uncertainties in the output from the GCMs

General Circulation Model estimates of climate variables remain uncertain because of some significant weaknesses of these models, which include (IPCC, 1995)

i) poor model representations of cloud processes;

ii) concern over the simulation of various feedback mechanisms in models, e.g. water vapour and warming, clouds and radiation, ocean circulation and ice, snow and cloud albedo (Carter,1998; Kandel, 2000);

iii) their coarse spatial resolution, at present at best employing grid cells of about 200 km horizontal dimension in model runs for which outputs are widely available for impact analysis;

iv) generalized topographic representation, disregarding some significant orographic features between GCM points;

v) problems in the parameterisation of subgrid scale atmospheric processes such as convection; and

vi) a simplified representation of land-atmosphere and ocean-atmosphere interactions.

Of particular concern over Africa are

i) the inability of GCMs to simulate El Niño / Southern Oscillation (ENSO) events realistically, especially in the light of some regional rainfall regimes in Africa being highly sensitive to the ENSO phenomenon (e.g. south-eastern Africa, coastal East Africa, parts of north-east Africa);

ii) the inability of GCMs to simulate the observed inter-annual and inter-decadal variability of rainfall; and

iii) the representation of land cover / climate interactions over Africa. Sensitivity experiments with climate models have shown that changes in land cover characteristics can have major feedbacks on continental scale climate if the perturbations are large enough (Ringius *et al.*, 1996). Since GCMs used for climate change experiments do not yet allow for land cover characteristics to change dynamically, either as a result of climate change or of human disturbance, there must be some caution applied when interpreting the results of GCM scenarios for Africa (Ringius *et al.*, 1996).

According to the UKMO (2000) the reason why climate predictions are so uncertain is that changes in climate feed back, either positively or negatively, on the original warming and that these feedbacks are poorly understood. Although they believe the most important feedbacks in the atmosphere, ocean, land surface and sea-ice are already included (albeit imperfectly) in the GCM, there are other feedbacks which should be taken into account, and this can only be done by including all components of the climate system in a fully interactive model. The IPCC (2000a) suggest that the greatest uncertainty in GCM simulations of future climatic conditions arises from inadequate understanding of cloud processes and cloud interactions with radiation and aerosols.

A sulphur cycle has been included recently in the HadCM3 GCM which simulates sulphate aerosol from natural and industrial $SO_2$ emissions. The UKMO (2000) state that their "next step is to add the carbon cycle and chemistry; climate change has the potential to disturb the natural carbon cycle in such a way as to alter atmospheric concentration of $CO_2$, and to disturb the chemistry of the atmosphere so as to alter concentrations of other greenhouse gases such as ozone and methane". Submodels currently under development will be incorporated (over the next few years) in the main model to form the first Hadley Centre Earth Systems Model. In future there is a plan to include feedbacks from socio-economic sectors such as agriculture and energy use (UKMO, 2000).

It is stated by Bonell *et al.* (1999) that the problem of uncertainty in the GCM results "can only be resolved by meteorologists and that the hydrological community cannot take direct action, except to bring to the attention of GCM modellers the need for improved land surface parameterisation of surface hydrology".

### 11.1.4 Natural climate variability

Climate varies naturally on multi-decadal time scales unrelated to anthropogenic influences. Thus, the determination of what constitutes natural climate variation and anthropogenically induced changes in climate is complex, in part because of limited long term records (> 100 years) of climate and that it may already contain an anthropogenic signal. Some attempt to

account for natural variability is important when developing climate scenarios (Hulme and Carter, 1999).

A 30 year data set is often used as the representative baseline period in climate impact assessments, however, in terms of multi-decadal variability a 30 year data set may prove to be an incorrect estimate of the longer term average climate (New, 2000).

### 11.1.5 Uncertainties in downscaling GCM output to a regional scale

A higher spatial resolution is required by most impact assessment models than is output by the GCM, as described in greater detail in Section 6.4 of Chapter 6. Therefore, various techniques are employed to interpolate the GCM information to a finer spatial resolution. However, it is unclear as to the best downscaling approach. Polcher (1999) suggests that the most simple method be used which creates the least number of new uncertainties.

It is not possible to validate the downscaling methods used and the overall uncertainties of downscaling GCM output to a finer spatial resolution are difficult to ascertain. However, Kilsby (1999) highlights that the uncertainty inherent in the GCMs outweighs the uncertainty derived from the downscaling technique used.

### 11.1.6 Uncertainties in the model used in the impacts assessments

The most widespread approach for estimating potential impacts of climate change involves the use of impact models. As previously mentioned in Chapter 4, these models vary in complexity from simple empirically based models to complex process based simulation models. All models have inherent uncertainties owing to errors in model structure, parameter values and model inputs (Schulze, 1998; Hulme and Carter, 1999). A model is a representation of the actual real world situation and uncertainties and errors are incurred in the use of a model in climate impact assessment or any other simulations. These include uncertainty in, *inter alia*, vegetation interactions and subsurface processes, according to Pittock and Jones (2000).

In many cases information on these uncertainties can be obtained from validation or sensitivity studies using the model (Arnell, 1999; Hulme and Carter, 1999). In addition, often only one model is used in a climate impact assessment, leading to uncertainty as to whether a different model would produce a different result (Arnell, 1999).

### 11.1.7 Uncertainties in the results from the impacts assessments

There is some doubt as to the reliability of present impact assessments. To predict the impact of climate change at any point in time is difficult because regional scale predictions are uncertain and understanding of some of the crucial processes is limited. Often dated GCM predictions are used, or the version of the GCM is not given in literature cited. Furthermore, very few studies have considered threshold responses to steadily increasing concentrations of greenhouse gases and to concentrations of $CO_2$ beyond a 2X $CO_2$ scenario.

The performance of a GCM at simulating present climate is sometimes compared to observations from present-day climate. However, measurement errors, interpolation errors and sampling errors lead to considerable uncertainty regarding the baseline climate information (Hulme and Carter, 1999) In the verification component of this study the output from present climatic conditions from the GCM was compared to observed climate in southern Africa and particularly poor correspondence was noted between the precipitation estimates from these two sources (cf. Chapter 6, Section 6.6).

Different GCM scenarios yield different results when used as input into models. Therefore, to use one GCM in climate impact assessment gives only one possible outcome in a range of outcomes. Various approaches have been developed to capture this range of responses and they vary from using all possible GCM results to using a selected subset of GCM simulation output. This allows for the generation of a range of future possible impacts (Hulme and Carter, 1999; Polcher, 1999).

### 11.1.8 Uncertainties in adaptative responses to climate change

The impact of climate change in the water and agricultural sectors will depend both on how systems change over time in response to changes in climate and how system managers adapt to climate change impacts, leading to further uncertainty (Arnell, 1999). Potential adaptation responses which could be considered in response to possible negative consequences of changes in climate are discussed in the following chapter.

## 11.2 Communication of Uncertainties to Stakeholders

When results of climate impact assessments are presented to stakeholders and users of the information, some indication of the uncertainty involved in the assessments should be provided (Risbey *et al.*, 2000; Viner, 2000b). However, in many instances stakeholders, decision makers and the public are more interested in environmental, social and economic risks associated with climate change rather than the scientific difficulties encountered in projecting and simulating potential changes in climate. There are arguments for both quantitative and qualitative indications of the uncertainties involved in a climate impact assessment as discussed below.

### 11.2.1 Quantitative measures of uncertainty

Leavesley (1999) suggests that quantitative measures of uncertainty in climate impact assessment results are needed. As the uncertainties involved in climate impact assessments appear to restrict their use, ideally some probability should be attached to the results from the assessments. The importance of thresholds should be emphasised and the robustness of the assessments should also be stressed (Viner, 2000b).

A method of quantifying uncertainty in a climate impact assessment could be through expert judgement of Monte Carlo sampling (Hulme and Carter, 1999). This approach involves the definition of prior probabilities of outcomes from the model, multiple simulations of the model using random samples of the inputs which fall within the predefined probability

distribution and lastly the definition of the distribution of the outcomes (Katz, 1999; New and Hulme, 1999).

### 11.2.2 Qualitative measures of uncertainty

Katz (1999) notes that it could be argued that a qualitative measure of uncertainty, rather than probabilities, should be presented to policy and decision makers with a climate impact assessment, thereby allowing better understanding of uncertainty. However, use of qualitative terms such as "unlikely" or "likely" could be considered subjective and therefore subject to a wide range of interpretations.

Although it is not realistic to include all uncertainties contained in any climate impact assessment, it is necessary to attempt to indicate what uncertainties have, or have not, been factored into the assessment (Hulme and Carter, 1999). Honkasalo (1999) reiterates the importance of stressing the dual nature of uncertainties from both incomplete knowledge and the unpredictability of natural and social systems.

## 11.3 Dealing with Uncertainty

Owing to the considerable uncertainty arising from the inconsistencies in the outputs from the GCMs, managers, decision makers and policy makers face equally high uncertainty in the task of formulating appropriate adaptation strategies and policy decisions.

According to Viner (2000b) the best method of dealing with uncertainty is

i) to perform sensitivity studies;
ii) improve techniques of downscaling GCM output to a finer spatial resolution;
iii) carry out Monte Carlo sampling from which probabilities for the results can be gained; and
iv) to incorporate different forcings, different GCMs and regional uncertainties into assessments.

It is important to stress that the confidence in the ability of GCMs to project future climates has increased. The understanding of climate processes has improved, resulting in improved simulations of water vapour, sea-ice and ocean heat transport dynamics (IPCC, 2000a).

Hulme and Carter (1999) believe that further advances in science and technology should reduce the uncertainty in climate impact assessments. However, they stress that the climate system is a complex, non-linear, dynamic system and that even with perfect models and unlimited computing power for a given scenario of forcing, a range of future climates will always to simulated (Hulme and Carter, 1999).

* * * * * * *

In this chapter some of the primary sources of uncertainties in climate impact assessments have been identified. These uncertainties are difficult to eliminate from the assessments, and thus methods of dealing with these uncertainties have been suggested. It is important to convey to stakeholders both the level of certainty as well as the assumptions made in the assessment where possible.

In the following chapter some potential adaptation strategies which could be employed in the water resources and agricultural sectors are given. Particular reference is made to adaptation strategies that could be employed in southern Africa considering the results obtained in this study.

# 12. POSSIBLE ADAPTATION MEASURES TO THE POTENTIAL IMPACTS OF CLIMATE CHANGE ON AGRICULTURE AND WATER RESOURCES IN SOUTHERN AFRICA

If climate change is considered inevitable, then it is probably inevitable that the sea level will rise, agricultural production will change, runoff and water supply will change and the location of forests and other terrestrial vegetation will alter (Tegart *et al.*, 1990). Society will have to adapt to these and other changes. According to Parry and Carter (1998) a major shortcoming of impact assessments to date has been their superficial treatment of adaptation and this has been due, in part, to its complexity.

According to Downing *et al.* (1997) the principal stakeholders in adapting to climate change can range from consumers and businesses to relief organisations and governments. The potential detrimental effects of climate change experienced by various sectors are likely to dictate their involvement in adapting to any negative consequences of changes in climate.

As already discussed in Chapter 3, the final step in climate impact assessment is the assessment of possible adaptation strategies in response to changes in climate (cf. Chapter 3, Section 3.7). In this chapter the adaption measures which could be applied to reduce any negative impacts of climate change on water resources and agriculture are initially reviewed (Sections 12.1 and 12.2). In Section 12.3 a range of policy options available in the water resources and agricultural sectors are identified and lastly some suggested adaptation strategies for southern Africa, considering the results obtained in this study and other studies, are suggested (Section 12.4).

## 12.1 Possible Adaptation Measures to the Potential Effects of Climate Change on Water Resources

Current water management strategies are generally planned and operated to serve the present range of climate variability, but also have some scope to respond to future perturbations

(Ringius *et al.*, 1996). Presently employed methods to cope with climate variability in southern Africa include the construction of dams, the use of irrigation systems, varying crop planting dates and planting a variety of crops.

However, flood control structures such as dams, spillways and floodwalls, are designed using statistics that are derived from historical data assuming stationarity of the long term climate. In addition, most hydraulic structures are expensive, publicly funded and essentially irreversible structures. These structures have a long life (20 - 200 years) and are expected to operate safely and efficiently under extreme flood and drought conditions (Loaiciga *et al.*, 1996). Potential scenarios of higher temperature, decreases or increases in precipitation and prolonged droughts are a cause for concern. While some regions may receive more streamflow, water scarcity, increased demand and water quality deterioration are very likely to be problems in the future with or without climate change (Ringius *et al.*, 1996).

Water management strategies need to be flexible enough to anticipate the additional stress which climate change may place on managing water in the future. For new hydraulic facilities, early planning for the hydrological impact of climatic changes could prevent their possible failure in future when conditions may change, and thus save expensive redesign or reconstruction. Implementing responses to climate change in the water sector takes a long time. There is a need for enhanced flexibility and advanced planning to decide on how to plan for climate change, given a range of potential climate scenarios. Managers should begin now to plan how the potential effect of climate change could be incorporated into their operating procedures (Ringius *et al.*, 1996).

Climate change may alter the magnitude, timing and distribution of storms that produce flood events, which implies that changes in flood frequency analysis of design floods will be necessary to account for the potential impact of climate change of flood events. Downstream flood protection can be maintained by incorporating expected climate change scenarios into reservoir operating rules, such as keeping reservoir water levels either higher or lower than at present (McAnally *et al.*, 1997). Potential adaptations should also be evaluated in the light of their economic consequences. For example, installation of irrigation systems may be costly

and require regional (rather than just local) planning and management. Furthermore, water for new systems may not be as readily available under changed climate conditions.

Benioff *et al.* (1996) suggest that three basic adaptations are possible in the water resources sector, *viz.* increase water supply, reduce water demand and manage supply and demand differently. Examples of possible adaptations include

i) increasing water supply: modify catchment vegetation, construct reservoirs, drain wetlands, reduce evaporation losses, develop groundwater supplies and use inter-basin transfers;

ii) reducing water demand: decrease the activities that require water, decrease the amount of water demand for each unit of economic activity, modify behaviour to use less water, re-use water and recycle water; and

iii) managing supply and demand differently: modify cropping patterns, apply conjunctive use of groundwater and surface water, apply daily to weekly to seasonal climate forecasts to manage water resources operations, provide more versatile inter-basin transfer schemes and more flexible operating rules for water systems.

## 12.2 Possible Adaptation Measures to the Potential Effects of Climate Change on Agriculture

Changes in temperature, precipitation and $CO_2$ concentrations were shown in this study to potentially have a marked effect on crop yields and their distribution patterns in the study area. Climate change is, furthermore, expected to have a host of effects on the economics of agriculture, including changes in farm profitability, prices, supply, demand, trade and comparative advantage (Kaiser *et al.*, 1993).

As the focus of this thesis has been on the refinement of modelling tools for application in assessing potential impacts of climate change, and not solely on the possible impacts themselves, only a brief summary of some of the adaptation strategies that could be considered at a farm scale are presented below.

The prospects for natural adaptation of crop species to climate change do not appear promising (IPCC, 1999). However, in the past the agricultural sector has shown remarkable capacity to adjust to social and environmental changes. Agricultural adaptation to climate change could take several forms including technological innovations, changes in land areas under specific crops and changes in modes of irrigation and scheduling.

Technological innovations include the development of new plant cultivars, or switching cultivars, for a particular crop. For example, if climate change were to affect the length of the growing season, then farmers could switch to a shorter-growing, higher yielding cultivar. Furthermore, if climate change was to affect the relative yield and profitability of one crop in favour of another, then farmers could respond by changing the crop mix planted. Finally, farmers could adjust their scheduling of field operations (e.g. plant dates) in response to changes in climate (Kaiser *et al.*, 1993).

## 12.3 Policy Options for Adaptation to Climate Change

One of the first steps in responding to climate change is to identify the policy options available to address the adverse effects of such change. All anticipatory adaptation policies should satisfy at least two criteria, *viz.* flexibility and the potential for benefits to exceed costs. There are many uncertainties regarding the regional impacts of climate change and, therefore, to address the broad range of uncertainties, anticipatory adaptation policies should be flexible. The objective of selecting an adaptation policy should be to enhance the ability to meet stated objectives under a wide range of climatic conditions. Thus, a policy may be either *robust*, implying that it allows the system to continue functioning under a wider range of conditions, or *resilient*, implying that it allows the system to quickly adapt to changed conditions (Smith and Lenhart, 1996).

In addition to being flexible and having the potential for benefits to be greater than costs, anticipatory adaptation options that meet the following criteria should be implemented sooner rather than later to address climate change. Adaptation policies should be implemented in anticipation if, firstly, there are net benefits independent of climate change and, secondly,

because they would be significantly less or ineffective if implemented as reactive policies, i.e. they are of high priority because of irreversible catastrophic impacts, long term decisions such as the construction of dams and bridges or unfavourable trends (Smith and Lenhart, 1996).

### 12.3.1 General policy options for adaptation to climate change

The following general policy options for adaptation to climate change are broad strategies which may be used to complement specific policies, as suggested by Smith and Lenhart (1996):

i) *Incorporate climate change in long-term planning*: Long-term planning for climate-sensitive resources should incorporate changes in conditions that will affect the services provided by those resources. Including climate change in long-term plans could result in changes being made that will enhance the ability of future generations to cope with these changes.

ii) *Keep an inventory of existing practices and decisions used to adapt to different climates*: An inventory may focus on actual social and economic decisions in light of variable climatic regimes over time or across regions.

iii) *Promote awareness of climatic variability and change*: Climatic variability and the potential risks of climate change are often not well understood by the public or by decision makers. Because climatic adaptation will affect the individual, organisational and policy levels, communication about the human significance of climatic variability is important at all levels in a community.

More specific policy options that could be applied in the water resources and agricultural sectors are suggested in the following sections.

### 12.3.2 Policy options for adaptation of water resources

i) *Plan and co-ordinate use of catchments*: Comprehensive planning across a catchment, ie. river basin, may allow co-ordinated solutions to problems of water quality and water supply. Planning can also help to address the effects of population growth, economic growth and changes in the supply of and demand of water.

ii) *Make marginal changes in construction of infrastructure*: In planned construction consider marginal increases in the size of dams or marginal changes in the construction of canals, pipelines, pumping plants and storm drainages.

iii) *Conserve water*: Reducing demand can increase excess supply, creating a greater margin of safety for future droughts. Demand for water may be reduced through a range of measures that encourage efficient water use including education, voluntary compliance, pricing policies, legal restrictions on water use, rationing of water or the imposition of water conservation standards on technologies.

iv) *Control pollution*: Polluting water so that it is unfit for drinking or other uses can have an effect that is similar to reducing water supply. Reducing water pollution effectively increases the supply of water. In turn, a larger water supply increases the safety margin for maintaining water supplies during droughts.

v) *Allocate water supplies by using market-based systems*: Market-based allocations are able to respond more rapidly to changing conditions of supply and also tend to reduce demand, thus conserving water. Consequently, market-based allocation increases both the robustness and the resiliency of the water supply system.

vi) *Adopt contingency planning for drought*: Plans for short-term measures to adapt to water shortages could help mitigate droughts. Planning could be undertaken for droughts of known, or greater, intensity and duration. The cost of developing contingency plans is relatively small compared with the potential benefits.

vii) *Use inter-basin transfers*: Transfers of water between catchments may result in more efficient water use under current and changed climate. Transfers also can be an effective short-term measure for responding to regional droughts or other problems of water supply.

viii) *Maintain options to develop new dam sites*: Keep options open to develop new dam sites, should they be needed. The number of sites that can be used efficiently as reservoirs is limited and removing structures once an area has been developed may be very costly or politically difficult.

ix) *Improve monitoring and forecasting systems for floods and droughts*: Climate change is likely to affect the frequency of floods and droughts. Monitoring systems will help in coping with these changes and will be beneficial without climate change.

### 12.3.3 Policy options for adaptation of agriculture

The following is a list of possible options for adaptation in the agricultural sector to potential effects of changes in climate (Smith and Lenhart, 1996).

i) *Develop new crop types and enhance seed banks*: The storage of a variety of seed types allows the opportunity for farmers to diversify .

ii) *Avoid monoculture and encourage farmers to plant a variety of heat and drought resistant crops*: Growing one crop only increases the farmers vulnerability to climate variability.

iii) *Increase efficiency of irrigation*: Efficient use of irrigation can reduce dependence of farmers on rainfall and runoff. Improvements allow greater flexibility by reducing water consumption with reducing crop yields.

iv) *Disperse information on conservation practices*: By employing conservation practices such as contour ploughing, terracing or using wind breaks, soil moisture contents can be increased and well as aiding in the reduction of soil erosion.

v) *Promote agricultural drought management*: Encourage management practices that recognise drought as part of a highly variable climate rather than treating it as a natural disaster.

## 12.4 Potential Adaptation Strategies for Southern Africa

According to Watson *et al.* (1997) the African continent is particularly vulnerable to the impacts of climate change because of factors such as widespread poverty, recurrent droughts, inequitable land distribution and over-dependence on rainfed agriculture. Resource poor farmers, land owners, people reliant on rainfed agriculture and subsistence agriculture could be considered particularly vulnerable and for these people the outcomes of adaptation strategies in respond to climate change could affect their livelihood (Downing *et al.*, 1997).

Ideal adaptation strategies include those that

i) have benefits for a number of objectives and stakeholders;

ii) are timed to maximise benefits; and

iii) are in the context of sustainable development (Downing *et al.*, 1997).

Cost effective strategies in adapting to climate change are of particular importance in a developing countries such as Lesotho, Swaziland and, up to a point, South Africa. The benefit of adaptation needs to be clear to encourage investment in climate change adaptation to be made. In certain instances the beneficiaries many be future generations and thus incentives may be necessary to encourage investment in adaptation strategies. An inexpensive strategy for southern Africa could be the establishment of food reserves which could act as buffers to potential increases in the variability of food production (Downing *et al.*, 1997).

The bulk of the responsibility for designing, evaluating and implementing strategic responses are governments, national research centres and aid organisations. Private water companies also play a role, however, this role could be considered less important than the development of a national strategy (Downing *et al.*, 1997).

The management of water in Africa is often poorly integrated with decisions being made from a host of organisations ranging from local users to those implementing international agreements. The focus should thus be on promoting flexibility in water management strategies to cope with a range of possible outcomes of a changing climate (Downing *et al.*, 1997). Southern Africa is highly dependent on agriculture and thus adaptation strategies need to be considered to ensure optimal production of staple crops.

Considering the suggestions made by Benioff *et al.* (1996) and Smith and Lenhart (1996) the following two tables (Table 12.1 and 12.2) were prepared to assess these potential adaptation strategies considering the results obtained in this and other studies.

Table 12.1 Review of potential adaptation policy options for the water resources sector in southern Africa considering the results obtained (modified from ideas by Benioff *et al.*, 1996; Smith and Lenhart, 1996)

| Policies | Assessment of Option Considering Results Obtained |
|---|---|
| Build reservoirs and dams | The building of new dams is highly dependent on the availability of sites and the costs involved<br>Considering the increases in evaporation simulated for a 2X $CO_2$ climate (cf. Figure 9.11) this is not considered to be a highly recommended option<br>Marginal increases in storage capacities of proposed dams could, however, be considered<br>Small dams could be advisable in areas which show a simulated increase in variability of rainfall (cf. Figures 6.18 and 6.19) |
| Drain wetlands | This is not considered to be a suitable strategy for southern Africa as wetlands dissipate flood peaks and increases in high magnitude events were simulated (cf. Figure 6.30) |
| Develop groundwater supplies | This is a suggested option, particularly for rural areas, as there are net benefits regardless of climate change and the cost of piped water is prohibitively high is some regions<br>Not recommended in Western Cape where significant reductions in percolation to vadose zone were simulated (cf. Figure 9.14) |
| Catchment planning and co-ordination | Comprehensive planning of both water quantity and quality aspects of large catchments is recommended and there are net benefits regardless of climate change |
| Contingency plans for drought | Droughts have had devastating effects on rural settlements and agriculture in the past and therefore this is a recommended adaptation policy for southern Africa<br>There are also net benefits regardless of climate change |
| Use inter-basin transfers | This is a suggested strategy as it is beneficial both in the short term for drought mitigation as well as in the long term<br>However there are ecological impacts to inter-basin transfers (Richter *et al.*, 1997) |
| Conserve water | By decreasing activities that require water and modifying consumer behaviour water can be conserved, however, this is not an easy option<br>Education required<br>Net benefits regardless of climate change |
| Control pollution | Recommended as it increases water available for use and reduces purification costs<br>Net benefits regardless of climate change |
| Seasonal rainfall / runoff forecasting | Of particular importance in southern Africa are changes in extremes such as floods and droughts, therefore, development of rainfall forecasts and early warning systems which are applicable to the water resources and agriculture sectors should be considered<br>However, forecasts need improvement to become applicable (cf. Schulze *et al.*, 1998) |

Table 12.2 Review of potential adaptation policy options for the agricultural sector in southern Africa considering the results obtained (modified from ideas by Benioff *et al.*, 1996; Smith and Lenhart, 1996)

| Policies | Assessment of Option Considering Results Obtained |
|---|---|
| **At a commercial farm scale** | |
| Develop new cultivars | Efforts to benefit from the potential positive effects of climate change should be investigated<br>This includes the potential benefits in the agricultural sector from $CO_2$ enrichment (cf. Chapter 2, Section 2.3.1.1) as shown particularly in the simulations of maize yield (cf. Figure 8.36)<br>Efforts to breed to cultivars which benefit from increased atmospheric $CO_2$ concentrations or that are suitable for a range of climatic conditions could be investigated<br>However, cost of development of these cultivars could result in expensive seed |
| Plant a variety of heat and drought resistant crops | Recommended to reduce risk<br>Net benefits regardless of climate change |
| Increase irrigation efficiency if areas are already using irrigation | This is recommended and would include strategies such as irrigating at night, which could go some way to counteracting higher expected evaporation rates (cf. Figure 9.11) and adjusting irrigation schedules to optimise water use<br>There are net benefits regardless of climate change |
| Change planting dates | This will be applicable in certain areas in under certain circumstances, however, may not be applicable in marginal areas<br>In these areas it may be necessary to switch to more water efficient crops such as sorghum (cf. Figures 8.23 and 8.24) or change to livestock |
| Implement irrigation | This is a costly approach and irrigation uses scarce water resources |
| **At the community farm scale** | |
| Conservation management | This includes soil conservation which could be beneficial regardless of climate change and generally results in increased soil moisture contents and decreased soil erosion and water conservation |
| Plant low water use crops | A suggested strategy, but may be determined by cost of plants as well as desire for certain crops for consumption |
| Crop-mix | More intra seasonal security expected |
| Inter-cropping | Recommended to reduce vulnerability of farmers |

According to Smith (1999), when screening possible adaptation measures the screening should be based on the following criteria:

i) Does the adaptation measure address high priority adaptation?

ii) Does the adaptation measure address targets of opportunity? In particular, are decisions being made now on infrastructure decisions or plans being revised.

iii) Is the adaptation measure likely to be effective?

iv) Are there any other benefits to the economy or environment, in particular, is the measure justified under present climatic conditions?

v) Will the adaptation be inexpensive to implement?

vi) Is the measure feasible? Are there significant barriers to overcome in implementation (which could include legal, social, cultural, market related or technological)?

From the results obtained in this study the possible water resources and agricultural adaptation measures considered suitable for southern Africa and given in Tables 12.1 and 12.2 were screened and the screened options for southern Africa are reflected in Table 12.3. There naturally is an element of subjectivity to this screening process.

Table 12.3 Screened adaptation measures for southern Africa following guidelines given by Smith (1999)

| Adaptation | High Priority | Target of Opportunity | Effective-ness | Other Benefits | Low Costs | Low Barriers |
|---|---|---|---|---|---|---|
| Develop groundwater supplies | ✔ | ✔ | ✔ | ✔ | ✗ (?) | ✔ |
| Catchment planning and co-ordination | ✔ | ✔ | ✔ | ✔ | ✗ (?) | ✗ |
| Contingency plans for drought | ✔ | ✔ | ✔ | ✔ | ✔ | ✔ |
| Inter-basin transfers | ✔ (?) | ✔ | ✔ | ✔ | ✗ | ✔ (?) |
| Control pollution | ✗ (?) | ✗ (?) | ✔ (?) | ✔ | ✗ | ✗ |
| Water conservation | ✔ | ✔ | ✔ | ✔ | ✗ (?) | ✗ |
| Improve monitoring and forecasting | ✗ (?) | ✔ | ✔ | ✔ | ✔ (?) | ✔ |
| Develop new cultivars | ✔ | ✔ | ✔ | ✔ | ✗ | ✗ |
| Improve irrigation efficiency | ✔ | ✔ | ✔ | ✔ | ✔ | ✗ |
| Change planting dates | ✗ | ✔ | ✔ | ✔ | ✔ | ✔ |
| Multi-cropping | ✔ | ✔ | ✔ | ✔ | ✔ | ✔ |
| Conservation management | ✔ | ✔ | ✔ | ✔ | ✔ | ✗ |
| Inter-cropping | ✔ | ✔ | ✔ | ✔ | ✔ | ✗ |

Therefore, three primary strategies that are suggested for the water resources sector in southern Africa are:

i) *Adopt contingency plans for drought*: Planning for short-term droughts with known or greater intensity or duration could assist in the mitigation of droughts. This is a low cost adaptation measure which is believed would be met with little resistance and would be effective.

ii) *Improve monitoring and forecasting for floods and droughts*: Improvements in weather monitoring and forecasting systems would assist considerably with management of high flows and droughts, regardless of climate change.

iii) *Use inter-basin transfers*: Inter-basin transfers are considered an effective short-term measure for addressing droughts and water supply on a regional scale. The prohibitive factor is the high cost involved.

At the commercial farm scale in southern Africa improvements in irrigation efficiency are recommended, as well as the planting of crops which benefit from $CO_2$ enrichment, have a low water use and are heat and drought resistant. Community farmers should practice conservation management and, if possible, introduce inter-cropping and multi-cropping to reduce the risk of negative consequences of climate change.

* * * * * * *

In this chapter some potential adaptation strategies in response to possible changes in climate were provided. These policy options could reduce the potential risks of climate change for southern Africa.

In the following chapter provides conclusions from the research undertaken in this study are presented and some suggested future improvements to the procedures developed here are made.

# 13. DISCUSSION AND CONCLUSIONS

The impacts of greenhouse gas emissions on the climate could be felt for several generations, even if emissions are reduced, owing to the long chemical half-life of many of these gases. The enhanced greenhouse effect has the potential to cause climatic change impacts across the range of human and natural systems. The assessment of potential impacts of anthropogenically induced changes in climate on agricultural and hydrological systems is subject to a range of uncertainties. These uncertainties arise in part from an inadequate understanding of biophysical processes, such as the complex mechanisms involved in the responses of biological systems, the uncertainties derived from inaccuracies of the General Circulation Model (GCM) output through incomplete understanding of the behaviour of the physical climate system and inaccuracies which arise through interpolation of the GCM output to a finer spatial resolution. In addition, there is the inability to accurately predict spontaneous and human induced adaptations to changes in climate.

The severity of the impacts will vary and not all impacts will constitute damage to the environment, with some sectors being more resilient and robust than others to climate change impacts, while some areas will be benefiting from changes in climate and others may suffer detrimental effects. Even small changes in average climatic conditions can result in significant changes in the frequency, magnitude and timing of hydrological responses. Water is a limiting resource for development in southern Africa and changes in the water supply could have major implications in most sectors of the economy, including the agricultural sector. In addition, developing countries are generally more vulnerable to changes in climate than developed countries owing to their poorer socio-economic and physical infrastructure and, in many cases, their dependency on natural resources and rainfed agriculture.

A wealth of literature has emerged over the past few years on the potential impacts of climate change on agrohydrological systems. However, although there is consensus on some aspects of climate change (as described in Chapter 2), there still appear to be major uncertainties in GCM output, especially when it is applied for climate change predictions at a regional level, in estimating changes in future water demands and in socio-economic and environmental

impacts of response strategies. Considering the uncertainties involved in climate change impact assessments (cf. Chapter 7) the results in this study should be viewed in the light of being within a range of possible outcomes, with the focus of this study having been on the refinements of some of the tools available to perform climate impact assessments with a diverse region, rather than on the impacts *per se*. It is important to develop the methodologies for climate change assessment as predictive tools for evaluating potential impacts. The refinements to modelling tools made in this study were designed to enable more dynamic and realistic simulations of potential impacts from changes in climate, as well as to facilitate a more flexible and efficient way of obtaining regional results.

The seven main steps identified by the IPCC (IPCC, 1994) in conducting climate impact assessments were used as a guide in this study (Chapter 3), bearing in mind the objectives laid out in the introduction (Chapter 1).

The first step is the definition of the problem and the identification of the main data requirements. To provide reference points against which to compare impacts of future climate predictions it is necessary to specify current baseline conditions. It is important to have a sufficiently long duration of current baseline information in order to include a wide range of climate anomalies from the average conditions, with the stationarity of data assumed. The quality of the data is also important and it is thus generally considered preferable to use a recent historical record for current climatic conditions, as these data are generally expected to be more accurate.

In this study precipitation and temperature information for the period 1950 - 1993 was used. The World Meteorological Organization's recommended period of record is 1961 - 1990 (Benioff *et al.*, 1996; Carter, 1998). However, a longer period of record may be preferable particularly in the drier parts of the study area owing to the higher rainfall variability in these areas. Schulze *et al.* (1995a) consider a rainfall record length of 40 years sufficient for the southern African region. This includes two "quasi" periodic fluctuations with approximately 20 year oscillations which have been observed by various researchers (Tyson, 1987). The baseline climate information for this study was extracted from the one minute by one minute of a degree (1' x 1') latitude / longitude gridded database established by the School of

Bioresources Engineering and Environmental Hydrology (School of BEEH) and described in detail in the *South African Atlas of Agrohydrology and -Climatology* (Schulze, 1997b). This gridded database of southern Africa was derived from various sources and is made up of 1' x 1' grid blocks, comprising 437 000 grid cells in a digital database covering South Africa, Lesotho and Swaziland (Chapter 5).

Southern Africa, which is defined in this study as the contiguous areas of South Africa, Lesotho and Swaziland, has been divided into 1946 relatively homogenous hydrological zones known as Quaternary Catchments. Information on soils, vegetation and climate for each Quaternary Catchment was available for each Quaternary Catchment from an existing database. The water resources component of this study and the detailed maize and winter wheat yield analyses was carried out at the Quaternary Catchment scale.

Towards the end of this study the procedure to estimate daily temperatures for each of the 1946 Quaternary Catchments was completed. Therefore, the option of using daily instead of monthly temperatures to simulate potential climate change impacts became available.

The second step in the seven-step IPCC system is the selection of the method to assess potential impacts of climate change (cf. Section 3.3 in Chapter 3). The most common method of assessing climate change impacts is the use of simulation models to simulate a variety of responses to climate change scenarios and this was the approach used in this study.

The third step in the IPCC approach is the testing of the method (cf. Chapter 3, Section 3.4). To assess potential impacts of climate change on hydrological responses in the study area the *ACRU* hydrological modelling system was selected and used in conjunction with the Quaternary Catchment Input Database. The widely used and verified *ACRU* model is considered suitable for climate impact assessments as it is a physical conceptual model which operates using a daily water budget, is sensitive to changes in climate and land use and does not require external calibration. There are several advantages to modelling climate change issues which include the ability to analyse the dynamic behaviour of complex systems, showing inter-relationships and feedbacks between various components and treating uncertainties explicitly.

Although *ACRU* has been used in previous climate impact assessments there were certain routines that either needed to be updated or modified to enable more realistic and dynamic simulations of the agrohydrological processes, including feedbacks, involved in changes in climate (Chapter 4).

The onset of a vegetation growth cycle, and hence the crop's water use coefficient, canopy interception loss and root development, is triggered largely by critical minimum temperatures. If temperatures are expected to increase in future then the monthly values for these variables in *ACRU* are expected to change. Therefore, various linear functions were incorporated into *ACRU* to represent the expected changes in these variables as a function of minimum temperature. Therefore, the monthly values of the water use coefficient, canopy interception loss and root development, under conditions of optimum soil water, are dynamically determined depending on minimum temperatures, thereby accounting for increases in temperature expected in a future climate and also for inter-seasonal climatic changes.

The mean monthly values of the water use coefficient, either generated in *ACRU* or input explicitly, are first converted to daily values by Fourier Analysis an then used to determine the maximum soil water evaporation and transpiration loss by vegetation on a daily basis. However, during a period of soil water stress the plant losses its ability to transpire at a maximum rate and also its ability to recover immediately after stress is relieved by rainfall. Previously, *ACRU* failed to account for daily stresses and recoveries and on any day of a given year the daily value of the water use coefficient ($K_d$) would therefore be the same. Equations describing these stresses and recoveries had previously been provisionally incorporated into a research version of *ACRU* (Kunz, 1993). However, the routines have since been revised and incorporated into the operational version of the model. These changes in $K_d$ were considered of particular importance when simulating hydrological processes in a perturbed climate in which influences of changes in evaporative demands and precipitation amounts have to be accounted for.

When exposed to higher concentrations of carbon dioxide ($CO_2$) plants respond by closing their stomata, with a resultant suppression of plant transpiration. This phenomenon is accounted for in *ACRU* through a percentage suppression of maximum transpiration under

conditions of elevated $CO_2$ concentrations. However, these values needed to be modified to reflect recent findings. The new maximum transpiration suppression estimates are, therefore, 15% for C3 plants and 22% for C4 plants.

In addition, modifications were made to the winter wheat submodel in *ACRU*. Each phenological growth stage was previously activated by number of days after planting, but the routine has been modified to allow the growth stages to be activated by a more dynamic accumulated degree days approach instead. In this way the lengths of the various growth stages as well as the length of the growing season will be adjusted depending on the temperature and therefore will change in a future, warmer climate. The suppression of transpiration resulting from increased atmospheric $CO_2$ under a future climate scenario was also included in the *ACRU* winter wheat submodel.

More recently emphasis has been placed on regional assessments of changes in climate to aid decision makers in those areas and to isolate which regions might be more severely affected by climate change impacts than others. According to Parry and Carter (1998), when undertaking Step 3 of the IPCC approach, it is also necessary perform sensitivity and threshold analyses. Sensitivity analyses were performed in the water resources component of the study. Threshold analyses of mean annual runoff, mean annual percolation to the vadose zone and median maize yield were carried out.

Sensitivity studies are often used in climate impact assessment to assess the sensitivity of a response to a range of plausible or incremental future perturbations. The output from various *ACRU* simulations was used to determine a sensitivity index for each Quaternary Catchment for the hydrological response in question. From the sensitivity studies undertaken it was concluded that runoff in the study area was highly sensitive to changes in precipitation, had was sensitive to changes in $CO_2$ and was not particularly sensitive to changes in temperature, except in the south of the Western Cape Province (cf. Section 9.4, Chapter 9). Percolation into the vadose zone was found to be highly sensitive to changes in precipitation. Sensitivity studies are useful to help in identifying areas of current and possible future vulnerability to climate change.

Threshold analyses are useful to ascertain at what stage during a long term change in climate the hydrological or agricultural system will start responding. The estimates of the threshold of runoff, percolation into the vadose zone and maize yield were achieved by performing three *ACRU* simulations in addition to the simulations of present and estimated future climatic conditions. These additional simulations represented $^1/_4$, $^1/_2$ and $^3/_4$ changes in climatic conditions between the present and a 2X $CO_2$ scenario, using output from a selected GCM and assuming a linear change in climate with time. Thus, the threshold analysis has allowed the identification of areas where changes in hydrological response could occur sooner, or later, than in other areas.

From the threshold study of runoff it can be concluded that the western half of the study area could experience a 10% decrease in runoff by the year 2015 already using climatic output from the HadCM2 GCM, excluding sulphates (HadCM2-S). Moving from the western to the eastern half of the study area the date when a 10% decrease in runoff occurs moves progressively later to 2060. There are some Quaternary Catchments in the north and east of the study area which were simulated to experience increases in runoff using output from this particular GCM. However, the date by which these increases are expected to occur is later rather than earlier.

In the threshold analysis of percolation to the vadose zone a scattered pattern of threshold levels of the hydrological response resulted. The catchments in the interior of southern Africa generally experienced a 10% decrease or increase in percolation to the vadose zone earlier than the coastal catchments (cf. Chapter 9, Section 9.5).

The threshold analysis of maize yield showed that in most catchments in the climatically suitable areas this staple crop was fairly robust to changes in climate and only showed a 10% increase in yield by 2060 (cf. Section 8.3.5 in Chapter 8).

Step 4 in the IPCC approach is the selection of quantitative representations of anticipated changes in climate (cf. Section 3.5 in Chapter 3). There are numerous ways in which climate change scenarios can be constructed, although the most common is the use of output from large scale GCMs (Chapter 6). The UKTR GCM, excluding sulphate forcing (UKTR-S) and

the HadCM2, both including and excluding sulphate forcing, were used for the agricultural impact assessments. These GCMs were used to compare results obtained by using output from the two versions of the Hadley Centre GCMs and the differences in results by including and excluding sulphate forcing in the GCM simulations. Four GCMs were used for the water resources component of the impact studies, *viz.* the 1998 version of the Climate Systems Model (CSM), two Hadley GCMs, one excluding and the other including sulphate feedbacks and the Genesis (1998) GCM. Using only one climate scenario would represent only one possible outcome within a range of possible outcomes. However, using several scenarios of future climate results in a range of possible outcomes without any quantified probability of the accuracy of the various outcomes.

The GCM output of precipitation and temperature that was provided was of a coarse spatial resolution. Therefore the climate change estimates needed to be prepared at a suitable resolution for agrohydrological impact studies. In a previous study in southern Africa carried out by Kunz (1993) temperature change algorithms were used to obtain estimates of future temperatures. However, it was decided that this technique needed improvement and refinement.

In this study the large grid cells output by the GCMs were downscaled by an interpolation procedure to a quarter of a degree by quarter of a degree ($^1/_4° \times {}^1/_4°$) grid scale by an inverse distance weighting technique in ARC/INFO. The $^1/_4° \times {}^1/_4°$ grid values were further disaggregated to 1' x 1' values, with each 1' x 1' grid cell retaining the magnitude of climate change calculated for the original $^1/_4° \times {}^1/_4°$ grid cell. The reason for this was that the bulk of the agricultural impact assessments which were carried out at a 1' x 1' grid resolution. Additionally, for the impact assessment in hydrology, which was undertaken on a catchment basis, the centroid of each of the 1946 Quaternary Catchments was determined and the magnitude of change in temperature and ratio change in precipitation of each Quaternary Catchment was obtained from the geometrically closest $^1/_4° \times {}^1/_4°$ GCM grid cell values.

All four GCMs simulated increases in 2X $CO_2$ temperatures from present temperatures. The two Hadley GCMs output both maximum and minimum temperatures separately for each month of the year, whereas the CSM (1998) and Genesis (1998) GCMs provided only mean

temperature change estimates per month. As would be expected, the potential changes in temperature were higher for HadCM2 where sulphate forcing was excluded compared with the simulations in which the effect of sulphate cooling was included. However, the generally higher increase in maximum temperatures over minimum temperatures was the opposite to what would have been anticipated according to the IPCC (1990). There appeared to be strong spatial patterns with higher temperatures in the north-central parts of the study area in the output from HadCM2. This could be attributed to the effect of continentality. The simulated changes in temperature of Genesis (1998) are higher than those of CSM (1998). However, the range of increase is greater by CSM (1998).

The GCMs predict both increases and decreases in precipitation in the summer months in the future. However, the two HadCM2 GCMs predict that most regions will experience decreases in rainfall whereas Genesis (1998) predicts that most regions could expect large increases in rainfall in the summer months. CSM (1998) predicts neither a large increase nor decrease in summer months' precipitation. However, this GCM simulated large decreases in the winter months' rainfall over the northern part of the study area. An overall decrease in winter precipitation is predicted by HadCM2-S with Genesis (1998) simulating general increases in winter rainfall for the study area. The discrepancies shown by the maps of seasonal changes in rainfall by the four selected GCMs reflect the uncertainties associated with using GCM output in climate change impacts assessments. Genesis (1998), in particular, seems to simulate a far greater increase in precipitation in the study area than the other GCMs.

General Circulation Models generally provide outputs from a simulation of present, or 'control', conditions and from a 'perturbation' experiment which assumes a climate associated with future greenhouse gas concentrations, usually for an effective doubling of $CO_2$ from pre-Industrial Revolution of 280 ppmv to the equivalent of 560 ppmv (2X $CO_2$). In order to assess how well GCMs might perform for scenarios of climate change, two comparative studies were performed on GCM output for present (i.e. 1X $CO_2$) conditions versus present climatic conditions from the baseline gridded database.

For the first verification study, residual grid values were created by subtracting precipitation or temperature output from HadCM2-S for a 1X $CO_2$ scenario from corresponding $^1/_4°$ grid

values of the baseline climate databases. The residuals illustrate the magnitude of errors which may be incurred as a result of the coarse resolution of the GCM output. HadCM2-S generally overestimates maximum summer temperatures, except over Lesotho, and both underestimates and overestimates minimum temperatures in July in the study area. This particular GCM generally underestimated rainfall in January, although rainfall along the eastern seaboard was overestimated. The magnitude of error for July by HadCM2-S was not very high, except in the south-western area where the GCM significantly overestimated rainfall.

Next, four sample GCM points were selected across southern Africa to represent four different climatic zones. Two studies were carried out, *viz.* a comparison of the monthly output from HadCM2-S to the observed monthly climate at the four points and, secondly, a comparison of the variability of the rainfall generated by the HadCM3 GCM (HadCM3-S) to the present observed rainfall variability (cf. Chapter 6, Section 6.6).

By comparing plots at each point of present temperature and rainfall for each month of the year from the baseline database against the estimated temperature and rainfall from HadCM2-S the relative inaccuracies of the GCM output were highlighted. The maximum and minimum temperature plots show a fairly good correspondence. There is only a weak relationship, however, between the precipitation estimates of this GCM and the observed climate at the four selected points. HadCM2-S consistently underestimated precipitation in the interior of the study area and overestimated precipitation in the winter rainfall region. The estimations of precipitation in the study area by this GCM, based on the four sample points, were on average too high.

From the analyses of monthly climate it can be concluded that significant errors have been identified in the GCM output for present, i.e. 1X $CO_2$, climatic conditions. If it is to be assumed that a similar magnitude and sign of error in the GCM estimates of 2X $CO_2$ climatic conditions will persist as in the GCM estimates for present climatic conditions, then it was considered preferable to use the differences between 2X $CO_2$ and 1X $CO_2$ climate scenarios for assessment of relative temperature change, and similarly to use the ratios between GCM

outputs for future and present rainfall, rather than absolute values generated by the GCMs, when undertaking the regional climate change impacts assessments.

The second component of the verification study involved the comparison of various statistics calculated from the HadCM3-S GCM output of daily rainfall for present climatic conditions and observed rainfall statistics. From this analysis it was concluded that the HadCM3-S has a reasonably good representation of the variability at three of the four points in the study area. The exception was the interior summer rainfall region and this is believed to be attributed to the coarse resolution of the GCM output. An averaging of high rainfall over the mountainous parts of Lesotho with lower rainfall amounts in the Free State appears to result in an overestimation of the mean rainfall and an underestimation of the number of days with no rainfall occurring in this GCM point located in the southern Free State.

Once the GCM output had been prepared and the *ACRU* model modified to enable more dynamic simulations of changes in climate, potential changes in both the agricultural and hydrological responses resulting from climate change in of southern Africa were assessed. This is the fifth step in the seven-step guide suggested by the IPCC (cf. Section 3.6 in Chapter 3).

In this study the maize yield, winter wheat yield and hydrological responses in the study area were simulated using the *ACRU* model at a resolution of the Quaternary Catchment. An *ACRU* Input Database has been established which contains the information required by the model. A modified structure of storing the input information in a spreadsheet and then exporting it to an easily accessible array has facilitated a more flexible and user friendly method of storing the input information and establishing *ACRU* input menus from a database at both the Quaternary Catchment, or the finer Quinary Catchment scale. The inputs for the Quaternary Catchment have been stored in this new database structure as a pre-populated database which can be accessed by multiple users and easily updated. The information contained in the Quaternary Catchment Input Database was updated and modified to allow a greater variety of choices when performing climate impact assessments at this scale.

These modifications included

i) the incorporation of the choice of a range of GCM output available as estimates of future climatic conditions;
ii) the option of performing a sensitivity or threshold analysis;
iii) the addition of other possible land uses besides veld in fair hydrological condition, such as veld in poor or good hydrological condition, which is useful in sediment yield analyses for example;
iv) the addition of the option of performing a crop yield analyses which could include an economic analysis;
v) the inclusion of an irrigation option which allows the simulation of potential changes in irrigation;
vi) the inclusion of the option of performing an extreme event analysis on rainfall, runoff or peak discharge; and
vii) the option of performing a sediment yield analysis.

The development of a user friendly interface has allowed the rapid selection of these new options, the automated creation of *ACRU* input menus and the streamlined simulation of agrohydrological responses. The output from the climate impact assessments is ideally displayed in the form of maps. The techniques that were previously available in the School of BEEH were modified and enhanced to enable more flexible and efficient ways of extracting the necessary output from the *ACRU* simulations to present using the ARC/INFO GIS or as a time series.

With these structures in place potential changes in hydrological response, irrigation water demand, sediment yield as well as winter wheat and maize yields for the entire study area or for groups of selected catchments could be determined efficiently.

Climate is the primary determinant of agricultural productivity. Thus, climate change is expected to influence agricultural production, as shown by the results presented in Chapter 8. The future estimates of temperature and precipitation from UKTR-S and the two HadCM2 GCMs were used to estimate potential changes in parameters important to agriculture as well as changes in yield and climatically suitable areas of selected pastures, crops and commercial

tree species. Most of these assessments were carried out using simple, unidirectional crop models at a 1' x 1' grid scale for southern Africa. The exceptions were the maize and winter wheat analyses which were carried out using models of intermediate complexity which included feedbacks at the Quaternary Catchment scale.

Temperature increases in southern Africa may have direct impacts in agriculture in some regions. A reduction in frost hazard and longer growing seasons will benefit agriculture in cooler regions and high elevations, but may extend the range of pests and disease vectors. However, these regions are relatively small in southern Africa, with the majority of areas, particularly in the semi-arid regions, most likely experiencing enhanced heat stress in future with the added risk of increased grassland (veld) fires. The effects of climate change on agricultural potential, without adaptation in management, are expected to be significant. Changes in regional productivity have the potential to affect both local and international markets.

Most agricultural production in the study area is rainfed production. Thus, changes in precipitation amounts will have a strong effect on crop production. However, current predictions of changes in precipitation in southern Africa are unreliable. From the research presented in was found that climate change will have mixed impacts on agricultural production in the study region with some regions benefiting from changes in climate and other regions showing decreases in yield and in climatically suitable growing areas. The results obtained using output from UKTR-S and HadCM2-S were very similar. By including sulphate feedback in the HadCM2 changes in yield and climatically suitable areas of the crop were simulated for a 2X $CO_2$ scenario.

Increases in $CO_2$ concentrations have been found to affect plant physiological processes (Section 2.3.1.1 in Chapter 2). The direct effects of $CO_2$ enrichment on plants tend to increase yields and reduce water use, as shown in the example using the *ACRU* maize yield model. Maize follows a C4 photosynthetic pathway and thus the effects of $CO_2$ enrichment on transpiration and, therefore, crop yields were found to be more significant than in the case of wheat which is a C3 plant. Although it is often suggested that $CO_2$ fertilisation should be taken into account when conducting climate impact assessments, considering the uncertainties

regarding crop response to $CO_2$ enrichment a conservative approach would be to assume no $CO_2$ fertilisation effect. This was the case in the modelling of potential changes in crop yields using the simple Smith (1994) yield models. In conclusion, it was shown that the combined effects of increased temperatures, changes in precipitation and $CO_2$ fertilisation on crop yields are expected to vary by crop and location.

The impact of increases in $CO_2$ concentrations on weeds seems uncertain at present, with estimates ranging from a 10% to an almost three-fold increase in biomass (IPCC, 1996b). Agricultural pests, overall, are likely to thrive under conditions of increasing $CO_2$ concentrations and increased temperatures, as shown in the simple example of potential changes in the number of life cycles per annum of the codling moth in the study area. All these changes combined could have major implications on food security, in some cases positive and in other cases negative.

Once the refinements to the *ACRU* model, the *ACRU* Input Database and the linkages between the database, model and GIS were complete, these refined modelling tools were applied to assess potential impact of climate change were applied at a Quaternary Catchment scale in the water resources component of the study. Southern Africa is considered vulnerable to changes in climate. Factors that contribute to vulnerability in water systems in southern Africa include high intra-seasonal and inter-annual variations in rainfall, which are amplified in runoff production, as well as high evaporation rates. Even without climate change, water supply in southern Africa is already predicted to be become of serious concern in the next half century.

Climate change is expected to alter the present distribution of hydrological resources in southern Africa and changes in water availability due to global warming are expected to add further pressure on the adaptability of water systems. Increased temperatures increase the atmospheric demand for water, evaporation from soils and open water surfaces and transpiration from plants. The extent to which precipitation change will offset the increased evapotranspiration in some areas is highly uncertain. It is likely that some regions will have significant decreases in moisture availability even when the direct effects of $CO_2$ enrichment are taken into account.

Previously only the option of simulating climate change impacts for the entire study area was available. Structures were therefore first established to allow the simulation of hydrological responses for a Primary, Secondary, Tertiary or Quaternary Catchment and then also options of selecting a large catchment or Water Management Area in southern Africa were introduced. This modification is useful in the performing regional assessments of changes in climate.

The hydrology of Quaternary Catchments can be simulated either on individual, lumped Quaternary Catchments which are unconnected hydrologically to their upstream Quaternary Catchments or as cascading Quaternary Catchments where the streamflow from one Quaternary Catchment cascades, as it would naturally, into the next downstream Quaternary Catchment. Previously the only option when conducting climate change impact assessments on water resources had been to simulate changes in hydrological responses on individual Quaternary Catchments. Techniques therefore had to be developed to facilitate the linking of Quaternary Catchments in *ACRU* to assess potential changes in accumulated runoff in large catchments. Once the sequencing of the Quaternary Catchments had been determined, the option of selecting a Quaternary Catchment which exited into the sea or another country, and determining the accumulated flow for that large catchment, was established through the use of the distributed mode function in *ACRU*. Alternatively, any Quaternary Catchment in southern Africa can be selected and the contributing catchments will automatically be identified. This option is particularly useful in determining the accumulated streamflow at any point in a large catchment.

Identical procedures were used for all the hydrological analyses over southern Africa, with the assumption of a single baseline land cover type, *viz.* grassland in fair hydrological condition, covering the entire study area. In addition, no anthropogenic perturbations such as abstractions from rivers or reservoirs, or inter-basin transfers were considered.

The changes in hydrological responses were calculated both as absolute differences between future and present values and the ratios of future hydrological response to the present responses. It is considered preferable to view the results presented in this study as comparative estimates, rather than assuming values to be absolute. From the water resources impact assessments it may be concluded that the spatial patterns resulting from the two

approaches of depicting absolute response changes and relative differences are dissimilar. There are also significant differences between the various components of the hydrological system to climate change. In addition, the GCM chosen had a significant influence on the results obtained for the water resources component of the study. The wide range of outcomes that are possible when using a selection of GCMs was observed in the water resources component of this study. The results obtained using Genesis (1998) were significantly different from the results from the other three GCMs and this GCM was therefore excluded from further analyses.

These assessments showed potential changes in the spatial patterns of hydrological responses in southern Africa resulting from climate change. They give an indication of where, within the study area, water resources are simulated to change more than elsewhere but give no indication of when during the year these changes could occur. Therefore, an assessment of potential changes in the temporal patterns of runoff was carried out. From these simulations it was concluded that there is an overall decrease in the duration of runoff during the year, an increase in the concentration of runoff in many areas and a change in the seasonality of runoff in the study area. Such changes could have significant implications for both agriculture and water resources in southern Africa.

Daily time series from the GCMs have recently become available and these are useful for analysis of variability and extreme events, where changes in day-to-day rainfall amounts and sequences are important. The potential for increases in flood and drought frequency and severity with climate change is of particular concern in sub-Saharan Africa, as the consequences of floods and drought to agriculture and settlement patterns are significant.

From the analysis of potential changes in rainfall variability, using daily precipitation output from HadCM3-S, it was concluded from the simulations that a decrease in mean precipitation and an increases in the coefficient of variation are likely. There were also increases in the number of days with no precipitation in the central regions in June and increases in rainfall events over 25 mm, which points to increases in extreme events at both ends of the spectrum. An increase in extreme events would increase financial demands on the public and private sectors to cover insured and uninsured weather related losses.

This study, through the linking of Quaternary Catchments, has facilitated the assessment of actual catchment hydrological problems. Two large catchments, *viz.* the Orange and Mgeni Catchments, were selected to assess the potential impact of climate change on individual catchment runoff and accumulated flows assuming a land cover of veld in fair hydrological condition at a Quaternary Catchment scale. Decreases in both mean annual runoff and mean annual accumulated runoff were simulated using output from HadCM2+S and HadCM2-S. However, the decreases in runoff were not as large when using output from HadCM2+S.

A detailed study was carried out on the Mgeni Catchment in South Africa. The 12 Quaternary Catchments have been divided into 137 subcatchments. The impact of climate change versus land use change on hydrological responses was assessed, assuming baseline land cover conditions represented by Acocks' (1988) Veld Types. The information on present land uses included input on dams, abstractions and transfers in this Catchment. From the results it was concluded that land use had a greater impact on changes in runoff and sediment yield in the Mgeni Catchment than climate change. Large increases in runoff and sediment yield were simulated in the more populated parts of the Catchment. Next, potential impacts of climate change on the water resources of the Catchment, assuming present land uses, were simulated using *ACRU*. Most subcatchments of the Mgeni were simulated to have a 10 - 30% decrease in mean annual runoff in a 2X $CO_2$ climate scenario. Decreases in mean annual accumulated runoff were also simulated for this Catchment. These could have significant implications for agricultural, domestic and industrial water users within the Catchment. In addition, decreases in sediment yield were simulated for a 2X $CO_2$ climate scenario in the Mgeni, which could result in improved water quality in the Catchment.

Potential changes in water supply from the Mgeni Catchment which supplies water to two large urban centres, *viz.* Durban and Pietermaritzburg, were investigated by assessing changes in the runoff feeding Midmar Dam from the Lions River Management Area. In the future increases in demand are expected from users of water supplied by this dam and reductions in runoff from this Management Area were simulated. This could indicate potential conflicts in water demand and supply from this dam under a future climate scenario. In addition, there were simulated to be changes in the monthly runoff amounts from the Lions River

Management Area. The greatest decreases in runoff were simulated to occur in the wet summer months.

Lastly in the seven-step approach (Steps 6 and 7) there is the need to evaluate adaptive responses (cf. Section 3.7 in Chapter 3). If climate change is inevitable, then it is probably inevitable that agricultural production will change, runoff and water supply will change and the optimum growth areas of plantations and crops will alter. Society will have to adapt to these and other changes. Only brief suggestions of possible adaptation measures to potential climate change impacts on agrohydrological systems were provided, as the focus of this thesis was on the refinement of the tools to assess climate change impacts, rather than on the impacts *per se*. Suggestions for potential adaptation strategies in the water resources sector for southern Africa include planning for droughts and floods, developing inter-basin transfers and improving monitoring and seasonal forecasting to assist with flood and drought management. Strategies which could be applied in the agricultural sector in southern Africa include improvement in irrigation efficiencies, planting crops and / or cultivars that are more suited to a warmer climate with enhanced atmospheric $CO_2$ concentrations and farming with new mixes of crops to reduce vulnerability to crop failure.

Although predictions regarding the magnitude and direction of changes in climate remain uncertain, the potential impacts of climate change on the agrohydrological system may be profound. Therefore, tools need to be continually developed to assist in climate impact assessments to provide policy makers with the necessary tools to develop strategies to review possible adaptation methodologies in response to potential changes in climate. Bearing in mind the modifications that were made to assist in climate impact assessments, the results obtained in this study and the uncertainties involved in climate change studies which have been highlighted, some recommendations for future research are presented.

There is a need, in future, to have configured Quaternary Catchments for southern Africa which include information on, *inter alia*, actual land uses, reservoirs, abstractions and return flows. This would enable more detailed simulations of potential changes in water demand and supply to be made as a result of climate change in the study area. In addition, studies on potential changes in water quality are needed. Water quality indices that are affected by

changes in temperature are, *inter alia*, phosphorus loadings and *E. coli* concentrations and the incidence of some water-borne diseases.

There are still many uncertainties in the magnitude and regional direction of climate changes. The climate output from the four GCMs, for example, produced significantly different simulation results of potential changes in hydrological responses when used as input in the *ACRU* model. Research goals should focus on possibly reducing, or eliminating, uncertainties through structured research. Therefore, more confidence in impacts studies would be gained once GCMs produce more uniform climate predictions.

The downscaling of GCM output to a finer spatial resolution for use in climate impact assessments is of particular importance. An inverse distance weighting technique was used in this study. However, this technique does not explicitly account for topographic influences for example. Although the interpolative downscaling techniques used in this study are considered satisfactory, improved downscaling by regional climate models would be recommended for future agrohydrological impact studies, particularly in the light of the dominant effect of precipitation on agrohydrological responses.

Sensitivity studies were performed on runoff and percolation into the vadose zone. Similar techniques could be applied to the agriculture sector to investigate, for example, the sensitivity of components of climate change on maize yields. Maize is the staple food in southern Africa and such a study may aid in the identification of certain areas being more vulnerable than others to elements of climate change, and thereby assist in regional planning for the future.

When modelling agrohydrological responses for potential future climatic conditions in this study the assumption was made of an instantaneous doubling of atmospheric $CO_2$ concentrations for future (2X $CO_2$) climatic conditions. This is clearly unrealistic, as greenhouse gas levels are increasing continuously and, therefore, in future it would be preferable to attempt to perform simulations which take these transient changes in climate into account. The threshold analysis did, however, go some way in addressing this problem.

In future more emphasis in the agricultural and water resources sectors needs be placed on possible adaptations to changes in climate through the analysis of areas sensitive, or vulnerable, to climate change and the subsequent analysis of potential adaptation strategies which could be used to offset any negative impacts.

The potential for climate to change has raised many questions for which there are no simple answers. Through the refinements of the tools available to assess climate change impacts it is hoped that, as the simulations of climate by the GCMs improve and more information becomes available on present climate inputs, the tools will be refined and readily available to re-assess potential impacts and facilitate efficient and realistic results to be used in decision making in southern Africa.

# 14. REFERENCES


Acock, B. (1990). Effects of Carbon Dioxide on Photosynthesis, Plant Growth, and Other Processes. *In*: Kimball, B.A., Heichel, G.H., Stuber, C.W., Kissel, D.E. and Ernst, S. (eds). Impact of Carbon Dioxide, Trace Gases, and Climate Change on Global Agriculture. American Society of Agronomy, Inc. (ASA), Special Publication 503. 45 - 60.

Acocks, J. P. H. (1988). Veld types of South Africa.. Botanical Research Institute, Pretoria. Botanical Survey of South Africa, Memoirs 57. pp 146.

Adams, R.M., Hurd, B.H., Lenhart, S. and Leary, N. (1998). Effects of global climate change on agriculture: An interpretative review. Climate Research, 11, 19 - 30.

Agrios, G.N. (ed). (1988). Plant Pathology. (3rd Edition). Academic Press, San Diego, California, USA. pp 627.

Arnell, N.W. (1995). Socio-Economic Impacts of Changes in Water Resources due to Global Warming. *In*: Oliver, H.R. and Oliver, S.A. (eds). The Role of Water and the Hydrological Cycle in Global Change. Series 1: Global Environmental Change, Vol. 31. Proceedings of the NATO Advanced Study Institute on the Role of Water and the Hydrological Cycle in Global Change, II Cicocco, Lucca, Italy. Springer, Berlin, Germany. 389 - 408.

Arnell, N.W. (1999). Uncertainty in Climate Change Impact Studies in the Water Sector. Proceedings of the ECLAT-2 Helsinki Workshop, Helsinki, Poland, 14 - 16 April 1999. 85 - 88.

Arnitt, R.A. (2000). Comparisons of statistical and dynamical downscaling for evaluating climate change impacts on water resources. Presentation at the International Workshop on Climatic Change: Implication for the Hydrological Cycle and for Water Management, Wengen, Switzerland.

Arnold, J.G., Williams, J.R., Srinivasan, R. and King, K..W. (1996). Soil and Water Assessment Tool: User Manual. USDA, Agricultural Research Service, Grassland, Soil and Water Research Laboratory. Texas A and M University, Texas, USA.

Ashton, P.J. (1996). Water Quality. *In*: Shackleton, L.Y., Lennon, S.J. and Tosen, G.R. (eds). Global Climate Change and South Africa. Environmental Scientific Association, Cleveland, South Africa. 74 - 75.

Bass, B.L. (1993). Summary Report on IGBP/BAHC Workshop on Focus 4: The Weather Generator Project. IGBP/BAHC Core Project Office, Department of Meteorology, Free University, Berlin, Germany.

Basson, M.S. (1997). Overview of Water Resources Availability and Utilisation in South Africa. CTP Book Printers (Pty) Ltd, Cape Town, South Africa. pp 72.

Bazzaz, F.A., Bassow, S.L., Berntson, G.M. and Thomas, S.C. (1996). Elevated $CO_2$ and Terrestrial Vegetation: Implications For and Beyond the Global Carbon Budget. *In*: Walker, B. and Steffen, W. (eds). The Terrestrial Biosphere and Global Change: Implications for Natural and Managed Ecosystems. International Geosphere-Biosphere Programme (IGBP) Science No. 1. Stockholm, Sweden. 43 - 76.

Benioff, R., Guill, S. and Lee, J. (1996). Vulnerability and Adaptation Assessments. Version 1.1. An International Handbook. Environmental Science and Technology Library, 7. Kluwer Academic Publishers, Dordrecht, The Netherlands. pp 421.

Beran, M. (1989). Hydrological Impacts - What if we are right? *In*: Berger, A., Schneider, S.H. and Duplessy, J.C. (eds). Climate and Geo-Sciences: A Challenge for Society in the 21st Century. NATO Advanced Study Institute Series C, Mathematical and Physical Sciences, 285. Springer, Berlin, Germany. 661 - 665.

Bergström, S., Carlsson, B., Gardelin, G., Lindström G. and Petterson, A. (2000). Climate change and water resources in Sweden - Analysis of uncertainties. Presentation at the

International Workshop on Climatic Change: Implication for the Hydrological Cycle and for Water Management, Wengen, Switzerland.

Bloomgarden, C.A. (1995). Protecting endangered species under future climate change: From single-species preservation to an anticipatory policy approach. Environmental Management, 19, 641 - 648.

Bonell, M., van Dam, J.C. and Jones, V. (1999). Conclusions and Recommendations. *In*: van Dam, J.C. Impacts of Climate Change and Climate Variability on Hydrological Regimes. Cambridge University Press, Cambridge, England. 123 - 128.

Bouten, W. and Goudriaan, J. (1994). Effects of $CO_2$ Fertilisation on Evapotranspiration. *In*: Oliver, H.R. and Oliver, S.A. (eds). The Role of Water and the Hydrological Cycle in Global Change. Series 1: Global Environmental Change, Vol. 31. Proceedings of the NATO Advanced Study Institute on the Role of Water and the Hydrological Cycle in Global Change, II Cicocco, Lucca, Italy. Springer, Berlin, Germany. 163 - 186.

Brinkop, S. (2000). Change in convective activity and extreme events in a transient climate situation. Presentation at the International Workshop on Climatic Change: Implication for the Hydrological Cycle and for Water Management, Wengen, Switzerland.

Carter, T.R. (ed). (1998). Preliminary Guidance Material on the Use of Scenario Data for Impact and Adaptation Assessment. Task Group on Scenarios for Climate Impact Assessment, Intergovernmental Panel on Climate Change. Agricultural Research Centre of Finland, Helsinki, Finland. pp 67.

Carter, T.R., Parry, M.L., Nishioka, S. and Harasawa, H. (1992). Preliminary Guidelines for Assessing Impacts of Climate Change. Environmental Change Unit, Oxford and Center for Global Environmental Research, Tskuba, Japan.

Carter, T.R., Parry, M.L., Harasawa, H. and Nishioka, S. (1994). IPCC Technical Guidelines for Assessing Climate Change Impacts and Adaptations. Intergovernmental Panel on Climate

Change, Department of Geography, University College London, England and Centre for Global Environmental Research, Tsukuba, Japan. pp 59.

Childs, S.W. and Hanks, R.J. (1975). Model of soil salinity effects on crop growth. Soil Science Society of America Journal, 39, 617 - 622.

Cohen, S.J. (1995). Potential Changes to Hydrologic Systems. *In*: Oliver, H.R. and Oliver, S.A. (eds). The Role of Water and the Hydrological Cycle in Global Change. Series 1: Global Environmental Change, Vol. 31. Proceedings of the NATO Advanced Study Institute on the Role of Water and the Hydrological Cycle in Global Change, II Cicocco, Lucca, Italy. Springer, Berlin, Germany. 373 - 388.

Conley, A.H. (1996). Impacts of Global Climatic Change on Water Resources and Catchments. *In*: Shackleton, L.Y., Lennon, S.J. and Tosen, G.R. (eds). Global Climate Change and South Africa. Environmental Scientific Association, Cleveland, South Africa. 55 - 57.

Darroch, M.A.G. (2000). Department of Agricultural Economics. University of Natal, Private Bag X01, Scottsville, 3209, South Africa. Personal communication.

Dent, M.C., Lynch, S.D. and Schulze, R.E. (1989). Mapping Mean Annual and Other Rainfall Statistics over Southern Africa. Water Research Commission, Pretoria, South Africa. Report 109/1/89. pp 230.

Domleo, F.B. (1990). Maize and Wheat Yield Simulation with the *ACRU* Model. Unpublished MSc dissertation, Department of Agricultural Engineering, University of Natal, Pietermaritzburg, South Africa. pp 117.

Doorenbos, J. and Kassam, A.H. (1979). Yield response to water. FAO Irrigation and Drainage Paper 33. FAO, Rome, Italy. pp 193.

Downing, T.E., Ringius, L., Hulme, M. and Waughray, D. (1997). Adapting to climate change in Africa. Mitigation and Adaptation Strategies for Global Change, 2, 19 - 44.

DWAF (Department of Water Affairs and Forestry). (1998). Mkomazi IFR Study. Starter document for IFR Workshop. Department of Water Affairs and Forestry, Pretoria, South Africa.

DWAF (Department of Water Affairs and Forestry). (2000). Department of Water Affairs and Forestry, Pretoria, South Africa. Personal communication.

El-Raey, M., Sasr, S., Desouki, S. and Dewikar, K. (1995). Potential impacts of accelerated sea level rise on Alexandria governate, Egypt. Journal of Coastal Resources, Special Issue, 14, 190 - 204.

Ennos, A.R. and Bailey, S.E.R. (1995). Adaptation, Behaviour and Evolution. *In*: Problem Solving in Environmental Biology. Longman, London, England. 22 - 23.

ESRI (Environmental Systems Research Institute). (1991). Performing Analysis with GRID. *In*: ARC/INFO User's Guide 6.0 Cell-Based Modelling with GRID. Environmental Systems Research Institute, Inc. 6-98 to 6-109.

FAO (Food and Agriculture Organisation). (1978). Report on the Agro-Ecological Zones Project, Vol. 1: Methodology and Results for Africa. Food and Agriculture Organisation of the United Nations, Rome, Italy. World Soil Resources Report, 48. pp 60.

Fishcer, G., Frohberg, K., Parry, M.L. and Rosenzweig, C. (1996). Impacts of potential climate change on global and regional food production and vulnerability. *In*: Downing, T.E. (ed.). Climate Change and World Food Security. NATO Advanced Study Institute Series 1, 37. 115 - 159.

French, G.T., Awosika, L.F., and Ibe, C.E. (1995). Sea level rise and Nigeria: Potential impacts and consequences. Journal of Coastal Resources, Special Issue, 14, 224 - 242.

Frigon, A. and Caya, D. (2000). Water resource simulations with the Canadian RCM. Presentation at the International Workshop on Climatic Change: Implication for the Hydrological Cycle and for Water Management, Wengen, Switzerland.

Gates W.L., Mitchell J.F.B., Boer G.J., Cubasch U. and Meleshko V.P. (1992). Climate Modelling, Climate Prediction and Model Validation. *In*: Houghton J.T., Callander B.A. and Varney S.K. (eds). Climate Change 1992: The Supplementary Report to the IPCC. pp 200.

Gibberd, V., Rook, J., Sear, C.B. and Williams, J.B. (1996). Drought Risk Management in Southern Africa: The Potential for Long Lead Climate Forecasts for Improved Drought Management. Natural Resources Institute, London, England. pp 43.

Gleick, P.H. (1990). Vulnerability of Water Systems. *In*: Waggoner, P.E. (ed). Climate Change and U.S. Water Resources. John Wiley & Sons Inc., New York, USA. 223 - 242.

Gleick, P.H. (ed.). (1993). Water in Crisis: A Guide to the World's Fresh-Water Resources. Oxford University Press, New York, USA. pp 498.

Gordon, C., Cooper, C., Senior, C.A., Banks, H., Gregory, J.M., Johns, T.C. and Mitchell, J.F.B. (2000). The simulation of SST, sea ice extents and ocean heat transports in a version of the Hadley Centre couple model without flux adjustments. Climate Dynamics (accepted).

Goudriaan, J. and Unsworth, M.H. (1990). Implications of Increasing Carbon Dioxide and Climate Change for Agricultural Productivity and Water Resources. *In*: Kimball, B.A., Heichel, G.H., Stuber, C.W., Kissel, D.E. and Ernst, S. (eds). Impact of Carbon Dioxides, Trace Gases and Climate Change on Global Agriculture. American Society of Agronomy, Inc. (ASA), Special Publication 53. 111 - 131.

Graedel, T.E. and Crutzen, P.J. (1993). Atmospheric Change - An Earth System Perspective. W.H. Freeman and Company, New York, USA. pp 443.

Graves, J. and Reavey, D. (1996). Global Environmental Change: Plants, Animals and Communities. Longman, London, England. pp 226.

Gyalistras, D. (1999). Techniques for Estimating Uncertainty in Climate Change Scenarios and Impact Studies: Quantitative Techniques. Proceedings of the ECLAT-2 Helsinki Workshop, Helsinki, Poland, 14 - 16 April 1999. 76 - 69.

Hanks, R.J. (1974). Model for predicting plant yield as influenced by water use. Agronomy Journal, 66, 660 - 665.

Hare, F.K. (1988). The Global Greenhouse Effect. *In*: WMO/OMM, No. 710. World Meteorological Organisation, Geneva. 59 - 69.

Herbert, M.A. (1992). Nutrition of eucalypts in South Africa. Institute for Commercial Forestry Research, Pietermaritzburg, South Africa. ICFR Bulletin Series, 27/92. pp 25.

Herbert, M.A. (1993). Site requirements of exotic hardwood species, Institute of Commercial Forestry Research, Pietermaritzburg, South Africa. ICFR Bulletin Series, 2/93. pp 17.

Hewitson, B.C. (1997). Climate System Analysis Group, Department of Environmental and Geographical Science, University of Cape Town, Private Bag, Rondebosch, 7701, South Africa. Personal communication.

Hewitson, B.C. (1999). Deriving Regional Precipitation Scenarios from General Circulation Models. Water Research Commission, Pretoria, South Africa. Report 751/1/99.

Hewitson, B.C., Lennard, C. and Joubert, A. (1998). Climate System Analysis Group, Department of Environmental and Geographical Science, University of Cape Town, Private Bag, Rondebosch, 7701, South Africa. Personal communication.

Honkasalo, A. (1999). Presenting Uncertainties in Future Climate Scenarios and their Impacts to Stakeholders I. Proceedings of the ECLAT-2 Helsinki Workshop, Helsinki, Poland, 14 - 16 April 1999. 98 - 100.

Hostetler, S. (1999). How can GCMs characterise extremes and variability and how are their variables downscaled to suit biological purposes? Presentation at 1999 Aspen Global Change Institute Workshop on "Ecological and Agricultural Consequences of Climatic Extremes and Variablity". Aspen, Colorado, USA, August 1999.

Hudson, D.A. (1997). Southern African climate change simulated by the GENESIS GCM. South African Journal of Science, 93, 389–403.

Hughes, A.D. (1992). Sugarcane yield simulation with the *ACRU* model. Unpublished MSc dissertation. University of Natal, Pietermaritzburg, Department of Agricultural Engineering, South Africa. pp 90.

Hulme, M. (1996). Climate Change and Southern Africa: An Exploration of Some Potential Impacts and Implications for the SADC Region. Climatic Research Unit, University of East Anglia, Norwich, England. pp 104.

Hulme, M. and Carter, T.R. (1999). Representing Uncertainty in Climate Change Scenarios and Impact Studies. Proceedings of the ECLAT-2 Helsinki Workshop, Helsinki, Poland, 14 - 16 April 1999. 13 - 39.

IBSNAT. (1989). Decision Support System for Agrotechnology Transfer. Department of Agronomy and Soil Science. College of Tropical Agriculture and Human Resources, University of Hawaii, Hawaii.

Idso, S.B. and Brazel, A.J. (1984). Rising atmospheric carbon dioxide concentrations may increase streamflow. Nature, 312, 51 - 53.

IPCC (Intergovernmental Panel on Climate Change). (1990). Climatic Change: The IPCC Scientific Assessment. Report prepared by Working Group II. Tegart, W.J., Sheldon, G.W. and Griffiths, D.C. (eds). Australian Government Publishing Service, Canberra, Australia. pp 22.

IPCC (Intergovernmental Panel on Climate Change). (1994). IPCC Technical Guidelines for Assessing Climate Change Impacts and Adaptations. Report prepared by Working Group II and WMO/UNEP. Carter, T.R., Parry, M.L., Harasawa, H. and Nishioka, S. (eds). University College, London, England and Center for Global Environmental Research, National Institute for Environmental Studies, Tsukuba, Japan. pp 59.

IPCC (Intergovernmental Panel on Climate Change) Agricultural Impacts. (1995). Working Group II, Sub-group D (Agriculture). Reilly, J. (ed). WMO/UNEP, Geneva, Switzerland. pp 188.

IPCC (Intergovernmental Panel on Climate Change). (1995). Climate Change 1995: Impacts, Adaptations and Mitigation. Summary for Policymakers. Contribution of Working Group II to the Second Assessment Report. Cambridge University Press, New York, USA. pp 22.

IPCC (Intergovernmental Panel on Climate Change). (1996a). Climate Change 1995: The Science of Climate Change. Contribution of Working Group I to the Second Report of the Intergovernmental Panel on Climate Change. Houghton, J.T., Meira Filho, L.G., Callander, B.A., Harris, N., Kattenburg, A. and Maskell, K. (eds). Cambridge University Press, New York, USA. pp 572.

IPCC (Intergovernmental Panel on Climate Change). (1996b). Climate Change 1995: Impacts, Adaptations and Mitigation of Climate Change: Scientific - Technical Analyses. Contribution of Working Group II to the Second Report of the Intergovernmental Panel on Climate Change. Watson, R.T., Zinyowera, M.C. and Moss, R.H. (eds). Cambridge University Press, New York, USA. pp 876.

IPCC (Intergovernmental Panel on Climate Change). (2000a). Summary for Policymakers. Contribution of Working Group I to the Third Report of the Intergovernmental Panel on Climate Changes. pp 12.

IPCC (Intergovernmental Panel on Climate Change). (2000b). Summary for Policymakers. Contribution of Working Group II to the Third Report of the Intergovernmental Panel on Climate Changes. pp 18.

Jones, P. D. (1994). Hemispheric surface air temperature variability - A reanalysis and an update to 1993. Journal of Climate, 7, 1794 - 1802.

Jones, R.N. (2000). An irrigation demand model for climate change analysis. Climate Research, 14, 89 - 100.

Jones, C.A. and Kiniry, J.R. (1986). CERES-Maize: A simulation model of maize growth and development. Texas A&M University Press, College Station, Texas, USA.

Joubert, A.M. and Hewitson, B.C. (1997). Simulating present and future climates of southern Africa using General Circulation Models. Progress in Physical Geography, 21, 51–78.

Joubert, A.M. and Tyson, P.D. (1996). Equilibrium and coupled GCM simulations of future southern African climates. South African Journal of Science, 92, 471 - 484.

Kaiser, H.M., Riha, S.J., Wilks, D.S. and Sampath, R. (1993). Adaptation to Global Climate Change at the Farm Level. *In*: Kaiser, H.M. and Drennen, T.E. (eds). Agricultural Dimensions of Global Climate Change. St. Lucie Press, Delray Beach, USA. 136 - 152.

Kandel, R. (2000). Global warming and changes in atmospheric water content and fluxes. Presentation at the International Workshop on Climatic Change: Implication for the Hydrological Cycle and for Water Management, Wengen, Switzerland.

Katz, R.W. (1999). Techniques for Estimating Uncertainty in Climate Change Scenarios and Impact Studies. Proceedings of the ECLAT-2 Helsinki Workshop, Helsinki, Poland, 14 - 16 April 1999. 40 - 55.

Kayane, I. (1996). An Introduction to Global Water Dynamics. *In*: Jones, J.A.A., Liu, C., Woo, M. and Kuing, H. (eds). Regional Hydrological Response to Climate Change. Kluwer Academic Publishers, The Netherlands. 25 - 38.

Kienzle, S.W., Lorentz, S.A. and Schulze, R.E. (1997). Hydrology and Water Quality of the Mgeni Catchment. Water Research Commission, Pretoria, South Africa, Report TT87/97. pp 88.

Kiker, G.A. (1999). School of Bioresources Engineering and Environmental Hydrology. University of Natal, Private Bag X01, Scottsville, 3209, South Africa. Personal communication.

Kilsby, C. (1999). Hydrological Impact Modelling and the Role of Downscaling. Proceedings of the ECLAT-2 Helsinki Workshop, Helsinki, Poland, 14 - 16 April 1999. 89 - 91.

Körner, C. (1993). $CO_2$ Fertilization: The Great Uncertainty in Future Vegetation Dynamics. *In*: Solomon, A.M. and Shugart, H.H. (eds). Vegetation Dynamics and Global Change. Chapman and Hall, London, England. 53 - 70.

Kundzewicz, Z.W. (2000). Floods in the context of climate change and variability. Presentation at the International Workshop on Climatic Change: Implication for the Hydrological Cycle and for Water Management, Wengen, Switzerland.

Kunz, R.P. (1993). Techniques to Assess Possible Impacts of Climate Change in Southern Africa. Unpublished MSc dissertation, Department of Agricultural Engineering, University of Natal, Pietermaritzburg, South Africa. pp 172.

Kunz, R.P. and Schulze, R.E. (1993). A Sensitivity Analysis of Runoff Production in Southern Africa to Global Climate Change. *In*: Proceedings of the Sixth South African National Hydrological Symposium, Department of Agricultural Engineering, University of Natal, South Africa. 203 - 210.

Leavesley, G.H. (1999). Overview of Models for Use in the Evaluation of the Impacts of Climate Change on Hydrology. *In*: van Dam, J.C. Impacts of Climate Change and Climate Variability on Hydrological Regimes. Cambridge University Press, Cambridge, England. 107 - 122.

Leggatt, J., Pepper, W.J. and Swart, R.J. (1992). Emissions Scenarios for the IPCC: An Update. *In*: Houghton J.T., Callander B.A. and Varney S.K. (eds). Climate Change 1992: The Supplementary Report to the IPCC. 69 - 95.

Levitt, J. (1980). Responses of Plants to Environmental Stress, Vol. 1. Chilling and Freezing and High Temperature Stresses, 2nd edition. Academic Press, New York, USA.

Linacre, E.T. (1984). Unpublished manuscript. School of Earth Sciences, Macquarie University, Sydney, Australia.

Linacre, E.T. (1991). Unpublished manuscript. School of Earth Sciences, Macquarie University, Sydney, Australia.

Lins, H.F., Shiklomanov, I.A. and Stakhiv, E.Z. (1991). Impacts on Hydrology and Water Resources. *In*: Jäger, J. and Ferguson, H.L. (eds). Climate Change: Science, Impacts and Policy. Proceedings of the Second World Climate Conference. Cambridge University Press, Cambridge, England. 87 - 107.

Lindsley-Noakes, G.C., Louw, M. and Allan, P. (1995). Estimating daily Positive Utah Chill Units using daily minimum and maximum temperatures. Journal of the South African Society of Horticultural Science, 5, 19 - 28.

Liu, C. (2000). Vulnerability of water resources to environmental changes: A case study on the Yellow River, China. Presentation at the International Workshop on Climatic Change: Implication for the Hydrological Cycle and for Water Management, Wengen, Switzerland.

Loaiciga, H.A., Valdes, J.B., Vogel, R., Garvey, J. and Schwarz, H. (1996). Global warming and the hydrologic cycle. Journal of Hydrology, 174, 83 - 127.

Lorentz, S.A. and Schulze, R.E. (1995). Sediment Yield. *In*: Schulze, R.E. Hydrology and Agrohydrology: A Text to Accompany the *ACRU* 3.00 Agrohydrological Modelling System. Water Research Commission, Pretoria, South Africa, Report TT69/95. AT16-1 to AT16-34.

Lowe, K.L. (1997). Agrohydrological Sensitivity Analysis with Regard to Projected Climate Change in Southern Africa. Unpublished MSc dissertation, School of Environment and Development, University of Natal, Pietermaritzburg, South Africa. pp 104.

MacIver, D.C. (ed). (1998). Summary of IPCC Workshop on Adaptation to Climate Variability and Change, San Jose, Costa Rica. Atmospheric Environment Service, Ontario, Canada. pp 55.

Manabe, S., Stouffer, R.J., Spelman, M.J., and Bryan, K. (1991). Transient response of a coupled ocean-atmosphere model to gradual changes of atmospheric $CO_2$. Part I: Annual mean response. Journal of Climate, 4, 785-818

Manning, W.J. and Tiedemann, A. (1994). Climate change: Potential effects of increased atmospheric carbon dioxide ($CO_2$), ozone ($O_3$), and ultraviolet-B radiation on plant diseases. Environmental Pollution, 88, 219 - 245.

McAnally, W.H., Burgi, P.H., Calkins, D., French, R.H., Holland, J.P., Hsieh, B., Miller, B., Thomas, J. (1997). Water Resources. *In*: Watts, R.G. (ed). Engineering Response to Global Climate Change: Planning a Research and Development Agenda. Lewis Publishers, Boca Raton, USA. 261 - 290.

Meier, K.B. (1997). Development of a Spatial Database for Agrohydrological Model Applications in Southern Africa. Unpublished MSc dissertation, Department of Agricultural Engineering, University of Natal, Pietermaritzburg, South Africa. pp 141.

Meier, K.B. and Schulze, R.E. (1995). A New Spatial Database for Modelling Hydrological Responses in Southern Africa. Proceedings of the Seventh National South African Hydrology Symposium. Institute of Water Research, Rhodes University, Grahamstown, South Africa. pp 16.

Midgley, D.C., Pitman, W.V. and Middleton, B.J. (1995). Surface Water Resources of South Africa 1990. Water Resources 1990 Joint Venture. Water Research Commission, Pretoria, South Africa.

Mirza, M.M.Q. (1998). Water Demand, Development and Management in a Warmer Climate in South Asia. *In:* Zebidi, H. (ed). Water a looming crisis? Proceedings of the International Conference on World Water Resources at the Beginning of the 21st Century. UNESCO, Paris, France, 3 - 6 June 1998.

Morehouse, B.J. and Diaz, H.F. (1999). Institutional, political implications of climate impacts on water management in transboundary regions. Presentation at the International Workshop on Climatic Change: Implication for the Hydrological Cycle and for Water Management, Wengen, Switzerland.

Murphy, J.M. and Mitchell, J.F.B. (1995). Transient response of the Hadley Centre coupled ocean-atmosphere model to increase carbon dioxide. Part 2. Spatial and temporal structure of the response. Journal of Climate, 8, 57 - 80.

New, M. (2000). Uncertainty in Representing Observed Climate. Proceedings of the ECLAT-2 Helsinki Workshop, Helsinki, Poland, 14 - 16 April 1999. 61 - 68.

New, M. and Hulme, M. (1999). Representing uncertainty in climate change scenarios: A Monte-Carlo approach. Submitted to Environmental Modelling and Assessment.

NWA (National Water Act). (1998). National Water Act, Act No. 36 of 1998. Government Printer, Pretoria, South Africa. pp 200.

Olesen, J.E. Jensen, T. and Peterson, J. Sensitivity of field-scale winter wheat production in Denmark to Climate Variability and Climate Change. Climate Research, 15, 221 - 238.

Ortmann, G. (1999). Department of Agricultural Economics. University of Natal, Private Bag X01, Scottsville, 3209, South Africa. Personal communication.

Parry, M. and Carter, T.R. (1998). Climate Impact and Assessment: A Guide to the IPCC Approach. Earthscan Publications, London, England. pp 166.

Parry, M., Carson, I., Rehman, T., Tranter, R., Jones, P., Mortimer, D., Livermore, M. and Little, J. (1999). Economic Implications of Climate Change on Agriculture in England and Wales, Research Report No. 1. Jackson Environmental Unit, University College, London, England. pp 114.

Patz, J.A., McGeehin, M.A., Bernard, S.M., Ebi, K.L., Epstein, P.R., Grambsch, A., Gubler, D.J., Reiter, P., Romieu, I., Rose, J.B., Samet, J.M. and Trtajn, J. (2000). Potential consequences of climate variability and change for human health in the United States. www.nacc.usgrcp.gov.

Peixoto, J.P. (1997). The Role of the Atmosphere in the Water Cycle. *In*: Oliver, H.R. and Oliver, S.A. (eds). The Role of Water and the Hydrological Cycle in Global Change. Series 1: Global Environmental Change, Vol. 31. Proceedings of the NATO Advanced Study Institute on the Role of Water and the Hydrological Cycle in Global Change, II Cicocco, Lucca, Italy. Springer, Berlin, Germany, 199 - 252.

Penman, H.L. (1948). Natural Evaporation from Open Water, Bare Soil and Grass. Proceedings of the Royal Society A193, London, England, 120 - 146.

Perks, L.A., Schulze, R.E., Kiker, G.A., Horan, M.J. C. and Maharaj, M. (2000). Preparation of Climate Data and Information for Application in Impact Studies of Climate Change Over Southern Africa. *ACRU*cons Report 32. Report to the South African Country Studies for Climate Change Programme. School of Bioresources Engineering and Environmental Hydrology, University of Natal, Pietermaritzburg, South Africa. pp 75.

Pielke, R.A. Sr. (2000a). Overlooked Issues in the US National Climate and IPCC Assessments. Preprints, 11th Symposium on Global Change Studies, California, USA, 32 - 35.

Pielke, R.A. Sr. (2000b). Department of Atmospheric Science, Colorado State University, Fort Collins, Colorado, 80523, United States of America. Personal communication.

Piltz, R. (ed). (1998). Our Changing Planet: The FY 1998 U.S. Global Change Research Program. A Report to the Subcommittee on Global Change Research, Committee on Environment and Natural Resources of the National Science and Technology Council. A Supplement to the President's Fiscal Year 1998 Budget.

Pittock, A.B. (1991). Developing Regional Climate Change Scenarios: Their Reliability and Seriousness. Hawkesburg Centenary Conference, University of Western Sydney, Sydney, Australia, 25 - 27.

Pittock, A.B. and Jones, R.N. (1998). "Adaptation To What and Why?" Background Paper for the IPCC Workshop on Adaptation to Climate Variability and Change, San Jose, Costa Rica. Draft paper. pp 31.

Pittock, A.B. and Jones, R.N. (2000). Climate and water resources in Australia : Managing uncertainty and risk. Presentation at the International Workshop on Climatic Change: Implication for the Hydrological Cycle and for Water Management, Wengen, Switzerland.

Pittock, A.B., Fowler, A.M. and Whetton, P.H. (1991). Probable changes in rainfall regimes due to the enhanced greenhouse effect. International Hydrology and Water Resources Symposium. Perth, 2 - 4 October 1991. 182 - 186.

Polcher, J. (1999). Climate Projections: Physical Uncertainties. Proceedings of the ECLAT-2 Helsinki Workshop, Helsinki, Poland, 14 - 16 April 1999. 69 - 70.

Reilly, J. (1996). Climate Change, Global Agriculture and Regional Vulnerability. *In*: Bazzaz, F. and Sombroek, W. (eds). Global Climate Change and Agricultural Production: Direct and Indirect Effects of Changing Hydrological, Pedological and Plant Physiological Processes. John Wiley & Sons, New York, USA. 238 - 265.

Richardson, E.A., Seeley, D.D. and Walker, D.R. (1974). A model for estimating the completion of rest for 'Redhaven' and 'Elberta' peach trees. Hortsceince, 9, 331 - 332.

Richter, R.B., Baumgartner, J.V., Wigington, R. and Braun, D.P. (1997). How much water does a river need? Freshwater Biology, 37, 231 - 249.

Ringius, L., Downing, T.E., Hulme, M., Waughray, D. and Selrod, R. (1996). Climate Change in Africa: Issues and Challenges in Agriculture and Water for Sustainable Development. CICERO Report, 8. University of Oslo, Oslo, Norway. pp 151.

Risbey, J.S., Kandlikar, M. and Karoly, D.J. (2000). A protocol to articulate and quantify uncertainties in climate change detection and attribution. Climate Research, 16, 61 - 78.

Ritchie, J.T. (1972). Model for predicting evaporation from a row crop with incomplete cover. Water Resources Research, 8, 1204 - 1213.

Roeckner, E., Arpe, K., Bengtsson. L., Christoph, M., Claussen, M., Düümenil, L., Esch, M., Giorgetta, M., Schlese, U. and Schulzweida, U. (1996). The Atmospheric General Circulation Model ECHAM4: Model Description and Simulation of Present-day Climate. Max-Planck-Institut füür Meteorologie, Hamburg, Germany, Report 218. pp 90.

Rosenberg, N.J., Kimball, B.A., Martin, P. and Cooper, C.F. (1990). From Climate Change and $CO_2$ Enrichment to Evapotranspiration. *In*: Waggoner, P.E. (ed). Climate Change and U.S. Water Resources. John Wiley & Sons Inc., New York, USA. 151 - 175.

Rosenzweig, M.L. (1968). Net primary production of terrestrial communities: Prediction from climatological data. The American Naturalist, 102, 67 - 74.

Rosenzweig, C. and Hillel, D. (1998). Climate Change and the Global Harvest: Potential Impacts of the Greenhouse Effect on Agriculture. Oxford University Press, New York, USA. pp 324.

Rooseboom, A. (1992). The development of the new sediment yield map of southern Africa. Water Research Commission, Pretoria, South Africa, Report 279/1/92.

Rowlands, I.H. (1998). Climate Change Cooperation in Southern Africa. Earthscan Publications Ltd, London, England. pp 186.

Russell, G.L., Miller, J.R. and Rind, D. (1995). A coupled atmosphere-ocean model for transient climate change studies. Atmosphere-Ocean, 33, 683-730.

Schönau, A.P.G. and Stubbings, J.A. (1987). In Forestry Handbook. SA Institute of Forestry, Pretoria, South Africa. 106 - 115.

Schulze, R.E. (1983). Agrohydrology and -Climatology of Natal. Water Research Commission, Pretoria, South Africa. pp 137.

Schulze, R.E. (1991). Global Climate Change and Hydrological Response: A Southern African Perspective. *In*: Proceedings of the Fifth South African National Hydrological Symposium. University of Stellenbosch, Stellenbosch, South Africa. 1-1 to 1-17.

Schulze, R.E. (1993). The greenhouse effect and global climate change: An agricultural outlook for Namibia. Presentation Association of Agricultural Economics in Namibia - Seminar on Challenges to Agriculture to the Year 2000 Within a Changing Environment.

Schulze, R.E. (1995a). Hydrology and Agrohydrology: A Text to Accompany the *ACRU* 3.00 Agrohydrological Modelling System. Water Research Commission, Pretoria, South Africa, Report TT69/95. pp 503.

Schulze, R.E. (1995b). Soil Water Budgeting and Total Evaporation. *In*: Schulze, R.E. Hydrology and Agrohydrology: A Text to Accompany the *ACRU* 3.00 Agrohydrological Modelling System. Water Research Commission, Pretoria, South Africa, Report TT69/95. AT7-1 to AT7-22.

Schulze, R.E. (1995c). Hydrology, Agrohydrology and Agrohydrological Simulation Modelling. *In*: Schulze, R.E. Hydrology and Agrohydrology: A Text to Accompany the *ACRU* 3.00 Agrohydrological Modelling System. Water Research Commission, Pretoria, South Africa, Report TT69/95. AT1-1 to AT1-14.

Schulze, R.E. (1997a). Impacts of global climate change in a hydrologically vulnerable region: Challenges to South African hydrologists. Progress in Physical Geography, 21, 113 - 136.

Schulze, R.E. (1997b). South African Atlas of Agrohydrology and -Climatology. Water Research Commission Report, Pretoria, Report, TT82/96. pp 276.

Schulze, R.E. (1998). Modelling Hydrological Responses to Land Use and Climate Change: A Southern African Perspective. Invited Paper at IGBP Scientific Advisory Council V Meeting, Nairobi, Kenya. *ACRU*cons Report 17. School of Bioresources Engineering and Environmental Hydrology, University of Natal, Pietermaritzburg, South Africa. pp 30.

Schulze, R.E. (1999). Transcending scales of space and time in impact studies of climate and climate change on agrohydrological responses. Submitted to Agriculture Ecosystems and Environment. pp 25.

Schulze, R.E. (2000a). Transcending scales of space and time in impact studies of climate and climate change on agrohydrological responses. Agriculture, Ecosystems and Environment, 82, 185 - 212.

Schulze, R.E. (2000b). Risk, uncertainty and risk management in hydrology: A southern African perspective focussing on impacts of land use, climate variability, climate forecasting and climate change. Presentation at the International Workshop on Climatic Change: Implication for the Hydrological Cycle and for Water Management, Wengen, Switzerland.

Schulze, R.E., Angus, G.R., Lynch, S.D. and Smithers, J.C. (1995b). *ACRU*: Concepts and Structure. *In*: Schulze, R.E. Hydrology and Agrohydrology: A Text to Accompany the *ACRU* 3.00 Agrohydrological Modelling System. Water Research Commission, Pretoria, South Africa, Report TT69/95. AT2-1 to AT2-26.

Schulze, R.E., Dent, M.C., Lynch, S.D., Schäfer, N.W., Kienzle, S.W. and Seed, A.W. (1995a). Rainfall. *In*: Schulze, R.E. Hydrology and Agrohydrology: A Text to Accompany the *ACRU* 3.00 Agrohydrological Modelling System. Water Research Commission, Pretoria, South Africa, Report TT69/95. AT3-1 to AT3-38.

Schulze, R.E., Domleo, F.B., Furniss, P.W. and Lecler, N.L. (1995d). Crop Yield Estimation. *In*: Schulze, R.E. Hydrology and Agrohydrology: A Text to Accompany the *ACRU* 3.00 Agrohydrological Modelling System. Water Research Commission, Pretoria, South Africa, Report TT69/95. AT19-1 to AT19-14.

Schulze, R.E., Hallowes, J.S., Lynch, S.D., Perks, L.A. and Horan, M.J.C. (1998). Forecasting seasonal runoff in South Africa: A preliminary investigation. Report to CRG / Eskom. pp 19.

Schulze, R.E., Kiker, G.A. and Kunz, R.P. (1993). Global climate change and agricultural productivity in southern Africa: Thought for food and food for thought. Global Environmental Change, 3, 330 - 349.

Schulze, R.E., Kiker, G.A. and Kunz, R. P. (1996). Global climate change and agricultural productivity. *In*: Shackleton, L.Y., Lennon, S.J. and Tosen, G.R. (eds). Global Climate Change and South Africa. Environmental Scientific Association, Cleveland, South Africa. 90 - 95.

Schulze, R.E. and Kunz, R.P. (1995). Reference Potential Evaporation. *In*: Schulze, R.E. Hydrology and Agrohydrology: A Text to Accompany the *ACRU* 3.00 Agrohydrological Modelling System. Water Research Commission, Pretoria, South Africa, Report TT69/95. AT4-1 to AT4-38.

Schulze, R.E. and Kunz, R.P. (1996). Climate Change Scenarios for Southern Africa: A 1993 View. *In*: Shackleton, L.Y., Lennon, S.J. and Tosen, G.R. (eds). Global Climate Change and South Africa. Environmental Scientific Association, Cleveland, South Africa. 5 - 8.

Schulze, R.E., Lecler, N.L. and Hohls, B.C. (1995c). Land Cover and Treatment. *In*: Schulze, R.E. Hydrology and Agrohydrology: A Text to Accompany the *ACRU* 3.00 Agrohydrological Modelling System. Water Research Commission, Pretoria, South Africa, Report TT69/95. AT6-1 to AT6-32.

Schulze, R.E. and Lynch, S.D. (1992). Distributions and Variability of Primary Production over Southern Africa as an index of Environmental and Agricultural Resource Determination. Proceedings of ICID International Symposium on impacts of Climate Variations and Sustainable Development in Semi-Arid Regions. Foraleza, Brazil. Vol III, 721 - 740.

Schulze, R.E., Lynch, S.D., Smithers, J.C., Pike, A. and Schmidt, E.J. (1995e). Statistical Output from *ACRU*. *In*: Schulze, R.E. Hydrology and Agrohydrology: A Text to Accompany the *ACRU* 3.00 Agrohydrological Modelling System. Water Research Commission, Pretoria, South Africa, Report TT69/95. AT21-1 to AT21-36.

Schulze, R.E. and Nortje, C. (2000). School of Bioresources Engineering and Environmental Hydrology. University of Natal, Private Bag X01, Scottsville, 3209, South Africa. Personal communication.

Schulze, R.E. and Perks, L.A. (2000). Assessment of the Impact of Climate Change on Hydrology and Water Resources in South Africa. *ACRU*cons 33. Report to the South African Country Studies for Climate Change Programme. School of Bioresources Engineering and Environmental Hydrology, University of Natal, Pietermaritzburg, South Africa. pp 70.

Schulze, R.E. and Schmidt, E.J. (1995). Peak Discharge. *In*: Schulze, R.E. Hydrology and Agrohydrology: A Text to Accompany the *ACRU* 3.00 Agrohydrological Modelling System. Water Research Commission, Pretoria, South Africa, Report TT69/95. AT12-1 to AT12-9.

Shackleton, L.Y., Lennon, S.J. and Tosen, G.R. (eds). (1996). Global Climate Change and South Africa. Environmental Scientific Association, Cleveland, South Africa. pp 160.

Shiklomanov, I.A. (1999). Climate Change, Hydrology and Water Resources: The Work of the IPCC, 1988 - 94. *In*: van Dam, J.C. Impacts of Climate Change and Climate Variability on Hydrological Regimes. Cambridge University Press, Cambridge, England. 8 - 20.

Simons, D.B. and Sentürk, F. (1992). Sediment Transport Technology: Water and Sediment Dynamics. Water Resources Publication, Denver, Colorado, USA..

Smith, J.B. (1999, in press). Setting Priorities for Adapting to Climate Change. The Environmental Professional.

Smith, J.M.B. (1994). Crop, Pasture and Timber Yield Estimate Index. Natal Agricultural Research Institute, Cedara, South Africa. Cedara Report, N/A/94/4. pp 82.

Smith, J.B. and Lenhart, S.S. (1996). Climate change adaptation policy options. Climate Research, 6, 193 - 201.

Smithers, J.C. and Schulze, R.E. (1995). *ACRU* Agrohydrological Modelling System: User Manual Version 3.00. Water Research Commission, Pretoria, South Africa, Report TT70/95. AM6-1 to AM6-188.

SRK and DWAF. (1994). Mr J. Stern. Steffan, Robertson and Kirstern, Johannesburg, South Africa. Personal communication. Cited in Meier, K.B. (1997). Development of a Spatial Database for Agrohydrological Model Applications in Southern Africa. Unpublished MSc dissertation, Department of Agricultural Engineering, University of Natal, Pietermaritzburg, South Africa. pp 141.

Stakhiv, E.Z. (1998). Induced Climate Change Impacts on Water Resources. *In:* Zebidi, H. (ed). Water a looming crisis? Proceedings of the International Conference on World Water Resources at the Beginning of the 21st Century. UNESCO, Paris, France, 3 - 6 June 1998.

Sulzman, E.W., Poiani, K.A. and Kittel, T.G.F. (1995). Modelling human-induced climatic change: A summary for environmental managers. Environmental Management, 19, 197 - 224.

Sys, C., Van Ranst, E., Debaveye, J. and Beenaert, F. (1993). Land Evaluation Part III Crop Requirements. General Administration for Development Cooperation, Brussels, Belgium. ITC Agricultural Publication, No. 7. pp 199.

Tergart, W.J., Sheldon, M. and Griffiths, D.C. (1990). Climate Change: The IPCC Impacts Assessment. Intergovernmental Panel on Climate Change. Australian Government Publishing Service, Canberra, Australia.

Thompson, G.D. (1976). Water use by sugarcane. South African Sugar Association Journal, 60, 593 - 600 and 627 - 635.

Thompson S.L. and Pollard D. (1995). A global climate model (GENESIS) with a land-surface-transfer scheme (LSX). Part One: Present day climate. Journal of Climate, 8, 732-761.

Tyson, P.D. (1987). Climatic Change and Variability in Southern Africa. Oxford University Press, Cape Town, South Africa. pp 220.

UKMO (United Kingdom Meteorological Office. (2000). http://www.met-office.gov.uk/sec5/CR_div/pubs/brochures/B1998/science.html

Valentin, C. (1996). Soil Erosion Under Global Change. *In*: Walker, B. and Steffen, W. (eds). Global Change and Terrestrial Ecosystems. University Press, Cambridge, England. 317 - 338.

Viner, D. (2000a). The Climate Impacts LINK Project. http://www.cru.uea.ac.uk

Viner, D. (2000b). Representing uncertainties and the application of climate scenarios and impact studies: The ELCAT-2 Project. Presentation at the International Workshop on Climatic Change: Implication for the Hydrological Cycle and for Water Management, Wengen, Switzerland.

Voss, R., May, W. and Roeckner, E. (2000). Simulated changes in extreme events associated with the hydrological cycle under enhanced greenhouse conditions. Presentation at the International Workshop on Climatic Change: Implication for the Hydrological Cycle and for Water Management, Wengen, Switzerland.

Watson, R.T., Zinyowera, M.C, Moss, R.H. and Dokken, D.J. (eds). (1997). Summary for Policymakers, The Regional Impacts of Climate Change: An Assessment of Vulnerability. A Special Report of IPCC Working Group II. http://www.ipcc.ch

Westmacott, J.R. and Burn, D.H. (1997). Climate change effects on the hydrologic regime within the Churchill-Nelson river basin. Journal of Hydrology, 202, 263–279.

Whitmore, J.S. (1971). South Africa's water budget. South African Journal of Science, 67, 166 - 176.

Wigely, T.L. and Jones, P.D. (1985). Influences of precipitation changes and direct $CO_2$ effects on streamflow. Nature, 314, 149 - 152.

Wilby, R.L., Hay, L.E. and Leavesley, G.H. (1999). A comparison of downscaled and raw GCM output: Implications for climate change scenarios in the San Juan River Basin, Colorado. Journal of Hydrology, 225, 67 - 91.

Williams, J.R. (1975). Sediment Yield Prediction with Universal Equation using Runoff Energy Factor. *In*: Present and Prospective Technology for Predicting Sediment Yields and Sources, USDA-ARS, 40, 244 - 252.

Wischmeier, W.H. and Smith, D.D. (1978). Predicting Rainfall Erosion Losses - A Guide to Conservation Planning. USDA, Washington DC, Agricultural Handbook. pp 537.

Wolfe, D.W. and Erickson, J.D. (1993). Carbon Dioxide Effects on Plants: Uncertainties and Implications for Modeling Crop Response to Climate Change. *In*: Kaiser, H.M. and Drennen, T.E. (eds). Agricultural Dimensions of Global Climate Change. St. Lucie Press, Delray Beach, USA. 153 - 178.

World Bank. (1992). World Development Report 1992. Oxford University Press, New York, USA.

World Climate News. (2000). World Climate News, 17.

Yarnal, B. (1998). Integrated regional assessment and climate change impacts in river basins. Climate Research, 11, 65 - 74.

Zalom, F.G., Goodell, P.B., Wilson, L.T., Barnett, W.W. and Bentley, W.J. (1983). Degree days: The calculation and use of heat units in pest management. University of California, Division of Agriculture and Natural Resources, Berkley CA, USA. Leaflet 21373. pp 11.

# APPENDIX

Table A1 Monthly values of the water use coefficient ($K_d$) used in *ACRU* to indicate whether veld is in either poor or good hydrological condition

| Hydrological Condition of Veld | Jan | Feb | Mar | Apr | May | Jun | Jul | Aug | Sep | Oct | Nov | Dec |
|---|---|---|---|---|---|---|---|---|---|---|---|---|
| Poor | 0.55 | 0.55 | 0.55 | 0.45 | 0.20 | 0.20 | 0.20 | 0.20 | 0.30 | 0.40 | 0.50 | 0.55 |
| Good | 0.75 | 0.75 | 0.75 | 0.65 | 0.40 | 0.20 | 0.20 | 0.20 | 0.30 | 0.60 | 0.65 | 0.70 |

Table A2 Monthly values of the leaf area index (LAI) used in *ACRU* to indicate whether veld is in either poor or good hydrological condition

| Hydrological Condition of Veld | Jan | Feb | Mar | Apr | May | Jun | Jul | Aug | Sep | Oct | Nov | Dec |
|---|---|---|---|---|---|---|---|---|---|---|---|---|
| Poor | 0.80 | 0.80 | 0.80 | 0.80 | 0.80 | 0.80 | 0.80 | 0.80 | 0.80 | 0.80 | 0.80 | 0.80 |
| Good | 1.50 | 1.50 | 1.50 | 1.50 | 1.50 | 1.50 | 1.50 | 1.50 | 1.50 | 1.50 | 1.50 | 1.50 |

Table A3 Monthly values of the coefficient of initial abstraction (COIAM) used in *ACRU* to indicate that veld is in poor hydrological condition

| Hydrological Condition of Veld | Jan | Feb | Mar | Apr | May | Jun | Jul | Aug | Sep | Oct | Nov | Dec |
|---|---|---|---|---|---|---|---|---|---|---|---|---|
| Poor | 0.10 | 0.10 | 0.15 | 0.25 | 0.25 | 0.25 | 0.25 | 0.25 | 0.25 | 0.20 | 0.15 | 0.10 |

Table A4 Modified values of the coefficient of initial abstraction (COIAM) for standard hydrological response simulations depending on which rainfall seasonality region the Quaternary Catchment falls into

| Rainfall Region | Jan | Feb | Mar | Apr | May | Jun | Jul | Aug | Sep | Oct | Nov | Dec |
|---|---|---|---|---|---|---|---|---|---|---|---|---|
| All year rainfall | 0.20 | 0.20 | 0.30 | 0.30 | 0.30 | 0.30 | 0.30 | 0.30 | 0.30 | 0.30 | 0.30 | 0.20 |
| Winter rainfall | 0.25 | 0.25 | 0.30 | 0.30 | 0.30 | 0.30 | 0.30 | 0.30 | 0.30 | 0.30 | 0.30 | 0.25 |
| Summer rainfall | 0.15 | 0.15 | 0.20 | 0.30 | 0.30 | 0.30 | 0.30 | 0.30 | 0.30 | 0.25 | 0.20 | 0.15 |

Table A5 List of Primary and Secondary Catchments that fall into different rainfall seasonality zones used to determine values of the coefficient of initial abstraction (COIAM)

| | |
|---|---|
| All year rainfall | Primaries : K, P |
| | Secondaries : J4, H8, H9, L7, L9, N3, N4 |
| Winter rainfall | Primaries : E, F, G |
| | Secondaries : H1, H2, H3, H4, H5, H6, H7, J1 |
| Summer rainfall | Primaries : A, B, C, D, M, Q, R, S, T, U, V, W, X |
| | Secondaries : remaining J, L and N catchments |

Table A6 Modified values of the water use coefficient ($K_d$), vegetation interception loss ($I_l$) and root fraction in the A horizon ($R_A$) when maize is planted in the catchment (Assumed plant date: 15 November)

| | Jan | Feb | Mar | Apr | May | Jun | Jul | Aug | Sep | Oct | Nov | Dec |
|---|---|---|---|---|---|---|---|---|---|---|---|---|
| $K_d$ | 1.10 | 0.95 | 0.46 | 0.20 | 0.20 | 0.20 | 0.20 | 0.20 | 0.20 | 0.20 | 0.49 | 0.98 |
| $I_l$ | 1.50 | 1.40 | 1.30 | 1.20 | 0.50 | 0.50 | 0.50 | 0.50 | 0.50 | 0.50 | 0.50 | 0.90 |
| $R_A$ | 0.90 | 0.90 | 0.90 | 0.94 | 1.00 | 1.00 | 1.00 | 1.00 | 0.92 | 0.92 | 0.90 | 0.90 |

Table A7 Inputs used in *ACRU* for the irrigation option

| *ACRU* Input | Assumption for Irrigation |
|---|---|
| Monthly value of the coefficient for initial abstraction for the irrigated area | 0.3 |
| Texture of soil in the irrigated area | Sandy clay loam |
| Soil water content at lower limit for the soil being irrigated | 0.160 $m.m^{-1}$ |
| Soil water content at the drained upper limit for the soil being irrigated | 0.260 $m.m^{-1}$ |
| Soil water content at saturation (i.e. porosity) for the soil being irrigated | 0.440 $m.m^{-1}$ |
| Water use coefficient for each month of the year | 0.8 |
| Interception loss for the crop under irrigation | 1.5 $mm.irrigation^{-1}$ or $mm.rainday^{-1}$ |
| Potential rooting depth of the irrigated crop under the prevailing conditions | 0.8 m |
| Soil depth to which the majority of soil water extraction takes place for a fully grown irrigated crop | 0.8 m |

Table A7 Inputs used in *ACRU* for irrigation option (cont.)

| *ACRU* Input | Assumption for Irrigation |
|---|---|
| Water use coefficient of the irrigated crop when the rooting depth reaches a maximum | 0.8 |
| Water use coefficient of the irrigated crop at which ground cover is a maximum | 0.8 |
| Maximum amount of ground covered by the irrigated crop | 100 % |
| Critical leaf water potential of the irrigated crop | -1000 kPa |
| Fraction of plant available water at which irrigation water is applied | 0.5 |
| Conveyance losses, i.e. the fraction of the irrigated water that is lost in conveying it from the source to the application point. | 0.1 |
| Spray evaporation and wind drift losses | 0.1 |



Table A8 Values of the vegetation interception loss used when a sediment analysis or extreme value analysis is performed

| | Jan | Feb | Mar | Apr | May | Jun | Jul | Aug | Sep | Oct | Nov | Dec |
|---|---|---|---|---|---|---|---|---|---|---|---|---|
| Vegetation interception loss for veld in poor hydrological condition | 0.80 | 0.80 | 0.80 | 0.80 | 0.80 | 0.80 | 0.80 | 0.80 | 0.80 | 0.80 | 0.80 | 0.80 |
| Vegetation interception loss for veld in good hydrological condition | 1.50 | 1.50 | 1.50 | 1.50 | 1.50 | 1.50 | 1.50 | 1.50 | 1.50 | 1.50 | 1.50 | 1.50 |

Table A9 Values of the coefficient of initial abstraction (COIAM) used when an extreme value analysis is performed

| | Jan | Feb | Mar | Apr | May | Jun | Jul | Aug | Sep | Oct | Nov | Dec |
|---|---|---|---|---|---|---|---|---|---|---|---|---|
| Coefficient of initial abstraction | 0.15 | 0.15 | 0.20 | 0.30 | 0.30 | 0.30 | 0.30 | 0.30 | 0.30 | 0.25 | 0.20 | 0.15 |